PROPERTIES AND BEHAVIOUR OF STRUCTURAL LIGHTWEIGHT (LYTAG - SAND) CONCRETE

BY

G. LAMBERT. B.Eng.

Thesis submitted for the degree of Doctor of Philosophy at the University of Sheffield

January 1982

To Ann

SUMMARY

Lytag is a synthetic lightweight aggregate which has been in commercial production for many years. Its production process involves sintering pulverised fuel ash at approximately 1200-1300^{o}C to produce spherical, chemically inert pellets with a porous structure, which is graded into coarse, medium and fine grades.

Concrete, produced with Lytag coarse and fine material, has been extensively studied to assess its basic material and structural properties. Few data, however, are available on concrete made with Lytag coarse material and natural sand fines. The aims of this investigation were basically two-fold. Firstly the material properties of Lytag-sand concrete were investigated and an extensive study of various properties such as strength, moduli of elasticity, Poisson's ratio, stress-strain characteristics, shrinkage, moisture movement and creep are reported. Secondly, the structural behaviour of reinforced Lytag-sand concrete T-beams failing in shear and flexure was also investigated.

As with all concretes, these properties are affected by the constituents which make up the concrete, in particular the aggregate. With this in mind microscopic examination of several Lytag pellets was carried out using a scanning electron microscope (S.E.M.) in order to observe some of the physical characteristics of Lytag aggregates in general. An attempt was then made to relate these characteristics to the water absorption of Lytag aggregates.

The test results show that concrete strengths of 60 N/mm^2 are easily obtainable using Lytag and sand, and that in general a lower cement content is required for Lytag-sand, than for other sand replaced lightweight concretes, in order to achieve a given compressive strength. Shrinkage and creep are comparable with the range of values obtained for concretes made with various dense aggregates but when compared to concretes made with good quality dense aggregates values of the order of 1.5 times the dense concrete values are to be expected.

The nominal ultimate shear stresses at failure, for the beams tested were significantly greater than the allowable shear stresses quoted in the British design code. The instantaneous deflection and crack widths at design service moment are within the maximum recommended values for serviceability and tests showed that Lytag-sand concrete has a high strain capacity in excess of 4000 microstrain.

Various empirical formulae and design equations are presented and conclusions are drawn at the end of each chapter concerned with test data. Limitations of the present investigation and proposals for future work are also discussed.

ACKNOWLEDGEMENTS

The author wishes to express his sincere thanks to Dr. R. N. Swamy for his constant supervision, valuable suggestions and general interest at all stages of this study. He also wishes to convey his thanks to Professor D. Bond and Professor T. H. Hanna, for their concern and encouragement.

The research was funded under a case award by S.R.C. and Messrs Lytag Ltd. to whom the author is indebted.

The author also wishes to acknowledge the assistance of the technical staff, in particular Mr. R. Newman, and of the secretarial staff of the department. Thanks are due to Linda Bell, Julia Hunter and Pam Pennington for their careful, accurate typing of the manuscript.

Finally the author wishes to acknowledge the interest and concern expressed by his parents, throughout this study and to thank his wife Ann for her patience and understanding in tolerating the authors preoccupation with his work.

CONTENTS

LIST OF FIGURES

LIST OF TABLES

LIST OF PLATES

NOTATION

Symbols which are used constantly throughout the thesis are defined below. Symbols which occur less frequently are defined as they appear.

A_{st} - area of tension reinforcement
a - distance between load point and support; shear span
b - section width
b_f - flange width
b_w - web width
C - concrete cover
d - effective depth of section
E_c - elastic modulus of concrete
E_D - dynamic modulus of elasticity
E_S - static modulus of elasticity
f_c' - cylinder crushing strength
f_{ct} - tensile strength of concrete
f_{cu} - cube crushing strength
f_{MR} - tensile strength by modulus of rupture test
f_{Sp} - tensile strength by split cylinder test
f_y - yield stress of tensile reinforcement
h - overall depth of section
I_c - moment of inertia of cracked transformed section
I_e - effective moment of inertia
I_g - moment of inertia of gross concrete section about the centroidal axis, neglecting reinforcement
L - effective span between supports
M - applied bending moments
M_c - moment due to tensile strength of concrete
M_{cr} - moment at first flexural crack
M_{exp} - experimental ultimate moment
M_f - calculate ultimate flexural moment
M_u - ultimate moment for shear beams
S_v - link spacing
t - time after loading or initial readings
U_w - concrete crushing strength
V - shear strength
V_{cr} - shear cracking strength
V_u - ultimate shear strength
v_c - maximum allowable concrete shear stress (CP110 (54))
v_{cr} - shear cracking stress
v_u - ultimate shear stress
x - neutral axis depth
Z - internal lever arm
ρ - longitudinal steel percentage
ρ_b - balanced steel ratio
ρ_f - longitudinal steel percentage based on flange width
ρ_w - longitudinal steel percentage based on web width

ABBREVIATIONS

A.C.I.	-	American Concrete Institute
B.R.S.	-	Building Research Station now known as Building Research Establishment (B.R.E.)
C.E.B.	-	Euro-International Committee for Concrete
C.L.	-	centre line
C.M.R.	-	constant moment region
C.T.H.R.	-	constant temperature and humidity room
D.O.E.	-	Department of the Environment
D.T.	-	diagonal tension
dia.	-	diameter
F.I.P.	-	International Federation for Prestressing
L.W.A.	-	lightweight aggregate
O.P.C.	-	ordinary portland cement
P.C.A.	-	Portland Cement Association
p.f.a.	-	pulverised-fuel ash
R.C.	-	reinforced concrete
R & D	-	research and development
RILEM	-	International Union for Materials Testing Laboratories
R.H.	-	relative humidity
S.E.M.	-	scanning electron microscope
U.W.I.S.T.	-	University of Wales Institute of Science and Technology
W.C.	-	web crushing

CHAPTER 1

INTRODUCTION

1.1 General Introduction

Concrete, either reinforced or prestressed, is perhaps the most widely used structural material; it is economical and the raw materials needed for the manufacture of its constituents are available in most countries throughout the world.

When compared to other building materials such as steel, however, the density of a crushed rock or gravel concrete is high in relation to its strength. Thus the availability of a structural concrete with reduced density has obvious advantages.

Structural lightweight concrete is not a new building material, on the contrary it has been in existence for a considerable number of years. Despite this, and the fact that many investigators have turned their attentions towards the properties and behaviour of lightweight concretes, both at home and abroad, it is still regarded with great caution by the majority of practicing engineers in this country.

To most engineers the word concrete describes a material consisting of cement, sand and crushed rock or gravel, with a certain water cement ratio, having an air dry density of approximately 2300-2400 kg/m^3 and able to achieve a wide range of strengths, 15 - 100 + N/mm^2, depending on the relative proportions of its constituents. Their only contact with lightweight concrete is in the form of concrete blockwork or floor and roof screeds. Thus an association is formed between lightweight and low strength.

It is true that not all lightweight concretes are suitable for reinforced or prestressed concrete work; however most lightweight aggregates are capable of producing concretes suitable for reinforced concrete members and several types of aggregate are capable of producing high strength concrete, 60 + N/mm^2, suitable for prestressing.

Several classifications exist for lightweight concrete and probably the most comprehensive is that put forward by Rilem (1).

The classification covers the following:

(a) type of lightweight concrete

(b) type of binder

(c) type of aggregate

(d) type of curing

(e) function.

For the purpose of this thesis, only lightweight aggregate concrete will be under consideration, unless otherwise specified. It shall be referred to simply as lightweight concrete while crushed rock or gravel concrete shall be referred to as dense concrete.

The first organised attempt to promote the use of lightweight concrete, in the UK, was undertaken by the British Reinforced Concrete Association who held a one-day symposium on 'Structural lightweight concrete' in June 1962. This was attended by over four hundred engineers from both the consulting and the contracting sections of the civil engineering industry. Over the next ten to fifteen years, numerous articles appeared in the various construction journals (2-9), heralding the advent of structural lightweight concrete. There have been two international congresses on lightweight concrete both held in London. The first was in 1968 and the second, CI80, in 1980. In addition to this researchers in the UK have been investigating the physical properties and characteristics of the various lightweight aggregates manufactured in this country (10-15), since the late fifties, but despite these attempts to educate the construction industry in the virtues of lightweight concrete, its use is still relatively limited in comparison to that of dense concrete.

Its early use as a structural material stemmed mainly from a need to solve specific problems such as a need to reduce a structures dead weight because of span or poor ground conditions, for example the prestressed cantilever roofs on the grandstands at Doncaster, Leopardstown and Goodwood racecourses, or the floor slabs of the new National Westminster bank tower in London. Present day design and construction knowledge, for lightweight concrete, stems mainly from the south east of England where the scarcity of good quality natural

aggregates has forced the construction industry to look at alternative sources of aggregates. It is now fair to say that several consultants, contractors and ready mix concrete companies are well experienced in the design and construction of lightweight concrete structures.

The use of lightweight concrete in the USA and Europe has shown that it has many advantages. Its lower density means that a structure's dead weight can be reduced with a consequent reduction in the size of foundations. Alternatively the dimensions of elements can be considerably enlarged without having to alter erection systems or craneage capacity; or the geometric shape of an element can be greatly simplified without increasing its overall weight. The density of lightweight concrete in air ranges between about 75-85% of that of dense concrete. When submerged under water, however, the density of lightweight concrete may be as low as 55% of that for dense concrete (15). This increased bouyancy has obvious advantages for use in marine structures such as offshore production platforms and floating docks. Further advantages include the fact that lightweight concrete is easier to handle enabling larger pours, free from construction joints to be undertaken. Lightweight aggregates tend to be less abrasive than dense aggregates thus reducing formwork and plant maintenance costs. Lightweight concrete shows better insulating and fire resistance properties and experience (16) has indicated that for a given fire endurance, the thickness of lightweight concrete required is approximately 20% less than traditional gravel concrete. Heat losses through solid lightweight concrete walls are reduced by between 20 and 50%, depending upon the density of the material. Also drilling, cutting and chasing of lightweight concrete is easier and therefore cheaper.

As with all materials, there are of course disadvantages, not least of which is the fact that per cubic metre lightweight concrete is generally more expensive than dense concrete.

This higher cost is made up, basically, of two components, namely:

(a) The higher haulage costs generally associated with lightweight aggregate delivery to site or ready mix plants. The relatively small number of plants

producing lightweight aggregates means that, generally, longer haulage distances are involved with delivery.

(b) The higher cement contents generally required to reach a given cube strength, in relation to the cement contents of a dense concrete of similar strength.

Investigations (17, 18) have shown that if a direct substitution of lightweight for dense concrete is made then costings will invariably favour dense concrete. It is only when the project as a whole is designed specifically with lightweight concrete in mind that the savings in foundations, steel and concrete quantities and handling and erection costs can be appreciated. In some cases savings are considerable. For example the One Shell Plaza in Houston, Texas was originally designed as a 35-storey building in dense concrete on a floating foundation. The design was changed to a 52-storey, 217 m high building in lightweight concrete, with no increase in the 18 m deep foundation despite the fact that it rests on a 600 m thick layer of clay.

Other disadvantages include lower sound absorption, higher creep and therefore prestress losses and greater deflections due to the lower modulus of elasticity.

Although individual brands of lightweight aggregates are very consistent in physical properties and characteristics substantial differences may occur between different brands. This has often been quoted as a measure of their potential unreliability, while the variation in quality, durability and long term behaviour of concretes made with dense aggregates from various sources, which is considerable, has been neglected. It is important however, that data be available for all lightweight aggregates and the concretes they produce. For this reason research projects to investigate the various commercially available lightweight aggregates in the UK have been undertaken.

1.2 Aims of this Investigation and Outline of Thesis

The purpose of this project was to investigate the properties and behaviour of concrete made with coarse sintered-pulverised fuel ash, Lytag, aggregate and natural sand fines. Chapter 2 is a literature review of available

information relevant to this project. Chapters 3-8 cover the various properties and characteristics investigated and Chapter 9 summarises the limitations of the present work, the overall conclusions and recommendations for future work.

Each of Chapters 3-8 covers a series of tests carried out to investigate a particular set of related properties and characteristics and the aims of each series of tests are described below.

Although Lytag has been commercially available since the early sixties no work has been reported on investigations of the microstructure of Lytag pellets. As a part of this project a study of the microstructure of Lytag pellets was made using a scanning electron microscope (S.E.M.) and this work is reported in Chapter 3 along with an attempt to relate, qualitatively, the water absorption characteristics of the pellets to their microstructure.

Chapter 4 covers mix design and strength characteristics of Lytag-sand concrete. A mix design chart is derived for compressive strengths ranging from 20 N/mm^2 up to 60 N/mm^2. Long term compressive strength characteristics and short term tensile strength characteristics are also reported.

Chapter 5 covers the short term deformation properties of Lytag-sand concretes for strengths ranging from 20 N/mm^2 up to 60 N/mm^2. The properties investigated included the static and dynamic moduli of elasticity and Poisson's ratio. A series of tests was also carried out to obtain the complete stress-strain curves for concretes of different compressive strength.

The results of a series of tests to investigate the long term deformation properties of Lytag-sand concrete are presented in Chapter 6. The shrinkage, creep and moisture movement properties were studied for three different concrete strengths. Shrinkage specimens were curved under four different conditions while creep specimens were cured under constant temperature and humidity only. For each cube strength studied, two specimens were loaded per creep rig with two rigs at different stress-strength ratio's being used. Moisture movement specimens were subjected to cyclic drying and wetting in order to determine its effect on the volume and density stability of the concrete.

Chapter 7 covers tests carried out to investigate the shear behaviour of

Lytag-sand concrete T-beams. Three of the more important parameters which effect the shear behaviour of reinforced concrete beams were varied, namely the shear span-effective depth ratio, the longitudinal steel percentage and the concrete strength. Four shear span-effective depth ratio's, six longitudinal steel percentages and three concrete strengths were investigated and a total of thirty three beams were tested.

The last chapter dealing with test data, Chapter 8, covers tests carried out to determine some of the flexural characteristics of Lytag-sand reinforced concrete T-beams. Two concrete strengths and six longitudinal steel percentages were used with a total of six beams being tested.

Conclusions are drawn at the end of each chapter with a summary of limitations of the present work, conclusions and recommendations for future work being presented in Chapter 9.

CHAPTER 2

LIGHTWEIGHT AGGREGATE CONCRETE: A LITERATURE REVIEW

2.1 Introduction

In this chapter, an up to date review of the literature available on structural lightweight concrete is presented. It begins with an account of the history and development of lightweight aggregate concrete which is followed by a review of past research in both the USA and the UK. The main conclusions concerning the general properties of lighweight concrete are summarised. This is followed by a review of past research concerned with investigating the effects of sand replacement on the properties and behaviour of lightweight concrete and again a summary of the main conclusions is presented. Finally a review of the various design procedures and guidelines for lightweight concrete, given in the American and European design codes, is presented.

2.2 History and Development

Lightweight concrete is by no means a new material. Probably its earliest use, in a structural form, was as far back as Roman times. In the second century AD the Romans constructed the Pantheon in Rome. The outstanding feature of this building is its 43 m diameter domed roof, composed almost entirely of cast-in-situ lightweight concrete made with pumice aggregate. A similar type of concrete was used in the construction of the Colosseum, also in Rome.

The first large scale use of lightweight aggregates, for concrete, occurred during the First World War when a number of lightweight concrete ships and barges were built in both the UK and USA. With the war over, however, and the shortage of steel no longer a problem, the use of lightweight concrete was all but abandoned.

Possibly the most important development in the history of lightweight concrete occurred in America. In 1918, Mr. S. J. Hayde patented a process for manufacturing lightweight aggregates by expanding clay in a rotary kiln. The market did not develop significantly until after 1945 when there was a rapid expansion in the use of lightweight concrete throughout the USA. In 1957 Shideler (19), reported that most of the 41 plants producing lightweight

aggregates from shales and clays, at that time, had only been built in the post-war years. There were also 18 plants producing lightweight aggregates from slag.

Despite the fact that at the turn of the century, clinker from the then new solid-fuel-fired power stations was being used on a commercial scale in the UK, it was not until 1944 that the first British Standard specification for clinker aggregate, BS 1165 (20), was published.

The first processed lightweight aggregate in Great Britain, foamed blast furnace slag, came into commercial production in 1935 and a covering British Standard, BS 877 (21), was published in 1939. However, it was not until the 1957 edition of CP114 (22), 'The Structural use of Reinforced Concrete in Buildings', that mention was made of foamed slag, to BS 877 (21), and natural pumice as allowable aggregates for use in structural lightweight concrete. Pumice had been imported in small quantities before 1939 when imports ceased. They did not restart until 1966.

In 1954 commercial production of an expanded clay aggregate, 'Leca', began in Britain. This was followed in 1957 by 'Aglite' a sintered colliery shale and clay mix; in 1961 by 'Lytag' a sintered pulverised-fuel ash and in 1966 by 'Solite' an expanded slate.

The revised edition of CP114, 1965 (22), stated that foamed slag to BS 877 (21), expanded clay, slate shale or slag, sintered pulverised-fuel ash and other types of suitable aggregate were now permissible materials for use as lightweight aggregates.

Thus, it can be seen that suitable standards covering quality control and design were slow in coming. This was probably due to the comparative abundance of natural gravels, sands and crushed rock was well as the lack of understanding of the potential of lightweight aggregates for use in structural concrete.

By the late fifties, early sixties, therefore, the UK was producing several lightweight aggregates but their use was restricted mainly to the production of lightweight concrete building blocks. Production has increased since then to some 1.5-2.0 million tonnes, annually.

2.2.1 Lightweight Aggregate Production in the UK

One of the advantages of lightweight aggregates is that they can be manufactured from a variety of waste materials which are produced in this country.

Table 2.1 lists the quantities, disposal and use of common waste materials produced in Great Britain in 1978 (23). Table 2.2 shows the estimated aggregate production (dense and lightweight) in Great Britain in 1978 (23). It can be seen that recycled waste materials only contribute a very small proportion of the sum total.

Table 2.3 and Figure 2.1 show the locations and annual productions of Britain's lightweight aggregate manufacturers (23). There are a total of 15 aggregate production plants in Great Britain grouped mainly in the North of England and the Midlands. This in itself may explain why the use of lightweight concrete is not more widespread. The cost of lightweight aggregates delivered to ready mix plant or to site is generally greater than for dense aggregate. This is accounted for mainly by the longer haulage distances associated with lightweight aggregate distribution. Coupled with this is the fact that many areas of the North of England and the Midlands, such as the Trent valley region, still have plentiful supplies of easily accessible sands and gravels.

However at a time when conservation of the landscape is such a prominent issue, it seems unthinkable that we should not utilise the vast spoils of potentially recyclable materials available in this country.

2.3 General Properties of Lightweight Aggregate Concrete

The state of the art in terms of the use of lightweight aggregate concretes is well advanced, and it is probably fair to say that more is known about individual lightweight aggregates than any single type of natural aggregate. This has been brought about by the detailed investigations of many different types of lightweight aggregates, reported by researchers in the USA and the UK. The realisation that different brands of lightweight aggregate exhibit their own individual characteristics has led to the production of data on each aggregate type.

Type	Production M. Tonnes per Year	Stockpile M. Tonnes	Amount Used M. Tonnes per Year	Use	Disposal M. Tonnes per Year
Colliery spoil	50	3250	7-8	LWA, bricks, fill	42 on land and sea
Pulverised fuel ash (pfa)	11	250	4-5	LWA, fill, cement replacement	5-6 lagoons and old workings
Furnace bottom ash	5.5	not known	most used	concrete, blocks, fill	lagoons
China clay waste	22	300	1.5	brick manufacture	tipping, lagoons
Blast furnace slag	10	not known	9	LWA, filter media, etc.	-

TABLE 2.1 APPROXIMATE QUANTITIES, DISPOSAL AND USE OF THE MAJOR WASTE MATERIALS IN GREAT BRITAIN (23) 1978

	Million Tonnes
Sand and gravel	110.0
Marine dredged aggregate	12.0
Crushed rock	100.0
Furnace bottom ash	5.5
Furnace clinker	0.5
Manufactured lightweight aggregates	1.5
	229.5

TABLE 2.2 ESTIMATE OF AGGREGATE PRODUCTION IN GREAT BRITAIN (23) 1978

Aggregate	No. of Plants	Location (Fig. 2.1)	Production (m^3 x 1000)
Aglite	1	1	200
Foamed slag	4	2,3,4,5	300
Foamed slag (pelletised) Lycrete, Pellite	4	8,9	300
Leca	1	6	250
Lytag	3	7	550
Sintag	1	10	200
Taclite	1	11	150
TOTAL	15	-	1950

TABLE 2.3 LOCATIONS AND ANNUAL PRODUCTION OF BRITAINS LIGHTWEIGHT AGGREGATE MANUFACTURERS (23) 1979

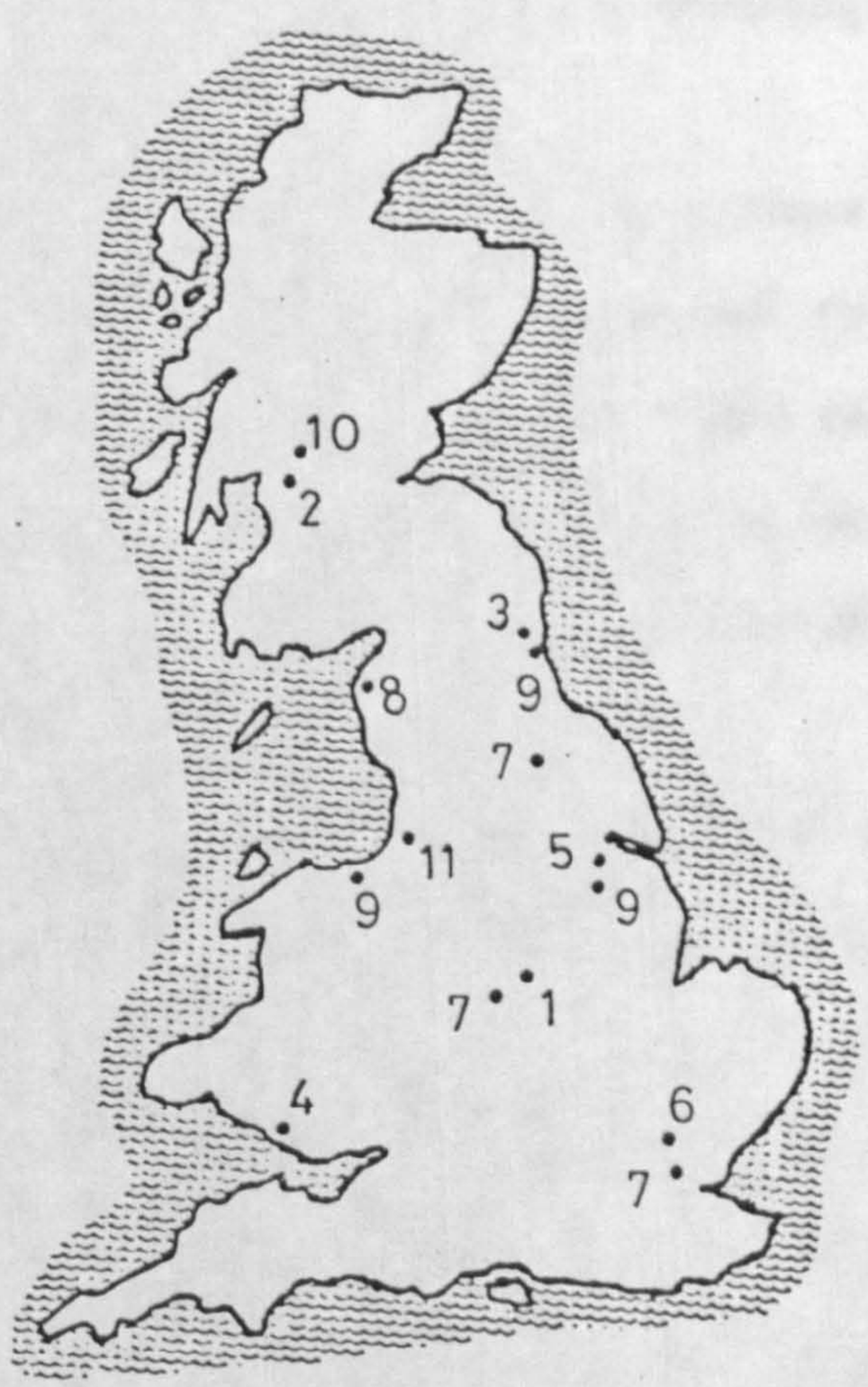

FIGURE 2.1

In this section a review of past research is presented. The following chapters each contain a comprehensive review of research relevant to the topic under discussion.

2.3.1 Previous Research in the United States

Probably the earliest investigators to concern themselves with the properties of lightweight concrete were Richart and Jensen (24), who carried out a series of tests on concrete made with Haydite aggregate. The investigation was divided into two groups of tests concerned with the properties of the aggregates themselves and the properties of concrete made with them. Their main conclusions include the following:

1. While concrete made with Haydite aggregate generally required greater water-cement ratios for similar mixes and equal slumps, the relation between compressive strength and water-cement ratio of Haydite concrete does not differ greatly from that for gravel concrete.
2. For beams without web reinforcement, which failed by diagonal tension, the ratio of the shearing unit stress to the compressive strength of control cylinders was practically the same for corresponding mixtures of gravel and Haydite concrete.
3. The ultimate strength of reinforced concrete columns made with Haydite concrete varied between 84 and 108% of the values for corresponding gravel concretes for tied and spiral reinforcement cages respectively.
4. The modulus of elasticity of Haydite concrete is approximately 55% of that for corresponding gravel concrete for the considerable range of mixtures and consistencies tested.

Washa, Kluge, Carlson and Valore (25) presented a condensed early history of the use of lightweight aggregates in 1956. Washa and Kluge (25) investigated the structural properties of lightweight concretes as part of the work of A.C.I. Committee 213 after 1948. Washa (25) concluded that:

1. The modulus of elasticity of structural lightweight concrete varies between about 50 and 67% of that for comparable gravel concrete.

2. Drying shrinkage is variable, for lightweight concrete, usually ranging between 0.01 and 0.50%.
3. The coefficient of thermal expansion of lightweight concrete is usually about equal to that of gravel concrete.

Kluge (25) attempted to correlate all the available test data, published and unpublished and presented this as a guide in the use of lightweight aggregate for structural concrete, in 1956. The main conclusions are as follows:

1. The unit weight of the concretes increased with increase in strength. At high strengths the rate of increase was relatively small.
2. The modulus of elasticity data for the various concretes considered showed similar values to those reported by Richart and Jensen (24).
3. The bond strengths reported vary widely, mainly because of a lack of standard test procedure. Calculated values of bond stress from pull out tests were 50% or more than required by ACI-318-51 (26).
4. There were very few data available on the shearing resistance of lightweight concrete. Shear strengths were 60 to 300% above those required by the 1951 ACI Building Code (26).

For a number of years tests were carried out on various lightweight aggregates at the Portland Cement Association. Early tests were reported by Shideler (19). An extensive series of tests were carried out on concretes made with eight different lightweight aggregates and one gravel aggregate. Concrete mixes were designed to produce compressive strengths of 21 N/mm^2 and 31 N/mm^2 for all aggregates and 48 N/mm^2 and 69 N/mm^2 for three selected aggregates.

Data reported include mix properties, compressive and flexural strengths, modulus of elasticity, bond, creep and drying shrinkage. The main conclusions are as follows:

1. The various lightweight aggregates produced concretes with unit weights ranging from 1440 to 1760 kg/m^3. Expanded shale aggregates from rotary kilns produced the lower weight concretes whereas expanded slag and sintered shale aggregates produced the heavier lightweight concretes.

2. For 21 and 31 N/mm^2 concretes, the modulus of elasticity varied between 53 and 82% of that for comparable gravel concretes.
3. The flexural strengths of the lightweight and sand and gravel concretes were approximately equal at early ages, but after 28 days the sand and gravel concrete showed greater strength gain with continuous moist curing than did the lightweight concrete.
4. Bond strengths of some of the lightweight concretes were approximately equal to those of the sand and gravel concretes. The position of the bar was an important factor in the development of bond. In the 21 and 31 N/mm^2 series, all specimens, with a single exception reached bond stresses in excess of 6 N/mm^2. For the high strength series all specimens failed at bond stresses in excess of 10 N/mm^2. .
5. The creep of lightweight aggregate concrete of 21 N/mm^2 was between 84-145% of that of comparable gravel concrete. For the 31 N/mm^2 concrete the range was between 100-175%, and for the 48.5 N/mm^2 concrete the range was between 95-110%.
6. In the lower strength series, 21 N/mm^2, at age 6 months the drying shrinkage of the lightweight concretes stored at 50% relative humidity was between 95 and 138% of that of the sand and gravel concrete.

In a follow up to Schidelers work at the P.C.A., Hanson (27,28) reported on the shear capacity of lightweight concrete beams. The test data showed a good correlation between the nominal unit shear strength of the beams and their associated split cylinder tensile strengths. Nominal unit shear strengths for the lightweight beams varied between 60 and 100% of the values for comparable gravel concrete beams.

Greib and Werner (29), reported results from an investigation into the effect of curing conditions on the tensile and compressive strength properties of various concretes. Tests were carried out on ten different types of lightweight aggregate concrete and comparable crushed rock and gravel concretes. Specimens were cured under two different environments, namely moist curing until testing at 28 days or moist curing for 7 days followed by air curing at

23°C and 50% relative humidity until testing at 28 days. The main conclusions are as follows:

1. The ratio between the average tensile splitting strength and the average flexural strength for specimens cured in moist conditions and tested between 7 days and 1 year was 67%, 62% and 76% for crushed stone, gravel concrete and lightweight concrete respectively. The ratio of the tensile splitting strength to compressive strength was 10.7%, 10.8% and 8.0% respectively.
2. For specimens cured in air after 7 days the 28 day tensile splitting, flexural and compressive strengths were 69%, 38% and 96% respectively of those for continuously moist cured specimens. One year values were 90%, 57% and 82% respectively.

In 1979, Committee 213 of A.C.I. published a report (30) giving guidelines for the use of structural lightweight aggregate concrete. The aim of the guide was to summarise the knowledge on lightweight concrete then available. The physical and mechanical properties of structural lightweight aggregate concretes, described in this report, can be summarised as follows:

1. Depending upon the source of material, structural grade lightweight concrete can be obtained with unit weights in the range 1440-1840 kg/m^2.
2. Generally the modulus of elasticity for structural lightweight concrete is considered to vary between 50% and 75% that of sand and gravel concrete of the same strength.
3. A wide band of creep values can be obtained for various lightweight concretes some higher, some lower than comparable gravel concretes. The spread of results reduces markedly as the 28 day compressive strength of the concrete increases.
4. Low strength lightweight concretes generally show higher shrinkage than comparable gravel concretes. At higher strengths, however, some lightweight concretes exhibit lower shrinkage.
5. Lightweight concretes show lower thermal conductivities and coefficients of thermal expansion. Heat losses through solid walls range between 50-80% of values for comparable gravel concretes, depending on density.

6. Structural lightweight concretes are more fire resistant than normal weight concretes because of their lower thermal conductivity, lower coefficient of thermal expansion and the inherent fire stability of an aggregate already burned to over 1100°C.

2.3.2 Previous Research in the United Kingdom

There are, today, a number of different brands of lightweight aggregates commercially available in the United Kingdom and these are listed in Table 2.4, along with some of their basic properties.

Lydon (13), published a review of research, in progress or planned, in 1976 along with a bibliography of selected publications dealing with lightweight concrete in the UK.

The Building Research Station were probably the first organisation to actively study a variety of commercially available lightweight aggregates, including foamed slag, Aglite, Leca and Lytag, back in the late 1950's. Work on mix design, lightweight aggregate production processes and the behaviour of concrete block walls have been reported as recently as the mid 1970's (13).

The bulk of the remaining work, either reported or in progress is being carried out by various research and educational establishments, mainly the Universities. Of these there are three which have reported work relevant to this project, namely Leeds, Sheffield and University of Wales Institute of Science and Technology, (UWIST).

2.3.2.1 Research at the Building Research Station (B.R.S.)

Early work at the B.R.S. was concerned with investigating a wide range of concretes made with various aggregates, as mentioned above, and the first results were reported by Short (31) in 1959. This was followed by reports from Teychenné (11,32), Grimer (10) and Taylor and Brewer (33).

Their conclusions can be summarised as follows:

1. The workability characteristics of lightweight aggregate concretes differ somewhat from those of sand and gravel concretes, but there is no difficulty in producing lightweight concrete suitable for full compaction under site conditions.

Aggregate		Average Oven Dry Bulk Density for Available Nominal Size Ranges		Air Dry Density kg/m^3	Strength Grade Range N/mm^2
Coarse Particle	Type	Coarse Grades	Fine Grades		
Rounded	Sintered p.f.a (Lytag)	12-5 mm 800 kg/m^3	< 5 mm 1050 kg/m^3	1530-1900	15-60
	Expanded clay (Leca)	20-10 mm 350 kg/m^3 10-3 mm 370 kg/m^3	3 mm 625 kg/m^3	1050-1600	7-15
	Pelletised expanded slag (Pellite, Lycrete)	14-5 mm 800 kg/m^3	< 5 mm 1000 kg/m^3	1400-2000	7-60
Irregular	Foamed slag	12-5 mm 700 kg/m^3	< 5 mm 900 kg/m^3	1400-2000	7-50
	Sintered shale (Aglite)	10-5 mm 700 kg/m^3	< 5 mm 900 kg/m^3	1450-1900	20-50
	Sintered p.f.a (Taclite)	12-5 mm 800 kg/m^3	< 5 mm 950 kg/m^3	Up to 1700	Up to 50
	Sintered colliery shale (Sintag)	12-5 mm 800 kg/m^3	< 5 mm 950 kg/m^3	Up to 1850	Up to 30

TABLE 2.4 BASIC PROPERTIES OF BRITISH MANUFACTURED LIGHTWEIGHT AGGREGATES

2. With a given lightweight aggregate, the main factor influencing the crushing strength is the water cement ratio.
3. Concrete made with Leca has a crushing ceiling of 30 N/mm^2. Any of the other lightweight aggregates can produce concrete with a 28-day crushing strength at least equal to that obtained with sand and gravel, but in some cases a higher cement content is required.
4. The concrete strength development up to 28 days is similar to that of gravel concrete, but there is generally a greater increase in strength at 1 year, particularly with Lytag.
5. In many cases the 28 day strength of air cured lightweight concrete is greater than that of water cured concrete. The increase in strength owing to the initial period of moist-air curing is less than with sand and gravel concrete.
6. The tensile strength, by the modulus of rupture test, of lightweight concretes may be greater than, or as low as 50% of, the values for comparable gravel concretes.
7. Modulus of elasticity varies between about 30% and 70% of that for comparable gravel concretes. The figure for Lytag concrete is about 60%.
8. The air dry density of lightweight concrete varies between about 1120-2080 kg/m^3, depending on the aggregate type and the cement content. The density range for Lytag concretes was 1600-1760 kg/m^3.
9. Deflections of lightweight concrete beams vary between 10-50% greater than those for comparable gravel concrete beams.
10. Bond strengths, by pull-out tests, vary between 50-75% of the values for comparable gravel concretes.
11. Shrinkage and moisture movement depend upon aggregate type and increase with increases in cement content and water/cement ratio. For a given cement content the lowest shrinkage values were obtained with Lytag concrete, the values being equal to the gravel concrete values.
12. The effect of the type of aggregate on the rate of penetration of a carbonation front is small by comparison with the effect of mix properties. For

Lytag concrete the rate is the same as for gravel concrete.

13. Steel embedded in lightweight concretes, with low cement contents and therefore low strengths, may be more prone to corrosion than with gravel concretes of similar strengths.
14. The shear strengths of rectangular beams made with Aglite varies between 78-88% of the values for comparable gravel concrete beams. For Lytag the variation is 83-93%.

2.3.2.2 Research at the University of Leeds

Work at Leeds University has been concentrated on two lightweight aggregates, namely Aglite and Lytag. Early results were published by Evans et al (34-38). Further results were published by Neville and Liszka (39) and by Brooks and Neville (40,41).

The main conclusions resulting from their work can be summarised as follows:

1. A cube crushing strength of approximately 50 N/mm^2 is obtainable with Aglite concrete and sufficiently high strengths for prestressing can be obtained with Lytag concrete.
2. The strength increase between 28 days and 6 months is greater for Lytag concrete than for comparable gravel concrete.
3. The tensile strength of Aglite concrete was 25-50% less than that for gravel concretes of comparable compressive strength. The tensile strength of Lytag concrete, by the modulus of rupture test decreased appreciably on drying.
4. The modulus of elasticity of Aglite concrete is approximately 60% of the value of comparable strength gravel concrete. The modulus of elasticity of Lytag concrete increases with an increase in crushing strength and the increase in modulus of elasticity, between 28 days and 6 months is greater for Lytag concrete than for gravel concrete.
5. The ultimate moments of reinforced concrete beams made with Aglite, Lytag and gravel concretes are satisfactorily predicted by Whitney's theory.
6. The compressive stress block of a Lytag concrete beam differed from that of a gravel concrete beam in the following respects:

(a) Maximum stress was not developed until a strain of 0.3% was reached (0.2% in gravel concrete).

(b) Maximum stress is developed nearer the compression face.

7. For Aglite concrete, the immediate deflections of beams reinforced with up to 4% steel are 10-25% greater than for comparable gravel beams. At working loads deflection may be as much as 40-50% greater.

   For Lytag concrete beams, the ratio of the total deflection at 750 days to the instantaneous deflection is less than for gravel concrete beams. Initial deformation of Lytag concrete was 1.5 to 2.0 times that of gravel concrete, while at 500 days the deformation of Lytag concrete was 1.0 to 1.5 times that of gravel concrete.

8. For similar crushing strengths, crack widths in Aglite concrete beams are approximately 50% wider and crack spacings approximately 60% closer than for gravel concrete beams.

9. Creep and shrinkage in Aglite and Lytag concrete is generally greater than in gravel concrete of similar strength.

10. The absorption of Aglite concrete was 30-40% higher than that of comparable gravel concrete, but permeability was much the same.

11. In 152 mm long pull-out test specimens, containing a single 12.5 mm diameter bar, for a maximum bond stress of 5.2 N/mm^2, the average stress with Aglite concrete was approximately 25% higher than with gravel concrete.

12. The shear cracking load of Aglite concrete beams was about 75% that of gravel beams of similar strength.

2.3.2.3 Research at the University of Sheffield

Work at Sheffield University was concentrated on investigating the properties of Solite lightweight aggregate concrete in the early seventies, while more recently, attention has focused on Lytag concrete. Swamy et al (42-47) published results of tests carried out by Ibrahim (48) and Bandyopadhyay (49) on Solite and Lytag concrete. More recent research, carried out by Ajibade (50), Jojagha (51), Sittampalam (52) and Winata (53), has been concerned only with Lytag concrete as Solite is no longer manufactured. The results of the various

investigators can be summarised as follows:

1. Both Lytag and Solite are capable of producing concrete with a cube strength in excess of 60 N/mm^2.
2. The use of high early strength cement can result in up to 50-60% of the 28 day cube strength being obtained within 24 hours.
3. Solite concrete requires approximately 25% less cement than Lytag and approximately 30-35% less than other lightweight aggregate concretes to achieve the same compressive strength at 28 days.
4. The air dry density of Solite and Lytag concrete varies between about 1600-1840 kg/m^3.
5. There is a reduction in both the tensile splitting and the flexural strength of concretes cured in air as opposed to those continuously moist cured.
6. The tensile splitting strength is approximately 76% of the flexural strength for Solite concrete.
7. The static modulus of elasticity of Lytag and Solite concrete is approximately 60-65% of that of comparable gravel concretes. The use of high early strength cement may further reduce the modulus of elasticity by up to 10%.
8. For Solite concrete, the compressive strength, flexural strength and dynamic modulus of elasticity were all reduced when pre-wetted as opposed to dry aggregates were used.
9. Solite concrete is more crack resistant than comparable gravel concrete. This is probably due to its lower modulus of elasticity and higher relaxation of stress due to higher creep.
10. Pull-out tests indicate that bond strengths for Solite concrete are approximately 96% of the values for gravel concrete.
11. When considering the durability of steel, the effect of the type of aggregate on the rate of penetration of the carbonation front was small by comparison with the effect of mix proportions.
12. With Solite concrete, no instance of damage due to corrosion was found in embedded steel bars after two years exposure to a severe industrial atmosphere.

13. The strain at maximum stress which Solite concrete specimens sustained under constant strain loading was between 0.3 and 0.33% while for gravel concrete the value was 0.25%.

14. The instantaneous deflection of Solite concrete beams at design load was 20-30% greater than that of comparable gravel concrete beams. Deflections can be satisfactorily estimated by methods employed in the design codes (26, 54) based on a cracked section.

15. The ultimate moment of resistance of Solite concrete beams can be satisfactorily calculated by using Whitney's theory.

16. Crack widths at working loads, for reinforced Solite concrete beams, were within the limits set by CP110 (54).

17. The shear cracking strength of Solite concrete T-beams was found to be identical to that of comparable gravel concrete beams.

18. It was found that the diagonal tension strength of Solite concrete T-beams is affected by the same variables as those effecting the resistance of gravel concrete beams. There is no fundamental difference in behaviour and modes of failure. The difference lies only in the type of aggregate used and its capacity to resist the shear failure.

19. The ultimate shear resistance of Solite concrete T-beams varies between 71 and 95% of that of comparable gravel concrete T-beams.

20. The main difference in shear failure between Solite and gravel concrete lies in the fact that diagonal cracks in lightweight concrete traverse the aggregate particles as well as the matrix, whereas for gravel concrete the crack results from a bond failure between the aggregate and the matrix which in turn results in the adjacent surfaces being irregular, interlocked and still capable of withstanding further load.

21. The shear cracking load is independent of the presence of vertical stirrups. The magnitude of the load causing the formation of initial cracks depends primarily on the strength of the concrete and to a lesser extent on the longitudinal steel ratio and the shear span - effective depth ratio.

22. Even the provision of a small amount of web steel effectively increases the

shearing strength of Solite concrete T-beams, and also prevents the sudden failures associated with shear.

2.3.2.4 Research at UWIST

Investigations at UWIST have covered a wide range of lightweight aggregates, namely, Aglite, foamed slag, Leca, Lytag, Solite and Taclite. Early work was reported by Lydon (12, 55-60) and was concerned mainly with the water absorption of various lightweight aggregates and its effect on the mix design process for lightweight aggregate concrete. Work has been continued by Balendran (61) who conducted an extensive series of tests to investigate the properties of high strength lightweight aggregate concretes made with Lytag and Taclite. They also contained natural sand fines and for this reason are discussed in Section 2.3.3. The results of the earlier work and the conclusions drawn from it, can be summarised as follows:

1. Different lightweight aggregates absorb water at different rates and in different amounts tending towards saturation values after quite long periods of time.
2. Without evacuation of entrapped air, immersed aggregates probably never become saturated at low pressure.
3. Lightweight aggregates absorb water rapidly and over a period of time. Rapid absorption is useful in that only a short contact time is required between aggregate and water before quasi-equilibrium is reached, so that most of the potential loss of concrete workability takes place during mixing.
4. The presence of internal water from lightweight aggregates may benefit concrete in full scale structures or structural elements, insofar as continued hydration of cement is concerned. But the behaviour of small elements can be apparently erratic and complex and test specimen results may need to be interpreted with caution.
5. Considerable loss of water can occur from lightweight concrete before measurable drying shrinkage occurs.

2.3.2.5 Research at John Laing Research & Development

Tests have been carried out at Laing R & D, since the early sixties into

the properties and behaviour of Lytag concrete and comparable strength gravel concrete. The results have been published in a series of internal reports (62). The main conclusions of this work can be summarised as follows:

1. The initial moisture content of Lytag fines has little effect on the strength and workability of concretes with the same total water/cement ratio.
2. For Lytag medium, the workability decreases slightly and the strength increases, when aggregates of increasing initial moisture content are used, until a critical value is reached after which strength and workability remain constant.
3. Creep tests on 76 x 76 x 406 mm prisms in axial compression and 102 x 102 x 762 mm beams, reinforced with 2-9.5 mm ϕ mild steel bars, in bending, revealed that the ratio of total to instantaneous deflection at approximately 18 months, is lower for Lytag concrete than for gravel concrete, despite Lytag concretes higher initial deflection.
4. For wet cured cubes, the rate of gain of strength after 28 days is greater for Lytag concrete than for comparable strength gravel concrete.

2.3.3 The Effect of Natural Sand Replacement of Lightweight Fines

The effect of sand replacement was first studied, to a limited extent, by Richart and Jensen (24), as a part of their series of tests of lightweight concrete made with Haydite aggregate. The most comprehensive investigation of the effect of sand replacement on the properties of lightweight concrete, made with various American aggregates, was undertaken by Hanson and Pfeifer (63-68), and their results were reported in a series of articles published over several years. Eleven lightweight aggregates were used and for each aggregate concretes with 33, 66 and 100% sand replacement were tested. The compressive strength range for 6 x 12 inch cylinders was approximately 20-45 N/mm^2. The conclusions of their work can be summarised as follows:

1. Most mix characteristics and concrete properties were improved by sand replacement with the exception of unit weight.
2. Sand replacement had a negligible effect on the gain of compressive strength between 7 and 28 days.

3. With 100% sand replacement:

   (a) The unit weight increased by 10-20%.

   (b) Total water requirement decreased by 12-25%.

   (c) For a given strength, cement contents are reduced.

   (d) Compressive strength increased by 12-64%.

   (e) The drying shrinkage decreased by 25-40% of the corresponding values for all-lightweight aggregate concretes, depending on aggregate type and cement content.

   (f) The modulus of elasticity increased by up to 50% depending on aggregate type.

4. With most concretes, rates of early age creep and shrinkage were generally reduced when the natural sand contents were increased.

5. With complete sand replacement creep values were reduced by 0-40% depending on aggregate type and concrete strength.

6. Partial or complete sand replacement can significantly improve the freezing and thawing resistance of lower strength concretes (21 N/mm^2). At higher strengths (42 N/mm^2) sand replacement produces only minor improvements.

7. The freeze-thaw durability of lightweight concretes, generally, is similar to that of gravel aggregate concrete over comparable strength ranges.

In the UK, many of the investigators, concerned with the properties and behaviour of lightweight concretes, carried out limited tests on lightweight concrete containing natural sand fines (11,31,40,41,48,49,60,62). The most comprehensive investigation to date was that made by Balendran (61). The main conclusions of the work carried out in the UK are summarised below:

1. Sand replacement increases density and reduces cement content for comparable compressive strengths.

2. Maximum strengths of 60-70 N/mm^2 are possible with several UK lightweight aggregates.

3. Sand replacement increases workability, tensile strength and modulus of elasticity.

4. The creep and shrinkage of concretes made with natural sand fines is reduced

in comparison to all lightweight concrete, and is more compatible with the range of values associated with the various types of dense aggregate concrete available.

5. Basic creep values for Lytag and Taclite concretes are 20-30% greater than comparable strength limestone concrete for the same coarse aggregate volume.
6. The freeze-thaw durability of lightweight concrete with natural sand fines is comparable with and in some cases superior to that of dense aggregate concrete.
7. Sand replacement reduces the penetration of a carbonation front into the concrete thus affording a greater degree of protection to the reinforcing steel.

2.4 Code Requirements

As with any building material, the results of research into the properties and behaviour of lightweight concretes, and the structural elements produced with such concretes, had to be condensed into easily managable guidelines to assist in the design process. The wide range of properties and characteristics, which are common between different brands of aggregate, have greatly complicated this task.

In Europe the job was undertaken by the Fédération Internationale de la Précontrainte (F.I.P.) in 1962. Subsequently, in 1966 a report of the F.I.P. Commission (69) was presented at their fifth congress in France. This was followed in 1972 by the European Concrete Committee (C.E.B.) Manual of lightweight concrete (70), revised in 1973 (70), and in 1974 by the European Cement Associations 'Lightweight aggregate concrete: Technology and World Applications' (71). Finally a combined C.E.B./F.I.P. manual was published in 1977 (72).

In the USA the task of collating the available data on lightweight aggregate concrete is the responsibility of the A.C.I. Committee - 213. Their most recent report was published in 1979 (30).

Both the British (54) and American (26) codes, as well as the recently introduced C.E.B.-F.I.P. 'Model code for concrete structures' (73) give limited recommendations for lightweight aggregate concrete leaving design to be based

on more specific data to be obtained, were possible from individual manufacturers.

Basic strength properties of various lightweight aggregates are well established, but continued investigation into the structural properties of elements made with lightweight concretes is required.

CHAPTER 3

THE MICROSTRUCTURE OF LYTAG AGGREGATE AND ITS RELATION TO WATER ABSORPTION

3.1 Introduction

Design using any material requires a fundamental understanding of the behaviour of that material so that it may be safely exploited to the full. In order to try and obtain a better understanding of the behaviour of concrete made with Lytag aggregate, an examination was made of the microstructure of Lytag pellets and the results are reported in this chapter. A literature search failed to reveal any reports of similar examinations of Lytag or of any of the other UK manufactured lightweight aggregates. Richart and Jensen (24) reported microscopic studies of Haydite aggregate but the maximum magnification used was only x 250 and this was only used to give an overall view of material passing a No. 200 sieve.

The description of the tests carried out to examine the microstructure is preceeded by a description of the raw materials and the manufacturing process of Lytag aggregate. The microstructure examination, using a scanning microscope, is then reported, followed by a series of tests to determine the water absorption characteristics of Lytag. The water absorption characteristics are then related to the observed microstructure.

3.2 Raw Materials and the Manufacture of Lytag

The manufacturing process of Lytag aggregate is outlined diagramatically in Figure 3.1.

The basic raw material used in the manufacture of Lytag is pulverised-fuel ash, pfa, and this is supplied directly, by means of a pipeline, from a C.E.G.B. power station to the nearby Lytag plant. The pfa inevitably contains some unburnt fuel but it is unlikely to be as high as 8% which is the approximate amount required for sintering to take place (74). This fuel deficiency is corrected by the addition of coal dust in the form of a slurry. The pfa and coal slurry are blended in screw mixers before being fed onto the pelletizers. The pelletizers consist of a tilted, rotating pan into which water sprays are directed. The ash mixture, which is fed continuously into the pelletizer,

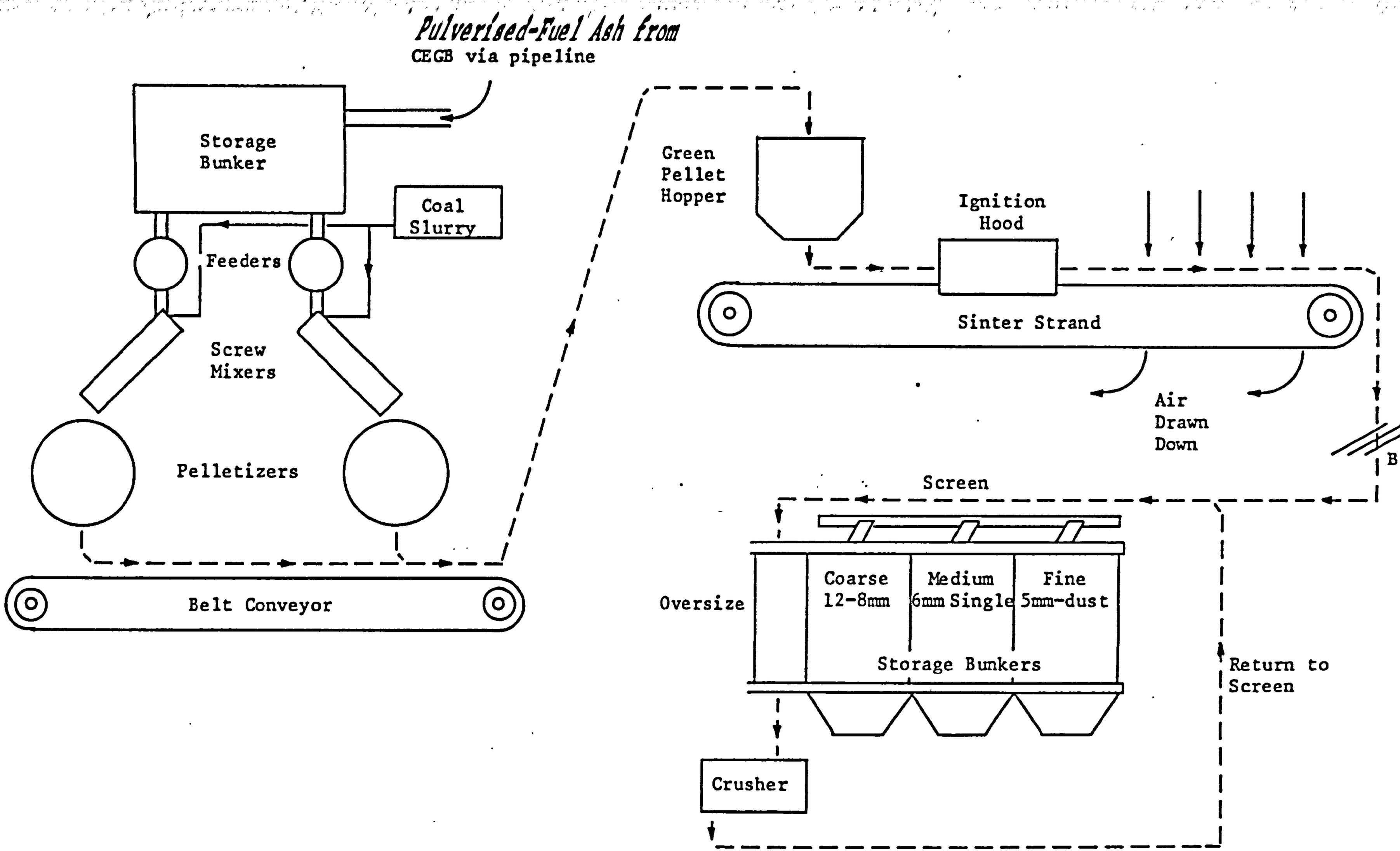

FIGURE 3.1 MANUFACTURING PROCESS FOR LYTAG AGGREGATE (62)

travels in a spiral path during which it forms into pellets which collect at the lower part of the pan and eventually spill over onto a belt conveyor. The blending of the raw materials is critical and it is only by careful control of the water and carbon contents of the ash mixture that it is possible to produce the strong spherical pellets which are subsequently sintered to produce maximum strength with minimum density and cost (75).

When conditions have been carefully adjusted, the pelletizers will produce pellets of remarkably constant size and will operate with little supervision. Adjustments of pan tilt, peripheral speed and pan depth can be used to produce pellets of different sizes.

The 'green' pellets are transferred by means of a belt conveyor to a storage hopper where they are fed onto the sinter strand. The pellet bed thickness is kept constant at approximately 300 mm. As the sinter strand progresses slowly forwards the pellet bed is ignited on its top surface as it passes under an oil fired ignition hood which is maintained at a temperature of 1200-1300^{o}C. Ignition time, which varies with the carbon content of the material, usually is about one minute. The pellets emerge from under the ignition hood in a partially sintered state and the 'flame front' is then forced to progress down through the pellet bed by drawing air down through it. By the time the material reaches the end of the sinter strand it is fully sintered.

The material falling off the strand is red-brown in colour and has the appearance of popcorn, i.e. a number of spherical globules stuck together at their points of contact. When dropping through grizzly bars the material easily shatters into separate spherical particles which are then transferred to a series of screens which grade the material into coarse, medium and fine grades, with any oversize material being returned to the screens via a crusher.

The process is continuous and it is possible for a factory to produce aggregate twenty four hours per day.

Pfa consists generally of spherical particles, some of which may be like glass and hollow and of irregularly shaped particles of unburnt fuel or carbon. It may vary in colour from light grey to dark grey or even brown. Its principal

constituents are, normally: silicon dioxide SiO_2 (about 30 to 60%), aluminium oxide Al_2O_3 (about 15 to 30%), carbon in the form of unburnt fuel (varies widely possibly up to as high as 30%), calcium oxide CaO (about 1 to 7%) and small quantities of magnesium oxide MgO and sulphur trioxide SO_3 (76).

Although sintered pfa is a coal residue and has the same basic mineral composition as furnace clinker, it differs from the latter in important respects (77):

(a) The fuel content of sintered pfa is negligible, whatever it might have been in the raw ash, whereas the fuel remaining in clinker may be very high, and sometimes of a chemically unstable nature.

(b) Becuase of the fineness of pfa, minerals such as pyrites and lime, which are potentially injurious substances, cannot, as in clinker, be present in high local concentrations but are uniformly distributed and thus harmless. Moreover, because of the fineness, any unstable minerals, if they were present, would be very reactive, and by quickly reaching their ultimate state would obviate such troubles as 'lime popping' and rust staining which could otherwise arise from delayed reaction.

The sintering process, therefore, produces a material which, like brick, is inert in the presence of most substances encountered in building and civil engineering, its chemical constituents being mainly silica and alumina.

A problem which has come to light over recent years, concerning the durability of concrete in general, is that of alkali aggregate reaction (78). With chemically inert materials such as Lytag, however, this problem should not arise.

3.3 The Microstructure of Lytag Aggregate

3.3.1 Aims of Tests

The aims of this series of tests were basically twofold; firstly to examine in detail the internal microstructure of Lytag pellets and secondly to relate the microstructure to the behavioural characteristics of the aggregate.

3.3.2 Details of Tests

3.3.2.1 Specimen Selection

Pellet specimens were selected at random from various parts of the stock-pile of a single batch of aggregate. Approximately one dozen specimens were selected initially. In order to observe the bond between the pellets and a sand cement mortar, several pieces of concrete from crushed cubes were also selected.

3.3.2.2 Specimen Preparation

From one pellet a thin section, approximately 30 μm thick was prepared and mounted on a glass slide. The remaining specimens were either sawn in half using a rotary diamond saw or fractured by means of a sharp blow with a hammer. The bond specimens were looked at in order to find areas where the aggregate-matrix boundary was clearly visible. A small area enclosing the required section was then cut from the concrete piece using a rotary diamond saw.

The various specimens for viewing under the scanning electron microscope (S.E.M.) were then cleaned using an ultrasonic cleaner and individually mounted on special holders which hold the specimen in place within the electron microscope. In order that the specimens may be viewed using the S.E.M. they must receive a conductive coating of a heavy metal. In this case gold was used.

3.3.2.3 S.E.M. Type

The machine used in this series of tests was a Philips PSEM 500X scanning electron microscope with a magnification range of x20 - x180,000.

3.3.3 Results of Investigation

A selection of the details seen under the S.E.M. are shown in Plates 3.1(b) - 3.8(d). Each plate is accompanied by a figure which indicates the magnification, e.g. x640 and by a scale, e.g. scale: 10 μm. The scale refers to the relative length of each of the individual segments of the dotted white line which is visible on each plate.

Plate 3.1(a) was produced by using a thin section of Lytag aggregate as a negative and printing the plate directly from it. The plate gives an overall view of the cross-section of a Lytag pellet and it can be seen that there is a thin

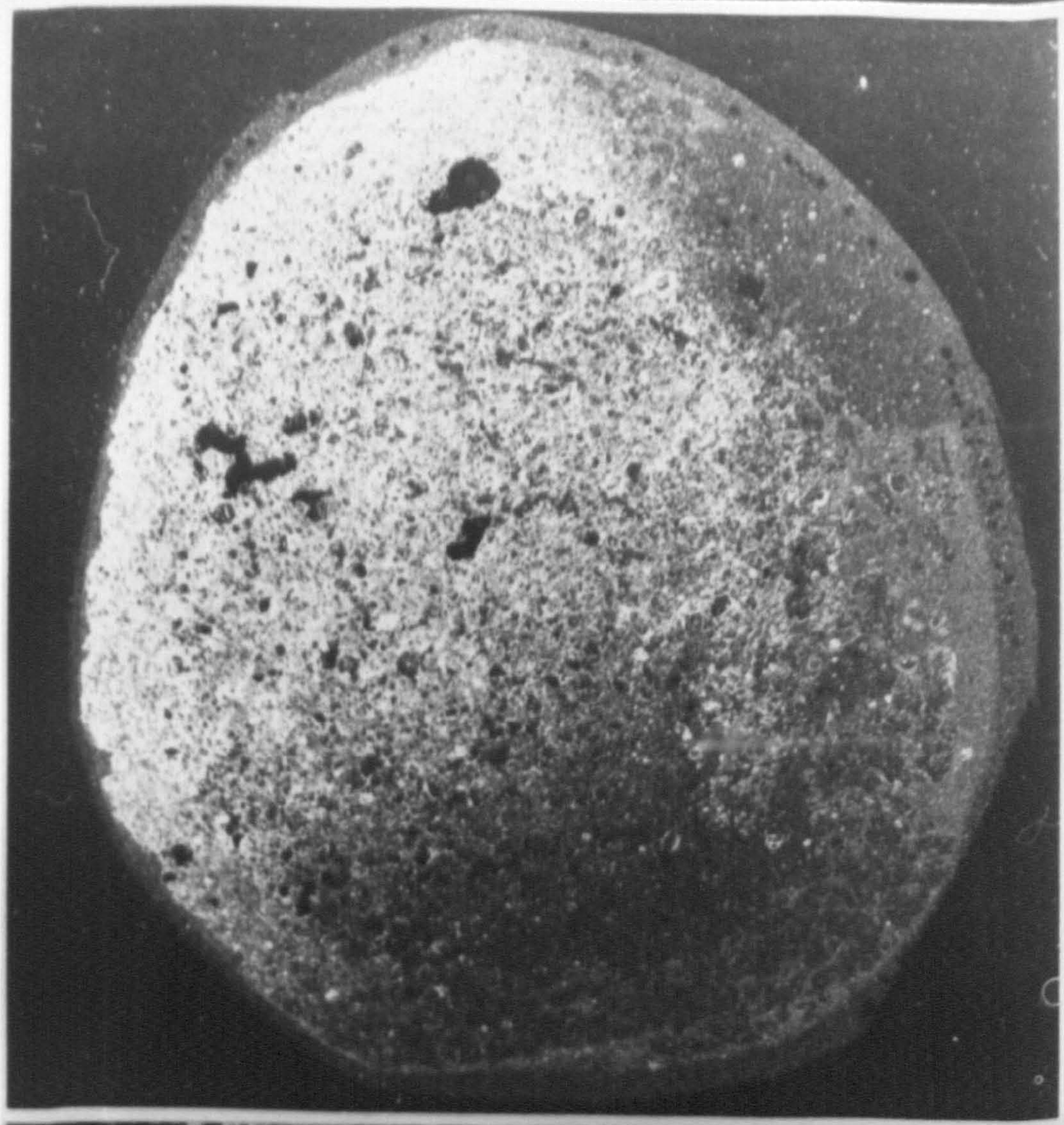

(a)

x 10 (approx)

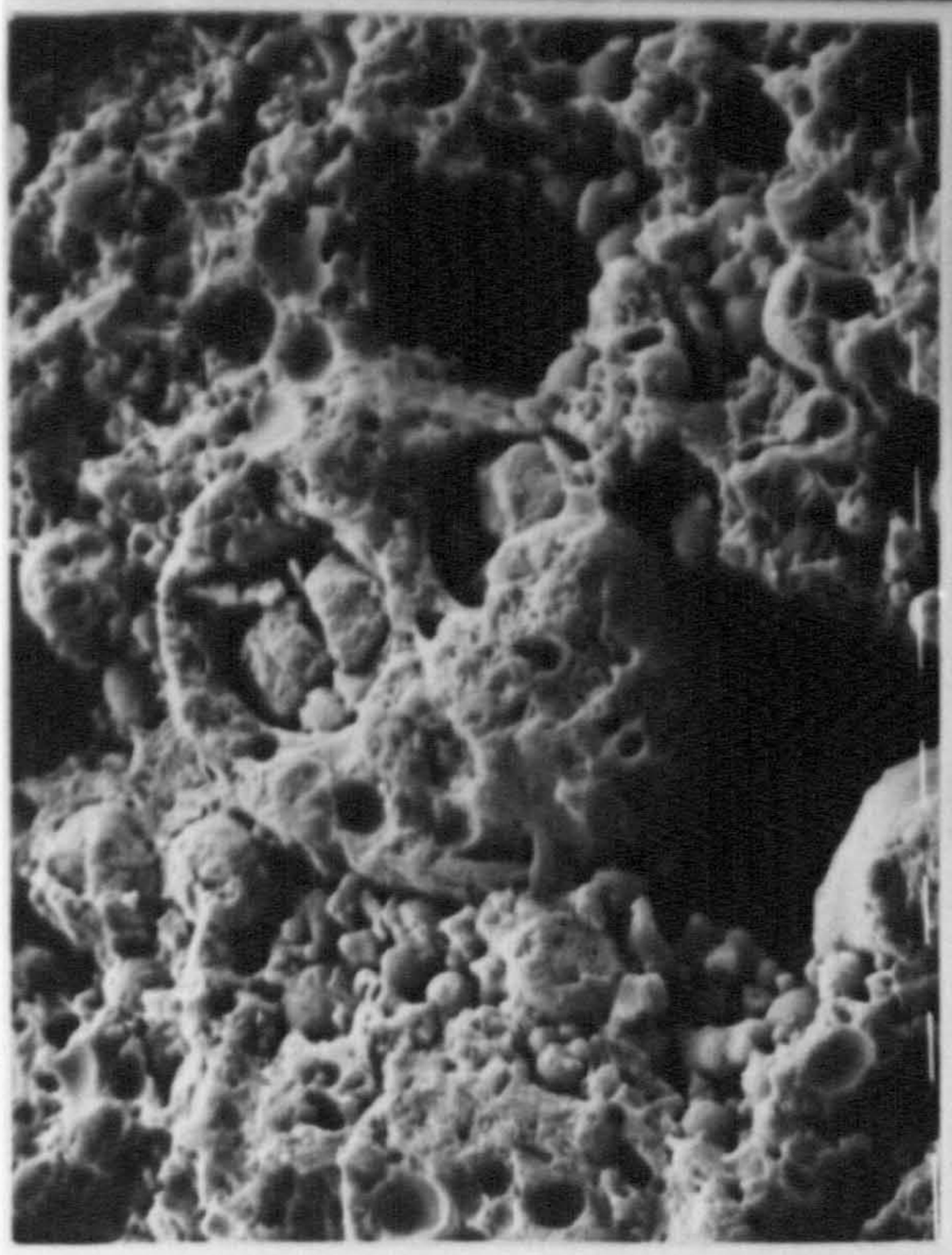

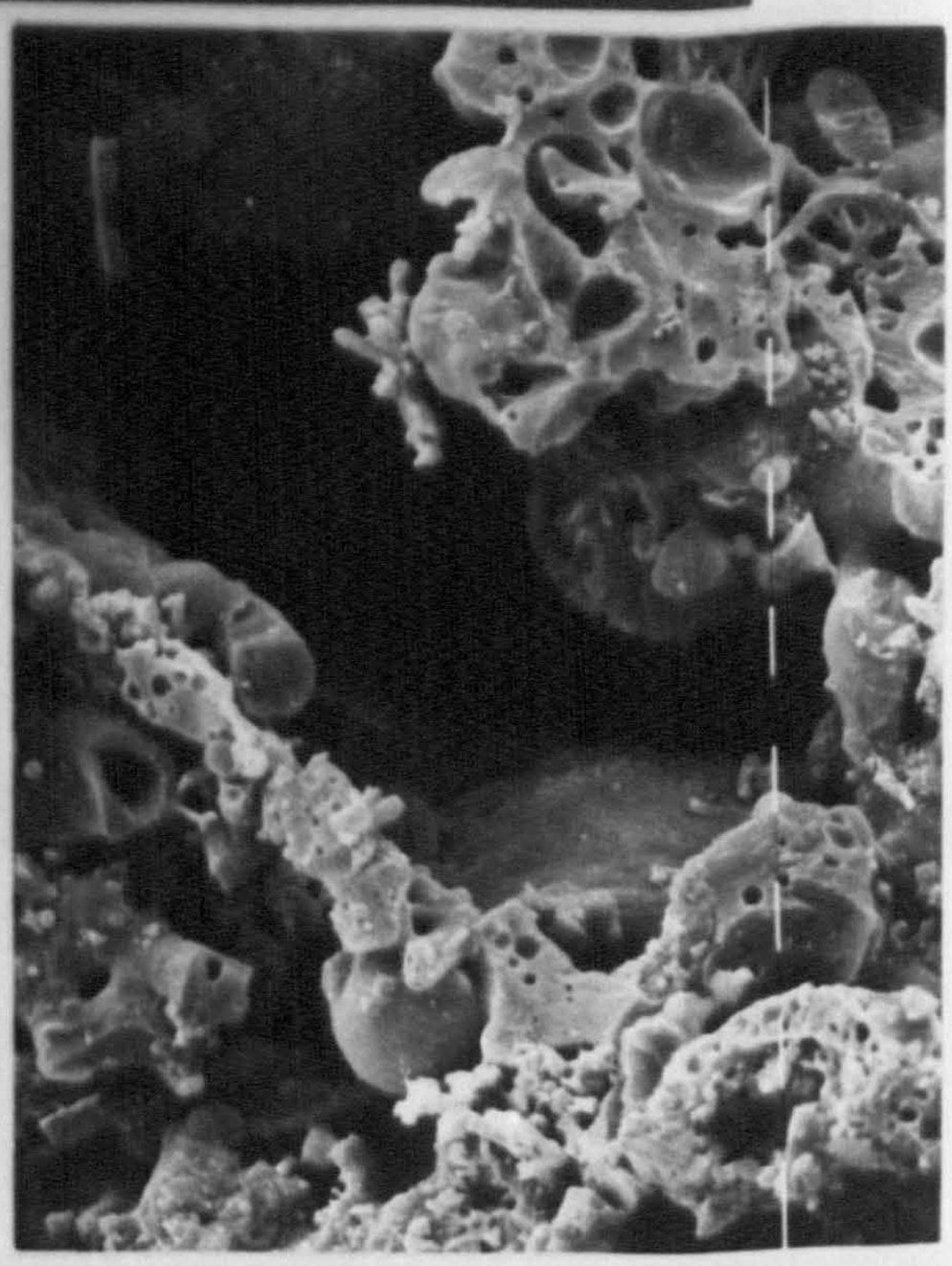

(b) x 640 Scale : 10 µm.

(c) x 640 Scale : 10 µm

PLATE 3.1 OVERALL VIEW OF LYTAG PELLET AND SURFACE PREPARATION

outer shell of variable thickness, ranging between approximately 0.15 and 0.5 mm, surrounding the bulk of the pellet. In reality this outer shell is an earthy red-brown in colour whilst the bulk of the pellet is blackish. The large voids towards the top left of the plate and the absence of the outer shell towards the bottom right are probably due to the cutting process. As was described in section 3.2 the raw ash and coal dust mixture is ignited under a firing hood and the combustion process is prolonged by drawing air down through the pellet bed as it passes along on the sintering grate. Thus the outer layer is probably the product of rapid heating to 1200-1300^{o}C followed by rapid cooling by the air flow. The remainder of the pellet burns and cools at a slower rate.

In order to examine the internal microstructure two types of surface were prepared as described in section 3.3.2. Plates 3.1(b) and 3.1(c) show the sawn and fractured surfaces respectively. Despite the ultrasonic cleaning of the specimens, it can be seen that the surface of the sawn specimen is littered with debris and that a great deal of detail has been obscured. The fractured surface on the other hand is much cleaner and the detail far easier to see. For this reason it was decided that the remainder of the tests would be carried out on fractured surfaces only.

In order to try and define a definite boundary between the two layers previously described all the prepared specimens, sawn and fractured were examined both at low and at high magnifications. No such visible boundary was found. Plates 3.2(a,b) and 3.2(c,d) show the edge region and central region of a fractured surface and a sawn surface respectively. Plate 3.2(a) shows the edge region to be made up of a honeycomb type structure with unreacted pfa cenospheres fused into it. Plate 3.2(b) shows an area of honeycombing photographed in the central area of a pellet. It should not be assumed from this plate that there were no unreacted pfa cenospheres towards the centre of the pellet, unreacted pfa was found but in general, the fused honeycombed areas were more evident than in the edge region.

Since the thin section, Plate 3.1(a) clearly showed a distinct boundary between the outer shell and inner area of the pellet, it was hoped that a sawn

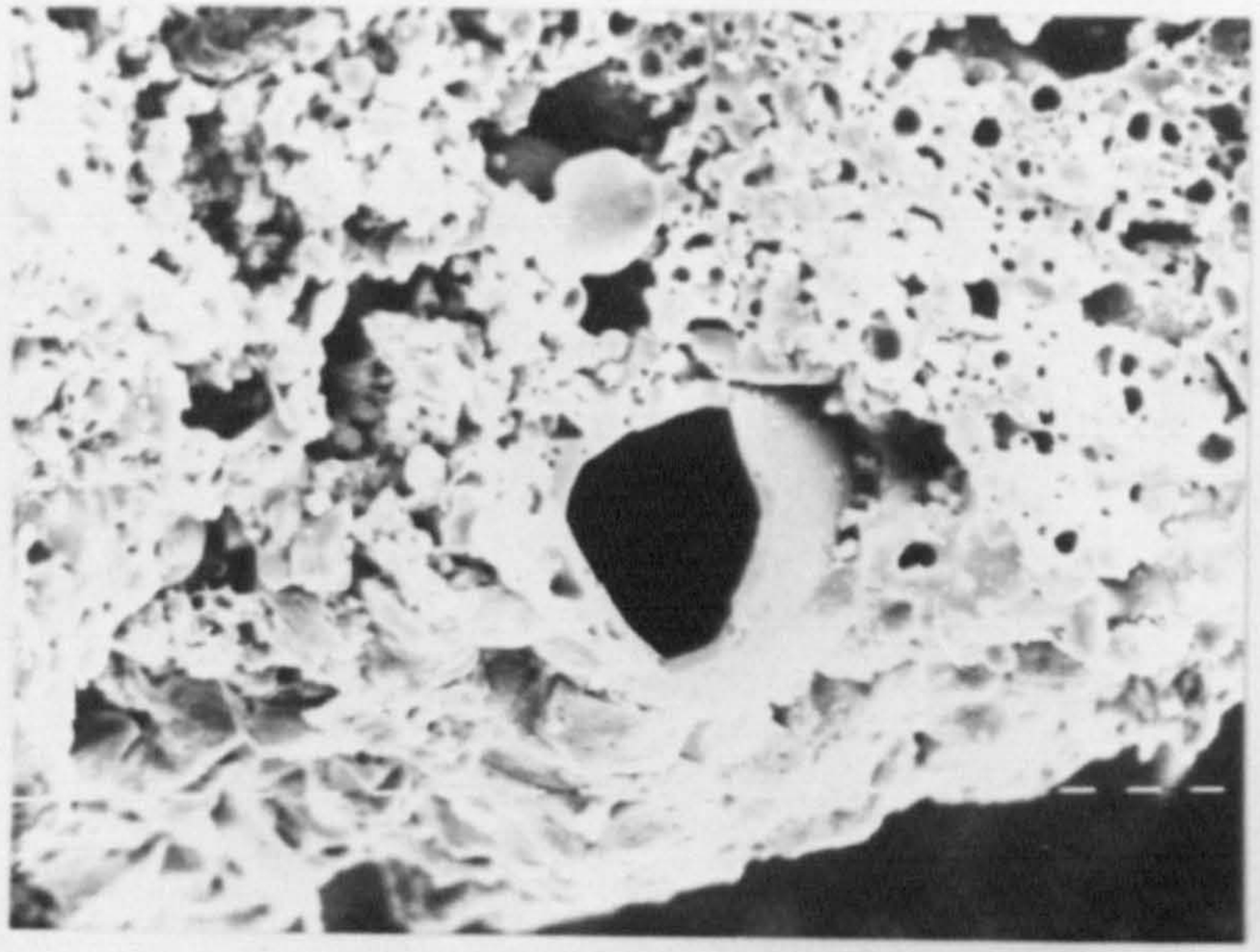

(a) x 320
Scale : 10 μm
Fractured
edge

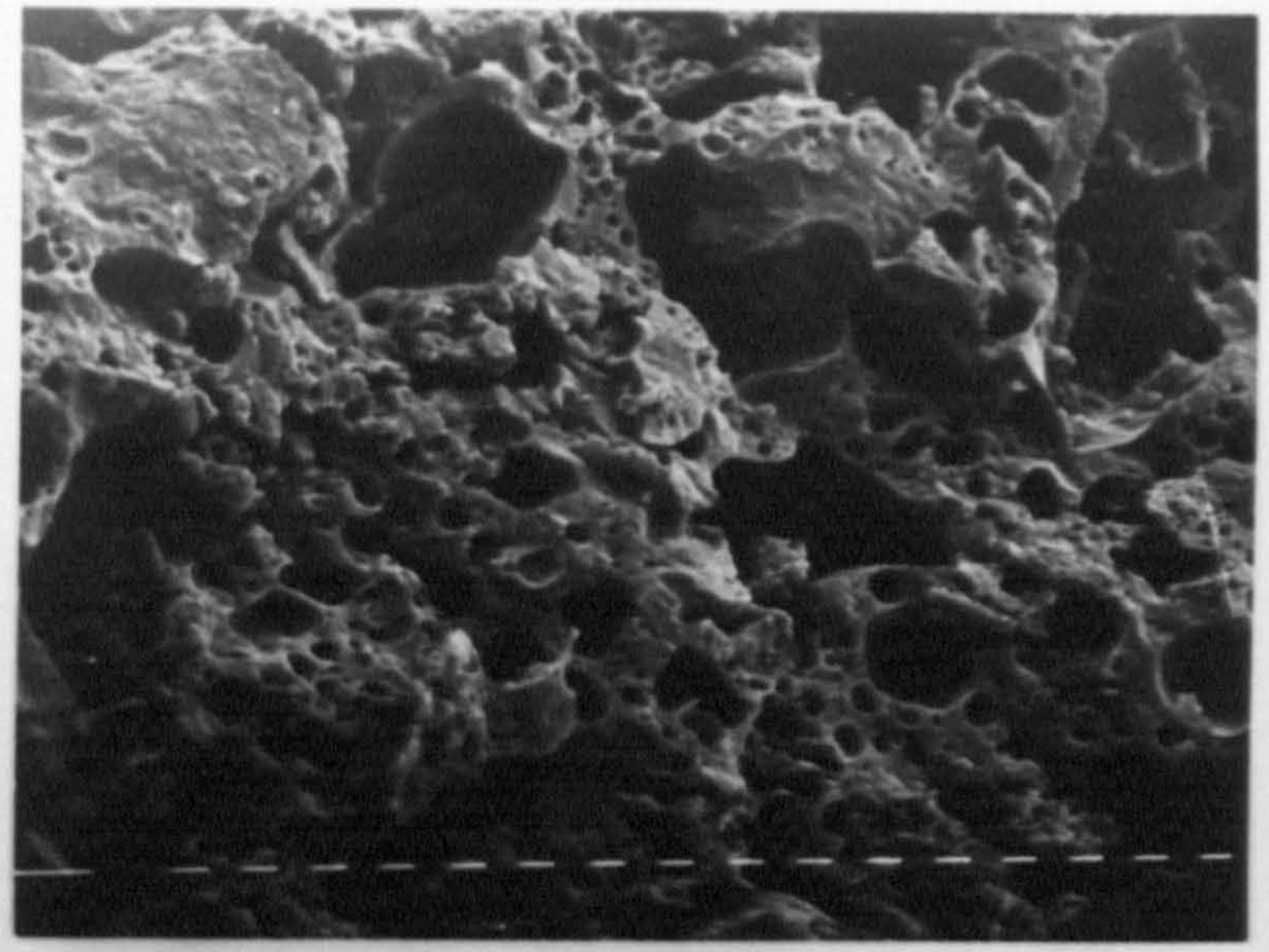

(b) x 320
Scale : 10 μm
Fractured
centre

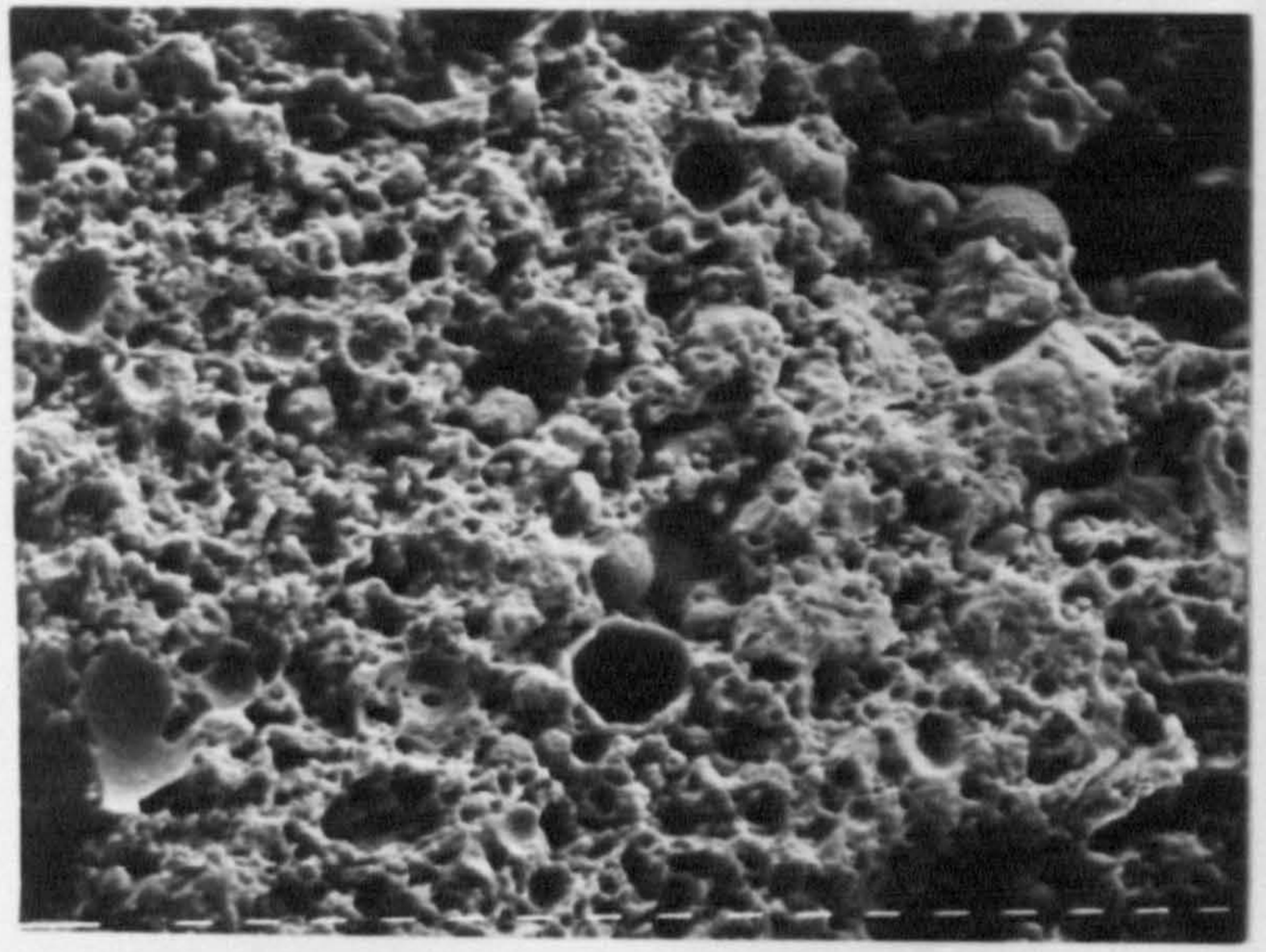

(c) x 320
Scale : 10 μm
Sawn
edge

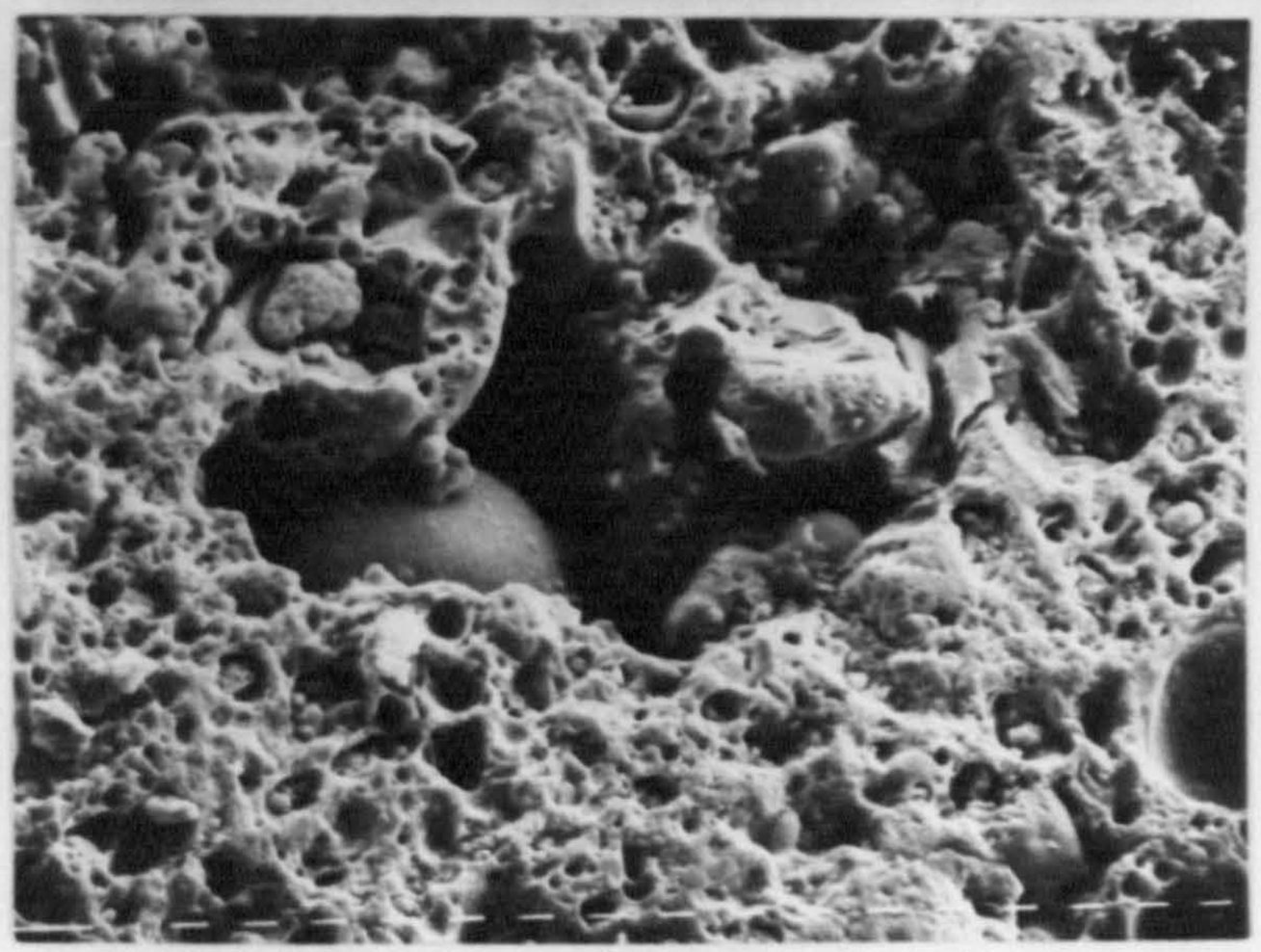

(d) x 320
Scale : 10 μm
Sawn
centre

PLATE 3.2 CROSS SECTIONAL SURFACE FEATURES

surface may reveal similar detail on a larger scale when viewed using the S.E.M. Plate 3.2(c) and (d) show the edge and central regions respectively of a sawn surface. They do, however, only serve as further evidence of the unsuitability of a sawn surface for detailed study as there is a great deal of debris present.

Of all the specimens examined only one small area of one particular pellet revealed a distinct boundary and this is shown in Plate 3.3(a). The bottom left hand corner of the plate indicates the outer edge of the pellet, moving inwards towards the top right hand corner. The outer layer appears to be a fused mass with little sign of voids and this may have been produced by momentary exposure to intense heat at that point. The total circumferencial length of this fused area was approximately 3-4 mm.

Plates 3.3(b), (c) and (d) show unreacted pfa cenospheres of various sizes and these were found throughout the cross-section of all the specimens viewed. It can be seen that the diameter of the cenospheres varies from approximately 75-100 μm in Plate 3.3(b) down to 3-4 μm in Plate 3.3(d). The overall structure of the pellets appears to be composed of the honeycomb type material, which is formed by the virtual melting of the various raw materials, with the unreacted pfa cenospheres fused into it. The honeycombing effect is certainly due to the presence of voids between the constituent materials in the 'green' pellet as well as the formation and expansion of gases and the vapourisation of the contained water, during the sintering process.

Plates 3.4(a)-(d) show the fractured surfaces at various magnifications and are included to show the void distribution and size range. Magnifications have purposely been kept low so as to give a general overall view rather than a view of a small area which would be the case at high magnification.

Plate 3.4(a) is a low magnification view and shows the very irregular surface of the fractured specimen. Only the larger voids are clearly visible on this plate but it can be seen that they are distributed fairly evenly throughout the cross-section. The largest voids appear to be of the order of 100-150 μm. Plates 3.4(b) and (c) are at a higher magnification and show several of the larger voids as well as the whole range of void sizes right down to those less

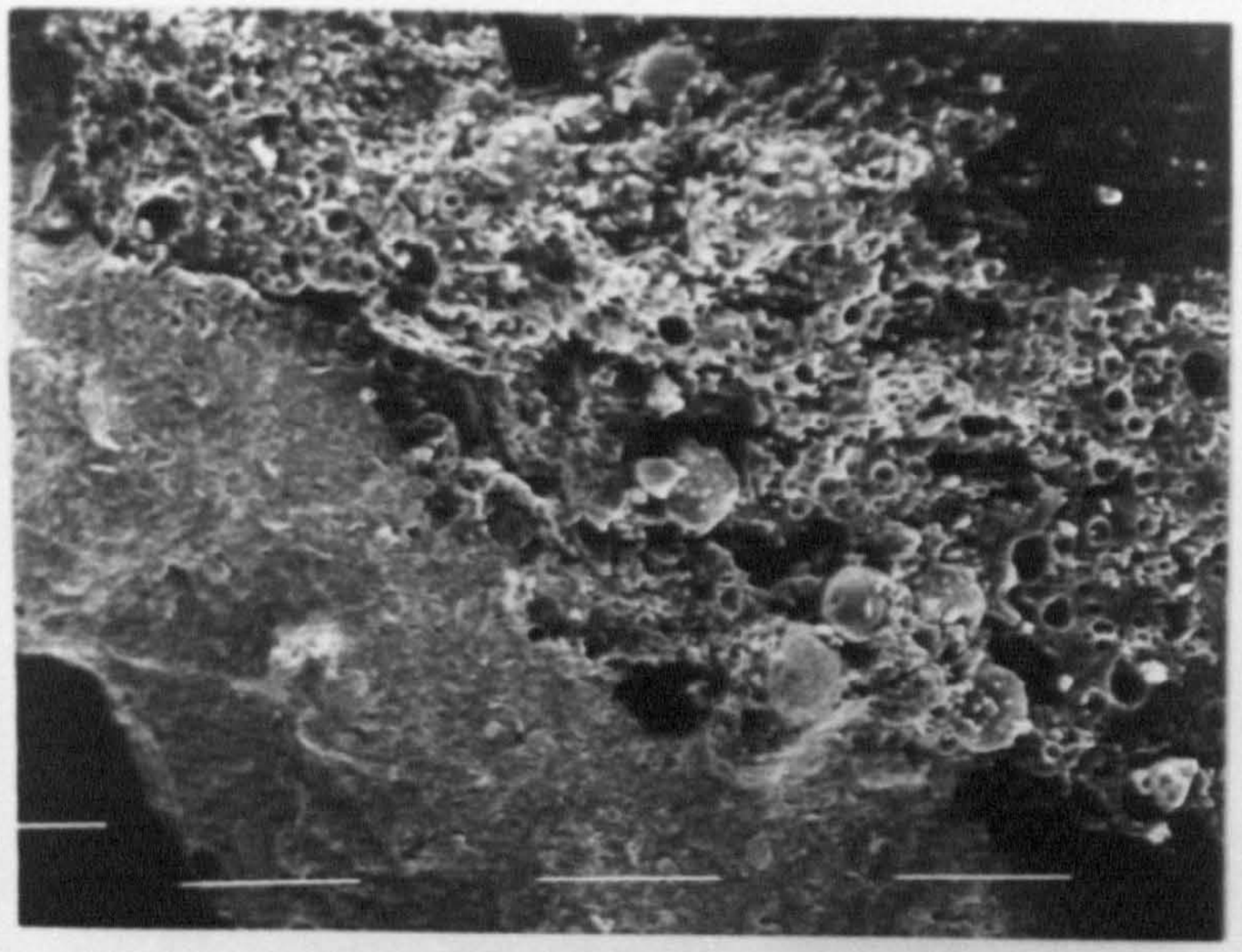

(a) x 160
Scale : 100 μm

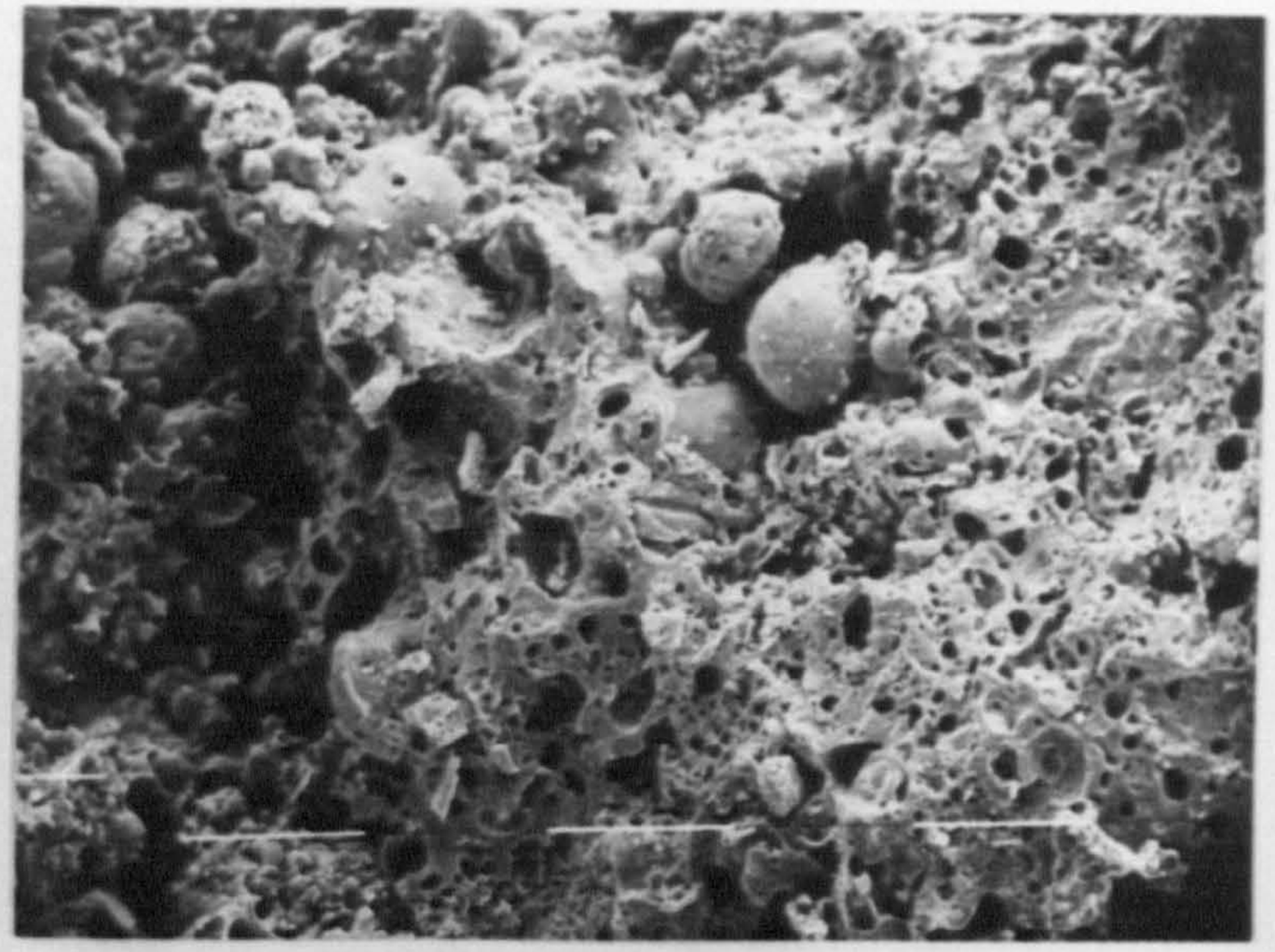

(b) x 160
Scale : 100 μm

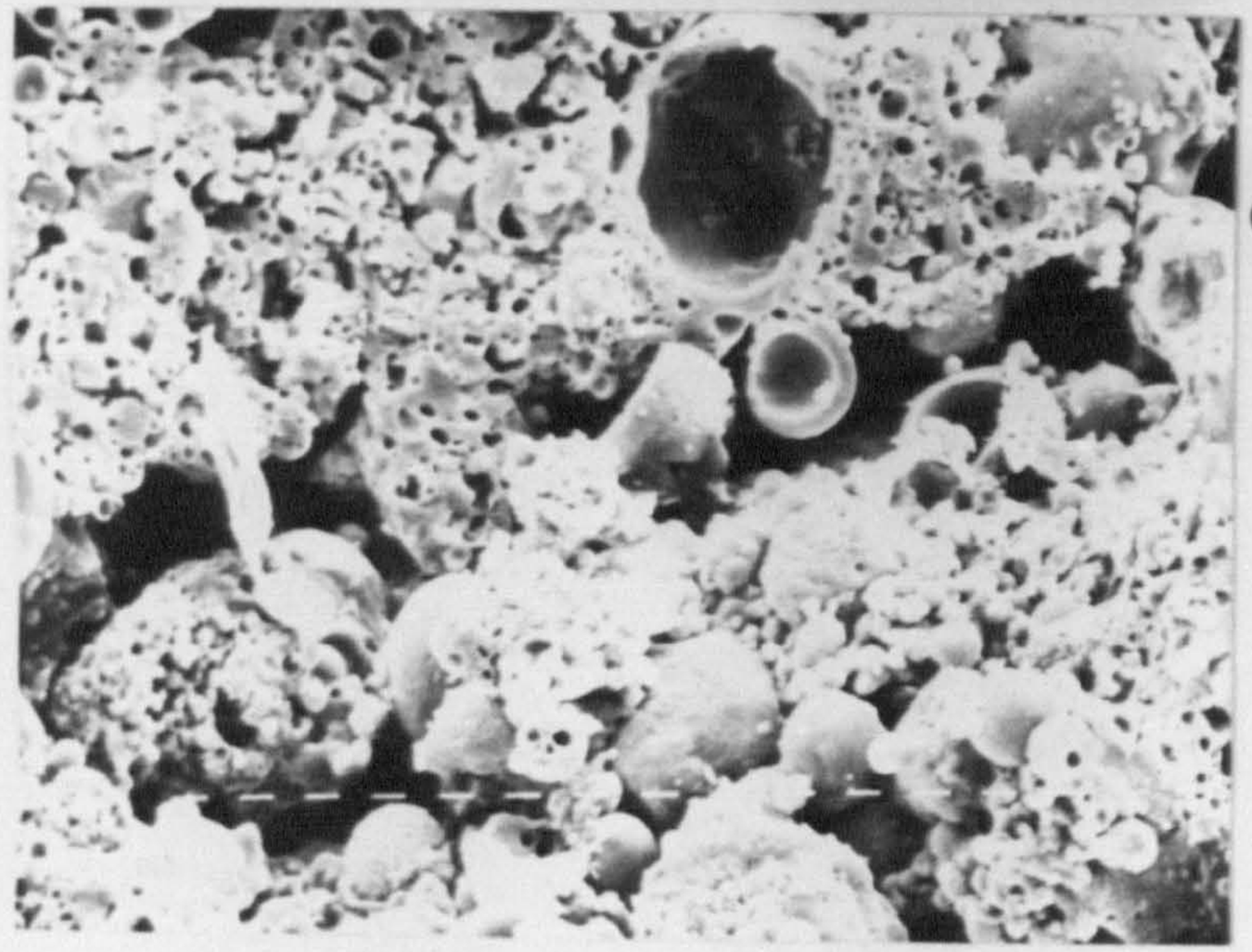

(c) x 320
Scale : 10 μm

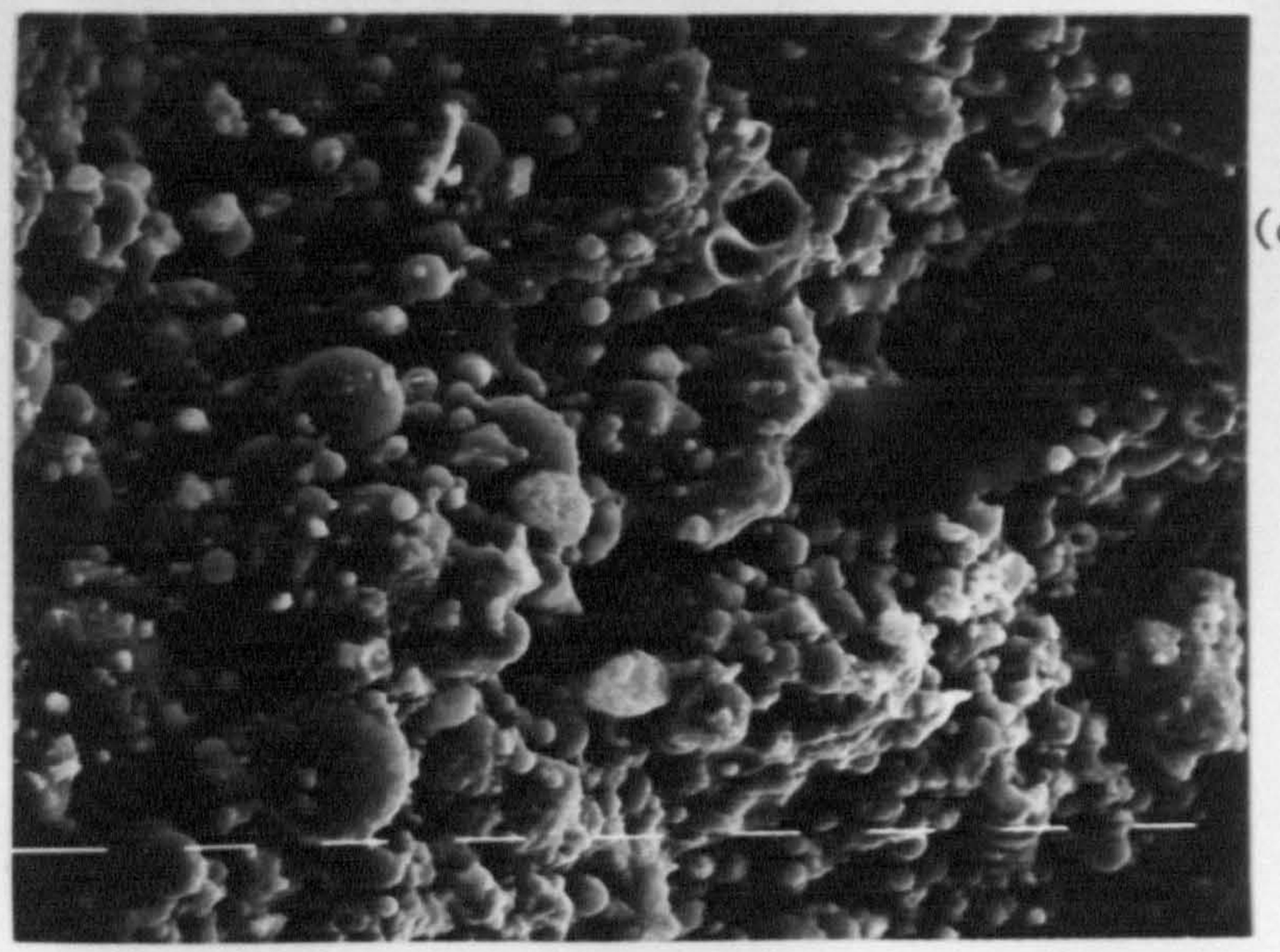

(d) x 640
Scale : 10 μm

PLATE 3.3 CROSS SECTIONAL SURFACE FEATURES

(a) x 20
Scale : 100 μm

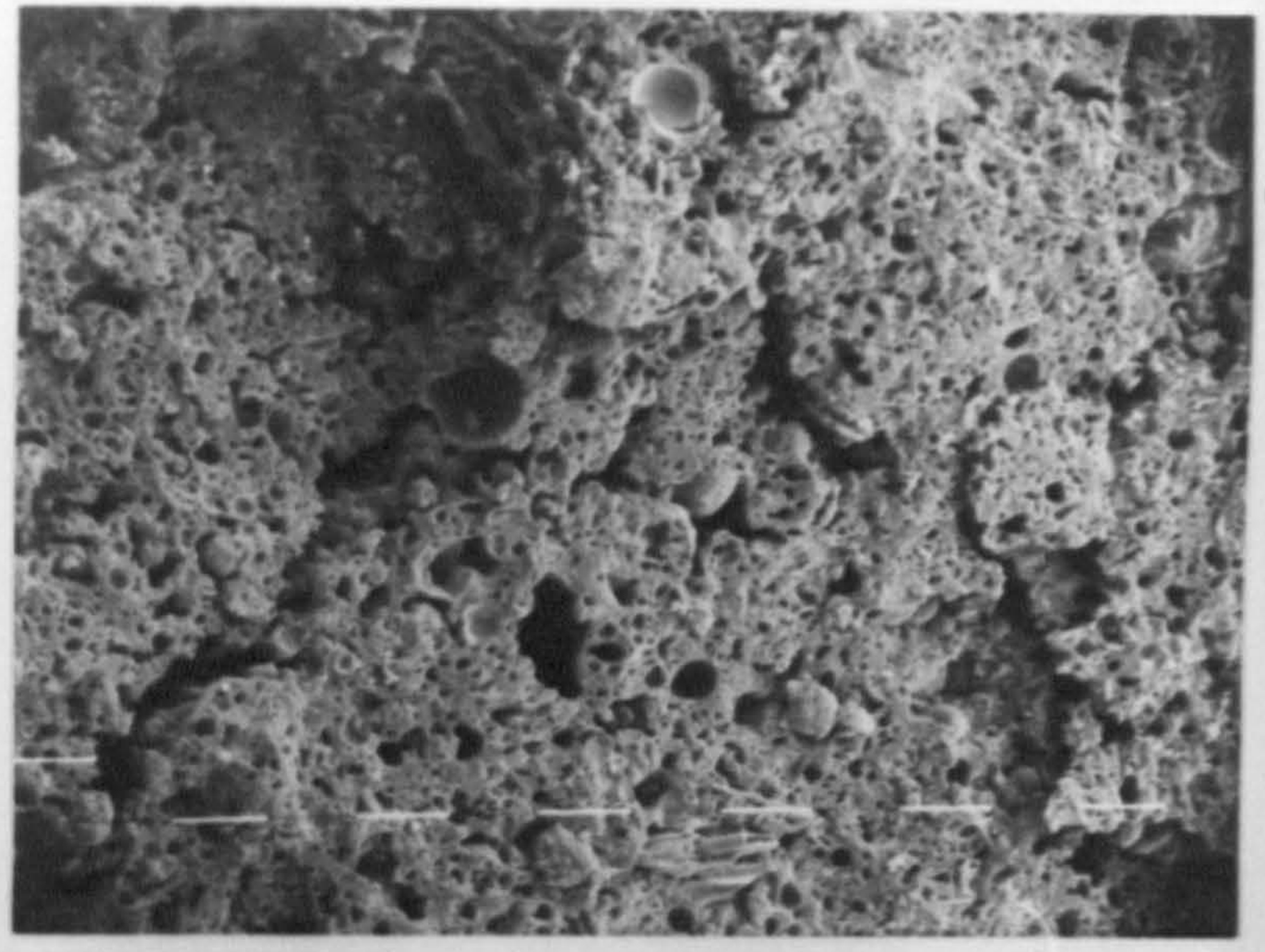

(b) x 80
Scale : 100 μm

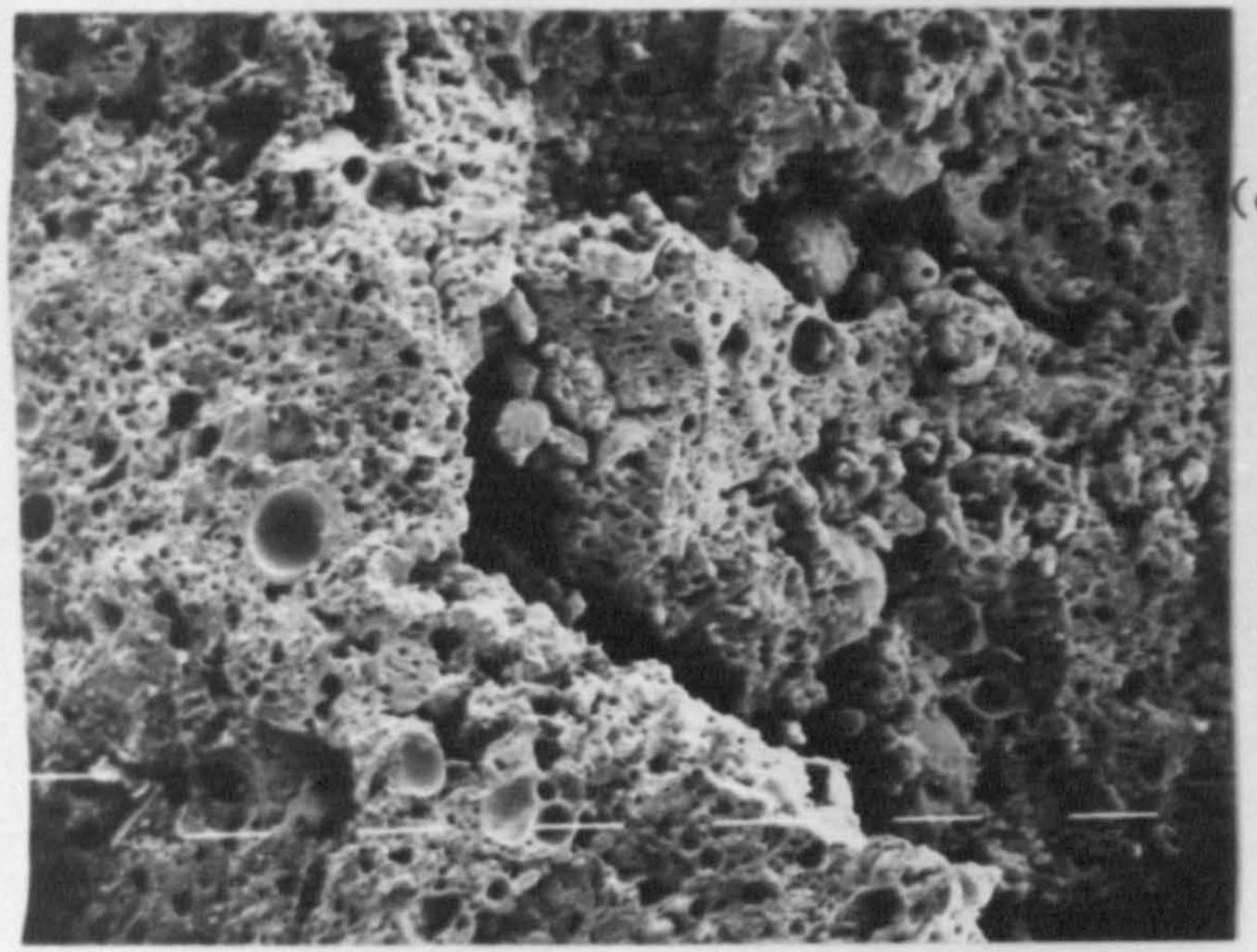

(c) x 80
Scale : 100 μm

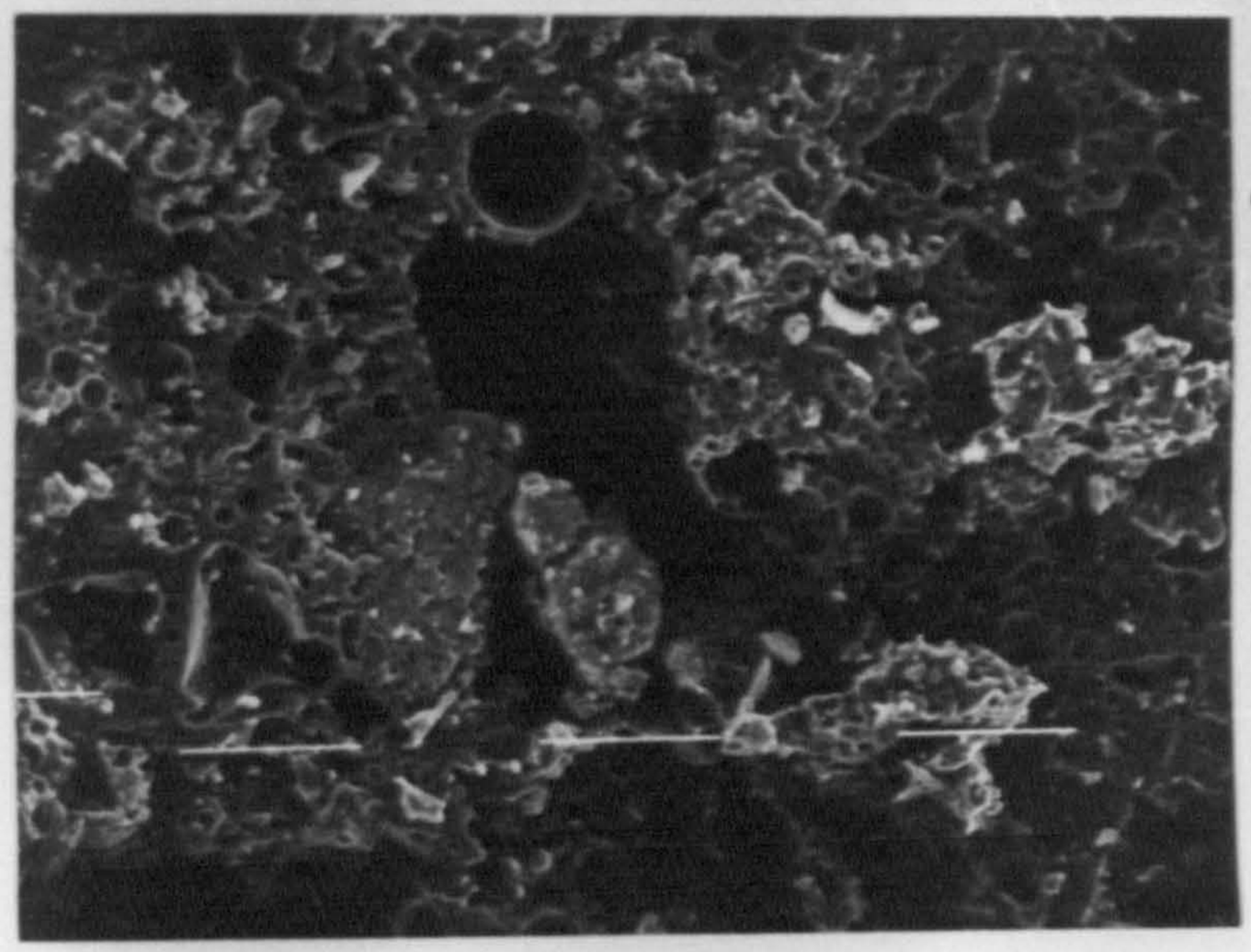

(d) x 160
Scale : 100 μm

PLATE 3.4 VOID DISTRIBUTION AND SIZE

than 10 μm. Again the distribution of the voids appears to be fairly even with the larger and smaller voids evenly mixed. Several spherical hollows are clearly visible and these appear to be either impressions left where cenospheres have been dislodged or the shells of broken cenospheres which are hollow, or both. Plate 3.4(d) is at a higher magnification again and shows again a large void, approximately 200 μm across, surrounded by smaller voids ranging in size from 75-100 μm down to less than 10 μm.

Plates 3.5(a)-(d) show in greater detail the structure of several large voids approximately 150-200 μm across. The four plates show that the voids are interconnected and that the overall structure of the pellet is a highly porous one. Plates 3.5(a) and (b) show voids which appear to have formed by gases escaping through a molten material. The honeycombing is visible both within the void itself and around the void on the fracture surface, and the internal surfaces are smooth and curved.

Plates 3.5(c) and (d) show voids which appear to have been formed by particles of the raw materials already forming the voids and then being fused into position during the sintering process.

Plates 3.6(a)-(d) concentrate on the structure of unreacted cenospheres. All four plates show that the cenospheres are hollow and of variable shell thickness. Within the shell itself smaller voids are also present. Plate 3.6(a) shows a cenosphere which has split cleanly, probably when the aggregate was fractured. X-ray spectrography showed a high silica content in the cenosphere which accounts for the clean fracture surface. A high silica content was found throughout the pellets generally and this also accoumts for the smooth clean fracture surfaces visible on many of the plates.

Plate 3.6(b) shows more voids within the shell wall of a cenosphere. The largest of these voids is approximately 10 μm across whereas the smallest is less than 1 μm.

Plates 3.7(c) and (d) show almost whole cenospheres which have fused into the surrounding material. They show the cenospheres to be hollow with a relatively thin shell containing some voids. These internal voids range in

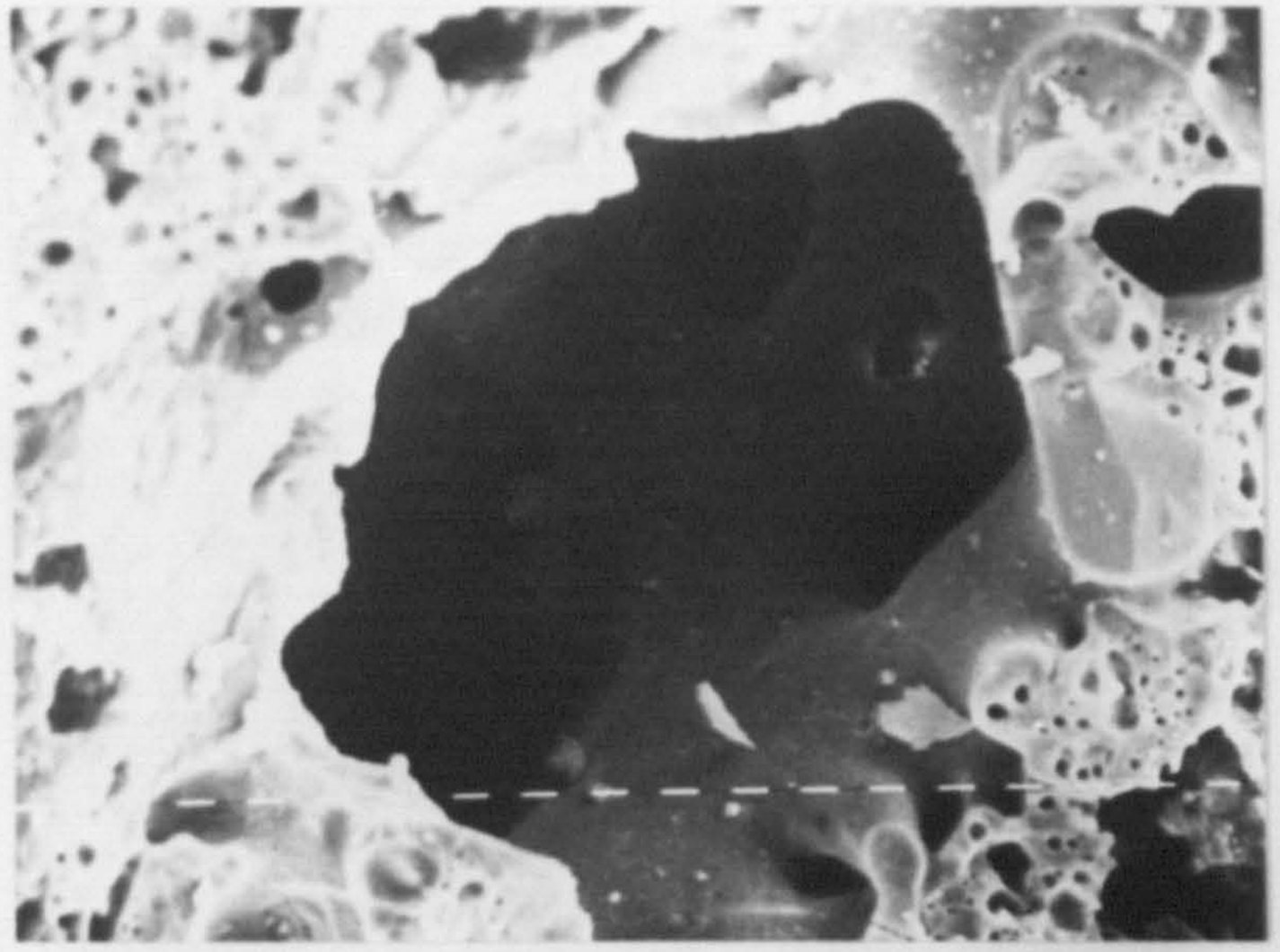

(a) x 320
Scale : 10 μm

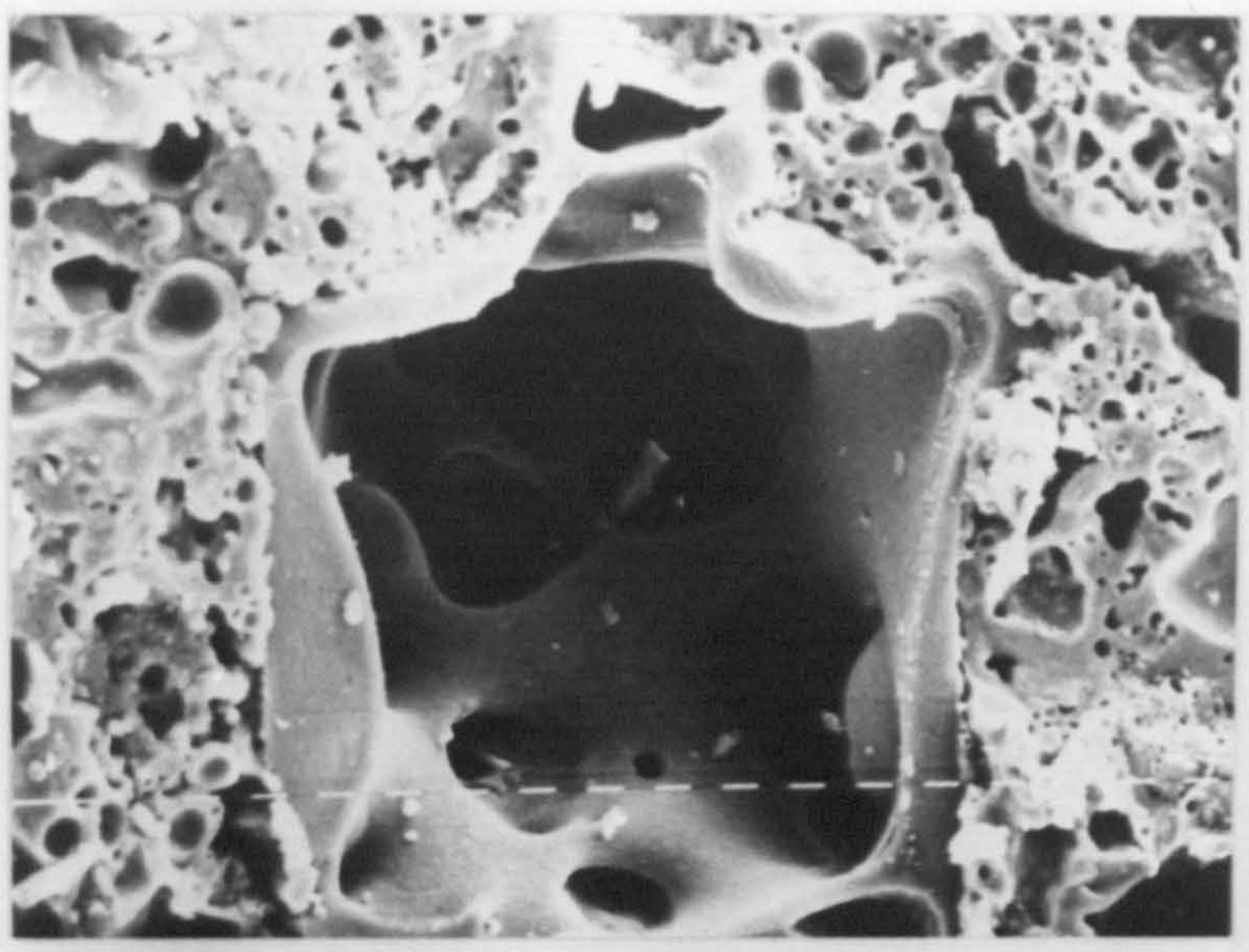

(b) x 320
Scale : 10 μm

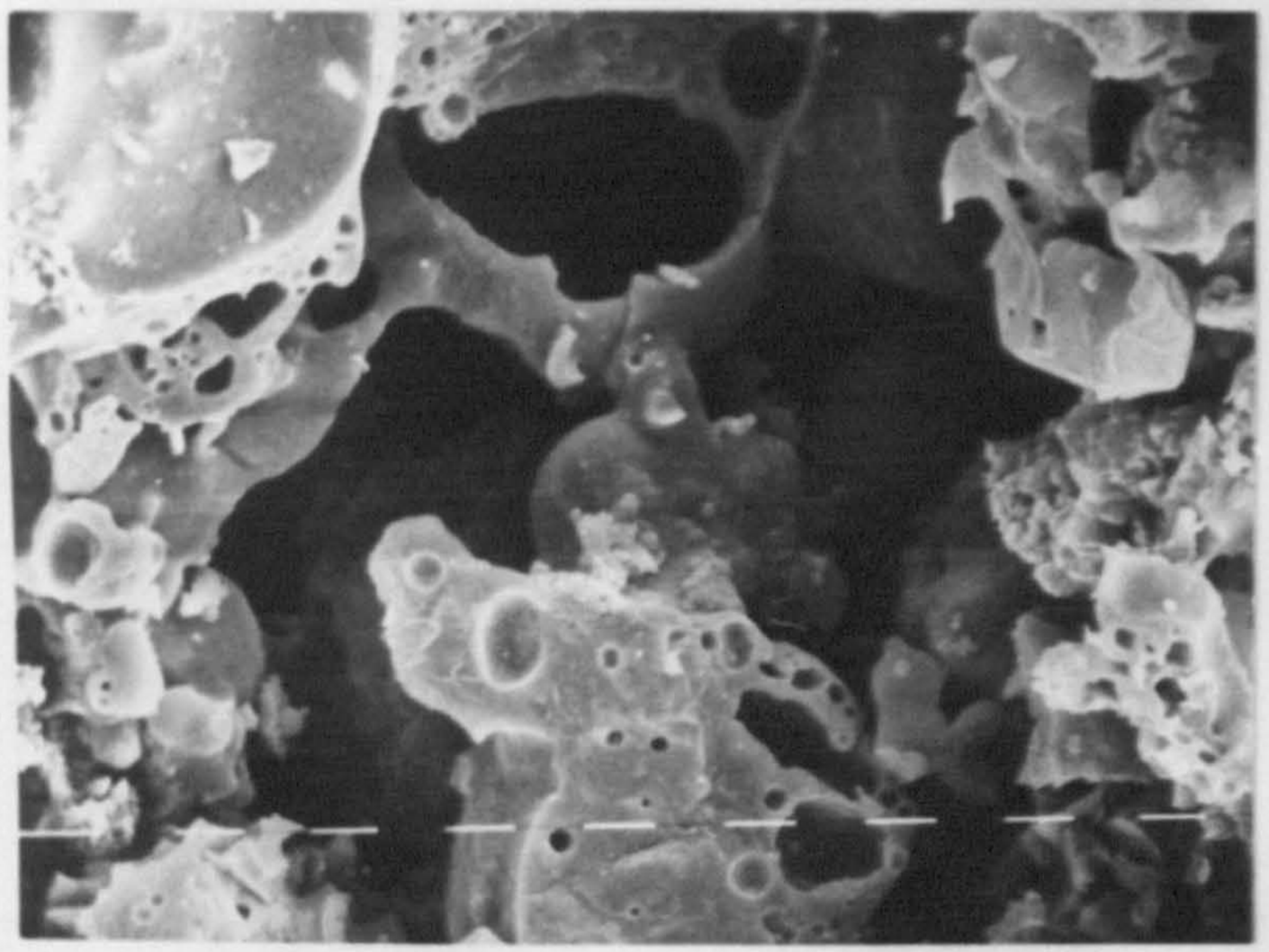

(c) x 640
Scale : 10 μm

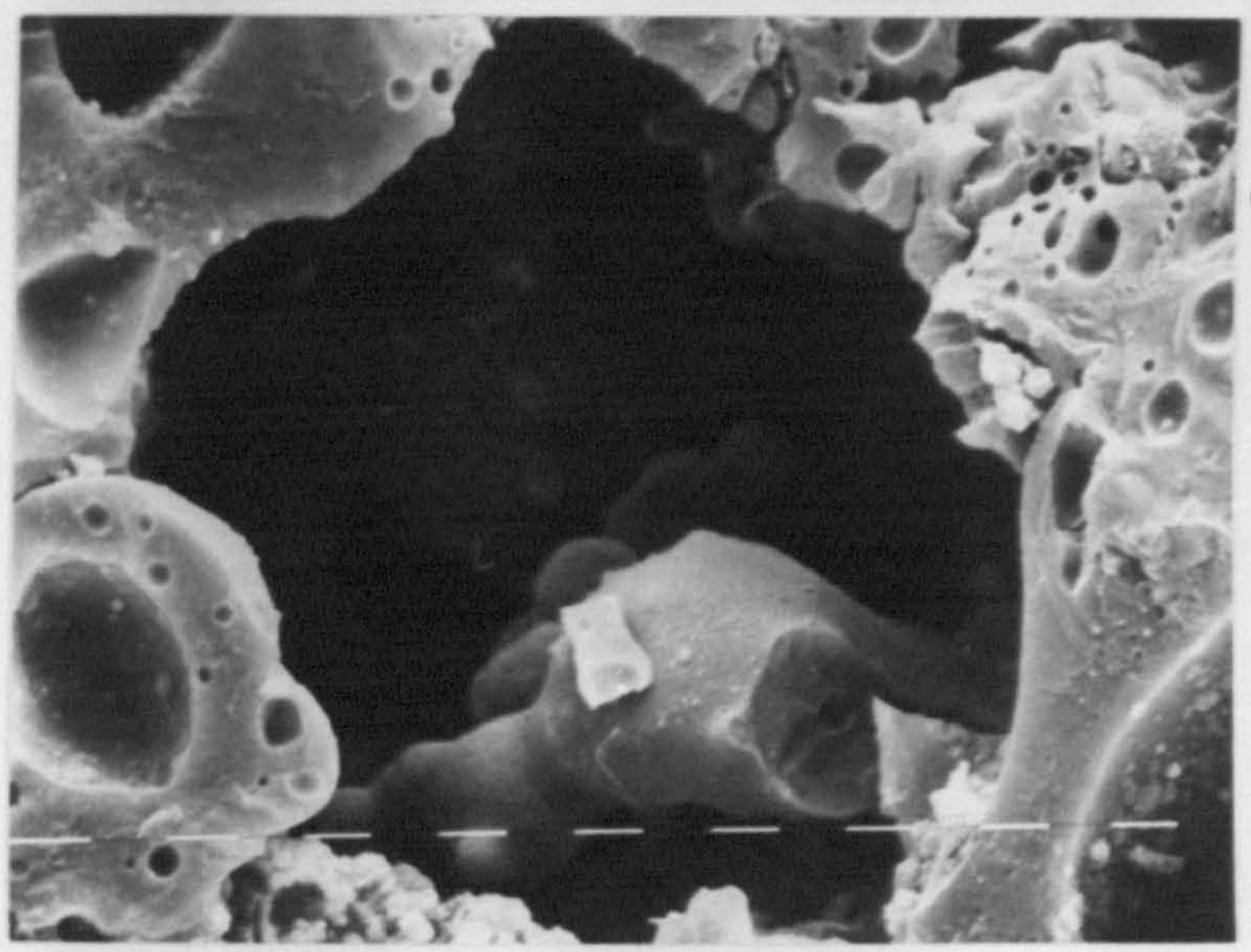

(d) x 640
Scale : 10 μm

PLATE 3.5 VOID SIZE AND STRUCTURE

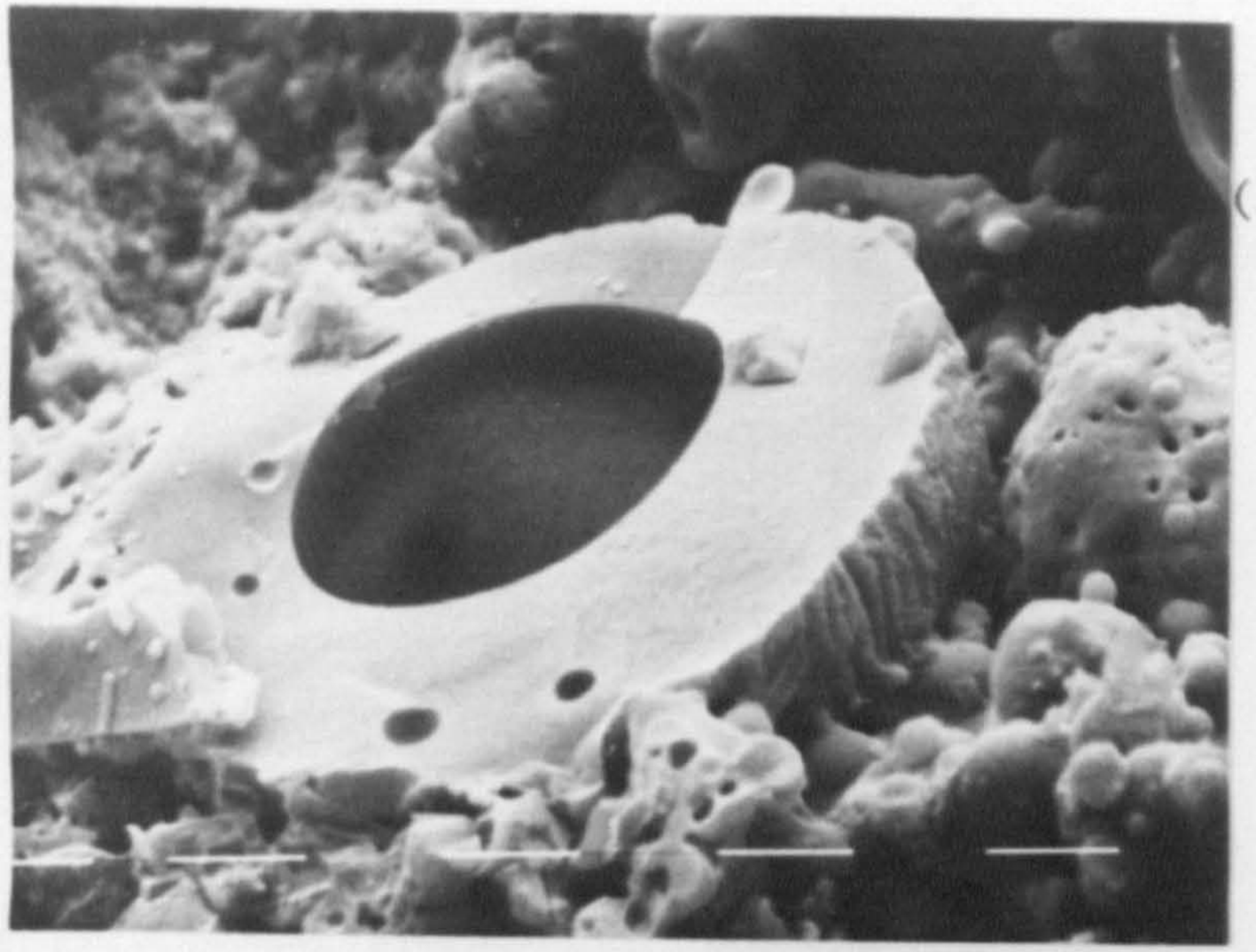

(a) x 1250
Scale : 10 μm

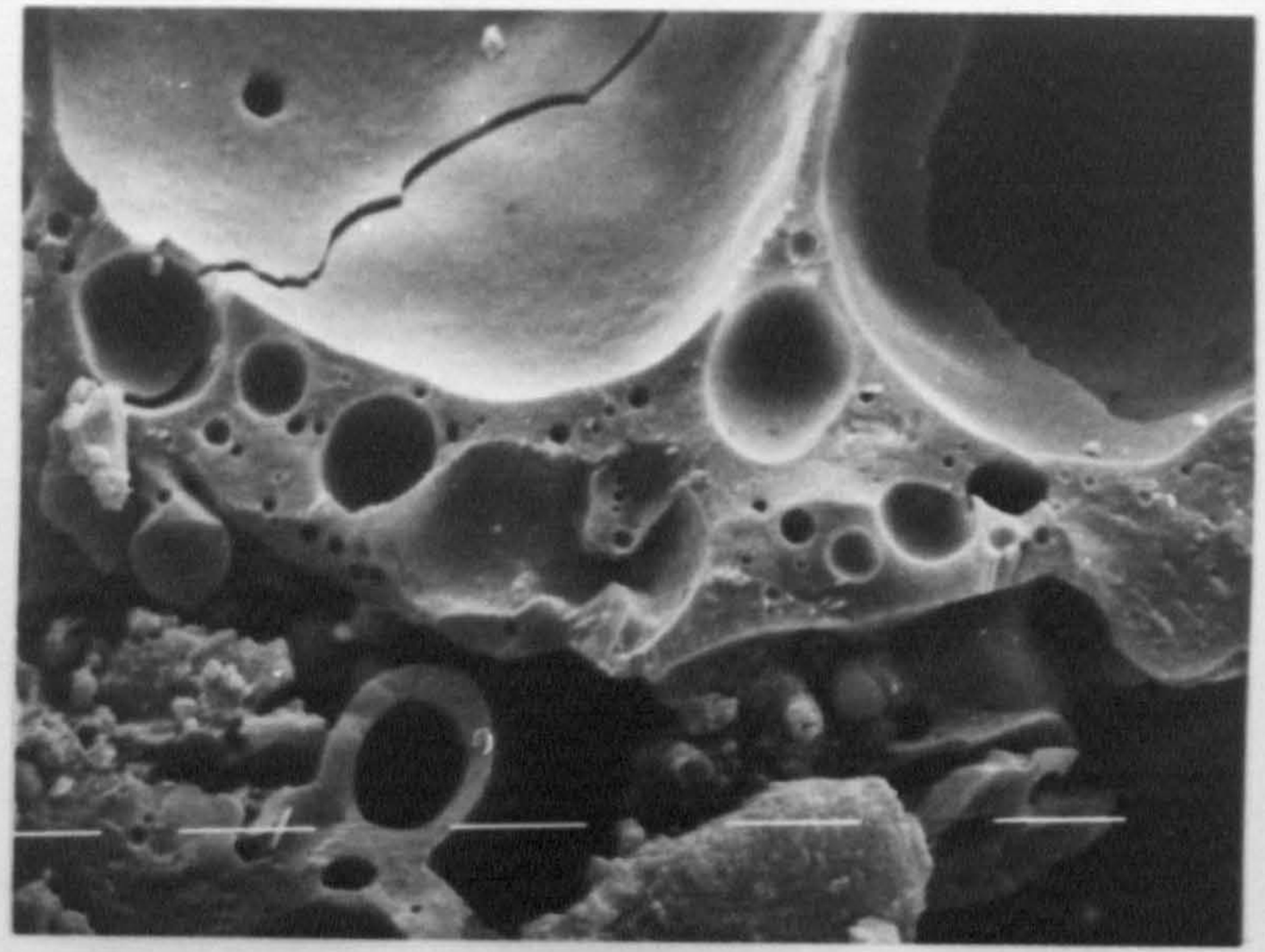

(b) x 1250
Scale : 10 μm

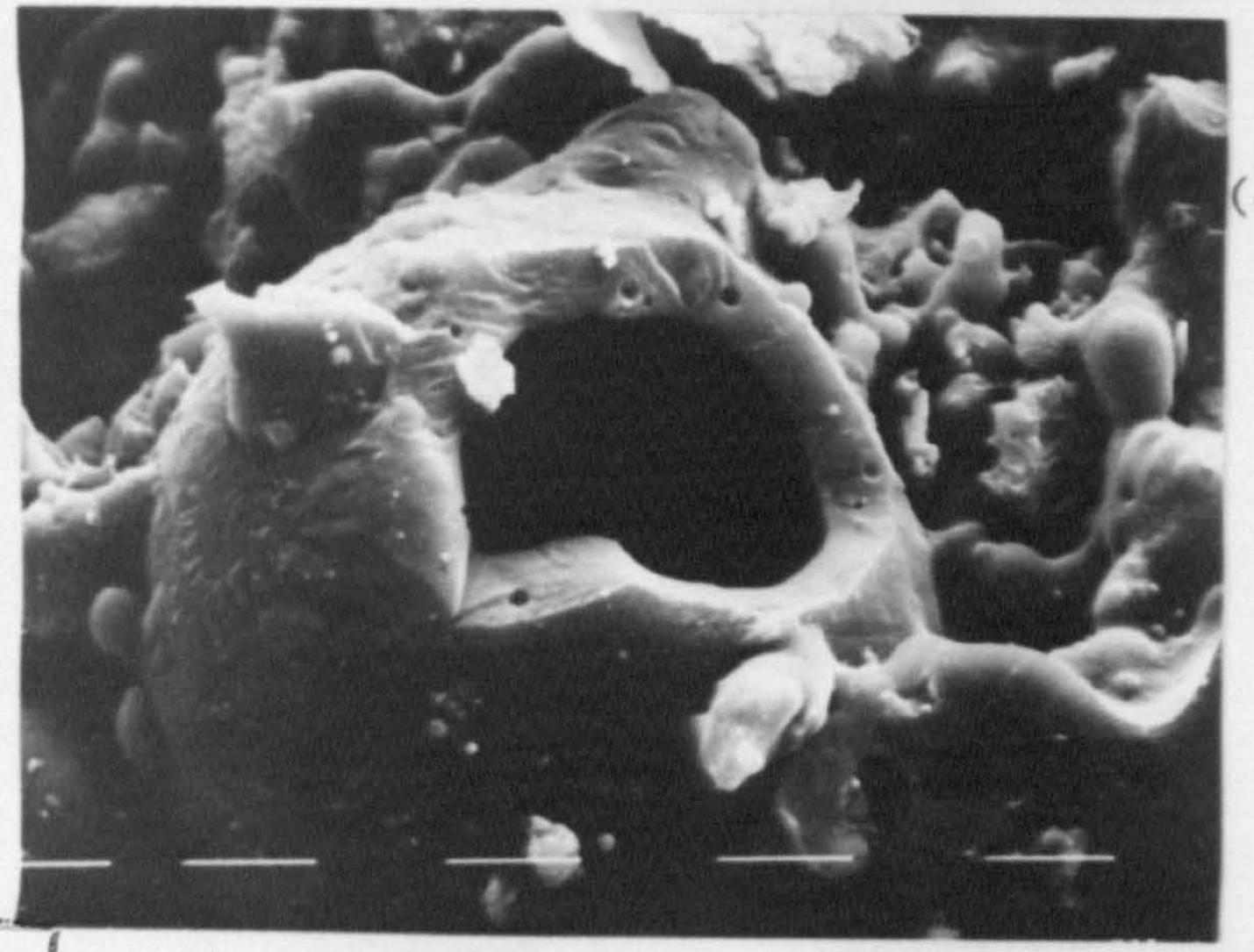

(c) x 1250
Scale : 10 μm

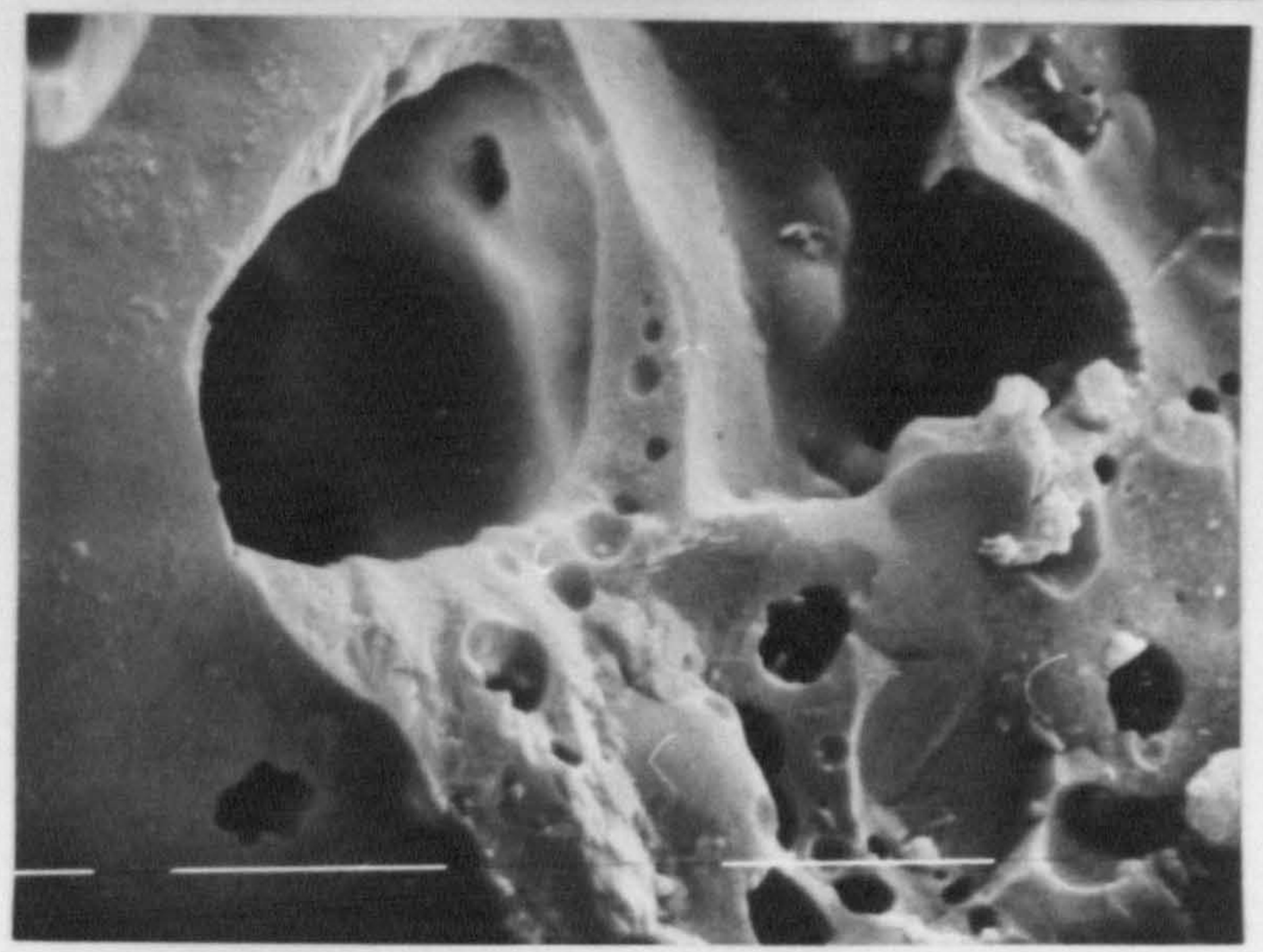

(d) x 2500
Scale : 10 μm

PLATE 3.6 VOID SIZE AND STRUCTURE

size from 3-4 μm down to 1 μm.

Plates 3.7(a)-(d) show some unusual features which were observed during the investigation. Plate 3.7(a) shows a piece of material peppered with small holes approximately 2-3 μm across. X-ray spectrography revealed that the major elements making up the material were silica and aluminium, with small amounts of magnesium, iron, potassium and calcium. This feature along with features shown in Plates 3.7(b)-(d) has probably resulted from a local 'hot spot' which occurred during sintering. The minerals became molten and escaping gases formed the holes which were preserved as the material cooled and solidified.

Plate 3.7(b) shows another mass of material which appears to have solidified to form a flaky type of structure. The chemical composition of this material was similar to that of the previous material but a higher silica content is reflected in the smooth clean fracture surface.

Plates 3.7(c) and (d) both show crystal type structures. The former were foumd as part of the general matrix of the pellet whereas the latter were found on the surface of an unreacted cenosphere. X-ray spectrography showed the mineral content to be similar to that of the material shown in Plate 3.7(a).

Finally Plates 3.8(a)-(d) show the interface between a Lytag pellet and sand cement matrix. The interface is easily visible and it can be seen that there is excellent bonding all along the surface line of the pellet. Low magnifications were only used to observe this feature since the very irregular fracture surface in the interface region meant that at high magnifications it was not possible to focus on both materials on either side of the interface.

3.4 Absorption Characteristics of Lytag

3.4.1 Experimental Details

The aim of this part of the investigation was to study the absorption characteristics of Lytag aggregate up to a period of twenty four hours.

Samples from four different batches of aggregates, delivered during the course of this project, were tested with the percentage absorption by weight being calculated for each batch after 30 seconds, 30 minutes and 24 hours immersion in water. The test method used was based on that described in BS 812:

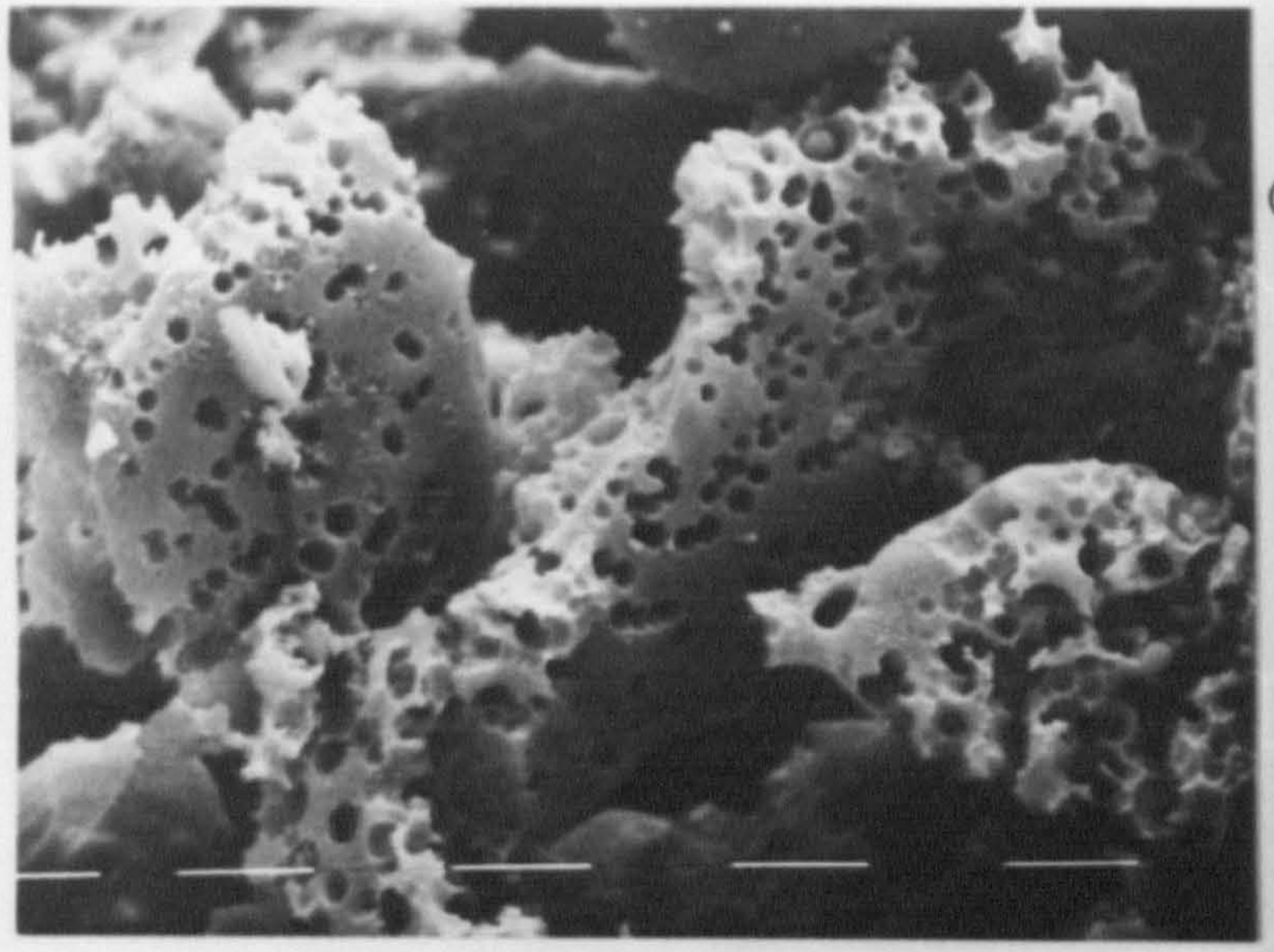

(a) x 1250
Scale : 10 μm

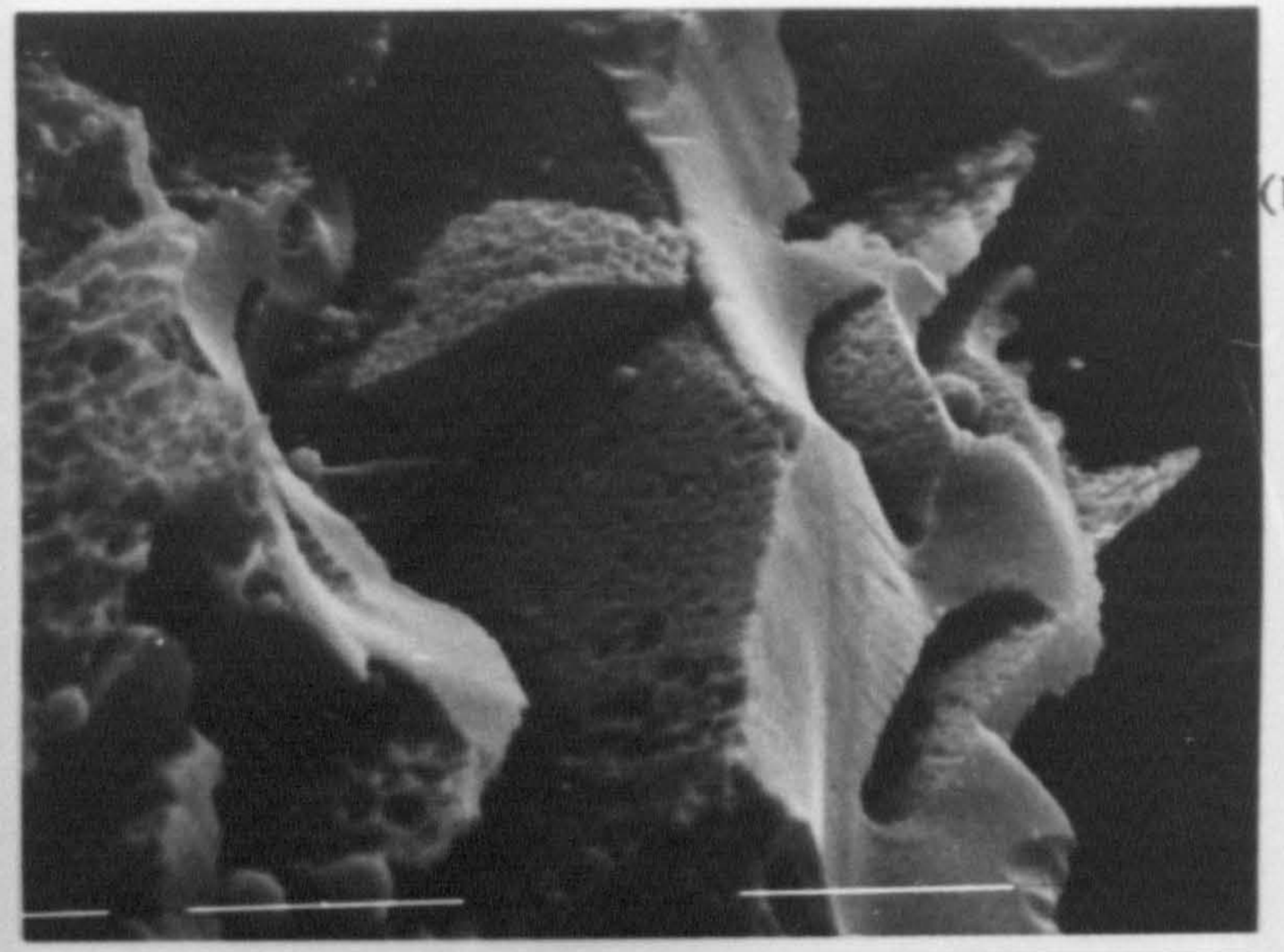

(b) x 2500
Scale : 10 μm

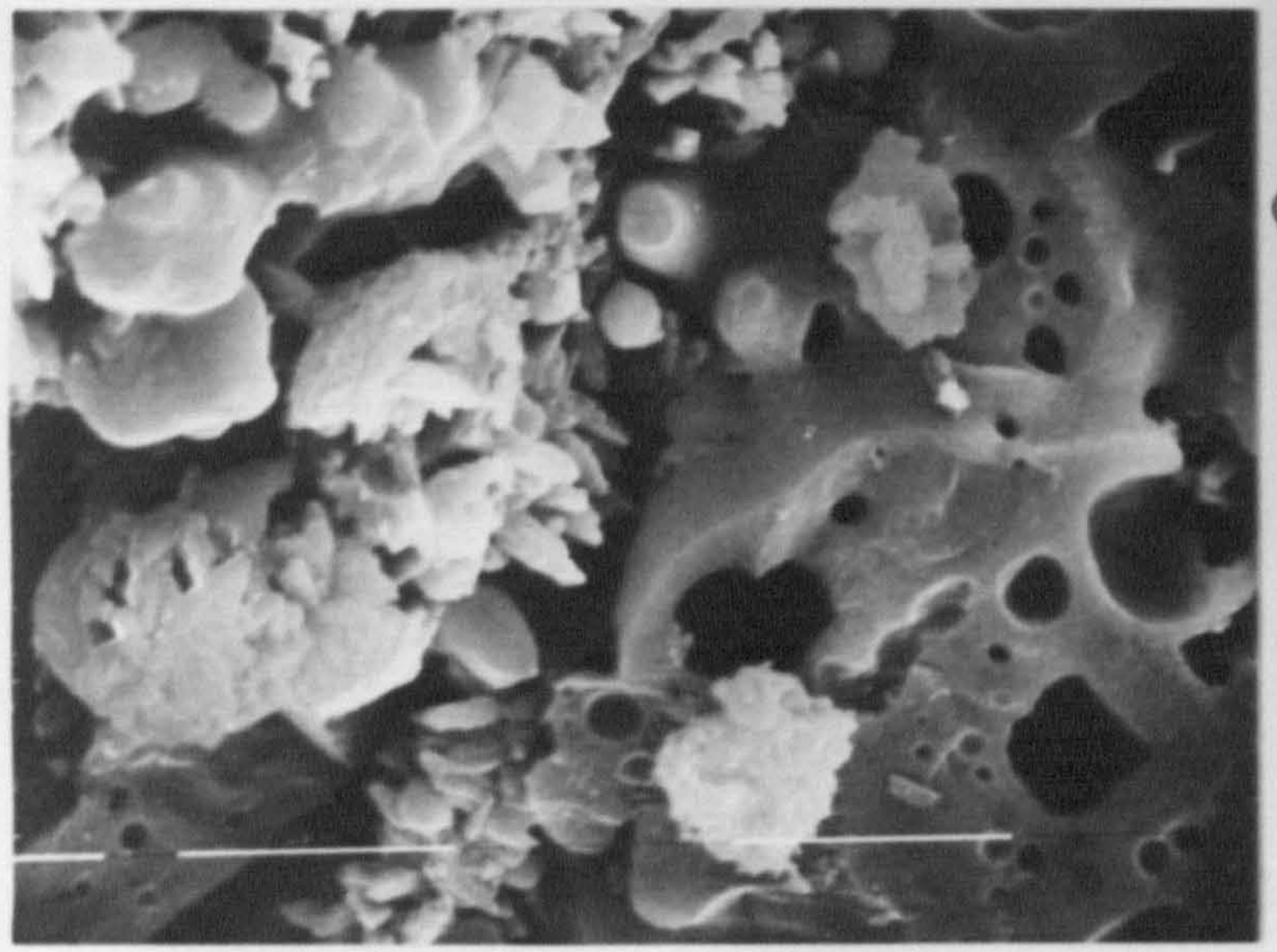

(c) x 2500
Scale : 10 μm

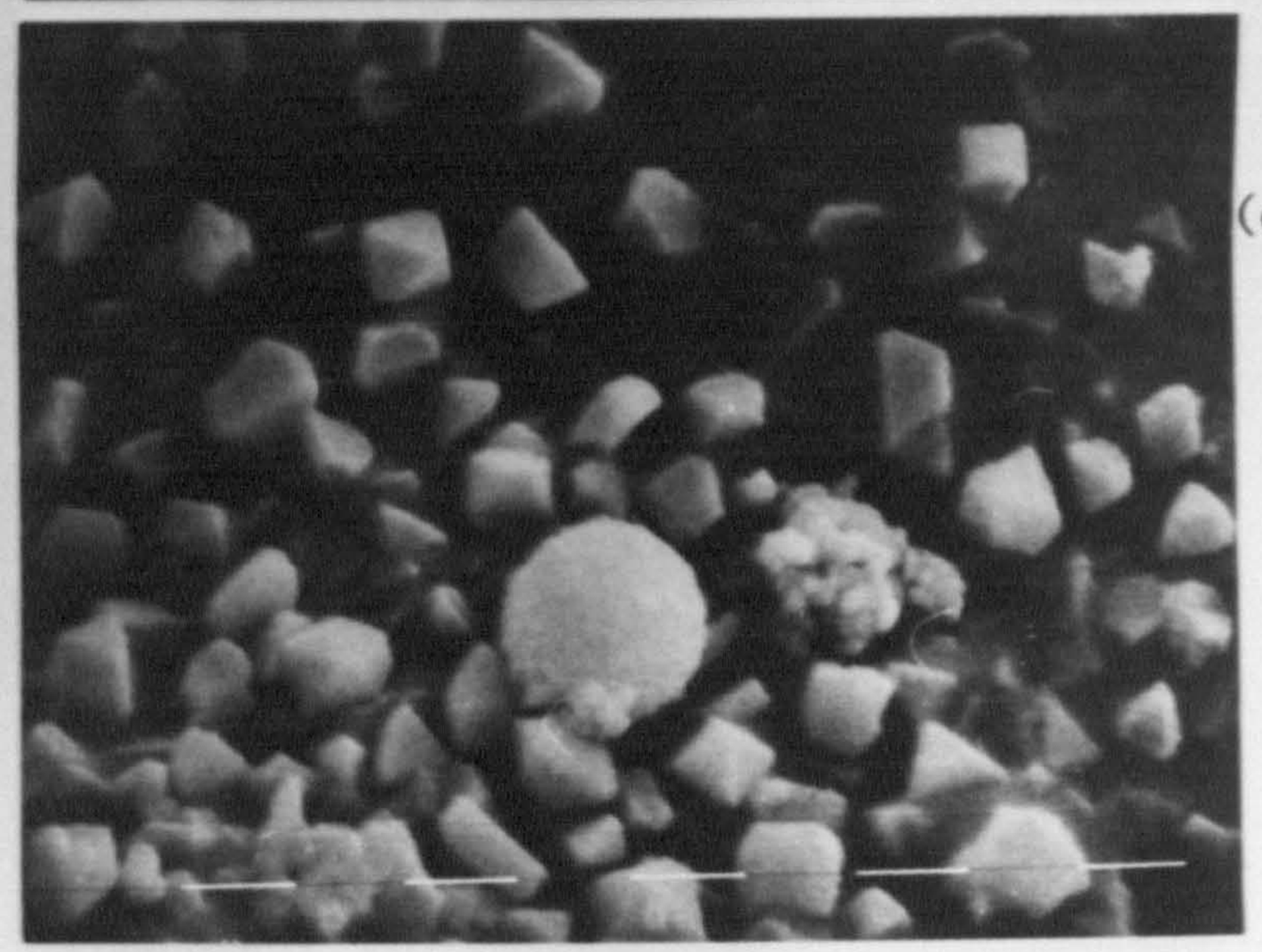

(d) x 10,000
Scale : 1 μm

PLATE 3.7 UNUSUAL FEATURES

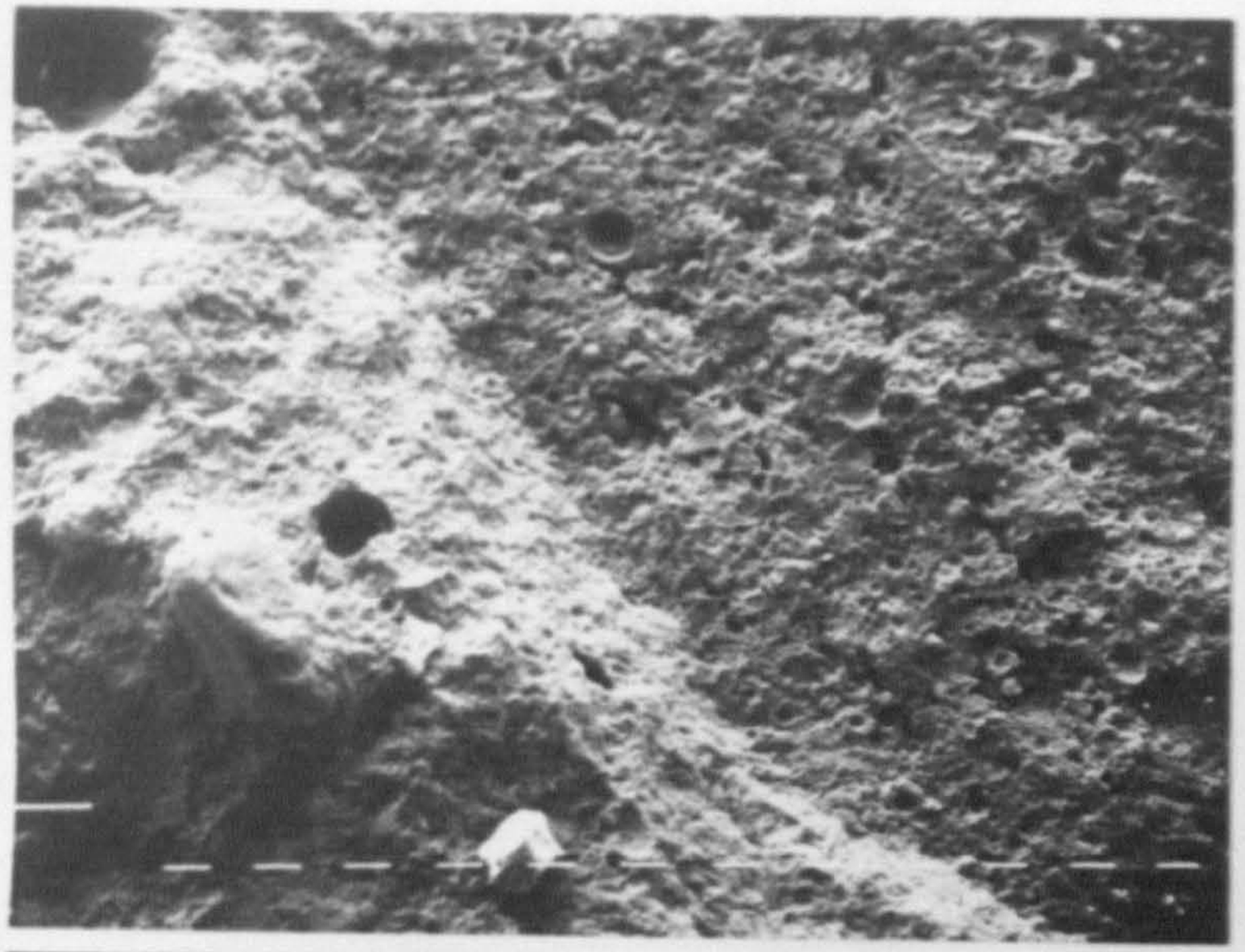

(a) x 40
Scale : 100 μm

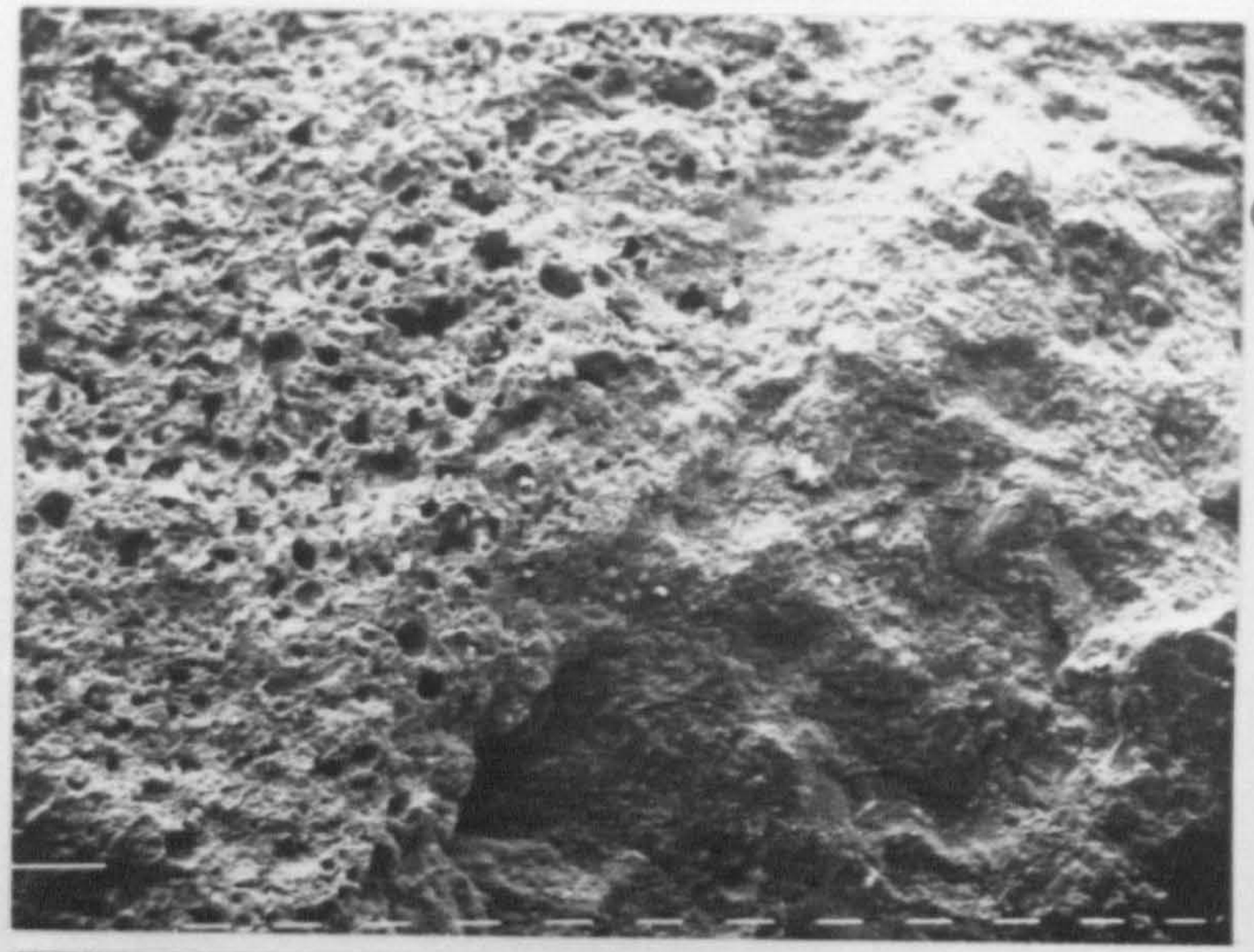

(b) x 40
Scale : 100 μm

(c) x 40
Scale : 100 μm

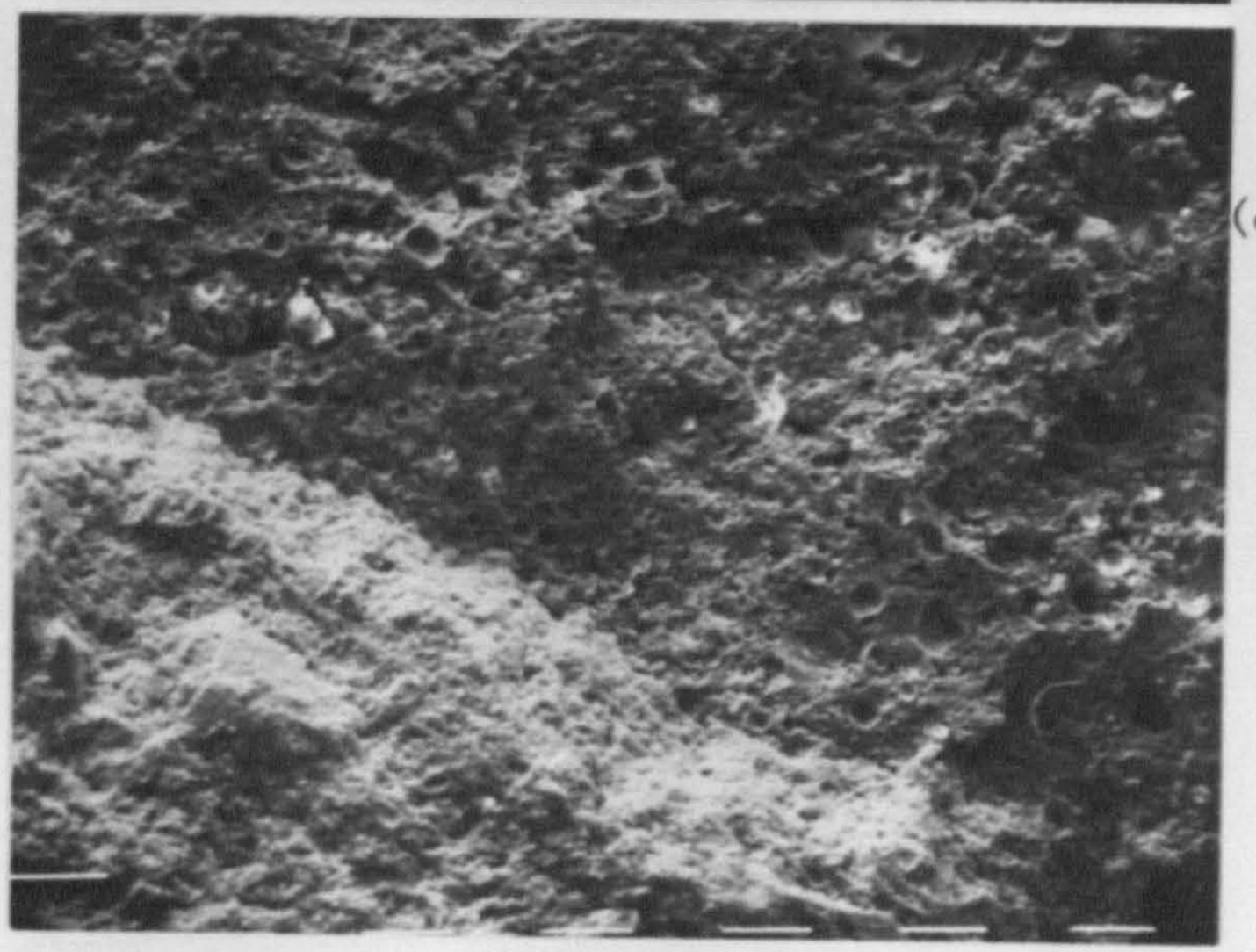

(d) x 80
Scale : 100 μm

PLATE 3.8 BOND BETWEEN AGGREGATE AND MATRIX

Part 2: 1975 (79), for aggregates between 40 mm and 5 mm.

Each batch sample of aggregate was individually washed on a 5 mm sieve to remove the finer particles, particularly the dust which would otherwise be lost during the test, thereby affecting the result. The sample was then drained and dried in an oven at $105^{o} \pm 5^{o}C$ for 24 hours. The sample was then removed from the oven and allowed to cool in the laboratory for approximately 1 hour. From each batch sample, three smaller samples of approximately 0.5 kg were obtained by using a sample divider. 30 s, 30 min and 24 hr absorption figures were each obtained from one of the three samples.

A dried sample was weighed and then placed in a gas jar. The sample was covered with water and timing started. The sample was aggitated to remove air bubbles by rapid clockwise and anti-clockwise rotation of the gas jar. At the end of the absorption period the sample was drained and then placed onto an absorbent cloth to remove the bulk of the surface water. The aggregate was then spread out on a second absorbent cloth to a depth of one pellet and exposed to the atmosphere until all visible films of water had disappeared. The sample was then weighed.

For the samples tested at 24 hrs, the procedure outlined in BS 812 (79) for measuring relative density was also carried out.

3.4.2 Discussion of Results

The results of the absorption test series are shown in Table 3.1 along with the results from other investigators (32, 61). The results for the four batches of aggregate tested by the author are consistent, with the maximum difference in absorption values of 1% occurring between batches B, D and A at 24 hours. The average values for the different periods of immersion compare favourably with the results of the other investigators. The differences which do occur are probably due to the subjective nature of absorption tests in general (12). Teychenné (32) and Balendran (61) do not give a description of the test method used to obtain absorption rates.

From this series of tests it can be seen that approximately 69% of the 24 hour absorption occurs within the first 30 s. Similar results have been

Lytag Batch	Water Absorption* (% of Dry Mass)				Relative Density*			Calculated Porosity** %
	30 Sec.	30 Min.	24 Hr.	6 Mth.	Oven Dried	Saturated Surface Dried	Apparent	
A	9.1	10.2	13.6	-	1.53	1.74	1.93	-
B	8.7	9.5	12.6	-	1.59	1.79	1.99	-
C	9.3	10.2	13.5	-	1.52	1.73	1.92	-
D	8.9	9.6	12.6	-	1.59	1.79	1.99	-
Average (Author)	9.0	9.9	13.1	-	1.56	1.76	1.96	-
Teychenné (32)	-	-	13.0	-	-	-	-	-
Balendran (61)	9.0 (10 Secs)	11.0	14.0	24.0	1.60	1.96	-	38

* See Reference (79)
** See Reference (80)

TABLE 3.1 ABSORPTION TEST RESULTS FOR LYTAG AND COMPARISON WITH OTHER INVESTIGATORS

reported by several investigators for various UK lightweight aggregates (32, 49, 61). Balendran continued his absorption tests up to 6 months and from his results was able to calculate the porosity of the aggregate based on a formula presented by Hosking (80). This formula depends on all the voids within an aggregate particle being saturated to be strictly accurate. This is obviously not the case with aggregates which contain completely sealed discrete voids and it has been suggested (60) that even an interconnected void structure is unlikely to become fully saturated at low pressure. Thus the calculated porosity value is likely to be slightly lower than the true porosity.

3.5 Relationship Between the Microstructure and Water Absorption of Lytag Aggregate

In common with other lightweight aggregates, the water absorption characteristics of Lytag follow two distinct phases, namely:

(a) the initial rapid absorption of water when dry aggregate is immersed, followed by;

(b) a much slower, prolonged period of absorption, tending towards a finite value after six to twelve months.

In terms of the microstructure of Lytag aggregate, this two phase phenomenon can be explained by the size range, structure and distribution of the voids within a Lytag pellet. The voids range in size from approximately 200 μm down to less than 1 μm. The larger voids are highly interconnected and very few voids are discrete and completely sealed. The only ones which do tend to fit these criteria are those within the unreacted pfa cenospheres. Also the voids are evenly distributed throughout the entire pellet with large, medium and small voids being thoroughly mixed.

Even the larger voids are so small that they will only become saturated by capillary action but on immersion in water the saturation of these larger voids will be rapid. Therefore within a few seconds of immersion the entire pellet will have water distributed throughout it by means of the larger and medium sized voids. Capillary action over a period of time will saturate the smaller voids until eventually a state of equilibrium is reached. With some of

the very small voids, however, it is probable that they will never become saturated under low pressure.

The above theory also applies, in reverse, to the drying out of a hardened lightweight concrete over a period of time. Water will tend to migrate relatively rapidly at first from the larger voids within the pellet into the cement matrix as the hydration process continues, followed by the slower more prolonged dissipation of water from the smaller voids within the aggregate. This gradual loss of water over a period of time is believed to enable the concrete to 'self repair' internal microcracking possibly caused by the application of loads to a member during construction, as the hydration process continues.

The observed high porosity of the aggregate is reflected in the calculated value for porosity, obtained by Balendran (61), of approximately 40% by volume.

3.6 Conclusions

The following conclusions can be derived from this part of the investigation:

1. In order to examine the microstructure of Lytag aggregates fractured surfaces rather than sawn surfaces should be used.
2. Although there is a distinct colour boundary between the thin outer layer of the pellet and its internal 'bulk', no such boundary occurs within the microstructure of the pellet.
3. The overall structure of a Lytag pellet is basically made up of unreacted cenospheres which are fused together at their points of contact and/or surroumded by a solidified honeycomb type structure probably formed when some of the raw materials became semi-molten and gases escaped through them.
4. The unreacted cenospheres range in diameter from approximately 75-100 μm down to less than 1 μm.
5. Voids range in size from approximately 200 μm down to less than 1 μm with all sizes being evenly distributed throughout the pellet.
6. The majority of the voids are interconnected although discrete voids do exist, mainly within the unreacted cenospheres.
7. X-ray spectrography revealed that the major chemical elements from which

Lytag pellets are composed are silica and alumina with smaller amounts of calcium, iron, magnesium and potassium.

8. An excellent bond forms between the pellets and a sand-cement matrix.
9. The 24 hr water absorption of Lytag aggregate is approximately 13% by weight.
10. Approximately 70% of the 24 hr water absorption occurs within 30 seconds for initially dry aggregates.

CHAPTER 4

MIX DESIGN AND STRENGTH CHARACTERISTICS OF LYTAG-SAND CONCRETE

4.1 Introduction

The mix design process and the strength characteristics of lightweight concrete are affected by the same parameters as those which affect dense concrete The lower modulus of elasticity of lightweight aggregates means that their role is not quite the same as for dense aggregates since there is a greater compatability, with respect to deformation behaviour, between lightweight aggregates and mortar than between dense aggregates and mortar. It is possible to produce structural lightweight concretes which are comparable with dense concretes, on a strength basis, but whose densities are 25-40% lower. Both density and strength are affected primarily by cement content, and thus by paste strength, and by water/cement ratio.

Although Lytag is not a new material, most of the research carried out on Lytag concrete has involved the use of Lytag fines as well as Lytag coarse material. Very little data are available for concretes made with Lytag coarse material and natural sand fines. The aim of this part of the investigation was to produce a mix design chart for concrete made with Lytag coarse material and natural sand fines using ordinary portland cement and having 28 day, air cured, cube strengths ranging from 20 N/mm^2 to 60 N/mm^2. The strength characteristics of these concretes were also investigated and results are reported of tests carried out to determine the crushing strength, flexural strength and tensile splitting strength at various ages and under different curing conditions.

4.2 Mix Design

The aim of mix design is to produce the most economical concrete mix which will give a required cube strength at a specified age and which is sufficiently workable to allow it to be easily placed and fully compacted. In certain cases other criteria such as the type of surface finish required, or the maximum shrinkage that can be allowed may govern the mix design process but in general the former criteria provide the basis for choosing the mix proportions for a particular grade of concrete.

In this respect, the mix design process for lightweight concrete is similar to that of dense concrete. There is however one major difference between the two, namely that all lightweight aggregates absorb considerably more water than conventional gravel or crushed rock aggregates. Typical 24 hour absorption figures for gravel or granite aggregates are 1.9 - 3.7% and 0.4 - 0.7% respectively depending on the maximum particle size (76). Typical figures for British lightweight aggregates vary between 13 - 24% depending on aggregate type (32). Thus an allowance must be made for water absorption by the aggregate and where aggregate is taken from a stock pile a measure of its moisture content must be obtained.

Dense concrete mix design was for a number of years based on Road Note 4 (81), but more recently this has been replaced by the D.O.E. mix design method (82). In formulating both of these mix design procedures, a considerable wealth of information on the mix proportions and the fresh and hardened concrete characteristics, of dense concretes, was drawn upon. The information available for lightweight concretes in general, although quite extensive, does not justify a similar national standard mix design procedure. Although concrete made with a given brand of lightweight aggregate generally shows a greater uniformity of physical and mechanical properties than for dense concretes, the variation between different brands, for say a given cement content, water/cement ratio and aggregate-cement content, can be quite considerable. Thus it seems more desirable to produce a simple mix design method for each brand of lightweight aggregate, in this case Lytag coarse and natural sand fines.

4.2.1 Experimental Programme

4.2.1.1 Materials

Ordinary portland cement, Lytag coarse aggregate and natural sand fines were used throughout this investigation. Several batches of all three materials were used during the course of the investigation but the source of each material was constant throughout. Details of all the materials are given in Table 4.1. A grading analysis of all batches of coarse and fine aggregate was carried out and typical grading curves are shown in Figure 4.1. All sand was dried using an

TABLE 4.1 DETAILS OF MATERIALS USED DURING INVESTIGATION

Material	Source	No. of Batches Used During Investigation	Nominal Size (mm)	Loose Dry Bulk Density (kg/m^3)	Fineness Modulus Range
O.P.C.	Blue Circle Cement Ltd, Hope Valley, Derbyshire	8	-	-	-
Lytag	Lytag Ltd, Rugeley, Staffordshire	5	14-5	830	5.96-6.07
Sand	Blue Circle Aggregates Ltd, Rugeley, Staffordshire	6	5-down	1560	2.74-2.92

NOTE Fineness modulus based on following set of sieves: 20, 14, 10, 5, 2.36, 1.18 mm and 600, 300, 150 μm.

FINES		COARSE	
o——o	Sample grading	□——□	Sample grading
o— —o	Grading limits for Zone 2 sand to BS 882 (83)	□— —□	Grading limits for 14 mm nominal graded aggregate to BS 3797 (85)

NOTES

(1) Sand sampled and tested in accordance with BS 812 (79) and BS 882 (83).

(2) Coarse aggregate sampled and tested in accordance with BS 3681 (84) and BS 3797 (85).

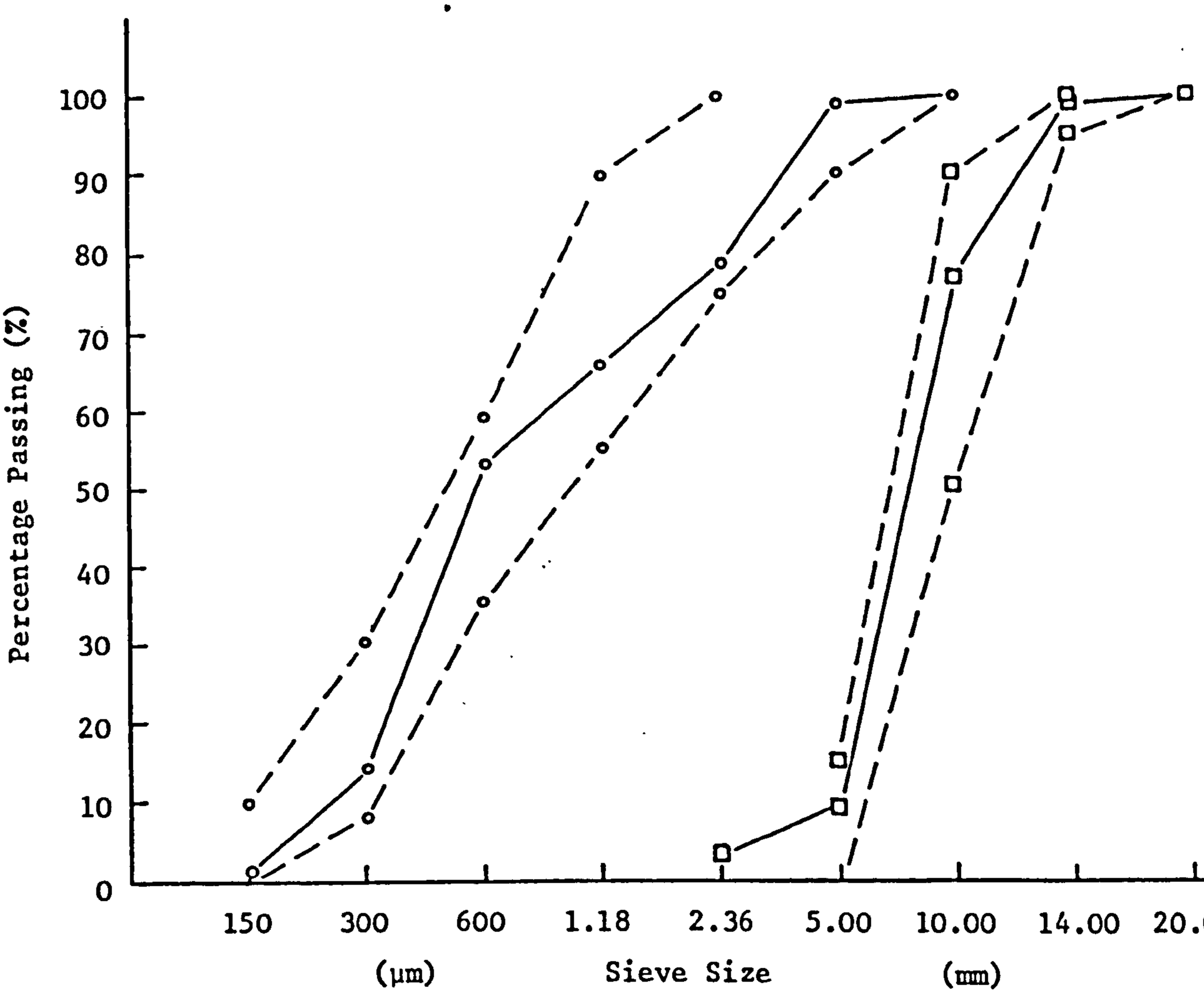

FIGURE 4.1 TYPICAL GRADING CURVES FOR LYTAG COARSE AGGREGATE AND NATURAL SAND FINES

electric sand drier and left to cool prior to use so that its moisture content could always be regarded as zero. The grading curve in Figure 4.1 is for sand dried in this way and then sieved in accordance with BS 882 (83). Coarse aggregate was stockpiled in the open air and the moisture content of several samples of the aggregate was measured immediately prior to use by means of a 'Speedy Moisture Tester'.

4.2.1.2 Mixing Procedure and Manufacture of Test Specimens

All concrete was mixed in a horizontal pan-type mixer. Several different methods of combining the constituents were tried but the following method was found to produce the most homogeneous mix. Firstly the Lytag was placed in the mixer and approximately one third of the mixing water added. The aggregate and water were mixed for approximately one minute to ensure that the absorbed moisture content of the aggregate was high (see Section 3.4). The cement and sand were then added and mixed for approximately 30 seconds. The remaining water was added and mixing continued for a further 90 seconds.

All specimens were cast in steel moulds which had been lightly oiled. Concrete was placed and compacted in two roughly equal layers. Two methods of compaction were used during initial mix design namely a high frequency vibrating table and a 25 mm diameter vibrating poker. As would be expected the method of compaction had little effect on the compressive strength of specimens provided that compaction was thorough. This is demonstrated in Figure 4.2 where specimens from the same mix but compacted by different methods are compared. After casting the specimens were left for approximately 2 hours before the surfaces were trowelled smooth. All the moulds were then covered with polythene sheet and left in the laboratory for approximately 24 hours before demoulding. All specimens were tested in accordance with BS 1881 (86) and at each age, three specimens were tested unless otherwise stated. The plotted and tabulated results are thus the average of three results.

4.2.1.3 Curing Conditions

In order to investigate the effect of curing conditions on the strength characteristics of Lytag-sand concrete, three curing regimes were used, namely:

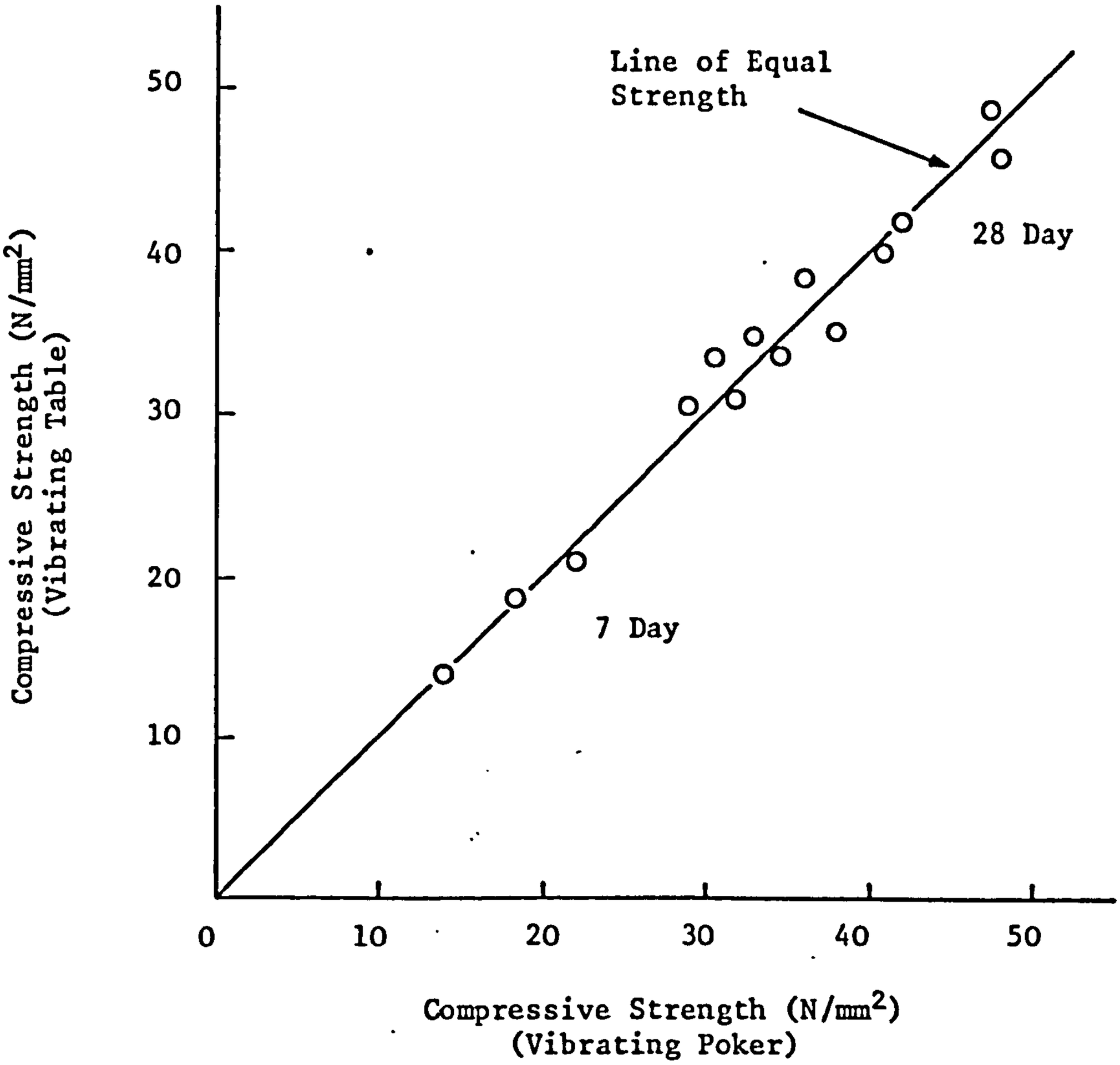

FIGURE 4.2 EFFECT OF COMPACTION METHOD ON THE 7 AND 28 DAY COMPRESSIVE STRENGTH OF AIR CURED CUBES

(i) Water at 22°C ± 3°C.

(ii) Uncontrolled laboratory condition.

(iii) Constant temperature and humidity room (C.T.H.R.) at a temperature of 16°C ± 0.5°C and 50 ± 2% relative humidity.

4.2.2 Test Results and Discussion

4.2.2.1 Trial Mixes

The initial trial mixes were designed with the aid of information supplied by Lytag Ltd. (62) (See Appendix A). The mixes given in this information are for commercial use and thus under laboratory conditions characteristic strengths were close to or in excess of the target strengths. The first series of trial mixes were aimed at producing 28 day cube strengths of 30, 40 and 60 N/mm^2 in order that some of the other testing programmes could be initiated.

The high effective water contents of early mixes, 180 kg/m^3, meant that slumps were very high and it was noted that the lower cement content mixes were prone to bleeding. The problem was discussed with Lytag Ltd. and it was pointed out that on site, for a given cube strength mixes have higher cement contents and generally there is a longer period of time between mixing and placing allowing more of the free water to be absorbed by the aggregate. Since this project as a whole was aimed at producing design data for concretes similar to those used commercially, it was decided to only reduce the effective water content to 175 kg/m^3. Also high workability mixes would be required for casting the beam specimens discussed in later chapters. Bleeding still occurred with the low strength mixes but was not excessive.

An allowance of 12% by weight, of dry Lytag, was made for water absorption by the aggregates. This was based on the 30 min absorption figure of 10% (Section 3.4) plus an allowance for the sand. A similar method is used commercially by Lytag (Appendix A).

It was also noted that the mixes were underyielding by approximately 2-3%. The mix proportions were adjusted accordingly.

Trial mixes for the 20 N/mm^2 concrete were cast at a later date.

4.2.2.2 Consistency of Results

The 30, 40 and 60 N/mm^2 trial mixes were all cast using the same batch of Lytag, batch 1 and a single batch of cement, as were several of the beam specimens for the shear series (see Chapter 7). When specimens were cast using the second and subsequent batches of aggregate and cement, it was found that consistent strength increases occurred. These were approximately 3 N/mm^2 for the 30 N/mm^2 mix and 5-6 N/mm^2 for the 40 N/mm^2 mix. The increase in strength for the 60 N/mm^2 mix was negligible since the ceiling strength of the aggregate was being approached for that cement content.

Since this strength increase was not discovered until after the second batches of aggregate and cement had been delivered, samples of the first batch of aggregate and cement were not available for test. The only means of comparing all five batches of aggregate was by their grading analysis and this is shown in Table 4.2. It can be seen that all five gradings are very similar. Table 4.3 shows the average compressive strength for the three mixes cast using different batches of aggregate and it can be seen that batches 2-5 produce reasonably consistent results and that it is batch 1 that is the odd one out. Since no samples of this batch of aggregate or the cement used were available for test it would be unwise to speculate as to the reasons why this should have occurred but this fact should be borne in mind when consulting the following chapters.

All five batches of aggregate have been used to produce concrete with 28 day cube strengths of 30 N/mm^2 and 40-45 N/mm^2 and the range of strength at various ages is shown in Figures 4.3 and 4.4 as a percentage of the 28 day strength. The effect of the initial moisture content of the aggregate on the compressive strength of various mixes is shown in Figure 4.5. There is no apparent variation in compressive strength as a result of the initial moisture content.

The mix proportions for the various strengths are shown in Table 4.4.

4.2.2.3 Effect of Coarse Aggregate on the Crushing Strength

The properties of lightweight aggregates which affect the compressive strength of the concretes produced with them can be listed as follows:

TABLE 4.2 LYTAG GRADINGS FOR BATCHES 1-5

Sieve Size (mm)	Percentage Passing (by Weight)					
	14 mm Nominal Graded Aggregate BS 3797 (85)	Batch 1	Batch 2	Batch 3	Batch 4	Batch 5
20	100	100	100	100	100	100
14	95-100	99	99	99	99	99
10	50-90	85	83	76	82	88
5	0-15	9	8	9	8	3
Fineness Modulus (See Note Table 4.1)	-	5.93	5.97	6.05	5.97	5.99

TABLE 4.3 AVERAGE COMPRESSIVE STRENGTH OF AIR CURED CONCRETE MADE WITH THE VARIOUS BATCHES OF AGGREGATE

Mix Proportions by Weight	28 Day Target Strength (N/mm^2)	Average Compressive Strength (N/mm^2)				
		Batch 1	Batch 2	Batch 3	Batch 4	Batch 5
1:2.85:2.84	30	30.5	32.5	32.1	31.9	33.0
1:1.94:2.14	40-45	39.6	46.2	45.4	46.2	47.0
1:1.06:1.47	60	58.0	-	59.0	-	60.0

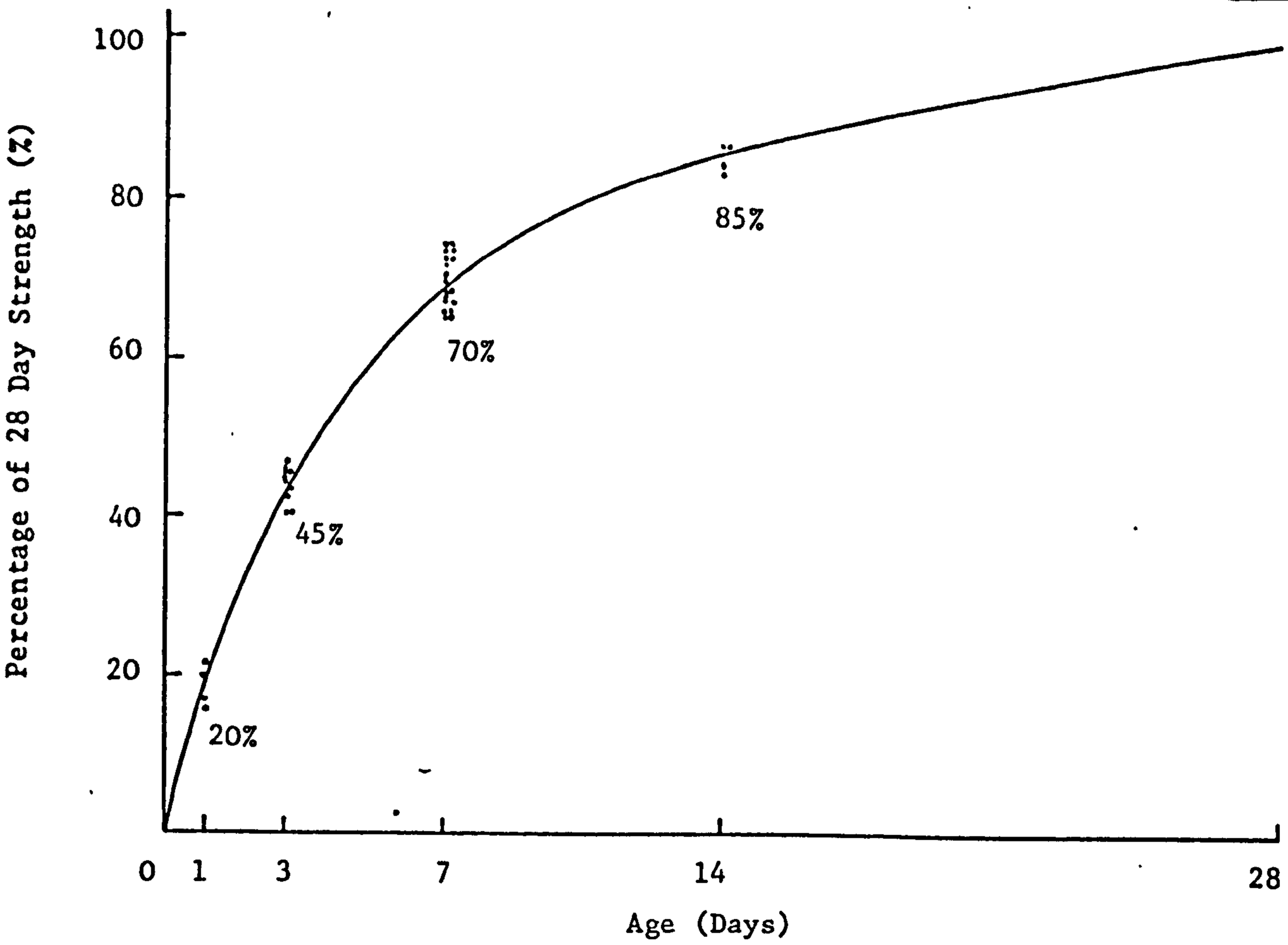

FIGURE 4.3 EARLY STRENGTH DEVELOPMENT FOR 30 N/mm^2 AIR CURED CONCRETE

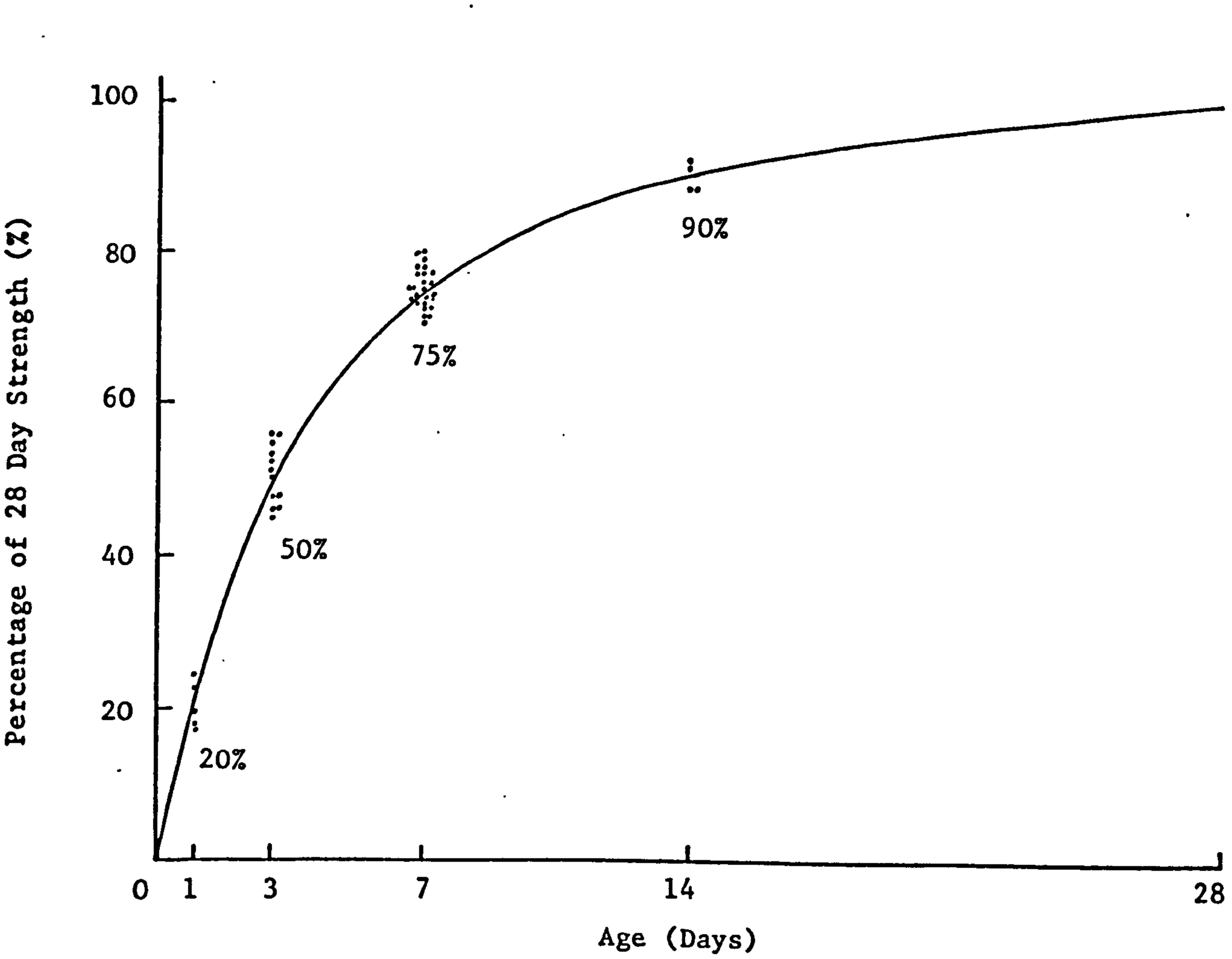

FIGURE 4.4 EARLY STRENGTH DEVELOPMENT FOR 45 N/mm^2 AIR CURED CONCRETE

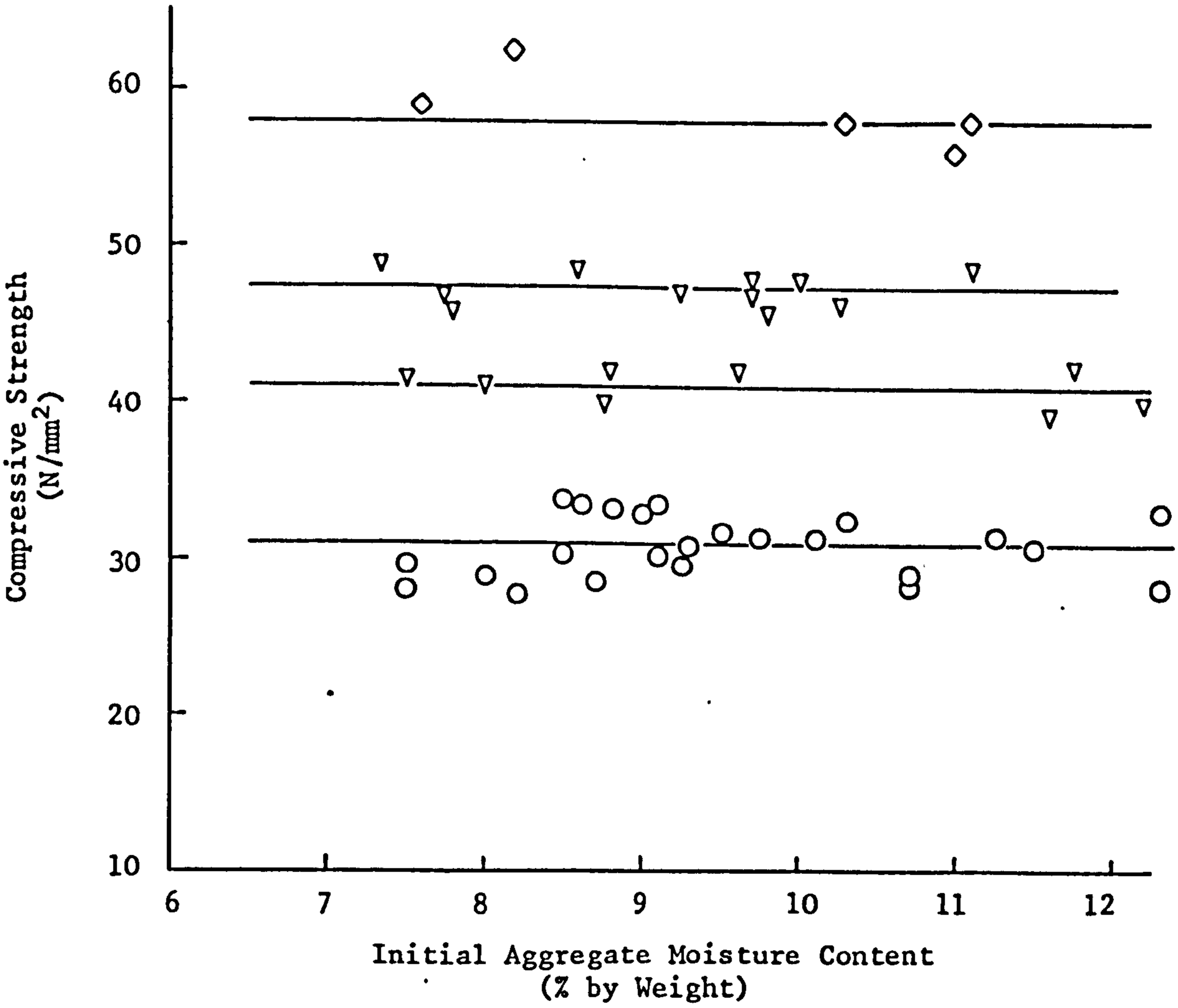

FIGURE 4.5 EFFECT OF INITIAL AGGREGATE MOISTURE CONTENT ON THE 28 DAY COMPRESSIVE STRENGTH OF AIR CURED CUBES

TABLE 4.4 MIX PROPORTIONS FOR VARIOUS STRENGTHS

28 Day Target Strength (N/mm^2)	Dry Weights per Cubic Metre (kg)			Free Water Content (kg)	Free Water/ Cement Ratio
	O.P.C.	Sand	Lytag		
30	250	715	715	175	0.70
45	335	645	715	175	0.53
60	485	515	715	175	0.36

(a) Particle strength.

(b) Modulus of deformation.

(c) Surface texture.

(d) Particle shape.

(e) Maximum dimensions and grading.

For dense aggregate the shape and surface texture of the aggregate affect compressive strength directly. The bond between the aggregate and the mortar matrix is stronger if the aggregate is angular in shape and/or rougher in surface texture. Failure occurs due to a breakdown of bond between aggregate and matrix. In the case of lightweight concrete the aggregate-matrix bond strength does not govern the concrete strength when taking an overall view. For example the strength of concretes made with different brands of aggregate is mainly a function of the particle strength of the various aggregates. Similarly the compressive strength ceiling is principally affected by aggregate particle strength. Within the strength range for a given brand of aggregate, however, the aggregate-matrix bond also influences compressive strength.

Plate 4.1 shows wet and dry cured cubes of various strength tested at 28 days. The cube strengths shown are based on 28 day wet cured cubes. It can be seen that as the cement content, and therefore the cube strength, increases, so does the proportion of fractured to unfractured aggregate particles.

It has been suggested that the aggregate-matrix bond in lightweight concrete is not a critical factor when considering compressive strength (70) and that aggregates having rounded spherical particles and a closed, smooth surface are desirable, since such material requires a lower effective water cement ratio than with angular, flat or elongated particles, in order to attain the same workability and compressive strength. With the higher strength concretes where particle fracture is high this may well be so, however, at lower strengths when aggregate-matrix bond failure is equal to or greater than particle fracture this will not be so.

4.2.2.4 Workability, Cement Content and Density

As with dense concrete, lightweight concrete must be sufficiently workable

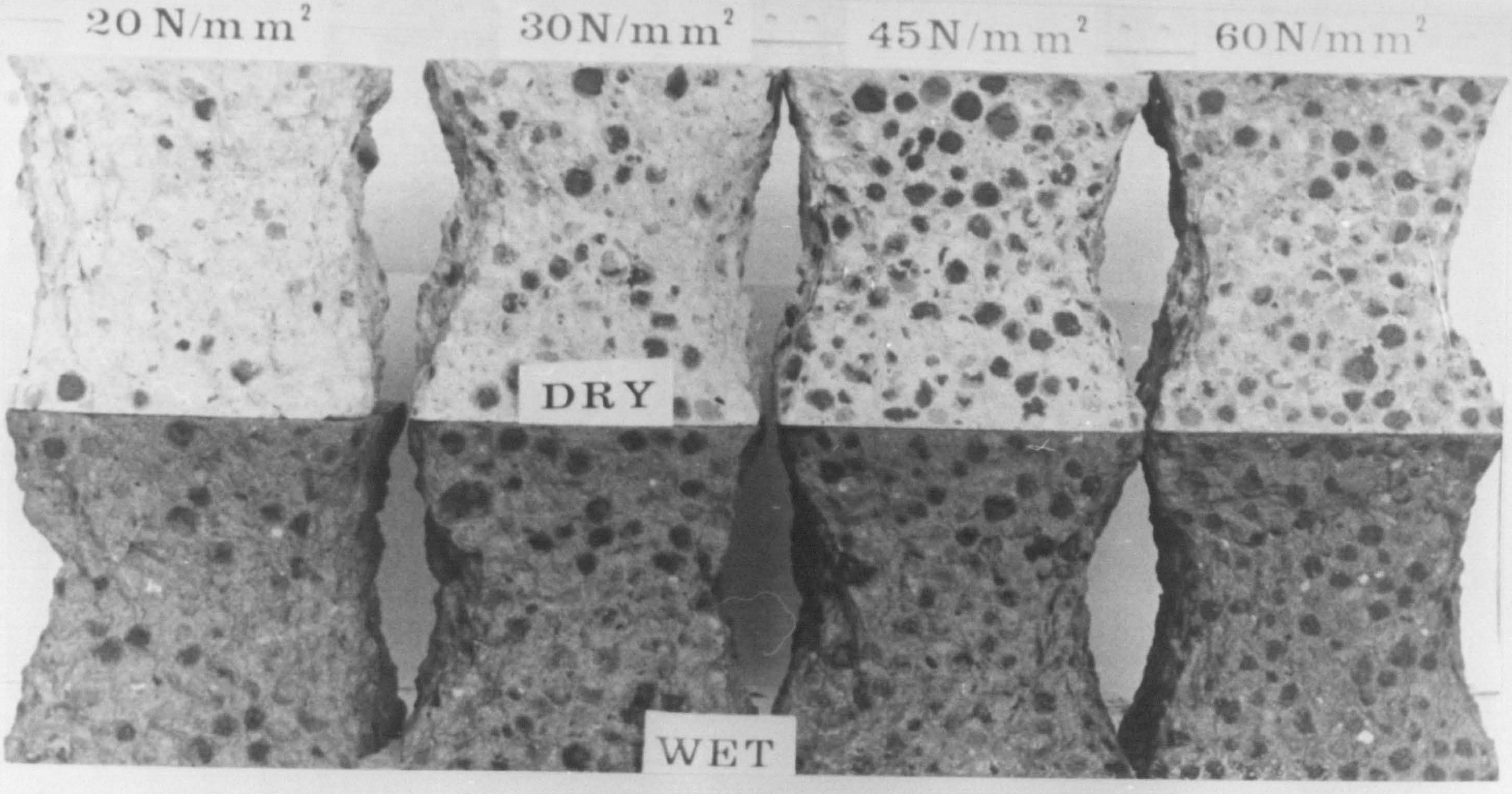

PLATE 4.1 AGGREGATE FRACTURE IN CUBES TESTED AT 28 DAYS

to allow it to be easily placed and compacted. The only test used to measure the workability of the various mixes was the slump test.

For the range of mixes tested, slumps were high and the test was not found to give consistent results. For a particular strength mix, slump could vary by + 25 mm, from the desired range of 75-100 mm and yet the average compressive strength would remain consistent. These variations are probably due to several variables the most important being the time between mixing and testing, and the initial moisture content of the aggregate.

Other investigators (11, 49) have suggested that the compacting factor and Vebe tests give more consistent results for lightweight concretes, however with high workability mixes, on site, it is doubtful whether these tests would provide adequate quality control.

The relationship between compressive strength and cement content varies according to the type of aggregate used. This is shown in Figure 4.6. It can be seen that of all of the coarse lightweight aggregate-natural sand fines mixes shown in Figure 4.6 Lytag requires less cement content to reach a given strength and for the high workability mixes used by the author the cement contents up to a cube strength of approximately 45 N/mm^2 are comparable with sand and gravel mixes (32). The Lytag-sand mixes of Balendran (61) are shown to require higher cement contents than those tested by the author up to a cube strength of approximately 50 N/mm^2. However, the mixes tested by Balendran (61) only had a maximum coarse aggregate volume concentration of 50%.

Figure 4.7 shows the relationship between compressive strength and total water cement ratio for sand and gravel (32), All-Lytag (62) and Lytag-sand concrete. For a given workability the total water/cement ratio should decrease when lightweight fines are replaced by sand. In Figure 4.7 the workability of the All-Lytag mixes shown was approximately 40-50 mm as opposed to the Lytag-sand mixes which had slumps of 75-100 mm.

Figure 4.8 shows the relationship between compressive strength and density for All-Lytag concrete and Lytag-sand concrete. It can be seen that sand replacement leads to an average increase in density of approximately 14%.

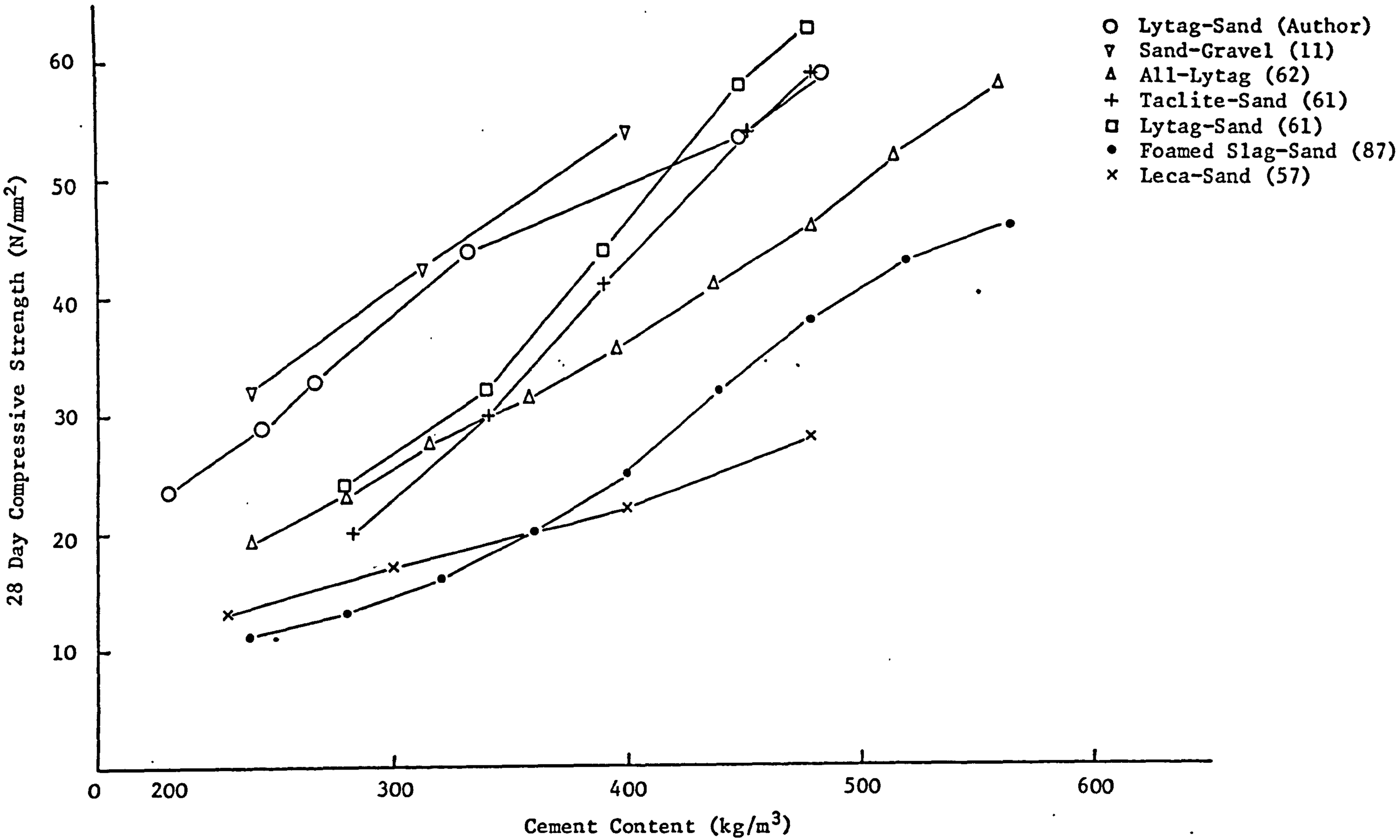

FIGURE 4.6 RELATIONSHIP BETWEEN COMPRESSIVE STRENGTH AND CEMENT CONTENT FOR VARIOUS LIGHTWEIGHT AGGREGATES

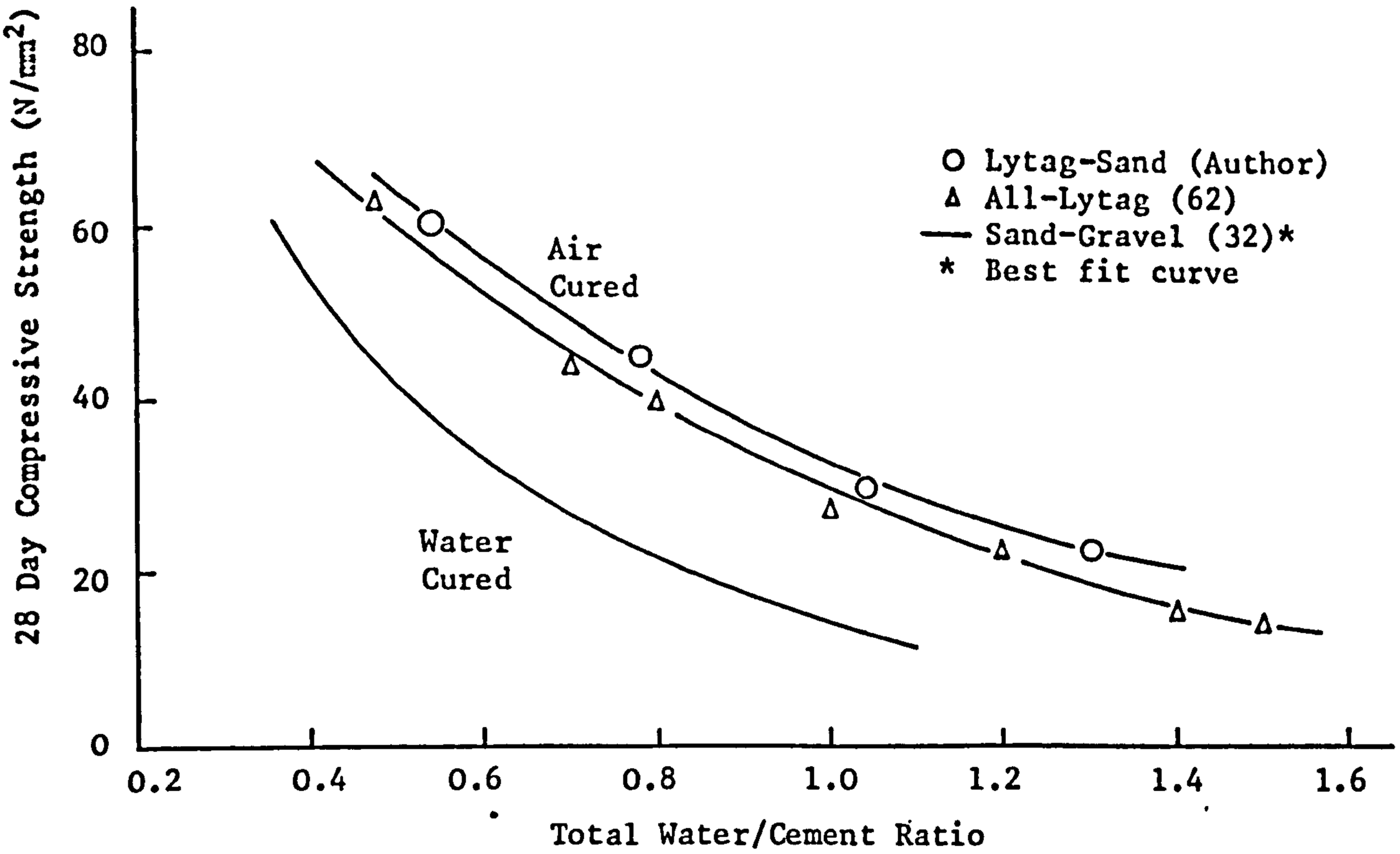

FIGURE 4.7 RELATIONSHIP BETWEEN COMPRESSIVE STRENGTH AND TOTAL WATER/CEMENT RATIO

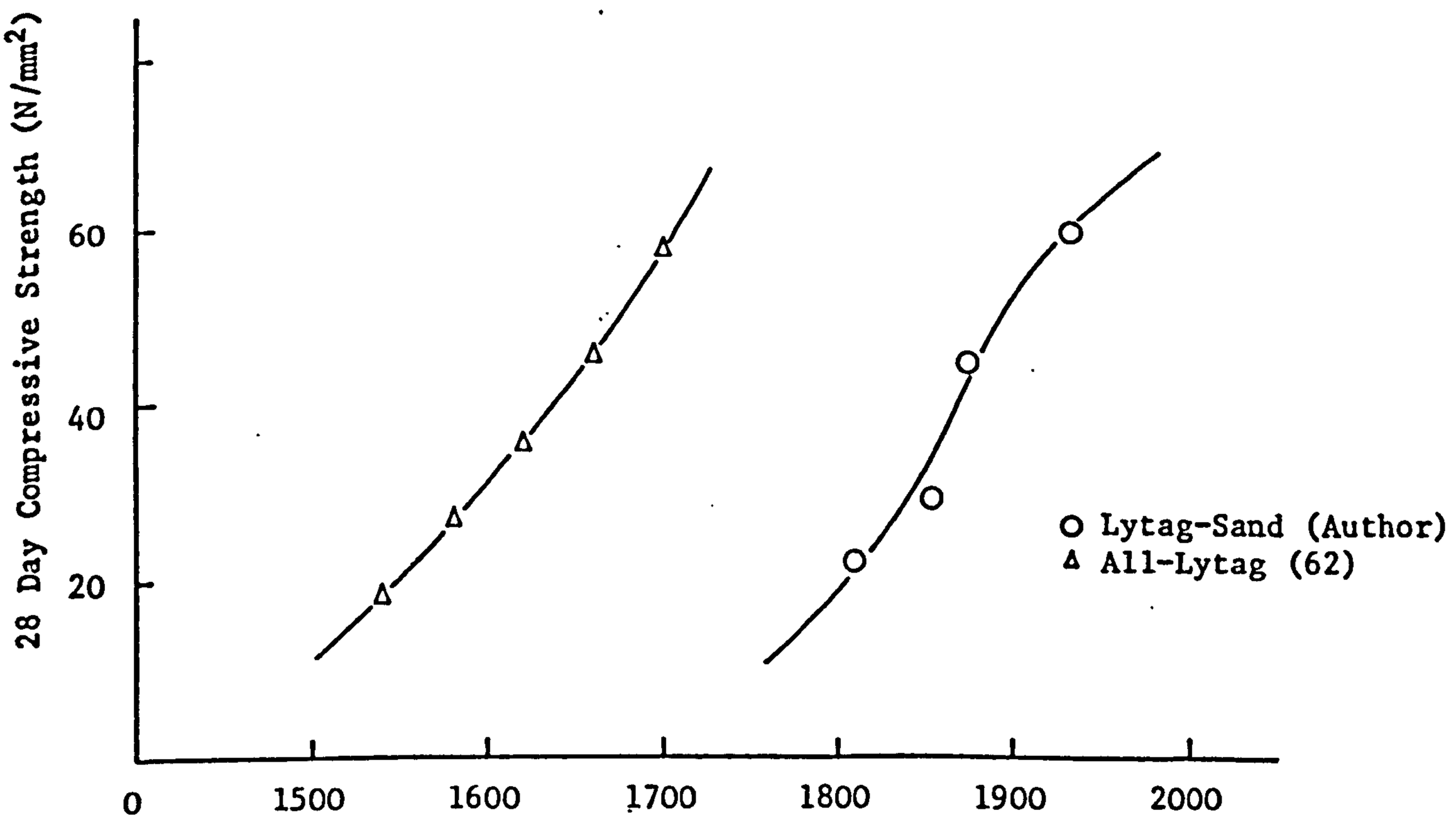

FIGURE 4.8 RELATIONSHIP BETWEEN COMPRESSIVE STRENGTH AND DENSITY

The grading of the aggregates, more particularly the fines, governs the workability of the concrete. Lytag is a spherical aggregate and thus the particle shape increases the workability of the concrete, for a given water cement ratio, as opposed to an angular shaped aggregate. This can, however, also result in the concrete having a 'harsh' under-fined appearance. The sand used was a coarse zone 2 sand to BS 882 (83) and this also helped to increase the 'harsh' appearance.

4.2.3 Mix Design Chart

As a result of the trial mixes prepared and tested during the early part of this research project it was possible to produce a mix design chart to aid with mix design during the remainder of the work. As more specimens were cast and tested for the different test series so their results were used to modify the mix design chart where need be. The design chart given in Figure 4.9 is thus the result of all the relevant data collected during this project.

The chart is a simple graphical and tabular approach based on a method suggested by Owens (88). Owens' method is based on the fact that for a given degree of workability over a range of cement contents, two factors remain fairly constant; water demand and the amount of coarse aggregate. The resultant chart provides a simple adequate technique for initial mix design. As was pointed out in the introduction to mix design, the variability between the various brands of lightweight aggregate means that it is unlikely that a suitably economical mix design procedure, covering all lightweight aggregates, could be derived. It seems more logical to produce a mix design chart for each brand of lightweight aggregate in order that it may be used most efficiently. Similar mix design charts have been produced by several investigators (49, 61) and thus the overall knowledge of lightweight concrete mix design is increasing.

4.3 Strength Characteristics

This section covers work carried out to investigate the compressive and tensile strength characteristics of Lytag-sand concrete. Long term compressive strength and short term flexural and tensile splitting strengths are reported and related to curing conditions.

Concrete Density (kg/m^3) at 28 days					
	Fresh	2035	2015	2010	1980
	Saturated	2050	2040	2030	2025
	Air Dried	1935	1875	1855	1810
	16°C & 50% R.H.	1935	1885	1850	1815
Total Water/Cement Ratio (By Weight)		0.54	0.78	1.04	1.30
Free Water/Cement Ratio (By Weight)		0.36	0.52	0.70	0.88

Materials

Cement : O.P.C.
Fines : Zone 2 sand
Coarse : Lytag 12mm

Notes

1. Air Cured Strength
2. Free Water = Total Water - 12% absorption, by weight of coarse aggregate
3. Effective water content = 175 kg/m^3
4. *Total Water to be added allowing 12% for aggregate absorption.

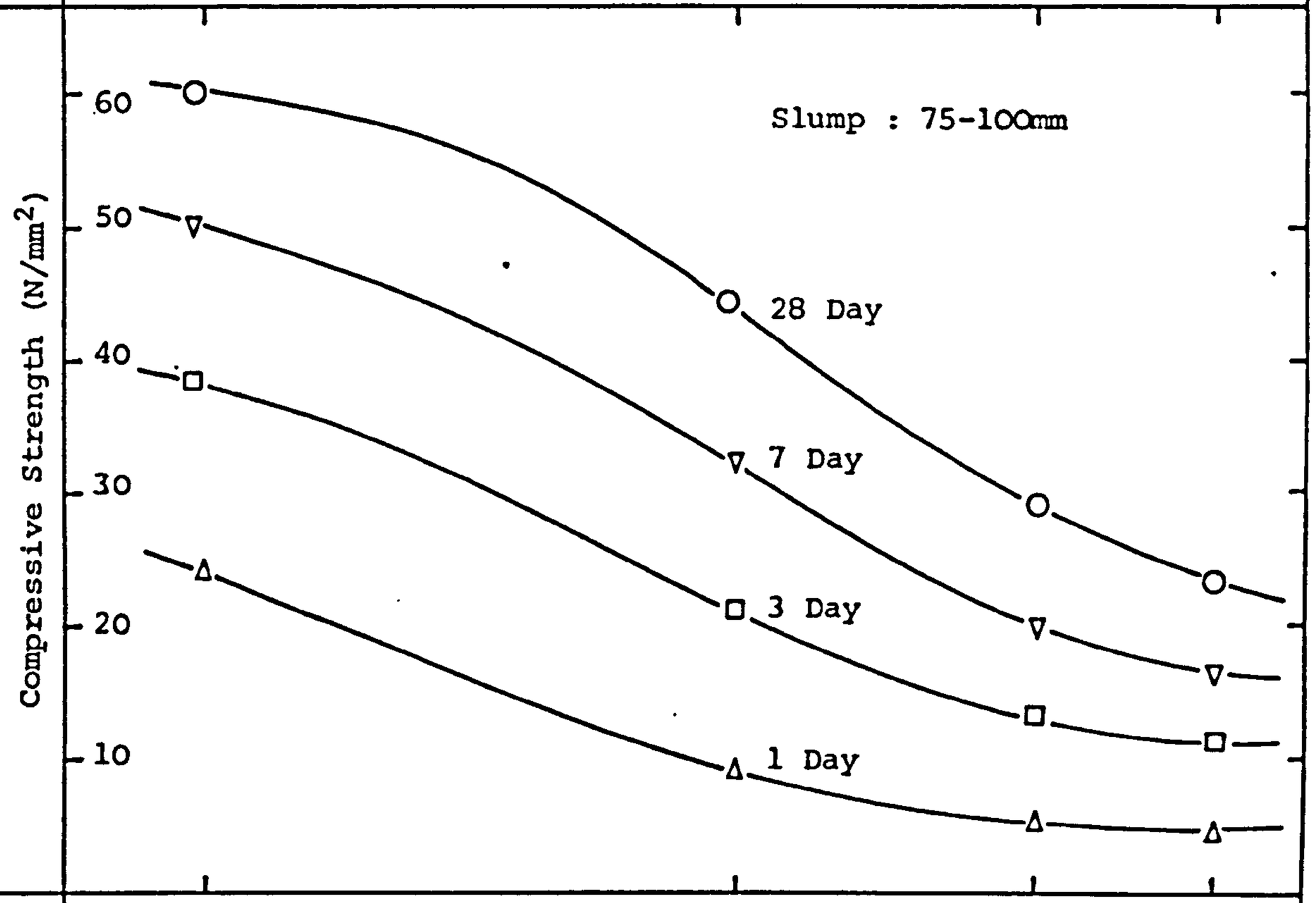

PROPORTIONS FOR ONE CUBIC METRE OF COMPACTED CONCRETE (kg)					
	CEMENT	485	335	250	200
	FINES	515	645	715	770
	COARSE	715	715	715	715
	WATER*	260	260	260	260

FIGURE 4.9 MIX DESIGN CHART FOR AIR CURED LYTAG-SAND CONCRETE

4.3.1 Experimental Programme

The materials used, mixing procedure and manufacture of the specimens were the same as those described in Section 4.2. Mix design was carried out in accordance with the mix design chart in Figure 4.9. Curing conditions were the same as those described in 4.2.1.3. Specimen sizes were as follows and all specimens were tested in accordance with BS 1881 (86):

(a) 100 x 100 x 100 mm Cubes: Compressive strength.

(b) 100 x 100 x 500 mm Prisms loaded at 1/3 points: Flexural strength.

(c) 100 mm dia. x 200 mm Cylinders: Tensile splitting strength.

4.3.2 Compressive Strength: Results and Discussion

Various investigators (11, 31, 34-38, 49, 61) have established that the compressive strength of lightweight concrete is affected by the same parameters as dense concrete and this was discussed in Section 4.2. In this section the effects of age and curing conditions on the compressive strength of Lytag-sand concrete are discussed.

4.3.2.1 Effect of Age and Curing Conditions on Compressive Strength

In order to study the effect of curing conditions on the compressive strength of Lytag-sand concrete three different curing regimes were used as described in Section 4.2.1.3. The effects of age and curing conditions on the compressive strength of Lytag-sand concrete are shown in Table 4.5 and Figures 4.10-4.13.

Figures 4.10-4.13 indicate that the higher the cement content and therefore the strength of the concrete, the greater the increase in strength up to 28 days. Similar effects were reported by Balendran (61) and Bandyopadhyay (49). After 28 days the water cured cubes continue to gain strength up to about one year after which the strength remains roughly constant. The maximum increase in strength expressed as a percentage of the 28 day strength varied between 111-138%. Balendran (61) reported similar strength increases for Taclite-sand concrete with strengths ranging from 110-140% of the 28 day strength at 18 months. Cubes stored in the constant temperature and humidity room showed a strength range between 101-112%, as a percentage of the 28 day strength, after 2 years.

TABLE 4.5 COMPRESSIVE STRENGTH DEVELOPMENT OF LYTAG-SAND CONCRETE

Age (Days)	Cement:Sand: Lytag Ratio (by Weight)	Total Water/ Cement Ratio	Compressive Strength (N/mm^2)		
			Water	Laboratory	C.T.H.R.
3	1:3.85:3.58	1.30	11.1	11.4	11.0
	1:2.77:2.78*	1.04	14.0	13.3	-
	1:2.60:2.68	1.00	14.5	13.5	12.6
	1:1.94:2.14	0.78	22.0	20.5	19.5
	1:1.07:1.48	0.54	29.0	31.0	29.0
7	1:3.85:3.58	1.30	14.8	15.7	14.8
	1:2.77:2.78	1.04	20.0	22.2	-
	1:2.60:2.68	1.00	24.0	22.0	19.6
	1:1.94:2.14	0.78	30.5	29.5	28.2
	1:1.07:1.48	0.54	46.5	46.5	45.0
14	1:3.85:3.58	1.30	17.7	19.3	18.5
	1:2.77:2.78	1.04	27.5	28.0	-
	1:2.60:2.68	1.00	28.5	26.0	26.6
	1:1.94:2.14	0.78	38.5	36.5	35.0
	1:1.07:1.48	0.54	51.5	54.5	55.7
28	1:3.85:3.58	1.30	19.5	22.5	22.0
	1:2.77:2.78	1.04	32.0	33.1	-
	1:2.60:2.68	1.00	32.5	31.0	29.9
	1:1.94:2.14	0.78	44.0	40.0	38.2
	1:1.07:1.48	0.54	56.0	58.0	57.4
91	-	-	-	-	-
	1:2.77:2.78	1.04	38.6	40.0	-
	1:2.60:2.68	1.00	35.5	36.5	-
	1:1.94:2.14	0.78	45.0	39.5	-
	1:1.07:1.48	0.54	60.0	56.5	-
182	-	-	-	-	-
	1:2.77:2.78	1.04	42.6	35.6	-
	1:2.60:2.68	1.00	39.0	41.0	-
	1:1.94:2.14	0.78	48.5	38.0	-
	1:1.07:1.48	0.54	61.5	56.5	-
365	-	-	-	-	-
	1:2.77:2.78	1.04	44.3	36.3	-
	1:2.60:2.68	1.00	40.0	29.5	-
	1:1.94:2.14	0.78	50.5	38.5	-
	1:1.07:1.48	0.54	62.0	56.0	-
766	-	-	-	-	-
	1:2.77:2.78	1.04	44.0**	37.0**	-
	1:2.60:2.68	1.00	40.5	31.0	33.4
	1:1.94:2.14	0.78	50.0	39.0	38.5
	1:1.07:1.48	0.54	61.0	54.0	58.2

* Batch 2 aggregate and cement.
** Tested at 635 days.

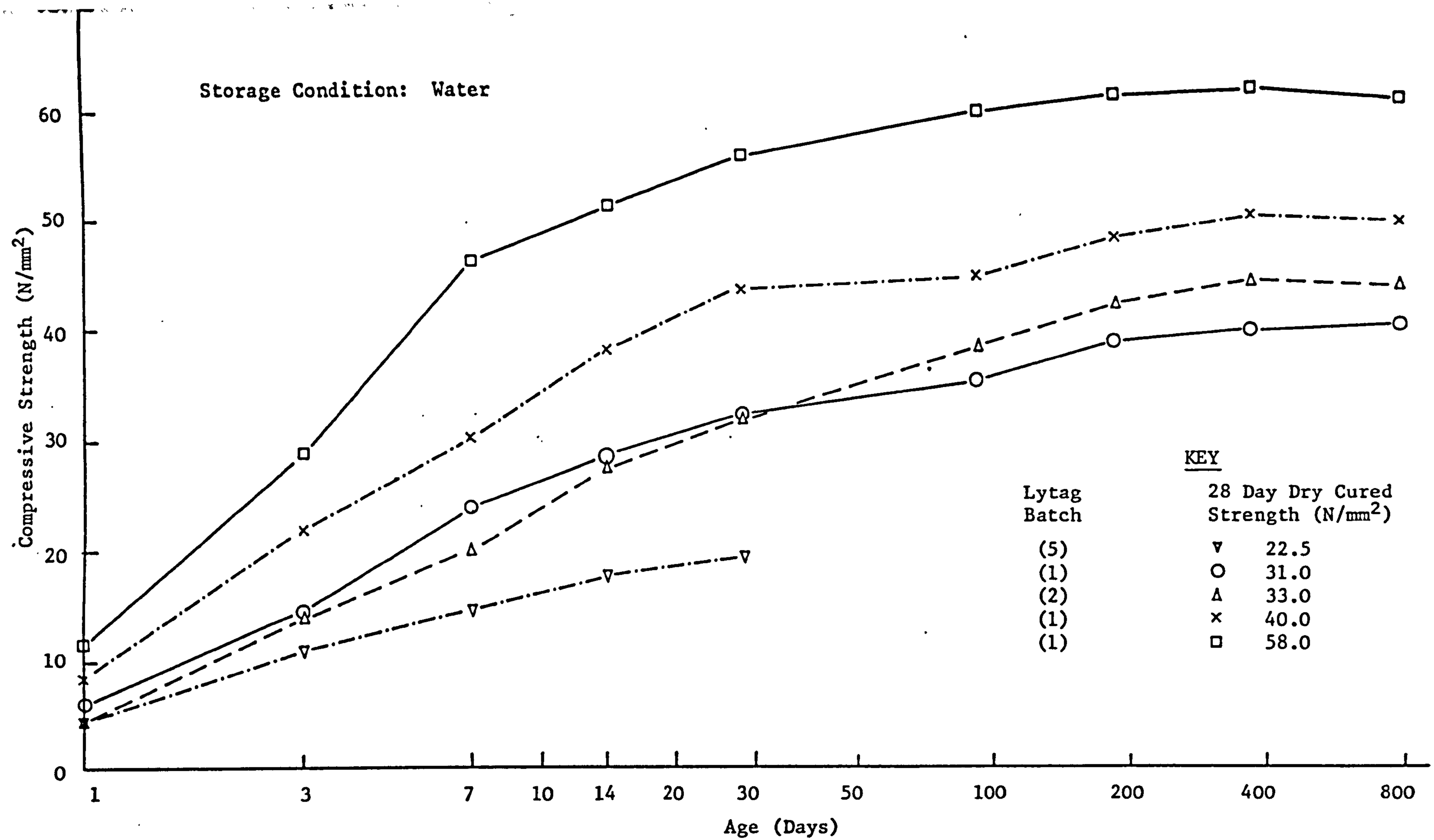

FIGURE 4.10 DEVELOPMENT OF COMPRESSIVE STRENGTH WITH AGE

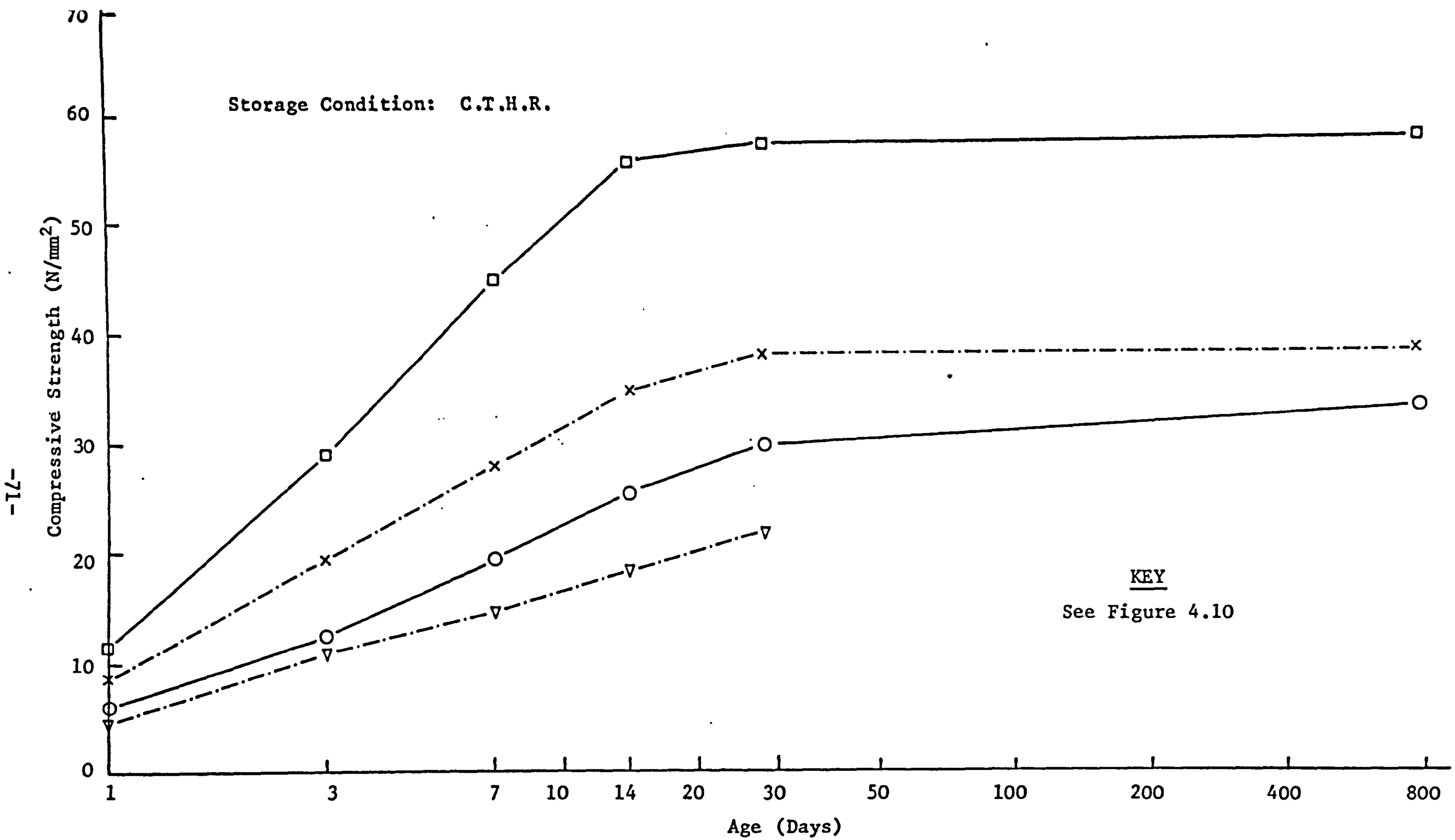

FIGURE 4.11 DEVELOPMENT OF COMPRESSIVE STRENGTH WITH AGE

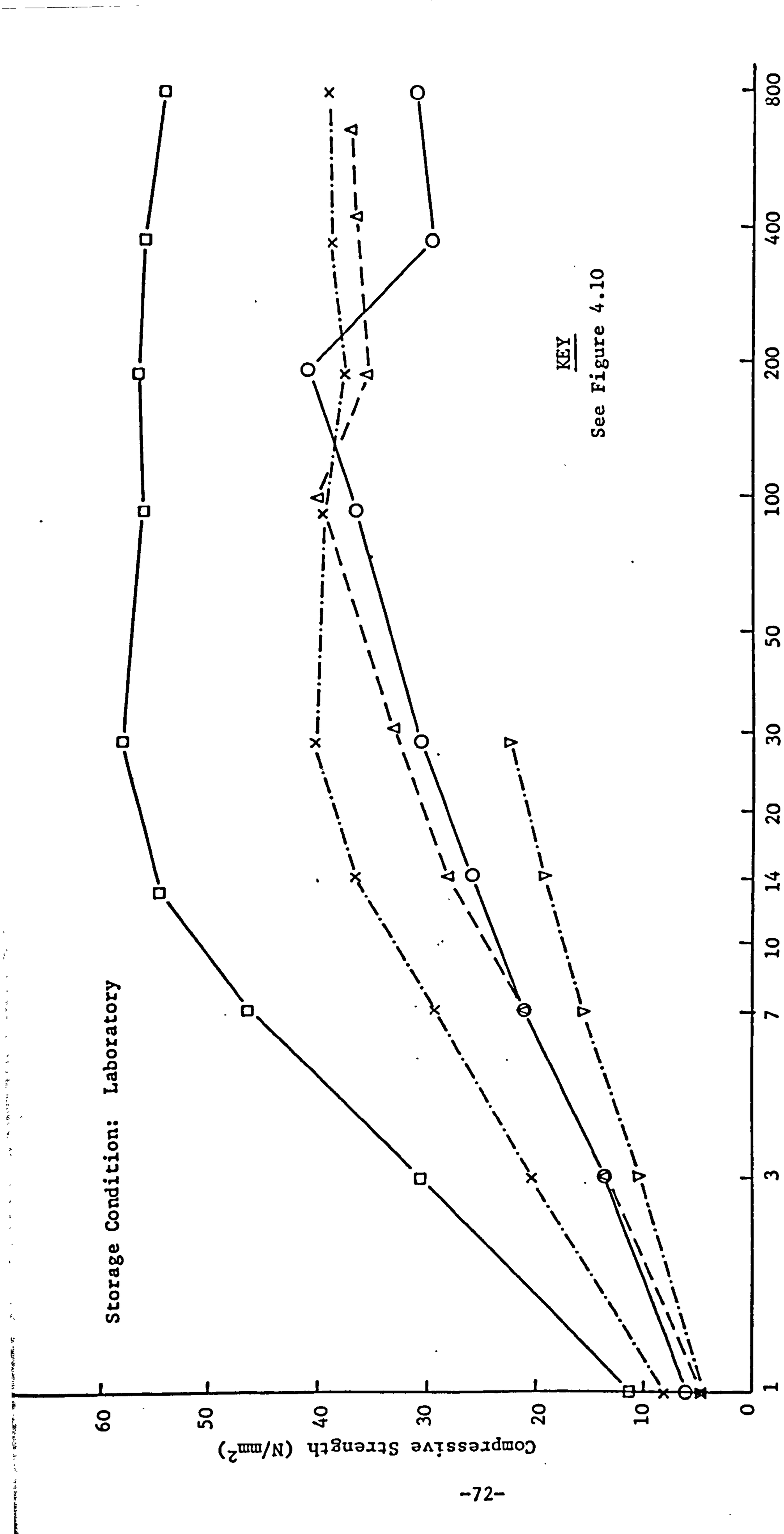

FIGURE 4.12 DEVELOPMENT OF COMPRESSIVE STRENGTH WITH AGE

Teychenné (11) reported an increase in strength up to 1 year for All-Lytag and Lytag-sand concretes stored at 18°C and 65% relative humidity. The 1 year strength expressed as a percentage of the 28 day strength varied between 130-156% for All-Lytag concrete and between 105-121% for Lytag-sand concrete. Balendran (61) reported similar characteristics for Taclite-sand concrete up to 18 months. The strength at 540 days expressed as a percentage of the 28 day strength varied between 109-115%. During the present work, however, the constant temperature and humidity room broke down on several occasions, generally for 2-3 days but in one case for 3 weeks, after the first 7-8 months of testing and this may have had an adverse effect on the specimens.

Figure 4.12 shows the strength with age of specimens stored in the uncontrolled laboratory environment. It can be seen that up to a period of two years there is a loss in compressive strength after a maximum value which occurs between 28 days and 6 months. Initially three sets of cubes were cast with batch 1 aggregates and cement. When the variation in strength was noticed between the first and second batches, Section 4.2.2.2, a second batch with a target strength of 30 N/mm^2 was cast. The 22.5 N/mm^2 mix was cast using batch 5 aggregate and results were only obtained up to a period of 28 days.

For the 60 N/mm^2 and 40 N/mm^2 mixes the maximum strength occurred between 1 and 3 months. With the 60 N/mm^2 mix the loss of strength is progressive with the two year strength being 93% of the 28 day strength. For the 40 N/mm^2 mix the maximum loss of strength occurs at 6 months when the strength is 95% of the 28 day strength. The 2 year strength is 98% of the 28 day strength and it is possible that the lower strength at 6 months was caused by the random selection of three weak cubes.

For the 30 N/mm^2 mix cast using batch 1 aggregate the strength increased up to a maximum 132% of the 28 day strength at 6 months after which there was a rapid fall off in strength, with the strength at 2 years being equal to the 28 day strength. The 30 N/mm^2 mix cast using batch 2 aggregate showed similar behaviour but in this case a maximum strength of 121% of the 28 day strength occurred at 90 days. The loss of strength after this period was less dramatic

than with the other 30 N/mm^2 mix and the strength never fell below the 28 day strength. The 2 year strength was 112% of the 28 day strength.

The variation in strength between aggregate and cement batches was again demonstrated by the two 30 N/mm^2 mixes, with the mix cast using batch 2 aggregate and cement having a slightly higher 28 day strength despite a slightly lower cement content.

In order to study further the effect of dry curing in an uncontrolled environment on the gain of compressive strength with age, further sets of cubes were cast using batch 2 and 3 aggregates and the results of these tests are shown in Figure 4.13. The strengths, at various ages, as a percentage of the 28 day strengths are shown in brackets. The results follow a similar pattern to those in Figure 4.12 except that for the 45 N/mm^2 concrete the strength gain continued up to 240 days.

Similar effects have been reported by other investigators (61, 89, 90) and it is suggested that the slow retrogression of strength may be associated with shrinkage-induced microcracks.

4.3.3 Tensile Strength: Results and Discussion

One of the basic properties of any concrete is its tensile strength which is an important criterion in designing for the serviceability limit state of cracking. The tensile strength of concrete is affected by three basic factors, namely:

(a) the tensile strength of the aggregate

(b) the tensile strength of the cement paste

(c) the aggregate matrix bond.

For lightweight concrete the tensile strength of the cement paste is generally higher than for dense concrete due to higher cement contents for a given compressive strength. The aggregate matrix bond strengths are generally higher for lightweight concrete as opposed to dense concrete (42) and hence the tensile strength of the concrete is therefore greatly influenced by the tensile strength of the aggregate.

This series of tests was aimed at studying the effect of curing conditions

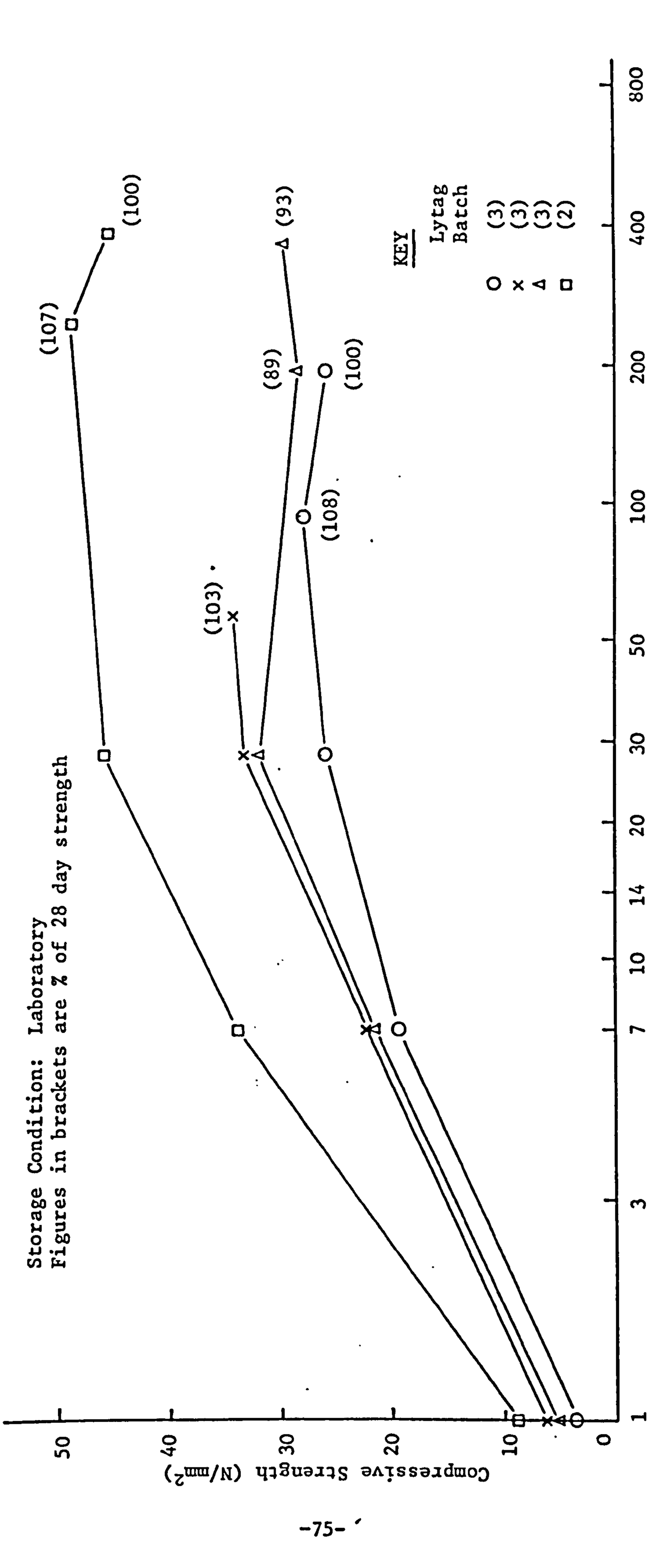

FIGURE 4.13 DEVELOPMENT OF COMPRESSIVE STRENGTH WITH AGE

on the tensile strength of Lytag-sand concrete up to 28 days. Relationships have been established between the tensile and compressive strengths and between the tensile splitting and flexural strengths and these are compared with published data.

4.3.3.1 Effect of Age and Curing Conditions on Tensile Strength

The effect of age and curing conditions on tensile strength is shown in Figures 4.14-4.15 and Tables 4.6-4.7. Figure 4.14 shows that the tensile splitting strength, f_{SP} increases up to an age of 28 days for water cured specimens. For dry cured specimens a similar increase up to 28 days is apparent for the lower strength concrete, 22.5 and 33.5 N/mm^2, but for higher strengths the behaviour is more erratic.

Table 4.6 indicates that the ratio of dry cured strength to wet cured strength, columns 6 and 7, initially increases up to a period of 3 days but then decreases to less than 100% at 28 days. An exception to this rule was the 22.5 N/mm^2 which showed a general increase up to 28 days. The rate of gain of strength is more rapid for the dry cured rather than the wet cured specimens, at early ages, up to 7 days, columns 8 and 9. The situation is then reversed as the higher strength dry cured concretes decrease in tensile strength, and the lower strengths decrease their rate of gain of strength. Columns 10, 11 and 12 show the ratio of the tensile splitting strength to the compressive strength for the various curing conditions up to 28 days. For the water cured specimens the ratio remains sensibly constant up to 28 days whereas for the dry cured specimens there is a marked decrease with increase in age. The exception again is the 22.5 N/mm^2 mix.

Figure 4.15 shows that the flexural strength by the modulus of rupture test, f_{MR}, behaves in a similar way to the tensile splitting strength, f_{SP}, for wet and dry cured specimens. The loss of flexural strength with the 64.0 N/mm^2 concrete is more marked than for tensile splitting strength but the strength is regained by 28 days.

Again Table 4.7 shows that the ratio of the dry cured strength to the wet cured strength, columns 6 and 7, is initially greater than 100% but decreases

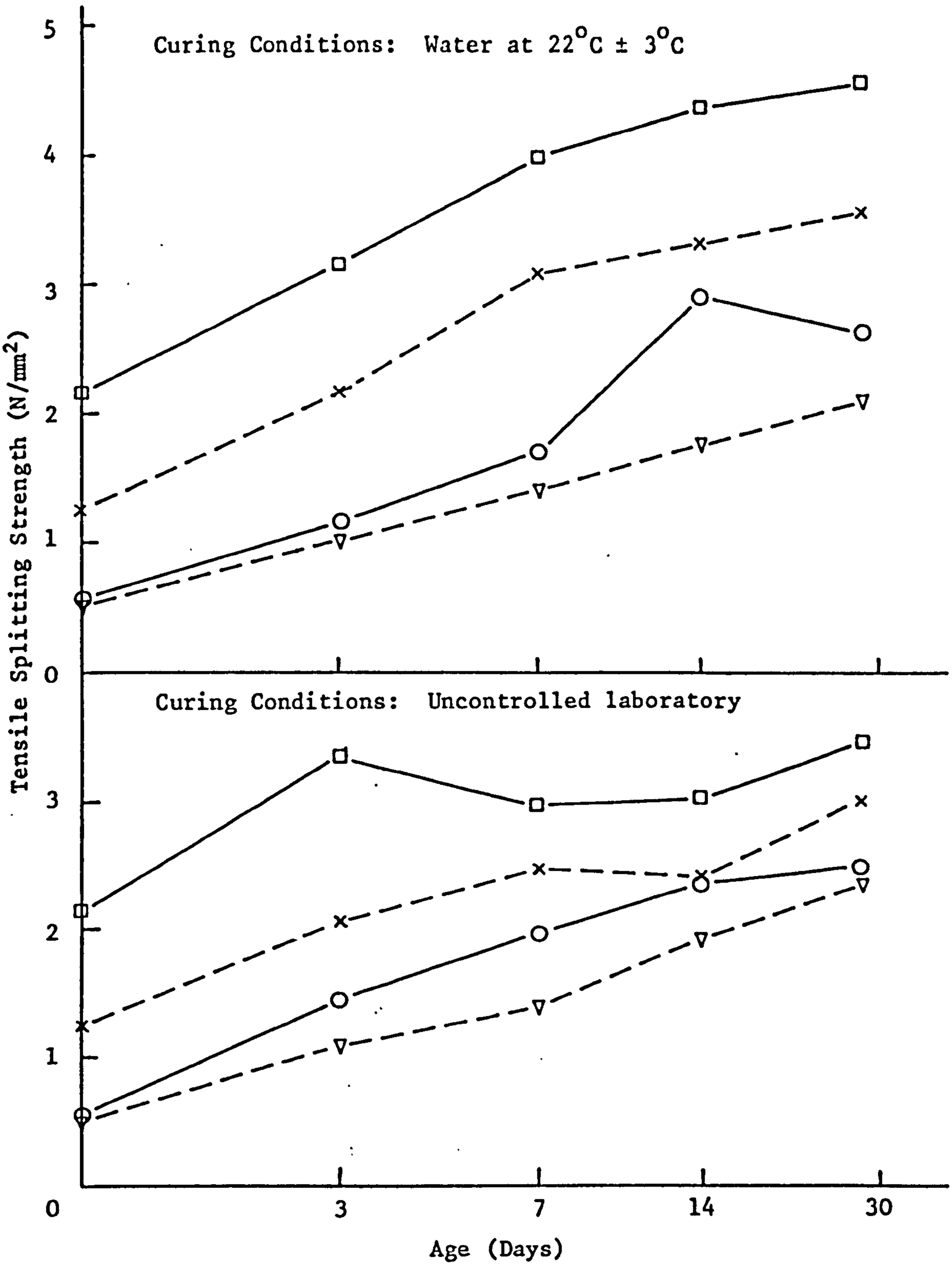

KEY

28 Day Dry Cured Strength (N/mm^2)	
▽	22.5
○	33.5
×	47.5
□	64.0

FIGURE 4.14 TENSILE SPLITTING STRENGTH DEVELOPMENT UP TO 28 DAYS

TABLE 4.6 EFFECT OF CURING CONDITION ON TENSILE SPLITTING STRENGTH OF LYTAG-SAND CONCRETE

28 Day Air Cured Cube Strength (N/mm^2)	Age (Days)	Tensile Splitting Strength (N/mm^2)			(4)/(3) (%)	(5)/(3) (%)	Percentage of 28 Day Strength (%)		Tensile Splitting Strength / Compressive Strength at age shown in Col. 2 (%)		
		Water	Laboratory	C.T.H.R.			Water	Laboratory	Water	Laboratory	C.T.H.R.
(1)	(2)	(3)	(4)	(5)	(6)	(7)	(8)	(9)	(10)	(11)	(12)
22.5	1	0.51	0.51	0.51	100	100	24	21	11	11	11
33.5	1	0.55	0.55	0.55	100	100	21	22	10	10	10
47.5	1	1.24	1.24	1.24	100	100	35	41	10	10	10
64.0	1	2.16	2.16	2.16	100	100	47	63	9	9	9
22.5	3	1.02	1.11	-	109	-	48	46	9	10	-
33.5	3	1.14	1.44	-	126	-	43	58	9	10	-
47.5	3	2.17	2.06	-	95	-	61	69	10	9	-
64.0	3	3.15	3.34	-	106	-	69	97	7	7	-
22.5	7	1.43	1.37	-	96	-	67	57	10	9	-
33.5	7	1.69	1.95	-	115	-	64	79	10	9	-
47.5	7	3.09	2.46	-	80	-	87	82	9	7	-
64.0	7	4.01	2.96	-	74	-	88	86	8	5	-
22.5	14	1.77	1.93	-	109	-	83	81	10	10	-
33.5	14	2.92	2.36	-	81	-	110	96	10	9	-
47.5	14	3.32	2.39	-	72	-	93	80	8	6	-
64.0	14	4.38	3.03	-	69	-	96	88	8	5	-
22.5	28	2.13	2.39	2.16	112	101	100	100	11	11	10
33.5	28	2.65	2.47	2.58	93	97	100	100	9	7	8
47.5	28	3.57	2.99	3.02	84	85	100	100	8	6	6
64.0	28	4.58	3.44	3.15	75	69	100	100	8	5	5

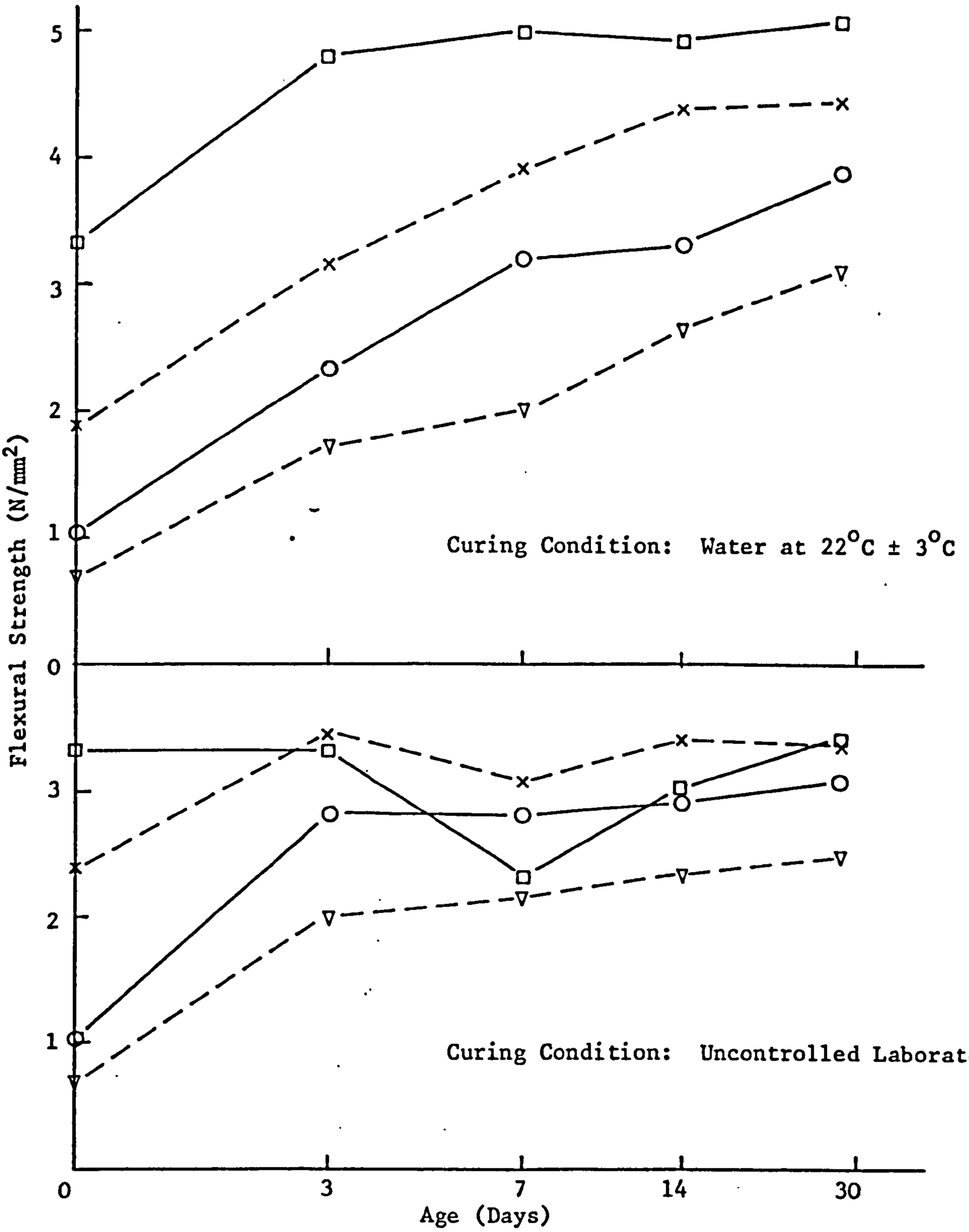

KEY

See Figure 4.14

FIGURE 4.15 FLEXURAL STRENGTH DEVELOPMENT UP TO 28 DAYS

TABLE 4.7 EFFECT OF CURING CONDITION ON FLEXURAL STRENGTH OF LYTAG-SAND CONCRETE

28 Day Air Cured Cube Strength (N/mm^2)	Age (Days)	Modulus of Rupture (N/mm^2)			(4)/(3) (%)	(5)/(3) (%)	Percentage of 28 Day Strength (%)		Modulus of Rupture / Compressive Strength at age shown in Col. 2 (%)		
		Water	Laboratory	C.T.H.R.			Water	Laboratory	Water	Laboratory	C.T.H.R.
(1)	(2)	(3)	(4)	(5)	(6)	(7)	(8)	(9)	(10)	(11)	(12)
22.5	1	0.68	0.68	0.68	100	100	22	27	15	15	15
33.5	1	1.09	1.04	1.04	100	100	27	34	19	19	19
47.5	1	1.88	1.88	1.88	100	100	92	56	15	15	15
64.0	1	3.32	3.32	3.32	100	100	65	98	13	13	13
22.5	3	1.72	2.00	-	116	-	55	81	15	18	-
33.5	3	3.32	2.80	-	121	-	60	91	14	15	-
47.5	3	3.16	3.44	-	109	-	71	102	12	13	-
64.0	3	4.80	3.32	-	69	-	94	98	11	7	-
22.5	7	2.00	2.16	-	108	-	64	87	14	14	-
33.5	7	3.20	2.80	-	88	-	82	91	14	12	-
47.5	7	3.92	3.08	-	79	-	88	92	11	8	-
64.0	7	5.00	2.28	-	46	-	98	67	10	4	-
22.5	14	2.66	2.32	-	87	-	85	94	15	12	-
33.5	14	3.32	2.91	-	88	-	86	95	13	14	-
47.5	14	4.40	3.39	-	77	-	98	101	11	8	-
64.0	14	4.93	3.03	-	61	-	97	89	9	5	-
22.5	28	3.12	2.48	2.40	79	77	100	100	16	11	11
33.5	28	3.88	3.08	2.80	79	72	100	100	13	9	9
47.5	28	4.48	3.36	3.56	75	79	100	100	11	7	8
64.0	28	5.08	3.40	2.84	67	56	100	100	9	5	5

with age to be less than 100% at 28 days. The exception this time is the 64.0 N/mm^2 mix which shows a dry cured to wet cured ratio to be less than 100% from 3 days on. Columns 8 and 9 show that the strength gain of wet cured specimens is fairly uniform up to 14 days with the exception of the 64.0 N/mm^2 mix whereas the strength gain of dry cured specimens is rapid up to 3 days followed by a very much slower rate of gain of strength. The ratio of the flexural strength to compressive strength at various ages is shown in columns 10, 11 and 12. As with the tensile splitting strength, the values for wet cured specimens decrease only slightly with age whereas the dry cured specimens show a much greater decrease with age especially with the higher strength concretes.

Similar results to these have been reported by several investigators (11, 28, 29, 49, 61).

The reduction in tensile strength, and subsequent recovery can be explained as follows. As the concrete dries out, differential moisture distribution occurs throughout the test specimen. This differential moisture distribution leads to differential shrinkage which in turn causes internal stress conditions and subsequent microcracking. When external load is applied a lower tensile strength is obtained because the specimen is already in a state of stress without a load. As the specimen becomes uniformly dry, the self-induced stress is relieved and the flexural strength regained.

Non-uniform moisture distribution affects the tensile strength in general although it appears to have a lesser effect on the tensile splitting strength than on the flexural strength.

Typical wet and dry cured specimens, tested at 28 days are shown in Plate 4.2.

4.3.3.2 Relationship Between Tensile and Compressive Strength

The relationship between tensile strength and compressive strength is generally expressed in the form

$$f_{ct} = a\, f_{cu}^{\,b} \qquad \ldots\ (4.1)$$

where f_{ct} is the tensile strength in N/mm^2

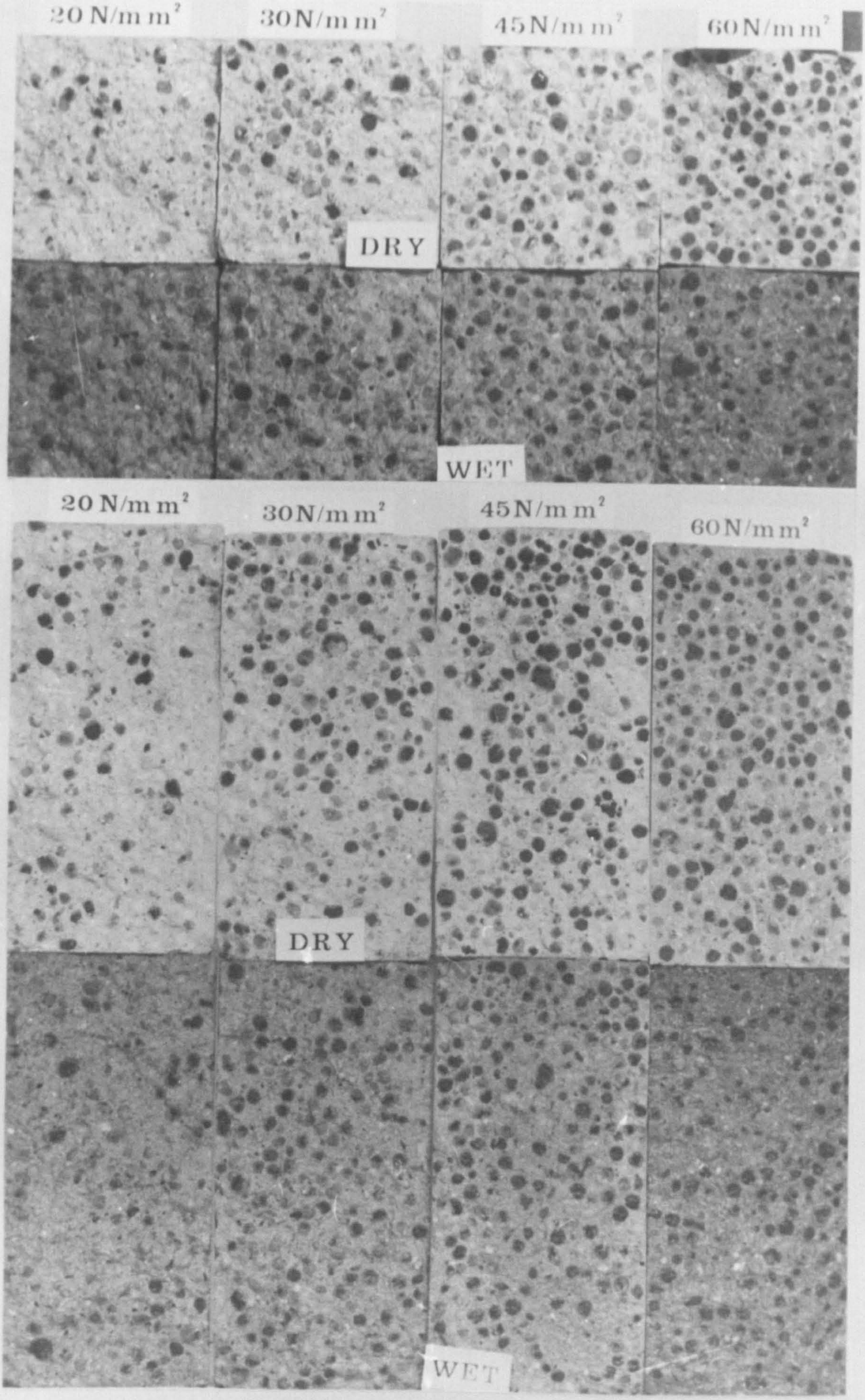

PLATE 4.2 AGGREGATE FRACTURE IN LYTAG-SAND CONCRETE PRISMS AND CYCLINDERS

f_{cu} is the cube strength in N/mm^2

a and b are constants.

Equation 4.1 is sometimes further simplified by setting b = 0.5. The variation of flexural strength and tensile splitting strength against compressive strength, for Lytag-sand concrete, is shown in Figures 4.16 and 4.17 respectively.

Figure 4.16 shows that there is a distinct difference between the flexural strength of wet cured specimens and that of dry cured specimens. Regression analysis produced the following equations:

$$f_{MR} = 0.90\ f_{cu}^{0.43} \quad \text{(wet)} \quad (r = 0.99) \qquad \ldots\ (4.2)$$

$$f_{MR} = 1.20\ f_{cu}^{0.26} \quad \text{(dry)} \quad (r = 0.65) \qquad \ldots\ (4.3)$$

where r is the correlation factor.

Combining the wet and dry cured specimen results gave the following equation:

$$f_{MR} = 1.07\ f_{cu}^{0.32} \quad (r = 0.52) \qquad \ldots\ (4.4)$$

In view of the difference between the wet and dry cured specimen results it would seem advisable to use separate equations for each condition.

Figure 4.17 indicates that the difference in tensile splitting strength between wet and dry cured specimens is not so great. Regression analysis of the data produced the following equations:

$$f_{SP} = 0.30\ f_{cu}^{0.64} \quad \text{(wet)} \qquad (r = 0.95) \qquad \ldots\ (4.5)$$

$$f_{SP} = 0.54\ f_{cu}^{0.45} \quad \text{(dry)} \qquad (r = 0.90) \qquad \ldots\ (4.6)$$

$$f_{SP} = 0.46\ f_{cu}^{0.51} \quad \text{(wet \& dry)} \quad (r = 0.86) \qquad \ldots\ (4.7)$$

It would seem that the relationship between tensile splitting strength and compressive strength can be adequately described by a single equation (4.7) covering wet and dry cured specimens.

4.3.3.3 Relationship Between Flexural Strength and Tensile Splitting Strength

The relationship between flexural strength and tensile splitting strength

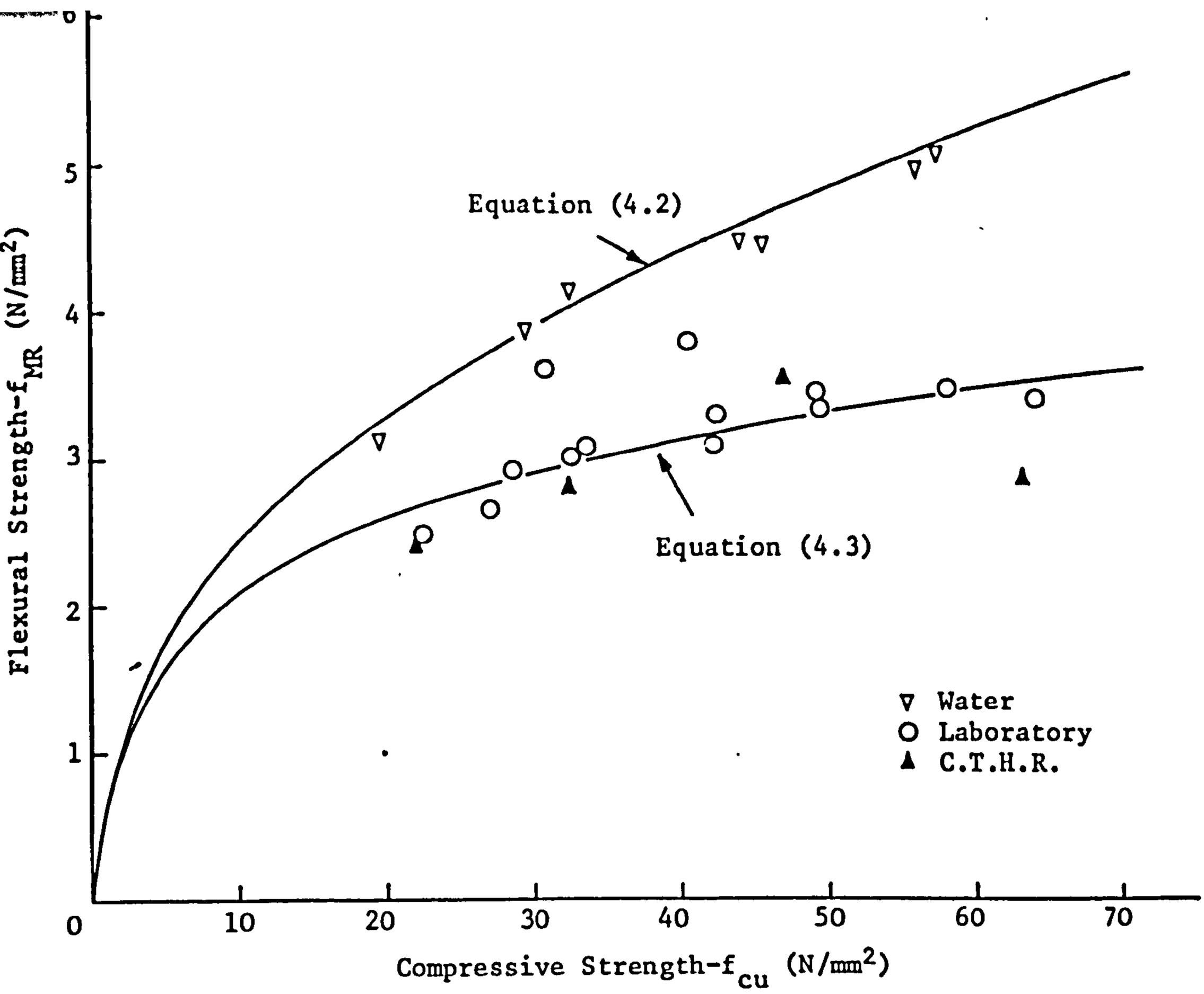

FIGURE 4.16 RELATIONSHIP BETWEEN FLEXURAL STRENGTH AND COMPRESSIVE STRENGTH FOR LYTAG-SAND CONCRETE AT 28 DAYS

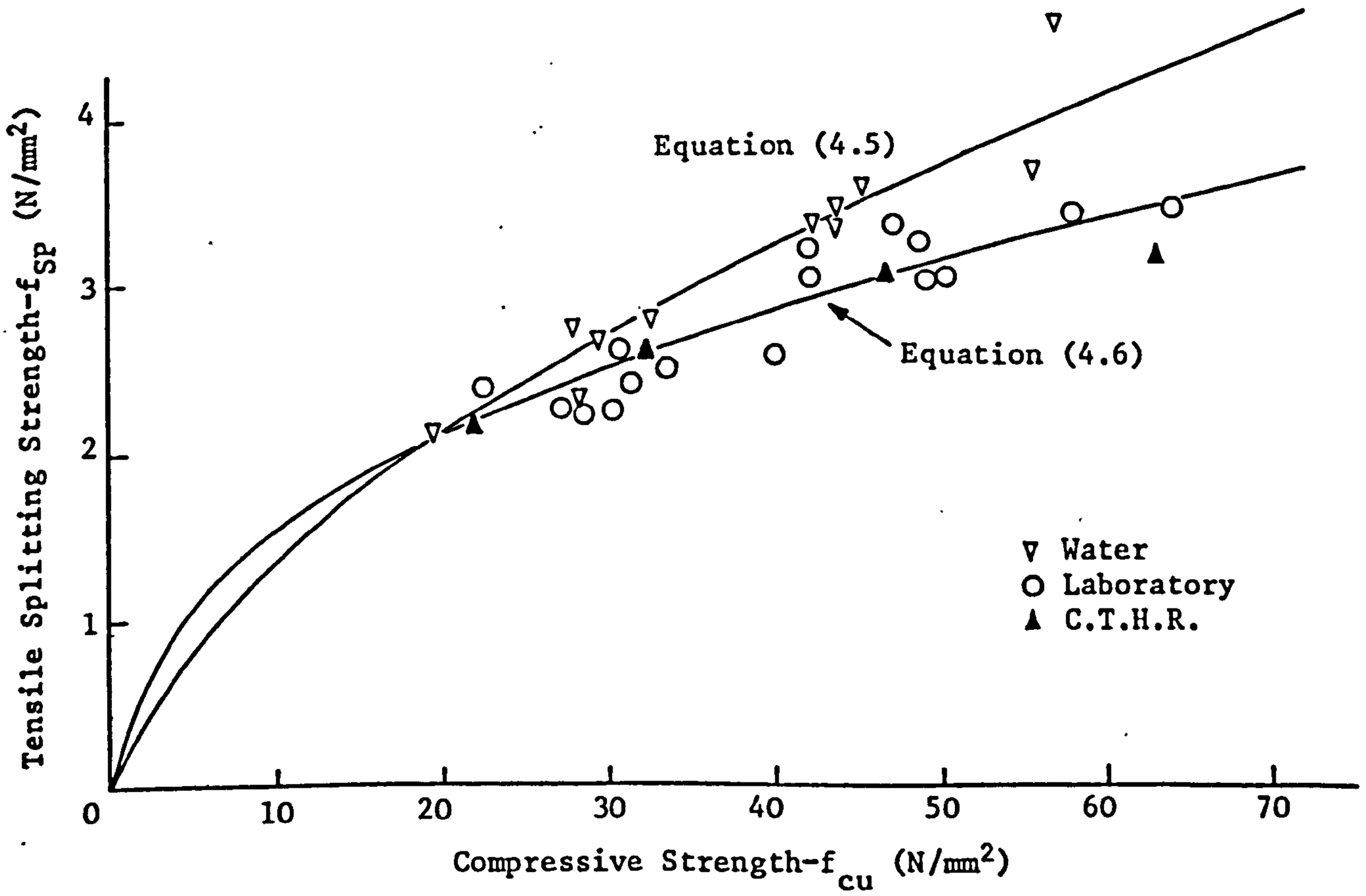

FIGURE 4.17 RELATIONSHIP BETWEEN TENSILE SPLITTING STRENGTH AND COMPRESSIVE STRENGTH FOR LYTAG-SAND CONCRETE AT 28 DAYS

is shown in Figure 4.18. The ratio of f_{SP} to f_{MR} for the range of mixes tested varied between 68-96%. Balendran (61) reported a range of 76-91% for Lytag-sand concrete. Regression analysis of the data shown in Figure 4.18 produced the following equations:

$$f_{MR} = 2.05\ f_{SP}^{0.64} \quad \text{(wet)} \qquad (r = 0.95) \qquad \ldots\ (4.8)$$

$$f_{MR} = 1.84\ f_{SP}^{0.52} \quad \text{(dry)} \qquad (r = 0.59) \qquad \ldots\ (4.9)$$

$$f_{MR} = 1.52\ f_{SP}^{0.76} \quad \text{(wet \& dry)} \qquad (r = 0.72) \qquad \ldots\ (4.10)$$

Again the unpredictability of dry cured specimens is reflected in the low correlation factor, and it is suggested that two separate equations be used to describe the effects of wet·curing and dry curing.

4.3.3.4 Comparison With Published Results

The results of the present investigation are compared with those of other investigators in Table 4.8. The majority of the investigators simplified the expressions describing the various relationships to parabolic forms although several investigators have used power functions.

Orangun (91) plotted the line given by the CP 114 (22) equation and showed that it fitted the results which he had obtained from tests. Teychenné (11) tested dense and lightweight concretes and produced several equations. By re-analysing his results for lightweight concrete with sand replacement, using a power equation, a set of equations has been produced which can be compared directly with the results obtained by the author. These equations along with those of other investigators generally indicate that sensibly accurate equations can be obtained for f_{SP} against f_{cu} with wet and dry cured specimens and for f_{MR} against f_{cu} and f_{SP} for wet cured specimens. For the dry cured specimens, however, correlation factors tend to be low and predictions using any of these equations should be assessed with caution.

4.4 Conclusions

The following conclusions can be drawn from this work:

1. Lytag-sand concrete developed 44-64% and 68-84% of 28 days' strengths at 3 and 7 days respectively. In general stronger concretes develop higher

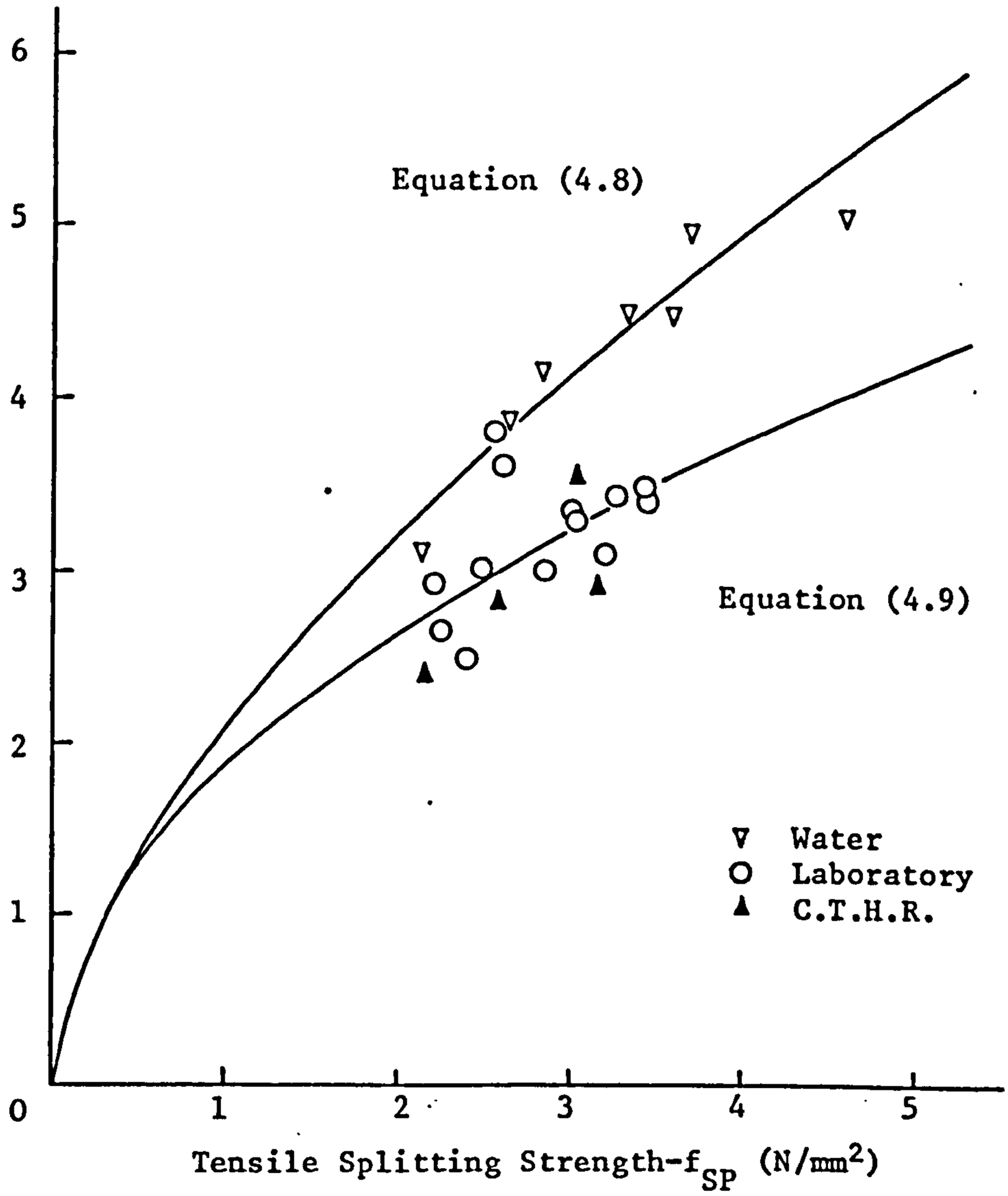

FIGURE 4.18 RELATIONSHIP BETWEEN FLEXURAL STRENGTH AND TENSILE SPLITTING STRENGTH FOR LYTAG-SAND CONCRETE, AT 28 DAYS

TABLE 4.8 COMPARISON OF TENSILE STRENGTH DATA WITH OTHER INVESTIGATORS

Author	Type of Concrete	Curing Condition	28 Day Cube Strength Range (N/mm^2)	Relationship	Correlation Factor - r	Comments
Orangun (91) 1963	Lytag - Lytag fines	Wet	20 - 60	$f_{MR} = 0.67\ f_{cu}^{0.50}$	-	As CP 114 (22)
Teychenné (11) 1967	Sand + gravel	Dry	7 - 40	$f_{MR} = 0.86\ f_{cu}^{0.50}$ $f_{MR} = 0.51\ f_{cu}^{0.50}$	- -	Upper and lower limit Central point load
	Aglite, foamed slag, Lytag	Dry	35 - 60	$f_{MR} = 9.01\ f_{cu}^{-0.27}$ $f_{MR} = 1.74\ f_{SP}^{0.60}$	0.37 0.80	Sand replacement
		Wet	13 - 64	$f_{MR} = 0.43\ f_{cu}^{0.63}$ $f_{MR} = 1.43\ f_{SP}^{1.06}$	0.94 0.98	
		Wet & dry		$f_{SP} = 0.49\ f_{cu}^{0.46}$	0.71	
	Aglite, foamed slag, Leca, Lytag	Dry	17 - 74	$f_{SP} = 0.54\ f_{cu}^{0.5}$ $f_{SP} = 0.37\ f_{cu}^{0.5}$	- -	Upper and lower limit
Short & Kinniburgh (77) 1968	Dense and lightweight	- -	- -	$f_{MR} = 0.66\ f_{cu}^{0.5}$ $f_{SP} = 0.42\ f_{cu}^{0.5}$	- -	Gravel, Aglite, foamed slag, Lytag
Komlos (92) 1970	Sand + gravel	Dry	21 - 43	$f_{MR} = 0.110\ f_{cu+1.70}$ $f_{SP} = 0.045\ f_{cu+1.25}$ $f_{MR} = 2.43\ f_{SP-1.15}$	0.93 0.94 0.96	Pozzolanic cement
Bandyopadhyay (49) 1974	Solite	Dry	21 - 60	$f_{MR} = 0.46\ f_{cu}^{0.5}$ $f_{SP} = 0.42\ f_{cu}^{0.5}$	- -	
		Wet	21 - 60	$f_{MR} = 0.75\ f_{cu}^{0.5}$ $f_{SP} = 0.54\ f_{cu}^{0.5}$ $f_{SP} = 0.76\ f_{MR}$	- -	

TABLE 4.8 COMPARISON OF TENSILE STRENGTH DATA WITH OTHER INVESTIGATORS - CONTINUED

Author	Type of Concrete	Curing Condition	28 Day Cube Strength Range (N/mm^2)	Relationship	Correlation Factor - r	Comments
Brooks & Neville (89) 1977	Dense and lightweight	Dry	20 - 80	$f_{MR} = 0.23\ f_{cu}^{0.75}$	-	Gravel, Aglite Lytag. Sand replacement
				$f_{MR} = 1.72\ f_{SP}^{0.87}$	-	
		Wet		$f_{MR} = 0.64\ f_{cu}^{0.55}$	-	
				$f_{MR} = 2.71\ f_{SP}^{0.62}$	-	
				$f_{SP} = 0.13\ f_{cu}^{0.80}$	-	
CEB-FIP (72) 1977	Lightweight	Wet and dry	-	$f_{MR} = 0.46\ f_{cu}^{0.67}$	-	
				$f_{SP} = 0.23\ f_{cu}^{0.67}$	-	
Balendran (61) 1980	Limestone, Lytag, Taclite	Wet	20 - 74	$f_{MR} = 0.39\ f_{cu}^{0.63}$	0.94	Sand replacement
				$f_{SP} = 0.13\ f_{cu}^{0.84}$	0.96	
				$f_{MR} = 1.81\ f_{SP}^{0.73}$	0.93	
Author 1981	Lytag	Dry	20 - 60	$f_{MR} = 1.20\ f_{cu}^{0.26}$	0.65	Sand replacement
				$f_{MR} = 1.84\ f_{SP}^{0.52}$	0.59	
		Wet		$f_{MR} = 0.90\ f_{cu}^{0.43}$	0.99	
				$f_{MR} = 2.05\ f_{SP}^{0.64}$	0.95	
		Wet & dry		$f_{SP} = 0.46\ f_{cu}^{0.51}$	0.86	

strengths at faster rates.

2. Lytag-sand concrete with a cement content of 485 kg/m^3 and a free water/cement ratio of 0.36 can achieve strengths up to 60 N/mm^2 at 28 days.
3. The initial moisture content of the coarse aggregate has little effect on compressive strength provided it is taken into account when computing the water to be allowed for aggregate absorption.
4. In general Lytag-sand concrete requires less cement than other sand replaced lightweight concretes in order to achieve a given compressive strength.
5. On average the increase in density of Lytag concrete by the addition of natural sand fines is approximately 14-15%.
6. The 28 day air-dry density of Lytag-sand concrete varies between 1810-1935 kg/m^3 for compressive strengths of 20-60 N/mm^2.
7. For water cured specimens compressive strength increases up to an age of 18 months after which it remains fairly constant. The strength at approximately 18 months expressed as a percentage of the 28 day strength varies between 111-138%.
8. For specimens stored under constant temperature and humidity conditions the strength at 2 years varies between 101-112% of the 28 day strength.
9. For specimens drying out under uncontrolled conditions a reduction in strength may be expected between 28 days and 2 years. After 2 years however the strength is approximately equal to that at 28 days. The maximum observed reduction in compressive strength was 7%.
10. The tensile strength of Lytag-sand concrete is affected by curing conditions at early ages.
11. For wet cured specimens the gain in tensile strength is progressive up to 28 days. For dry cured specimens initial strength gain is very rapid often followed by a loss in tensile strength after 2-3 days. The tensile strength is however generally regained as the specimen becomes uniformly dried out.
12. For the concretes investigated, a power law type of curve was able, in general, to sensibly describe the relationships between the various strengths, namely flexural, tensile splitting and compressive. While good correlation

was observed for wet cured specimens, dry cured specimens showed a greater variability.

CHAPTER 5

SHORT TERM DEFORMATION PROPERTIES OF LYTAG-SAND CONCRETE

5.1 Introduction

The series of tests described in this chapter were designed to provide information about some of the short term deformation properties of Lytag-sand concrete. The properties investigated were the elastic moduli, static and dynamic, Poisson's ratio and the complete stress-strain curve.

The static modulus of elasticity and Poisson's ratio were determined up to a stress equal to one-third of the cube strength. The dynamic modulus of elasticity was determined by an electrodynamic method. The complete stress-strain curve was determined by a technique developed by Wang et al (93) which involves modifying a constant loading rate test machine, by means of a case hardened, steel tube, in order that it becomes a constant strain rate test machine.

It is generally stated that the modulus of elasticity of lightweight concrete varies between 50-75% of that for dense concrete when compared on a compressive strength basis. The modulus of elasticity is an important characteristic which is used in the determination of the deflection of reinforced and prestressed concrete under short-term and long-term loading. In prestressed concrete the loss of prestress due to elastic deformation of concrete also depends on the elastic modulus.

The value of Poisson's ratio is generally not critical in engineering design although in some cases a knowledge of its value is required. In two dimensional stress analysis of a slab or shell, the distribution of moments is modified due to the Poisson's ratio effect. It may also be used to assess spalling effects due to thermal movement (94) and in the study of the formation and propagation of microcracks in concrete, by fracture mechanics (95, 96).

The accurate knowledge of the ascending and descending portions of the stress-strain curve for concrete is necessary since part of the concrete compression zone is usually in this range of strains near to failure.

5.2 Experimental Programme

5.2.1 Outline of Tests

Static and dynamic modulus of elasticity tests were carried out in accordance with BS 1881 (86). Four concrete strengths of 20, 30, 45 and 60 N/mm^2 were chosen based on the 28 day strength of wet cured cubes. For each cube strength two static modulus and three dynamic modulus specimens were tested. Static modulus tests were carried out at 3, 7, 14 and 28 days while dynamic modulus tests were carried out at 1, 3, 7, 14 and 28 days.

Poisson's ratio was calculated from lateral and longitudinal strain measurements taken on the static modulus specimens.

Determination of the complete stress-strain curves for the various concrete strengths mentioned was carried out at 28 days. For each strength three specimens, which had been stored in water up to 28 days, were tested. The plotted results are thus the average of three specimens.

5.2.2 Dimensions of Test Specimens

The sizes of the various test specimens were as follows:

(a) 100 x 100 x 300 mm prisms : static modulus of elasticity and Poisson's ratio.

(b) 100 x 100 x 500 mm prisms : dynamic modulus of elasticity.

(c) 75 x 75 x 300 mm prisms : complete stress-strain curve.

5.2.3 Curing Conditions

For the static and dynamic modulus of elasticity tests three specimens, at each strength, were placed in the following environments, along with their companion 100 mm cubes:

(a) Water at $22^{o}C \pm 3^{o}C$.

(b) Uncontrolled laboratory.

(c) Constant temperature and humidity room (CTHR) at a temperature of $16^{o}C \pm 0.5^{o}C$ and 50 ± 2% relative humidity.

The complete stress-strain curve specimens were stored in condition (a) until capping and testing at 28 days.

5.2.4 Manufacture of Test Specimens

For each concrete strength, all the test specimens for the various tests were cast at the same time. All specimens were cast in steel moulds which had been lightly oiled.

Mixing was carried out in accordance with the method described in 4.2.1.2 and concrete was placed in two roughly equal layers and compacted by means of a high frequency vibrating table. The surfaces of the specimens were trowelled smooth approximately two hours after casting. The moulds were then covered with polythene sheet and left in the laboratory for 24 hours before the specimens were demoulded and placed in their respective curing environments.

5.2.5 Instrumentation and Test Procedure

5.2.5.1 Static and Dynamic Moduli of Elasticity and Poisson's Ratio

The static modulus of elasticity was measured by means of a demec extensometer with a gauge length of 100 mm. Demec discs were fixed about the centre of the specimen, along the longitudinal axis and on two opposite faces. The demec gauge had a sensitivity of 16.2×10^{-6} m/m per division. To determine Poisson's ratio, two additional demec discs were placed at 50 mm apart in the lateral direction, at the centre of the specimen and on the same two faces as the longitudinal demec discs. The 50 mm demec gauge had a sensitivity of 19.8×10^{-6} m/m per division.

The dynamic modulus of elasticity was determined by an electrodynamic method. The apparatus used consisted of an electro-magnetic exciter unit, an electro-magnetic pick up unit, a digital counter unit, a variable frequency oscillator and a cathode ray oscilloscope. The exciter unit was driven by the variable frequency oscillator and connected in parallel with the digital counter unit. This measured the frequency of oscillation of the exciter unit to an accuracy of 1 Hz. The specimen under test was supported at its centre and the exciter unit was placed in contact with one end and the pick up unit with the other. A good contact between the units and the specimen was ensured by means of a small dab of grease. The signal generated by the exciter

unit propagated within the specimen and was received by the pick up which was in turn connected to the oscilloscope to give a visual display. The frequency of excitation was varied until resonance was obtained at the fundamental, i.e. the lowest, frequency of the specimen. Resonance was indicated by the maximum height of the trace on the oscilloscope.

5.2.5.2 Complete Stress-Strain Curves

Details of the equipment used in this series of tests are given in Figure 5.1. The technique was developed by Wang et al (93) and involves modifying a machine designed to give a constant rate loading in order that it can provide a constant rate of straining. Several investigators have developed techniques to obtain the complete stress-strain curve for concrete (97-100). Some of these techniques are costly, require testing machines which may not be available in a normal quality control laboratory or require expensive modifications to a standard testing machine.

The technique developed by Wang et al (93) was fairly simple and involved loading a concrete cylinder in parallel with a steel tube which had been case hardened so that its stress-strain curve was linearly elastic up to a strain of 0.006. During loading the vertical strains in the steel tube were measured by two foil-type electrical resistance strain gauges. These strains gave not only the amount of load taken by the steel tube, but were also used to obtain nominal strains in the concrete. Thus knowing the total load and the corresponding steel strain, the stress-strain relationship, for the concrete under test, was obtained.

The Authors did however point out that although the method was simple it did have certain limitations:

(a) the testing machine must apply load to both the steel tube and the concrete; thus the size of the specimen is limited by the capacity of the machine.

(b) the limit of 0.006 for final strain may be too small when concrete is confined with lateral reinforcement.

(c) the definition of strain is such that the deformations of the thin capping material and those of the end zones of the concrete specimen, where a purely

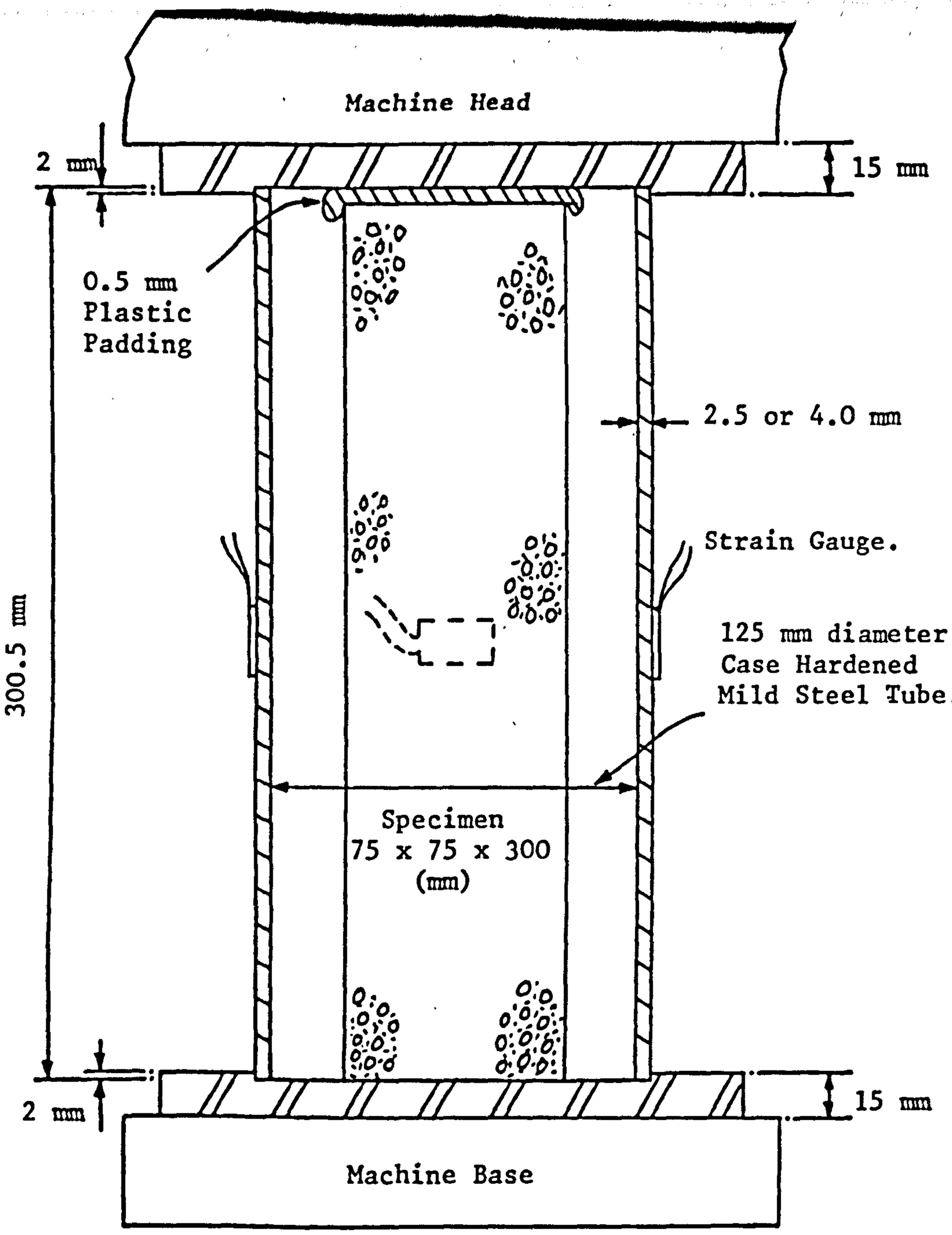

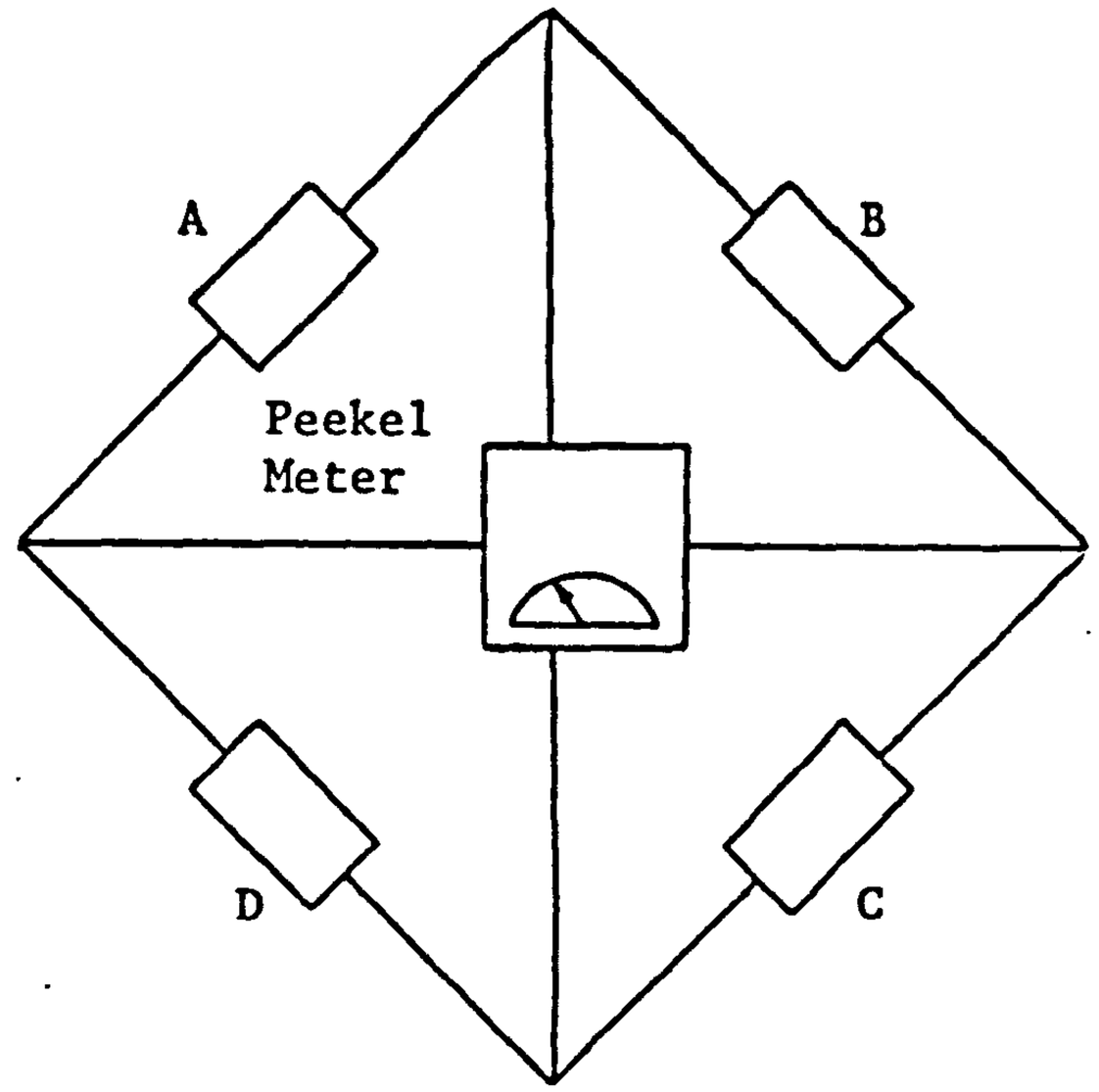

KEY

A and C - Vertical Gauges.
B and D - Horizontal Gauges.

Peekel meter reading = A + B + C + D
= 2 x vertical strain (1 +ν)
ν = Poisson's ratio for steel.

FIGURE 5.1 TEST APPARATUS FOR THE COMPLETE STRESS-STRAIN CURVE

uniaxial state of stress does not exist, are included.

(d) the presence of the steel tube precludes any observation of the failure modes of the test specimen during testing.

The steel tubes used in this investigation had nominal wall thickness of approximately 2.5 mm and 4.00 mm, an internal diameter of 100 mm and a length of 300.5 mm. Four epoxy backed foil-type electrical resistance strain gauges were attatched to the outside of each steel tube and connected to form a full Wheatstone bridge as shown in Figure 5.1. This is a very sensitive arrangement since it is temperature compensating as all the gauges are applied to the same material and subject to the same environment. Two gauges were arranged in the vertical direction and two in the horizontal direction and this configuration results in a strain reading on the strain indicator equivalent to

2x vertical strain x (1+ Poisson's ratio for steel)

The tubes were calibrated with the aid of a demec extensometer with a gauge length of 100 mm and a sensitivity of 16.2×10^{-6} m/m per division. The Wheatstone bridge circuit was connected to a Peekel T200 strain indicator.

The tube in use was calibrated before and after each series of tests on the different strength concretes. In order to test a specimen it would be placed inside the steel tube and capped with plastic padding which was in turn covered with aluminium foil. The top plate was positioned and the rig loaded in the test machine until a strain of 20×10^{-6} registered on the strain indicator. The rig was kept loaded for approximately 15 minutes to allow the capping material to harden. It was then removed from the machine, still intact, and left for a further 60 minutes before testing. The rate of straining used during testing was approximately 10 microstrain per second.

5.3 Test Results and Discussion

5.3.1 Static and Dynamic Modulus of Elasticity

The development of the static and dynamic moduli of elasticity, up to 28 days and under different curing conditions is shown in Table 5.1 and Figures 5.2 - 5.3. The results of other investigators (11, 61) are also shown in Figures 5.2 - 5.3. The results show a general increase in elastic

TABLE 5.1 DEVELOPMENT OF MODULI OF ELASTICITY WITH AGE

Age (Days)	28 Day Compressive Strength		Static Modulus at 1/3 rd Cube Strength			Dynamic Modulus		
	Wet (N/mm^2)	Dry (N/mm^2)	Water (kN/mm^2)	Laboratory (kN/mm^2)	C.T.H.R. (kN/mm^2)	Water (kN/mm^2)	Laboratory (kN/mm^2)	C.T.H.R. (kN/mm^2)
1	19.5	22.5	-	-	-	11.0	11.0	10.5
	29.5	33.5	-	-	-	12.5	12.5	13.0
	45.5	47.5	-	-	-	16.0	16.5	16.0
	59.0	64.0	-	-	-	19.5	20.0	19.5
3	19.5	22.5	12.0	11.5	12.5	17.0	16.0	15.5
	29.5	33.5	14.0	14.0	14.0	18.0	18.0	18.0
	45.5	47.5	15.0	15.5	15.0	21.5	21.5	21.0
	59.0	64.0	17.5	18.0	18.0	25.0	24.5	24.5
7	19.5	22.5	12.5	12.5	13.0	20.0	17.5	17.5
	29.5	33.5	15.5	15.5	15.5	21.5	20.5	20.0
	45.5	47.5	18.0	17.5	17.0	24.0	23.5	23.0
	59.0	64.0	20.0	19.5	19.0	26.5	25.5	25.5
14	19.5	22.5	14.5	14.0	15.0	21.5	18.0	18.5
	29.5	33.5	17.0	16.5	16.5	23.0	21.5	21.0
	45.5	47.5	19.0	18.5	19.0	25.5	24.0	23.5
	59.0	64.0	21.0	20.0	20.5	27.5	26.0	26.0
28	19.5	22.5	15.5	14.0	16.0	22.5	18.0	18.5
	29.5	33.5	18.0	17.5	17.5	24.5	21.5	21.5
	45.5	47.5	20.0	19.0	19.5	26.0	24.0	24.0
	59.0	64.0	22.0	21.5	21.5	28.5	26.0	26.0

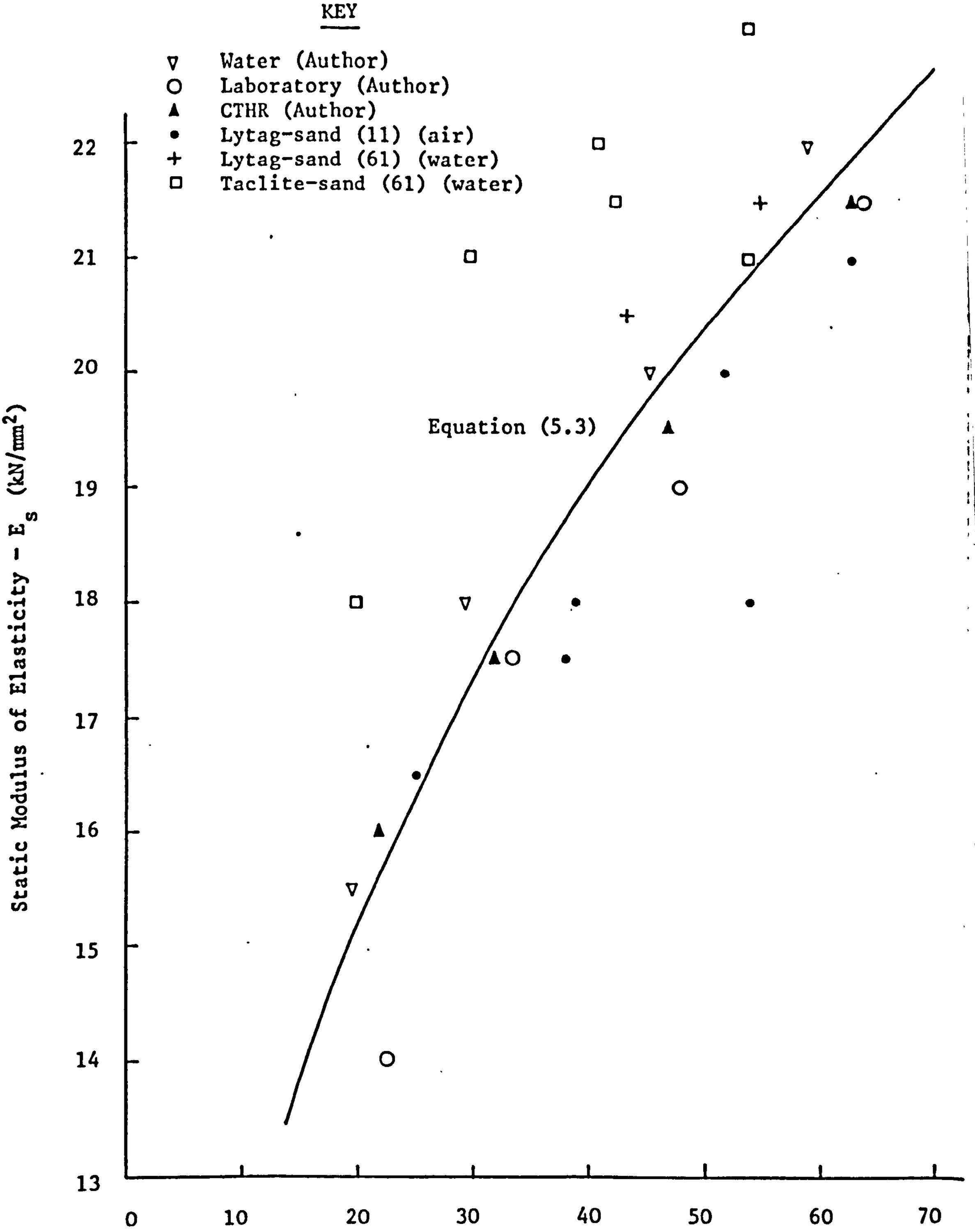

FIGURE 5.2 VARIATION OF STATIC MODULUS OF ELASTICITY WITH COMPRESSIVE STRENGTH AT 28 DAYS

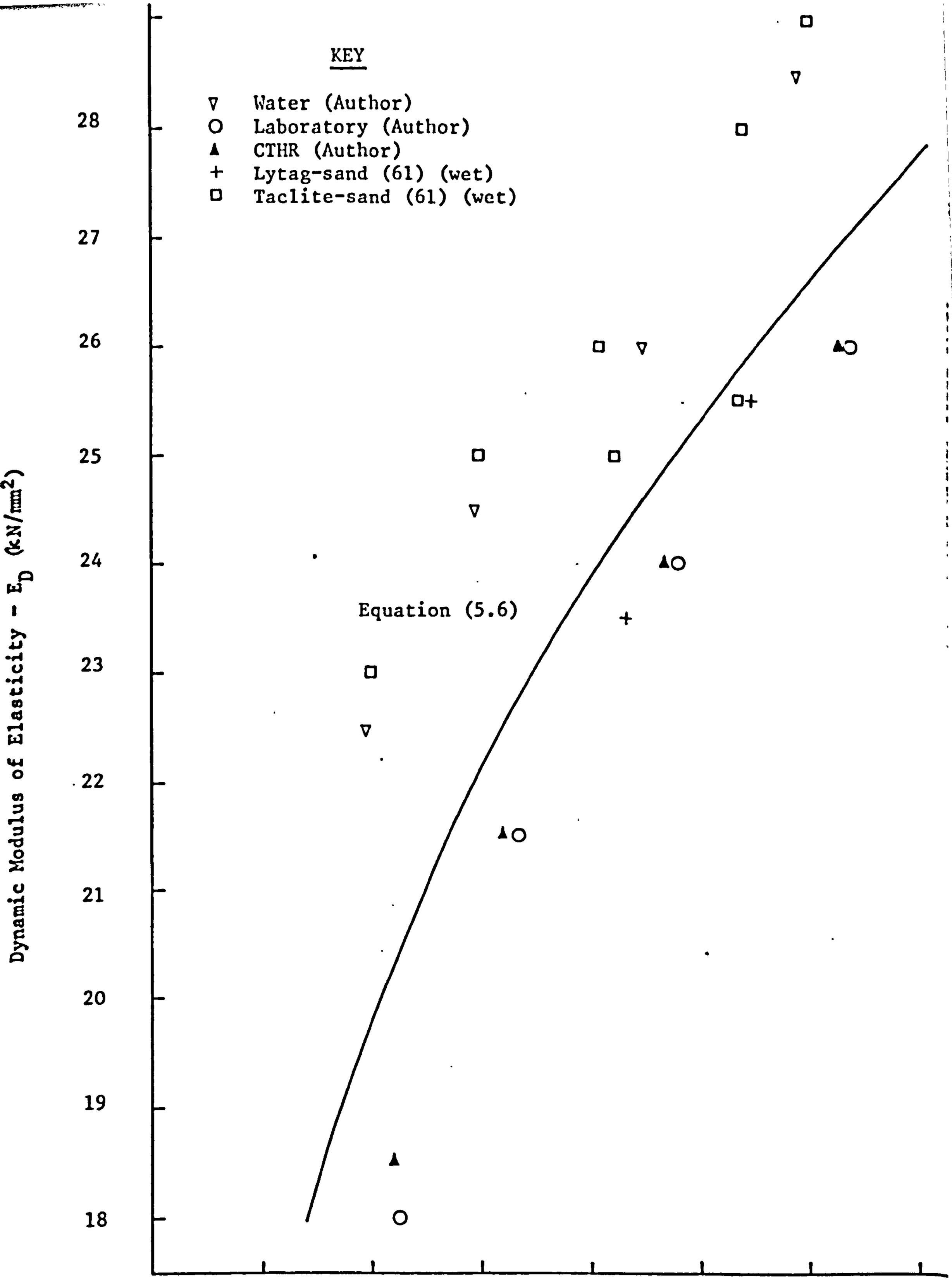

FIGURE 5.3 VARIATION OF DYNAMIC MODULUS OF ELASTICITY WITH COMPRESSIVE STRENGTH AT 28 DAYS

moduli with increasing strength.

Table 5.1 indicates that the static modulus of elasticity of wet cured specimens is consistently higher than that for dry cured specimens by approximately 5% on average. This is reflected in Figure 5.2, but there is a distinct difference between Lytag-sand concrete and Taclite-sand concrete.

The dynamic modulus of elasticity of wet cured specimens is also consistently higher than that of dry cured specimens, by approximately 15% on average. This is reflected in Figure 5.3 and is consistent with Balendrans results for Taclite-sand concrete. The average ratio of the static modulus to the dynamic modulus of elasticity for all the 28 day results given in Table 5.1 is 79%.

5.3.1.1 Relationship between Moduli of Elasticity and Compressive Strength

The modulus of elasticity is primarily dependent on the compressive strength of the concrete and the modulus of elasticity of the aggregate. To a lesser extent, the conditions of curing, age of concrete, mix proportions and type of cement are also factors which affect the elastic modulus.

For the purposes of design it is convenient to be able to estimate the elastic modulus of a particular type of concrete with only a knowledge of its compressive strength. Two basic forms of equation are generally accepted to adequately describe the relationship between elastic modulus E_c and compressive strength f_{cu}:

$$E_c = a f_{cu}^{\,b} \qquad \ldots\ (5.1)$$

or

$$E_c = \bar{c} + d\, f_{cu} \qquad \ldots\ (5.2)$$

where a, b, c and d are constants.

Equation (5.2) possibly over-simplifies the relationship since it implies that a concrete with zero compressive strength has an elastic modulus c, which is obviously incorrect. Equation (5.1) is sometimes simplified by setting b = 0.5.

Regression analyses, of the 28 day results shown in Table 5.1, based on equation (5.1) produced the following:

Static modulus: $E_S = 5.82\ f_{cu}^{0.32}$ (wet + dry) (r = 0.95) .... (5.3)

where r = correlation factor.

Dynamic modulus $E_D = 12.34\ f_{cu}^{0.2}$ (wet) (r = 0.99) .... (5.4)

$E_D = 6.57\ f_{cu}^{0.33}$ (dry) (r = 0.99) .... (5.5)

$E_D = 8.81\ f_{cu}^{0.27}$ (wet + dry) (r = 0.81) .... (5.6)

If the results of other investigators (11, 61) on Lytag-sand concrete, shown in Figure 5.2, are included, equation (5.3) becomes:

$$E_S = 6.16\ f_{cu}^{0.30} \quad (r = 0.91) \qquad \ldots. (5.7)$$

If the results for Taclite-sand concrete (61) are also included, the equation becomes:

$$E_S = 6.84\ f_{cu}^{0.28} \quad (r = 0.79) \qquad \ldots. (5.8)$$

It is, therefore, apparent that the static modulus of elasticity can be accurately predicted from the compressive strength, for either wet or dry cured specimens, by means of a single equation (5.8).

By a similar analysis of all the results shown in Figure 5.3 equation (5.4) becomes:

$$E_D = 13.82\ f_{cu}^{0.17} \quad (r = 0.82) \qquad \ldots. (5.9)$$

and equation (5.6) becomes:

$$E_D = 9.92\ f_{cu}^{0.24} \quad (r = 0.77) \qquad \ldots. (5.10)$$

Again sufficiently accurate prediction can be achieved by the use of a single equation (5.10).

5.3.1.2 Relationship between Dynamic and Static Moduli of Elasticity

It has been suggested that it may be more convenient to estimate the static modulus of elasticity from the more easily measured dynamic modulus of elasticity by means of a linear equation. CP110 (54) suggests that for normal concrete the equation is:

$$E_S = 1.25\ E_D - 19 \qquad \ldots. (5.11)$$

Regression analysis of the data shown in Figure 5.4 produced the following equation:

$$E_S = 0.93\ E_D - 2.56 \quad (r = 0.93) \qquad \ldots\ (5.12$$

Similar equations have been presented by other investigators (49, 61). It is suggested that equation (5.12) could be used for sand replaced lightweigh concrete in general in the absence of more accurate information.

5.3.1.3 Comparison of the Static Modulus of Elasticity with Published Results

Figure 5.5 shows the relationship between static modulus of elasticity and cube strength obtained by several investigators (11, 61) and compared with the relationship predicted by CP110 (54) assuming a lightweight concrete density of 1875 kg/m^3. In general the CP110 (54) values over-estimate the elastic modulus of sand replaced lightweight concrete by some 10% on average.

The effect of sand replacement on the elastic modulus of Lytag concrete is to increase its value by 20-25% on average. Similar results have been reported by Balendran with increase in elastic modulus of 10-30% for sand replacement.

The values predicted by equation (5.3) suggest that the elastic modulus of Lytag-sand concrete is approximately 60% of that of dense concrete, given in CP110 (54).

5.3.2 Static Poisson's Ratio

Poisson's ratio is extremely complex and variable in nature and is probably the most difficult of the elastic constants to measure. Since the . value for concrete generally lies between 0.1 and 0.2 difficulty is usually experienced in accurately measuring the lateral strains. A typical strain curve for the determination of Poisson's ratio is shown in Figure 5.6 and the results of this investigation are shown in Table 5.2.

Figure 5.7 shows the relationship between static Poisson's ratio and cube strength. The results appear to be random, and the only conclusion that can be drawn from this set of results is that the value of Poisson's ratio for

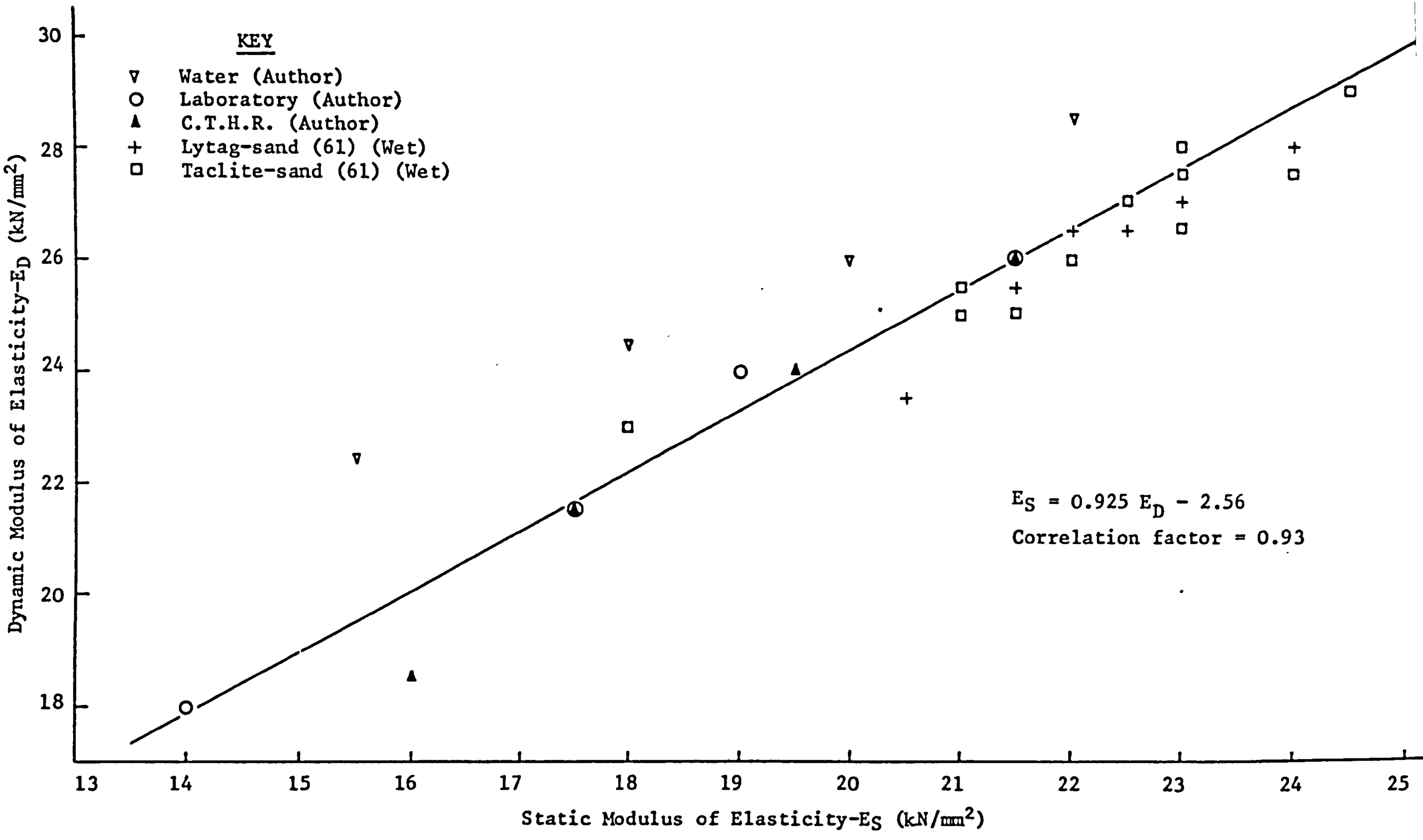

FIGURE 5.4 RELATIONSHIP BETWEEN STATIC AND DYNAMIC MODULI OF ELASTICITY

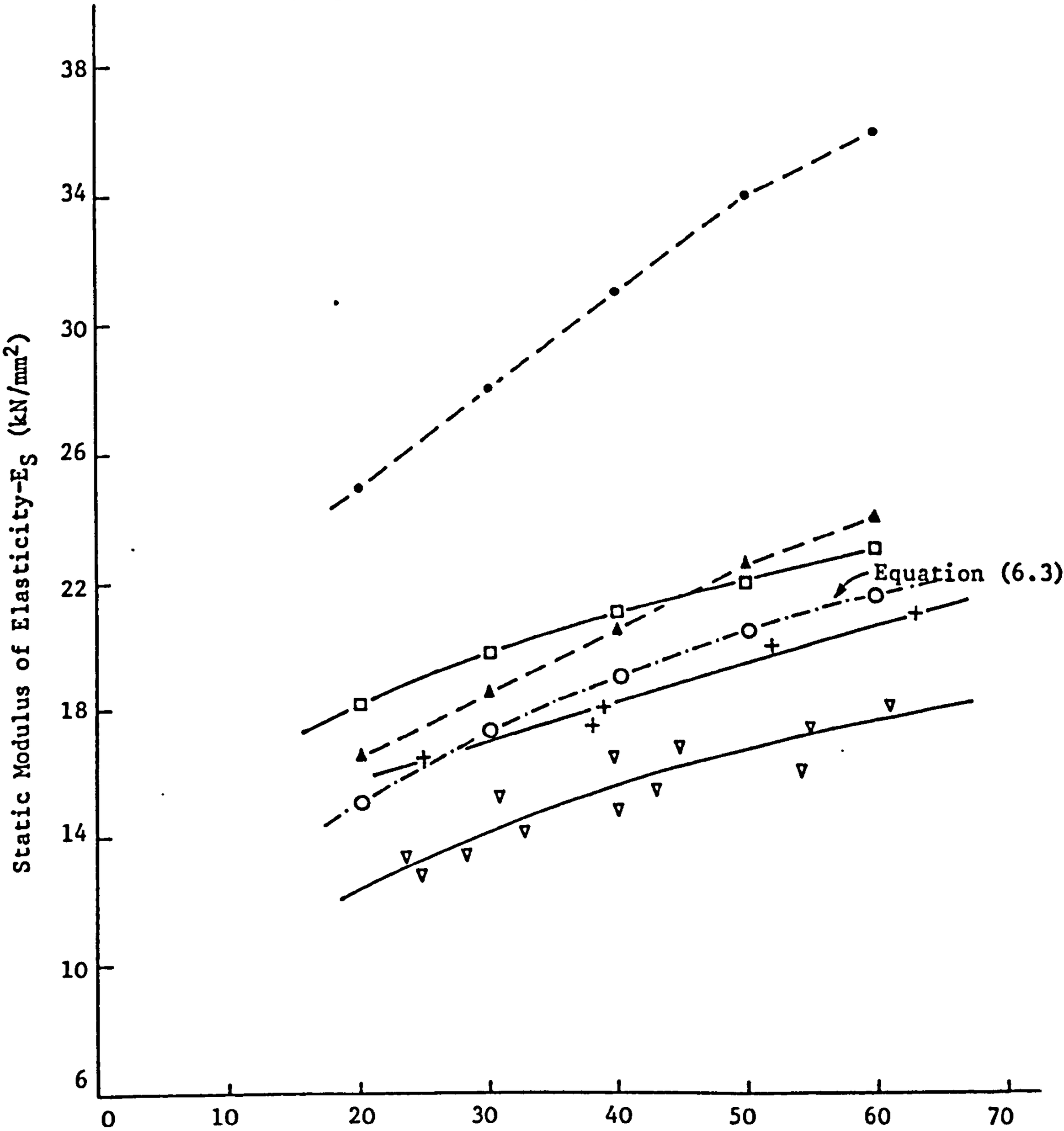

FIGURE 5.5 COMPARISON OF STATIC MODULUS OF ELASTICITY WITH PUBLISHED RESULTS

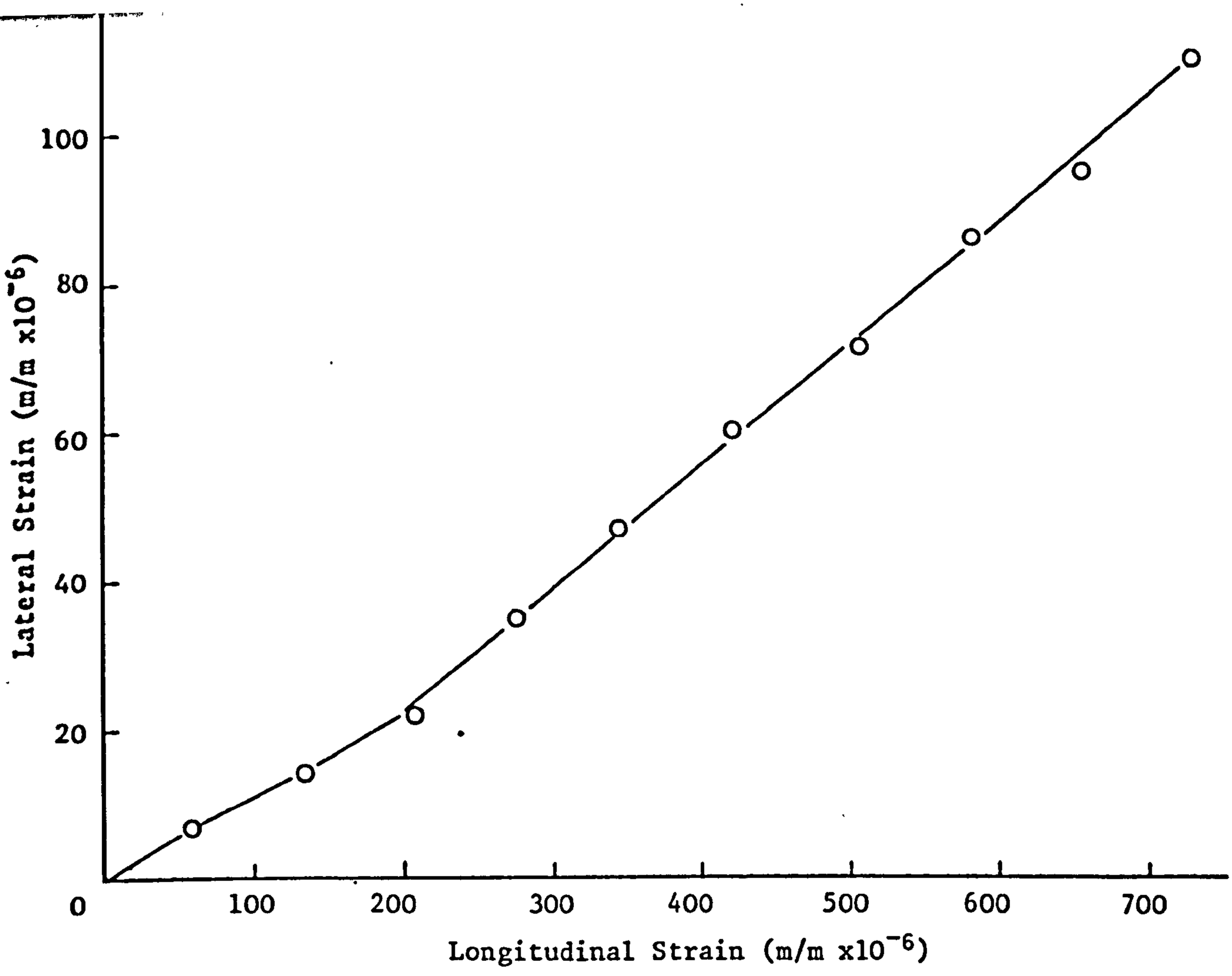

FIGURE 5.6 TYPICAL STRAIN CURVE FOR DETERMINATION OF POISSON'S RATIO FOR LYTAG-SAND CONCRETE IN UNIAXIAL COMPRESSION

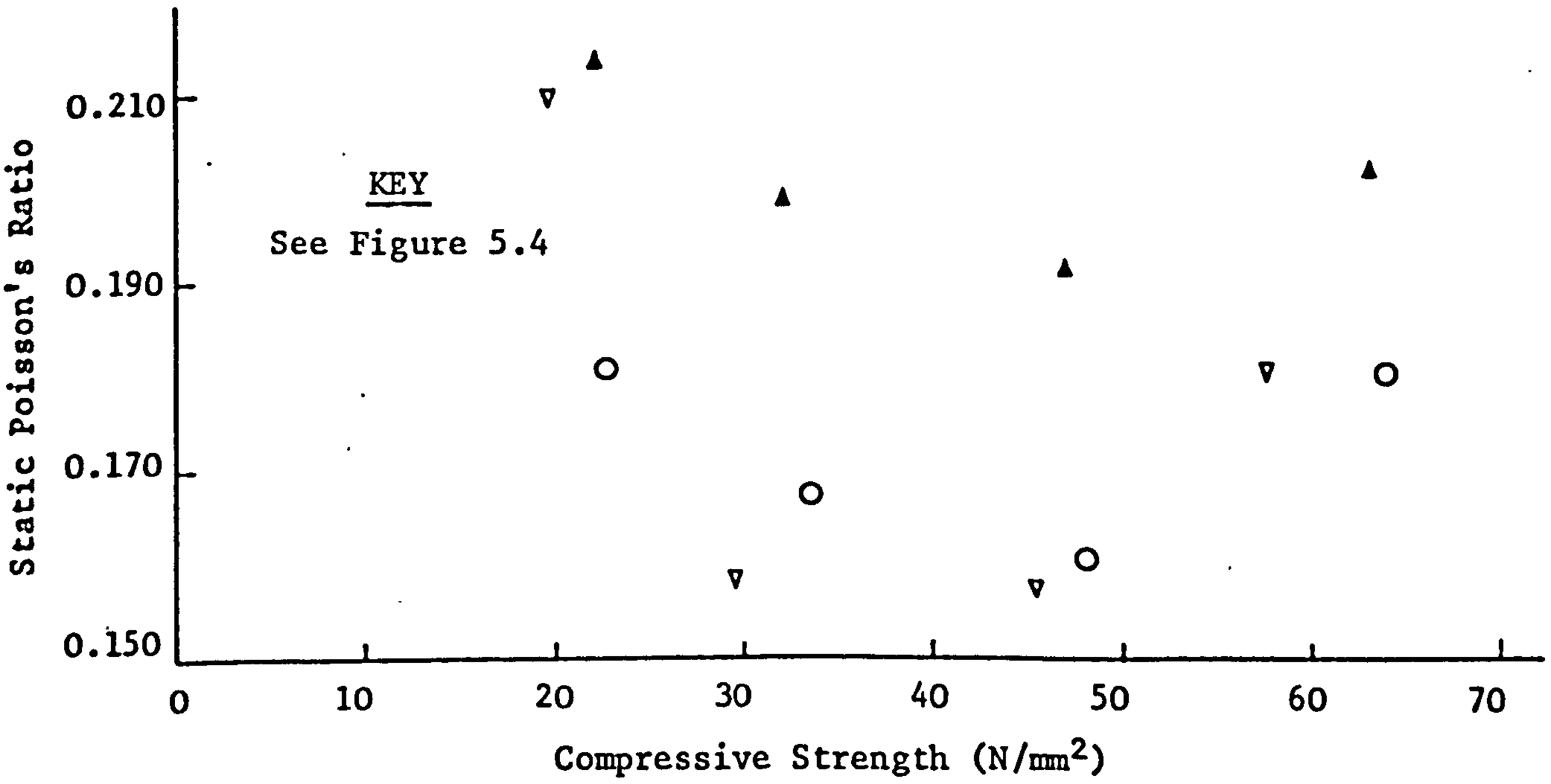

FIGURE 5.7 STATIC POISSON'S RATIO v COMPRESSIVE STRENGTH

TABLE 5.2 DEVELOPMENT OF STATIC POISSON'S RATIO (AT $^1/_3$ rd CUBE STRENGTH)

Age (Days)	28 Day Compressive Strength (N/mm^2)		Static Poisson's Ratio		
	Water	Laboratory	Water	Laboratory	CTHR
3	19.5	22.5	0.101	0.116	0.109
	29.5	33.5	0.074	0.111	0.117
	45.5	47.5	0.119	0.122	0.116
	59.0	64.0	0.145	0.161	0.169
7	19.5	22.5	0.117	0.152	0.142
	29.5	33.5	0.100	0.133	0.147
	45.5	47.5	0.109	0.152	0.139
	59.0	64.0	0.142	0.196	0.193
14	19.5	22.5	0.146	0.157	0.152
	29.5	33.5	0.140	0.162	0.197
	45.5	47.5	0.142	0.157	0.190
	59.0	64.0	0.148	0.207	0.200
28	19.5	22.5	0.210	0.181	0.212
	29.5	33.5	0.159	0.168	0.199
	45.5	47.5	0.157	0.161	0.192
	59.0	64.0	0.181	0.180	0.202

Lytag-sand concrete lies between 0.16 and 0.21 i.e. 0.185 ± 0.025.

5.3.2.1 Comparison with Published Results

Balendran (61) reported results of an extensive series of tests to determine the static Poisson's ratio of Lytag-sand, Taclite-sand and limestone-sand concretes, in tension and compression. Values reported for Lytag-sand concrete in compression varied between 0.17 and 0.19 and are comparable with the average results given in 5.3.2. Swamy and Bandyopadhyay (44) reported values of static Poisson's ratio for Solite concrete at 28 days varying between 0.19 and 0.22. Shideler (19) reported values of 0.16 to 0.21 for different American lightweight concretes. European and American codes of practice (26, 54, 73) recommend a value of 0.2. For sand replaced lightweight concretes a value of 0.19 would seem to be appropriate.

5.3.3 The Complete Stress-Strain Curve

The load-strain calibration curves for the two tubes are shown in Figure 5.8 and the Peekel meter calibration curves in Figure 5.9. From these two figures it can be seen that the elastic limit of both tubes was approximately 4000 microstrain. It was not possible to obtain a sensibly linear relationship above this strain and any attempt to do so resulted in high residual strains of the order of 50-100 microsctrain on unloading.

The 2.5 mm tube was used to test the 20, 30 and 45 N/mm^2 specimens, with the 4.0 mm tube being used to test the 60 N/mm^2 specimens. The results of the investigation are shown in Figure 5.10. Each curve is the average of three specimens, and the maximum stress as a percentage of the cube strength is shown. This figure remains sensibly constant at 83 ± 2% for the four concrete strengths tested.

The ascending portions of the curves behaved in a manner similar to those for the static modulus of elasticity tests and elastic moduli calculated from the curves compared favourably with the values given in Table 5.1, ranging between 14.0 kN/mm^2 and 22.0 kN/mm^2 for concrete strengths of 20-60 N/mm^2 respectively.

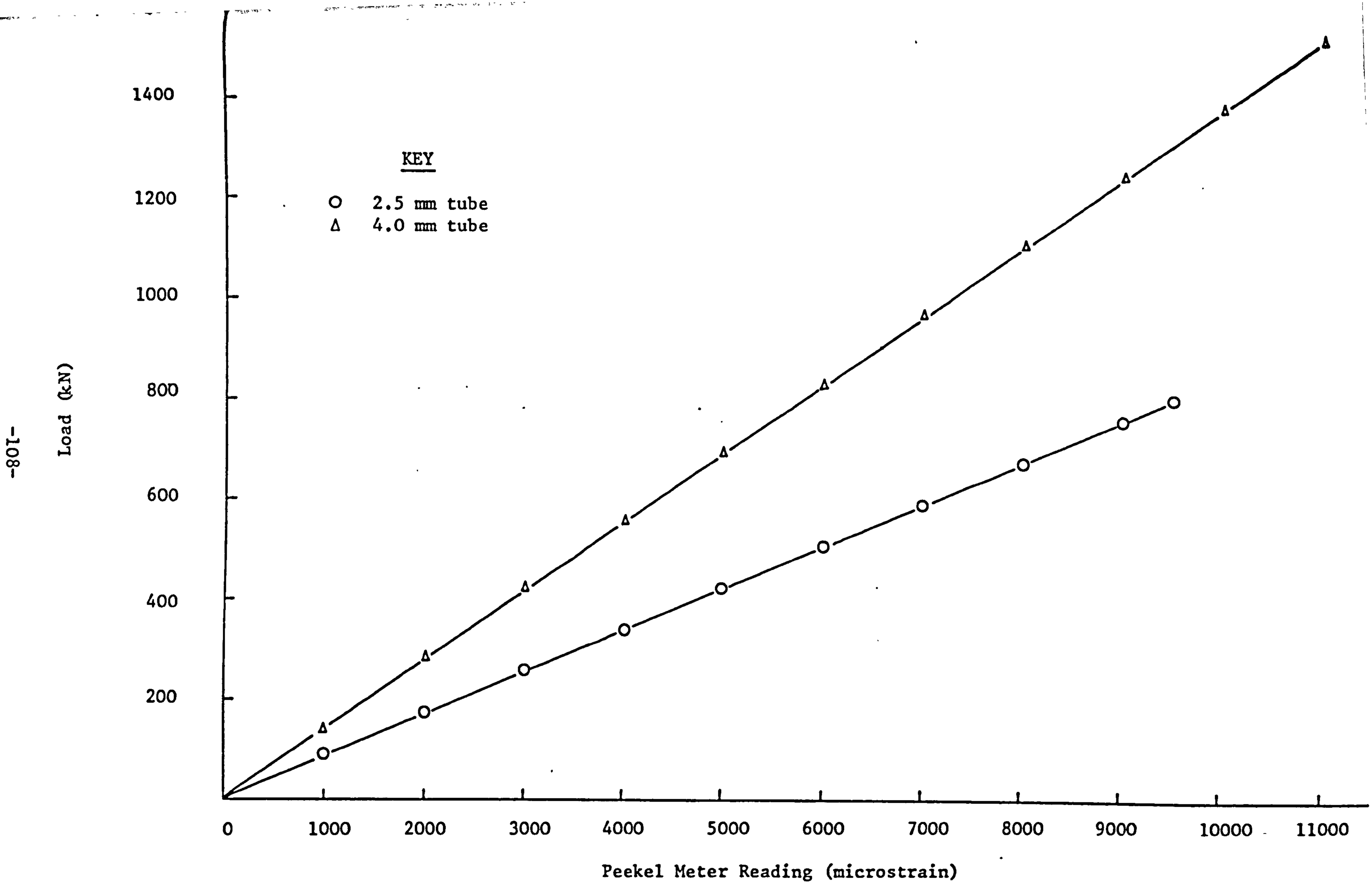

FIGURE 5.8 LOAD CALIBRATION CURVES FOR CASE HARDENED STEEL TUBES

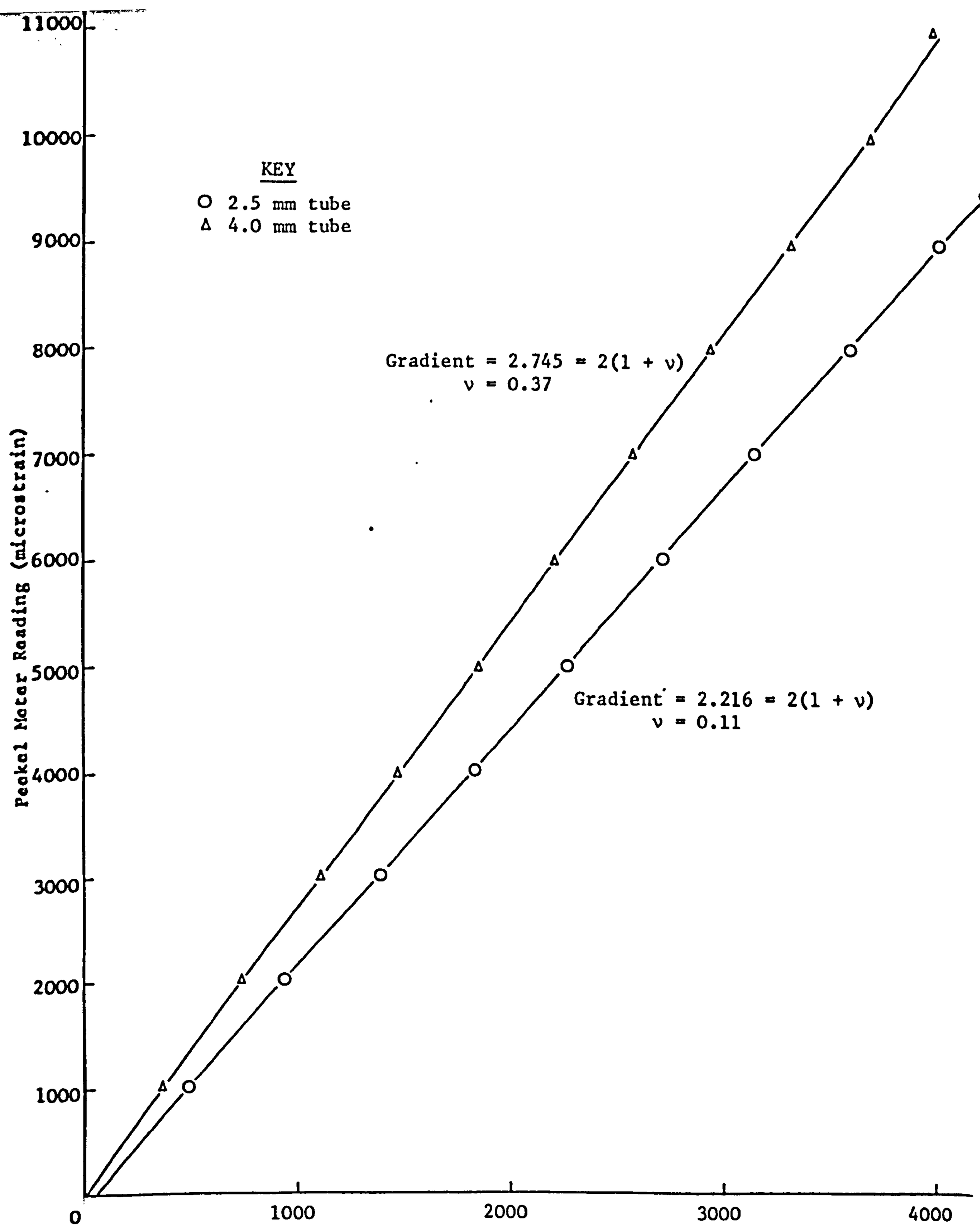

FIGURE 5.9 PEEKEL METER CALIBRATION CURVES

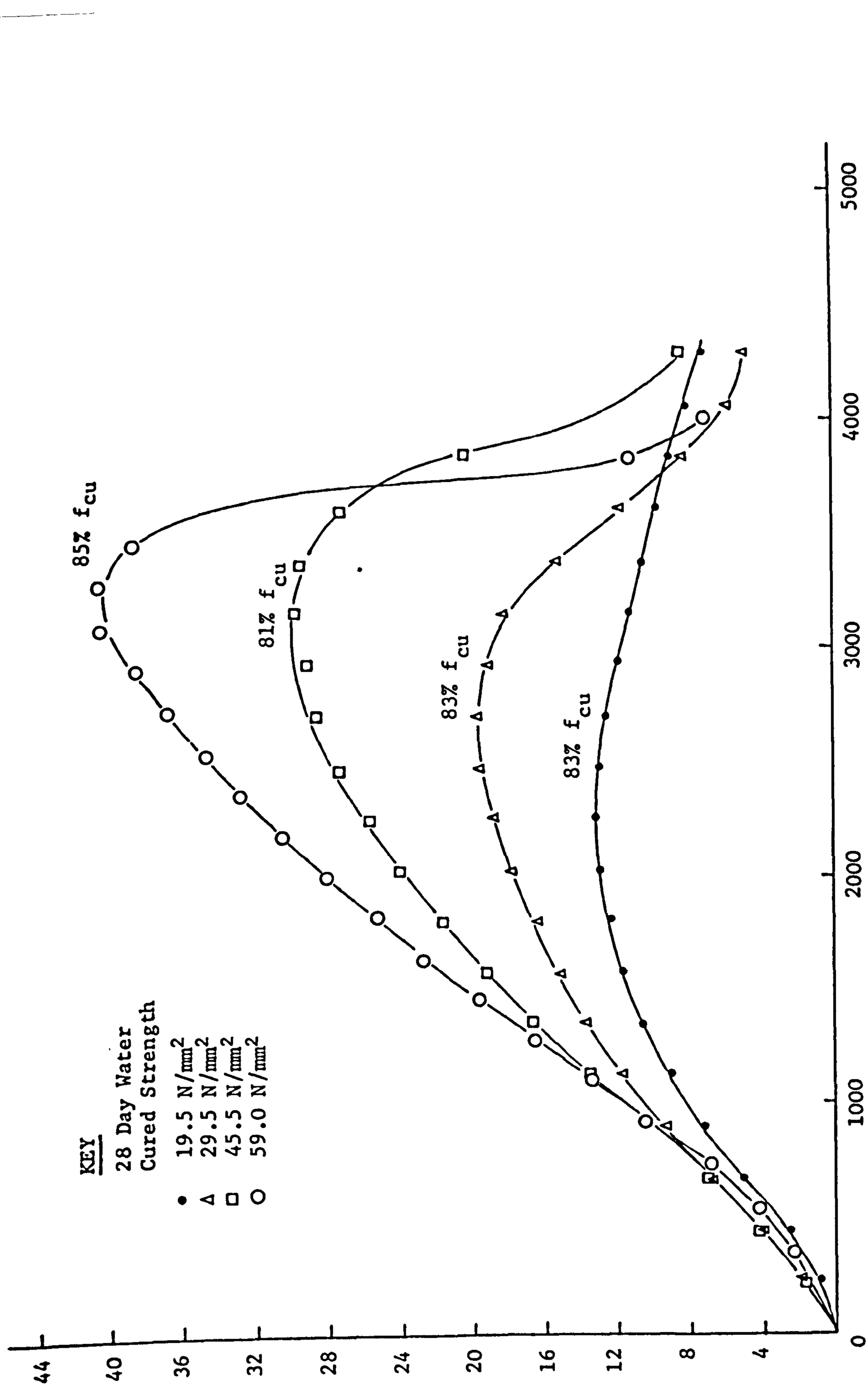

FIGURE 5.10 STRESS-STRAIN CURVES FOR LYTAG-SAND CONCRETE

With the exception of the 20 and 30 N/mm^2 specimens, the descending portion of the stress-strain curve was more difficult to control. After the peak stress had been reached the stress would begin to decrease gradually with increasing strain. The strain would then suddenly increase for no corresponding increase in total load. In some cases the total load indicated on the machine slightly decreased. This sudden energy release has obviously affected the shape of the descending portion of the curve. The lightweight concretes tested by Wang et al (93) showed that the rate of decrease in stress, after the peak stress, increases with increasing concrete strength, and this is also shown in Figure 5.10. However, the decrease in stress is more rapid for the higher strength concretes in Figure 5.10 than for equivalent strength concretes tested by Wang et al (93).

The machine used for testing the specimens has a listed capacity of 2500 kN. During testing it was found that at loads above 1100 kN, the machine lacked fine control and was subject to surges. This only affected the tests on the 60 N/mm^2 concrete and is therefore the reason for the lack of control during the descending portion of the stress-strain curve.

The results shown in Figure 5.10 show that for wet cured cube strengths from 20-60 N/mm^2 the strain at maximum stress for Lytag-sand concrete varies between 2250 and 3250 microstrain. Tests on all Lytag concrete (62) produced strains of between 2500 - 3500 microstrain for maximum concrete stresses of 25-30 N/mm^2. The results of the tests by Wang et al (93) indicate that the strain for American lightweight concretes varies between 2750 - 3750 micro-strain for maximum stresses between 20-55 N/mm^2.

The lower strain capacity of the specimens tested during this series of tests can be explained by the fact that the nominal concrete strains measured include the strains in the end regions of the specimen and the capping material. It has been shown (101) that the measured strains in a specimen near to failure are very much dependent on the location of the strain measuring device. A suggested improvement to the method used in the present investigation would be to attatch electrical resistance strain gauges to the surface of the concrete

specimen and bring the wires out through a hole and groove in the base plate. The gauges could be attached to the central region of the specimen thus ensuring that only uniaxial compressive strains are obtained.

It has been suggested (93) that the above method is a relatively cheap way of accurately obtaining the stress-strain curves for concrete by modifying a constant loading rate test machine. In this series of tests, several problems were encountered:

(a) A tube which was linear elastic up to 6000 microstrain could not be produced.

(b) For the higher strength concretes, 45 and 60 N/mm^2, difficulty was experienced in controlling the rate of straining after the peak stress had been reached.

The test method can provide a means of modifying a constant load rate test machine to a constant strain rate test machine but in order to obtain stress-strain curves for concretes with strengths in excess of 30 N/mm^2 using 75 x 75 x 300 mm specimens, the steel tube should have a wall thickness of at least 4.0 mm and the test machine a minimum capacity of 2500 kN. The quality of the test machine and the workmanship on the steel tube and end platens is very important.

The failure modes of the specimens tested during this series of tests are shown in Plate 5.1.

5.4. Conclusions

The following conclusions can be drawn from the series of tests described in this chapter:

1. The static modulus of elasticity of wet cured Lytag-sand concrete is approximately 5% greater than for dry cured concrete.
2. The dynamic modulus of elasticity of wet cured Lytag-sand concrete is approximately 15% greater than for dry cured concrete.
3. The relationship between static modulus of elasticity and cube strength, for sand replaced lightweight concrete, is $E_s = 6.84\ f_{cu}^{0.28}$.

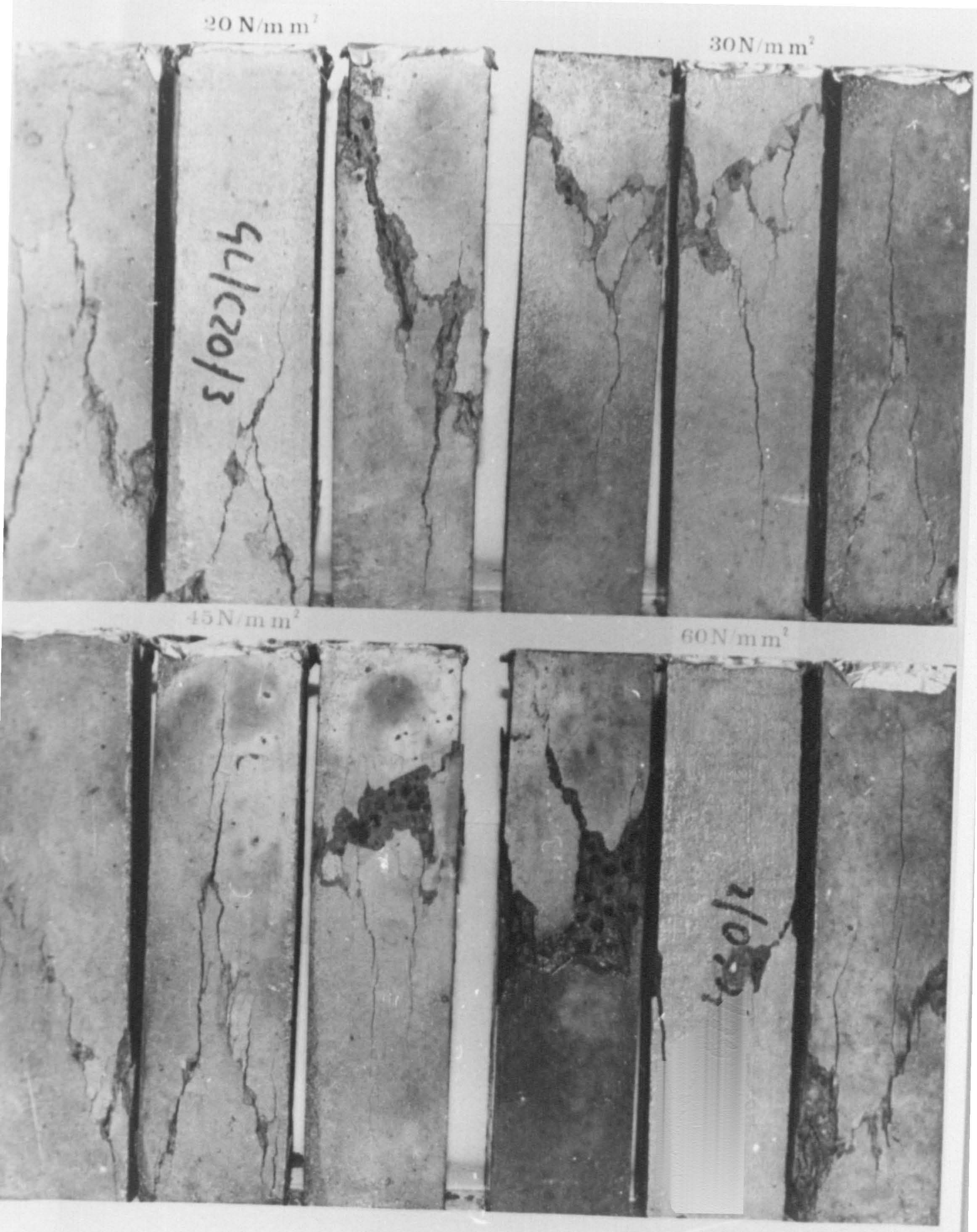

PLATE 5.1 COMPLETE STRESS-STRAIN CURVE SPECIMENS

4. The relationship between the dynamic modulus of elasticity and cube strength, for sand replaced lightweight concrete, is $E_D = 9.92\ f_{cu}^{0.24}$.
5. The static modulus of elasticity can be estimated from the dynamic modulus of elasticity by the equation $E_s = 0.93\ E_D - 2.56$.
6. The effect of replacing Lytag fines with natural sand, on the elastic modulus of Lytag concrete is to increase its value by 20-25%.
7. The elastic modulus of Lytag-sand concrete is approximately 60% of that of dense concrete as given in CP110 (54).
8. Static Poisson's ratio for Lytag-sand concrete varies between 0.16 and 0.21 and for design purposes, the value of Poisson's ratio for sand replaced lightweight concrete, in general, can be taken as 0.19.
9. For specimens with a length to width ratio of 4.0, tested in compression, the ratio of the maximum stress to that of 100 mm cubes is approximately 83%
10. The strain at maximum stress for Lytag-sand concrete in compression, varies between 2250-3250 microstrain for cube strengths of 20 to 60 N/mm^2 respectively.

CHAPTER 6

SHRINKAGE, MOISTURE MOVEMENT AND CREEP CHARACTERISTICS

6.1 Introduction

This chapter is concerned with the time dependent deformation properties of loaded and unloaded specimens. Drying shrinkage is a feature of all cement composites and is a direct result of moisture loss as the material dries out and matures. For concrete elements subjected to periodic wetting and drying, corresponding expansions and shrinkages occur and this is generally known as moisture movement. Whereas shrinkage and moisture movement are characteristics not dependent on the specimen being externally stressed, creep is the time dependent deformation resulting directly from an applied stress. Time dependent deformations are important since they affect the behaviour of an element during its life. They are directly linked with cement paste, with the coarse and fine aggregate fractions in a concrete mix merely serving to modify these deformations.

Neat cement paste has a high drying shrinkage and creep but the addition of a semi-rigid aggregate has a restraining effect on the shrinkage and creep of the paste. Since lightweight aggregates are generally weaker than dense aggregates and exhibit lower elastic moduli, it could be expected that shrinkage and creep in lightweight concretes will be greater than that of equivalent dense concrete mixes. Many investigators (38, 40, 41, 46, 102-106) have, however, shown that in general shrinkage and creep in lightweight concrete may be greater than or less than that of dense concrete. Concretes produced with various brands of lightweight aggregates may show widely varying shrinkage and creep properties. Similar variations may also occur between dense aggregates from different sources (40, 41, 106).

In this chapter the shrinkage, moisture movement and creep characteristics of Lytag-sand concrete are investigated, the main parameters being concrete strength, curing conditions and for the creep specimens, stress-strength ratio.

6.2 Review of Previous Research

Many investigators have turned their attentions towards time dependent deformations in concrete and a considerable amount of published literature is

available (107-109). This work has led to a better understanding of these phenomena but has also highlighted their complex interdependant nature and their complex relationship to the physical and mechanical characteristics of concrete in general. The results of many of these investigators have been collated to indicate the effects of the various parameters on the time dependent deformation properties of concrete (105) and these are discussed below.

6.2.1 Type of Cement

Cement type and its fineness have an important influence on the shrinkage and creep properties of concrete due to the different rates of hydration. Tests (110) have shown that the shrinkage of concrete made with very fine cement with a specific surface area of 7420 cm^2/kg is approximately 20% greater than that of ordinary cement concrete, 2770 cm^2/kg, for the same water-cement ratio and low workability. For high workability mixes, however, the increase in shrinkage was approximately 42%. It is generally agreed (105) that an increase in the rate of shrinkage produces a corresponding increase in the rate of creep. For the same water-cement ratio the creep of the concrete made with the very fine cement was higher at early ages, but after 1000 days it was less than that of the ordinary cement concrete.

6.2.2 Cement-Aggregate Ratio

Tests (19, 110-112) show that an increase in the aggregate concentration produces a decrease in the shrinkage and creep of concrete with age.

6.2.3 Water-Cement Ratio

For a constant cement content and cement-aggregate ratio, an increase in the water cement ratio produces a corresponding increase in shrinkage and creep. Bennet and Loat (110) showed that for O.P.C. concrete an increase in water-cement ratio from 0.3 to 0.375 resulted in increases in shrinkage and creep of 20% and 35% respectively. For very fine cement concrete these increases will be of the order of 40% and 66% for an increase in water-cement ratio from 0.375 to 0.525. Similar results were obtained by Evans and Kong (113).

6.2.4 Aggregate Properties

Aggregate properties have a significant effect on the shrinkage and creep

of concrete. Tests (114) have shown that various dense aggregates show a wide range of shrinkage and creep values for similar strength mixes. Aggregate quality is of prime importance, the shrinkage and creep of a limestone or quartz aggregate concrete could be of the order of half that of a sandstone aggregate concrete (114). Tests on various American lightweight aggregates (115) showed a considerable scatter of shrinkage and creep results whereas the results of tests on British lightweight aggregates (48, 91, 116) show comparatively less scatter. The lower modulus of elasticity of lightweight aggregates has led in the past to a general assumption that the shrinkage and creep of lightweight concrete will in general be greater than that of dense concrete. However the test results show that the range of values of shrinkage and creep obtainable with lightweight concretes is similar to that for various dense concretes (41, 91, 114-116).

6.2.5 Curing Conditions

Temperature and relative humidity effect the shrinkage and creep of dense and lightweight concrete. Troxell et al (114) showed that the shrinkage and creep of dense concrete increased with decrease in humidity. Also for dense concrete, Nasser and Neville (117-118) showed that creep is a function of temperature for new as well as old concrete. Mullen and Dolch (119) and Ross (120) showed that when concrete has completed its shrinkage (i.e. dried in an oven at 110°C) creep under load was negligible. Tests (46, 49, 61) have also shown that the shrinkage of concrete stored in an uncontrolled environment is less than for constant temperature and humidity conditions.

Water curing increases the volume of cement gel formed and can lead to increased shrinkage of cement paste and concrete (121). This increase can be explained by a reduction in the restraint offered by the cement clinker as its volume diminishes with age. It has been suggested that this effect can be reversed with prolonged curing since the cement gel undergoes a slow change in structure (121).

The effect of relative humidity on shrinkage and creep has been studied by A.C.I. Committee 209 (122).

6.2.6 Specimen Geometry

It has been recognised for many years that specimen size, or more specifically the exposed surface area to volume ratio, has a considerable effect on the shrinkage characteristics of concrete (104, 123-125). Ultimate shrinkage is thought, by some (123, 125), to decrease with increasing size, whereas others (126-129), maintain that it is independent of size. Creep is affected to a lesser extent and it has been suggested that in mass concrete size effects are negligible (105).

6.2.7 Age at Loading

Age at loading is important when considering prestress losses which occur at transfer. The age at loading indirectly determines the specimen's strength and, therefore, the stress-strength ratio. Tests (124) on dense concrete loaded to the same sustained stress at different ages showed an increase in creep as the age at loading decreased. This is to be expected since the stress-strength ratio increases with decreasing age. The greater increase in strength which occurred between 7 and 28 days as opposed to 28 and 90 days resulted in a greater difference between the creep of specimens loaded at 7 and 28 days than those loaded at 28 and 90 days.

The influence of age at loading for ages greater than 28 days has been found to be negligible (105, 130).

Balendran (61) showed that for specimens loaded at 7 days and 28 days to the same stress-strength ratio, of 0.25, the basic creep of sealed specimens of the former was approximately 12% less than that of the latter. The author explained this by the fact that for the specimens loaded at 7 days there was a higher gain in strength under load and, therefore, the average gain of strength over the loading period was greater and the basic creep lower. However, the specific basic creep of the 7 day specimens was approximately 15% greater than that for the 28 day specimens.

6.2.8 Stress-Strength Ratio

The majority of the early work carried out on creep of concrete involved loading specimens to a stress of less than one-third of the cube strength since

the applied stresses in the majority of structural members used in practice are of this order of magnitude.

Tests (61, 105, 110, 116) have shown that in general the relationship between stress-strength ratio and creep is linear for values of stress-strength ratio between 0.25 and 0.5.

6.3 Experimental Programme

6.3.1 Outline of Tests

The aim of this series of tests was to provide design data on the time-dependent deformations of Lytag-sand concrete. For shrinkage specimens the effects of concrete strength (i.e. cement content) and curing conditions were investigated. For moisture movement specimens subjected to periodic wetting and drying, concrete strength was the only variable. With the creep specimens, the limitations of facilities and resources meant that a single curing regime, namely constant temperature and humidity, only was used with the variables being concrete strength and stress-strength ratio.

6.3.2 Mix Design and Specimen Size and Manufacture

Mixes were designed, with the aid of the information given in Chapter 4, to produce concrete strengths of 30, 45 and 60 N/mm^2 for specimens stored in the C.T.H.R.

The specimens consisted of 500 x 100 x 100 mm prisms for the time-dependent deformation tests and 100 mm cubes for compressive strength.

Shrinkage and moisture movement specimens, for each strength, were cast together along with companion cubes. The creep specimens along with their companion shrinkage specimens and cubes were cast at later dates. All specimens were cast in lightly oiled steel moulds, in two roughly equal layers, and were compacted by means of the high frequency vibrating table. The specimen surfaces were trowelled smooth approximately 2 hours after casting, the moulds were covered with polythene sheeting and left in the laboratory for 24 hours before demoulding.

6.3.3 Curing Conditions

6.3.3.1 Shrinkage Specimens

Shrinkage specimens were cured under the following curing conditions:

(a) Water at $22^{o}C \pm 3^{o}C$.

(b) Uncontrolled laboratory.

(c) Constant temperature, $16^{o}C \pm 0.5^{o}C$, and humidity, 50% ± 2%, room, C.T.H.R.

(d) Outside under a lean-to roof, sheltered from the rain and sun but subject to temperature and relative humidity variations.

6.3.3.2 Moisture Movement Specimens

Moisture movement specimens were alternately cured in conditions (a) and (b).

6.3.3.3 Creep Specimens

Creep specimens were cured under condition (c), both prior to and after loading.

6.3.4 Loading Conditions for Creep Specimens

A typical creep rig is shown in Figure 6.1. For each concrete strength, the specimens were loaded as near to 28 days as was practically possible. Prior to loading the concrete strength was obtained by crushing three cubes which had been stored with the specimens. Two stress strength ratio's of 0.3 and 0.5 were chosen for each concrete strength and thus the stress to be applied could be calculated. These stress-strength ratio's were chosen since they cover the limits used in design recommendations, from one-half the cube strength at transfer to one-third the strength in bending at working load, according to CP 110 (54) and stress of the order of 0.6 x the cylinder strength at transfer and 0.45 x cylinder strength at working load, according to A.C.I. (26).

6.3.5 Instrumentation and Test Procedure

6.3.5.1 Shrinkage and Moisture Movement Specimens

The shrinkage and moisture movement specimens were demoulded approximately 24 hours after casting. Demec discs were attached to the four faces of each specimen over a gauge length of 305 mm. Initial strain readings were taken within one hour of demoulding and thus the plotted and tabulated strains are

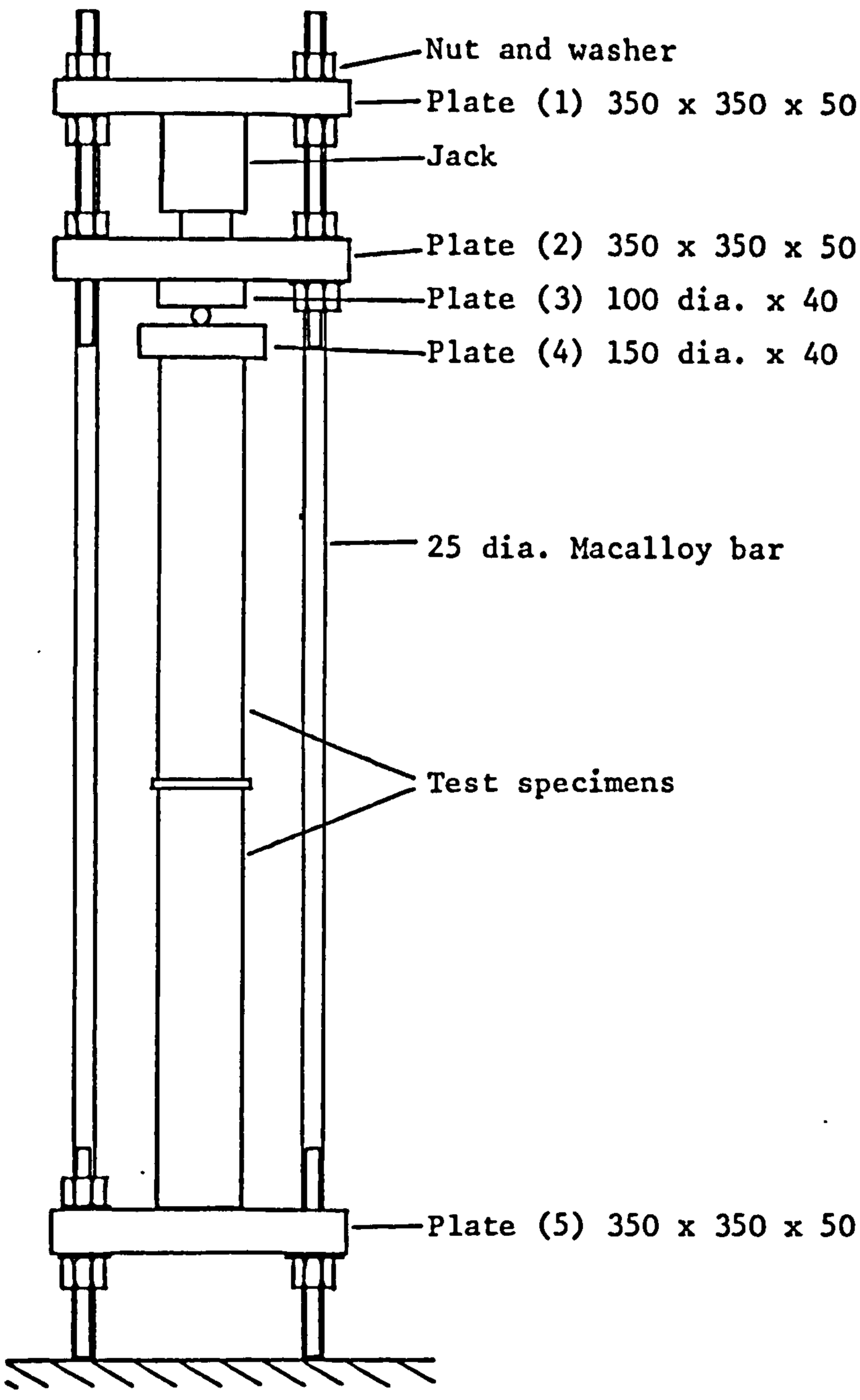

FIGURE 6.1 TYPICAL CREEP RIG

those which occurred after this time. For each curing condition two specimens were prepared, the plotted and tabulated results are thus the average of eight readings.

For the shrinkage specimens readings were taken at close intervals at early ages but the period between readings was gradually increased as the specimens matured. The maximum interval between readings was three months.

The moisture movement specimens were initially stored in the uncontrolled laboratory condition after demoulding. They were left there until the decrease in density as a percentage of the density at demoulding was approximately 0.01% per day on average. They were then transferred to the water tank and left until the increase in density as a percentage of the density at demoulding was approximately 0.01% per day on average. This resulted in a period of approximately 60 days drying and 45 days wetting for the first cycle, and these periods were maintained during subsequent cycles.

All strain measurements were made using a Demec Extensometer with a gauge length of 305 mm, and a sensitivity of 6.55×10^{-6} m/m per division.

6.3.5.2 Creep Specimens

As with the shrinkage specimens, demec discs were fixed to all four faces of each specimen over a 305 mm gauge length and initial strain readings taken within one hour of demoulding. Demec discs were also attached to the Macalloy bars on each creep rig. At approximately 28 days after casting two specimens were arranged in their respective rigs as shown in Figure 6.1. With the rig unloaded, strain readings were taken in the specimens and the Macalloy bars. The rig was then loaded in three stages by means of a calibrated jack, with the variation in strain readings on each being checked at each stage. When the required stress had been applied to the specimens and the concrete strains measured, the strains in the Macalloy bars were read. Plate (2) was then tightened down and the jack released. The strains in the Macalloy bars were checked to ensure that they were sensibly the same as those under the jack load.

The required stress was maintained on the rig by periodically reloading, frequently at first but less frequently as the age since loading increased. The

maximum period between reloading was three months.

6.4 Test Results and Discussion

6.4.1 Shrinkage

Shrinkage test details are shown in Table 6.1. The shrinkage-time curves are shown in Figures 6.2-6.4 and shrinkage data at different ages is shown in Table 6.2.

The results show that the cement content and water-cement ratio have a significant effect on the shrinkage of Lytag-sand concrete. Shrinkage, and expansion for water stored specimens, increases with increasing cement content and decreasing water-cement ratio. Similar findings have been reported for all-Solite concrete (49) and for Taclite, Lytag and limestone concretes with natural sand fines (61).

The effect of curing conditions is less pronounced at lower cement contents but does become more marked with increasing cement content, and therefore, strength. For the 30 N/mm^2 concrete, the shrinkage at last reading, for the specimens stored outside was about 83% of the shrinkage for the specimens stored under constant temperature and humidity conditions. For the 60 N/mm^2 concrete the corresponding value was 74%. Other investigators (49, 61) have reported a lower shrinkage for externally stored specimens with the values, as a percentage of the constant temperature and humidity stored specimens being 40%, or less. However, these specimens were stored on a roof, subject to rain and direct sunlight. The aim of the work reported here is to simulate the conditions under which external elements, such as bridge beams, will be expected to perform. While it is true that, for example in a bridge, the edge beams will be subjected to rain and direct sunlight the remainder of the structure will only be subjected to air temperature and humidity variations. Thus the expected shrinkage of such elements will be greater than shown by the above mentioned investigators (49, 61).

For the specimens stored in the C.T.H.R. and the laboratory there is little difference in the shrinkage at last reading although the seasonal temperature and humidity fluctuations are reflected in the laboratory stored specimens.

TABLE 6.1 DETAILS OF MIX PROPORTIONS, CURING CONDITIONS AND TEST DATA FOR SHRINKAGE TESTS

Specimen No.	28 Day Cube Strength (N/mm^2)	Cement Content (kg/m^3)	Cement:Sand: Lytag Ratio by Weight	Total Water/ Cement Ratio	Curing Conditions	Age at Last Reading (Days)	Shrinkage at Last Reading ($m/m \times 10^{-6}$)
SH 30-1	32.0	255	1:2.78:2.80	1.02	Water	536	-140
SH 45-1	44.5	335	1:1.93:2.13	0.78		533	-130
SH 60-1	58.0	485	1:1.06:1.47	0.54		501	-170
SH 30-2	29.5	255	1:2.78:2.80	1.02	Laboratory	536	595
SH 45-2	43.0	335	1:1.93:2.13	0.78		533	750
SH 60-2	59	485	1:1.06:1.47	0.54		501	915
SH 30-3	31.0	255	1:2.78:2.80	1.02	C.T.H.R.	536	660
SH 45-3	44.0	335	1:1.93:2.13	0.78		533	810
SH 60-3	58.5	485	1:1.06:1.47	0.54		501	980
SH 30-4	30.5	255	1:2.78:2.80	1.02	External	536	550
SH 45-4	41.0	335	1:1.93:2.13	0.78		533	660
SH 60-4	58.0	485	1:1.06:1.47	0.54		501	730

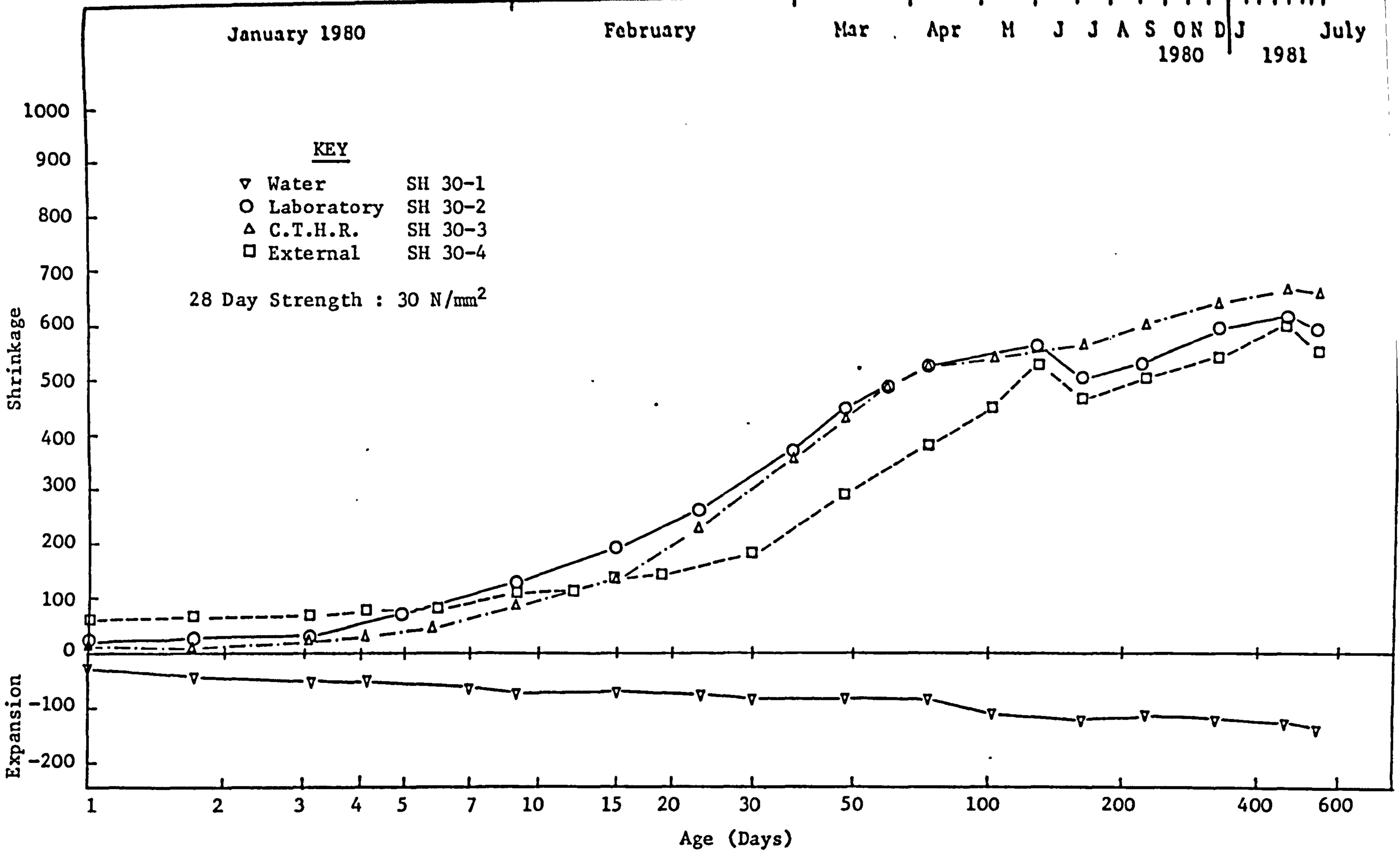

FIGURE 6.2 SHRINKAGE AND EXPANSION WITH TIME

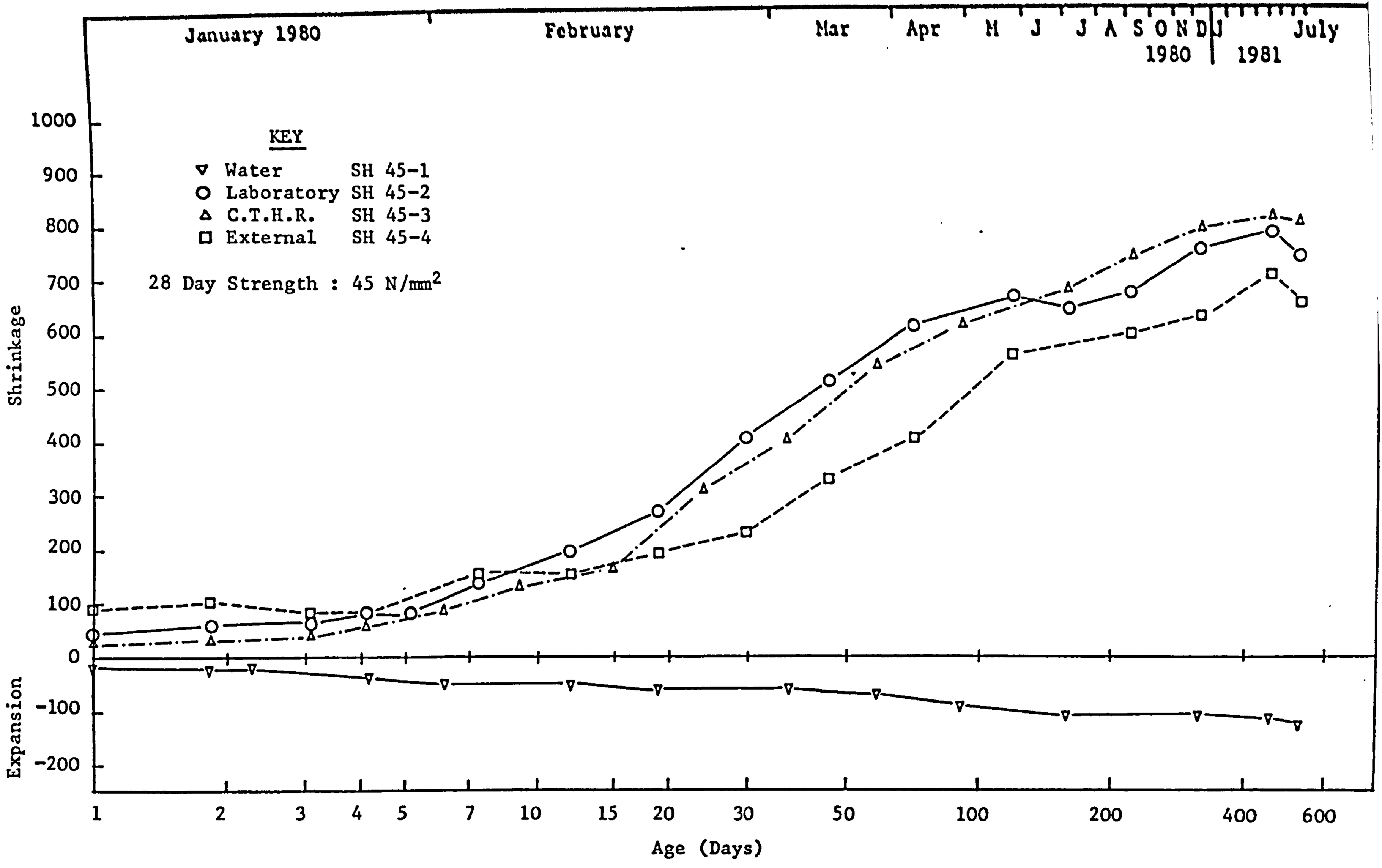

FIGURE 6.3 SHRINKAGE AND EXPANSION WITH TIME

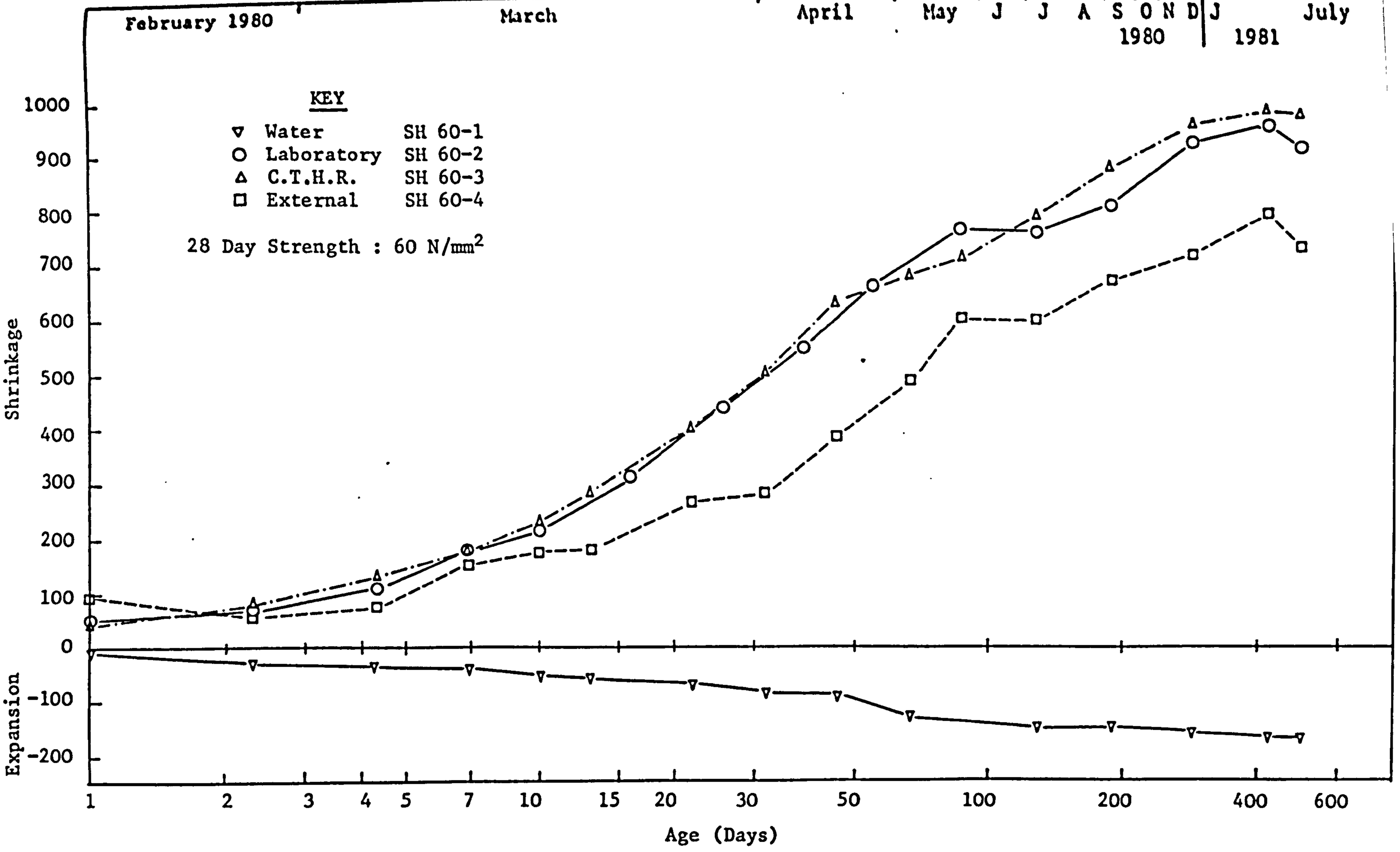

FIGURE 6.4 SHRINKAGE AND EXPANSION WITH TIME

TABLE 6.2 SHRINKAGE AT DIFFERENT AGES OF LYTAG-SAND CONCRETE

Specimen No.	Curing Conditions	Shrinkage Strain at 500 Days ($m/m \times 10^{-6}$)	Shrinkage Strain at 1 Month ($m/m \times 10^{-6}$)	Col. 4 / Col. 3 (%)	Shrinkage Strain at 3 Months ($m/m \times 10^{-6}$)	Col. 6 / Col. 3 (%)	Shrinkage Strain at 6 Months ($m/m \times 10^{-6}$)	Col. 8 / Col. 3 (%)	Shrinkage at Strain 1 Year ($m/m \times 10^{-6}$)	Col. 10 / Col. 3 (%)
1	2	3	4	5	6	7	8	9	10	11
SH 30-1	Water	-135	-85	63	-100	74	-120	89	-125	93
SH 45-1		-125	-60	48	-95	76	-110	88	-115	92
SH 60-1		-170	-80	47	-140	82	-150	88	-165	97
SH 30-2	Laboratory	605	325	54	540	89	510	84	600	99
SH 45-2		765	410	54	645	84	660	86	770	101
SH 60-2		915	480	52	770	84	805	88	945	103
SH 30-3	C.T.H.R.	665	305	46	535	80	575	86	650	98
SH 45-3		815	360	44	620	76	710	87	805	99
SH 60-3		980	485	49	720	73	870	89	975	99
SH 30-4	External	575	180	31	425	74	475	83	560	97
SH 45-4		685	230	34	475	69	590	86	665	97
SH 60-4		730	280	38	605	83	670	92	765	105

Specimens continuously moist cured showed expansive strains due to the absorption of moisture by the cement gel. At last reading the expansion varied between 16-21% of the shrinkage under constant temperature and humidity conditions.

Table 6.2 shows the shrinkage at various ages as a percentage of the 500 day shrinkage. For each curing condition this ratio remains remarkably constant regardless of the compressive strength of the concrete.

6.4.2 Moisture Movement

For exposed elements subjected to periodic drying and wetting there will be corresponding shrinkage and expansion. This reversal in strain, due to varying moisture content in the element, is known as moisture movement. The aim of this series of tests was to estimate the maximum probable moisture movement which could occur in Lytag-sand concrete exposed to the weather. The periods of wetting and drying were chosen as described in 6.3.5.1 and were approximately 45 and 60 days respectively. Although in this country it is rare to see prolonged periods of sunshine it is not unusual during the summer months to have two consecutive months during which very little rain falls. Similarly it is not unusual to have two consecutive months during which rain persistently falls and the relative humidity is high.

Figure 6.5 shows the effect of continuous drying or wetting on the volume-density relationship. In the case of drying specimens it can be seen that an appreciable reduction in density, due to water loss, can occur before any appreciable shrinkage takes place. This can be accounted for by the fact that the absorbed water contained within the aggregate particles migrates into the mortar as the specimen dries thus reducing the early shrinkage. Similar observations have been made by other investigators (60, 61). Balendran (61) suggested that the moisture contribution from the aggregate is a function of its particle shape and surface texture. The author based this statement on results for Taclite and Lytag concretes. Despite the fact that the rate of and capacity for water absorption is similar for both aggregates, greater moisture loss occurred from the rounded fine pored Lytag aggregate than from the more irregular

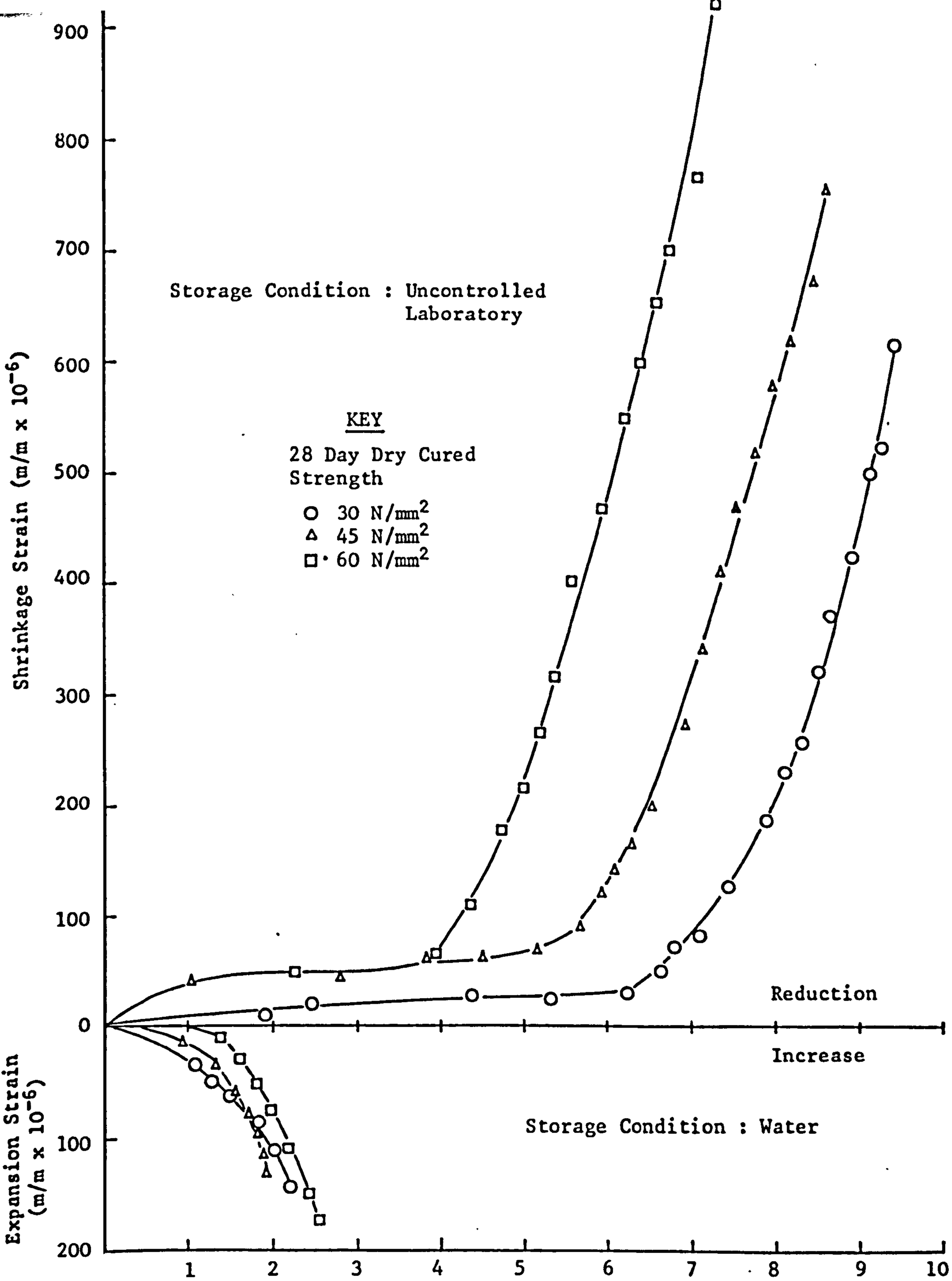

FIGURE 6.5 VARIATION OF SHRINKAGE AND EXPANSION WITH DENSITY

Taclite aggregate, with its larger surface pores which could be blocked by mortar.

Figures 6.6-6.8 show the shrinkage and expansion of continuously dry cured and wet cured specimens and the moisture movement associated with cyclic wetting and drying. For the 30 and 45 N/mm^2 concrete specimens five drying and wetting cycles were completed but unfortunately the 60 N/mm^2 specimens were accidentally destroyed after only two cycles had been completed. The figures show that after two or three cycles, the moisture movement occurring between extremes of wetting and drying remains sensibly constant and reflects the seasonal variations associated with the continuously dry cured specimens in the uncontrolled laboratory environment. The moisture movement appears to be of the order of 300-350 x 10^{-6} m/m for the various concrete strengths.

Figures 6.9-6.11 show the variation in density associated with the moisture movement indicated in Figures 6.6-6.8 respectively. Again it can be seen that after the second or third cycle, the density variation between extremes of wetting and drying remains sensibly constant. The variation in density is, however, dependent on the concrete strength with approximately 6.5% density variation for the 30 N/mm^2 concrete as opposed to approximately 3.5% for the 60 N/mm^2 concrete.

6.4.3 Creep

Details of the creep tests are given in Table 6.3. Test results are shown in Figures 6.12-6.13 with the creep at various ages shown in Table 6.4. One year creep coefficients are shown in Table 6.5 and the elastic strains at loading and unloading along with creep recovery are shown in Table 6.6.

The results show the effect of some factors on creep and these are discussed below.

6.4.3.1 Water-Cement Ratio

Figures 6.12 and 6.13 show that the effect of increasing the water-cement ratio is to increase the creep. An increase in the total water-cement ratio from 0.54 to 1.02 produced increases of 32% and 23% in the one year creep values for stress-strength ratio's of 0.3 and 0.5 respectively. Similar effects have

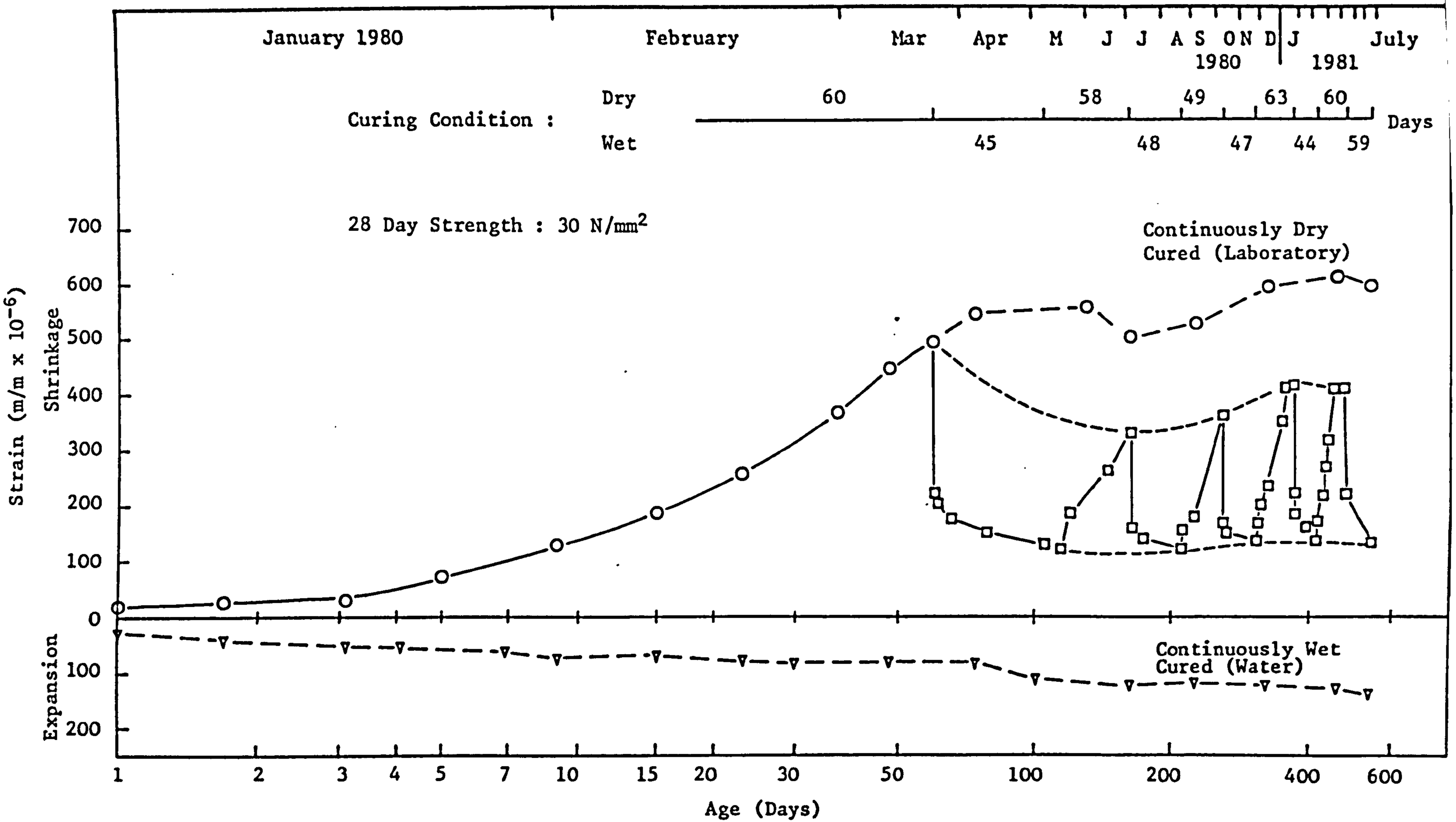

FIGURE 6.6 MOISTURE MOVEMENT WITH TIME

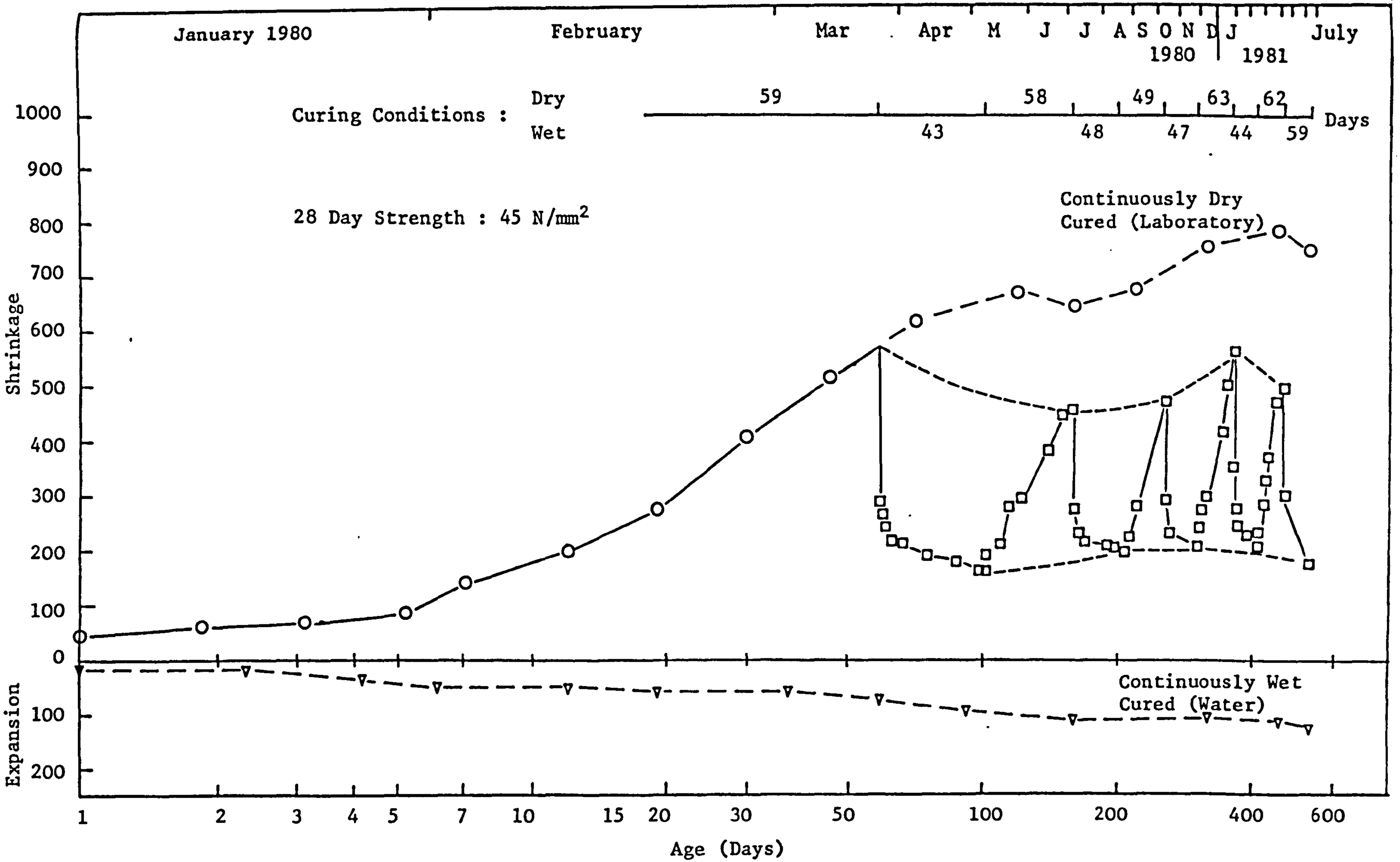

FIGURE 6.7 MOISTURE MOVEMENT WITH TIME

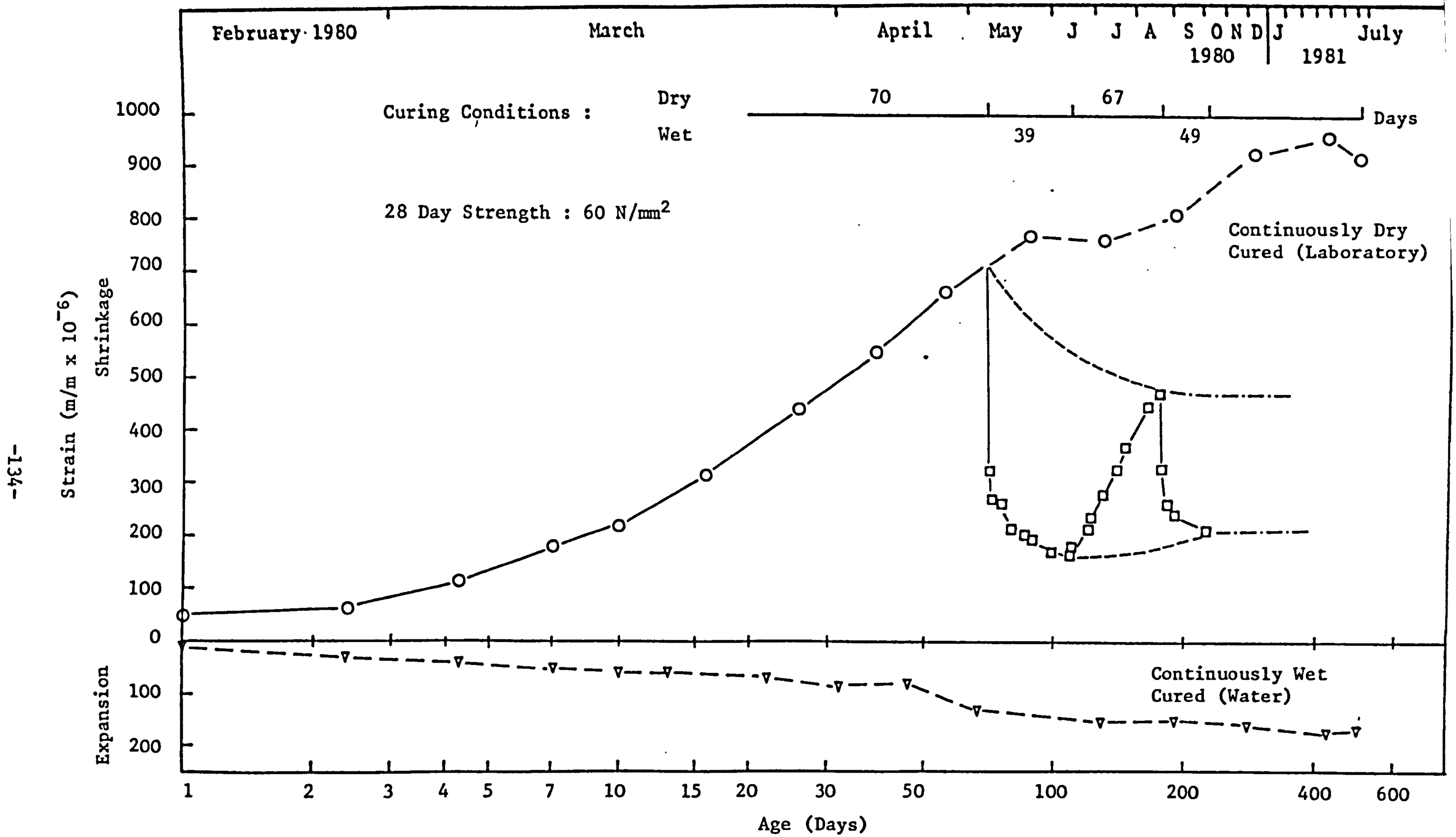

FIGURE 6.8 MOISTURE MOVEMENT WITH TIME

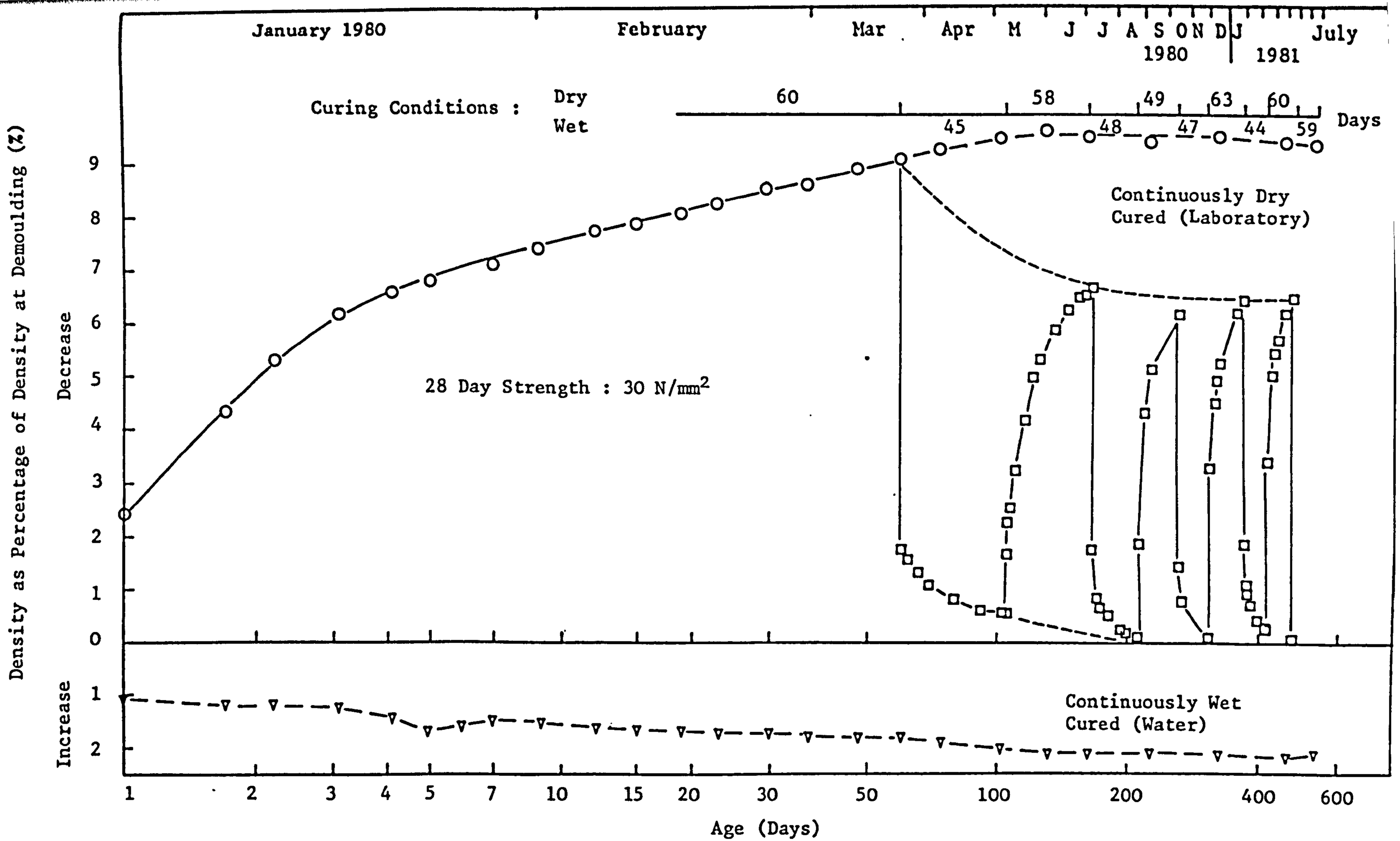

FIGURE 6.9 DENSITY VARIATION WITH TIME

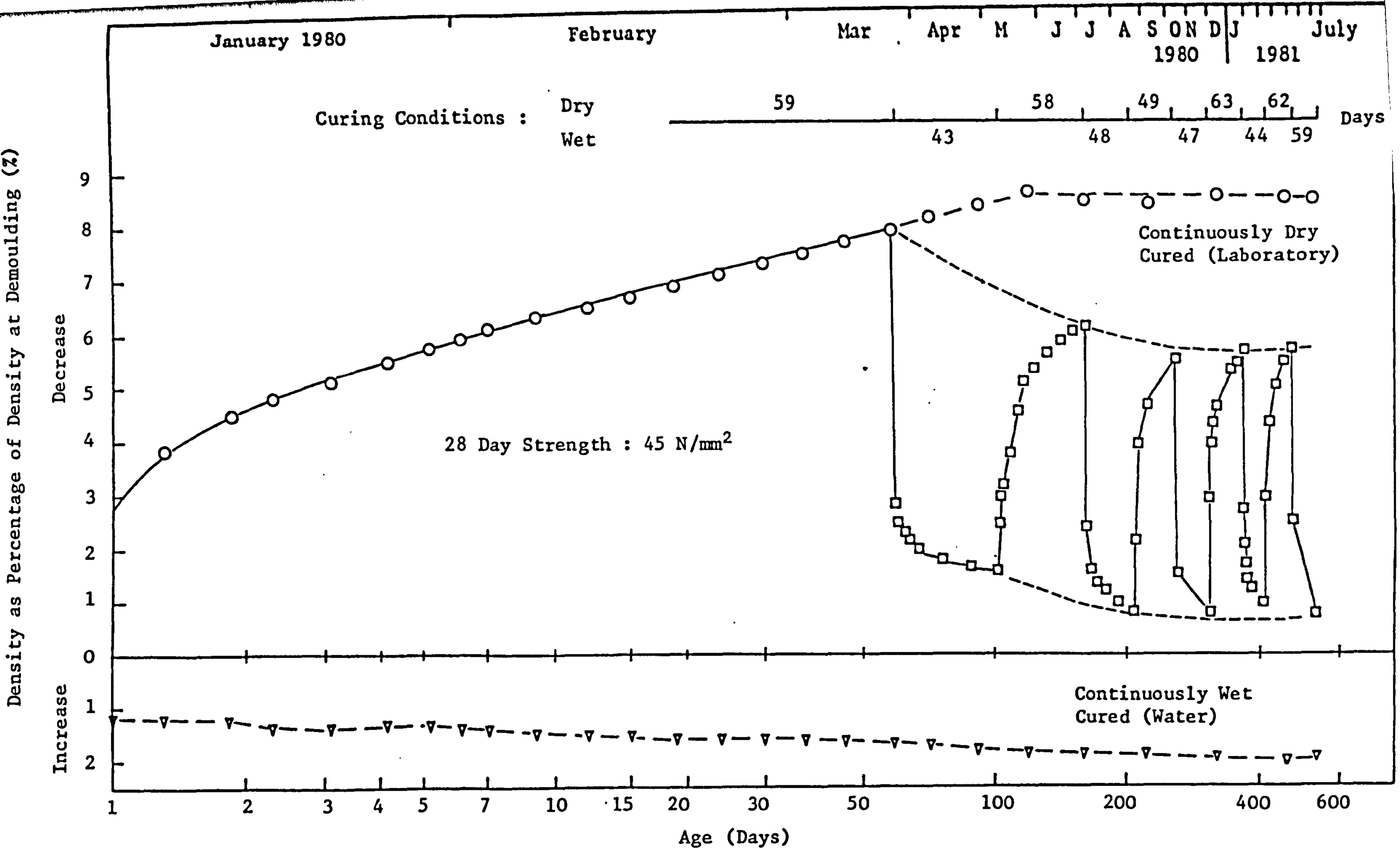

FIGURE 6.10 DENSITY VARIATION WITH TIME

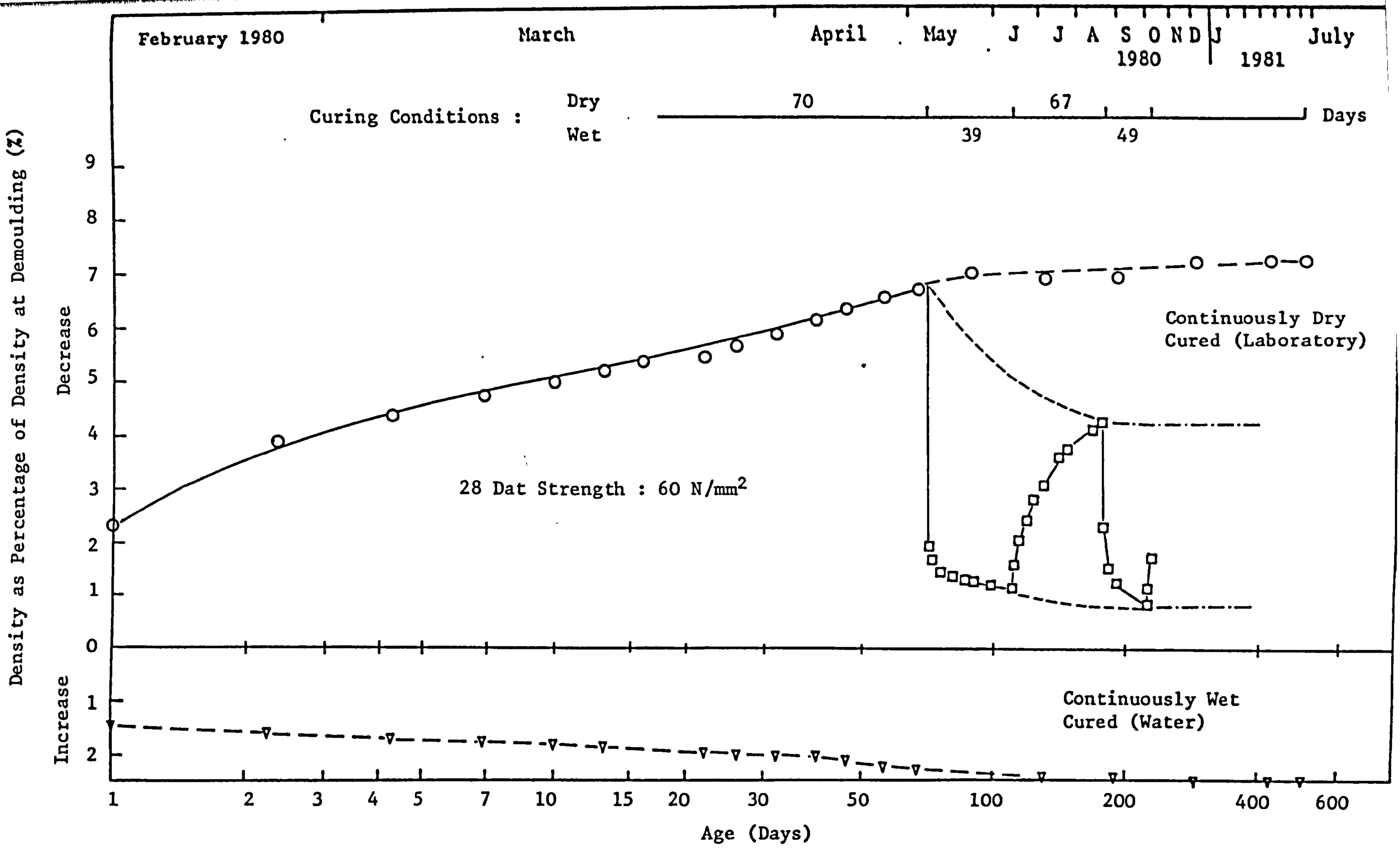

FIGURE 6.11 DENSITY VARIATION WITH TIME

TABLE 6.3 DETAILS OF LOADING CONDITIONS FOR CREEP TESTS

Creep Rig No.	Age at Loading (Days)	Cube Strength at Loading (N/mm^2)	Loading Stress (N/mm^2)	$\frac{\text{Stress}}{\text{Strength}}$
CR 30-1	30	31.5	8.8	0.28
CR 30-2	32	31.5	16.0	0.51
CR 45-1	27	43.0	12.2	0.28
CR 45-2	27	43.0	20.6	0.48
CR 60-1	30	59.0	16.2	0.27
CR 60-2	29	59.0	27.7	0.47

Notes

1. Mix proportions are the same as those given in Table 6.1.

2. All creep rigs were kept in the constant temperature and humidity room at 16 ± 0.5°C and 50 ± 2% relative humidity.

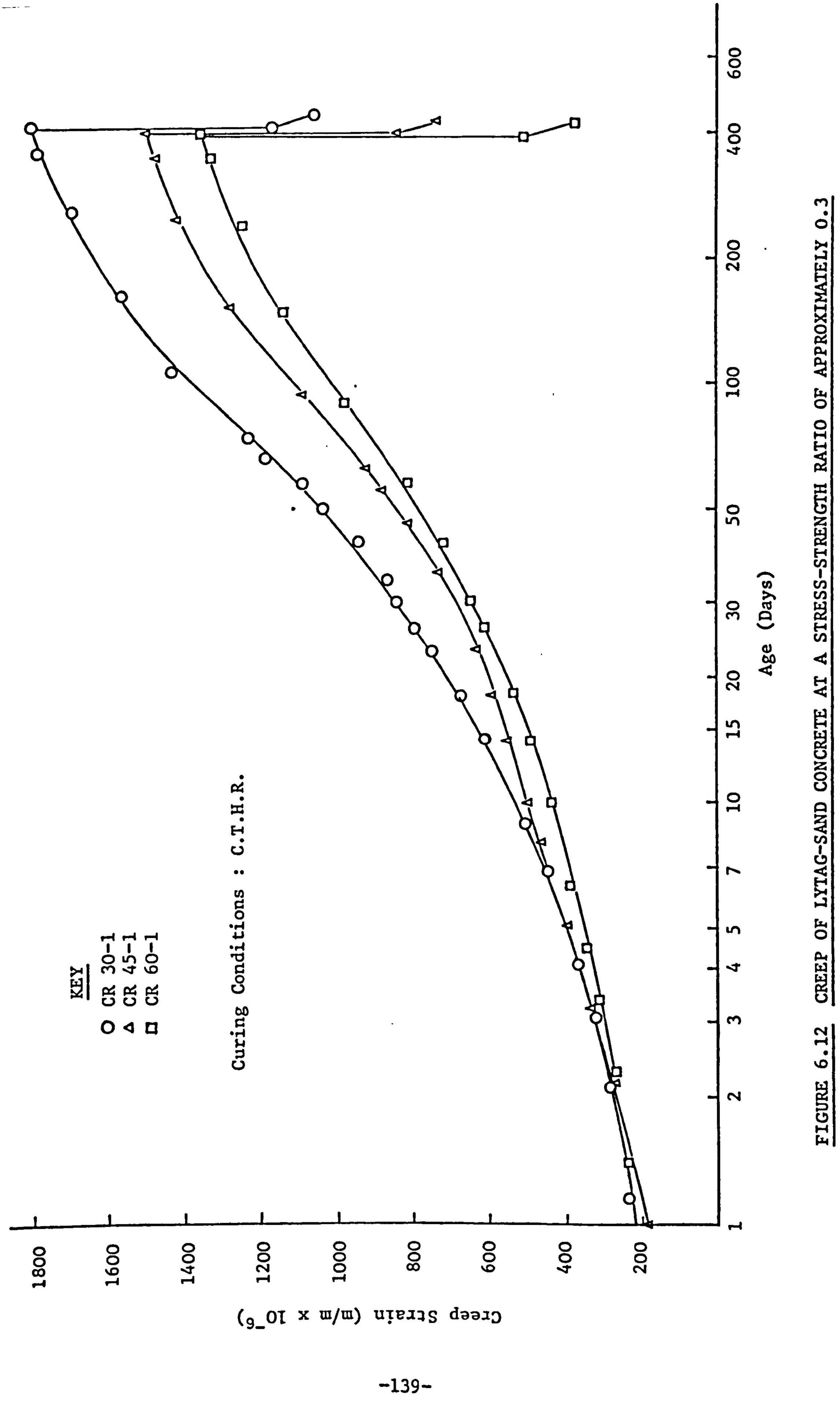

FIGURE 6.12 CREEP OF LYTAG-SAND CONCRETE AT A STRESS-STRENGTH RATIO OF APPROXIMATELY 0.3

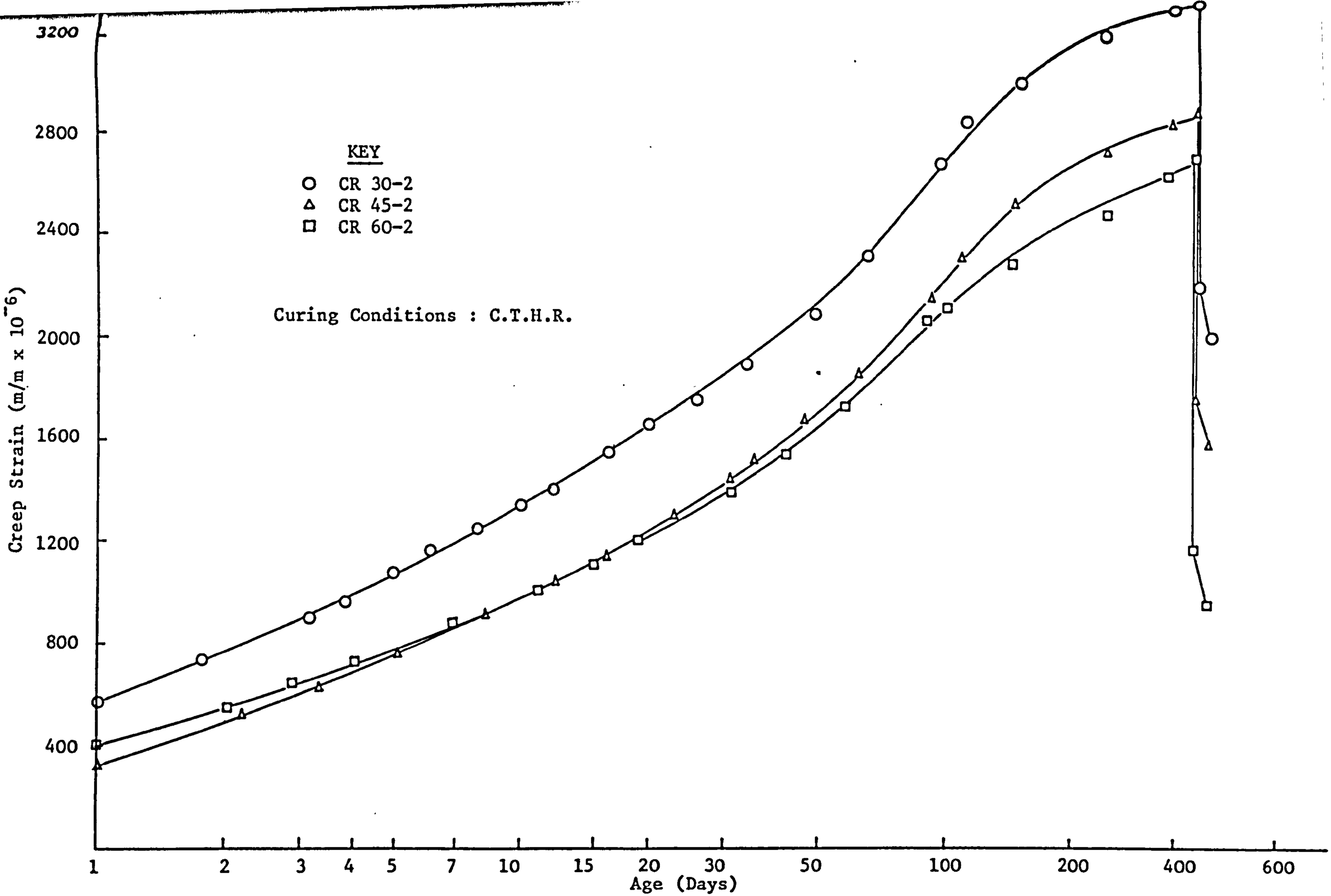

FIGURE 6.13 CREEP OF LYTAG-SAND CONCRETE AT A STRESS-STRENGTH RATIO OF APPROXIMATELY 0.5

TABLE 6.4 CREEP STRAIN OF LYTAG-SAND CONCRETE AT DIFFERENT AGES

Creep Rig No.	Creep Strain at 365 Days (m/m x 10^{-6})	Creep Strain at 1 Day (m/m x 10^{-6})	Col. 3 / Col. 2 (%)	Creep Strain at 7 Days (m/m x 10^{-6})	Col. 5 / Col. 2 (%)	Creep Strain at 30 Days (m/m x 10^{-6})	Col. 7 / Col. 2 (%)	Creep Strain at 90 Days (m/m x 10^{-6})	Col. 9 / Col. 2 (%)	Creep Strain at 180 Days (m/m x 10^{-6})	Col. 11 / Col. 2 (%)
1	2	3	4	5	6	7	8	9	10	11	12
CR 30-1	1780	235	13	446	25	844	47	1340	75	1606	90
CR 45-1	1500	196	13	455	30	690	46	1085	72	1345	90
CR 60-1	1340	230	17	403	30	654	49	990	74	1200	90
CR 30-2	3290	568	17	1210	37	1845	56	2600	79	3040	92
CR 45-2	2850	313	11	860	30	1430	50	2145	75	2645	93
CR 60-2	2660	404	15	880	33	1390	52	2070	78	2400	90

TABLE 6.5 ONE YEAR CREEP COEFFICIENTS FOR LYTAG-SAND CONCRETE

Creep Rig No.	Instantaneous Elastic Strain ($m/m \times 10^{-6}$)	Modulus of Elasticity from Col. (2) (kN/mm^2)	Creep Strain at 365 Days ($m/m \times 10^{-6}$)	Specific Creep at 365 Days (10^{-6} per N/mm^2)	Creep Coefficient: $\frac{\text{Col. (4)}}{\text{Col. (2)}}$
(1)	(2)	(3)	(4)	(5)	(6)
CR 30-1	497	17.7	1780	202	3.58
CR 45-1	626	19.5	1500	127	2.40
CR 60-1	710	22.8	1340	83	1.89
CR 30-2	1030	15.5	3290	206	3.19
CR 45-2	1138	18.1	2850	138	2.50
CR 60-2	1310	21.1	2660	96	2.03

TABLE 6.6 ELASTIC STRAIN AT LOADING AND UNLOADING

Creep Rig No.	Instantaneous Elastic Strain ($m/m \times 10^{-6}$)	Age at Unloading (Days)	Instantaneous Recovery ($m/m \times 10^{-6}$)	Col. 4 / Col. 2 (%)	Final Creep Prior to Unloading ($m/m \times 10^{-6}$)	Creep Recovery at 28 Days After Unloading ($m/m \times 10^{-6}$)	Col. 7 / Col. 6 (%)
1	2	3	4	5	6	7	8
CR 30-1	497	400	629	127	1800	110	6
CR 45-1	626	389	660	105	1501	104	7
CR 60-1	710	384	862	121	1371	132	10
CR 30-2	1030	396	1102	107	3302	195	6
CR 45-2	1138	389	1106	97	2868	183	6
CR 60-2	1310	385	1539	117	2724	230	8

been reported by other investigators (110, 113).

6.4.3.2 Stress-Strength Ratio

The effect of stress-strength ratio on creep is shown in Figures 6.12 and 6.13 and Table 6.5. For a given concrete strength the absolute values of creep increase with increasing stress-strength ratio but the one year values of specific creep and creep coefficient remain sensibly constant. A similar effect is apparent in Balendrans results (61) on Taclite concrete, for stress-strength ratio's of 0.25 and 0.33. The results in Table 6.5 would tend to suggest that the assumption of a linear relationship between creep and stress-strength ratio for values of stress-strength ratio between 0.25 and 0.5 is valid. Bennet and Loat (110) in their tests on dense concrete have shown that a linear relationship exists between values of stress-strength ratio of 0.33 and 0.5. Jones and Hirsch (104) have shown that with expanded clay concrete the limit of proportionality is 0.57 whereas Hardwick (116) in his tests on Aglite concrete showed the limit of proportionality to be 0.42.

6.4.3.3 Elastic Strains and Creep Recovery

Table 6.6 shows the instantaneous elastic strain at loading and the instantaneous recovery at unloading along with the creep recovery after 28 days. One interesting point to arise from this series of tests is that in all but one case, the elastic strain at unloading, is greater than the elastic strain at loading. This is contradictory to the results of Balendrans tests (61) which showed that for sand replaced Taclite, Lytag and limestone concretes the opposite was true. For the Lytag-sand specimens tested by Balendran (61), with a cube strength of 60 N/mm^2 and loaded to a stress-strength ratio of 0.25 at 28 days and allowed to dry under constant temperature and humidity conditions, the ratio of recovery strain to loading strain was 0.97. For the specimens tested by the author, the equivalent ratio is of the order of 1.20. The reason for this could possibly be explained by the mix proportions. Balendrans mix proportions for a cube strength of 60 N/mm^2 were 1:1.56:1.29 by weight of cement, sand and Lytag coarse with a total water-cement ratio 0.55. The mix proportions used by the author were 1:1.06:1.47 and 0.54 respectively, Table 6.1.

Thus it can be seen that the mix used by the author contained a higher volume of Lytag coarse material and a lower volume of sand fines. The lower modulus of elasticity of Lytag as opposed to sand may be the reason for the above phenomenon.

Balendrans results (61) indicated that the majority of creep recovery occurs within 28 days of unloading. Table 6.6 shows that the creep recovery after 28 days as a percentage of the creep at unloading varies from 6-10%. In general the higher the concrete strength the higher the percentage creep recovery.

6.4.4 Comparisons of Shrinkage and Creep with Published Data

Shrinkage and creep data from this and other investigations are listed in Table 6.7.

6.4.4.1 Shrinkage

Table 6.7 indicates that a wide range of shrinkage values exists for both lightweight and dense aggregate concretes. In general the range of values for lightweight concretes is 153-1200 x 10^{-6} m/m and for dense concrete 200-1420 x 10^{-6} m/m. Thus it can be seen that in both dense and lightweight concrete it is not possible to come to any general conclusions valid for all types of concrete and that for both dense and lightweight concrete, shrinkage is a function of many variables including mix proportions, aggregate type and quality, cement type and curing conditions.

In general, Lytag-sand concrete compares favourably with dense concretes on a shrinkage basis. The results obtained by the author are similar to those of Brooks and Neville (40, 41), for Lytag-sand concrete, using rapid hardening cement and with those of Orangun (91) for all-Lytag concrete. Balendrans results (61) are, however, approximately 35% lower than the results of the present investigation for a concrete strength of 60 N/mm^2. The reason for this difference is probably due to the mix proportions. The cement contents for Balendrans (61) tests and the authors tests on 60 N/mm^2 concrete are 450 and 485 kg/m^3 respectively. The total water-cement ratio's are 0.55 and 0.54 respectively and, therefore, the total water content of the authors mixes is

TABLE 6.7 COMPARISON OF SHRINKAGE AND CREEP WITH PUBLISHED DATA

Investigators	Concrete Type	Cube Strength at 28 Days (N/mm^2)	Curing Conditions	Age at Last Reading (Days)	Age at Loading (Days)	Stress-Strength Ratio	Specific Creep ($\times 10^{-6}$ per N/mm^2)	Shrinkage ($m/m \times 10^{-6}$)
Shideler (19)	Various L.W.A.	31*	21°C & 50% R.H.	365	7	0.15-0.20	120-210	670-900
	"	46*	"	"	"	0.32-0.40	60-75	510-600
	Expanded Slate	30*	"	"	"	0.18	120	850
	Gravel	29*	"	"	"	0.19	120	665
	"	49*	"	"	"	0.39	67	505
Troxell et al (114)	Limestone	-	21°C & 50% R.H.	30 Years	28	-	112	650
	Gravel	-	"	"	"	-	172	880
	Sandstone	-	"	"	"	-	272	1280
Best & Polivka (102)	Expanded Shale	20.5*	21°C & 50% R.H.	520	42	0.4	103-145	520-620
	"	34.5*	"	"	"	"	75-100	330-425
	Gravel	20.5*	"	"	"	"	140	940
	"	34.5*	"	"	"	"	88	920
Hardwick (116)	Aglite	24-34.5	19°C & 70% R.H.	540	7-8	0.28-0.54	138-161	700
Orangun (91)	Lytag	34-42	19°C & 70% R.H.	540	28	0.20-0.36	87-100	630-960
Teychenné (11)	Aglite	235-710+	to BS 1881 (86) Procedure	-	-	-	-	400-1200
	Foamed Slag	235-890+		-	-	-	-	350-950
	Leca	300-415+		-	-	-	-	550-700
	Lytag	235-650+		-	-	-	-	200-850
	Sand & Gravel	235-415+		-	-	-	-	200-350

TABLE 6.7 COMPARISON OF SHRINKAGE AND CREEP WITH PUBLISHED DATA - CONTINUED

Investigators	Concrete Type	Cube Strength at 28 Days (N/mm^2)	Curing Conditions	Age at Last Reading (Days)	Age at Loading (Days)	Stress-Strength Ratio	Specific Creep ($\times 10^{-6}$ per N/mm^2)	Shrinkage ($m/m \times 10^{-6}$)
Swamy & Ibrahim (46)	Solite with Very Fine Cement	32.5-52	$16^{\circ}C$ & 50% R.H.	567-686	1 & 28	0.34-0.53	87-126	805
		45.5-52	28 Days in M.R. then C.T.H.R.	645-686	28	0.35-0.38	74-96	720
		52	Laboratory	595	-	-	-	681
		52	Outside	692	-	-	-	634
Bandyopadhyay (49)	Solite	21-60	$16^{\circ}C$ & 50% R.H.	630&730	-	-	-	550-690
	"	"	Outside	"	-	-	-	153-182
		"	Laboratory	540&630	-	-	-	506-690
Brooks & Neville (40, 41)	Lytag++	17.6-31.2**	$22^{\circ}C$ & 60% R.H.	1800	14	0.3	83-265	680-1180
	Aglite++	18.2-23.5**	"	"	"	"	63-168	475-590
	Gravel++	14.7-36.8**	"	"	"	"	98-500	760-1020
	Gravel++	14.6-36.6**	"	"	"	"	74-370	770-1420
Balendran (61)	Taclite	20-60	$21^{\circ}C$ & 66% R.H.	365&600	28	0.25-0.33	67-68	555-700
	Lytag	60	"	"	"	0.25	59	640
	Limestone	72	"	"	"	"	41	510
Author	Lytag-Sand	31-59	$16^{\circ}C$ & 50% R.H.	365-536	27-32	0.27-0.51	83-206	660-980
		30.5-58	Outside	501-536	-	-	-	550-730
		29.5-59	Laboratory	"	-	-	-	595-915

* - Cylinder crushing strength (N/mm^2)
\+ - Cement content (kg/m^3)
++ - Rapid hardening cement and sand fines
** - 14 day strength.

higher. As was explained in 6.4.3.3 the Lytag volume was higher and the sand volume lower for the authors mixes.

The mixes used in this project were similar to those used commercially by Lytag Limited. Thus it can be seen that when research is being carried out with the aim of providing design data for practical application, the materials used and mix proportions should simulate as closely as possible those that will be used on site.

The present design codes (26, 54) do not specify shrinkage values for lightweight concretes, but suggest that in general the shrinkage of lightweight concrete will be greater than that of dense concrete and that specific design data should be obtained from aggregate manufacturers where possible. CEB-FIP (73) states that the shrinkage of lightweight concrete may vary between 1.0 and 1.5 times that of dense concrete. In view of the data shown in Table 6.7, these values would seem reasonable.

6.4.4.2 Creep

Values of total specific creep obtained during this investigation compare favourably with those obtained by Brooks and Neville (40, 41) but are again greater than those of Balendran (61) for a cube strength of 60 N/mm^2. The reasons for this are the same as those given in 6.4.4.1. The values obtained are also similar to those obtained by Orangum (91) for all-Lytag concrete but here again the mixes used had lower water-cement ratios.

The test results of Brooks and Neville (40, 41) are interesting in that they show a wide variation in specific creep values for dense concretes. The two dense aggregates used were North Notts gravel, considered to be a good aggregate and Stourton, a rather poor quality rounded aggregate. The specific creep was, however, higher in the North Notts aggregate concrete than the Stourton aggregate concrete. This is further evidence that even with dense concretes creep is not consistent and is difficult to predict without test data relating to the type of concrete in question.

CP 110 (54) states that creep will, in general, be greater than that for dense aggregate concrete and that reference should be made to specialist

information to ascertain values. Balendran's results (61) showed that the creep of Lytag concrete was approximately 40% greater than that of a good quality limestone aggregate concrete. In view of this a value of 1.5 times the values for dense concrete given in CP 110 would seem appropriate.

6.5 Prediction of Shrinkage and Creep

Creep prediction methods generally take two forms, namely:

(a) a creep time relationship in the form of an equation which usually requires the determination of one or more constants experimentally;

(b) a standard creep curve which can be modified by a series of correction factors to allow for mix proportions, storage conditions etc.

Method (b) does not require experimental data, but is generally less accurate than the empirical equation, method (a).

In the analysis of the shrinkage and creep results obtained during this investigation a hyperbolic type equation was found to suitably describe the data. The form of the equation, as suggested by Ross (131), is

$$C = \frac{t}{a + bt} \qquad \ldots\ (6.1)$$

where C = creep or shrinkage ($m/m \times 10^{-6}$)

t = time after loading for creep or after initial readings for shrinkage (days)

a and b are constants.

If equation (6.1) is rearranged into the following,

$$\frac{t}{C} = bt + a \qquad \ldots\ (6.2)$$

it can be seen that a plot of t/C against t will result in a straight line of slope b and intercept a. It can also be seen from equation (6.1) that as t tends to infinity the limiting value of $C = 1/b$.

Typical curves for determining the constants a and b are shown in Figures 6.14 and 6.15. The constants predicted by this method along with the measured and predicted values of shrinkage and creep at different ages are given in Table 6.8.

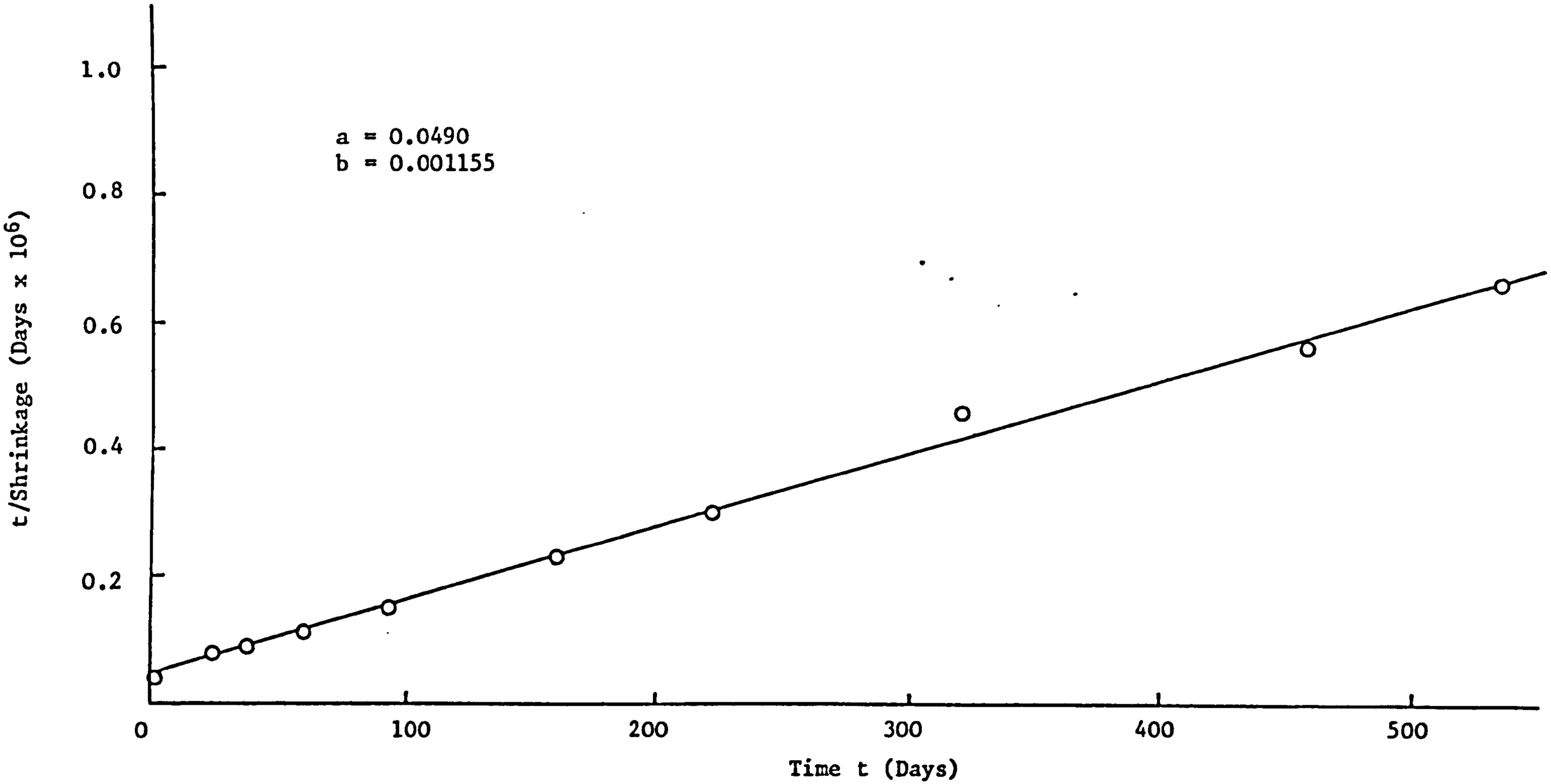

FIGURE 6.14 TYPICAL DETERMINATION OF SHRINKAGE CONSTANTS FOR EQUATION (6.1)

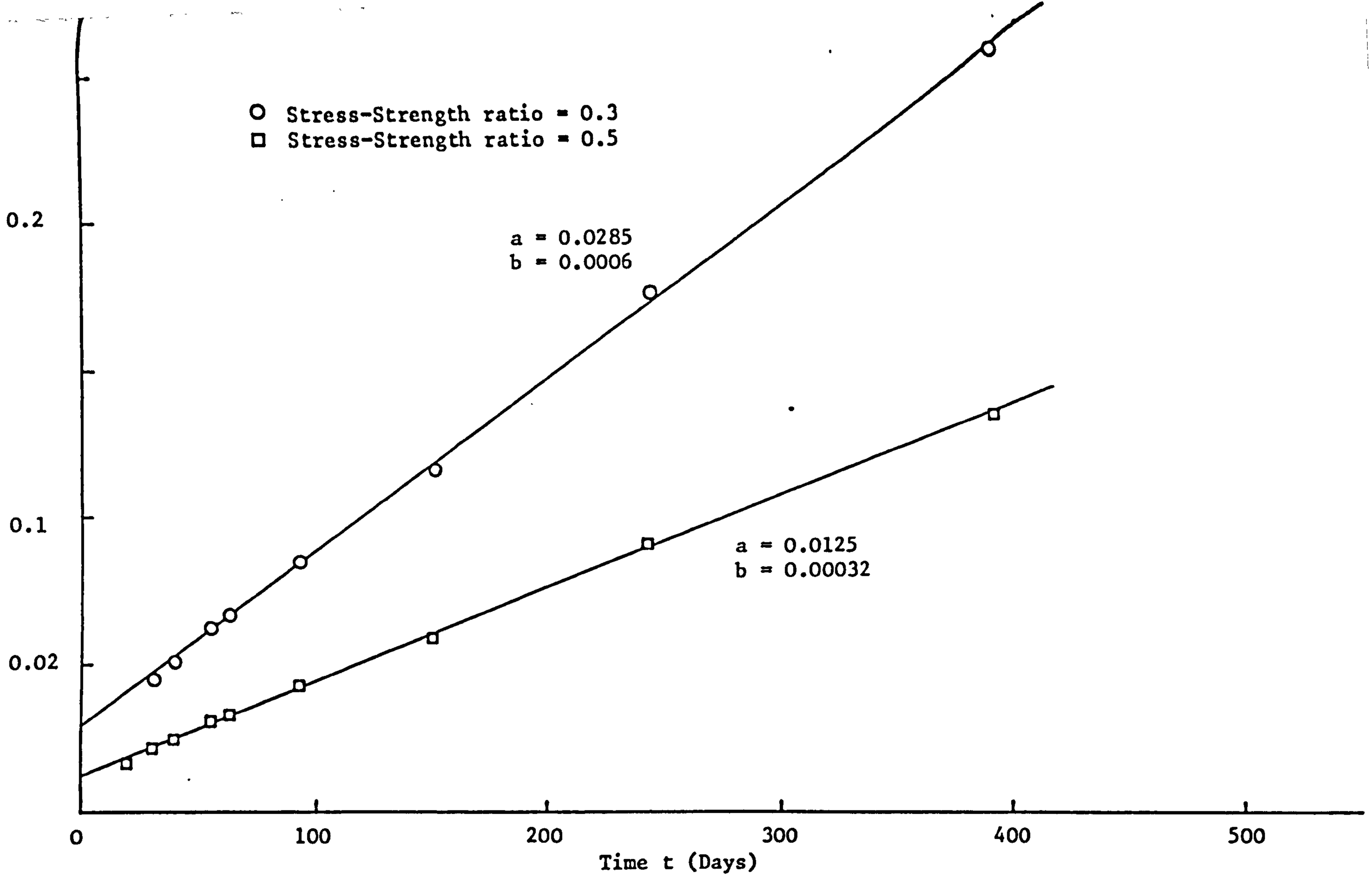

FIGURE 6.15 TYPICAL DETERMINATION OF CREEP CONSTANTS FOR EQUATION (6.1)

TABLE 6.8 COMPARISON OF PREDICTED AND MEASURED SHRINKAGE AND CREEP VALUES

28 Day Cube Strength (N/mm^2)	Shrinkage Specimen No.	Age (Days)	Constants for Equation 6.1		Shrinkage Strain ($\times 10^{-6}$)		Creep Specimen No.	Constants for Equation 6.1		Creep Strain ($\times 10^{-6}$)	
			a x 10^2	b	Measured	Calculated		a x 10^2	b	Measured	Calculated
30	SH 30-3	30	530	1400	305	315	CR 30-1	215	500	845	820
		90			535	505				1340	1355
		180			575	590				1605	1615
		365			650	645				1785	1790
		∞			-	715				-	2000
	-	30	-	-	-	-	CR 30-2	81	285	1840	1800
		90								2600	2665
		180								3040	3030
		365								3290	3255
		∞								-	3510
45	SH 45-3	30	490	1155	360	360	CR 45-1	285	600	685	645
		90			620	590				1085	1090
		180			710	700				1345	1320
		365			805	775				1495	1475
		∞			-	865				-	1665
	-	30	-	-	-	-	CR 45-2	125	320	1430	1355
		90								2150	2180
		180								2650	2570
		365								2850	2825
		∞								-	3125
60	SH 60-3	30	350	940	485	475	CR 60-1	295	670	655	605
		90			720	750				985	1000
		180			870	880				1215	1200
		365			975	965				1340	1330
		∞			-	1065				-	1495
	-	30					CR 60-2	130	340	1390	1295
		90								2070	2065
		180								2410	2425
		365								2660	2665
		∞								-	2940

Predicted values compare well with measured values, especially at ages greater than 90 days.

Table 6.9 shows the predicted ultimate creep, specific creep and creep coefficient for the specimens tested during this investigation.

6.6 Design Recommendations for Shrinkage of Lytag-Sand Concrete

The basic shrinkage coefficients for Lytag-sand concrete may be taken from Table 6.8 when time equals infinity. To use these values in design, appropriate correction factors should be applied. The final shrinkage coefficient, S, may be determined by the relationship:

$$S = S_c K_h K_d K_s K_c \quad \ldots\ldots (6.3)$$

where S = final value of shrinkage

S_c = basic shrinkage coefficient for non-reinforced concrete (Table 6.8)

K_h = influence of environmental humidity

K_d = influence of the smallest dimension of the element

K_s = influence of the longitudinal steel percentage

K_c = influence of the composition of concrete.

6.6.1 Basic Shrinkage (S_c)

During construction most concrete elements are exposed to the weather which decreases the effect of unrestrained shrinkage in general. After completion however most elements are protected from the weather and are often subject to warm dry atmospheres associated with central heating. Hence the estimated ultimate shrinkage given in Table 6.8 may be taken as the basic shrinkage coefficient S_c.

6.6.2 Relative Humidity Coefficient (K_h)

A study of the variation of shrinkage for different relative humidities has been made by A.C.I. Committee 209 (122). For relative humidities within the range H = 50 to 80% this variation may be expressed as follows:

$$K_h = 1.50 - 0.01\,H \quad \ldots\ldots (6.4)$$

TABLE 6.9 PREDICTED ULTIMATE VALUES OF CREEP, SPECIFIC CREEP AND CREEP COEFFICIENT

Creep Rig No.	Constants for Equation (6.1)		Predicted Ultimate Creep ($m/m \times 10^{-6}$)	Predicted Ultimate Specific Creep (10^{-6} per N/mm^2)	Predicted Ultimate Creep Coefficient
	$a \times 10^2$	b			
CR 30-1	215	500	2000	227	4.02
CR 30-2	81	285	3510	219	3.41
CR 45-1	285	600	1665	136	2.66
CR 45-2	125	320	3125	152	2.75
CR 60-1	295	670	1495	92	2.11
CR 60-2	130	340	2940	106	2.24

For H = 80 to 100%

$$K_h = 3.50 - 0.035\ H \qquad \ldots\ (6.5)$$

6.6.3 Smallest Dimension Coefficient (K_d)

Shrinkage is influenced by the shape and minimum dimensions of the element. A.C.I. (122) suggest that for elements with a minimum thickness of 200-225 mm this effect can be neglected. Branson and Christiason (132) suggested the following equation for K_d:

$$K_d = 1.17 - 0.029\ T \qquad \ldots\ (6.6)$$

where T is the thickness in inches.

If this equation (6.6) is modified to take account of the test specimen dimension of 100 mm it becomes

$$K_d = 1.17 - 0.0017\ T \qquad \ldots\ (6.7)$$

where T is the thickness in mm.

6.6.4 Longitudinal Steel Percentage Coefficient (K_s)

C.E.B.-F.I.P. (133) recommends the following equation for determining K_s:

$$K_s = \frac{100}{100 + m\rho} \qquad \ldots\ (6.8)$$

where m = the plastic modular ratio with regard to the effect of creep

ρ = the longitudinal steel percentage.

In calculating the plastic modular ratio the effective or reduced modulus for concrete E_c' is taken. The effective modulus E_c' is given by:

$$E_c' = E_c \left(\frac{1}{1 + C_t}\right) \qquad \ldots\ (6.9)$$

where E_c = elastic modulus of concrete at time of application of load

C_t = creep coefficient (see Table 6.9).

6.6.5 Composition of Concrete (K_c)

Mix proportions greatly effect the shrinkage of concrete. Higher cement contents and water cement ratio's increase shrinkage. Martin (134) suggested

the following equation:

$$K_c = 1 + 0.055 \frac{(f_c' - 3000)}{1000} \quad \ldots\ldots (6.10)$$

where f_c' = cylinder crushing strength in imperial units.

Modifying the equation to take account of the cube strength f_{cu} in S.I. units equation (6.10) becomes:

$$K_c = 1 + 0.055 \frac{(f_{cu} - 25.86)}{8.62} \quad \ldots\ldots (6.11)$$

6.7 Conclusions

6.7.1 Shrinkage

1. Regardless of curing condition the shrinkage of Lytag-sand concrete increases with increasing cement content.
2. Shrinkage specimens cured outside, protected from direct rain and sunlight, show a lower ultimate shrinkage than for internally cured specimens. The shrinkage varied between 74 and 83% of the values for specimens stored under constant temperature and humidity conditions.
3. Specimens cured continuously under water expand with age. At an age of approximately 500 days the expansion as a percentage of the shrinkage of specimens under constant temperature and humidity conditions was 16-21%.
4. The shrinkage of Lytag-sand concrete may be greater than or less than that of dense concrete, depending on the dense aggregate type, for similar mix proportions. In the absence of more accurate information values of 1.0 to 1.5 times the value for an equivalent strength dense concrete may be used.
5. Regardless of concrete strength and curing condition the ratio of the shrinkage at various ages to the shrinkage at 500 days remains sensibly constant particularly at ages of 90 days or more.
6. The shrinkage-age relationship for Lytag-sand concrete is adequately predicted by means of a hyperbolic type equation.

6.7.2 Moisture Movement

1. In lightweight concrete, a considerable moisture loss can occur before any appreciable shrinkage takes place, due to the migration of water absorbed

in the aggregate, into the cement-sand mortar.

2. For a 60 day drying and 45 day wetting cycle, the moisture movement in Lytag-sand concrete is of the order of 300-350 m/m x 10^{-6}, for concrete strengths of 30 to 60 N/mm^2 respectively.

6.7.3 Creep

1. Creep in Lytag-sand concrete increases with increasing water-cement ratio. An increase in the total water-cement ratio from 0.54 to 1.02 produced increases of 32% and 23% respectively in the one year creep values for stress-strength ratio's of 0.3 and 0.5 respectively.
2. The creep of Lytag-sand concrete is directly proportional to stress-strength ratio for values of stress-strength ratio between 0.3 and 0.5.
3. For high volume concentrations of aggregate, the elastic recovery of Lytag-sand concrete, at unloading, will generally exceed the elastic strain at loading.
4. The creep recovery after 28 days as a percentage of the creep at unloading varied from 6-10% depending on concrete strength.
5. As with shrinkage, the creep of Lytag-sand concrete may be greater than or less than that of comparable strength gravel concrete. In the absence of more accurate information values of 1.0 to 1.5 times the value for an equivalent strength dense concrete may be used.
6. The creep-age relationship for Lytag-sand concrete is adequately predicted by means of a hyperbolic equation.
7. As with shrinkage the creep at various ages expressed as a percentage of the creep at 1 year remains sensibly constant especially at ages of 90 days or more.

CHAPTER 7

SHEAR STRENGTH OF LYTAG-SAND R.C. T-BEAMS WITHOUT WEB REINFORCEMENT

7.1 Introduction

When the design of a reinforced concrete structure is undertaken an inherent part of the design procedure is the provision of an adequate factor of safety against any mode of failure which may occur, under the forces acting upon the structure, during its lifetime. One such mode of failure is the so called "shear failure". In reality this is a failure under combined shearing force and bending moment, plus, occasionally, axial load, or torsion, or both. Shear failures reduce the flexural capacity of members, and considerably reduce their ductility. They are, therefore, undesirable, especially since a reduction in ductility may lead to a sudden, brittle type, of failure.

Whilst the principle characteristics of the failure mechanism have been generally recognised for many years now (135, 136), the complexity of the problem is so great that as yet, no general analytical method for the determination of the various forces causing failure has been formulated. Most of the special methods rely on numerous simplifying assumptions.

From a designers viewpoint the following questions are raised:

(a) For a beam with a specific type of loading, geometry and material properties, what is the minimum amount of web reinforcement necessary to increase the shearing strength of that beam to a particular value V, greater than its cracking strength V_{cr}?

(b) For the above beam, what is the minimum amount of web reinforcement necessary to develop its full flexural strength?

Although no general analytical method has been developed which enables the magnitudes of the various forces, acting on a beam section at shear failure, to be calculated, adequately safe design procedures have been developed over the years. The large number of independent parameters influencing the shear failure mechanism has led investigators to derive empirical or semi-empirical equations based on the parameters investigated during their research.

The parameters effecting the shear failure mechanism in normal weight

concrete have been sufficiently well summarised in several publications (137-139), and comparisons of shear failures and their influencing factors, between dense aggregate and lightweight aggregate concrete beams of similar design, indicate that the general behaviour of lightweight concrete is similar to that of its denser counterpart.

The differences which have been observed relate mainly to the magnitude of diagonal tension resistance. So far as the mechanism of shear failure is concerned, there appears to be no significant difference between dense and lightweight aggregate concretes, except for the shear contribution through aggregate interlock.

In a gravel concrete beam a diagonal crack tends to result from a breakdown in the bond between the aggregate and the matrix. Relative slippage causes the irregular faces of the crack to separate slightly. Tensile stresses created in the steel bars by the crack opening induce clamping forces between the crack faces that in turn develop shear resistance, 'aggregate interlock'. The tensile and compressive strengths of lightweight aggregates are, however, generally less than those of crushed rock and gravel aggregates. Thus, a diagonal crack forming in a lightweight concrete beam will fracture a much higher percentage of the aggregate particles with the result that the crack faces are much smoother. Consequently there is a reduction in the shear resistance through aggregate interlock.

Although much research has been carried out on both rectangular and T-sections for dense aggregate concretes (138-142) investigators concerned with shear in lightweight concrete have concerned themselves mainly with rectangular sections and few data are available on the shear resistance of lightweight concrete T-beams (45, 49).

Rectangular sections offer an opportunity to study the basic phenomena of shear resistance and shear failure in relatively clear and simple circumstances. In practice, however, the use of T-sections as part of a composite beam slab construction is far more common.

The aim of this investigation is to observe the effect of varying some

of the more important parameters, which affect shear failure, on Lytag-sand concrete T-beams, in order to obtain much needed design data for lightweight concrete T-sections. The results are then compared with existing U.S. and European codes of practice. The results obtained by Bandyopadhyay (49) for Solite lightweight aggregate concrete T-beams and their gravel comparison specimens are also compared with the data obtained for the Lytag-sand beams.

7.2 Shear in Lightweight Concrete: Review of Past Research

Richart and Jensen (24) in 1930, were probably the first investigators to study the shear resistance of beams made with lightweight aggregate concrete. Test specimen details are given in Table 7.1. The authors reported that for beams without web reinforcement, which failed by diagonal tension, the ratio of the shearing unit stress to the compressive strength of control cylinders was practically the same for corresponding mixtures of gravel and Haydite concrete.

For beams with web steel, the authors argued that the unexpectedly high strength of the web steel meant that its full strength was not developed in any beam of this group and that, therefore, the recorded shearing stresses did not represent the full web resistance of these beams.

In 1958, Hanson (27), reported results from shear tests on beams made with seven different types of U.S. lightweight aggregates and a single type of gravel aggregate, Table 7.1. None of the beams contained web reinforcement. A comparison of ultimate loads with diagonal cracking loads showed that the spread of nominal unit shear would be nearly doubled if computed on the former rather than the latter. The author felt that this had contributed to the wide range of shear values reported in the literature for beams without web reinforcement. It was also observed that the longer span beams generally failed completely at the formation of the initial diagonal crack. The ability of the shorter spans to achieve stress redistribution after diagonal cracking was materially effected by the chance location of the crack. Thus he argued that the load at diagonal cracking should be considered as the ultimate load for beams without web reinforcement.

TABLE 7.1 TEST DETAILS FOR VARIOUS INVESTIGATORS

Investigator	Aggregate Type		Beam X-Section	Loading Arrangement	No. of Beams Without Web Steel	No. of Beams With Web Steel	Total	a/d Ratio	Compressive Strength Range 6" x 12" Cylinders f_c' (N/mm^2)	ρ (%)	Ultimate Shear Stress (N/mm^2)
	Coarse	Fine									
Richart & Jensen, 1931 (24)	Gravel	Sand	1	2	6	0	6	1.5	17.0-32.5	2.8	2.59-3.53
	Haydite	Sand	1	2	6	6	12	1.5	19.5-29.0	2.8	2.92-4.79
	Haydite	Haydite	1	2	6	0	6	1.5	12.5-22.5	2.8	1.79-2.31
							24				
Hanson, 1958 (27)	Gravel	Sand	1	2	5	0	5	2.5	25.5-73.5	2.5 & 5.0	
	U.S. L.W.A.'s	L.W. Fines	1	2	16	0	16	2.5	20.5-56.5	2.5 & 5.0	
Hanson, 1961 (28)	Gravel	Sand	1	2	5	0	5	2.5 & 5.0	21.0-31.0	1.25 & 2.50	0.83-2.15+
	U.S. L.W.A.'s	L.W. Fines	1	2	31	0	31		21.5-35.5		0.60-1.56+
							57				
Ferguson & Thompson, 1959 (143)	Expanded Shale	Expanded Shale	-	-	12	0	12	3.5 to 7.0	20.0-34.0	0.70 to 1.50	0.68-0.97+
							12				
Taylor & Brewer, 1963 (33)	Gravel	Sand	1	1	12	0	12	3.8	28.0-38.0*	1.9 Plain or 1.2 % Cold Worked	0.96-1.23
	Aglite	Aglite	1	1	12	0	12	3.8	25.5-38.5*		0.83-1.14
	Lytag	Lytag	1	1	12	0	12	3.8	27.0-39.0*		0.88-1.24
							36				
Evans & Dongre, 1963 (35)	Gravel	Sand	1	2	2	2	4	3.8	24.5-46.5*	5.7 plus 1.92 Compression Steel	1.63-1.67
	Aglite	Aglite	1	2	10	10	20	3.8	25.0-40.0*		1.15-1.71
							24				

TABLE 7.1 TEST DETAILS FOR VARIOUS INVESTIGATORS - CONTINUED

Investigator	Aggregate Type		Beam X-Section	Loading Arrangement	No. of Beams Without Web Steel	No. of Beams With Web Steel	Total	a/d Ratio	Compressive Strength Range 6" x 12" Cylinders (f_c' (N/mm^2)	ρ (%)	Ultimate Shear Stress (N/mm^2)
	Coarse	Fine									
Ivey & Buth, 1967 (144)	U.S. Lightweight Aggregates	Sand Lightweight Fines	1	2	3	0	3	3.3	25.5-28.0	0.95 & 1.48	0.84-0.97
			1	1	4	0	4	3.3	24.5-29.5	1.27	0.83-0.92
			1	2	19	0	19	2.5-5.0	19.0-32.5	0.95 & 2.10	0.68-2.48
							26				
Bandyopadhyay, 1974 (49)	Gravel	Sand	2	2	12	0	12	1.5 to 6.0	40.0-42.0*	1.64 to 2.70**	1.93-9.45++
	Solite	Solite	2	2	12	16	28		36.0-40.0*		1.65-8.07++
							40				

Beam X-Section Type

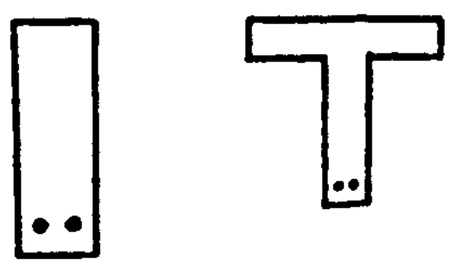

1. 2.

Loading Arrangement

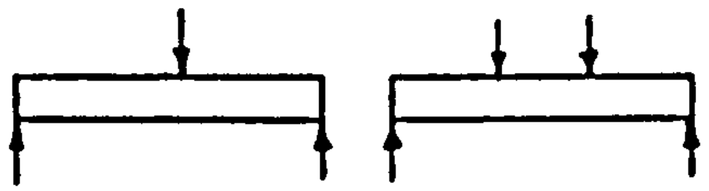

1. 2.

* Cube Strength f_{cu}.

\+ Based on diagonal cracking rather than failure load.

** Based on flange width times effective depth.

++ Based on rib width times effective depth.

A comparison of nominal unit shear strength as a function of concrete strength for all the different types of concrete showed that six of the lightweight aggregates produced concretes with shear strengths of approximately 75% of that of the comparable gravel concrete. The seventh lightweight aggregate produced a concrete with a shear strength equal to that of the gravel concrete. The shear strengths of Richart and Jensens (24) lightweight beams for comparable cylinder strengths are approximately 65% greater than Hansons (27), however, the moment shear ratio of the latter series of beams is greater than for the former; (Table 7.1).

Hanson's test beams were characterised by comparatively high steel percentages and a low moment-shear, a/d, ratio. In their discussion of this paper, Ferguson and Thompson (143) presented test data on the ultimate shear strength of twelve lightweight concrete beams made with a single type of aggregate, but with lower steel percentages and higher a/d ratio's; Table 7.1. The indicated shear strengths of these beams were lower than those reported by Hanson (27), and the authors suggested that the effects of steel percentage and moment-shear ratio may be more pronounced in lightweight than in dense aggregate concrete. At a later date, Ferguson furnished unpublished results (28) of fifteen additional beams using the same lightweight aggregate. These later findings corroborated the indicated low diagonal tension resistance of long span, low steel percentage lightweight beams, for the particular aggregate used.

In an attempt to clarify the situation, Hanson initiated a further series of tests which were reported in 1961 (28). As well as confirming some of his earlier findings the author also reported that a good correlation was found between the nominal unit shear strength of the beams and the accompanying split-cylinder tensile strengths of dry concretes, and that the split-cylinder and beam tests showed that the nominal unit shear strength of concrete containing a particular lightweight aggregate is determined by the characteristic level of tensile strength associated with the aggregate. The unit shear strengths of lightweight concrete beams varied from approximately 60-100% of the values for comparable gravel concrete beams depending on the lightweight aggregate considered

and on the beam characteristics.

Brewer in his discussion of this paper presented data from tests being carried out on concretes, made with two U.K. lightweight aggregates, and comparable sand-gravel concretes. The results were later published by Taylor and Brewer (33) in 1963. Details of the specimens are given in Table 7.1. The authors' main conclusions are summarised below:

1. The diagonal-cracking loads for the lightweight concrete beams ranged from 78-93% of the average values determined for the comparable gravel concrete beams.
2. The diagonal-cracking loads of beams reinforced with cold worked deformed bars were approximately 10% lower than for beams reinforced with plain mild steel bars.
3. The diagonal-cracking load for a particular type of beam increased with increasing concrete strength. The rate of increase was similar for all types of concrete.
4. The recommendations of CP 114 (22) regarding shear in beams without shear reinforcement did not give an adequate safety margin against failure for either gravel or lightweight concrete beams.

Evans and Dongre (35) also published shear test data, for lightweight concrete beams, in 1963; Table 7.1. It was shown that the relationship between diagonal cracking stress v_{cr} and cylinder crushing strength f_c' for gravel beams could be represented by the equation

$$v_{cr} = 0.04\ f_c' + 100 \qquad \ldots\ (7.1)$$

Since the split cylinder strength of Aglite concrete was about 75% of that for the comparable gravel concrete, the equation for Aglite concrete was modified to

$$v_{cr} = 0.03\ f_c' + 75 \qquad \ldots\ (7.2)$$

The authors argued that this equation was proved accurate by the test results for rectangular beams without web reinforcement and recommended that the allowable shear stress for Aglite concrete should be 0.41 N/mm^2 (60 psi) provided

that the works cube strength was 21 N/mm^2 (3000 psi) or more. Shear reinforcement was to be provided if the unit shear stress exceeded 0.41 N/mm^2.

For beams with 0.26% of mild steel stirrups as web reinforcement the results obtained showed an improvement of approximately 33% in the diagonal cracking load. Thus it was suggested that the relationship between diagonal cracking stress and the cylinder strength may be represented by the equation

$$v_u = 0.04\ f_c' + 100 \qquad \ldots\ (7.3)$$

It has since been established (139) that there is little correlation between cube strength and the nominal shear stress at which diagonal tension cracks occur. The permissible shear stress is related in terms of $\sqrt{U_w}$. In view of this fact it appears that the above equations, both for beams with and without web reinforcement, are no longer valid.

Ivey and Buth (144), reported tests carried out on twenty six lightweight concrete beams, in 1967; Table 7.1. The main variables were a/d ratio, steel percentage, three different types of aggregates and the beam cross-section. Their primary consideration was not in reiterating the previously proven effects of concrete strength, a/d ratio and steel percentage on the shear capacity, but the comparison of the test data collected during their test programme with the then existing ACI 318-63 design requirements (26) and its proposed amendments.

The previously shown effects of tensile strength, a/d ratio and steel percentage were again demonstrated. The tests meant to show the effect of beam size on shear resistance proved inconclusive and the authors suggested that if such an effect was present it was probably small.

Bandyopadhyay (49), published results, in 1974, of tests on lightweight concrete and gravel concrete T-beams, as detailed in Table 7.1. For beams without web reinforcement, he showed the effect of a/d ratio and steel percentage on the shear resistance of lightweight and dense aggregate concrete beams. The author also made the following conclusions:

1. The shear cracking strength of Solite concrete beams was equal to that of comparable gravel concrete beams.

2. Shear cracking strength of both Solite and gravel concrete beams is independent of the provision of vertical stirrups but depends on the concrete strength, a/d ratio and longitudinal steel percentage.
3. The diagonal tension strength of Solite concrete is effected by the same variables as those effecting the resistance of dense aggregate concrete. There is no fundamental difference in behaviour and modes of failure. The difference lies only in the types of aggregate used and its ability to resist the shear failure.
4. The ultimate shear resistance of Solite concrete T-beams varied between 71 and 95% of comparable gravel concrete T-beams.

For beams with web reinforcement, the authors most important conclusion was that such beams did not exhibit the sudden collapse mode associated with beams without web steel. This fact warrants the provision of nominal web reinforcement in all beams regardless of the value of the nominal shearing stresse

7.3 Shear in Lightweight Concrete: U.S. and European Design Recommendations

Excellent reviews of shear theories and their historical development, from the turn of the century until the early seventies, are given in several publications (136, 138, 139). The large number of differing theories which have been put forward indicate the complexity of the problem.

7.3.1 U.S. Design Code Recommendations

The first clauses relating to the shear strength of lightweight concrete beams were included in the 1963 revision of the ACI building code, ACI 318-63 (26). The ultimate strength design equation, for the nominal shear stress at shear cracking, in dense aggregate concrete was:

$$v_{cr} = \phi \ (1.9 \sqrt{f_c'} + 2500 \ \rho \ \frac{V_d}{M}) \qquad \ldots\ (7.4)$$

Following the studies of Hanson (28) and Ferguson and Thompson (143) it was suggested that equation (7.4) could be modified by the use of a correction factor for lightweight concrete. It would thus become:

$$v_{cr} = 0.75 \ \phi \ (1.9 \sqrt{f_c'} + 2500 \ \rho \ \frac{V_d}{M}) \qquad \ldots\ (7.5)$$

for all lightweight concrete or:

$$v_{cr} = 0.85\ \phi\ (1.9\ \sqrt{f_c'} + 2500\ \rho\ \frac{V_d}{M}) \qquad \ldots\ (7.6)$$

for partially sand replaced lightweight concrete.

Ivey and Buth (144) proposed an alternative to this method. They advocated the recognition of the splitting tensile strength, f_{SP}, as the concrete strength parameter rather than disguising it with F_{SP} (where $F_{SP} = f_{SP}/\sqrt{f_c'}$).

ACI 318-63 (26) ultimate strength design equation for lightweight concrete was:

$$v_{cr} = \phi\ (0.28\ F_{SP}\ \sqrt{f_c'} + 2500\ \rho\ \frac{V_d}{M}) \qquad \ldots\ (7.7)$$

The authors suggested that f_{SP} might be substituted for $F_{SP}\ \sqrt{f_c'}$ in equation (7.7) to give;

$$v_{cr} = \phi\ (0.28\ f_{SP} + 2500\ \rho\ \frac{V_d}{M}) \qquad \ldots\ (7.8)$$

With a value of $F_{SP} = 6.7$, equation (7.7) becomes identical to the normal weight concrete equation (7.4).

A comparison of equations (7.5), (7.6), (7.7) and (7.8) revealed that the 0.75, 0.85 procedure, equations (7.5) and (7.6) were the most conservative (36% or 60% including ϕ). Next came the existing code equations (7.7), (21% or 42% including ϕ). Equation (7.8) was the least conservative (7% or 26% including ϕ).

The revised code ACI 318-71 (26) suggested that from investigations (27, 28) one of the following modifications should apply when lightweight concrete is used:

(a) The provision for v_{cr} shall be modified by substituting $f_{SP}/6.7$ for $\sqrt{f_c'}$ but the values of $f_{SP}/6.7$ should not exceed $\sqrt{f_c'}$.

(b) When f_{SP} is not specified the term $\sqrt{f_c'}$ shall be multiplied by 0.75 for all lightweight concrete and 0.85 for sand-lightweight concrete. Linear interpolation may be used when partial sand replacement is used. It should be noted that the factors 0.75 and 0.85 apply only to the terms containing $\sqrt{f_c'}$ in the equation.

The above method was retained when A.C.I. revised their building code in 1977 (26).

7.3.2 U.K. Design Code Recommendations

The first British design code which contained clauses relating to lightweight concrete was the 1957 revised edition of CP 114 (22). For dense concrete, the permissible shear stress was based on the cube strength. If the shear stress acting on the section exceeded this value then the whole shearing force was to be provided for by the tensile resistance of the shear reinforcement acting in proper combination with the compression in the concrete. Even with the whole shearing force provided for in this way, the calculated shear stress was not to exceed four times the permissible shear stress for the concrete alone.

For lightweight concrete beams shear reinforcement was to be provided to resist the total shear force at any cross-section but again the calculated shear stress on the section was not to exceed four times the permissible shear stress for concrete alone.

The procedure recommended in CP 110 (54) is based on calculating the shear stress acting on a section and comparing this value with a maximum permissible value of nominal ultimate shear stress v_u given in the code. The values given in the code are based on the formula $v_u = 0.75 \sqrt{f_{cu}}$ with a limiting value of 4.75 N/mm^2. If the calculated shear stress is greater than the value of v_u given then the section must be revised. If not it is compared with a table of ultimate shear stress which increase with increasing concrete strength and/or longitudinal steel percentage up to a maximum value of 1.00 N/mm^2. If the calculated shear stress is greater than the corresponding ultimate shear stress v_c then shear reinforcement must be provided to carry the excess shear force above that which can be carried by the concrete. If the calculated shear stress exceeds half the value of v_c but does not exceed v_c then nominal links should be provided.

7.3.3 CEB-FIP Design Recommendations

In the 1978 CEB-FIP Model Code, (73), for the designing of web reinforcement for dense concrete elements two methods are proposed. The Standard Method

is a semi-empirical method based essentially on test results. The 'Refined Method' is theoretically based on the plastic analysis of a truss model (145) which has been checked and calibrated using a series of test results. It is applied to more specialised cases such as main girders in buildings and bridges and in particular to cases involving combined bending, torsion and shear.

For lightweight concrete, however, only the 'Standard Method' applies with various modifications to the dense concrete design equations. Design according to the 'Standard Method' is based on the following procedure, for dense concrete.

Firstly the resistance to shear, V_{Rd}, of an element, is considered to comprise the resistance V_{wd} carried by truss action (inclined concrete struts and shear reinforcement) and the resistance V_{cd} attributed to the shear resistance of the concrete compression zone and secondary effects. The design shear force V_{Sd} is thus given by:

$$V_{Sd} \leq V_{Rd} = V_{wd} + V_{cd} \qquad \ldots\ (7.9)$$

V_{wd} is given by:

$$V_{wd} = \frac{A_{sw}}{s} \cdot 0.9\ d\ f_{ywd}\ (1 + \cot \alpha)\ \sin \alpha \qquad \ldots\ (7.10)$$

where A_{sw} - cross-sectional area of web reinforcement

s - spacing of web reinforcement

d - effective depth of beam

f_{ywd} - design stress of web reinforcement

α - angle of inclination of web reinforcement.

V_{cd} is given by:

$$V_{cd} = 2.5 \cdot \tau_{Rd} \cdot b_w \cdot d \qquad \text{where } \tau_{Rd} = 0.25\ f_{ctd}$$

and f_{ctd} is the design concrete tensile strength

b_w is the width of the web.

As with CP 110 (54), the shear resistance reaches an upper limit

controlled by crushing of the concrete compression diagonals given by:

$$V_{Rd} = 0.30\ f_{cd} \cdot b_w \cdot d \qquad \ldots\ (7.11)$$

where f_{cd} is the design concrete stress in compression.

For lightweight concrete equation (7.11) is altered to

$$V_{Rd} = 0.20\ f_{cd} \cdot b_w \cdot d \qquad \ldots\ (7.12)$$

7.4 Details of Experimental Test Programme

7.4.1 Aim of Tests

The aim of this series of tests was to investigate the effects of varying three of the more important parameters known to effect the mechanism of shear failure, in beams without web reinforcement, and to compare the results with present U.S. and European design codes. The parameters studied are as follows:

7.4.1.1 The Concrete Strength

Two concrete strengths were originally chosen to represent both an average and a higher value likely to be found in reinforced concrete structures generally. The strengths chosen were 30 N/mm^2, series LS4-LS6, and 40 N/mm^2, series LS1-LS3. Despite the fact that strengths lower than 30 N/mm^2 were unobtainable is the cement contents listed in CP 110 were adhered to, two beams with cube strengths of 20 N/mm^2, S5 and S6 were later added to the test series.

7.4.1.2 The Percentage of Longitudinal Reinforcement

For the two concrete strengths of 30 and 40 N/mm^2 steel percentages of 0.29% (LS6), 1.14% (LS5), 1.87% (LS4) and 1.14% (LS3), 1.87% (LS2), 3.01% (LS1) respectively were decided on initially. However, when the results from the initial series of tests, LS1-LS6, were analysed, it was decided to cast further specimens with steel percentages of 0.57% for the 30 N/mm^2 concrete, S1 and S2, and 0.7% for the 40 N/mm^2 concrete, S3 and S4. For the 20 N/mm^2 concrete, S5 and S6, a steel percentage of 0.29% was used. All steel percentages are based on the flange width times the effective depth, b_f d.

7.4.1.3 The Shear Span-Effective Depth (a/d) Ratio

For series LS1-LS6, four a/d ratio's were chosen, namely 1.5, 3.0, 4.5

and 6.0, making a total of 24 beams in all. For the additional six beams tested, S1-S6, a/d ratio's of 3.0 and 4.5 were used.

Details of all beams are given in Table 7.2 and Figures 7.1 and 7.2.

7.4.2 Design of Beams

In order that a useful comparison between Lytag concrete T-beams and those of Solite and gravel, tested by Bandyopadhyay (49), could be made the beams for this series of tests were designed to have roughly similar dimensional properties to those of the previous tests (49).

In all the test specimens the web width b_w, flange width b_f, flange thickness t, and the effective depth d, were kept constant. For series LS1-LS6 the overall depth h was also kept constant. Thus the following ratio's remained constant:

(a) Flange width/web width ratio (b_f/b_w = 3.0) (= 3.0 for Bandyopadhyay (49)).

(b) Effective depth/flange thickness ratio (d/t = 2.37) (= 2.50 for (49)).

(c) Flange thickness/overall depth ratio (t/h = 0.32) (= 0.31 for (18)).

N.B. (c) only applies to series LS1-LS6 and not to S1-S6.

The value of b_f/b_w = 3.0 was chosen since previous research (142) has shown that significant increases in shear resistance are not always obtained with corresponding increases of b_f/b_w greater than 3.0. The web width b_w was chosen to allow the largest bar size used, ϕ 20 mm, to be accommodated in accordance with the spacing and cover requirements of CP 110 (54).

With the overall depth kept constant in series LS1-LS6, this meant that the cover to the main steel in series LS2-LS6, Figure 7.1, was in excess of that required by CP 110 (54). This was commented upon during the investigation (146) and it was decided to repeat the tests on two beams which had excessive cover in order to try and discover whether or not this resulted in any significant increase in the shear resistance of these beams. The repeat tests (with the correct cover to all longitudinal steel) were carried out on specimens similar to LS5-2 and LS6-2 and these specimens were labelled LS5-2R and LS6-2R respectively. Specimens S1-S6 had the correct cover to all reinforcement as defined in CP 110 (54).

TABLE 7.2 DETAILS OF LYTAG-SAND CONCRETE T-BEAMS

Beam No.	28 Day Cube Strength (N/mm^2)	ρ_b* (%)	ρ (%) Based on Flange Width	$\frac{\rho}{\rho_b}$ (%)	a/d Ratio	Number and Diameter of Main Steel (mm)	h (mm)	c (fig) (mm)
LS1-1	40.0	3.10	3.01	97	1.5	4-20 & 2-16	241	20
2	38.0	3.10	3.01	97	3.0	4-20 & 2-16	241	20
3	37.5	3.10	3.01	97	4.5	4-20 & 2-16	241	20
4	42.0	3.10	3.01	97	6.0	4-20 & 2-16	241	20
LS2-1	39.5	3.10	1.87	60	1.5	2-20 & 2-16	241	38
2	48.0	3.10	1.87	60	3.0	2-20 & 2-16	241	38
3	47.0	3.10	1.87	60	4.5	2-20 & 2-16	241	38
4	41.5	3.10	1.87	60	6.0	2-20 & 2-16	241	38
LS3-1	46.0	3.10	1.14	37	1.5	2-20	241	51
2	46.0	3.10	1.14	37	3.0	2-20	241	51
3	48.0	3.10	1.14	37	4.5	2-20	241	51
4	45.5	3.10	1.14	37	6.0	2-20	241	51
						2-20		
LS1-2R	46.0	3.10	3.01	97	3.0	4-20 & 2-16	241	20
LS2-2R	47.0	3.10	1.87	60	3.0	2-20 & 2-16	241	38
S3	47.5	3.10	0.70	23	3.0	2-12 & 2-10	215	15
S4	47.0	3.10	0.70	23	4.5	2-12 & 2-10	215	15
LS4-1	30.0	2.40	1.87	77	1.5	2-20 & 2-16	241	38
2	31.0	2.40	1.87	77	3.0	2-20 & 2-16	241	38
3	30.4	2.40	1.87	77	4.5	2-20 & 2-16	241	38
4	29.0	2.40	1.87	77	6.0	2-20 & 2-16	241	38
LS5-1	27.5	2.40	1.14	47	1.5	2-20	241	51
2	25.5	2.40	1.14	47	3.0	2-20	241	51
3	29.5	2.40	1.14	47	4.5	2-20	241	51
4	32.5	2.40	1.14	47	6.0	2-20	241	51
LS6-1	31.5	2.40	0.29	12	1.5	2-10	241	56
2	32.0	2.40	0.29	12	3.0	2-10	241	56
3**	33.5	2.40	0.29	12	4.5	2-10	241	56
4	-	2.40	0.29	12	6.0	2-10	241	-
LS5-2R	34.0	2.40	1.14	47	3.0	2-20	210	20
LS6-2R	33.5	2.40	0.29	12	3.0	2-10	200	15
S1	30.5	2.40	0.57	24	3.0	4-10	215	15
S2	31.5	2.40	0.57	24	4.5	4-10	215	15
S5	23.5	1.64	0.29	18	3.0	2-10	200	15
S6**	23.5	1.64	0.29	18	4.5	2-10	200	15

* Based on CP 110 (54) parabolic stress block, see Appendix B.

** Flexural failure.

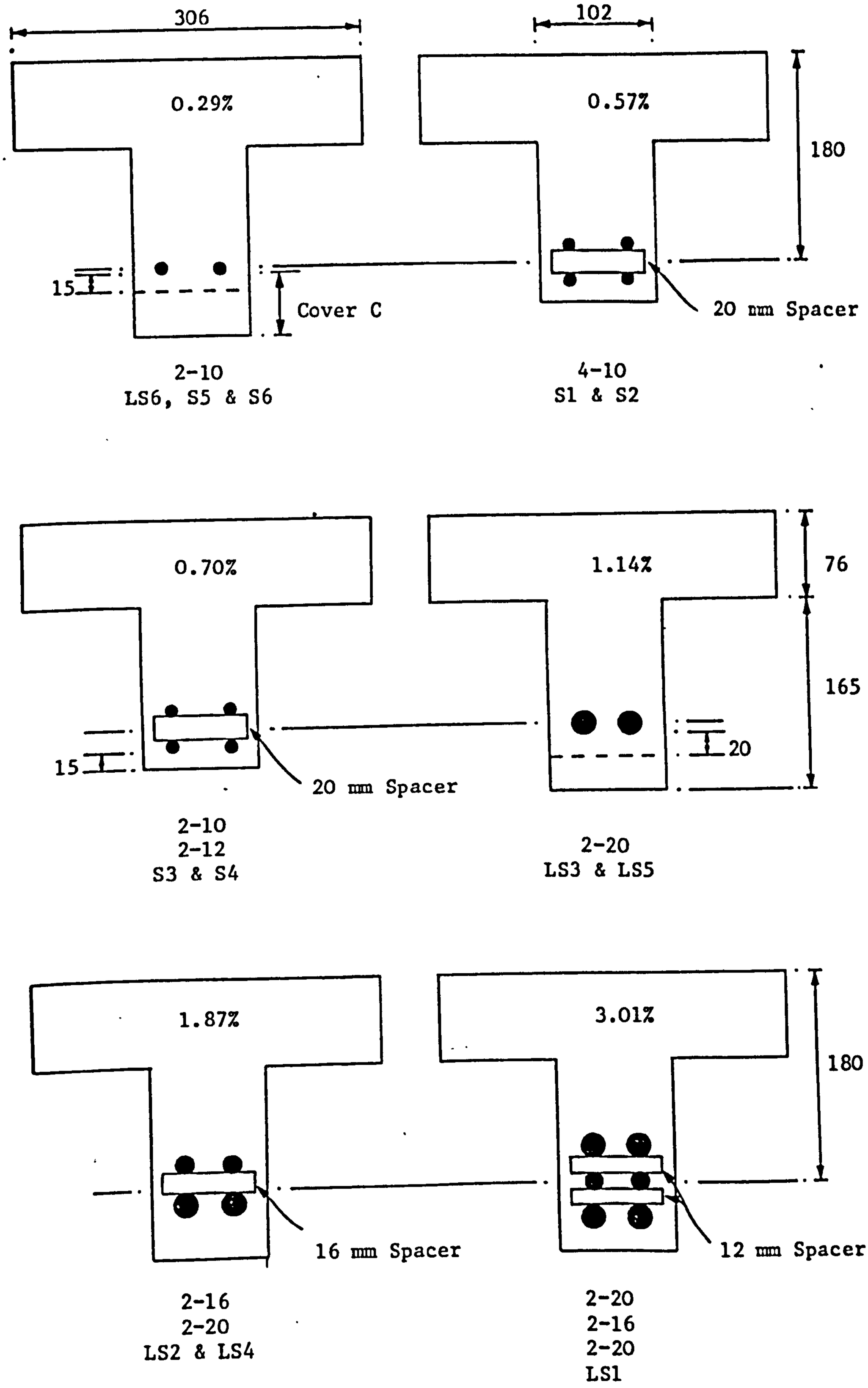

FIGURE 7.1 LONGITUDINAL REINFORCEMENT DETAILS FOR SHEAR SPECIMENS

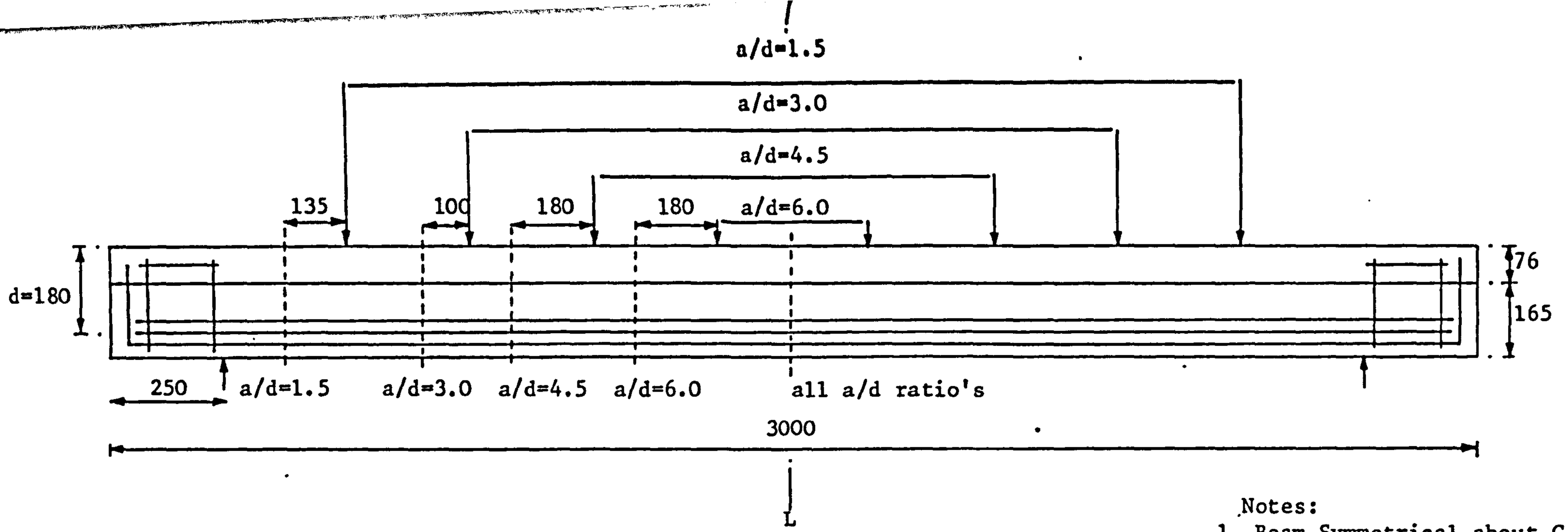

Notes:
1. Beam Symmetrical about C.L.
2. All dimensions in m.m.
3. --- C.L of Demec extensometer readings

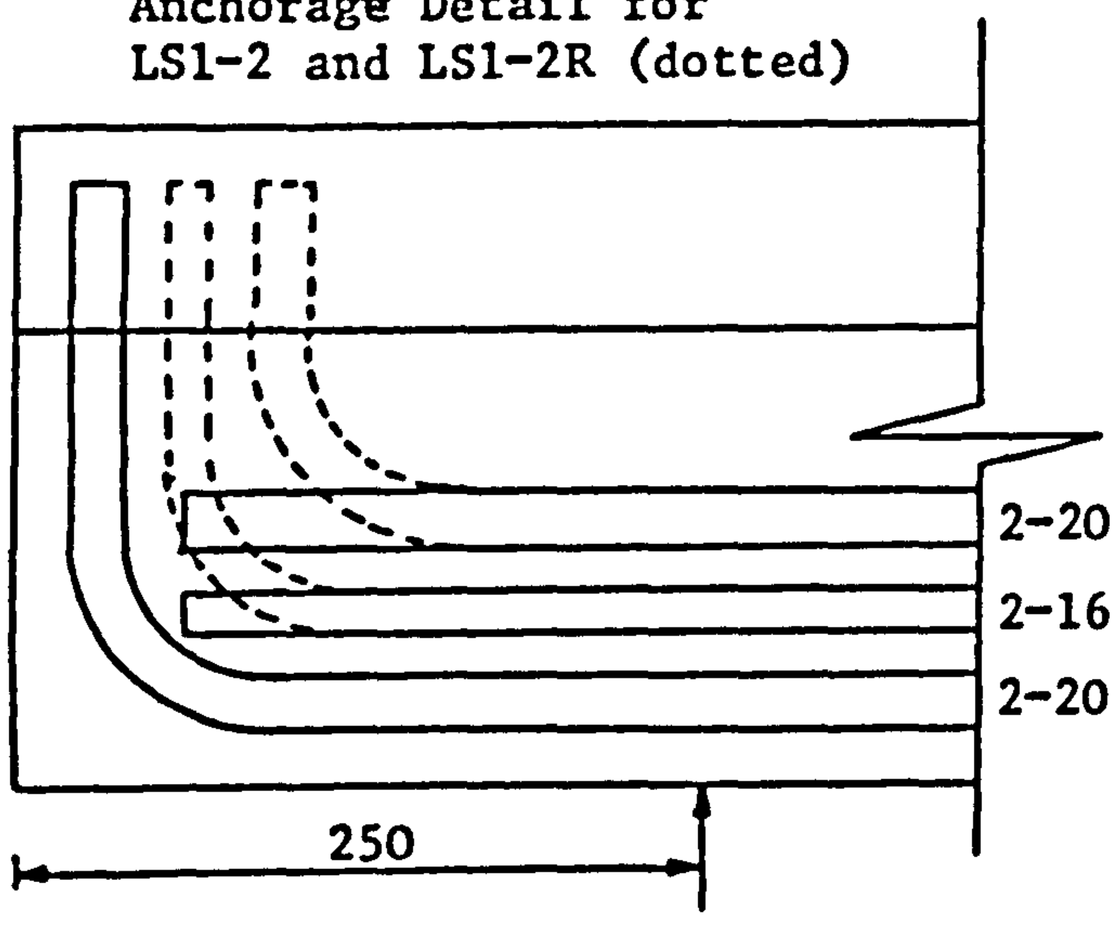

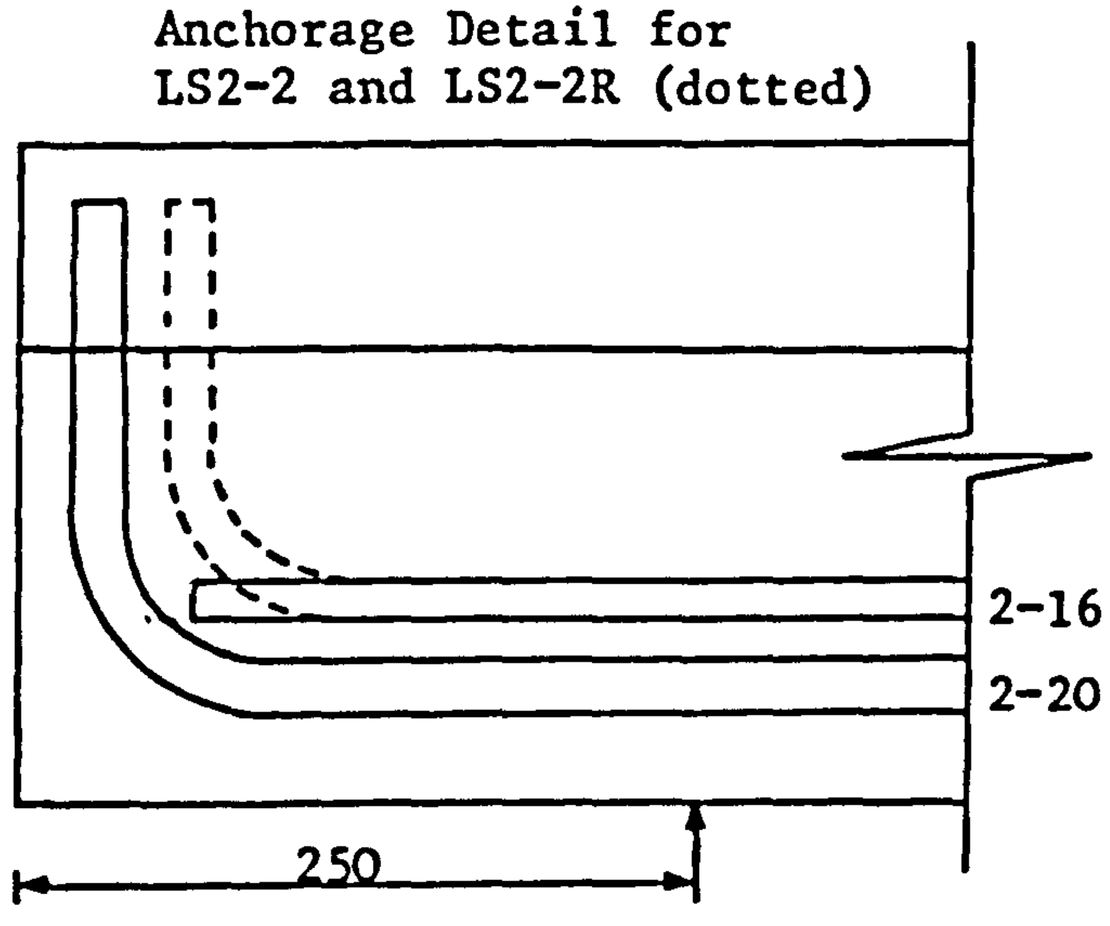

FIGURE 7.2 GENERAL REINFORCEMENT DETAILS FOR SHEAR SPECIMENS

The length of all the beams was kept constant at 2.5 m between supports. The beams projected beyond the supports by 0.25 m to allow adequate anchorage of the longitudinal steel.

For the beams in series LS2-LS6 all the longitudinal steel had effective anchorage lengths in accordance with CP 110 (54), i.e. not less than 12 times the bar diameter, ϕ, beyond the support. For series LS1, the top layer of 20 mm ϕ bars were shorter than required by CP 110 (54) by some 2 ϕ. It was suggested (147) that this may have led to premature anchorage failure of these specimens despite the fact that in none of the tests was there any signs of distress in the anchorage zone prior to failure. In order to investigate this a beam similar to LS1-2, labelled LS1-2R was cast and tested, the only difference being that all three layers of steel ended with L-type bends in the anchorage zone. A second beam similar to LS2-2 labelled LS2-2R was also cast and tested; in this case both layers of steel again ended with L-type bends in the anchorage zone (see Figure 7.2). Despite the fact that LS2-2 had adequate anchorage, LS2-2R was cast to see if the addition of a further L-type bend had any significant effect on the ultimate capacity of the beam.

The size of the beams used in the test programme represented one half scale models of normal laboratory prototypes, which have been shown to simulate well the deformation and strength characteristics of laboratory prototypes in every respect (141, 148). None of the beams contained web reinforcement.

7.4.3 Materials

The longitudinal reinforcement in all beams consisted of hot-rolled deformed high tensile steel with a characteristic yield stress of approximately 465 N/mm^2. A typical stress/strain curve for the steel is shown in Figure 7.3. Concrete mixes were designed to achieve 28 day cube strengths of approximately 20, 30 and 40 N/mm^2. As was explained in Chapter 4 problems of consistency occurred with the 40 N/mm^2 mixes with the average of all the test beams being slightly greater than 45 N/mm^2. The mix proportions by weight of OPC : natural sand : Lytag 12 mm, were as follows:

(a) 20 N/mm^2; 1 : 3.73 : 3.48.

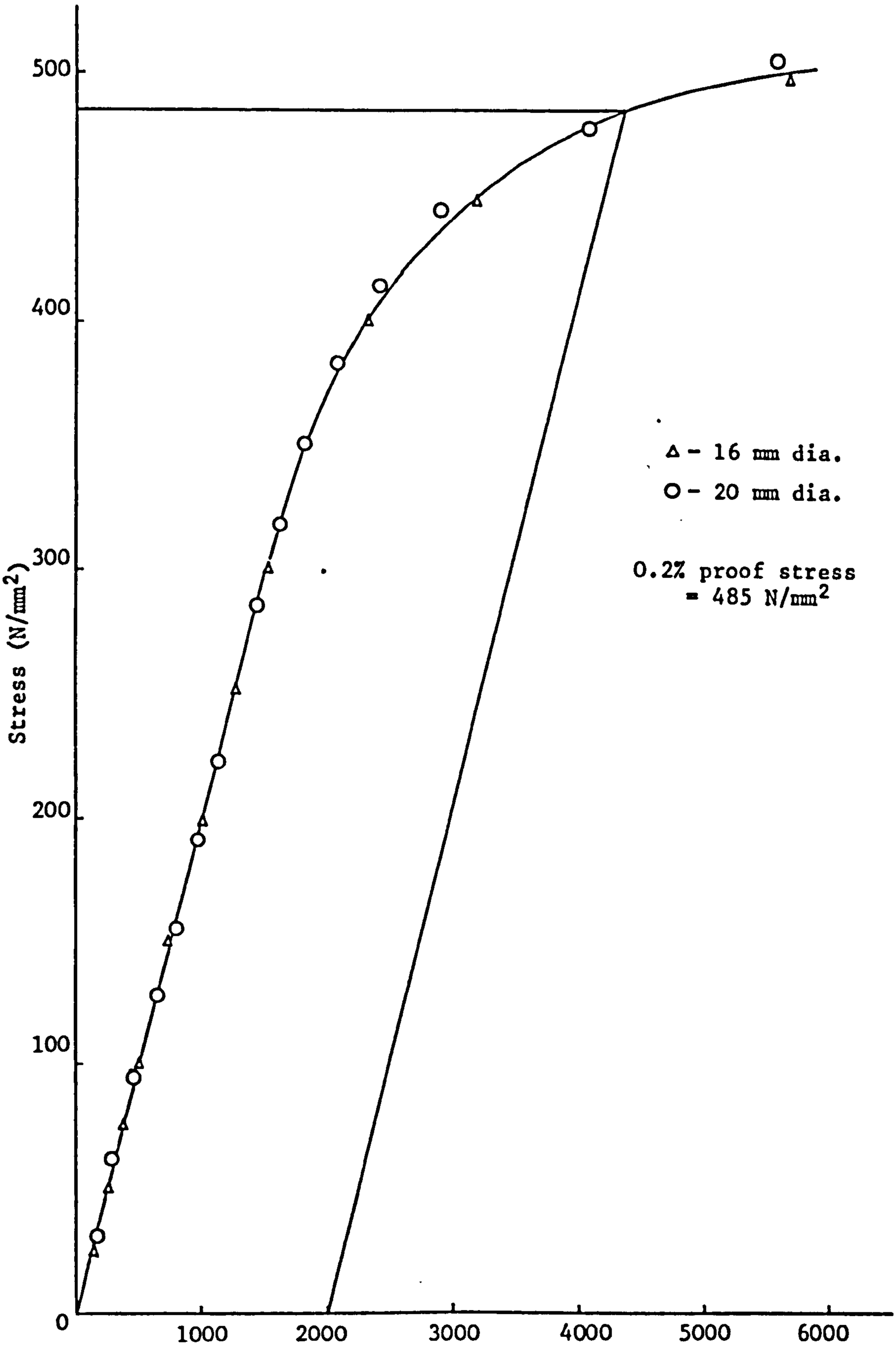

FIGURE 7.3 STRESS STRAIN CURVE FOR TENSILE STEEL

(b) 30 N/mm^2; 1 : 2.86 : 2.86.

(c) 40 N/mm^2; 1 : 1.93 : 2.13.

The effective water/cement ratio·s were 1.26, 1.04 and 0.78 respectively.

7.4.4 Manufacture of Beams

All beams were cast using the same steel mould which was fabricated using standard plate, channel and angle sections. All joints were sealed with tape and the mould was lightly oiled before each beam was cast. All reinforcing steel was allowed to rust slightly.

Each beam required two batches of concrete. These were mixed in a horizontal, pan-type mixer. The mould was placed on a high frequency vibrating table and concrete from the first batch was placed until it just covered the reinforcement. This was then vibrated by means of the table whilst at the same time a 10 mm ϕ steel rod was used to ensure that the concrete was sufficiently well compacted around the main steel. Aggregate distribution and the degree of compaction obtained are indicated by Plate 7.1. The remainder of the first batch was then placed and compacted. The second batch was placed in two layers and compacted by means of the vibrating table and a hand held poker vibrator. 100 mm cubes from each batch were also cast with each beam. The beam and control specimens were left for approximately 2-3 hours after casting before the surfaces were trowelled smooth. They were then covered with polythene sheeting. Specimens were demoulded at 2 days and left to dry in the laboratory. All beams and their companion cubes were tested at 28 days ± 1 day.

7.4.5 Loading Arrangement

Details of the test rig and loading arrangement are given in Figure 7.4. Load was applied at two symmetrical load points by means of a steel spreader beam. At each load point, load was transferred to the beam over the web by means of a 110 x 50 mm wide bearing plate. The jack load was measured directly from a load indicator dial.

7.4.6 Instrumentation and Measurements

For beams LS1-LS6, steel strains were measured in both shear spans and in the constant moment region by means of electrical resistance strain gauges.

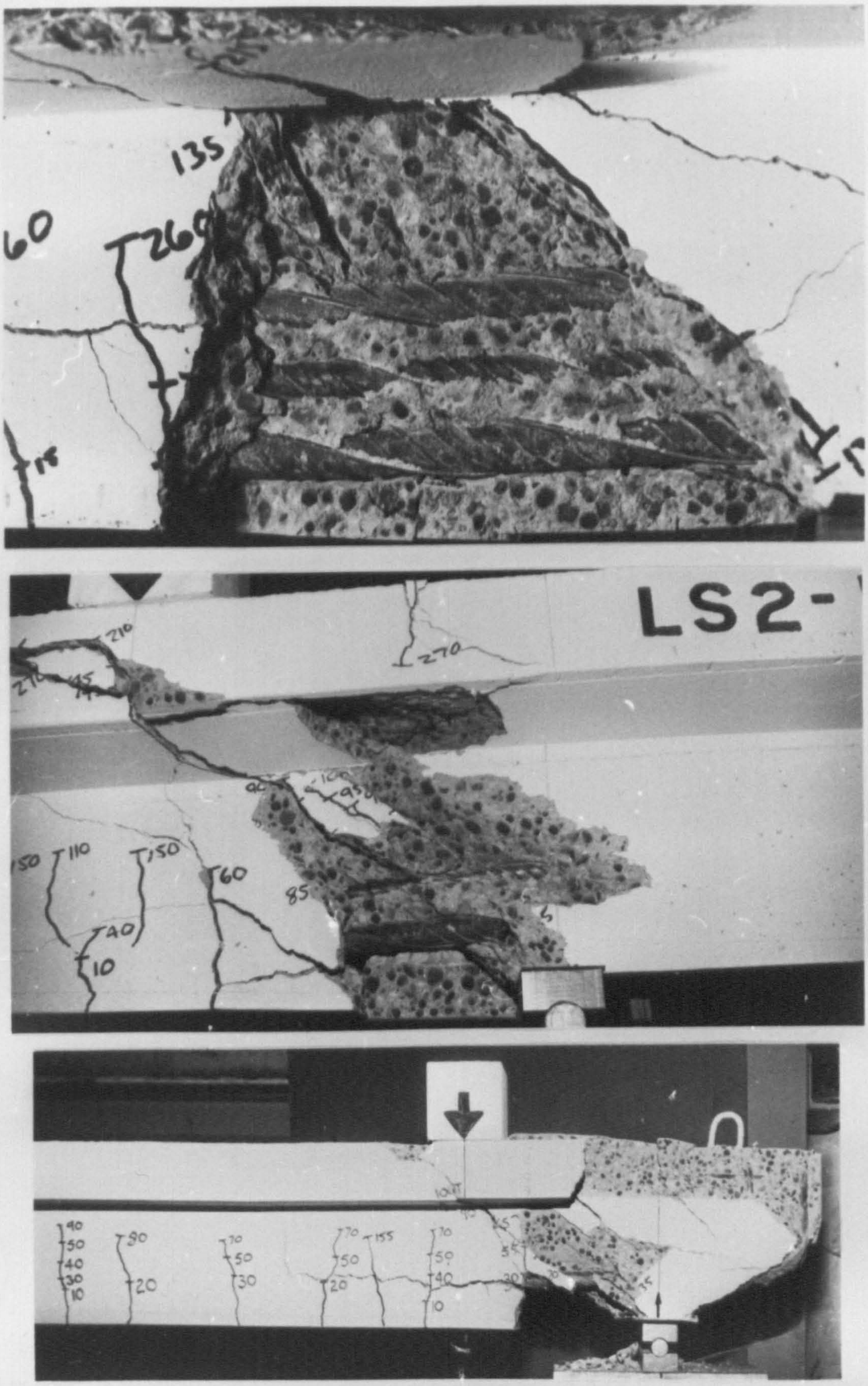

PLATE 7.1 AGGREGATE DISTRIBUTION AND CONCRETE COMPACTION IN SHEAR BEAMS

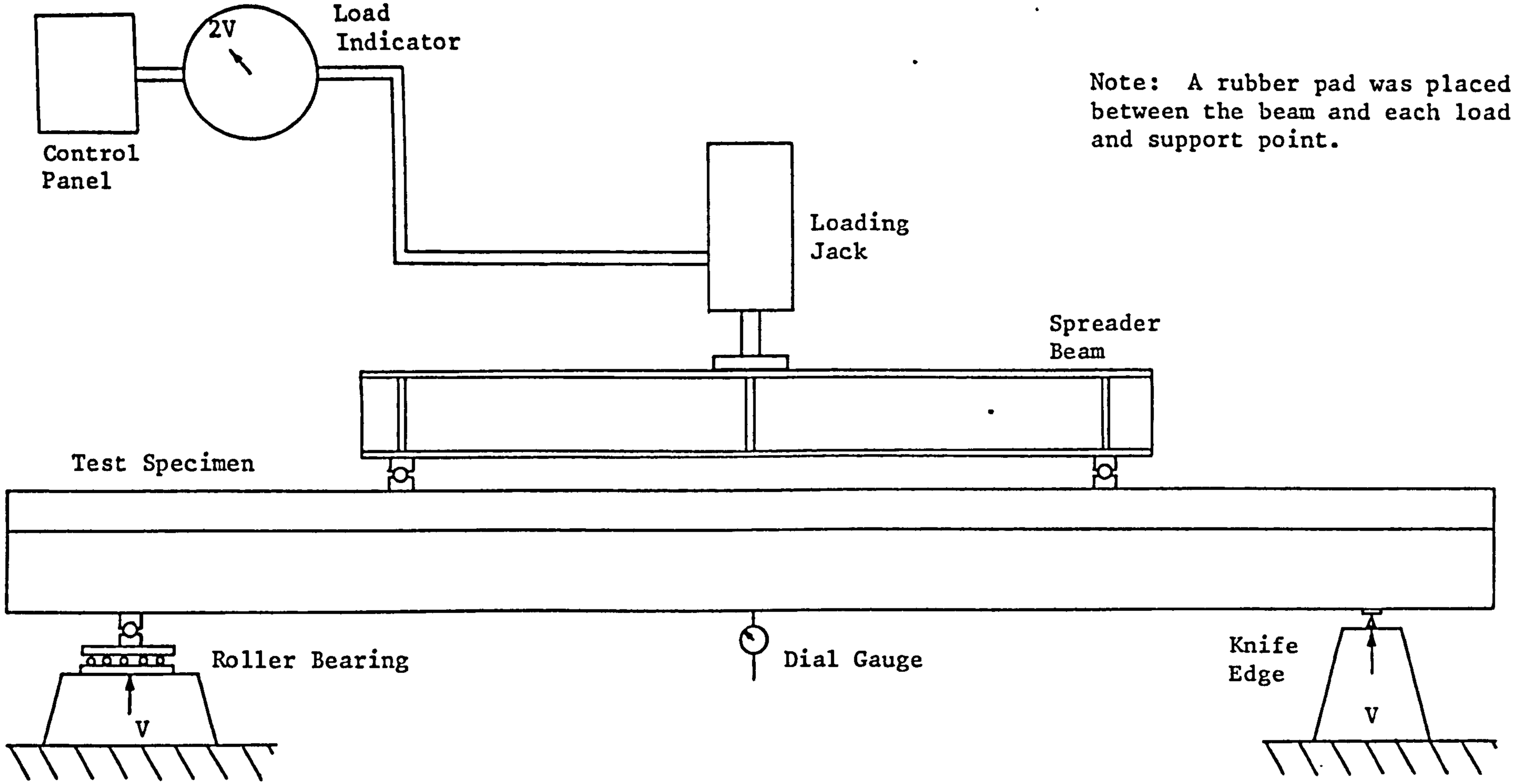

Note: A rubber pad was placed between the beam and each load and support point.

FIGURE 7.4 TEST RIG DETAILS

All gauges were placed on the same bar, and where more than one layer of reinforcement was involved, the bar was always positioned on the bottom layer in order that the probable maximum steel strains which occurred could be measured. Gauge locations varied depending on the a/d ratio of the test specimens.

Concrete strains were measured in both shear spans, near to the load point, and in the constant moment region by means of a Demec extensometer with a gauge length of 100 mm. The centre lines of the three locations used for each a/d ratio are shown in Figure 7.2. For each location four strain readings were taken across the top of the flange, at 60 mm centres, four on the side of the flange, at 20 mm centres, and three on the side of the web. Mid-span deflection was measured by means of a dial gauge accurate to 0.01 mm. For beams S1-S6, concrete and steel strains in the constant moment region and mid-span deflection only were recorded. To aid the observation and recording of cracks the entire beam was whitewashed prior to testing.

The beams were loaded in increments of V = 2.5 KN, Figure 7.4, and load at first diagonal crack and failure was noted. Strain and deflection measurements were taken at various intervals depending on the expected diagonal cracking and failure loads. Measurements were taken as near to failure as was practically possible and safe.

On the formation of a diagonal crack, the load indicated on the machine console would drop. The load would then be gradually brought back up to the diagonal cracking load and the incremental loading continued until failure. For the beams with longer a/d ratio's failure generally occurred before a return to the diagonal cracking load was achieved. Thus the diagonal cracking load and the failure load were the same.

7.5 Test Results and Discussion

7.5.1 Effect of Anchorage and Cover

It was mentioned in section 7.4 that the beams in series LS1 did not exactly meet the anchorage requirements according to CP 110 (54). It was suggested (147) that this may have led to premature anchorage failure in these beams. In order to investigate this, a beam similar to LS1-2 was tested with full anchorage to all steel. For comparison purposes a beam similar to LS2-2 was also tested with additional L-type bends in the anchorage zone despite the fact that the steel in LS2-2 was anchored according to CP 110 (54), (see Figure 7.2).

For the beams in series LS1-LS6, the overall depth of the beam, h, was kept constant and therefore beams LS2-1 to LS6-3 had excessive cover to the longitudinal reinforcement. It was suggested (146) that these beams may show a higher resistance to shearing, than similar beams with cover according to CP 110 (54), due to increased dowel action. In order to investigate this, beams similar to LS5-2 and LS6-2 were tested with the correct cover to all main steel (see Figure 7.1 and Table 7.2). All repeat beams were given the same beam numbers as their counterparts with the addition of the letter 'R'. The beams chosen for repeat tests were those with an a/d ratio of 3.0 since these specimens showed the highest shear capacity of the beams which behave as true 'beams' rather than 'short beams' or 'corbels', i.e. a/d $\leq$ 1.5. The results of the repeat tests are shown in Table 7.3.

For the anchorage tests, LS1-2 and LS2-2, it is apparent that the provision of L-type bends to all main steel, Figure 7.2, increases the load at diagonal cracking by 6-7% and the ultimate load by 8-12%. Despite the fact that for beam LS2-2 the minimum anchorage length was 12 times the bar diameter for all steel, in accordance with CP 110 (54), the addition of two L-type bends to the 16 mm diameter bars, Figure 7.2, increased the ultimate load capacity by 8%. It should be noted that none of the beams in series LS1 or LS2 showed any signs of distress in the anchorage zone prior to failure and this variation in shear capacity is probably due to the variation between two test specimens which can be expected

TABLE 7.3 EFFECT OF ANCHORAGE AND COVER ON ULTIMATE SHEAR STRENGTH

Beam No.	Compressive Strength (N/mm^2)	Load at 1st Diagonal Crack (kN)	Percentage Increase (%)	Ultimate Load (kN)	Percentage Increase (%)
LS1-2	38.0	85.0	-	130	-
LS1-2R	47.0	90.0	6	145	12
LS2-2	48.0	70.0	-	111	-
LS2-2R	47.0	75.0	7	120	8
LS5-2	25.5	50.0	-	72.5	-
LS5-2R	34.0	55.0	10	79.0	9
LS6-2	32.0	58.2	-	58.5	-
LS6-2R	33.5	48.0	-18	48.0	-18

when dealing with a variable material. Hanson (28) noted that for beams without web steel, the longer span beams generally failed completely at the formation of the initial diagonal crack and suggested that the ability of the shorter span beams to achieve stress redistribution after diagonal cracking was materially affected by the chance location of the diagonal crack. Although the cracking patterns and modes of failure, for both the above mentioned sets of beams, were similar, this may be an explanation for the increase of approximately 10% in the ultimate shear strength.

The effect of cover to the main steel is also shown in Table 7.3. The results of the two repeat beams appear to be contradictory, with LS5-2R showing a greater ultimate shear strength than LS5-2, despite less cover to the main steel, whereas LS6-2R shows a decrease in ultimate shear strength for a decrease in cover, as compared with LS6-2.

For LS5-2 and LS5-2R there is a large difference in concrete cube strength but as is shown in section 7.5.3.6.3 the effect of concrete strength on ultimate shear strength is generally small. The increased strength due to decreased cover may be due to flexural cracking in the shear span. For the beam with smaller cover, a higher shear force is required to initiate tensile cracking in the concrete since the distance from the centroid of the tensile steel to the extreme tensile concrete fibre is less. Thus for a given shear force the crack height should be less and this was borne out to some extent by an examination of the cracking patterns in the two beams. For smaller crack heights, the area of concrete resisting the shear force will be greater and thus the ultimate capacity will be increased. When the small increase due to concrete strength is taken into account, however, the variation in ultimate load capacity between the two beams will be very small.

For beams LS6-2 and LS6-2R a difference in the cracking patterns at failure was observed. The failure mode of LS6-2 was similar to those of the other beams tested at an a/d ratio of 3.0, (see Figure 7.15 (b)), with the failure plane reaching the web-flange junction near to the load point. For LS6-2R, however, the failure plane reached the web-flange junction near the centre

of the shear span. Thus it can be seen that for the low steel percentage used in these beams the chance location of the diagonal crack has significantly affected the ultimate shear strength.

The results of the tests to observe the effect of anchorage and cover on the ultimate shear strength were very limited and thus only limited conclusions can be drawn from them.

The fact that there were no signs of distress in the anchorage zones of the beams in series LS1 and LS2, prior to failure, tends to suggest that the increased capacity of approximately 10% for LS1-2R and LS2-2R is due to material variations typically associated with such tests.

Series LS6 suggests that for very low steel percentages the failure strength of an unreinforced web may be unpredictable.

7.5.2 Deformation Characteristics

7.5.2.1 Mid-Span Deflection

A selection of the mid-span deflection measurements taken during this series of tests is shown in Figures 7.5-7.7. Figure 7.5 shows the effect of a/d ratio on mid-span deflection for series LS3. The results are typical of all the beam series tested and indicate that for a given longitudinal steel percentage and concrete strength the deflection at any given load decreased with decreasing a/d ratio with a large decrease from a/d of 3.0 to 1.5. Similar results were reported by Bandyopadhyay (49) for Solite and gravel concrete T-beams.

Figures 7.6 (a) and (b) show the effects of longitudinal steel percentage on mid-span deflection for beams with an a/d ratio of 4.5 and concrete strengths of 30 or 45 N/mm^2. The variation in mid-span deflection between beams with different steel percentages is more marked for the higher a/d ratio's of 4.5 and 6.0, but the relationship between the beams shown in Figures 7.6 (a) and (b) is typical of all a/d ratio's. As would be expected, for a given load, the mid-span deflection decreases with increasing steel percentage and therefore beam stiffness. Similar results were again reported by Bandyopadhyay (49) for Solite and gravel concrete T-beams.

Figure 7.7 shows the effect of concrete strength on mid-span deflection

Series LS3

$$\frac{100\ A_{st}}{b_f d} = 1.14$$

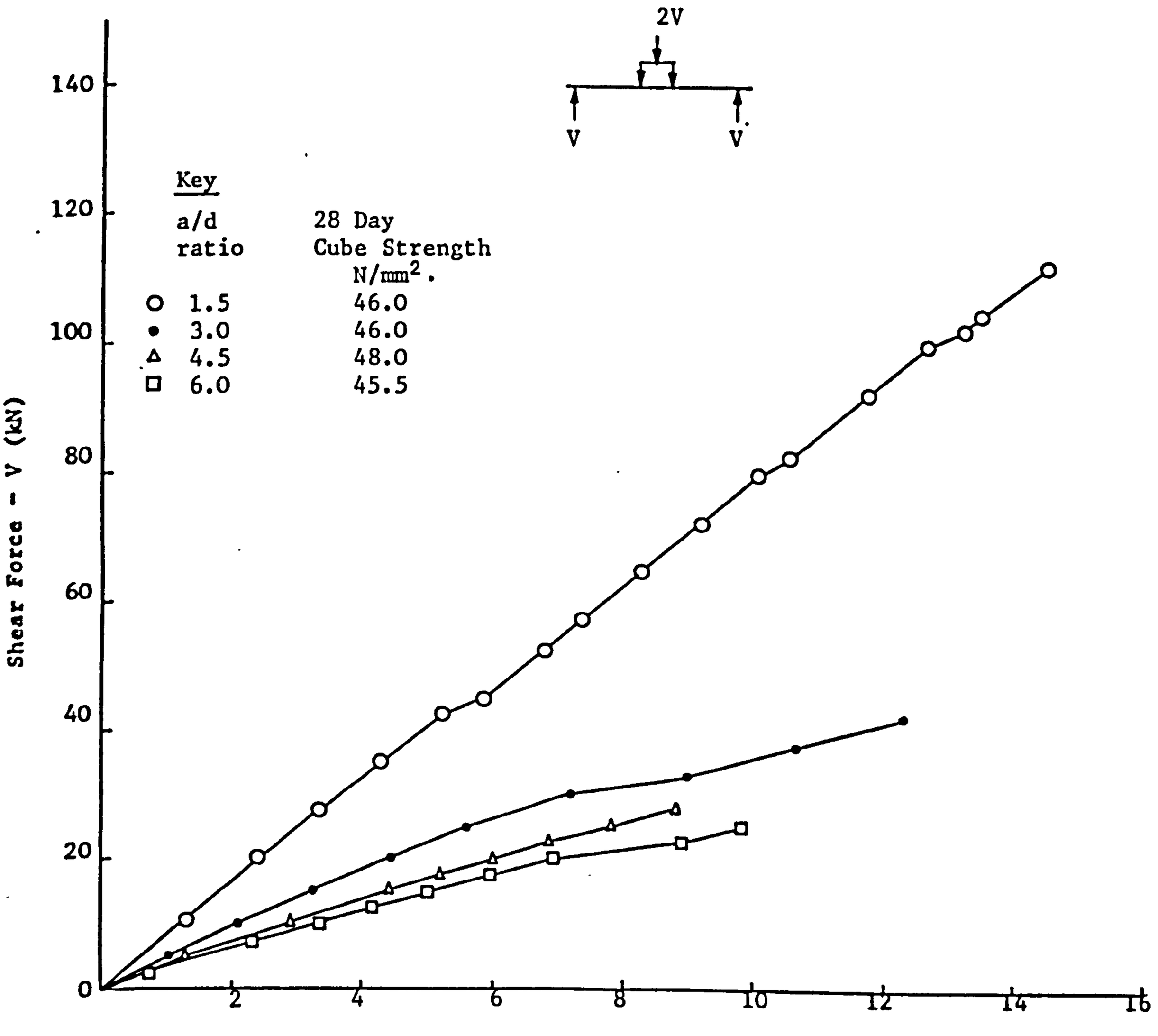

FIGURE 7.5 EFFECT OF a/d RATIO ON MID-SPAN DEFLECTION

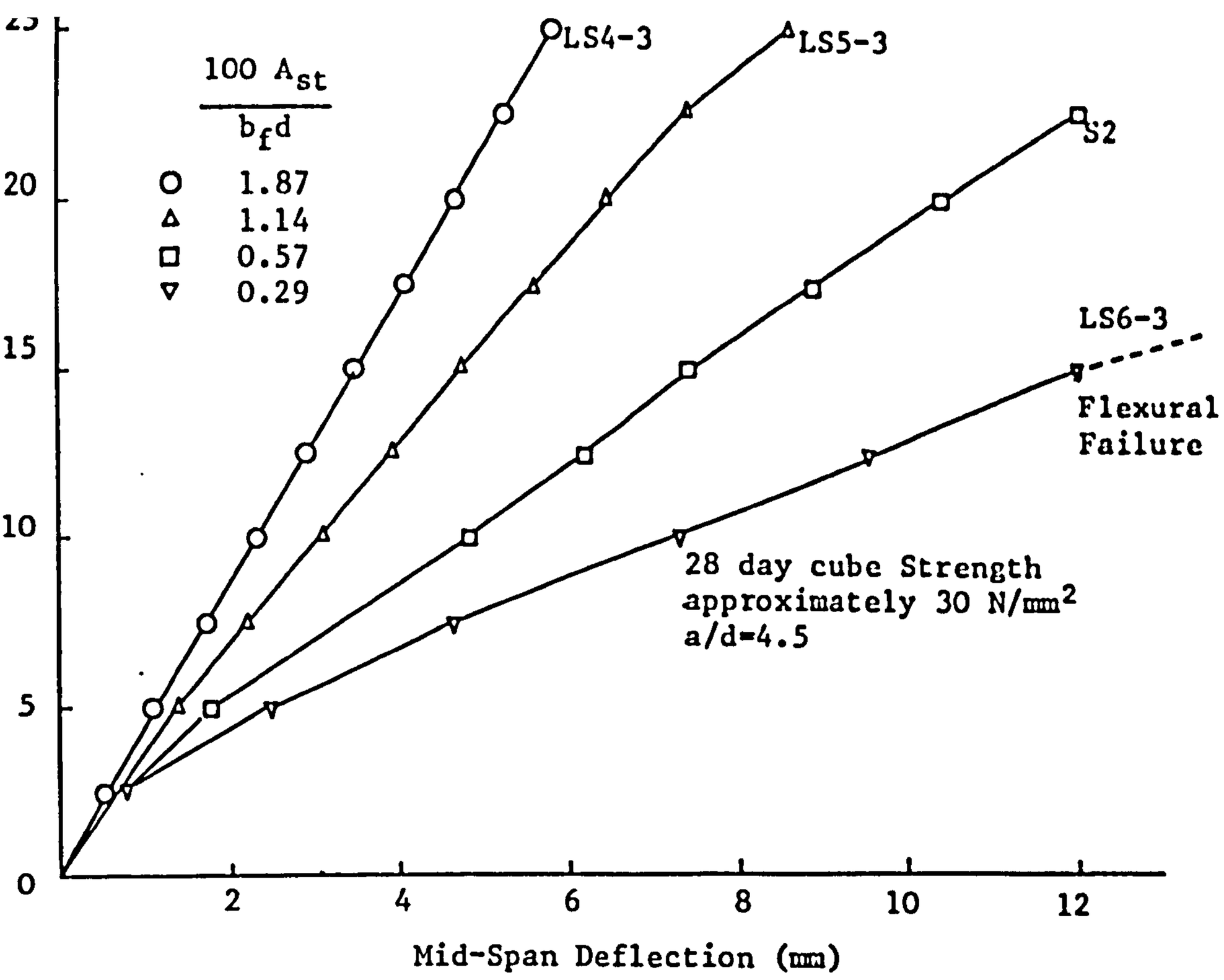

FIGURE 7.6(a) EFFECT OF LONGITUDINAL STEEL ON MID-SPAN DEFLECTION

FIGURE 7.6(b) EFFECT OF LONGITUDINAL STEEL ON MID-SPAN DEFLECTION

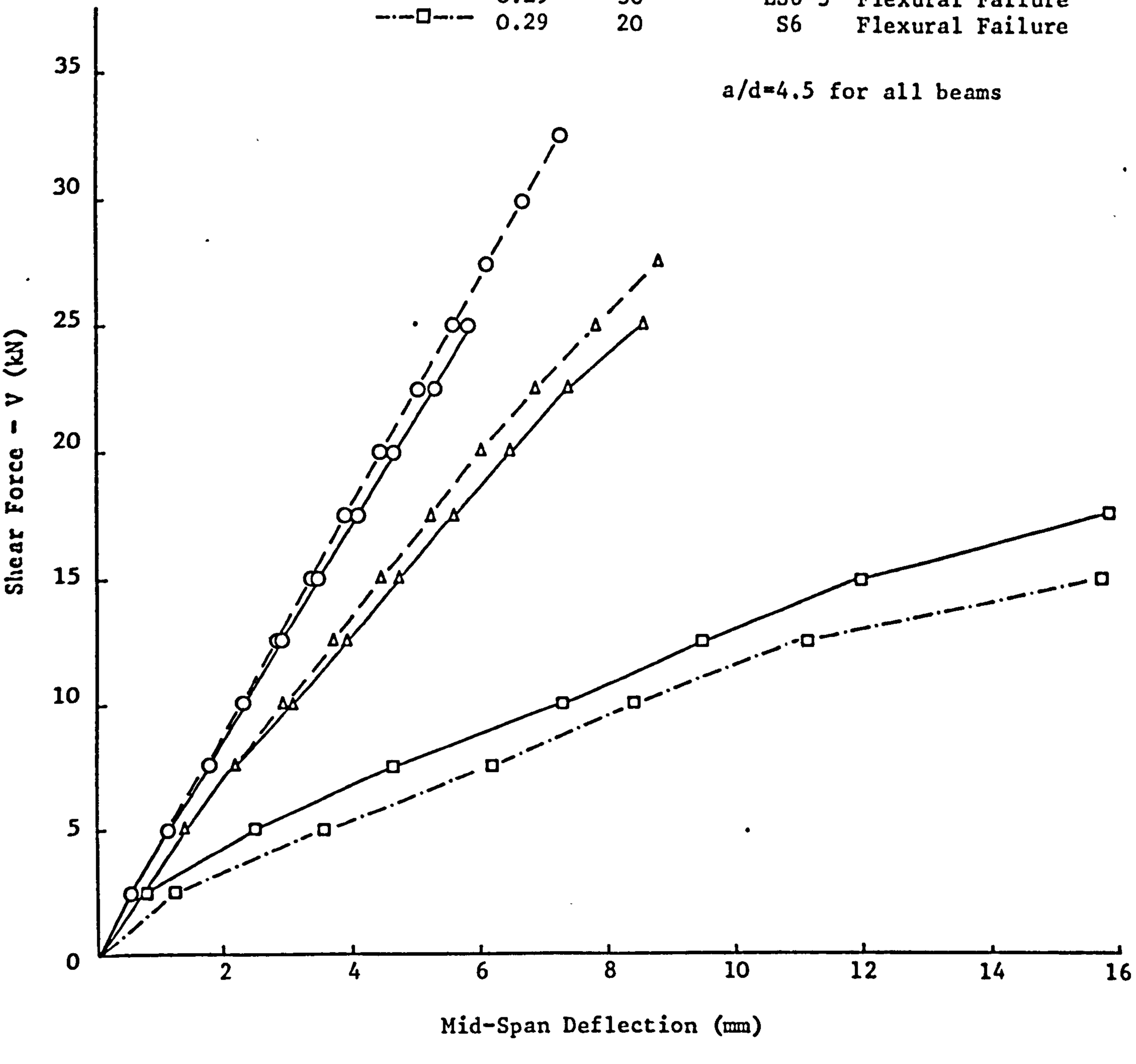

FIGURE 7.7 EFFECT OF CONCRETE STRENGTH ON MID-SPAN DEFLECTION

Series LS3

$$\frac{100\ A_{st}}{b_f d} = 1.14$$

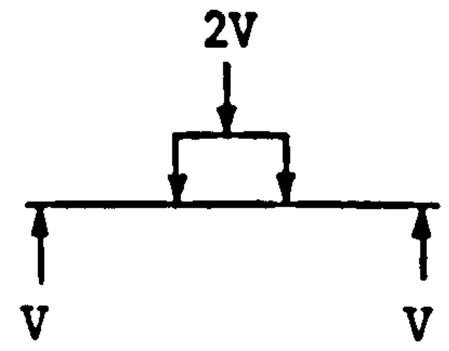

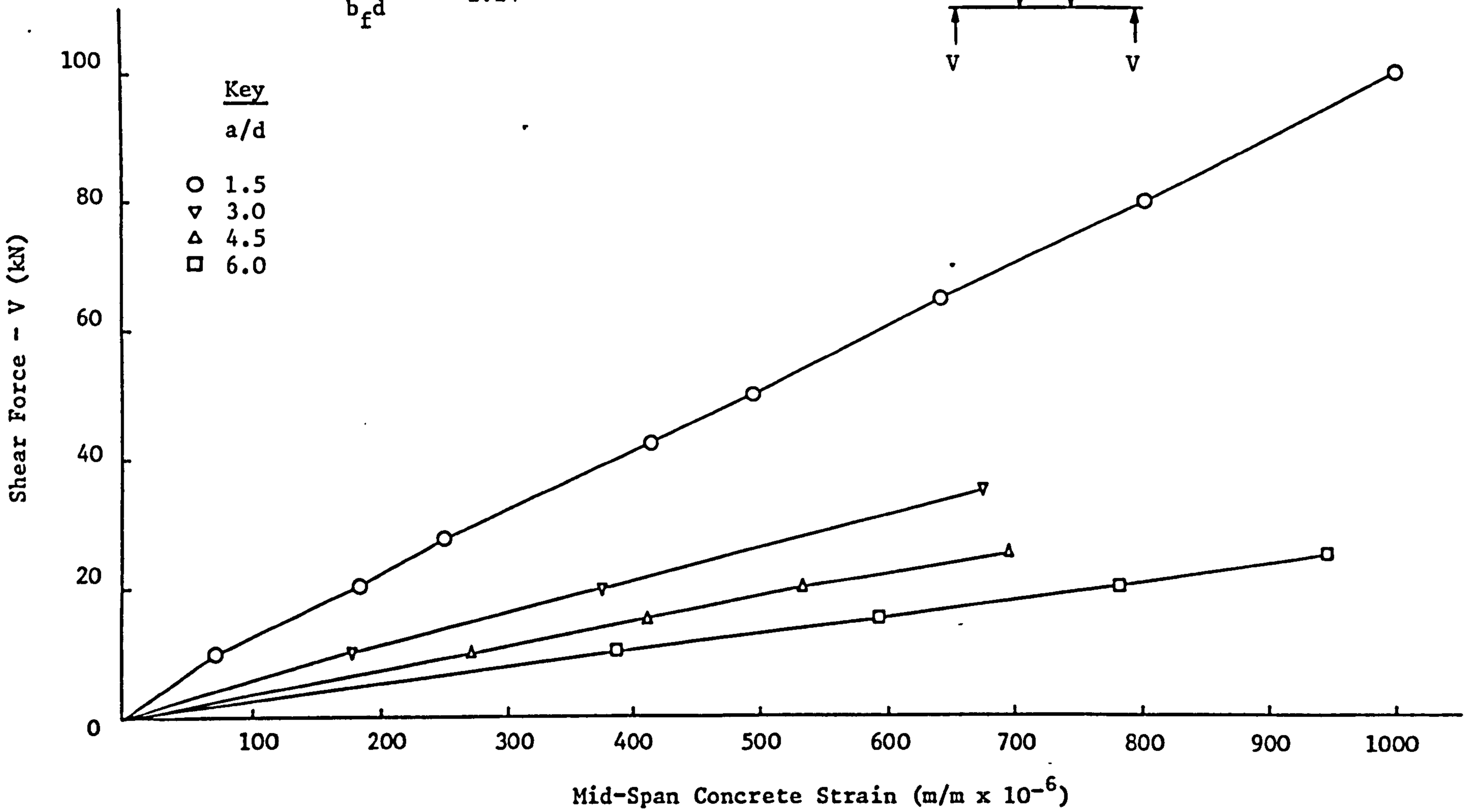

FIGURE 7.8 EFFECT OF a/d RATIO ON MID-SPAN CONCRETE STRAIN

KEY

	ρ %	Cube Strength N/mm²	Beam No.	
—— O ——	1.87	45	LS2-3	
—— O ——	1.87	30	LS4-3	
—— △ ——	1.14	45	LS3-3	
—— △ ——	1.14	30	LS5-3	
—— □ ——	0.29	30	LS6-3	Flexural Failure
—·— □ —·—	0.29	20	S6	Flexural Failure

a/d = 4.5 for all beams

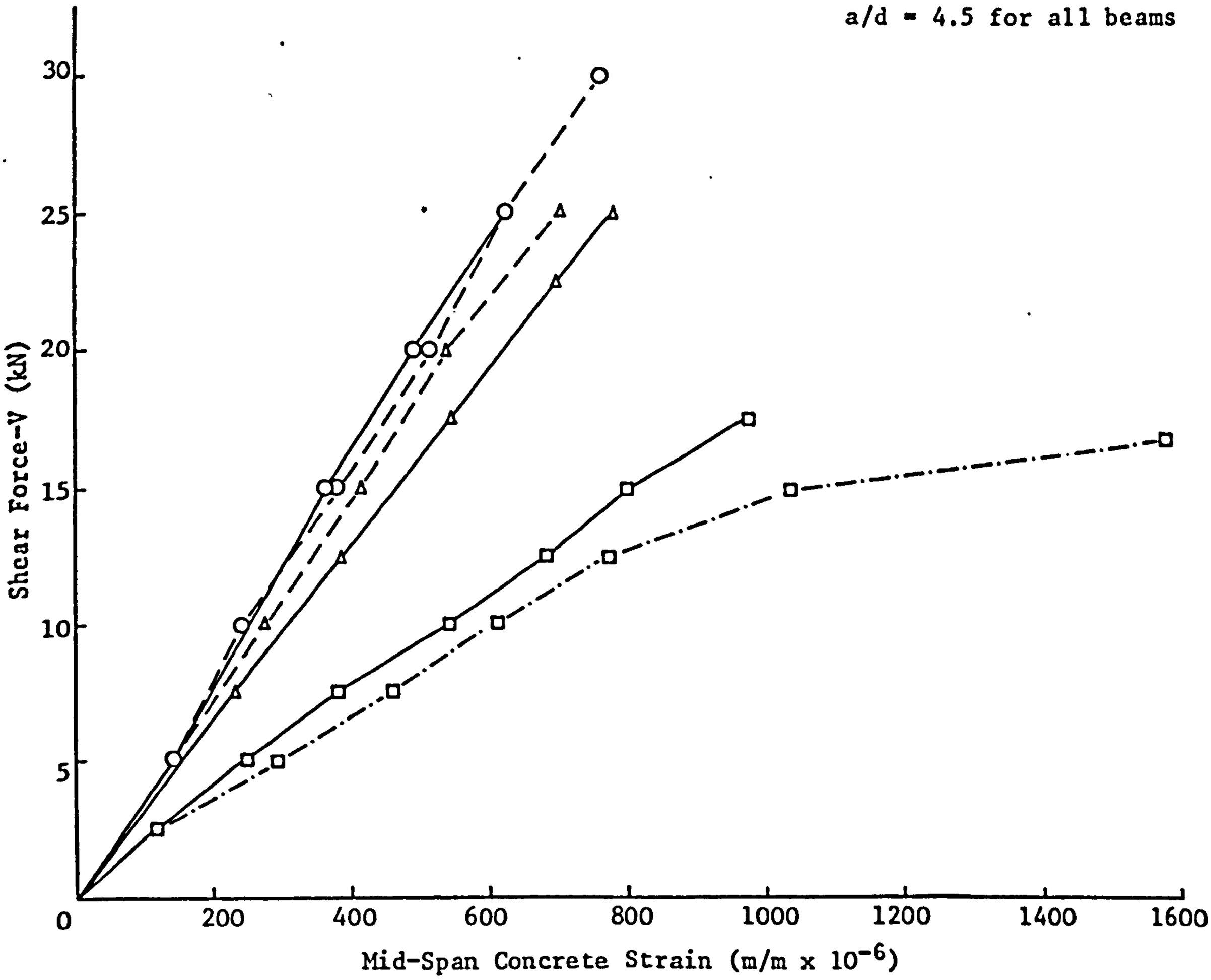

FIGURE 7.10 EFFECT OF CONCRETE STRENGTH ON MID-SPAN CONCRETE STRAIN

7.5.2.3 Concrete Strain Near Load Points

Several investigators (49, 142, 149-151) have reported the presence of tensile strain and of vertical cracks extending from the compression face in the shear span, near to the load points, for dense concrete beams. This is due to a stress redistribution in the shear span after the formation of a diagonal crack but is generally only associated with the shorter shear spans. In order to investigate the effects of diagonal crack formation on the concrete near to the load point, strain measurements were taken using a Demec extensometer with a gauge length of 100 mm. The locations of the demec points for the various a/d ratio's are shown in Figure 7.2. A typical set of strain measurements from the top face of the beam near to the load point, for series LS2 is shown in Figure 7.11 It can be seen that for a/d ratio's of 1.5 and 3.0, the formation of the diagonal crack leads to a reversal of strain which progressively increases with increasing load. For a/d ratio's of 4.5 and 6.0 the formation of the diagonal crack resulted in failure and thus any strain reversal which may have occurred is irrelevant. These results are generally in agreement with the findings of other investigators (49, 149-151).

The formation of vertical cracks extending from the top face of the compression flange was observed in many of the beams after failure. These cracks generally formed towards the middle of the shear span and can be explained by the fact that at the instant of failure the shear plane passes from close to the support to close to the load point with contact being maintained only over a small zone of the concrete flange, immediately next to the load and by the tensile steel. As the section of beam below the diagonal crack moves downwards, the tensile steel pulls the anchorage zone towards the centre of the beam and the section of beam above the diagonal crack is forced to bend upwards and thus crack. The structure becomes a mechanism and collapse occurs. For very short shear spans, a/d = 1.5, the tensile cracks form prior to failure and thus high tensile strains are recorded particularly if a crack lies within the zone over which strains are being measured.

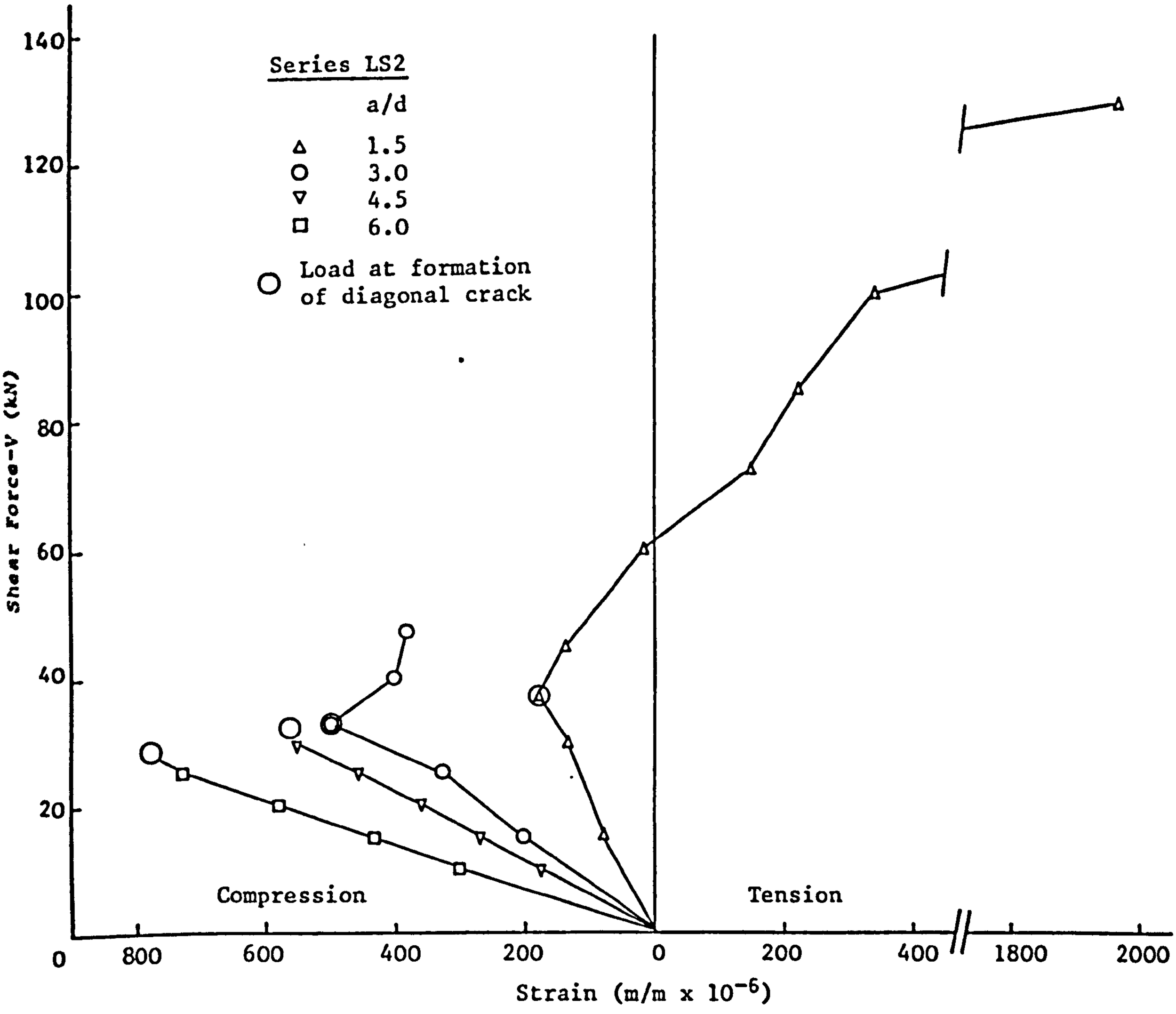

FIGURE 7.11 TYPICAL VARIATION OF CONCRETE STRAIN NEAR LOAD POINT IN FAILED SHEAR SPAN

7.5.2.4 Strain Distribution over the Depth of Section in the Failed Shear Span

The strain distributions across the depth of the section at various load increments are shown in Figures 7.12 and 7.13 for a/d ratio's of 1.5 and 6.0 respectively. These results are typical of the results obtained for all beams tested in the shear beam series.

For the a/d ratio of 1.5, Figure 7.12, it can be seen that the strain variation is complex. Strain redistribution is not apparent immediately after formation of the diagonal crack but near to failure it can be seen that the maximum compressive strain occurs within the web of the beam and that only small strains occur near the top face of the compression flange.

For the a/d ratio of 6.0, Figure 7.13, it can be seen that the section is behaving according to standard beam theory with concrete strains increasing towards the extreme compression fibre and plane sections remaining sensibly plane. The neutral axis position is constant and, along with the low maximum compressive strains recorded, is an indication of the low percentage of the flexural capacity of the beam at which failure occurred.

7.5.2.5 Steel Strains

Graphs of steel strain against load are not shown since they only reflect the previously shown trends of a/d ratio, longitudinal steel percentage and concrete strength. Instead the maximum recorded values of steel strain are shown in Table 7.4 along with other data. An examination of the strains occurring in the constant moment region indicates that in general steel strains were of the order of 50-75% of the 0.2% proof strain and that it was only in beams in series LS6 and S6 that the steel yielded.

For steel strains within the primary (failed) and secondary (unfailed) shear spans, the maximum recorded strain generally occurred adjacent to the load point but, for any particular beam the maximum recorded strain did not necessarily occur in the primary span. In many cases the strains recorded in the shear spans exceeded those in the constant moment region, but with the exception of beam LS3-1 and series LS6 no recorded strain was greater than 0.2%.

KEY

	Percentage of failure load
○	22%
△	34%
□	40%
▽	80%

Diagonal crack occurred at 36% of failure load

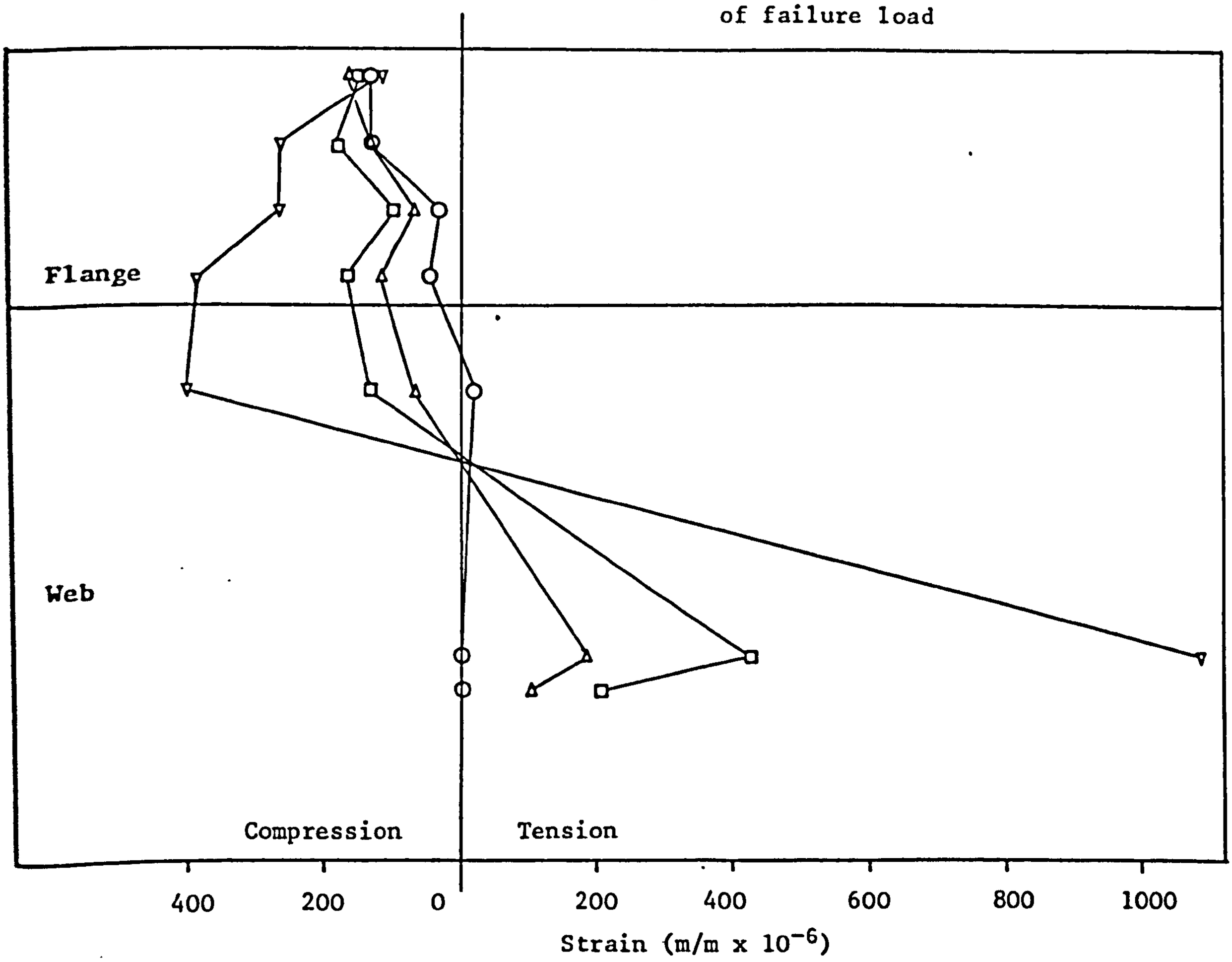

FIGURE 7.12 STRAIN VARIATION WITH DEPTH IN BEAM LS3-1

KEY

	Percentage of failure load
○	38%
△	57%
□	78%
▽	95%

Diagonal cracking load and failure load are equal

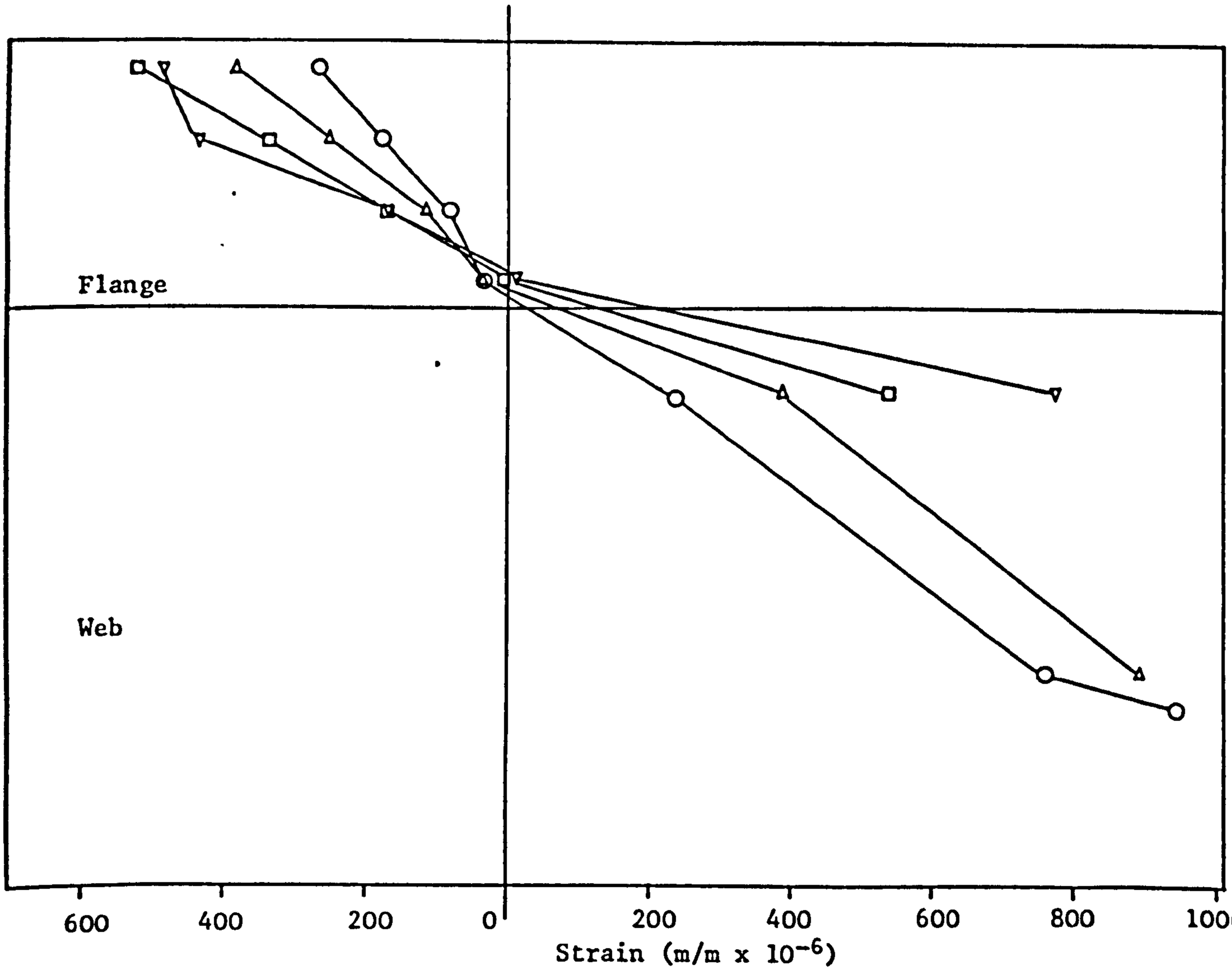

FIGURE 7.13 STRAIN VARIATION WITH DEPTH IN BEAM LS3-4

TABLE 7.4 TEST DATA FROM T-BEAMS

Beam No.	Shear Force at Failure (kN)	Maximum Recorded Steel Strain (m/m x 10^{-6})				Maximum Recorded Concrete Strain (m/m x 10^{-6})				Shear Force at 1st Diagonal Crack (kN)	% of Failure Load	Shear Force at 2nd Diagonal Crack (kN)**	% of Failure Load
		% of Failure Load	Primary Shear Span*	C.M.R.*	Secondary Shear Span*	% of Failure Load	Primary Shear Span	Mid Span	Secondary Shear Span				
LS1-1	150.0	93	-	1110	1900 S	75	470	775	235	45.0	30	50.0	33
2	65.0	96	860 S+	960	880 L+	88	-200	-800	-315	42.5	65	42.5	65
3	37.5	67	440 L	570	450 L	67	-425	-625	-400	37.5	100	37.0	99
4	37.0	95	900 L	1120	885 L	88	-815	-920	-800	37.0	100	-	-
LS2-1	140.5	96	1410 L	1380	1450 L	93	1970	-1165	440	37.5	27	40.0	28
2	55.5	95	970 L	1110	1120 S	86	-385	-755	304	32.5	59	32.5	59
3	32.5	92	680 L	890	720 L	92	-590	-755	-555	32.5	100	32.5	100
4	29.9	92	1080 L	1100	1075 L	84	-755	-825	-695	29.9	100	-	-
LS3-1	125.0	92	2200 L	1800	1700 L	80	10	-995	145	37.5	30	45.0	36
2	45.0	89	1100 L	1230	900 L	78	-295	-675	-140	25.0	56	25.0	56
3	27.5	91	1050 L	1210	845 L	91	-580	-695	-590	25.0	91	27.5	100
4	26.4	95	1400 L	1500	-	95	-760	-945	-685	26.4	100	-	-
S3	32.5	85	-	1050	-	92	-	-690	-	25.0	77	-	-
S4	26.9	93	-	1400	-	93	-	-875	-	25.0	93	-	-
LS4-1	97.5	97	1090 L	1085	1220 L	77	315	-600	50	40.0	41	45.0	46
2	52.5	95	1240 S	1305	1100 L	67	-750	-650	-490	30.0	57	32.5	62
3	31.0	81	580 L	825	650 L	81	-485	-620	-510	26.5	85	27.5	89
4	26.5	94	1100 L	1055	1250 L	75	-595	-730	-560	22.5	85	-	-
LS5-1	110.8	90	1710 L	1500	1430 L	77	275	-950	205	35.0	32	35.0	32
2	36.3	97	1320 L	1150	1200 L	97	-680	-770	-125	25.0	69	25.0	69
3	26.5	85	1080 L	1150	1100 L	94	-630	-775	-725	25.0	94	-	-
4	24.0	94	1200 L	1600	1100 L	94	-930	-920	-820	22.5	94	-	-
LS6-1	61.8	97	3070 L	9300	8500 L	81	350	-890	-75	25.0	40	-	-
2	29.3	85	2580 L	4350	2400 L	85	-135	-970	-365	22.5	76	25.0	85
3	20.5	85	-	7100	-	85	-	-970	-	-	-	-	-
4	-	-	-	-	-	-	-	-	-	-	-	-	-
S1	28.0	98	-	1500	-	98	-	-745	-	20.0	71	25.0	89
S2	25.0	-	-	-	-	90	-	-915	-	25.0	100	-	-
S5	19.7	89	-	1280	-	89	-	-650	-	17.5	89	-	-
S6	19.0	92	-	12800	-	92	-	-1775	-	-	-	-	-

* Primary Shear Span - Span in which failure occurred
Secondary Shear Span - Span which did not fail
** 2nd diagonal crack refers to the crack formation in the 2nd shear span

C.M.R. - Constant Moment Region
+ S - Near Support
L - Near Load

The data shown in Table 7.4 along with the previously discussed figures all combine to indicate the brittle failure mode associated with shear failures. In general, such failures are sudden and catastrophic.

7.5.3 Strength Characteristics

7.5.3.1 Introduction

The beam strength results are shown in Tables 7.4-7.6 and the failure modes of the test specimens are shown in Plates 7.2-7.3. The loads at first diagonal crack, V_{cr}, and at failure, V_u, in the Tables are the observed experimental values. The ultimate moment M_u is based on the failure load V_u and the flexural moment M_f was calculated from the CP 110 parabolic stress block, ignoring the material safety factors, (see Appendix B). The aim of this section on strength characteristics is to compare the ultimate shear stress with those of the various design codes (26, 54, 73) and to develop an empirical formula to predict the ultimate shear stress of a section without any web reinforcement.

7.5.3.2 Flexural Cracking

Only minor attention was paid to flexural cracking in the constant moment region since beams without web reinforcement are never designed in practice and, therefore, crack width, spacing and height data from these tests would be of little use. Flexural cracks were marked at each load increment throughout the length of the beam with attention being paid to crack formation and propagation within the shear spans.

Initial flexural cracks formed in the constant moment region and as the load increased, these cracks propagated towards the web flange junction and new cracks formed, both in the constant moment region and in the shear spans. With the exception of series LS6, flexural cracks did not propagate up to the web flange junction in the constant moment region. With the shorter shear spans ($a/d \leq 3.0$), however, it was not unusual to find flexural cracks which had formed directly under the loading point propagating into the flange. In general, flexural crack propagation was rapid at first but slowed down and in many cases ceased at medium to high loads, for beams which did not fail at the formation of the initial diagonal crack.

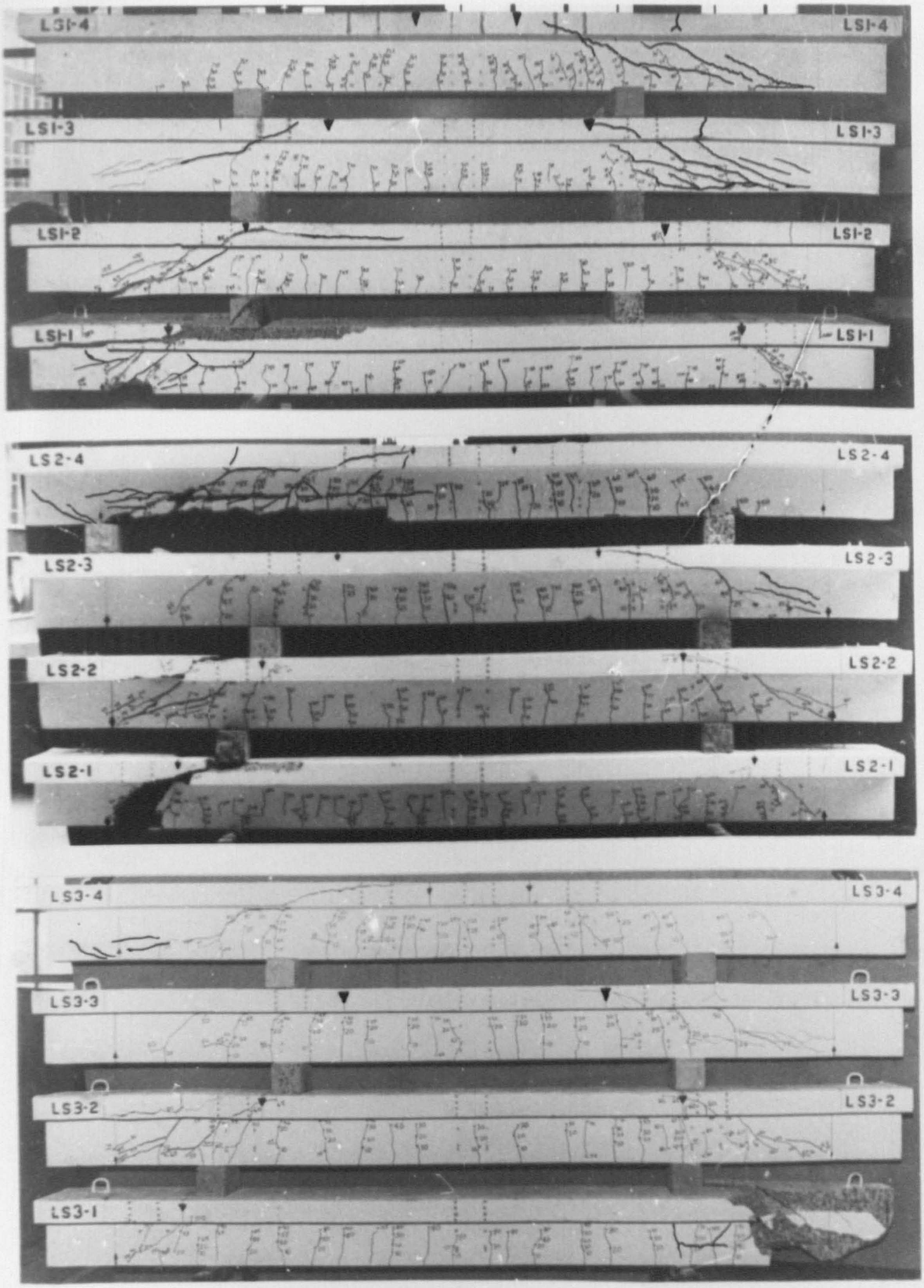

PLATE 7.2(a) FAILURE MODES FOR LYTAG-SAND CONCRETE T-BEAMS IN SHEAR

PLATE 7.2(b) FAILURE MODES FOR LYTAG-SAND CONCRETE T-BEAMS IN SHEAR

PLATE 7.2(c) FAILURE MODES FOR LYTAG-SAND CONCRETE T-BEAMS IN SHEAR

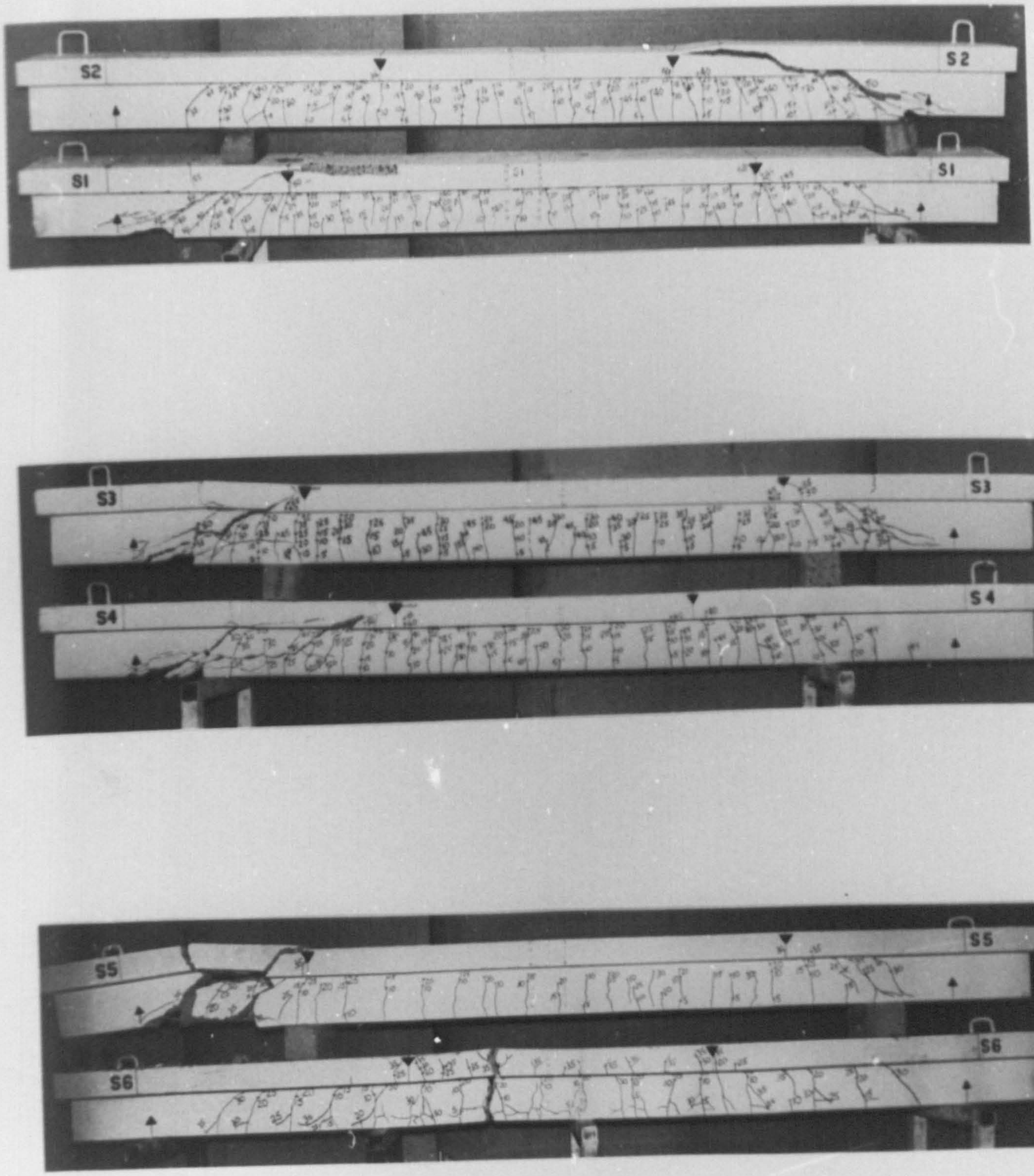

PLATE 7.2(c) FAILURE MODES FOR LYTAG-SAND CONCRETE T-BEAMS IN SHEAR

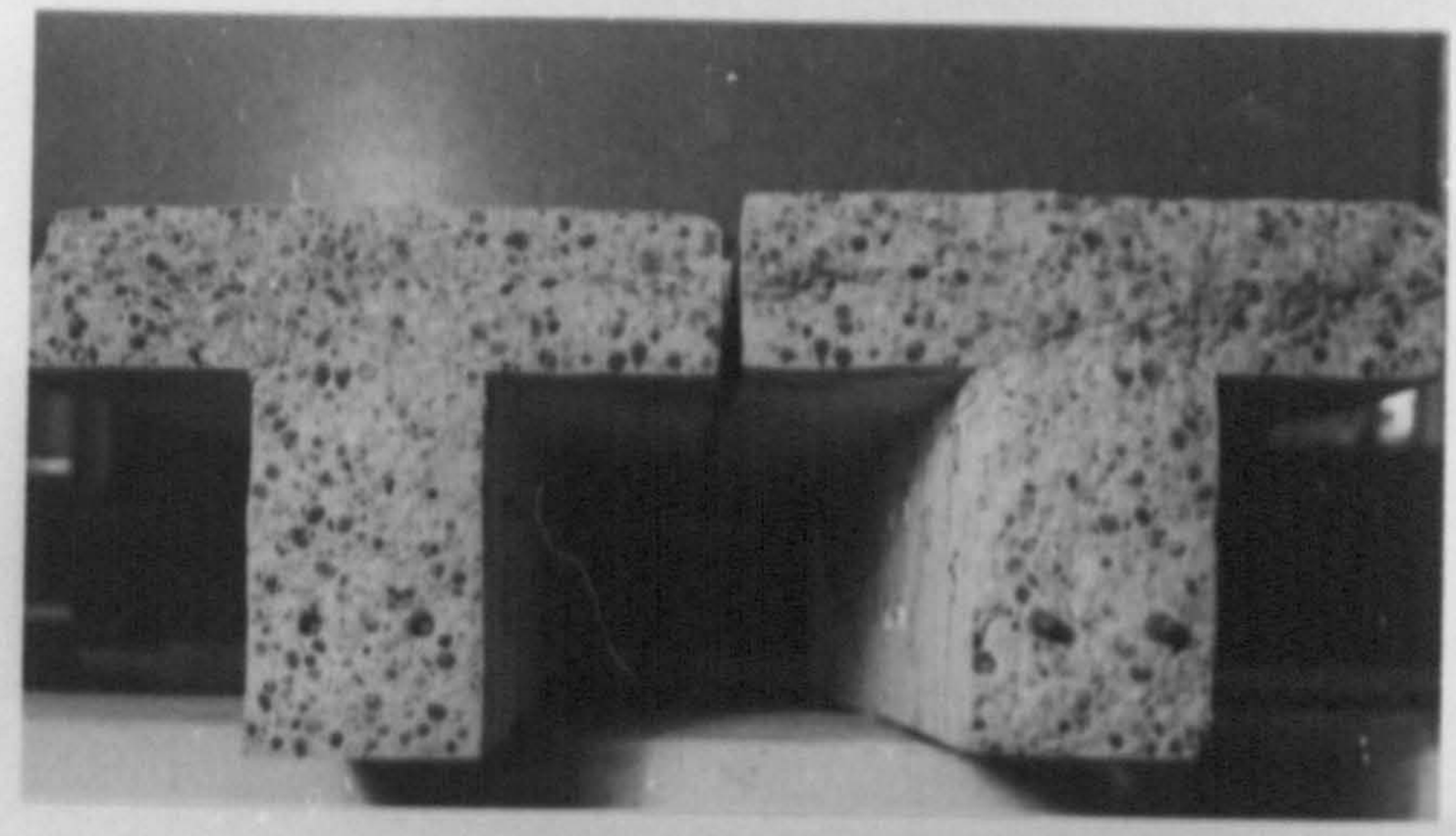

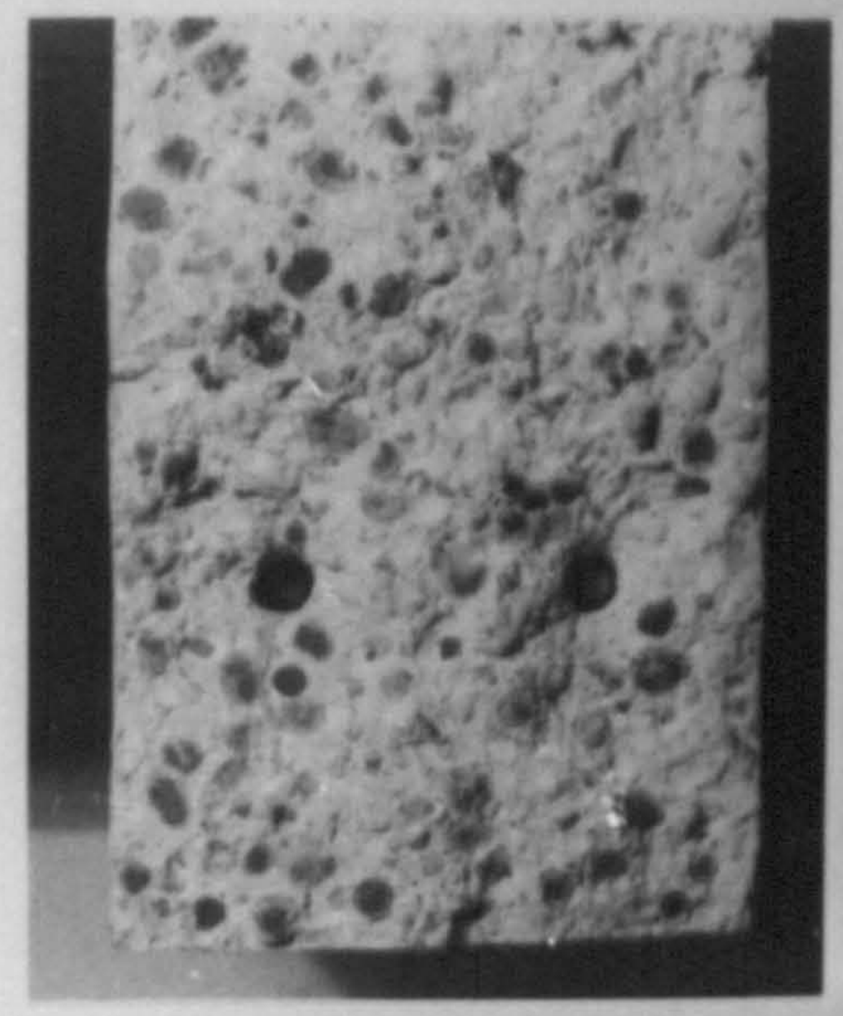

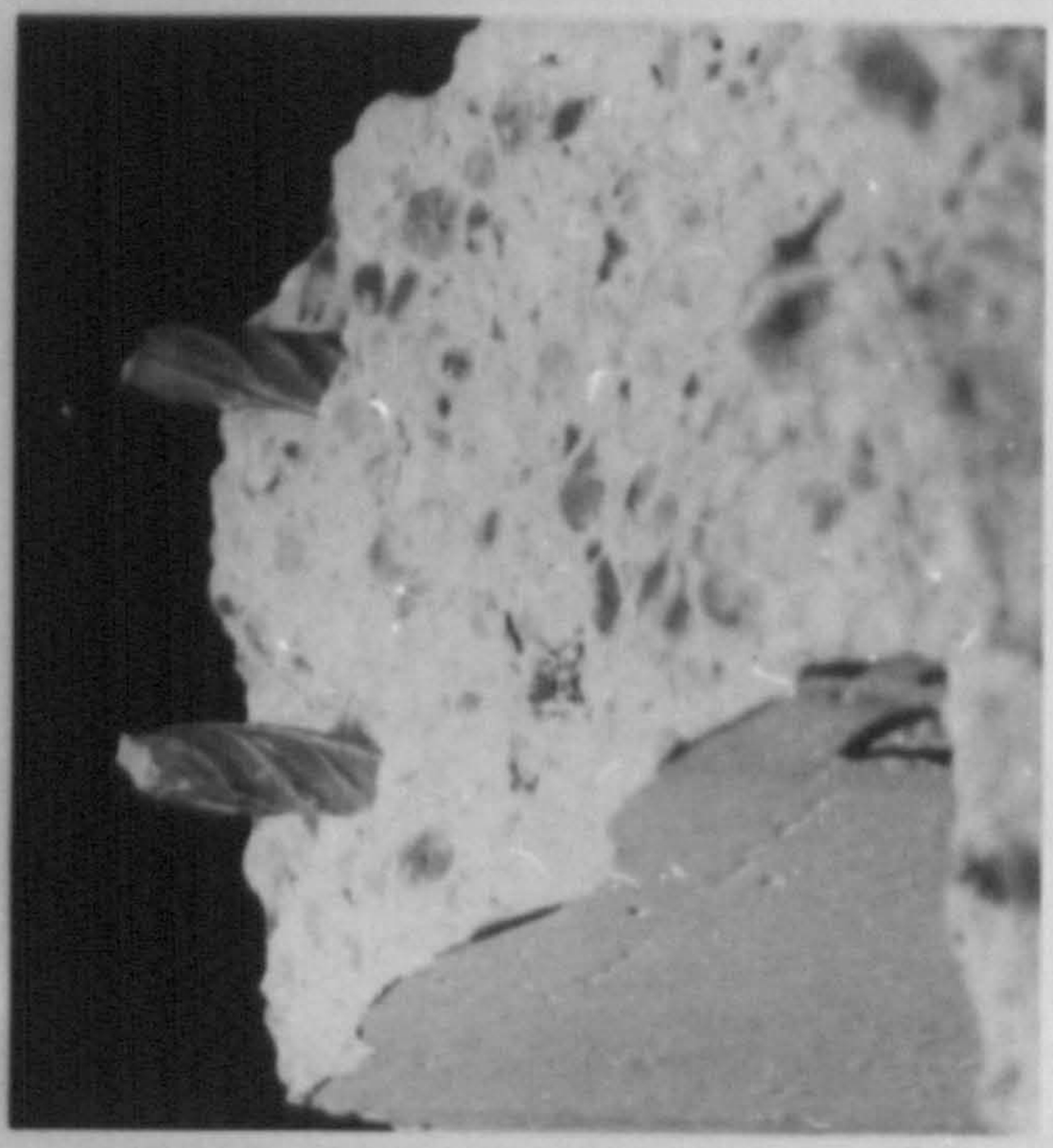

PLATE 7.3 FAILURE MODE FOR BEAM LS6-3

7.5.3.3 Diagonal Cracking

For the purposes of this thesis a diagonal crack is defined as an inclined crack which extends up towards the loading point and down towards the support. For the shorter shear spans ($a/d \leq 3.0$) the diagonal cracks tended to form in the web, in the shear span, independent of any flexural cracks. For a/d ratio's greater than 3.0, the diagonal cracks tended to form as an extension of a flexural crack.

It is worth noting that the span in which the first diagonal crack formed, the primary span, was not necessarily the span in which failure occurred. Also, in general the head of the critical crack immediately prior to failure was at a distance of approximately 1.0 to 1.5 times d from the load point.

7.5.3.4 Diagonal Cracking and Ultimate Load

Values of diagonal cracking load V_{cr} and ultimate load V_u are presented in Table 7.5. In converting the diagonal cracking and ultimate loads to stresses a problem is encountered with flanged sections. Design recommendations (26, 54, 73) are based on nominal shear stress which is calculated on the section width, for a rectangular section, or the rib width for a flanged section times the effective depth. This method has, not surprisingly, produced a wide range of safety margins when compared with actual test results. An added complication is introduced with flanged sections, such as T-beams, since the above method does not take account of the shear resistance of the concrete in the compression flange outstands. For design purposes this results in a conservative design since the actual nominal shear stress in the concrete will be less than the assumed value. For analysis purposes, however, neglecting the compression flange concrete will result in higher calculated values of nominal concrete shear stress at failure for test specimens, than actually exist.

Figure 7.14 shows the calculated nominal ultimate shear stresses for the beams in series LS3, based on the rib width times the effective depth and on the actual cross-sectional area of the beam down to the centroid of the tension steel. For the reasons already given the former calculation is incorrect but the latter calculation is also incorrect since it assumes that the cracked concrete in the

TABLE 7.5 STRENGTH CHARACTERISTICS OF T-BEAMS

Beam No.	a/d Ratio	Cube Strength (N/mm^2)	V_u (kN)	V_{cr} (kN)	$v_u = \frac{V_u}{b_w d}$ (N/mm^2)	$v_{cr} = \frac{V_{cr}}{b_w d}$ (N/mm^2)	M_u Measured (kNm)	M_f * Calculated (kNm)	$\frac{M_u}{M_f}$
LS1-1	1.5	40.0	150.0	45.0	8.17	2.45	40.50	102.03	0.40
2	3.0	38.0	65.0	42.5	3.54	2.31	35.10	100.12	0.35
3	4.5	37.5	37.5	37.5	2.04	2.04	30.38	99.61	0.30
4	6.0	42.0	37.0	37.0	2.02	2.02	39.96	103.75	0.39
LS2-1	1.5	39.5	140.5	37.5	7.65	2.04	37.94	71.84	0.53
2	3.0	48.0	55.5	32.5	3.02	1.77	29.97	74.34	0.40
3	4.5	47.0	32.5	32.5	1.77	1.77	26.33	74.09	0.36
4	6.0	41.5	29.9	29.9	1.63	1.63	32.29	72.52	0.45
LS3-1	1.5	46.0	125.0	37.5	6.81	2.04	33.75	47.96	0.70
2	3.0	46.0	45.0	25.0	2.45	1.36	24.30	47.96	0.51
3	4.5	48.0	27.5	25.0	1.50	1.36	22.28	48.15	0.46
4	6.0	45.5	26.4	26.4	1.44	1.44	28.51	47.91	0.60
S3	3.0	47.5	32.5	25.0	1.77	1.36	17.55	30.40	0.58
S4	4.5	47.0	26.9	25.0	1.46	1.36	21.79	30.38	0.72
LS4-1	1.5	30.0	97.5	40.0	5.41	2.18	26.33	67.36	0.39
2	3.0	31.0	52.5	30.0	2.86	1.63	28.35	67.96	0.42
3	4.5	30.5	31.0	26.5	1.69	1.44	25.11	67.61	0.37
4	6.0	29.0	26.5	22.5	1.44	1.23	28.62	66.72	0.43
LS5-1	1.5	27.5	110.8	35.0	6.03	1.91	29.92	44.93	0.67
2	3.0	25.5	36.3	25.0	1.98	1.36	19.60	44.33	0.44
3	4.5	29.5	26.5	25.0	1.44	1.36	21.47	45.44	0.47
4	6.0	32.5	24.0	22.5	1.31	1.23	25.92	46.09	0.56
LS6-1	1.5	31.5	61.8	25.0	3.37	1.36	16.69	12.72	1.31
2	3.0	32.0	29.3	22.5	1.60	1.23	15.82	12.73	1.24
3	4.5	33.5	20.5+	-	1.12	-	16.61	12.75	1.30
4	6.0	-	-	-	-	-	-	-	-
S1	3.0	30.5	28.0	20.0	1.53	1.09	15.12	24.56	0.62
S2	4.5	31.5	25.0	25.0	1.36	1.36	20.25	24.61	0.82
S5	3.0	23.5	19.7	17.5	1.07	0.95	10.64	12.58	0.85
S6	4.5	23.5	19.0+	-	1.03	-	15.39	12.58	1.22

* Based on CP 110 parabolic stress block (See Appendix B)
\+ Flexural failure

tensile zone is capable of carrying its full share of the shear, as does the method for rectangular sections. Thus the true shear stress, in the concrete, at failure must lie somewhere between these two extremes.

For comparison purposes with the various design codes (26, 54, 73), the shear stresses at diagonal cracking and at failure have been calculated based on the rib width times the effective depth.

7.5.3.5 Modes of Failure

In any multi-phase system under combined bending and shear, cracking, in particular diagonal cracking is a complex phenomenom. It is not uncommon for several secondary modes of failure to occur simultaneously at the failure stage. The difficulty in identifying and establishing the correct mode of failure in all cases along with the subjective nature of such identifications has resulted in the generalised use of the term 'diagonal tension failure' to cover all failures which occur as a result of combined bending and shear stresses and, which do not exhibit the ductile characteristics associated with flexural failure. Diagonal cracking data, along with the influence of a/d ratio and steel percentage, on the failure mode of Lytag-sand concrete T-beams, are shown in Table 7.6. The influence of a/d ratio on the diagonal crack formation and failure mode is shown in Figures 7.15 (a)-(d).

For a/d ratio's of 1.5 and 3.0, Figures 7.15 (a) and (b), the initial diagonal crack formed independently of any flexural cracks. With increasing load the crack, or cracks, propagated upwards towards the web-flange junction and downwards towards the support. With the short shear span, a/d = 1.5, the crack generally reached the web-flange junction and then proceeded to travel horizontally along the junction before propagating up into the flange just behind the load point. At failure a shear plane formed in the flange which extended down to meet the main diagonal crack near to where it reached the web-flange junction. Concrete spalling along the flange and at the support generally occurred and in general severe crushing of the concrete web was apparent. With a/d = 3.0, more than one diagonal crack generally formed. The critical crack, at failure, extended from near the support up through the web and the flange and

TABLE 7.6 INFLUENCE OF a/d AND ρ ON FAILURE MODE

Beam No.	ρ (%)	a/d Ratio	Cube Strength N/mm²	V_{cr} (kN)	$\frac{V_{cr}}{V_{cr}(L)}$ *	V_u (kN)	$\frac{V_u}{V_u(L)}$ *	Failure Mode
LS6-1	0.29	1.5	31.5	25.0	1.00	61.8	1.00	W.C.
LS5-1	1.14	1.5	27.5	35.0	1.40	110.8	1.79	"
LS3-1	1.14	1.5	46.0	37.5	1.50	125.0	2.02	"
LS4-1	1.87	1.5	30.0	40.0	1.60	97.5	1.58	"
LS2-1	1.87	1.5	39.5	37.5	1.50	140.5	2.27	"
LS1-1	3.01	1.5	40.0	45.0	1.80	150.0	2.43	"
S5	0.29	3.0	23.5	17.5	1.00	19.7	1.00	D.T.
LS6-2	0.29	3.0	32.0	22.5	1.29	29.3	1.49	"
S1	0.57	3.0	30.5	20.0	1.14	28.0	1.42	"
S3	0.70	3.0	47.5	25.0	1.43	32.5	1.65	"
LS5-2	1.14	3.0	25.5	25.0	1.43	36.3	1.84	"
LS3-2	1.14	3.0	46.0	25.0	1.43	45.0	2.28	"
LS4-2	1.87	3.0	31.0	30.0	1.71	52.5	2.66	"
LS2-2	1.87	3.0	48.0	32.5	1.86	55.5	2.82	"
LS1-2	3.01	3.0	38.0	42.5	2.43	65.0	3.30	"
S6	0.29	4.5	23.5	-	-	19.0	1.00	Flexural
LS6-3	0.29	4.5	33.5	-	-	20.5	1.08	"
S2	0.57	4.5	31.5	25.0	1.00	25.0	1.32	D.T.
S4	0.70	4.5	47.0	25.0	1.00	26.9	1.42	"
LS5-3	1.14	4.5	29.5	25.0	1.00	26.5	1.39	"
LS3-3	1.14	4.5	48.0	25.0	1.00	27.5	1.45	"
LS4-3	1.87	4.5	30.4	26.5	1.06	31.0	1.63	"
LS2-3	1.87	4.5	47.0	32.5	1.30	32.5	1.71	"
LS1-3	3.01	4.5	37.5	37.5	1.50	37.5	1.97	"
LS6-4	0.29	6.0	-	-	-	-	-	-
LS5-4	1.14	6.0	32.5	22.5	1.00	24.0	1.00	D.T.
LS3-4	1.14	6.0	45.5	26.4	1.18	26.4	1.10	"
LS4-4	1.87	6.0	29.0	22.5	1.00	26.5	1.10	"
LS2-4	1.87	6.0	41.5	29.9	1.33	29.9	1.25	"
LS1-4	3.01	6.0	42.0	37.0	1.64	37.0	1.54	"

D.T. = Diagonal Tension W.C. = Web Crushing

* Strengths compared with lowest steel ratio in group

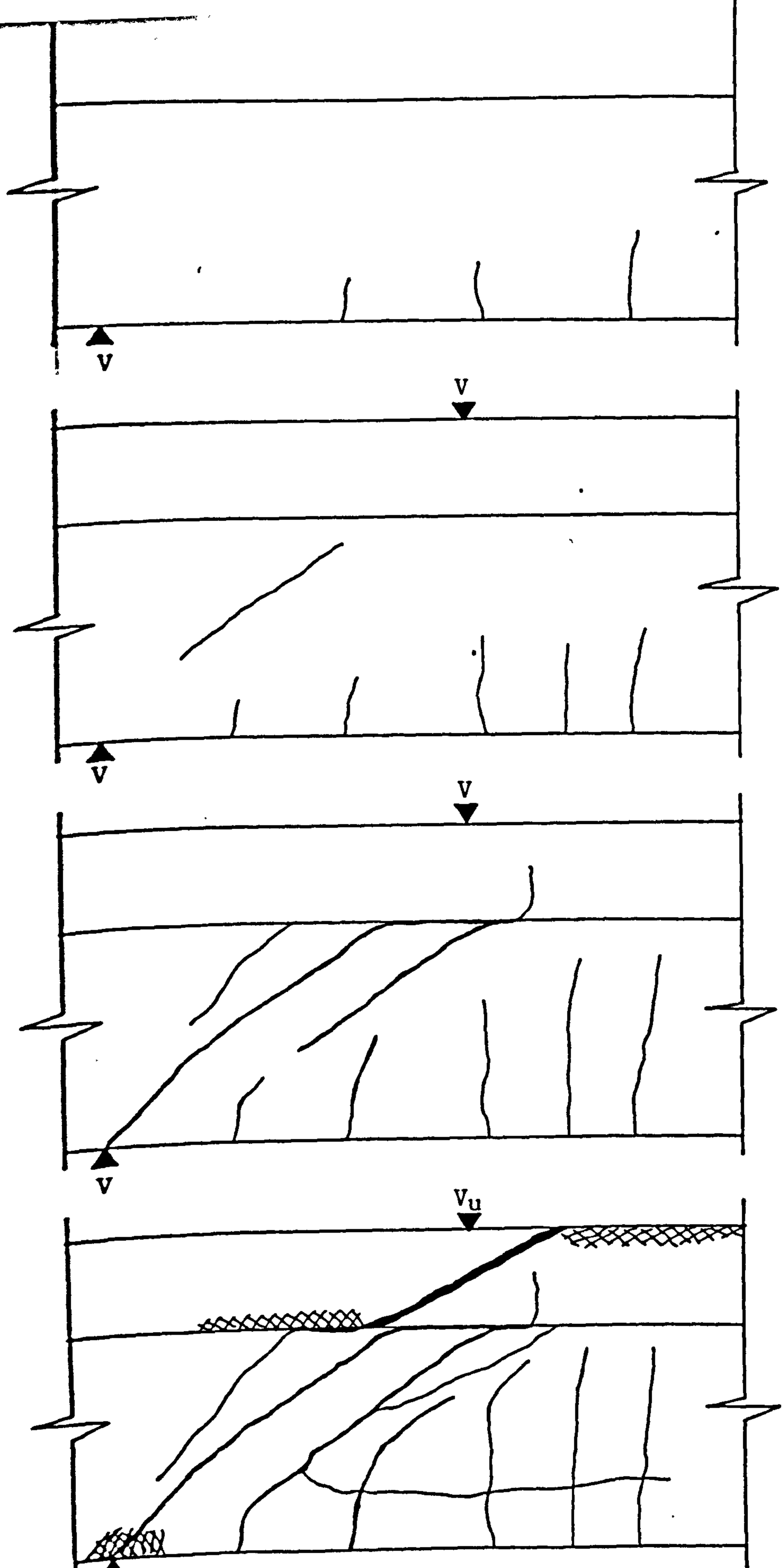

$V = (5\text{-}15\%)\ V_u$:

First flexural cracks appear in the shear span.

$V = (30\text{-}40\%)\ V_u$:

Diagonal tension crack appears in web independently from any flexural cracks.

$V = (40\text{-}65\%)\ V_u$:

Diagonal crack extends down to support and up to flange. Crack extends horizontally along web flange junction before propagating into flange.

Failure:

Failure plane forms on initial diagonal crack and extends through flange. Failure explosive with concrete crushing.

FIGURE 7.15(a) DIAGONAL CRACKING PATTERN AND FAILURE MODE

a/d = 3.0

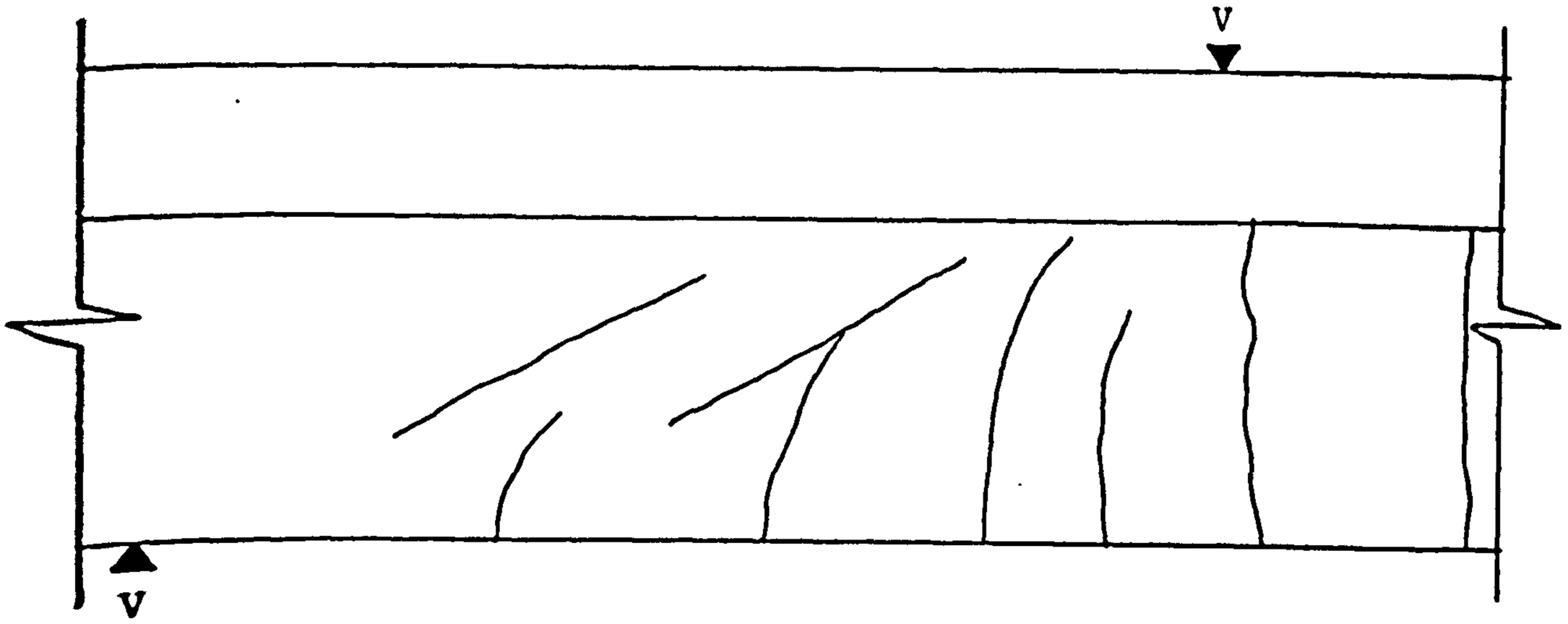

V = (50-70%) V_u: Diagonal tension cracks form, 1st crack generally independent of flexural cracks.

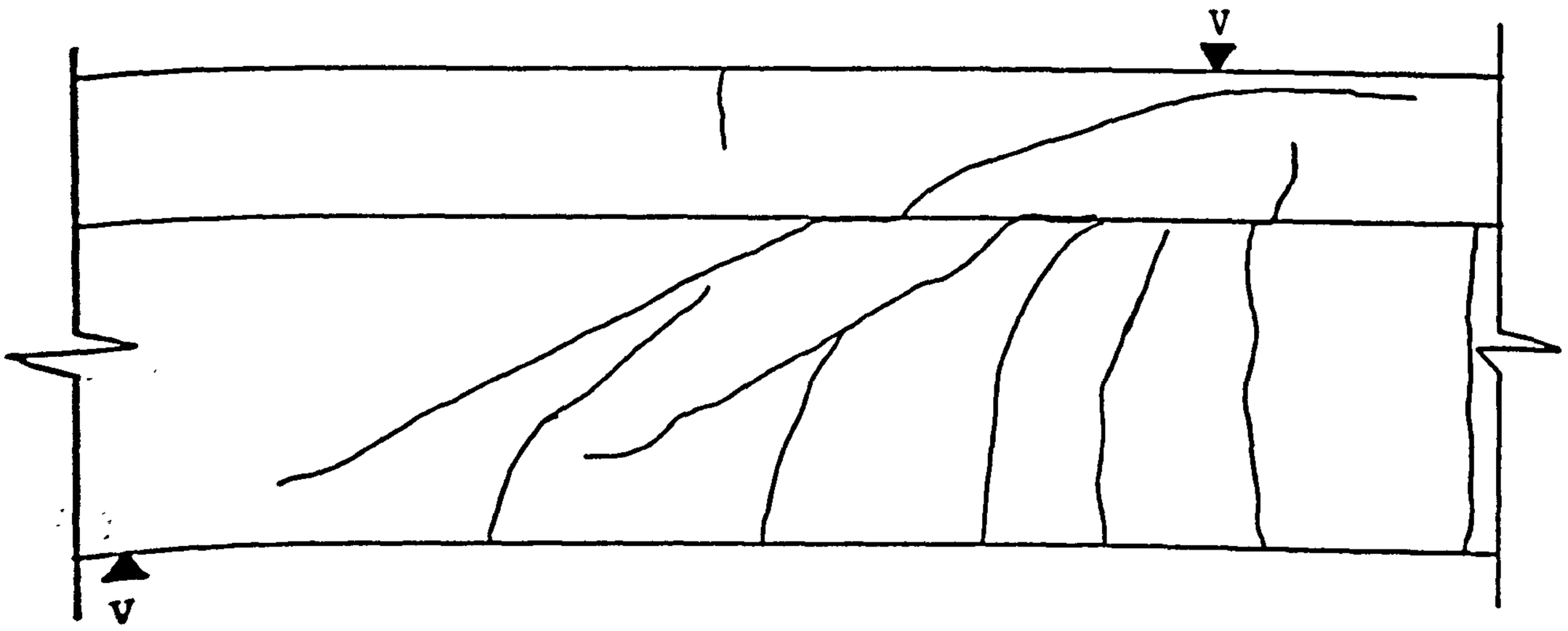

V = (70-95%) V_u: Fatal crack extends up into flange under load point. Tensile crack appears on upper face of flange, approximately at mid-span.

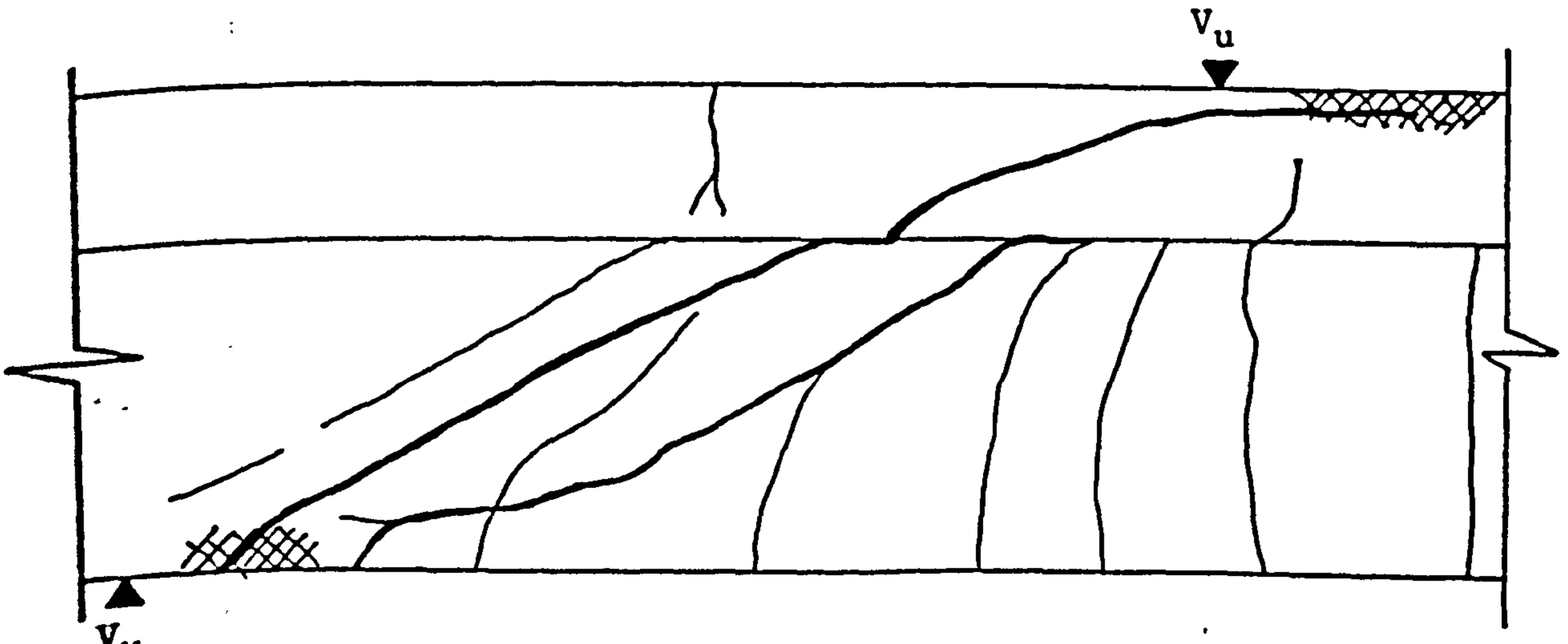

Failure: Fatal crack opens up and mechanism forms. Concrete crushing occurs near support. Fatal crack does not extend down to support.

FIGURE 7.15(b) DIAGONAL CRACKING PATTERN AND FAILURE MODE

a/d = 4.5

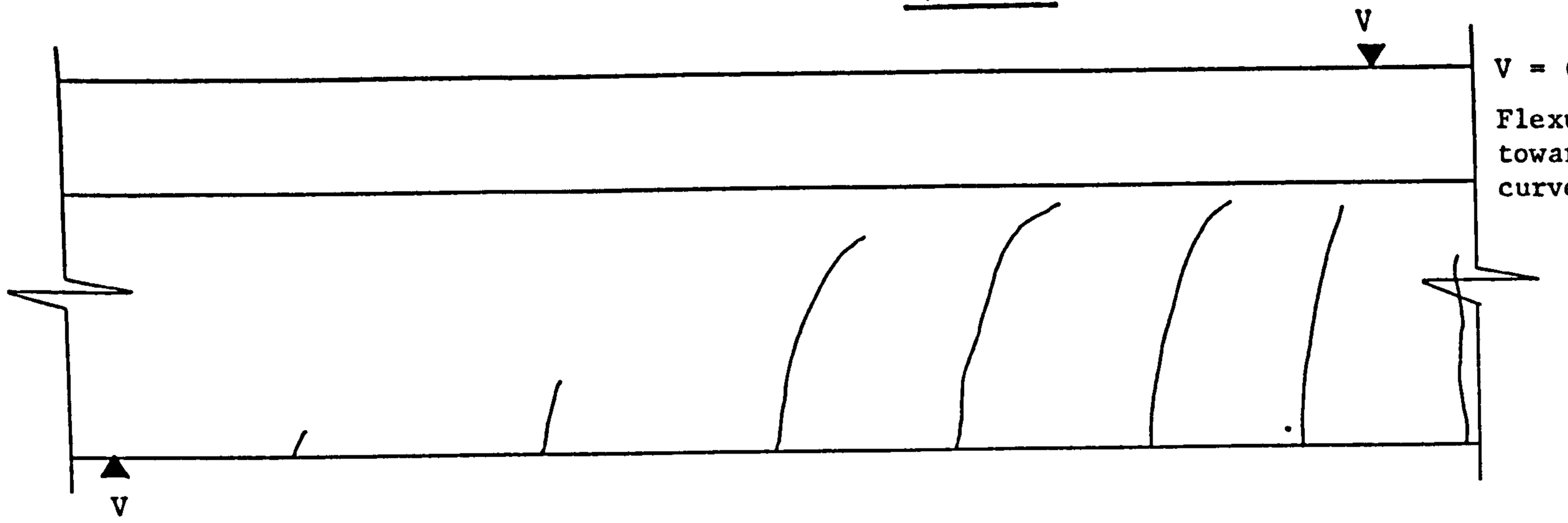

V = (80-95%) V_u:

Flexural cracks extend up towards flange and begin to curve towards load point.

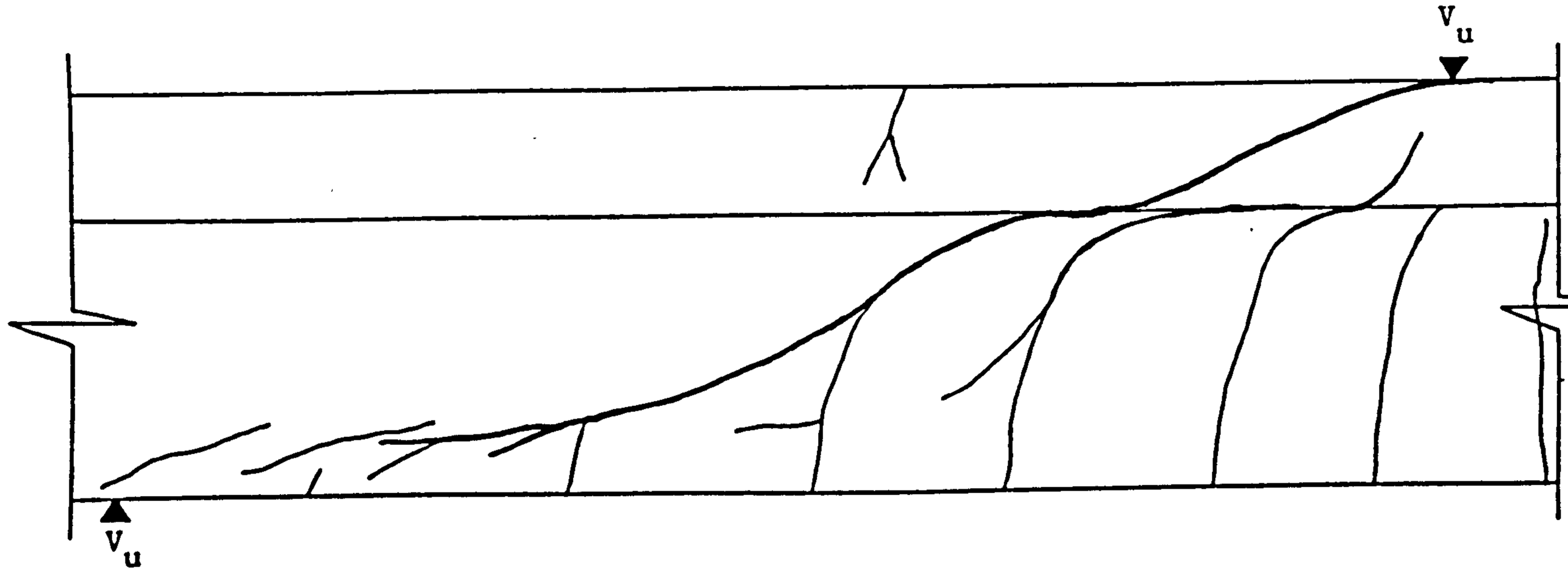

Failure:

Diagonal crack forms as an extension of a flexural crack and rapidly extends into flange and under load point. Failure occurs on or shortly after formation of crack. Tensile crack may or may not form in compression force. May get double failure plane as with a/d = 6.0.

FIGURE 7.15(c) DIAGONAL CRACKING PATTERN AND FAILURE MODE

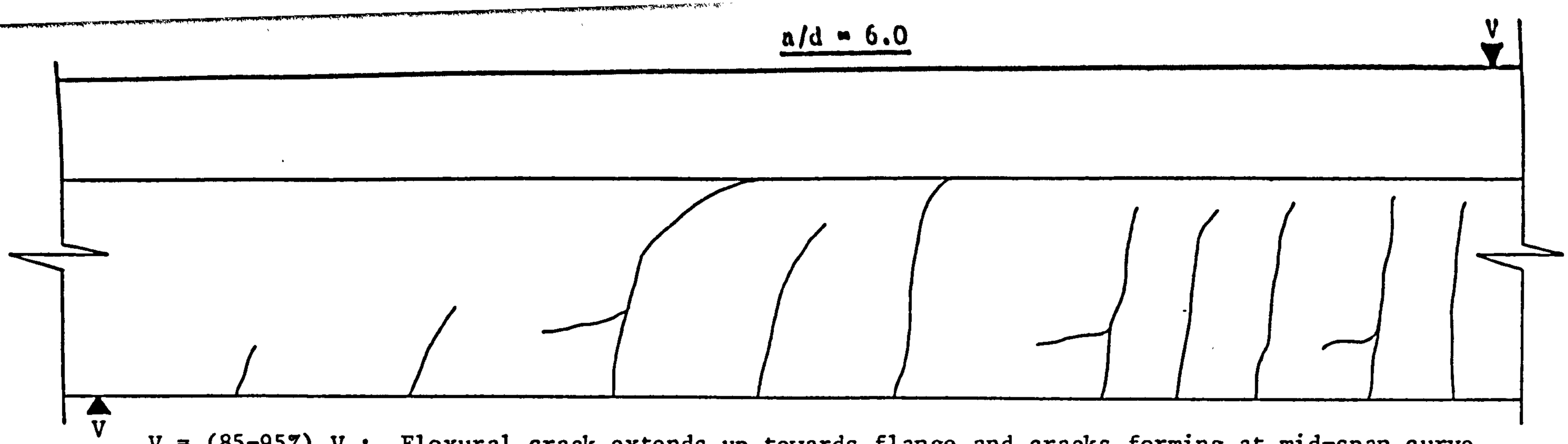

V = (85-95%) V_u: Flexural crack extends up towards flange and cracks forming at mid-span curve towards load point. Horizontal cracks may also form at top of tension steel.

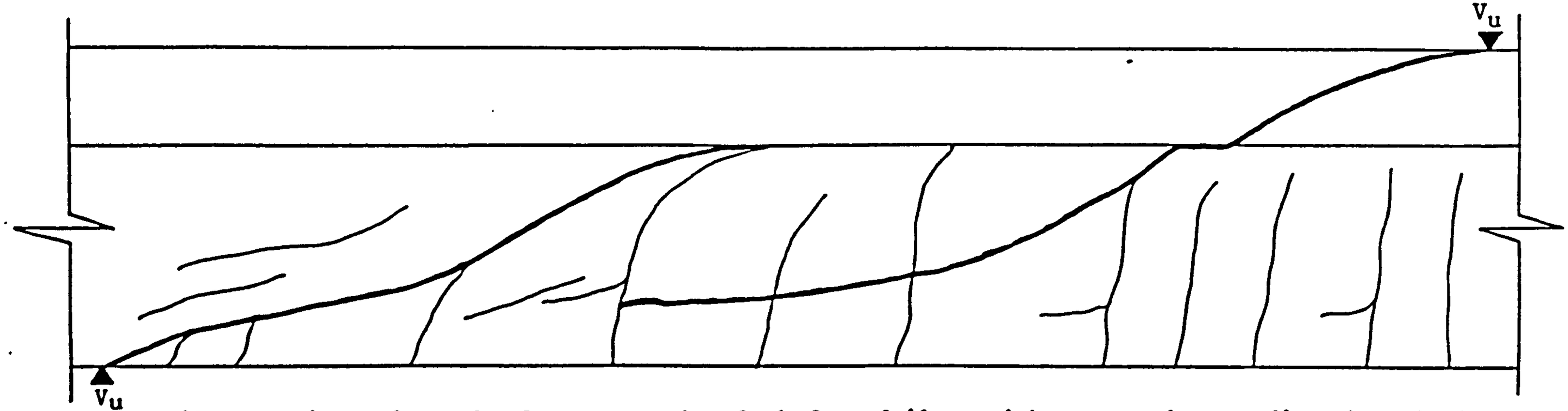

Failure: Diagonal cracks form at or shortly before failure with one crack extending through the flange towards the load point. May get single failure plane as with a/d = 4.5.

FIGURE 7.15(d) DIAGONAL CRACKING PATTERN AND FAILURE MODE

under the load point. Concrete spalling generally occurred on the top of the flange and close to the support where the base of the diagonal crack emerged.

For the longer shear spans with a/d ratio's of 4.5 and 6.0, the diagonal cracks formed as extensions of flexural cracks. A flexural crack would begin to curve towards the load point. Suddenly an increase in load would cause the crack to develop right up to the load point and back towards the support. Failure occurred either along a single shear plane as indicated in Figure 7.15 (c) or along two shear planes, as shown in Figure 7.15 (d) for both a/d ratio's.

For beams with a/d ratio's of 1.5 and 3.0, the formation of the initial diagonal crack was followed by the formation of a second diagonal crack or cracks in the other shear span. With further increase in load, both cracks extended towards the load point and immediately prior to failure, the head of the crack reached to within 15-30 mm (approximately) of the top of the flange. Failure at the compression face always involved destruction of the concrete close to the upper end of the diagonal tension crack, in particular, around the loading block. A side view of the beams shows the diagonal cracks reaching the top surface of the flange behind the load point, in general. This is due to the fact that the loading block only extended over the width of the rib and not the flange.

Similar failure modes have been observed by several investigators (49, 141, 152) for both lightweight and dense concrete T-beams in shear. Thus it can be concluded that the failure mode of Lytag-sand concrete T-beams and their diagonal tension strength are affected by the same variables as those which affect dense concrete T-beams. The difference lies only in the type of aggregate used and its ability to resist shear failure.

7.5.3.6 Ultimate Shear Resistance

7.5.3.6.1 Influence of Shear Span - Effective Depth (a/d) Ratio

The influence of the a/d ratio on the load at first diagonal crack and at failure, for the beams tested in this investigation, is shown in Figures 7.16 (a)-(c). Also plotted on these figures are the permissible concrete shear stresses according to the various design codes (26, 54, 73). In all cases, the

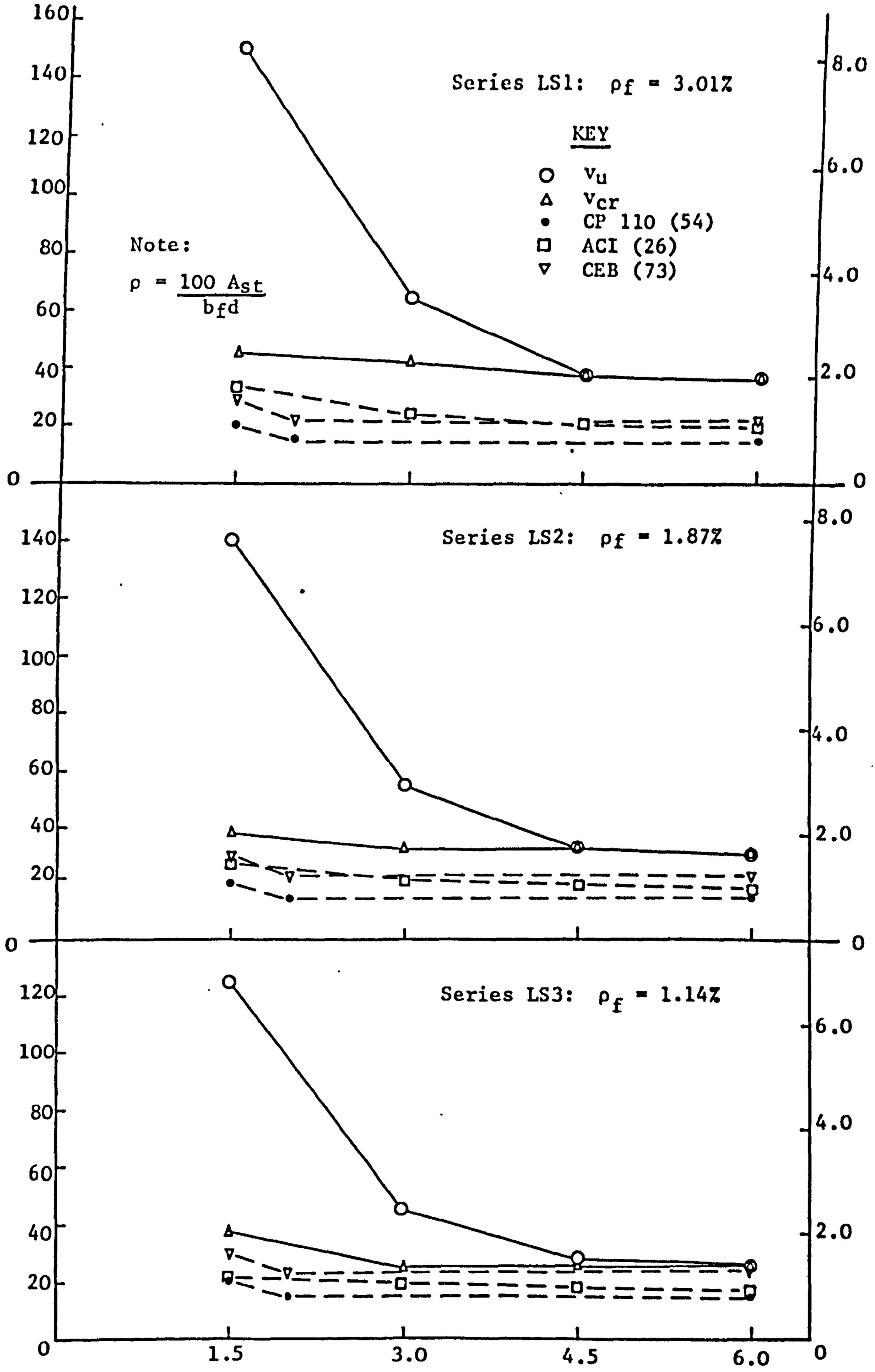

FIGURE 7.16(a) INFLUENCE OF a/d RATIO AND ρ ON SHEAR CRACKING AND ULTIMATE SHEAR STRENGTH FOR CONCRETE STRENGTH OF 40-45 N/mm^2

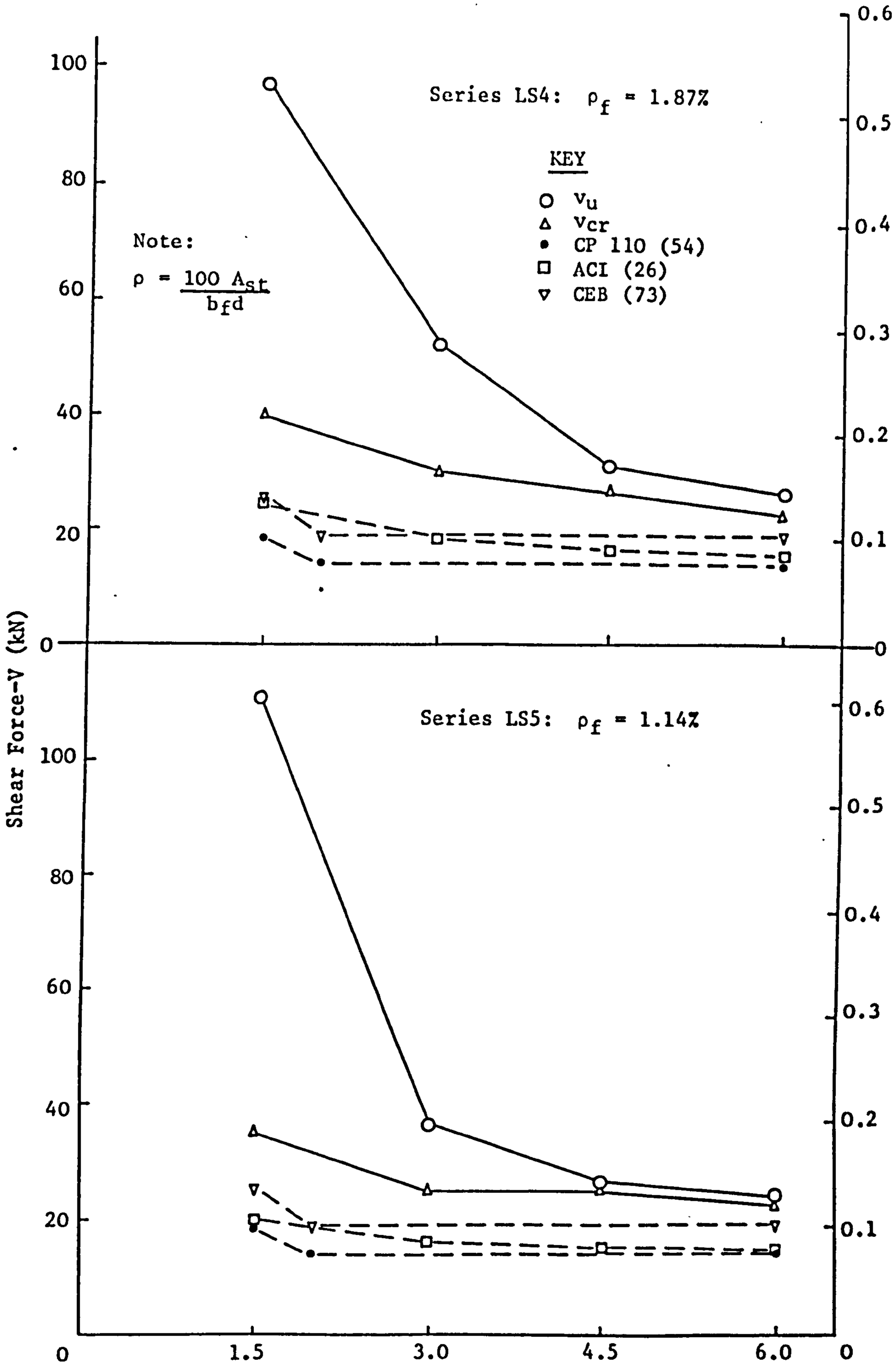

FIGURE 7.16(b) INFLUENCE OF a/d RATIO AND ρ ON SHEAR CRACKING AND ULTIMATE SHEAR STRENGTH FOR CONCRETE STRENGTH OF 30 N/mm²

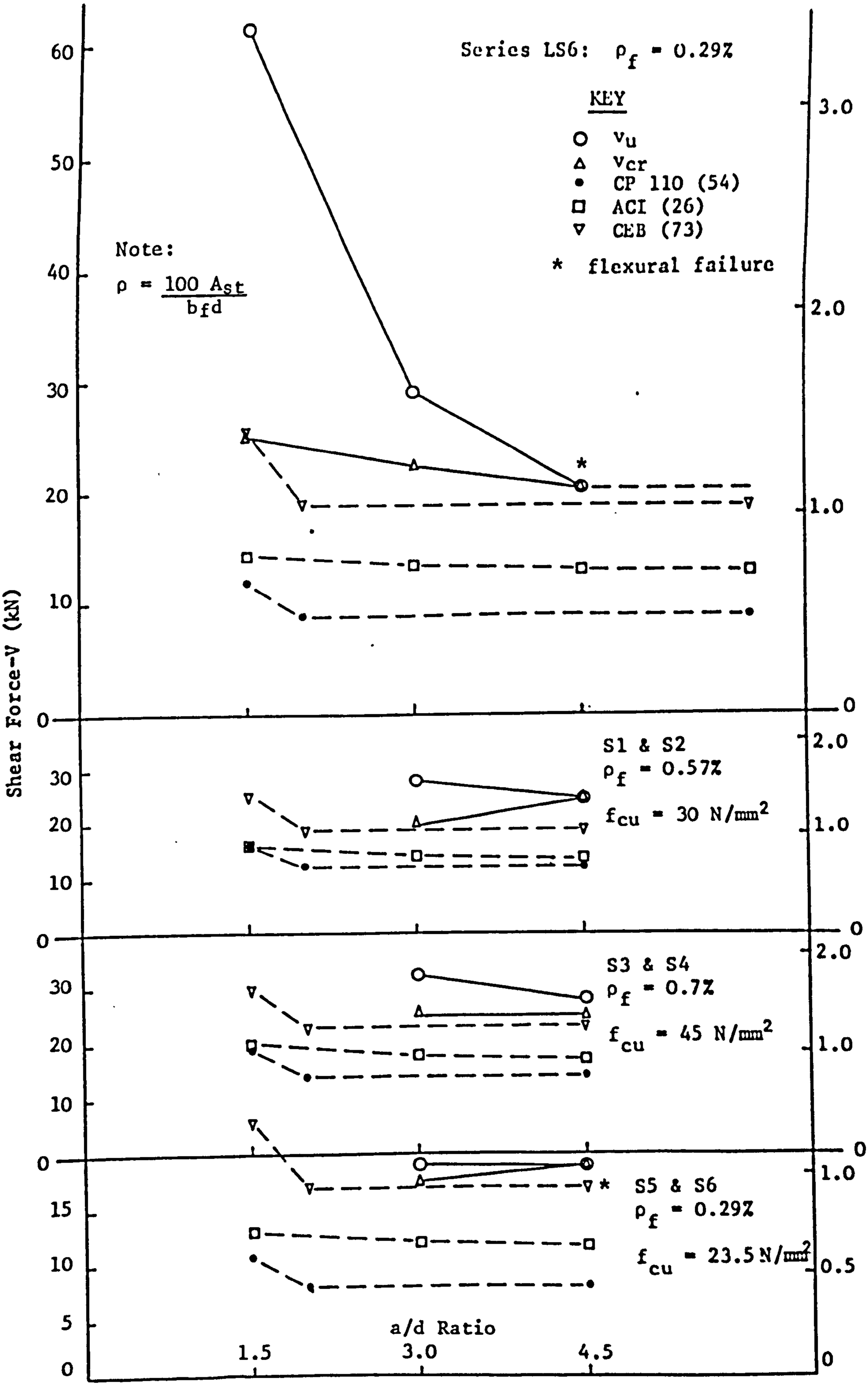

FIGURE 7.16(c) INFLUENCE OF a/d RATIO ON SHEAR CRACKING AND ULTIMATE SHEAR STRENGTH FOR SERIES LS6 AND S1-6

CP 110 (54) values are the most conservative. C.E.B.-F.I.P. (73) values are independent of longitudinal steel percentage and thus for a given concrete strength the gap between the C.E.B-F.I.P. (73) value and the test value decreases with decreasing steel percentage.

For a/d ratio's of 1.5 and 3.0, the ultimate load always exceeds the diagonal cracking load whereas for a/d ratio's of 4.5 and 6.0 failure occurs at or shortly after the diagonal cracking load. The effect of a/d ratio on ultimate shear strength is marked with true beam-type failures occurring at a/d ratio's of 4.5 and greater and arch action or strut-type failures (151) occurring at a/d ratio's of 3.0 and less; with a transition zone somewhere between these two values. Similar results have been reported by other investigators (49, 141-143, 151).

7.5.3.6.2 Influence of Longitudinal Steel Percentage

The effect of longitudinal steel percentage on the ultimate shear capacity is shown in Figures 7.17 (a) and (b). The effect becomes more pronounced as the a/d ratio and the area of longitudinal steel decrease but is less dramatic than that due to a/d ratio alone.

7.5.3.6.3 Influence of Concrete Strength

The influence of concrete strength on the ultimate shear capacity, for different steel percentages and a/d ratio's, is shown in Figure 7.18. Overall it appears that the effect of concrete strength on ultimate shear capacity is negligible.

The marked differences which occur between specimens LS2-1 and LS4-1 as indicated by the line marked a-b in Figure 7.18 are due to the uncharacteristically weak behaviour of beam LS4-1 which failed at an unexpectedly low load. This is clearly shown in Figure 7.19 (b) where the value of M_u/M_f for LS4-1 is lower than would be expected. No explanation can be offered for this lower strength.

The large difference in ultimate shear stress for beams LS6-2 and S5, as indicated by line c-d in Figure 7.18 can possibly be explained by the composition of the concrete for beam S5. The concrete strength for this beam at testing was

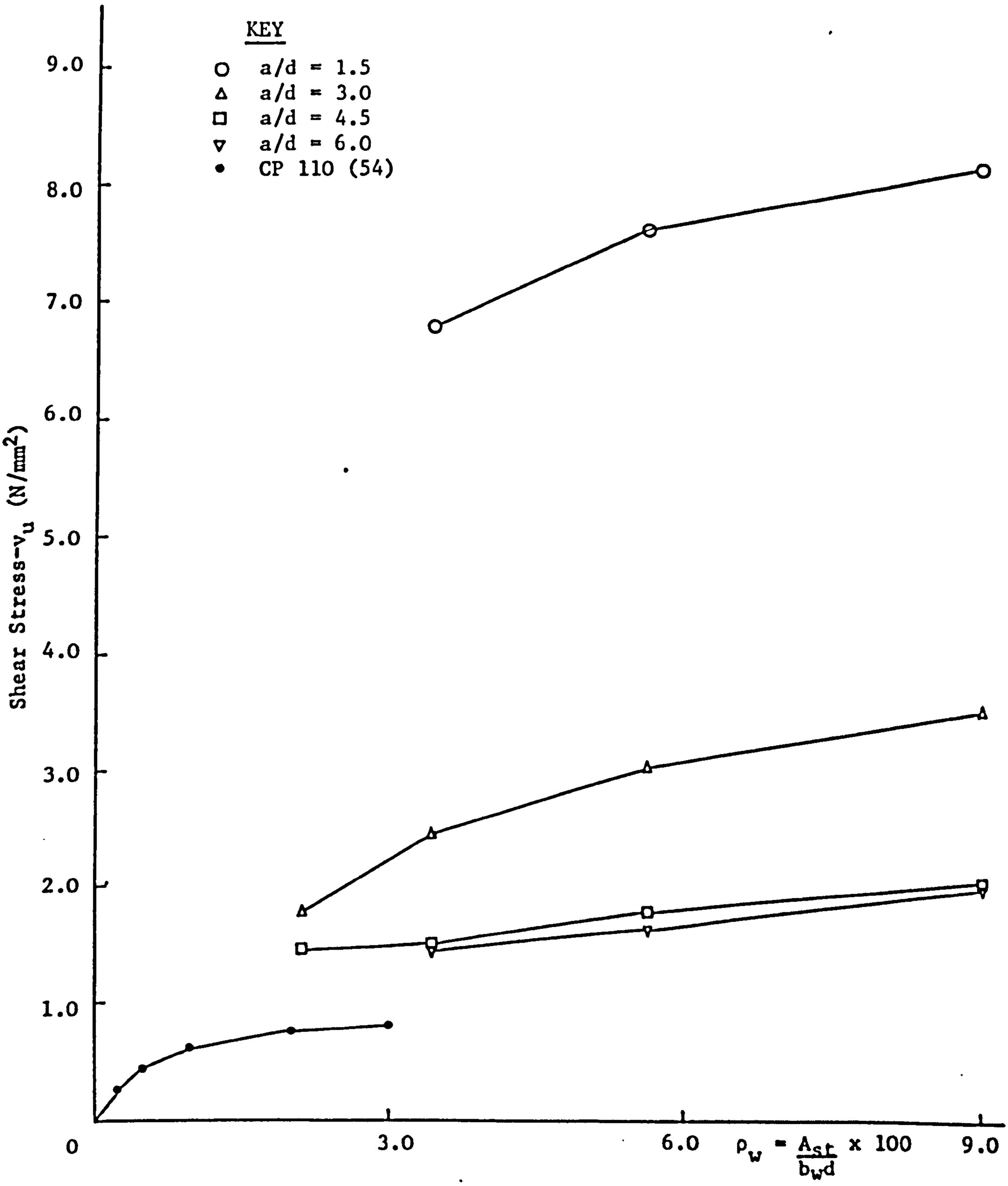

FIGURE 7.17(a) INFLUENCE OF LONGITUDINAL STEEL PERCENTAGE ON SHEAR STRESS AT ULTIMATE LOAD FOR CONCRETE STRENGTH 40-45 N/mm^2

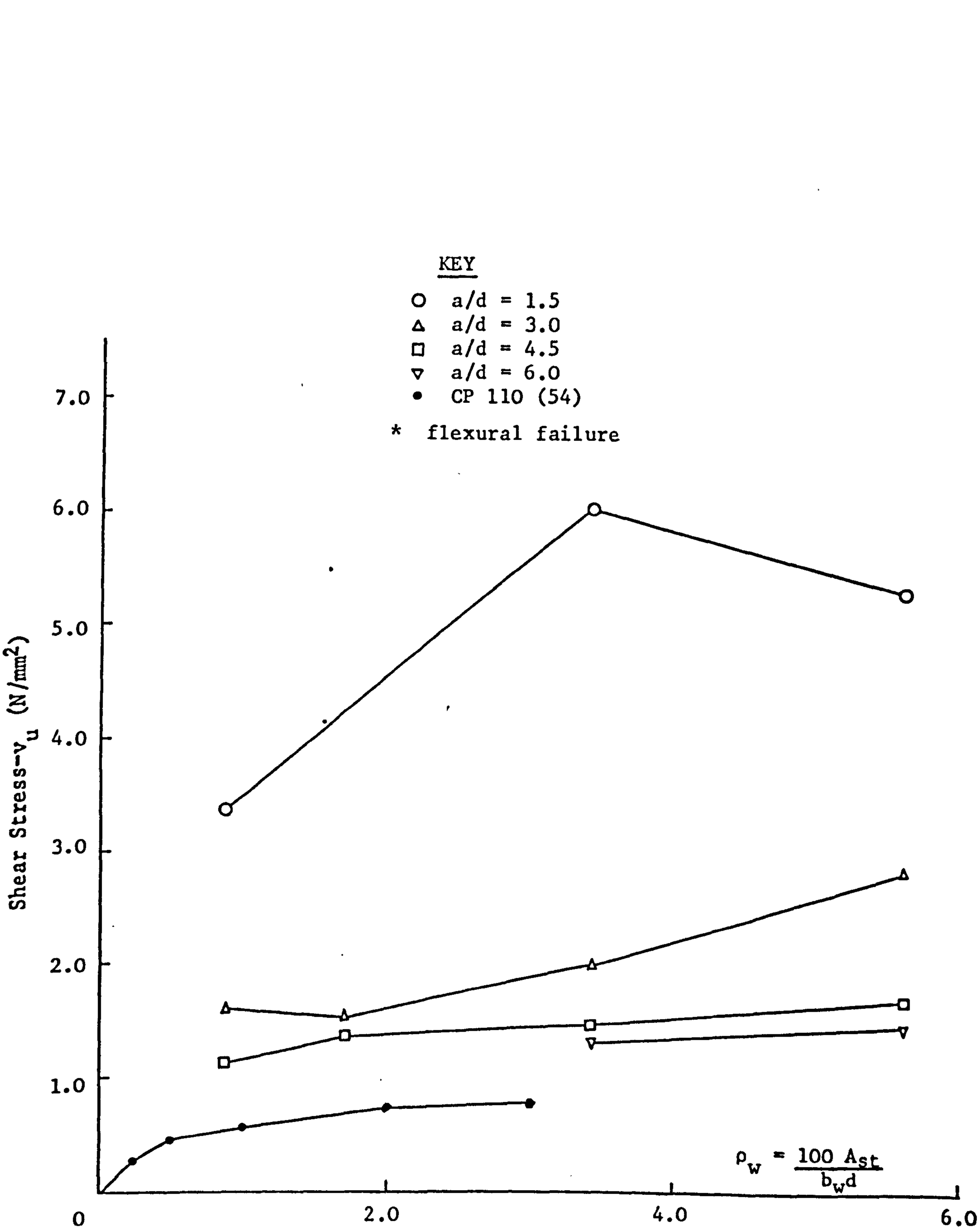

FIGURE 7.17(b) INFLUENCE OF LONGITUDINAL STEEL PERCENTAGE ON SHEAR STRESS AT ULTIMATE LOAD FOR CONCRETE STRENGTH 30 N/mm^2

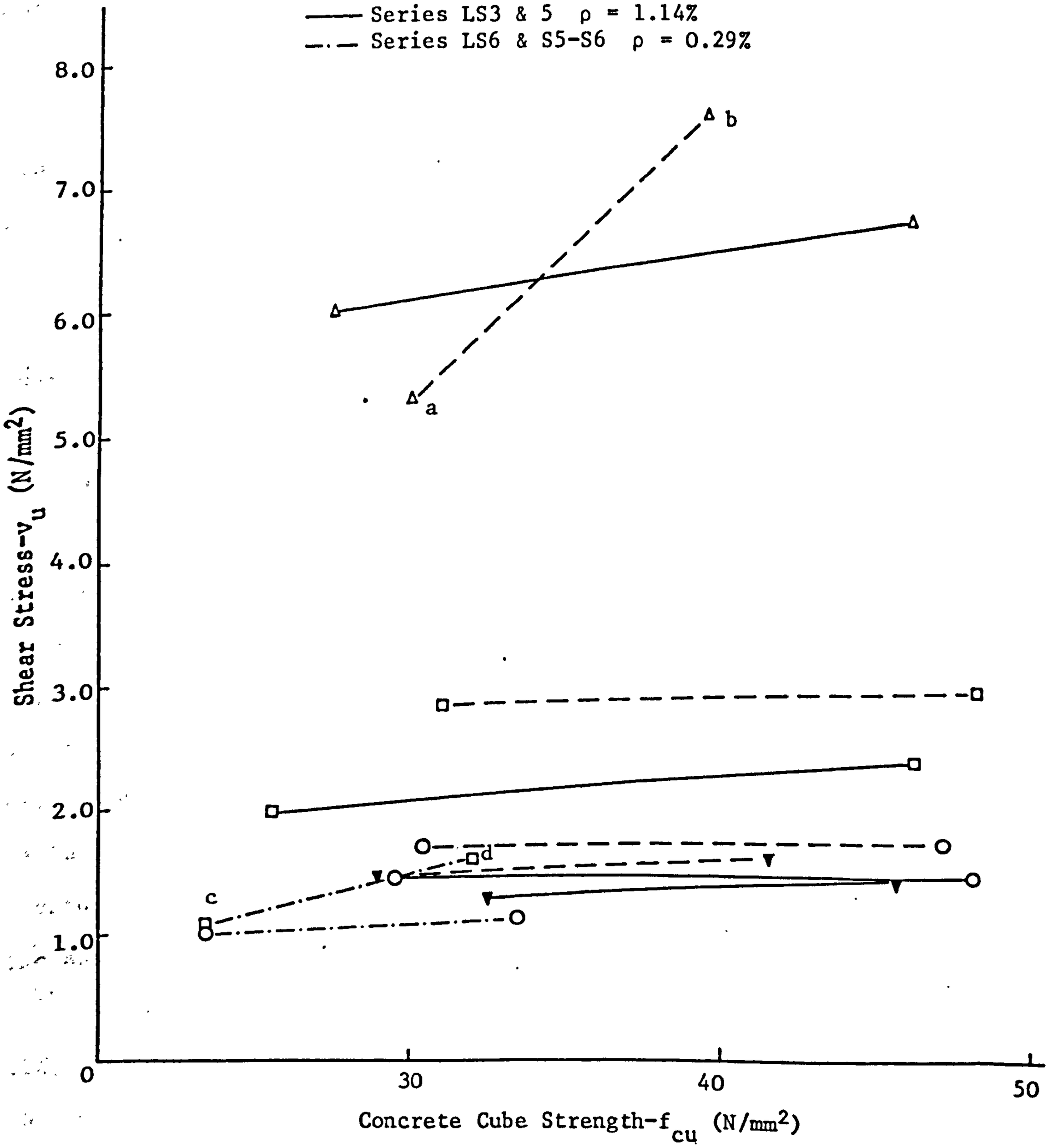

FIGURE 7.18 INFLUENCE OF CONCRETE STRENGTH f_{cu} ON SHEAR STRESS AT ULTIMATE LOAD

23.5 N/mm^2 and in order to achieve this low strength a very low cement content was used. At an a/d ratio of 3.0, the combined shearing and compressive stresses in the web region can produce high concrete stresses which for this low cement content and therefore quality concrete could have resulted in the lower failure load.

Neglecting these two sets of results, the maximum variation, from the mean, in ultimate shear strength for a cube strength range of 25.5-46 N/mm^2, LS3-2 and LS5-2, is 21%. The average variation is approximately 10%.

7.5.3.6.4 Influence of Ultimate Moment of Resistance

The ultimate moments at failure (M_u) of all the beams are shown in Table 7.5 along with the theoretical flexural moments on the CP 110 stress block (see Appendix B). The ratio's of M_u to M_f are plotted against a/d ratio in Figures 7.19 (a) and (b).

Figures 7.19 (a) and (b) show that the ratio of M_u/M_f decreases as a/d ratio increases from 1.5. At a value of a/d between 3.0 and 4.5, approximately, a lower bound value of M_u/M_f is reached after which for increasing a/d ratio a corresponding increase in M_u/M_f is observed. The significance of this feature is that for a/d ratio's of approximately 6.0 or greater, depending on the steel percentage, the theoretical flexural strength of the beam is attained despite the fact that no shear reinforcement is present. The significance of the longitudinal steel percentage on M_u/M_f for beams without web reinforcement is also apparent from Figures 7.19 (a) and (b).

For series LS6 where the recorded steel strains shown in Table 7.4 exceed 0.2%, the theoretical flexural capacity is exceeded before shear failure occurs.

7.6 Comparisons with Published Data

7.6.1 Comparison Between Lytag-Sand, All-Solite and Gravel-Sand T-Beams

In order to assess the shear capacity of Lytag-sand concrete in terms of all-lightweight concrete and dense concrete, some of the results from the present investigation were compared with results from the investigation carried out by Bandyopadhyay (49). In their tests to assess the influence of flange width on the shear behaviour of reinforced concrete T-beams, Swamy et al (142)

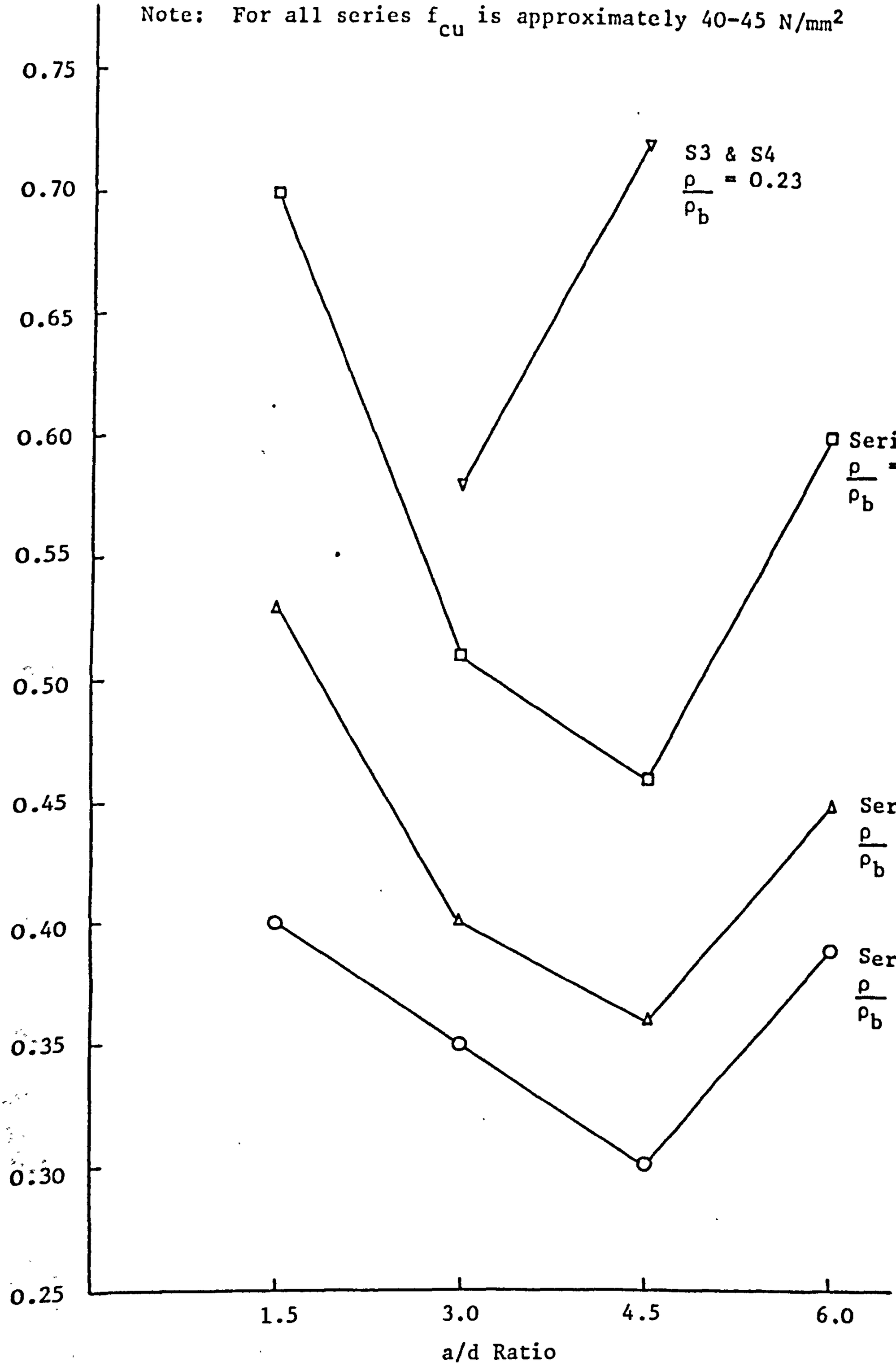

FIGURE 7.19(a) INFLUENCE OF a/d RATIO AND ρ ON THE ULTIMATE MOMENT CAPACITY OF T-BEAMS WITHOUT STIRRUPS

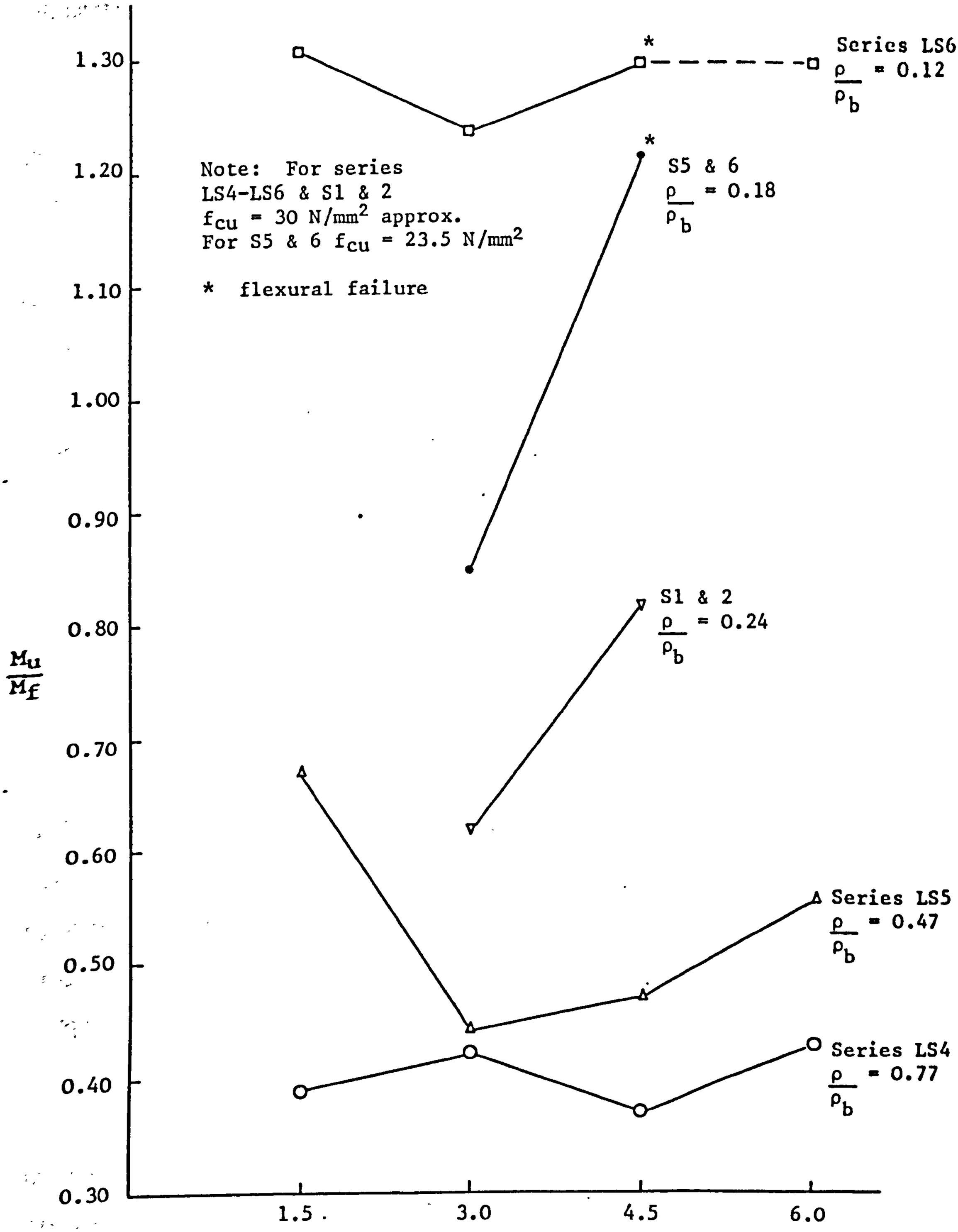

FIGURE 7.19(b) INFLUENCE OF a/d RATIO AND ρ ON THE ULTIMATE MOMENT CAPACITY OF T-BEAMS WITHOUT STIRRUPS

suggested that in order to make meaningful comparisons between beams failing in shear, of different cross-sections, the ratio of the tensile steel to that required for a balanced section should be used as a basis for the comparison. This approach has been used to compare two sets of test results from this project with two sets of results from investigation (49). The results are shown in Figure 7.20. For both sets of results the concrete cube strength is approximately 40 N/mm^2. The ratio of the tensile steel to the balanced steel is slightly greater for the Lytag-sand beams than for the Solite and gravel beams.

The results indicate that the shear strength of Lytag-sand concrete is generally lower than that of Solite or gravel concrete. At an a/d ratio of 6.0 the shear strength of the Lytag-sand concrete is approximately 75-85% of that for the gravel concrete. For lower a/d ratio's the corresponding range of values increases. Tests reported by Swamy and Bandyopadhyay (45) for All-Lytag concrete T-beams which were compared with equivalent gravel concrete and Solite concrete beams showed that for a/d ratio's of 4.5 and 6.0, the shear strength of Lytag-sand concrete lay between that for Solite and gravel. This tends to suggest that, because of the complexity of the shear type of failure and the inter-relationship between the various parameters effecting shear, the only reliable way to compare the performance of concretes made with different types of aggregate is by testing identical beams; that is beams of the same cross-sectiona properties and having the same longitudinal reinforcement ratio and concrete strength.

7.6.2 Comparison Between Various U.K. and U.S. Lightweight Concretes

In order to try and draw some conclusions for lightweight concretes in general, the results of several U.K. (33, 49, 62) and U.S. (28, 144) investigators are plotted in Figures 7.21-23. Figure 7.21 shows the shear stress at ultimate load against longitudinal steel percentage. The wide scatter of points obtained reflects the various a/d ratio's (not less than 2.5), concrete strengths, beam cross-sectional characteristics and aggregate properties all of which influence shear capacity. Two things are,however, apparent from this figure; firstly there is a general reduction in shear capacity with reducing steel percentage and

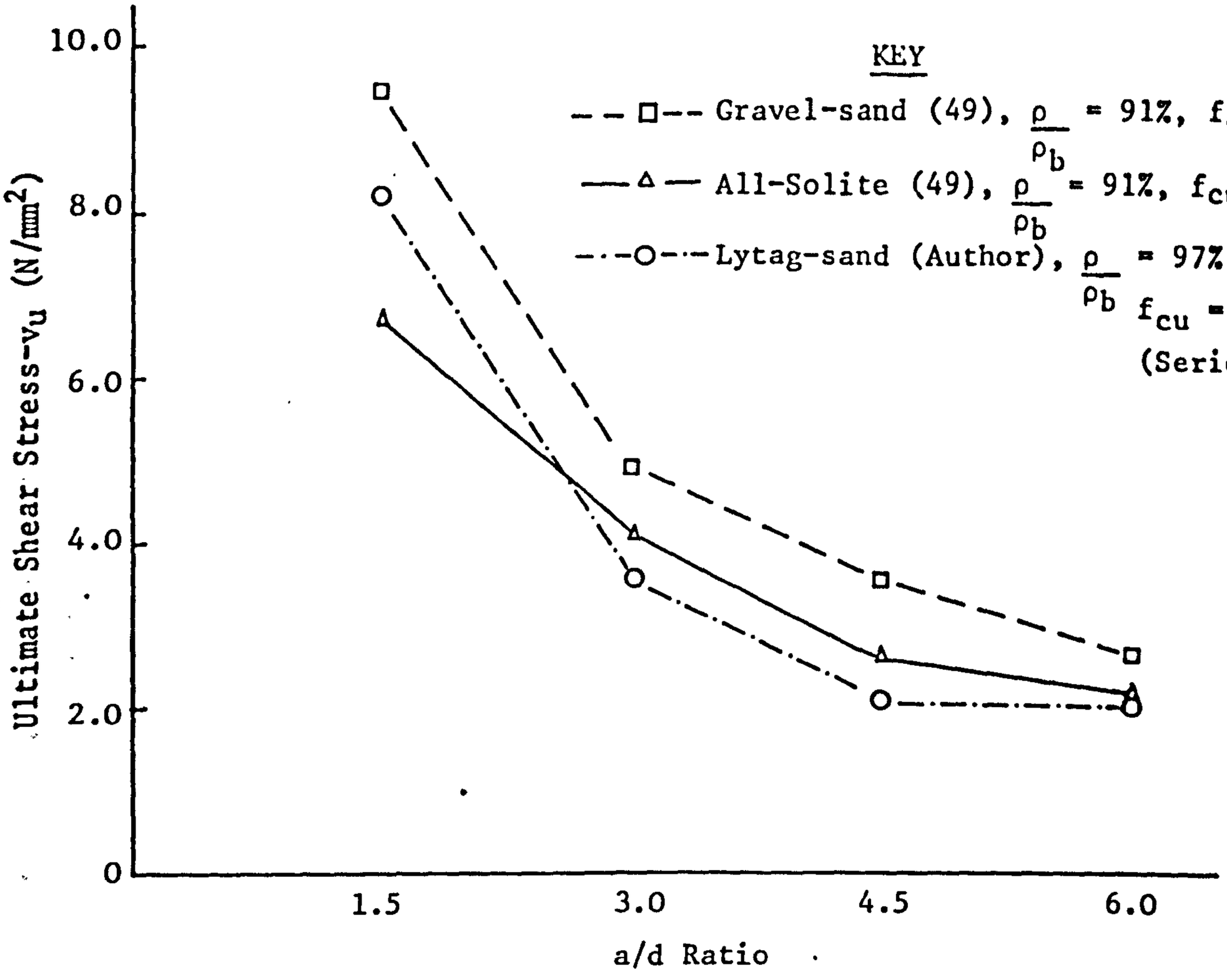

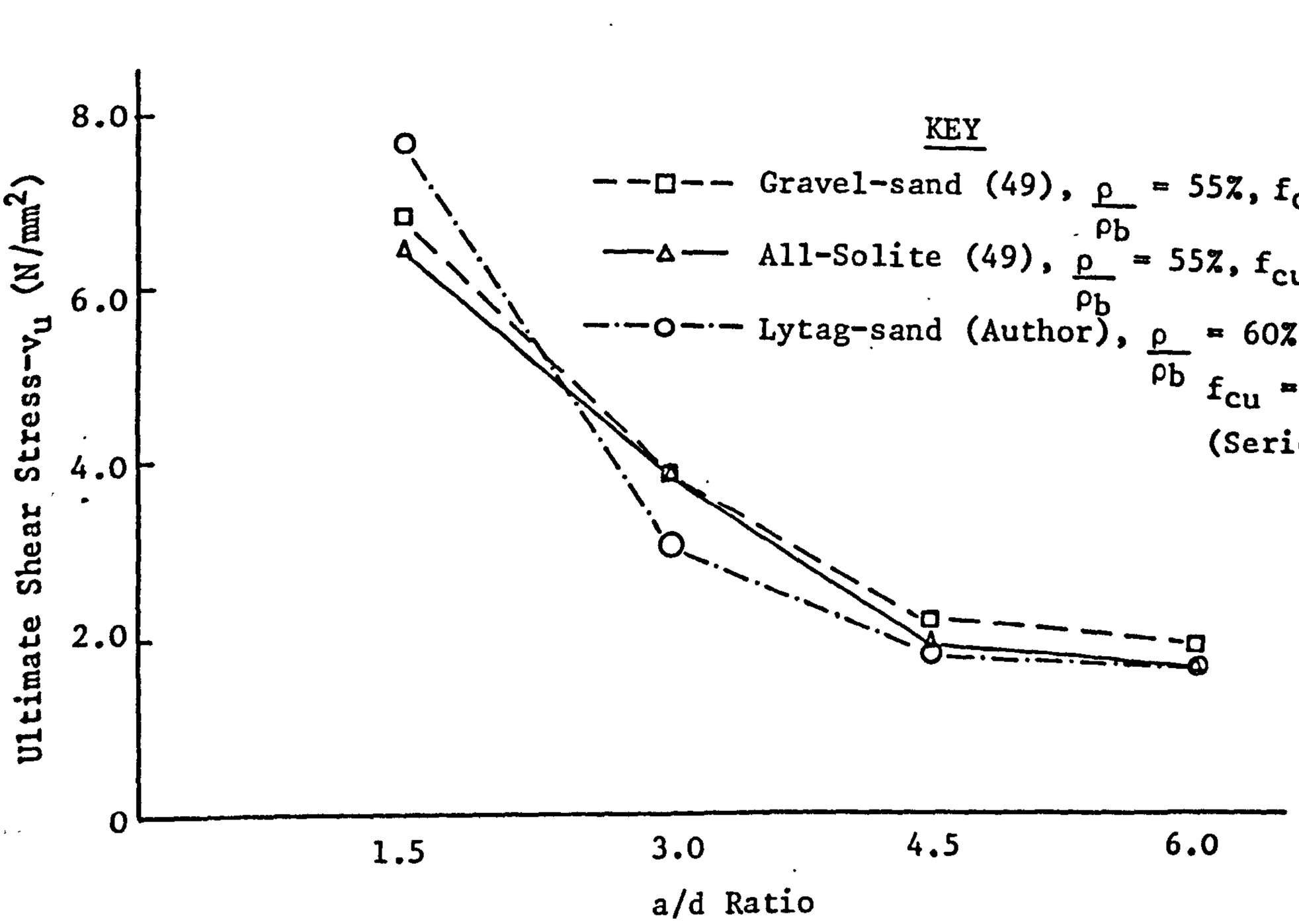

FIGURE 7.20 COMPARISON OF LYTAG-SAND, ALL-SOLITE (49) AND GRAVEL-SAND (49) CONCRETE T-BEAMS

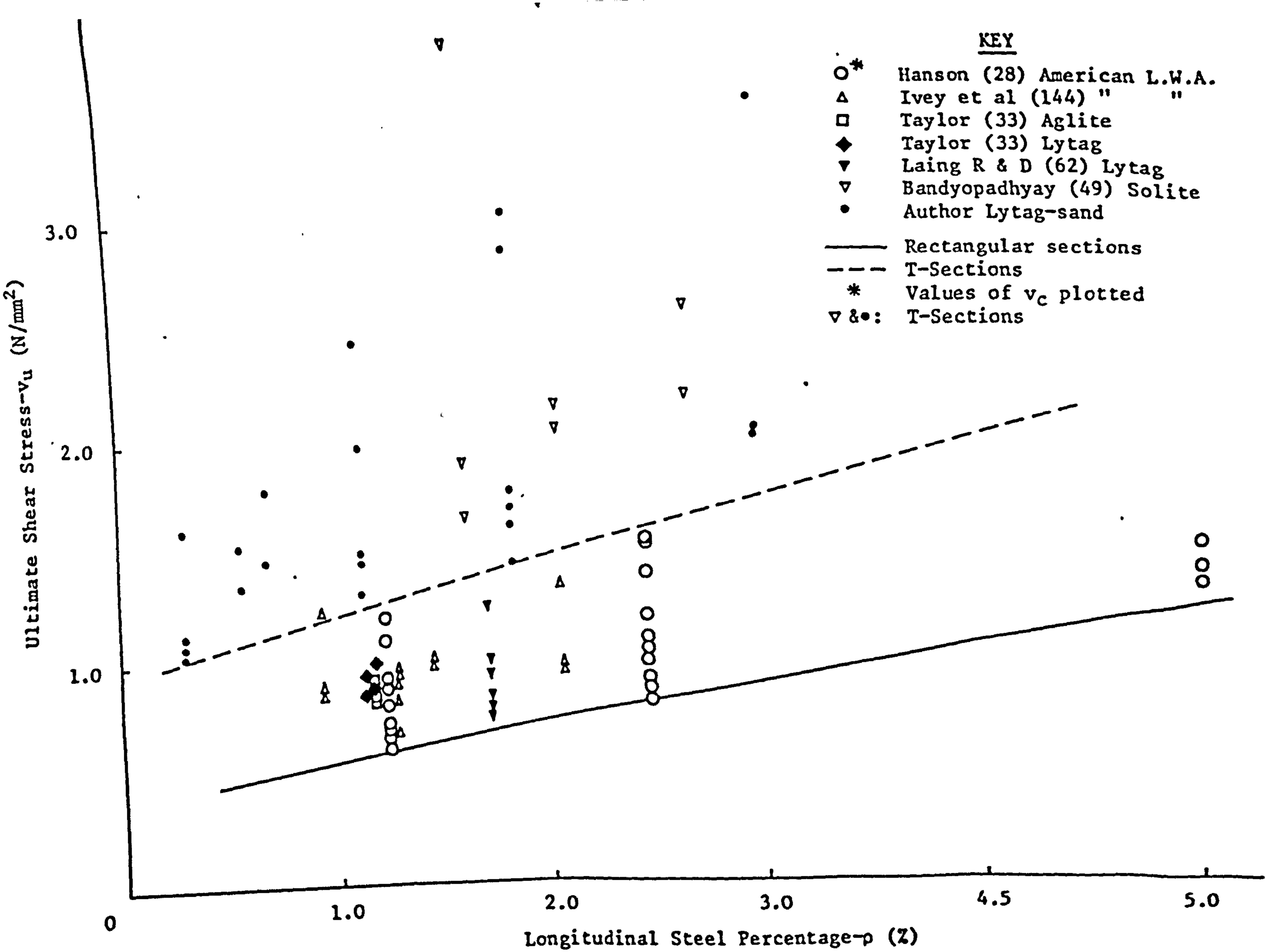

FIGURE 7.21 INFLUENCE OF STEEL PERCENTAGE ON SHEAR STRESS

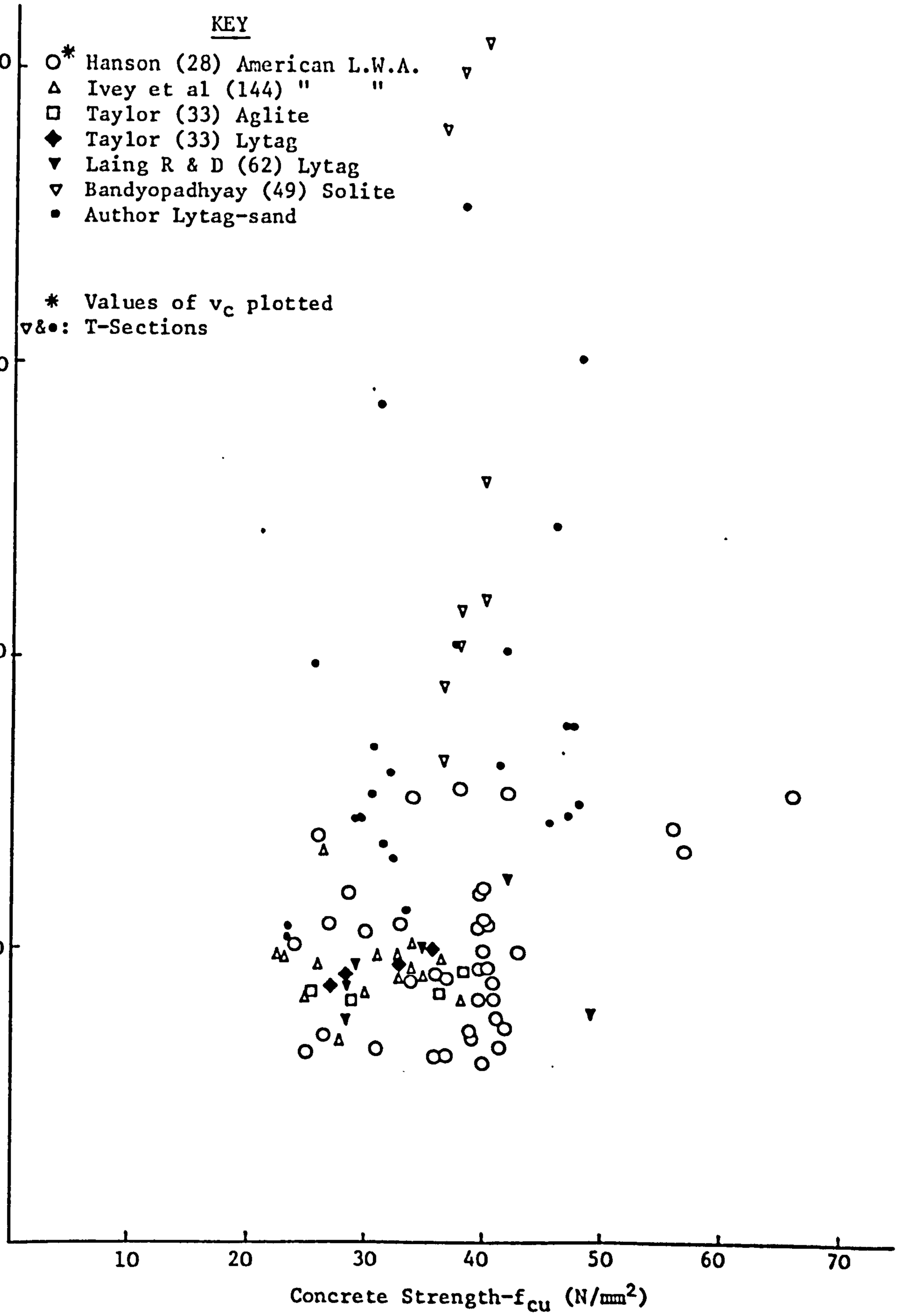

FIGURE 7.22 INFLUENCE OF CONCRETE STRENGTH ON SHEAR STRESS

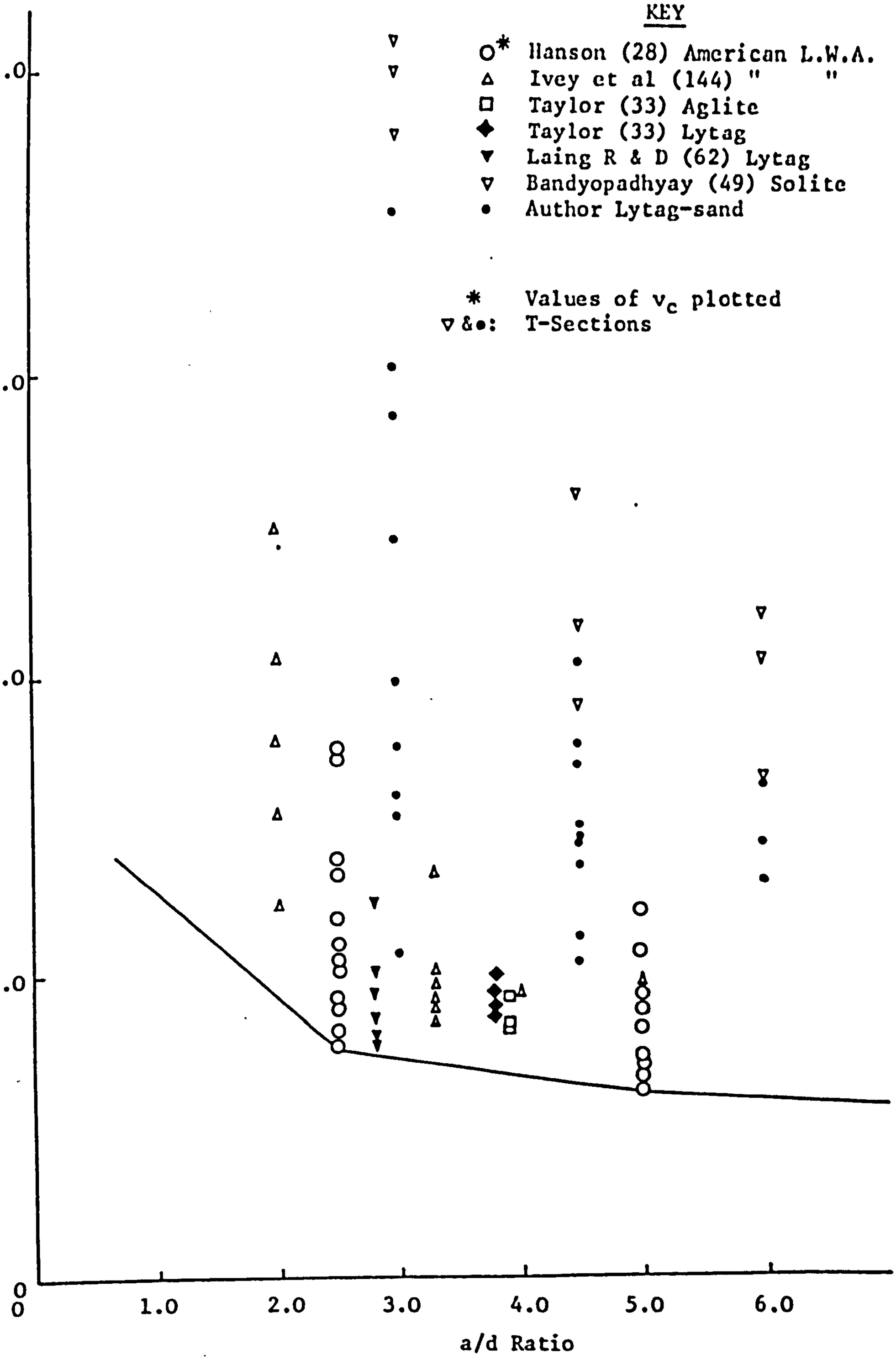

FIGURE 7.23 INFLUENCE OF a/d RATIO ON SHEAR STRESS

secondly the shear capacity of a flanged section is greater than of a rectangular section, a fact ignored by the various design codes (26, 54, 73).

Similar effects are apparent in Figures 7.22 and 7.23 which show the influence of concrete strengths and a/d ratio respectively. The influence of concrete strength, if any, is difficult to ascertain and if Hanson's (28) results for the shear stress at diagonal cracking are discarded, there is a general trend of increasing shear strength for increasing concrete strength. However, it is generally agreed that at higher a/d ratio's, the diagonal cracking load and the failure load are similar. Many of Hanson's (28) results are for beams with an a/d ratio of 5.0 and their inclusion is therefore valid. One interpretation of the results shown in Figure 7.22 is that the wide range of shear stresses for various concrete strengths indicates that the influence of a/d ratio and steel percentage on shear strength is more important. This would agree with the results of the present investigation. Whereas, it is generally acknowledged that the diagonal cracking stress is a function of the tensile strength of the concrete, which is in turn a function of compressive strength, such effects may well be limited when ultimate loads are considered.

Finally the influence of a/d ratio on shear stress is shown in Figure 7.23. The established relationship of increasing shear strength with decreasing a/d ratio is reiterated here. Again the increased shear strength of a flanged section is apparent.

From Figures 7.20-7.23 it is obvious that a complex relationship exists between the various parameters which affect shear in reinforced concrete beams. While each individual set of results may show the influence of the various parameters studied, on shear strength a comparison between the results of various investigators is extremely difficult and such comparisons should be viewed with caution. One of the main problems in comparing results is the accurate calculation of the shear carried by the concrete at failure. The assumption of a nominal unit shear stress is probably the main cause for the wide scatter of results obtained.

For Lytag-sand concrete the implication of Figure 7.20 is that the shear

strength is in some cases considerably lower than that of gravel concrete. However, as was mentioned in 7.6.1 direct comparisons between beams which are not identical in cross-sectional properties, appears to be unreliable. A limited series of tests between directly comparable gravel concrete and Lytag-sand concrete T-beams would help to alleviate any uncertainty.

7.7 Development of Design Equations

7.7.1 Introduction

Only a minimal amount of research has been carried out on the shear behaviour of lightweight concrete T-beams made with U.K. aggregates and, therefore, only a limited amount of data is available. The primary consideration of this investigation was to produce design data for Lytag-sand concrete T-beams and for lightweight concrete in general.

7.7.2 Design Criteria

It is now well established that for beams without web reinforcement and for a/d ratio's less than or equal to 6.0, the primary mode of failure is by diagonal tension cracking.

The data plotted in Figures 7.21 to 7.23 show that there is little correlation between any of the individual parameters, known to affect shear strength, and the shear capacity of sections without web reinforcement. Tests (28), however, have shown that there is an extremely good correlation between the shear capacity of an unreinforced web and the tensile splitting strength of concrete cylinders, which in turn is a function of the cube strength.

7.7.2.1 Design Equation for Beams Without Web Reinforcement and Shear Span - Effective Depth Ratio's ≥ 3.0

In an attempt to try and allow for the effects of a/d ratio, longitudinal steel percentage and concrete strength on the shear capacity of beams, Bower and Viest (153) suggested the following equation for dense concrete:

$$\frac{v_{cr}}{\sqrt{f_c'}} = \frac{V_{cr}}{b\ d\sqrt{f_c'}} = 1.9 + 2500\ \frac{\rho_d}{\frac{M}{V}\sqrt{f_c'}} \leq 3.5 \qquad \ldots\ (7.13)$$

where the units are imperial,

$$\text{and} \quad \frac{M}{V} = \frac{M_{max}}{V} - d \geq \frac{M_{max}}{V} - \frac{a}{2} \qquad \ldots\ (7.14)$$

In applying this form of equation to lightweight concrete Hanson (28), found that the constants in equation (7.13) varied widely due to the various characteristics of each lightweight aggregate used. Hence if a single pair of constants were chosen to provide a design equation which safely covered all lightweight aggregates, then such an equation would be extremely conservative for some aggregates. This is due to the variable diagonal tension resistance of concretes made with different lightweight aggregates.

7.7.2.2 Design Equation for Lytag-Sand Concrete T-Beams

By using the value of tensile splitting strength in equation (7.13) as opposed to $\sqrt{f_c'}$, design equations were derived for Lytag-sand concrete and also other British lightweight aggregates. The equations take the form of:

$$\frac{v_u}{f_{SP}} = c_1 + c_2 \frac{\rho\ Vd}{M\ f_{SP}} \qquad \ldots\ (7.15)$$

where c_1 and c_2 are constants. The data from investigations (28, 33, 49, 62, 144) are plotted along with the data from this investigation in Figure 7.24. Values of f_{SP} for Lytag-sand concrete were obtained using equation 4.6. The ultimate shear stress, v_u, was used instead of the diagonal cracking stress, v_{cr}, since beams with long spans generally fail at the formation of the diagonal cracks but for short shear spans v_{cr} grossly underestimates the shear capacity of the section. Although it is generally stated that this excess shear capacity is unpredictable and therefore unsafe, some excess strength will always be available and the equations derived here aim to take this into account. For Lytag-sand concrete the equation is

$$v_u = 0.365\ f_{SP} + 39.80 \frac{\rho\ Vd}{M} \qquad \ldots\ (7.16)$$

Using a single overall partial safety factor of 1.25, the design equation becomes:

$$v_u = 0.292\ f_{SP} + 31.83 \frac{\rho\ Vd}{M} \qquad \ldots\ (7.17)$$

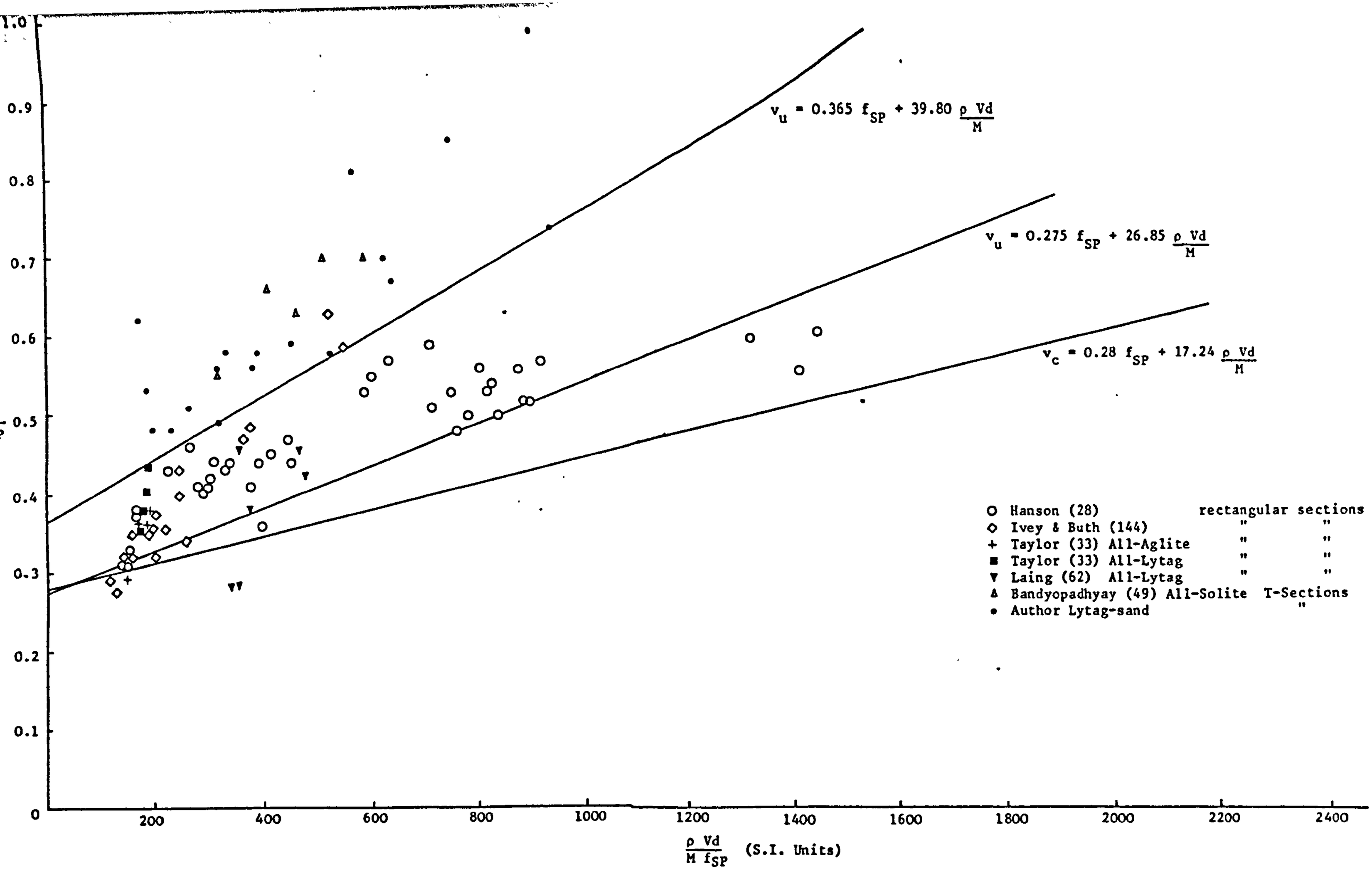

FIGURE 7.24 DERIVATION OF EQUATIONS FOR BEAMS WITHOUT WEB REINFORCEMENT

Equations (7.16) and (7.17) also provide a lower bound for the All-Solite concrete T-beams tested by Bandyopadhyay (49).

7.7.2.3 Design Equation for All Lightweight Concretes

For all British and American lightweight concretes (28, 33, 49, 62, 144) rectangular and T-sections, the lower bound equation is

$$v_u = 0.275\ f_{SP} + 26.85\ \frac{\rho\ Vd}{M} \qquad \ldots\ (7.18)$$

below which only 11 out of 107 points fall. If a partial safety factor of 1.25 is applied the equation becomes:

$$v_u = 0.22\ f_{SP} + 21.48\ \frac{\rho\ Vd}{M} \qquad \ldots\ (7.19)$$

below which only 2 points fall.

Also shown in Figure 7.24 is the line given by the equation suggested by Ivey and Buth (144) and Bandyopadhyay for diagonal cracking stress:

$$v_{cr} = 0.28 + 17.24\ \rho\ \frac{Vd}{M} \qquad \ldots\ (7.20)$$

which with a partial safety factor becomes:

$$v_{cr} = 0.22\ f_{SP} + 13.80\ \rho\ \frac{Vd}{M} \qquad \ldots\ (7.21)$$

7.8 Comparison Between Experimental and Theoretical Results

Table 7.7 shows the relationship between experimental results and predicted values using equations 7.16, 7.18 and 7.20. Considering first of all the diagonal cracking stress it can be seen that the values predicted by equation 7.20 are greater than the experimental values in all but two cases, with safety factors ranging from 1.19 to 1.80. The two cases where the safety factor was less than 1.00 are characterised by high steel percentages and low a/d ratio (a/d = 1.5) and were able to sustain loads of 3.3 and 3.75 times the diagonal cracking load.

Using equation 7.18 to predict the ultimate shear stress at failure it can be seen that all beams had a safety factor greater than 1.00 with the range being 1.35 to 3.34. This equation is far too conservative for beams with short

TABLE 7.7 COMPARISON BETWEEN EXPERIMENTAL AND THEORETICAL RESULTS FOR BEAMS WITHOUT WEB REINFORCEMENT

Beam No.	v_{cr} (N/mm^2)	v_u (N/mm^2)	Eqn. (7.20) (N/mm^2)	Col. 2 / Col. 4	Eqn. (7.18) (N/mm^2)	Col. 3 / Col. 6	Eqn. (7.16) (N/mm^2)	Col. 3 / Col. 8
1	2	3	4	5	6	7	8	9
LS1-1	2.45	8.17	2.87	0.85	4.01	2.04	5.83	1.40
2	2.31	3.54	1.56	1.48	1.98	1.79	2.81	1.26
3	2.04	2.04	1.22	1.67	1.45	1.41	2.03	1.00
4	2.02	2.02	1.12	1.80	1.28	1.58	1.78	1.13
LS2-1	2.04	7.65	2.08	0.98	2.78	2.75	4.01	1.91
2	1.77	3.02	1.35	1.31	1.60	1.89	2.24	1.35
3	1.77	1.77	1.13	1.57	1.27	1.39	1.75	1.01
4	1.63	1.63	1.00	1.63	1.10	1.48	1.50	1.09
LS3-1	2.04	6.81	1.63	1.25	2.05	3.32	2.92	2.33
2	1.36	2.45	1.14	1.19	1.29	1.90	1.78	1.38
3	1.36	1.50	1.03	1.32	1.11	1.35	1.51	0.99
4	1.44	1.44	0.96	1.50	1.01	1.43	1.37	1.05
S3	1.36	1.77	1.04	1.31	1.13	1.57	1.54	1.15
S4	1.36	1.46	0.96	1.42	1.00	1.46	1.35	1.08
LS4-1	2.18	5.31	1.49	1.46	1.91	2.78	2.73	1.95
2	1.63	2.86	1.00	1.63	1.15	2.49	1.60	1.79
3	1.44	1.69	0.98	1.47	1.12	1.51	1.55	1.09
4	1.23	1.44	0.88	1.40	0.98	1.47	1.34	1.07
LS5-1	1.91	6.03	1.46	1.31	1.88	3.21	2.69	2.24
2	1.36	1.98	0.94	1.45	1.10	1.80	1.53	1.29
3	1.36	1.44	0.86	1.58	0.94	1.53	1.29	1.12
4	1.23	1.31	0.84	1.46	0.90	1.46	1.22	1.07
LS6-1	1.36	3.37	0.91	1.49	1.01	3.34	1.39	2.42
2	1.23	1.60	0.79	1.56	0.82	1.95	1.11	1.78
3	-	1.12	-	-	-	Flexural Failure		
4	-	-	-	-	-	-	-	-
S1	1.09	1.53	0.91	1.20	0.97	1.58	1.33	1.15
S2	1.36	1.36	0.80	1.70	0.83	1.64	1.12	1.21
S5	0.95	1.07	0.70	1.36	0.73	1.47	0.99	1.08
S6	-	1.03	-	-	-	Flexural Failure		

a/d ratio's since it is based on rectangular sections rather than T-sections. One method of allowing for this may be to use the approach adopted by CP 110 (54) for a/d ratio's less than 2.0 where the shear stress is multiplied by a factor equal to two times d/a.

Using equation 7.16, the predicted values approximate much more closely to the experimental values but again the factor of safety for a/d = 1.5 is high, ranging between 1.40 and 2.42. Again this could be allowed for by using the factor 2d/a. For a/d ratio's of 3.0 to 6.0, only one result has a safety factor less than 1.00, but many have safety factors less than 1.25. If a partial safety factor of 1.25 is applied to equation (7.16) to get equation (7.17) then the values predicted by this equation would be adequately safe for all the beams tested.

7.9 Comparison Between CP 110 (54) Ultimate Shear Stresses and Equation (7.17)

An attempt has been made to predict the ultimate shear strength of Lytag-sand concrete T-beams using equation (7.17) and to compare these values with those given in CP 110 (54). The results are shown in Table 7.8. In this comparison the lowest concrete strength of 15 N/mm^2 is disregarded. For equation (7.17), values of f_{SP} were calculated from equation (4.6) and the value of M/Vd was taken as 5, i.e.

$$\frac{M_{max}}{V} - d = a - d = 6 - 1 = 5.0 \qquad \text{(See equation (7.14))}$$

The present code does not allow any increase in the shear stress for members where the concrete strength and steel percentage, based on the web width exceed 40 N/mm^2 and 3% respectively. While the results of this investigation suggest that increasing the concrete strength above 40 N/mm^2 will have little effect on the shear stress, this and another investigation (49), indicate that an upper limit of 3% of longitudinal steel, based on the web width, is totally inadequate for T-sections. In practice steel percentages greater than 3% are often used in T-sections and thus the present code (54) requirements will tend to produce very conservative sections. In Table 7.8 predicted shear stresses for steel percentages up to 5%, based on the web width, are shown. The values

TABLE 7.8 ULTIMATE SHEAR STRESSES FOR LYTAG-SAND CONCRETE T-BEAMS

100 $\frac{A_{st}}{b_w d}$	Concrete Characteristic Compressive Strength (N/mm^2)			
	20	25	30	40
0.25	0.62 (0.28)*	0.69 (0.28)	0.75 (0.28)	0.85 (0.28)
0.50	0.64 (0.36)	0.70 (0.40)	0.76 (0.44)	0.86 (0.44)
1.00	0.67 (0.48)	0.74 (0.52)	0.79 (0.56)	0.89 (0.60)
2.00	0.73 (0.64)	0.80 (0.68)	0.86 (0.72)	0.96 (0.76)
3.00	0.80 (0.68)	0.86 (0.72)	0.92 (0.76)	1.02 (0.80)
4.00	0.86 -	0.93 -	0.98 -	1.08 -
5.00	0.93 -	0.99 -	1.05 -	1.15 -

* Numbers in brackets are values given in CP 110 (54)

shown in Table 7.8 apply to members subjected to shear and moment only. It should also be noted that these values are based on a typical T-section and that for sections with thin webs or for rectangular sections, these values will not apply.

7.10 Conclusions

In this chapter work carried out to investigate the shear behaviour of Lytag-sand reinforced concrete T-beams, without web steel, is reported. From the work reported the following conclusions are drawn:

1. From an analysis of the deformation characteristics, it is evident that for beams failing in shear the failure mode is brittle and very sudden. None of the characteristic ductility associated with a flexural failure is shown.
2. In general, the head of the critical diagonal tension crack, immediately prior to failure is situated at a distance approximately equal to 1.0 to 1.5 times d, from the load point.
3. The mode of failure of a beam without web reinforcement is primarily dependent on the a/d ratio and the longitudinal steel percentage. At short a/d ratio's (a/d = 1.5) the failure mode is a result of diagonal tension cracking and crushing of the concrete compression struts. At a/d ratio's greater than 1.5 diagonal tensile cracking is the predominant mode of failure.
4. For beams with an a/d ratio $\leq$ 3.0, the ultimate load was, in all cases, greater than the diagonal cracking load. For beams with an a/d ratio greater than 3.0, failure occurred at or shortly after the diagonal cracking load had been reached.
5. The ultimate shear resistance of reinforced lightweight concrete T-beams is dependent on two main parameters; namely the a/d ratio and the longitudinal steel percentage. The influence of concrete strength is generally minimal.
6. For all the beams tested in this investigation, the ultimate shear stress at failure was significantly greater than the allowable shear stresses quoted in CP 110 (54).

7. The ultimate shear stress of a Lytag-sand reinforced concrete T-section can be predicted from the equation

$$v_u = 0.292\ f_{SP} + 31.83\ \frac{\rho\ Vd}{M} \qquad \ldots\ (7.17)$$

8. For T-sections, the ultimate shear stresses permitted in CP 110 (54) are too conservative and shear stresses for values of longitudinal steel percentage, based on the web width, greater than 3% should be included.

CHAPTER 8

SHORT-TERM FLEXURAL BEHAVIOUR OF LYTAG-SAND CONCRETE T-BEAMS

8.1 Introduction

The last chapter described tests to evaluate the shear capacity of Lytag-sand concrete. In this chapter a limited series of tests designed to examine the flexural capacity of Lytag-sand reinforced concrete T-beams is described and the results reported.

Present day design in the U.K., based on the ultimate limit state principle, involves designing for the ultimate load case; then checking the serviceability limit states of cracking and deflection under working load. The lower modulus of elasticity of lightweight concrete, as opposed to dense concrete, generally results in larger deflections under load.

Richart and Jensen (24) were probably the first investigators to study the flexural characteristics of reinforced lightweight concrete beams but many investigators have since followed (25, 31, 34-38, 48). The various conclusions drawn by each of the investigators are summarised in Chapter 2.

The aims of this limited series of tests were to compare the flexural characteristics of Lytag-sand concrete T-beams to the values given in the various design codes (26, 54, 73).

8.2 Experimental Programme

8.2.1 Details of Tests

Six reinforced concrete T-beams were tested in all; three with a concrete cube strength of approximately 30 N/mm^2 and three of approximately 45 N/mm^2. For each concrete strength three longitudinal steel percentages of approximately 12, 25 and 45% of the balanced steel ratio were chosen. Details of the beams are shown in Figures 8.1 and 8.2 and Table 8.1. All beams contained shear reinforcement designed in accordance with CP 110 (54) and some typical reinforcement cages are shown in Plate 8.1.

8.2.2 Materials

8.2.2.1 Concrete

Concrete mixes were designed according to the information given in

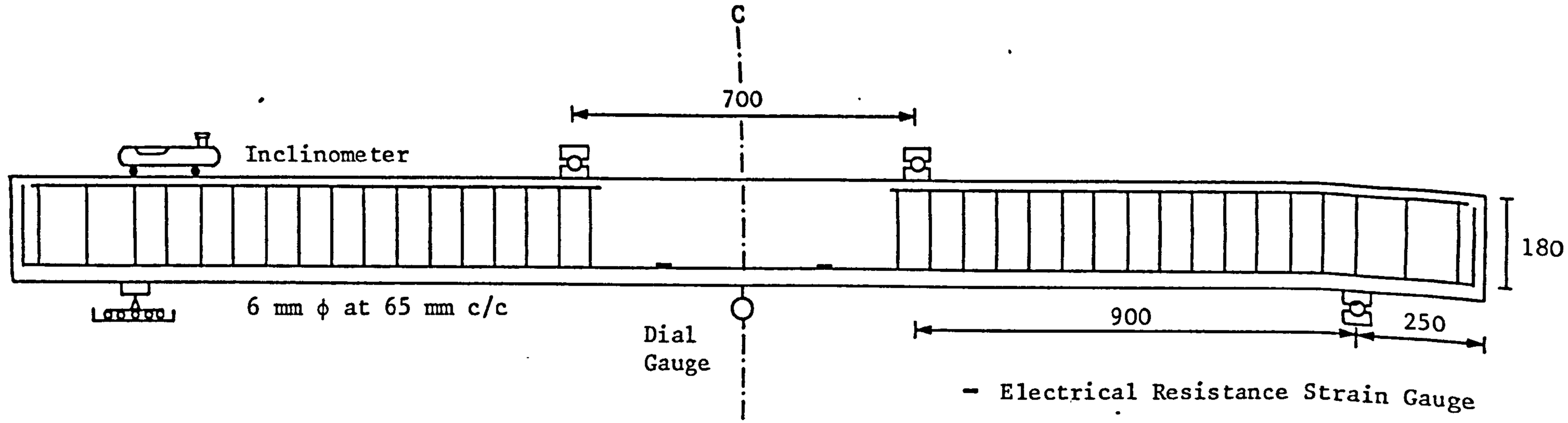

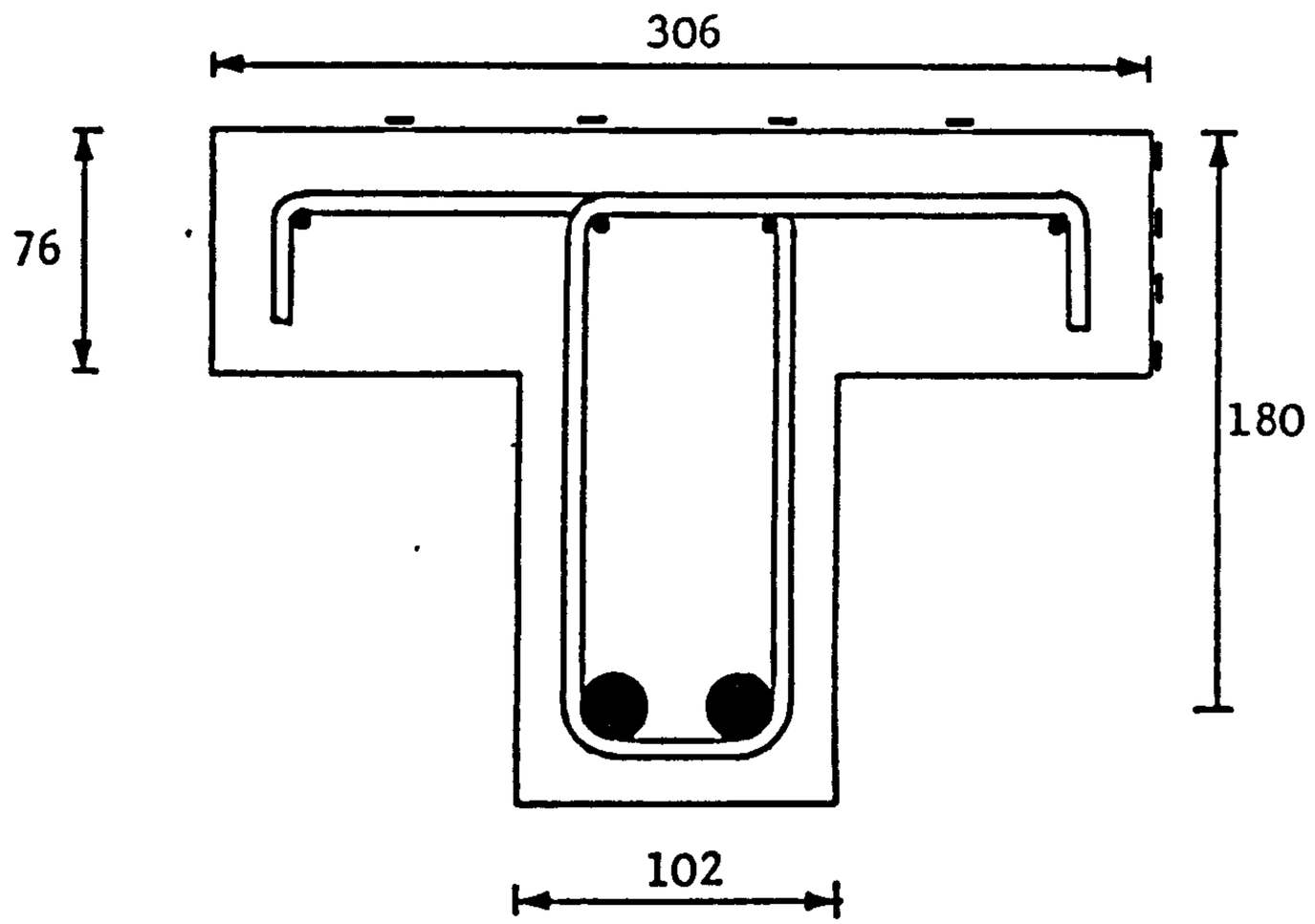

Notes:

1. All dimensions mm.
2. Cover to all steel according to CP 110 (54).
3. Stirrup spacing according to CP 110 (54).
4. Yield stress of longitudinal steel f_y = 465 N/mm^2.
5. All beams symmetrical about centre line CL.

FIGURE 8.1 GENERAL REINFORCEMENT DETAILS FOR FLEXURAL SPECIMENS

Beam No.	F3	F2	F1
ρ_f:	1.14%	0.57%	0.29%
f_{cu} = 30 N/mm^2	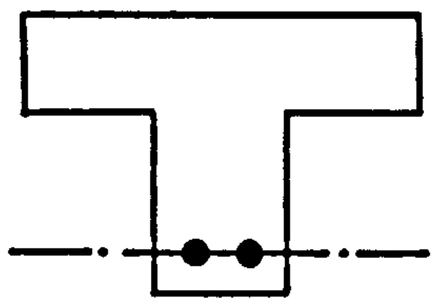	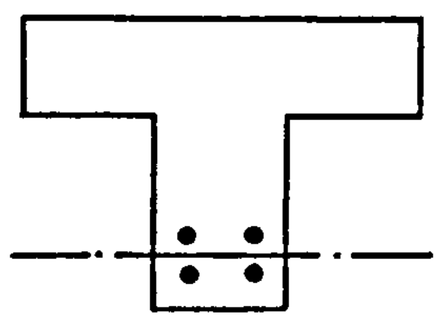	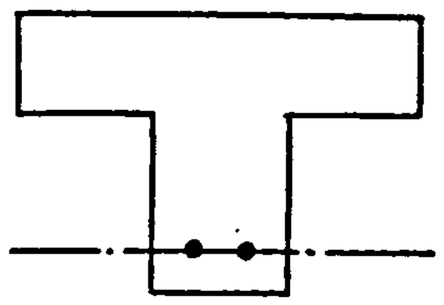
Bar No. & Type	2-20	4-10	2-10
Beam No.	F6	F5	F4
ρ_f:	1.46%	0.82%	0.41%
f_{cu} = 45 N/mm^2	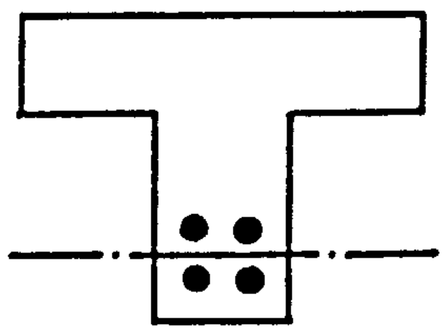	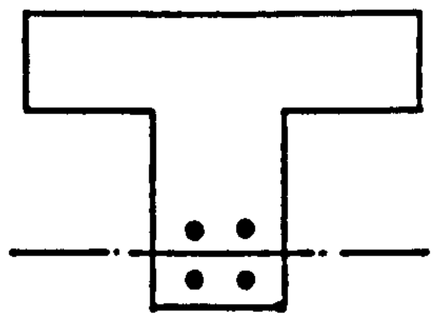	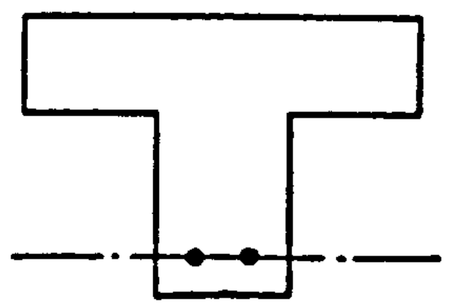
Bar No. & Type	4-16	4-12	2-12

Note: Cover to all steel according to CP 110 (54)

FIGURE 8.2 LONGITUDINAL REINFORCEMENT DETAILS FOR FLEXURAL SPECIMENS

TABLE 8.1 DETAILS OF LYTAG-SAND R.C. T-BEAMS

Beam No.	28 Day Dry Cured Strength (N/mm^2)	b_f x d (mm^2)	b_w x d (mm^2)	Reinforcement Number and Size (mm)	Yield Stress f_y (N/mm^2)	$\rho_f = \frac{A_{st}}{b_f d}$ (%)	$\rho_w = \frac{A_{st}}{b_w d}$ (%)	ρ_b CP 110 (54) (%)	$\frac{\rho_f}{\rho_b}$	S_v (mm)
F1	27.5	306 x 180	102 x 180	2-10	465	0.29	0.86	2.40	0.12	65
F2	28.5	306 x 180	102 x 180	4-10	465	0.57	1.71	2.40	0.24	135
F3	32.0	306 x 180	102 x 180	2-20	465	1.14	3.42	2.40	0.48	135
F4	46.0	306 x 180	102 x 180	2-12	465	0.41	1.23	3.49	0.12	45
F5	43.5	306 x 180	102 x 180	4-12	465	0.82	2.46	3.49	0.23	100
F6	44.0	306 x 180	102 x 180	4-16	465	1.46	4.38	3.49	0.42	135

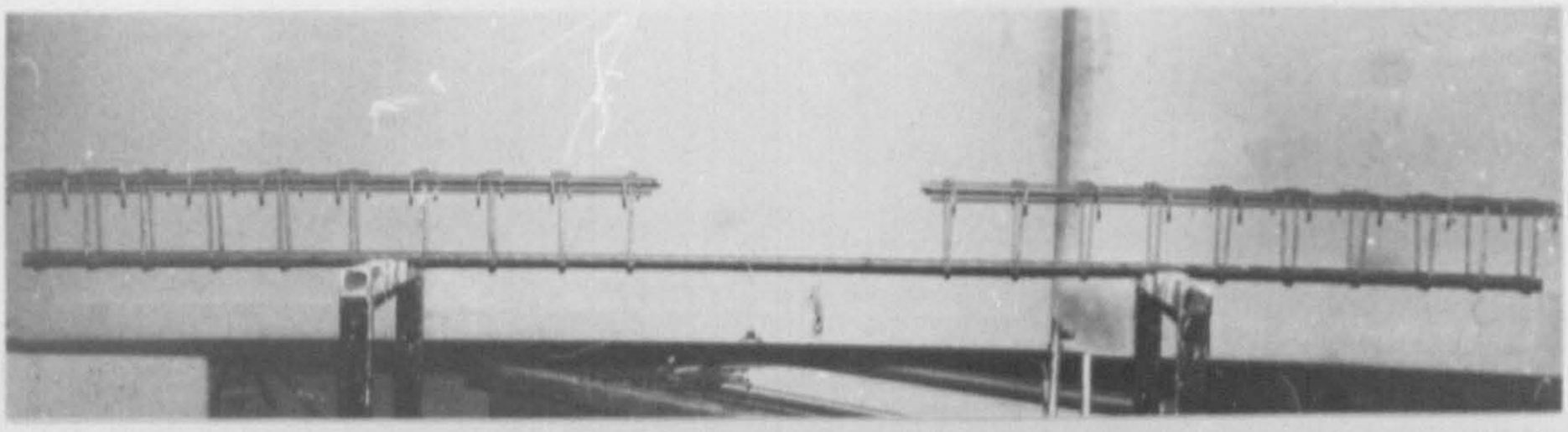

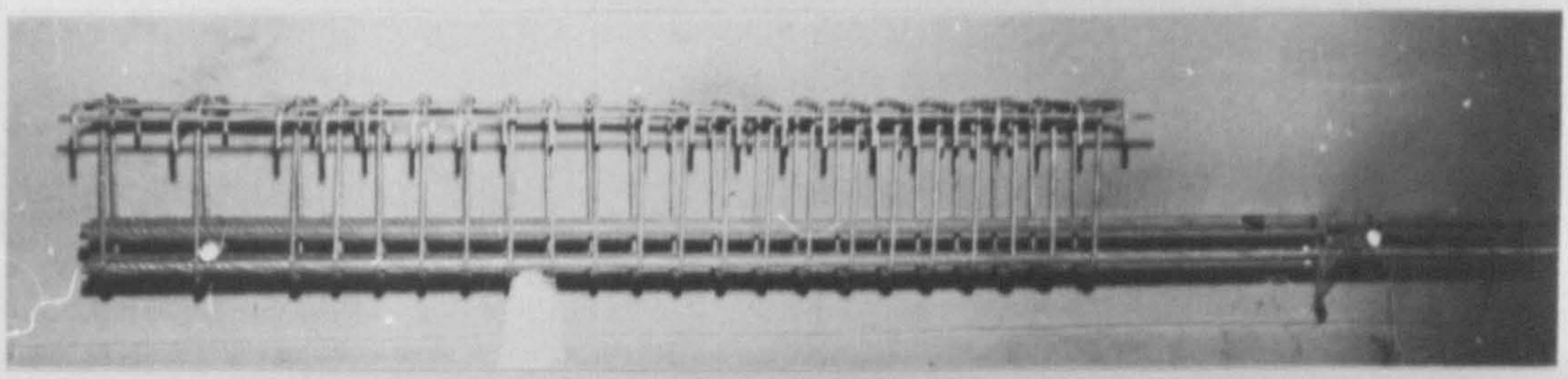

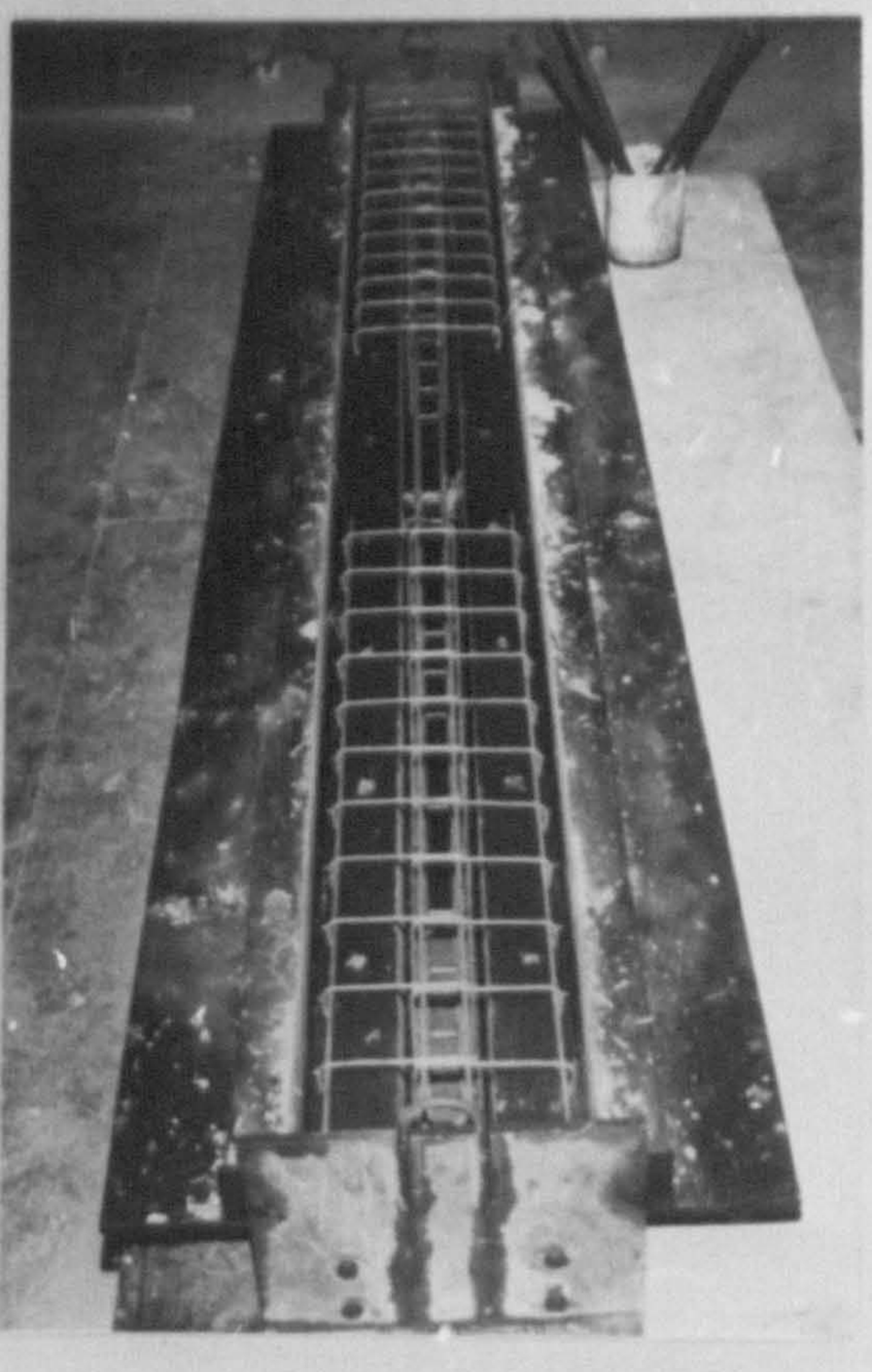

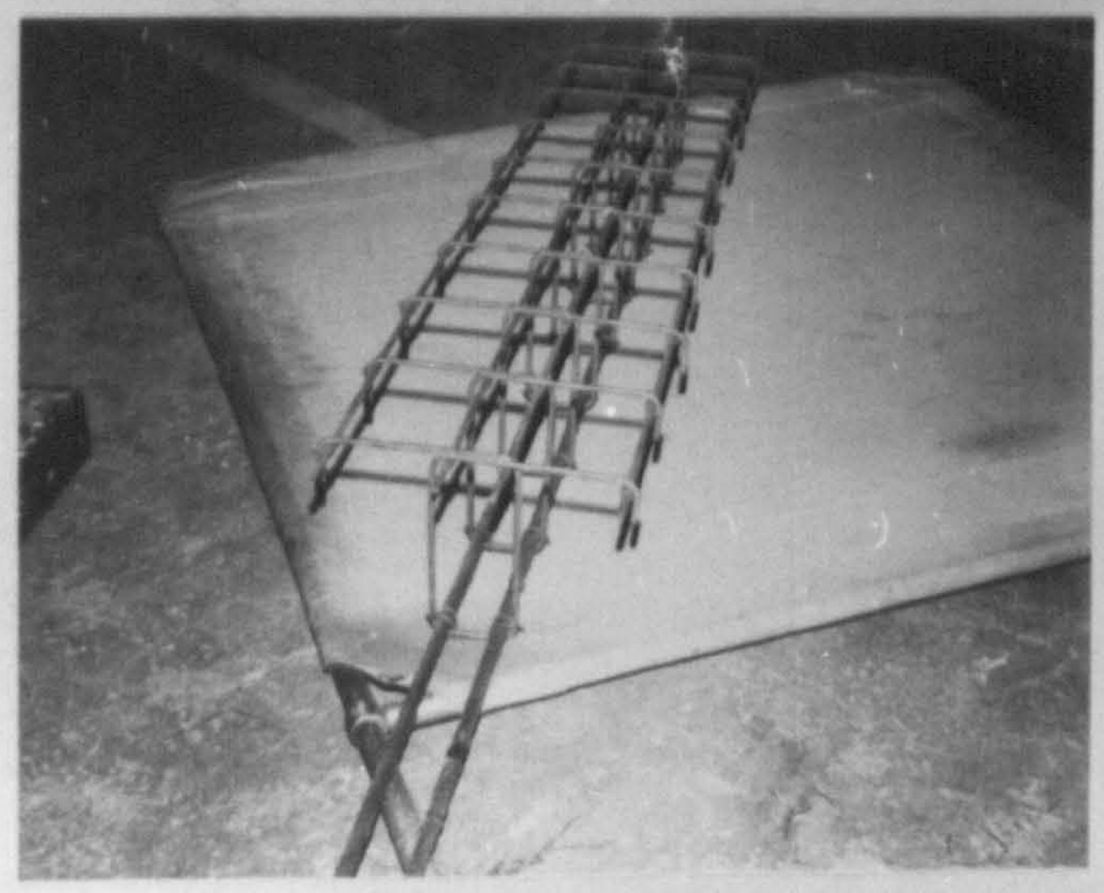

PLATE 8.1 TYPICAL REINFORCING CAGES FOR FLEXURAL T-BEAMS

Chapter 4. The mixes were designed to have dry cured cube strengths of 30 or 45 N/mm^2 at 28 days. O.P.C. was used throughout and the mix proportions were as follows:

f_{cu} = 30 N/mm^2 : 1 : 2.78 : 2.80 (cement : sand : Lytag)

f_{cu} = 45 N/mm^2 : 1 : 1.93 : 2.13

with total water-cement ratio's of 1.02 and 0.78 respectively.

8.2.2.2 Steel

The tensile reinforcement used in all the beams consisted of hot-rolled, cold worked, high tensile steel with a characteristic yield stress of 465 N/mm^2. A typical stress-strain curve for the steel is shown in Figure 7.3. Web reinforcement consisted of 6 mm diameter mild steel stirrups, as shown in Figure 8.1, and was provided in all beams in the region of the shear span. Stirrups were not provided in the flexural region of the beams.

8.2.3 Beam Design

Design of the test specimens was based on the CP 110 (54) parabolic stress block (see Appendix B) with the concrete materials factor of 1.5 removed, i.e. the maximum compressive stress = 0.67 f_{cu}. For each concrete strength the balanced steel ratio was calculated from which three areas of tensile steel, approximately equal to 12, 25 and 45% of the balanced steel ratio, were calculated. From this information the ultimate flexural moment M_f and the ultimate shear force V_u were calculated, from which shear reinforcement was designed in accordance with CP 110 (54).

8.2.4 Manufacture of Beams

All beams were cast using the same mould that was used for the beams in the shear series, described in Chapter 7. Two batches of concrete were required for each beam. Concrete was placed so that it just covered the tensile steel and was vibrated using a high frequency vibrating table. A 10 mm diameter rod was used to ensure that good compaction was obtained around the tensile steel. The remainder of the first batch of concrete was then placed and vibrated, followed by the second batch which was placed and vibrated in two roughly equal layers using the vibrating table and a 25 mm diameter vibrating poker.

With each beam, three 100 mm cubes were also cast for compressive strength tests. After casting the beam and cubes were left for approximately two hours before the surfaces were trowelled smooth. The specimens were then covered with polythene sheeting and left in the laboratory for two days before demoulding. After demoulding the specimens were stored in the laboratory until testing at approximately 28 days.

8.2.5 Instrumentation

Prior to casting electrical resistance strain gauges, with a gauge length of 7 mm, were fixed to the tensile bars in the pure bending region of the beams. The gauges were staggered to avoid loss of bond at one section. A Brüel and Kjaer, type 1516 strain gauge recorder with a maximum sensitivity of 5 microstrain and capacity of 30,000 microstrain was used to monitor the strain gauges.

In order to measure concrete strains a Demec extensometer with a gauge length of 100 mm and a sensitivity of 16.2×10^{-6} m/m was used. Demec discs were fixed as shown in Figure 8.1 about the centre line of the beam.

A dial gauge with a sensitivity of 0.01 mm per division and a total travel of 25 mm was used to measure central deflection. An inclinometer with a range of -2 to $+3^{o}$ was used to measure end rotations and a hand microscope with an illuminated scale, marked in 0.02 mm divisions, was used to measure crack widths.

8.2.6 Testing and Measurements

The test rig used for testing the flexural beams was the same as that shown in Figure 7.4. Prior to testing the beams were whitewashed to aid crack detection. All the beams were tested at the same shear span - effective depth ratio (a/d = 5.0). Load was applied in increments of 2.5 kN and crack development was marked at each load stage. Deflection, strains, crack widths and rotations were measured at various loads depending on the calculated flexural capacity and design load.

8.3 Calculation of Design Moment, Central Deflection and Ultimate Moment

8.3.1 Design Moments

For the reinforced T-sections tested during this part of the investigation, the design moments, for the serviceability limit states, were based on the ultimate design moments calculated from the CP 110 (54) simplified stress block. By using these equations, the ultimate design moment M_f was taken as the lesser of

$$M_f = 0.87\ f_y\ A_{st}\ z \qquad \ldots\ (8.1)$$

or

$$M_f = 0.15\ f_{cu}\ bd^2 \qquad \ldots\ (8.2)$$

where

$$z = \left(1 - \frac{1.1\ f_y\ A_s}{f_{cu}\ b.d}\right)d \qquad \ldots\ (8.3)$$

The calculated ultimate design moment is equivalent to the moment caused by 1.4 times dead load, plus 1.6 times the imposed load. Since for the beams tested, the dead load is the beam weight, then the serviceability design moment is given by $M_f/1.6$.

8.3.2 Central Deflection

Two methods were used to calculate the central deflection, as described in the American and U.K. design codes (26, 54).

8.3.2.1 CP 110 (54) Method

The instantaneous deflection at the centre of a simply supported beam, according to CP 110 (54) can be calculated from the equation

$$\Delta = K\ L^2\ \frac{1}{r_b} \qquad \ldots\ (8.4)$$

where Δ = central deflection

L = effective span of beam

$\frac{1}{r_b}$ = curvature at mid span

K = a constant dependent on the shape of the bending moment diagram.

Under this loading condition $K = 0.10648$.

For the partially cracked section considered in this case, the curvature at mid-span is given by

$$\frac{1}{r_b} = \frac{M_{net}}{E_c\ I_c} \qquad \ldots\ (8.5)$$

where E_c = modulus of elasticity of concrete (Table 5.1)

I_c = second moment of area of the transformed concrete section

$$M_{net} = M - M_c \qquad \ldots\ (8.6)$$

where M = applied moment at section considered

M_c = moment due to tensile strength of concrete; assumed to be 1 N/mm^2 at the centroid of the tension steel.

8.3.2.2 A.C.I. Standard Method (26)

The A.C.I. method of calculating deflection is based on the effective moment of inertia of the section, I_e, as follows, with a limiting value equal to Ig:

$$I_e = \left(\frac{M_{cr}}{M}\right)^3 Ig + \left[1 - \left(\frac{M_{cr}}{M}\right)^3\right] I_c \qquad \ldots\ (8.7)$$

where Ig = moment of inertia of gross concrete section about the centroidal axis, neglecting reinforcement

I_c = moment of inertia of the cracked transformed section

M = maximum applied moment at stage for which deflection is being calculate

$$M_{cr} = \frac{f_r\ Ig}{yt} \qquad \ldots\ (8.8)$$

$f_r = 7.5\ f_{SP}/6.7 \leq 7.5 \times 0.083 \sqrt{f_c'}$ for lightweight concrete.

y_t = distance from controidal axis of gross cross section, neglecting reinforcement to extreme fibre in tension.

Having calculated the value of I_e then the central deflection is calculated from

$$\Delta = \frac{K\ M\ L^2}{E_c\ I_e} \qquad \ldots\ (8.9)$$

8.3.3 Ultimate Moments

The ultimate moment of the test beams was calculated by two methods using the CP 110 (54) parabolic stress block, without the safety factors (see Appendix B), or Whitney's theory (154) which has been adopted by A.C.I. (26).

8.3.3.1 CP 110 (54) Method

When using the CP 110 (54) parabolic stress block, without the safety factors, the ultimate moment of resistance M_f of a beam is given by

$$M_f = f_y A_{st} \left[1 - \frac{k_2 f_y}{k_1 f_{cu}} \rho\right] d \quad \ldots\ldots (8.10)$$

where

$$k_1 = 0.67 (1 - \sqrt{f_{cu}}/43.1) \quad \ldots\ldots (8.11)$$

$$k_2 = \frac{\left[2 - \frac{\sqrt{f_{cu}}}{14.4}\right]^2 + 2}{4\left[3 - \frac{\sqrt{f_{cu}}}{14.4}\right]} \quad \ldots\ldots (8.12)$$

8.3.3.2 Whitney's Method (154)

For a section where the depth to the neutral axis, x, calculated from

$$x = \frac{A_{st} f_y}{0.85 f_c' b} \quad \ldots\ldots (8.13)$$

lies within the flange, then the ultimate moment of resistance M_f is given by

$$M_f = A_{st}.f_y.d \left[1 - \frac{0.59 A_{st}.f_y}{f_c' b d}\right] \quad \ldots\ldots (8.14)$$

where f_c' is the cylinder compressive stress taken as $0.85 f_{cu}$ for this investigation.

8.4 Test Results and Discussion

The main test results from this investigation are summarised in Tables 8.2 to 8.5. The failure modes and cracking patterns, of the six beams tested, are shown in Plate 8.2. The test results are discussed in the following sections and were appropriate are compared with design codes (26, 54).

8.4.1 Deflection

The load deflection curves for the beams are shown in Figures 8.3(a) and (b)

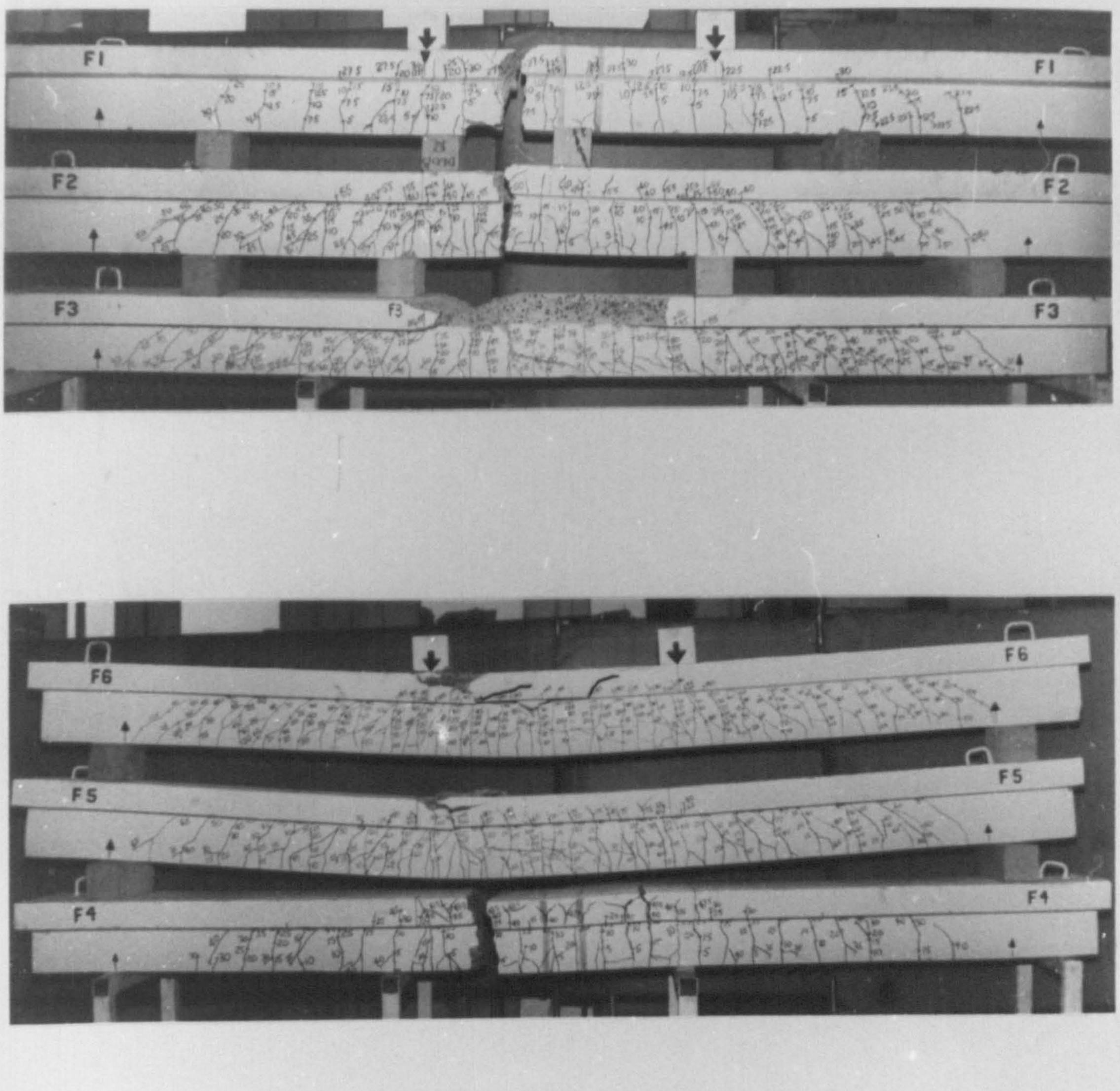

PLATE 8.2 FAILURE MODES FOR LYTAG-SAND CONCRETE T-BEAMS IN FLEXURE

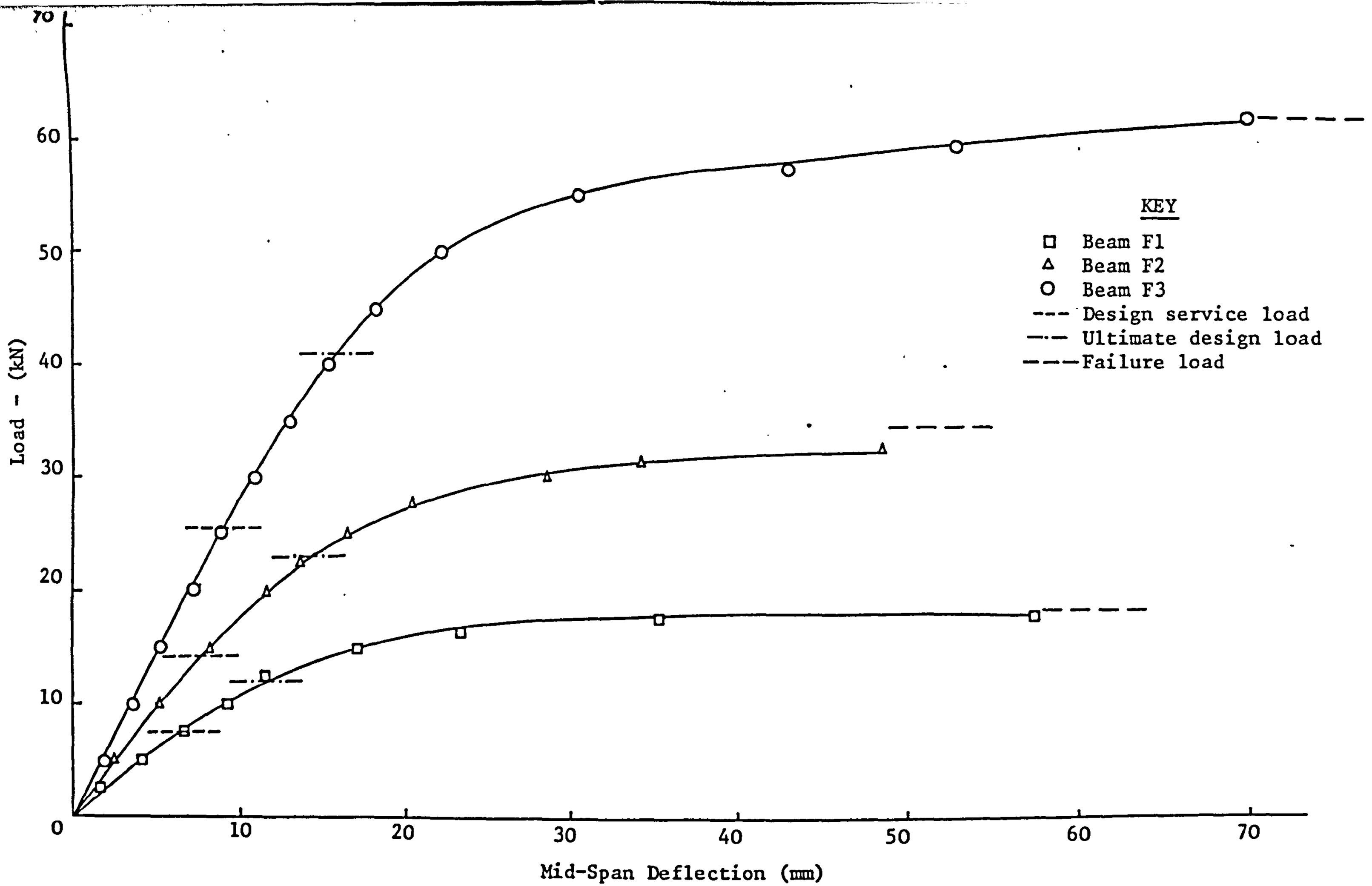

FIGURE 8.3(a) LOAD-DEFLECTION CURVES FOR T-BEAMS

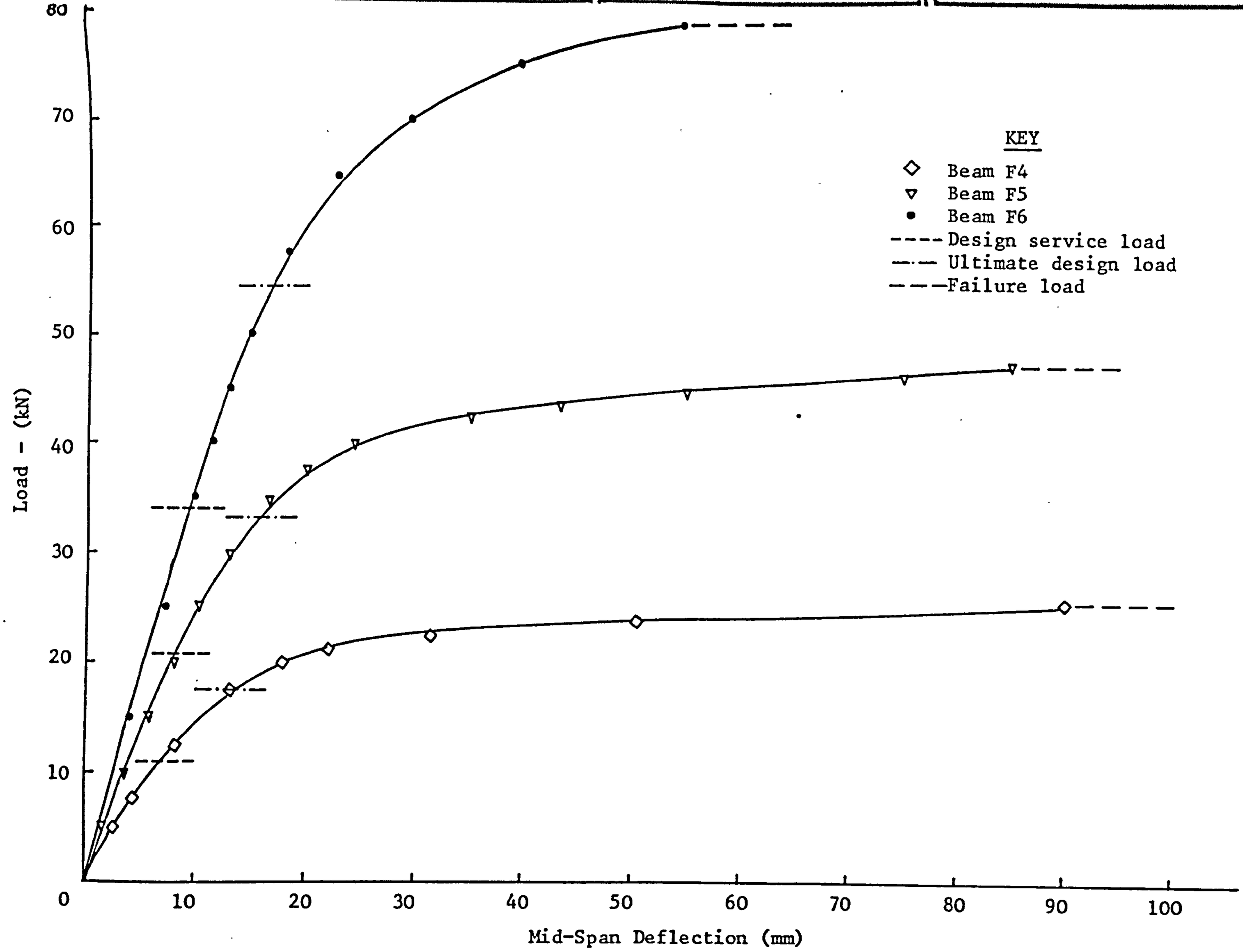

FIGURE 8.3(b) LOAD-DEFLECTION CURVES FOR T-BEAMS

For each beam the points on the curve corresponding to the design service load and the ultimate design load, calculated in accordance with 8.3.1, are shown. Results for measured and calculated deflections at design service load are shown in Table 8.2. For the concrete strengths and steel percentages used during this investigation, the central deflection under the design service load varies between 6.3 and 9.25 mm. The span deflection ratio's at the permissible working load vary between 270 and 396.

8.4.1.1 Comparison Between Measured and Predicted Deflections at Design Load

The deflections predicted using the design equations described in section 8.3.2 are compared with the test values, in Table 8.2. Both the CP 110 and A.C.I. (26, 54) equations underestimate the deflection at mid-span but for low steel percentages the CP 110 (54) equation grossly underestimates deflection. The A.C.I. equation gives closer values for the range of steel percentages and concrete strengths tested though they are still below the measured values.

If the CP 110 (54) equation is used without the allowance for moment due to the tensile strength of the concrete then the predicted values lie much closer to the actual measured values. From Plate 8.2 it can be seen that the crack specings are very close, even at the working load and thus the assumption that the concrete in tension is unable to resist moment is valid.

Several investigators have reported that the deflection of lightweight concrete beams is, in general, greater than that of comparable gravel concrete (35, 49). This is generally agreed to be due to the lower elastic modulus of lightweight concrete. From a designers point of view, however, a direct comparison between lightweight and dense concretes is not appropriate since lightweight concrete is a material in its own right and therefore should be designed with its own specific properties in mind.

8.4.2 Cracking Properties

During this investigation the crack widths at various load increments, along with the moment at first flexural crack and the number of cracks between the load points, at the design service moment M, were measured. The results

TABLE 8.2 DEFLECTION CHARACTERISTICS OF LYTAG-SAND R.C. T-BEAMS

Beam No.	Calculated Design Service Moment M (kNm)	Deflection at M From Test (mm)	Calculated Deflection at M (mm)			Col. 4 / Col. 3 (%)	Col. 5 / Col. 3 (%)	Col. 6 / Col. 3 (%)	Span / Col. 3 (%)	Deflection Prior to Failure (mm)
			CP 110 (54)	A.C.I. (26)	CP 110 (54)*					
1	2	3	4	5	6	7	8	9	10	11
F1	6.79	6.3	2.95	5.52	6.19	0.47	0.88	0.98	396	57.3
F2	12.90	7.5	4.79	6.60	6.72	0.64	0.88	0.90	333	48.2
F3	23.00	8.8	6.40	7.18	7.18	0.73	0.82	0.82	284	69.8
F4	9.76	6.75	4.25	6.19	6.49	0.63	0.92	0.96	370	90.0
F5	18.70	8.00	5.82	7.19	7.23	0.73	0.90	0.90	312	85.0
F6	30.5	9.25	6.91	7.83	7.84	0.75	0.85	0.85	270	55.0

* Neglecting the tensile strength of the concrete.

are shown in Table 8.3

The moment at first crack is based on the load at which the first flexural crack was observed in the pure bending region. It is a very subjective measurement since it relies on the ability of the observer to spot the first crack. It should be noted, however, that the observed values of the flexural cracking moment, from tests, vary between 63 and 83% of the values calculated from equation (8.8).

With regard to crack widths and spacings, it should be recognised that such data are notoriously subject to inherent experimental scatter. The duplication of tests is essential if valid conclusions are to be drawn. Most investigators who report cracking data, emphasize that maximum and minimum values of crack width and spacing may vary considerably from the mean.

From Table 8.3 it can be seen that the range of maximum crack widths under working load is from 0.10 to 0.18 mm and is well within the durability requirements given in CP 110 (54).

Average crack spacings vary between the approximate limits of 45-70 mm. Evans and Orangun (36) reported tests on twenty All-Lytag, rectangular, reinforced concrete beams in which maximum crack widths varied between 0.088 and 0.254 mm with average crack spacings of 62.5-157 mm for beams reinforced with square twisted bars. The smaller crack spacings of the present investigation have resulted in the smaller crack widths at working load, when compared to investigation (36), but may result in a slight increase in deflection due to a slight decrease in the stiffness of the beams.

8.4.3 End Rotations

The average values of end rotation for all beams tested in this series are shown in Figures 8.4 (a) and (b) against load. They show that in general the end rotation and therefore the curvature of the beams is directly proportional to the applied load up to working loads, after which the ductile behaviour of the beams leads to large increases in curvature for small increases in load.

TABLE 8.3 CRACK CHARACTERISTICS OF LYTAG-SAND R.C. T-BEAMS

Beam No.	Moment at 1st Crack M_{cr} (kN-m)	Calculated Design Service Moment M (kN-m)	Experimental Ultimate Moment M_{exp} (kN-m)	Crack Widths at M (mm)			No. of Cracks Between Loading Points at M	Maximum Crack Width Near Failure (mm)	$\frac{M}{M_{cr}}$
				Minimum	Maximum	Mean			
F1	2.03	6.79	16.3	0.10	0.18	0.14	11	1.46	3.35
F2	2.25	12.90	31.0	0.06	0.10	0.09	12	1.50	5.73
F3	2.25	23.00	55.8	0.08	0.14	0.10	12	0.80	10.22
F4	2.25	9.76	23.1	0.04	0.10	0.09	13	0.94	4.34
F5	2.25	18.70	42.8	0.04	0.12	0.10	16	0.65	8.31
F6	3.38	30.50	70.5	0.08	0.14	0.11	11	0.64	9.02

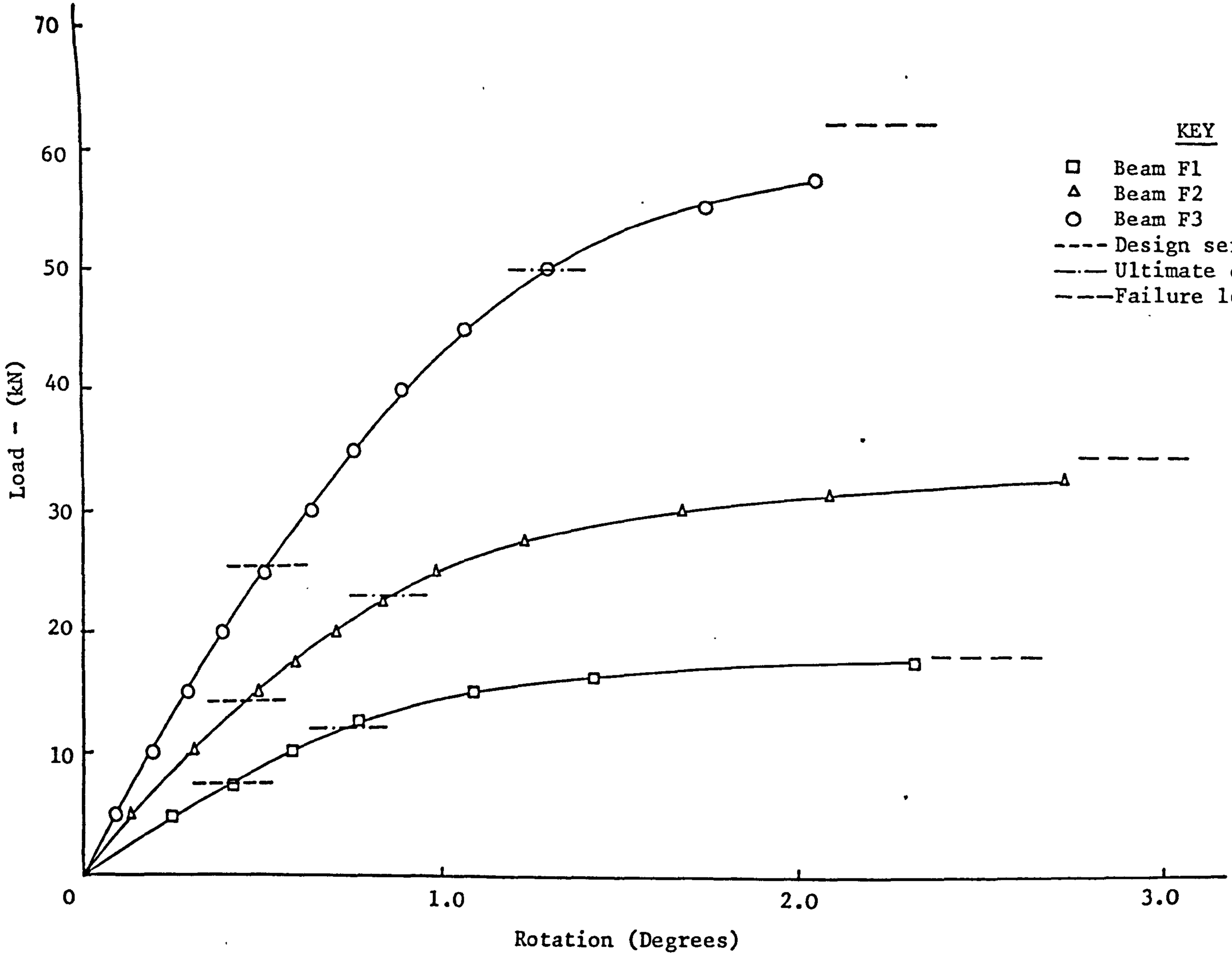

FIGURE 8.4(a) LOAD ROTATION CURVES FOR T-BEAMS

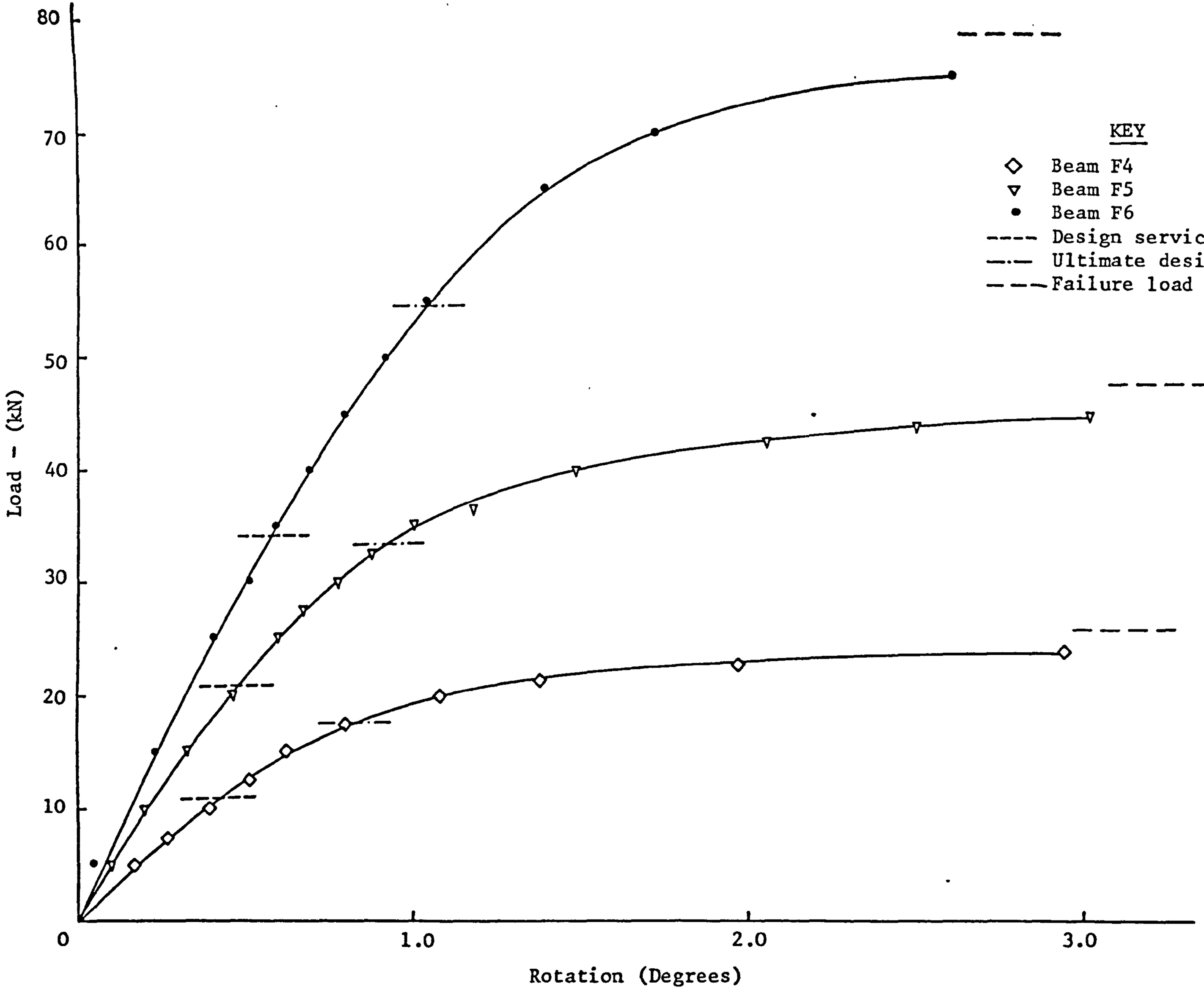

FIGURE 8.4(b) LOAD ROTATION CURVES FOR T-BEAMS

8.4.4 Design and Ultimate Moments

Table 8.4 shows the design moment at working load calculated from the CP 110 (54) simplified stress block, along with the experimental and calculated ultimate flexural moments.

The beams tested in this series show load factors ranging from 2.29 to 2.40. The ratio's of the experimental ultimate moment to the calculated ultimate moment based on CP 110 (54) and A.C.I. (26), without the safety factors, range from 1.18-1.28 and 1.17-1.28 respectively. With the inclusion of the safety factors in the design ultimate moment equations, these ratio's increase and therefore the design equations become more conservative.

The results of Table 8.4 show that the design of Lytag-sand concrete T-beams in flexure, according to design codes (26, 54) will provide an adequate load factor against failure.

8.4.5 Strain Distribution Over Depth of Section at Mid-Span

The strain distributions are shown in Figures 8.5(a)-(f), for the beams tested during this investigation, both at working load and shortly before failure. The high tensile strains at ultimate load result from the formation of cracks within the gauge length. For this reason web strains are not recorded for the load case shortly before failure.

From the strain distributions shown it can be seen that the assumption that plane sections remain plane is a valid one certainly within the compression flange.

Referring to Plate 8.2 it can be seen that for beams F1, F2 and F4 which failed by fracture of the reinforcing steel that the yield strain of the concrete, in the compression zone, was not reached. For beams F3, F5 and F6, however, it is apparent that high concrete strains, greater than 4000 μs, were reached in the compression flange, prior to failure by concrete crushing. This indicates that Lytag-sand concrete has a high strain capacity which adequately exceeds the value generally taken as the failure strain in design (54).

8.4.6 Compressive Concrete Strain at Mid-Span

The variation of mid-span concrete strain with load is shown in

TABLE 8.4 EXPERIMENTAL AND CALCULATED MOMENTS

Beam No.	Design Moment M (kN-m)	Ultimate Flexural Moment M_f CP 110 (54) (kN-m)	Ultimate Flexural Moment M_f ACI (26) (kN-m)	Experimental Ultimate Moment M_{exp} (kN-m)	Load Factor $\frac{M_{exp}}{M}$	$\frac{\text{Col. 5}}{\text{Col. 3}}$	$\frac{\text{Col. 5}}{\text{Col. 4}}$
1	2	3	4	5	6	7	8
F1	6.79	12.7	12.7	16.3	2.40	1.28	1.28
F2	12.90	24.5	24.7	30.9	2.40	1.26	1.25
F3	23.00	45.6	46.1	55.8	2.43	1.22	1.21
F4	9.76	18.3	18.4	23.1	2.37	1.26	1.26
F5	18.70	35.4	35.6	42.8	2.29	1.21	1.20
F6	30.50	59.6	60.2	70.5	2.31	1.18	1.17

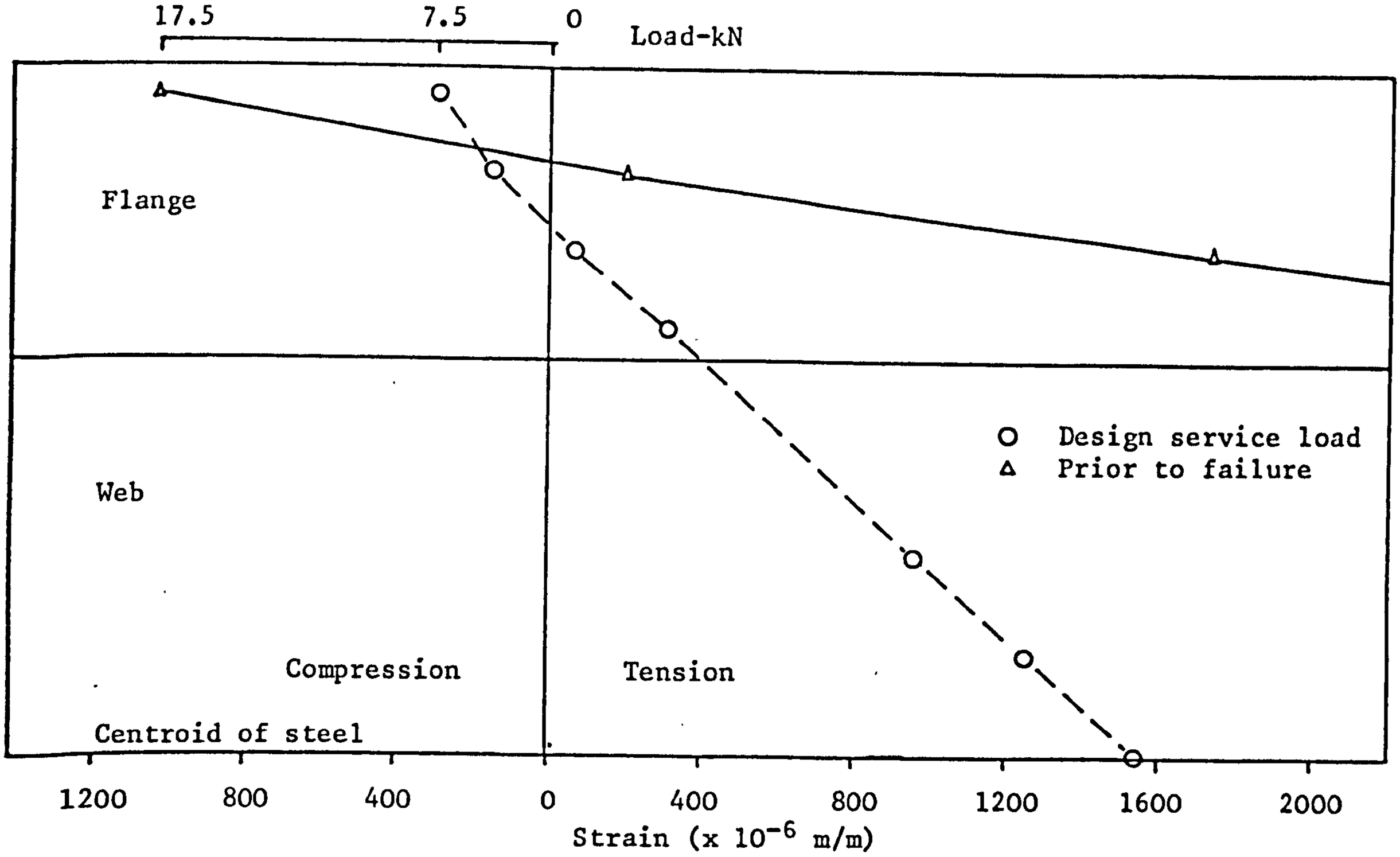

FIGURE 8.5(a) FLEXURAL STRAIN DISTRIBUTION FOR BEAM F1

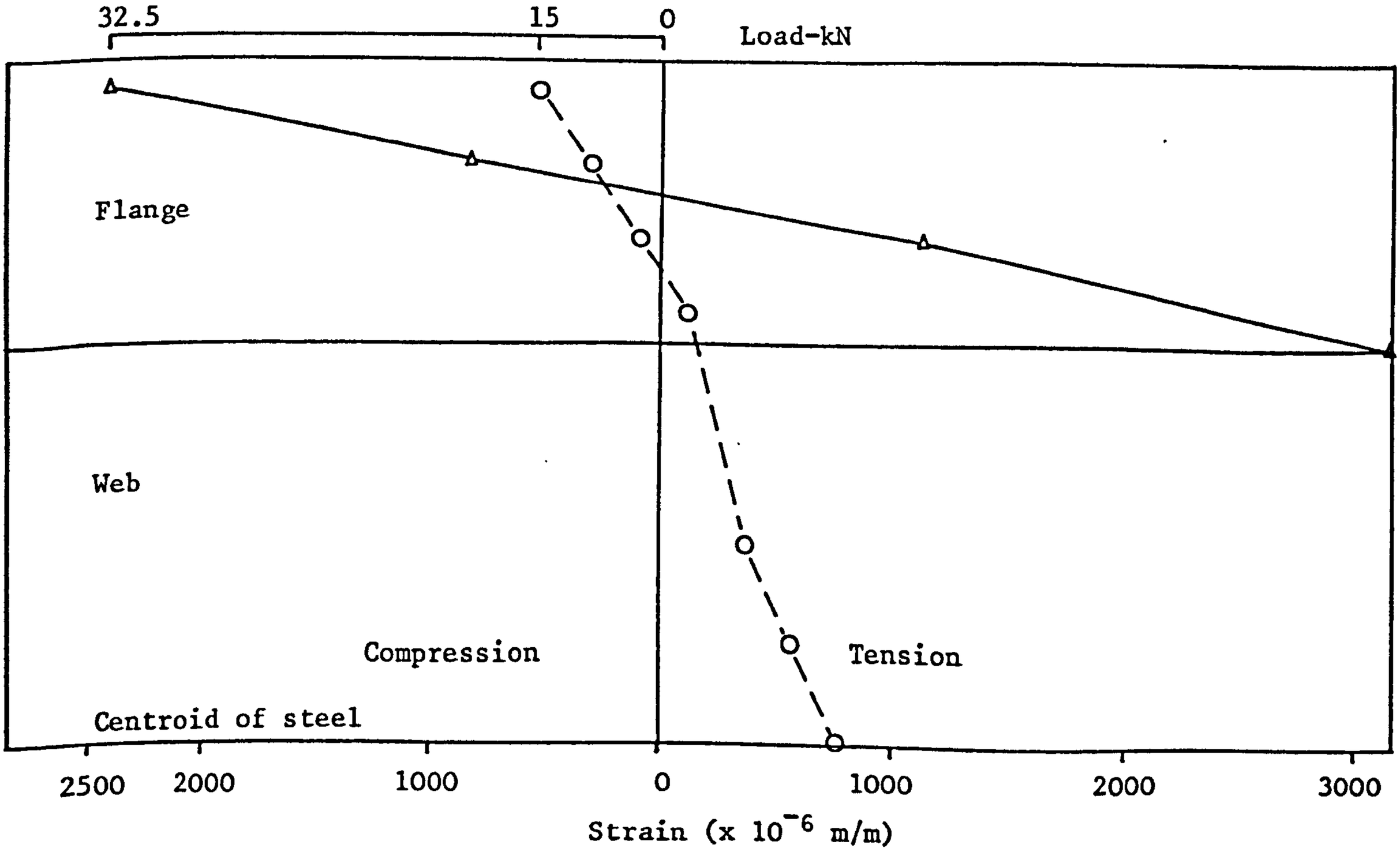

FIGURE 8.5(b) FLEXURAL STRAIN DISTRIBUTION FOR BEAM F2

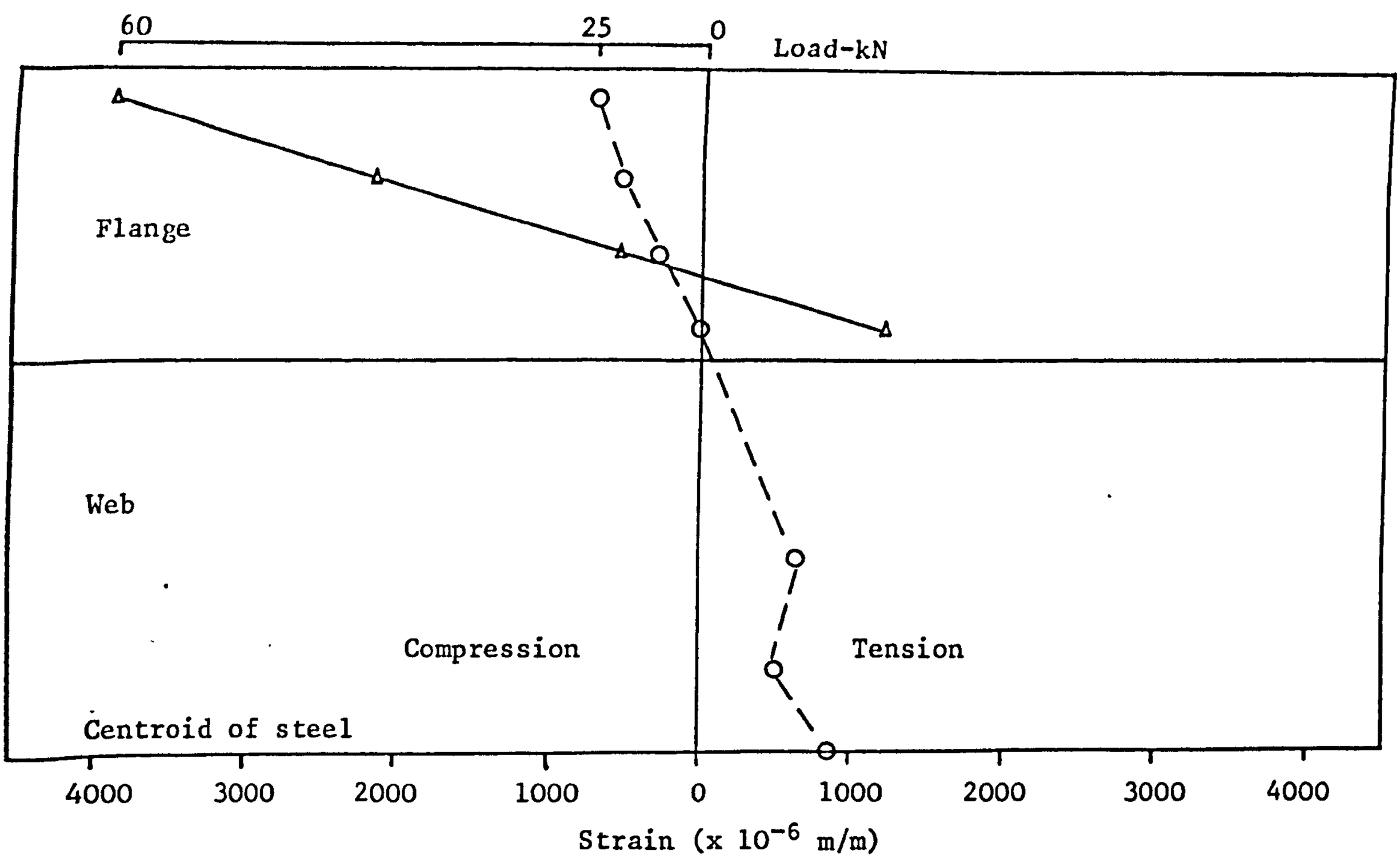

FIGURE 8.5(c) FLEXURAL STRAIN DISTRIBUTION FOR BEAM F3

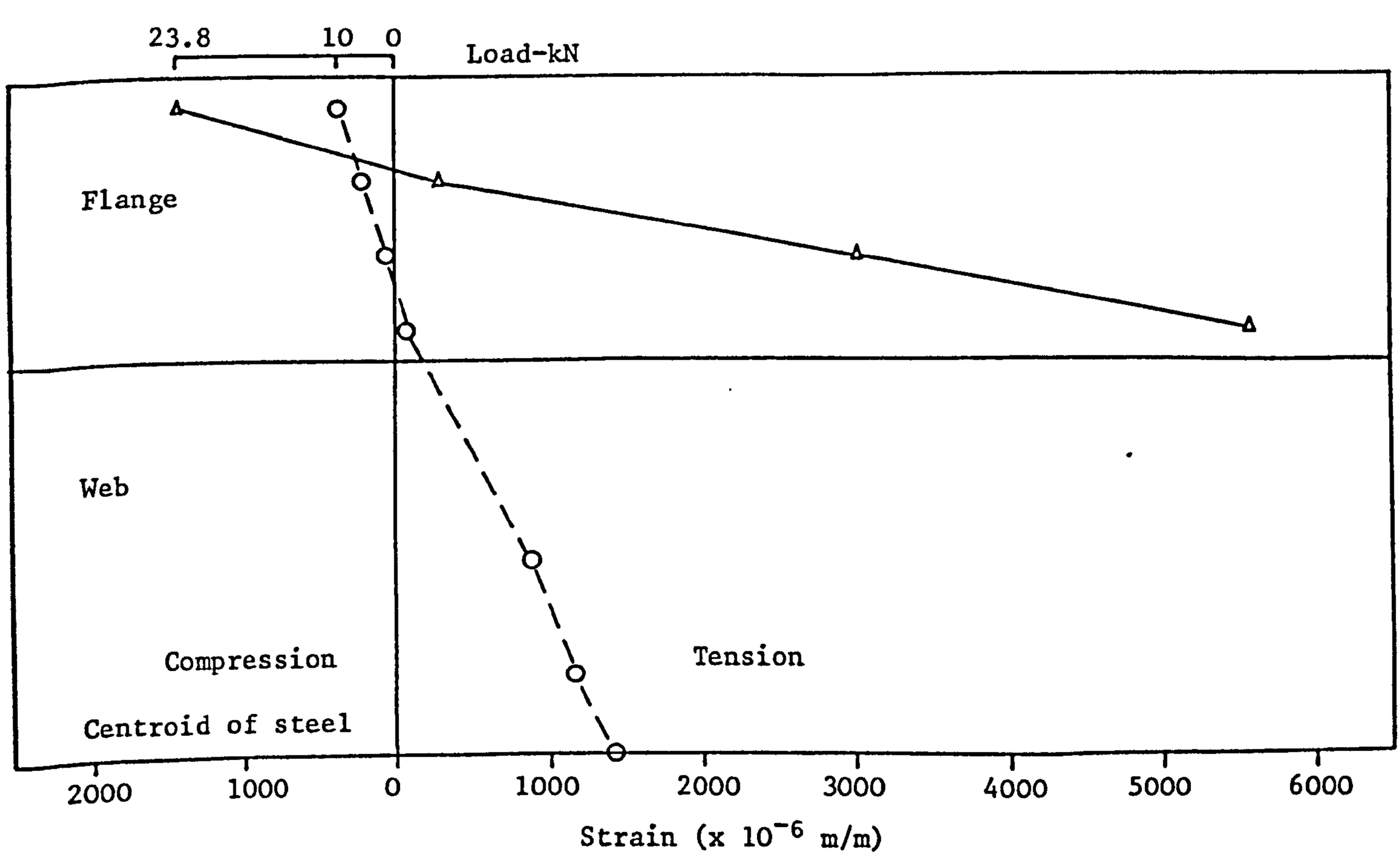

FIGURE 8.5(d) FLEXURAL STRAIN DISTRIBUTION FOR BEAM F4

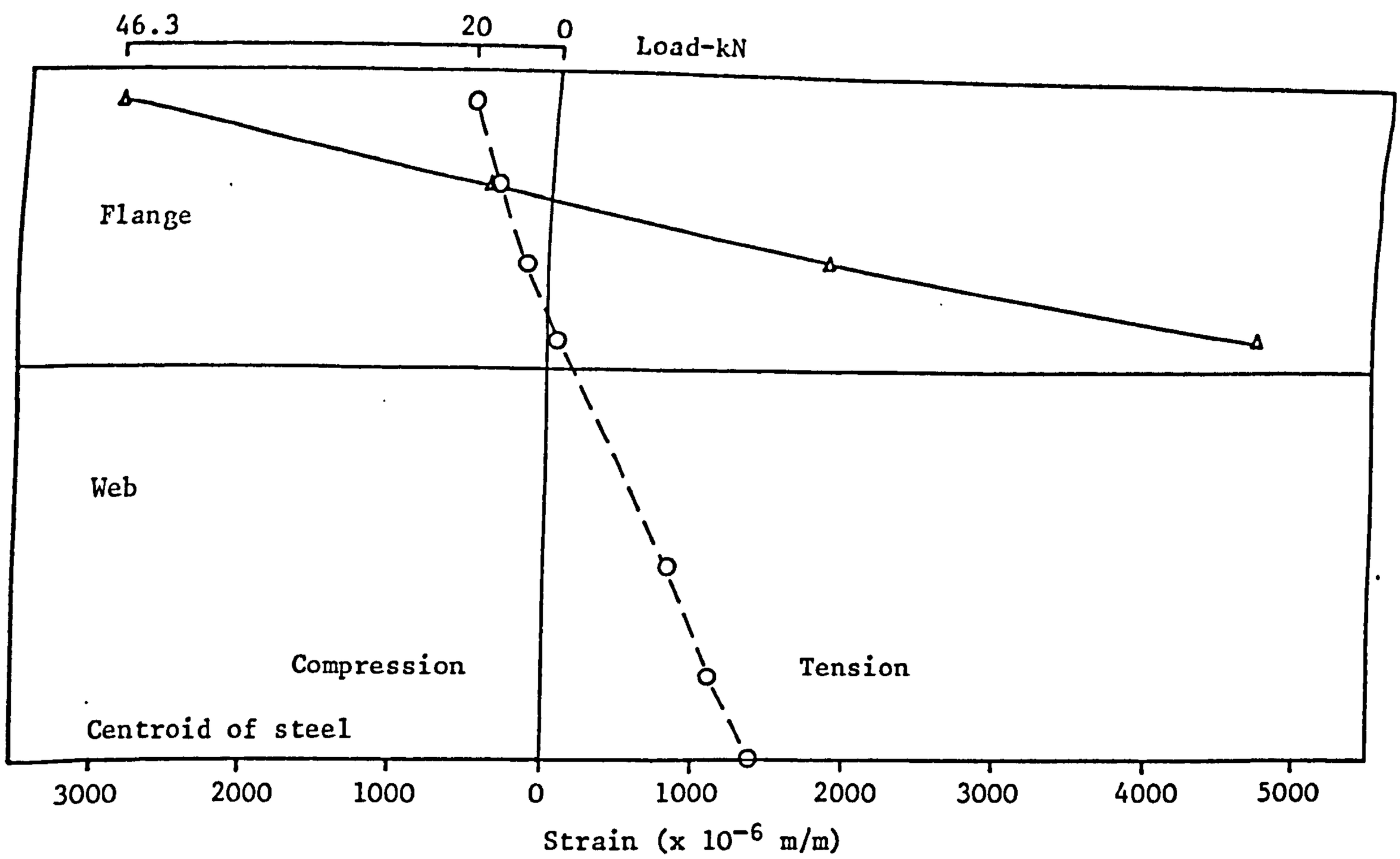

FIGURE 8.5(e) FLEXURAL STRAIN DISTRIBUTION FOR BEAM F5

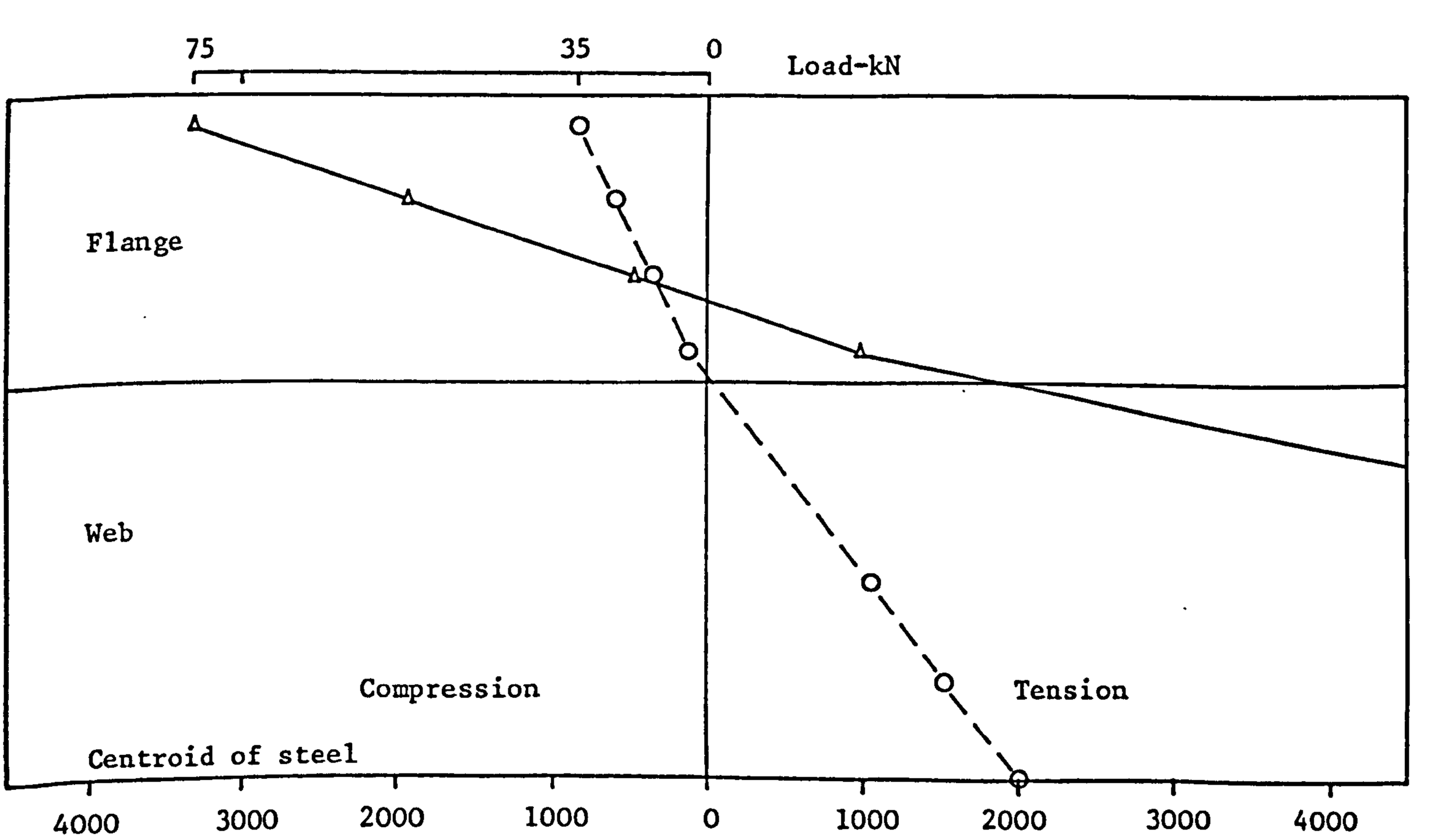

FIGURE 8.5(f) FLEXURAL STRAIN DISTRIBUTION FOR BEAM F6

Figures 8.6(a) and (b). The values shown are the averages of four readings taken across the top face of the compression flange.

The strains at working load range from approximately 425-925 microstrain. Again for the beams which failed by crushing of the concrete compression zone it can be seen that concrete strains in excess of 4000 microstrain were recorded prior to failure. The maximum recorded concrete strains prior to failure are listed in Table 8.5.

8.4.7 Tensile Steel Strain

The measured steel strains for each beam, in the pure bending region of the beam, are plotted against load in Figures 8.7(a) and (b). The measured steel strains at working load vary from 800-1400 microstrain. For the beams which failed by fracture of the steel, it can be seen that where the strain gauges remained operational, extremely high strains were recorded prior to failure.

The results of the rotation, strain distribution, compressive concrete strain and steel strain measurements discussed in sections 8.4.3 to 8.4.7 all indicate the ductile nature of the beams tested. It is obvious that Lytag-sand reinforced concrete T-beams can be adequately designed for safety according to the U.K. and American design codes (26, 54).

Values of maximum measured deflection, rotation, concrete strain and steel strain along with the design moment at service load and the ultimate moment, for each beam are shown in Table 8.5.

8.4.8 Modes of Failure

The general mode of failure for each of the beams tested is shown in Plate 8.2. For the beams which failed by crushing of the compression zone concrete, details of the failure zones are shown in Plate 8.3. Typical, fractured reinforcement bars removed from beams F1, F2 and F4 are shown in Plate 8.4.

The compression zone failures are typical of any T-section, without compression reinforcement, and show the large zone of the compression flange which is destroyed by concrete crushing at failure. The tensile steel specimens shown in Plate 8.4 show typical ductile characteristics for steel with a

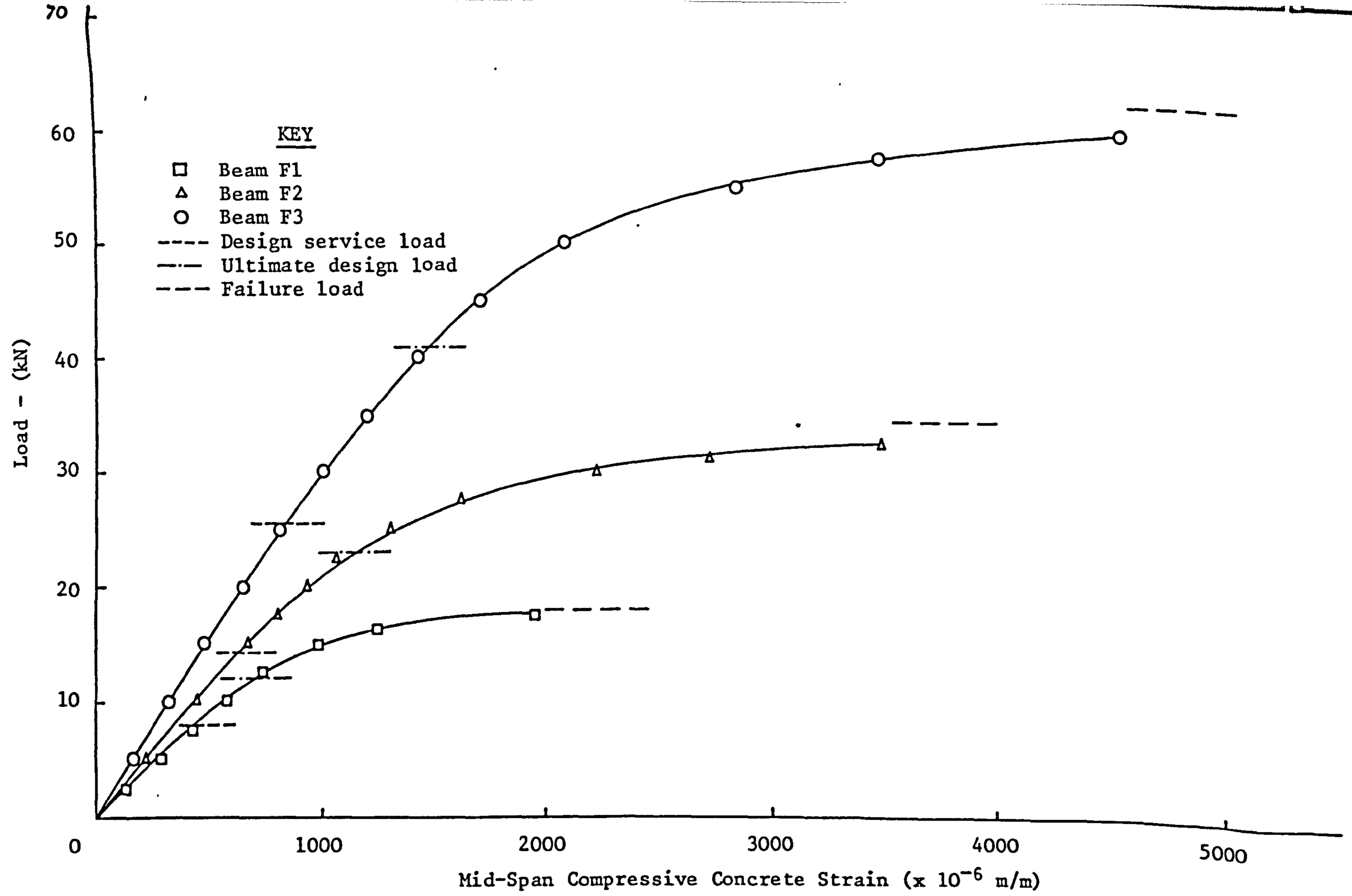

FIGURE 8.6(a) LOAD, MID-SPAN CONCRETE STRAIN CURVES

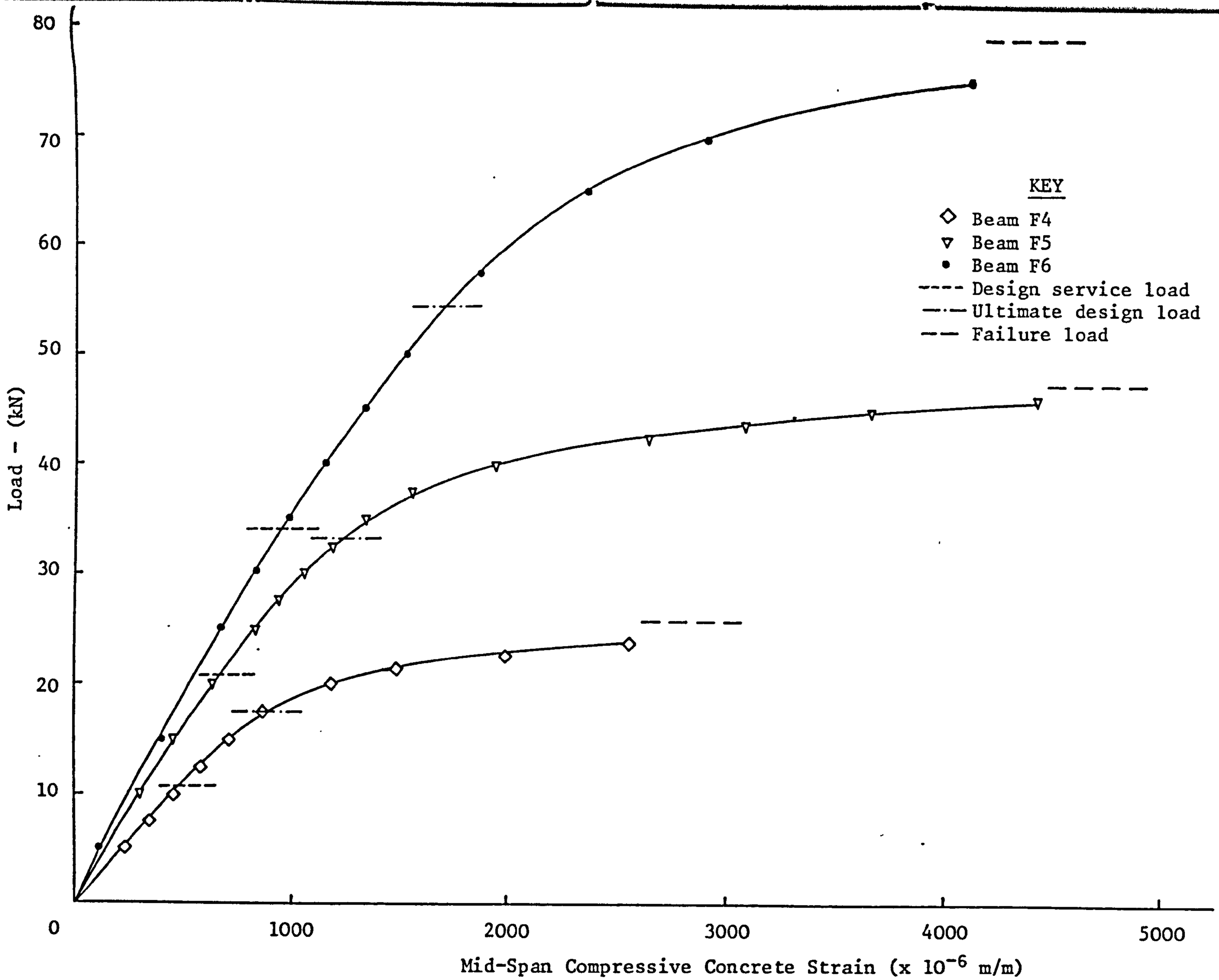

FIGURE 8.6(b) LOAD, MID-SPAN CONCRETE STRAIN CURVES

TABLE 8.5 MAXIMUM RECORDED DEFLECTION, ROTATION AND STRAINS

Beam No.	Calculated Design Service Moment M (kN-m)	Experimental Ultimate Moment M_{exp} (kN-m)	Maximum Recorded Deflection (mm)	Maximum Recorded Rotation	Maximum Recorded Compressive Concrete Strain (x 10^{-6} m/m)	Maximum Recorded Steel Strain (x 10^{-6} m/m)
F1	6.79	16.3	57.3	2^{o} 23'	1960	11700*
F2	12.90	30.9	48.2	2^{o} 45'	3550	17000*
F3	23.00	55.8	69.8	2^{o} 04'	4550	10000
F4	9.76	23.1	90.0	3^{o} 01'	2610	14000*
F5	18.70	42.8	85.0	3^{o} 01'	4420	28000
F6	30.50	70.5	55.0	2^{o} 41'	4200	15500

* Beams failing by steel fracture

Note: The maximum recorded values listed were measured at a load corresponding to approximately 95% of the failure load.

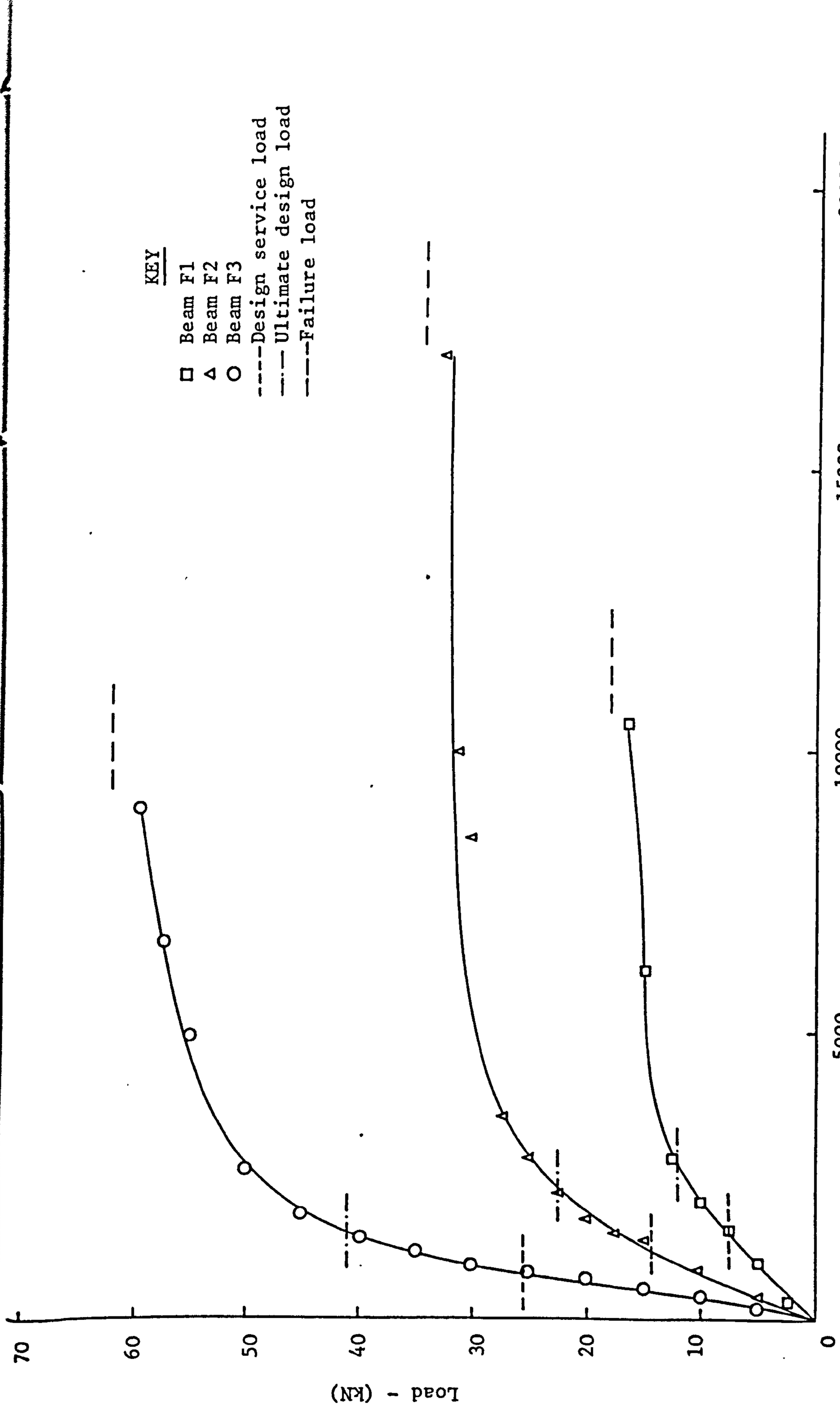

FIGURE 8.7(a) LOAD-TENSILE STEEL STRAIN CURVES

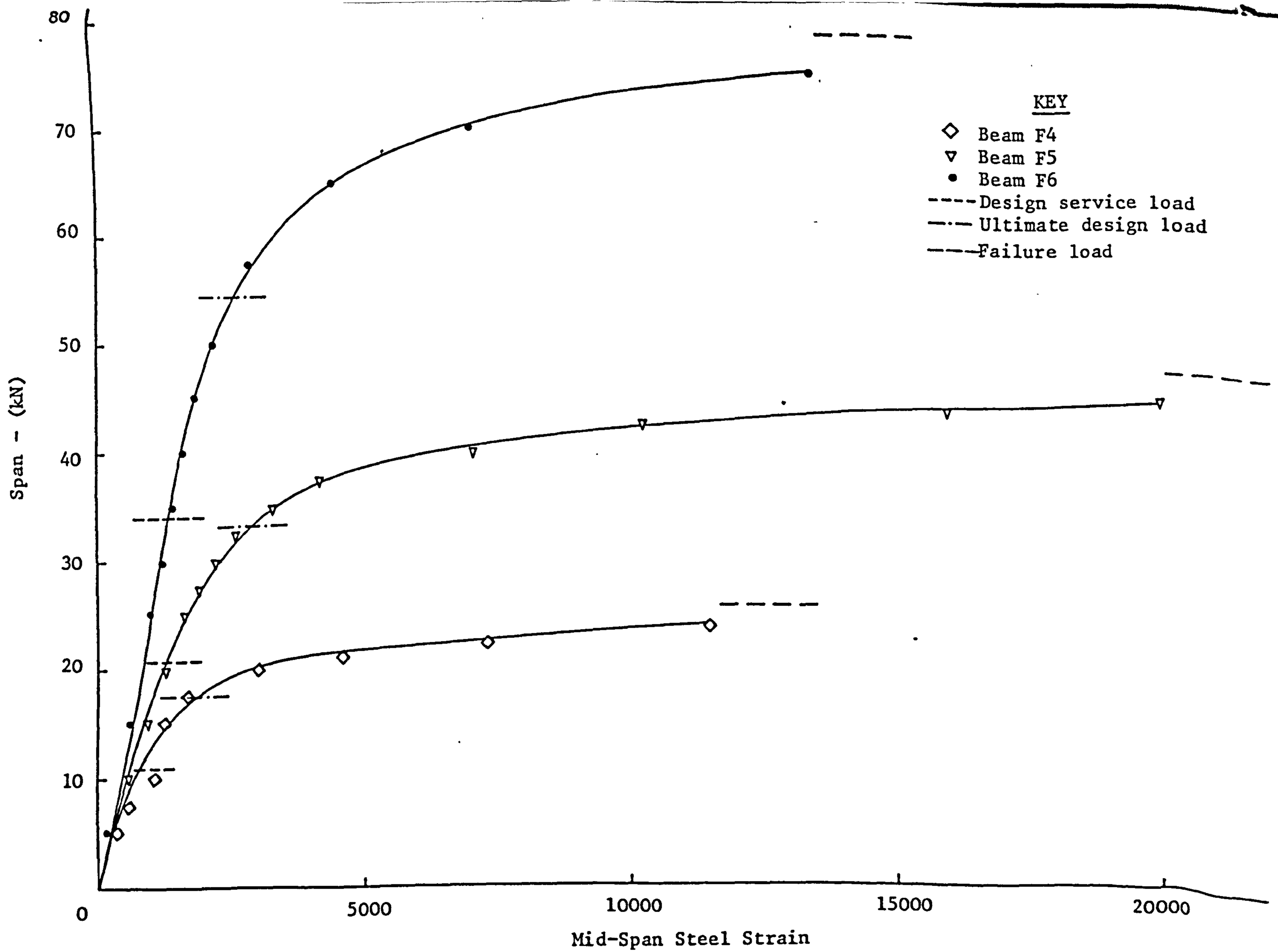

FIGURE 8.7(b) LOAD-TENSILE STEEL STRAIN CURVES

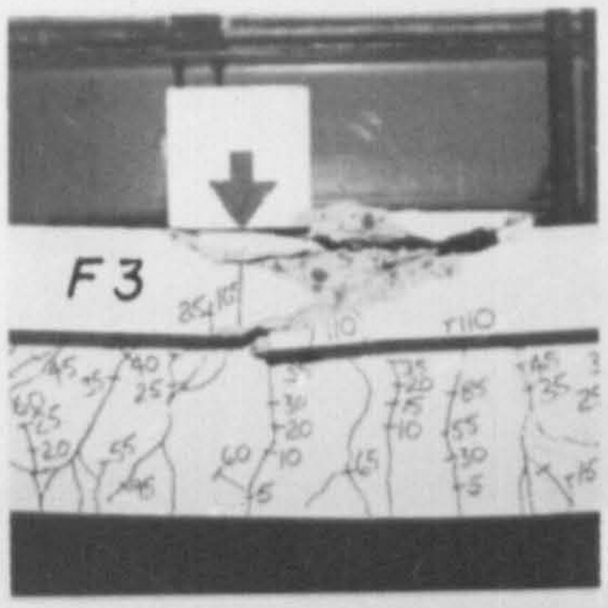

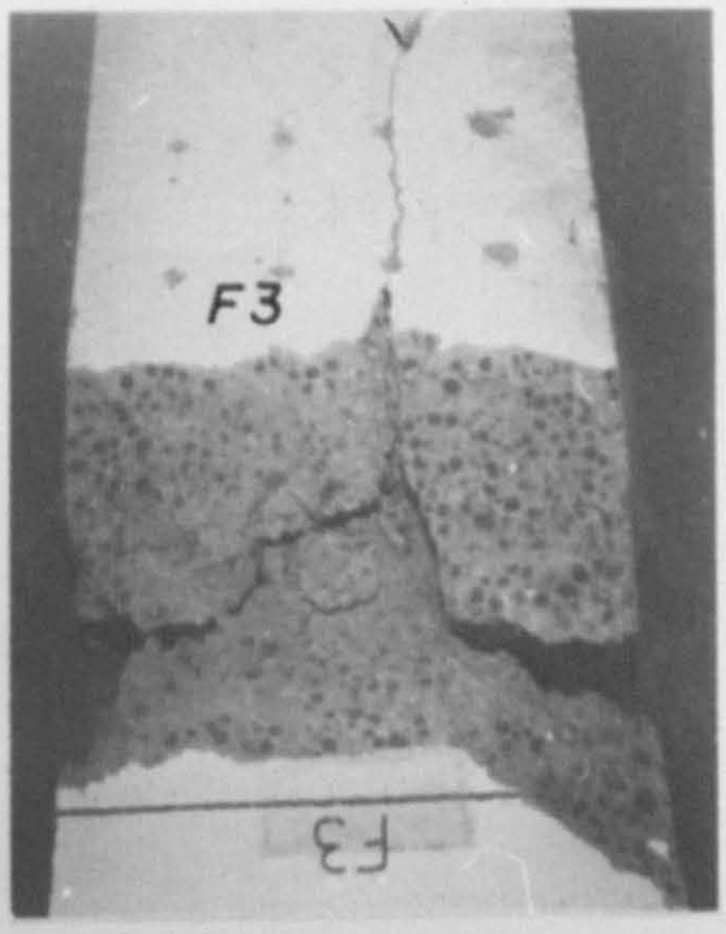

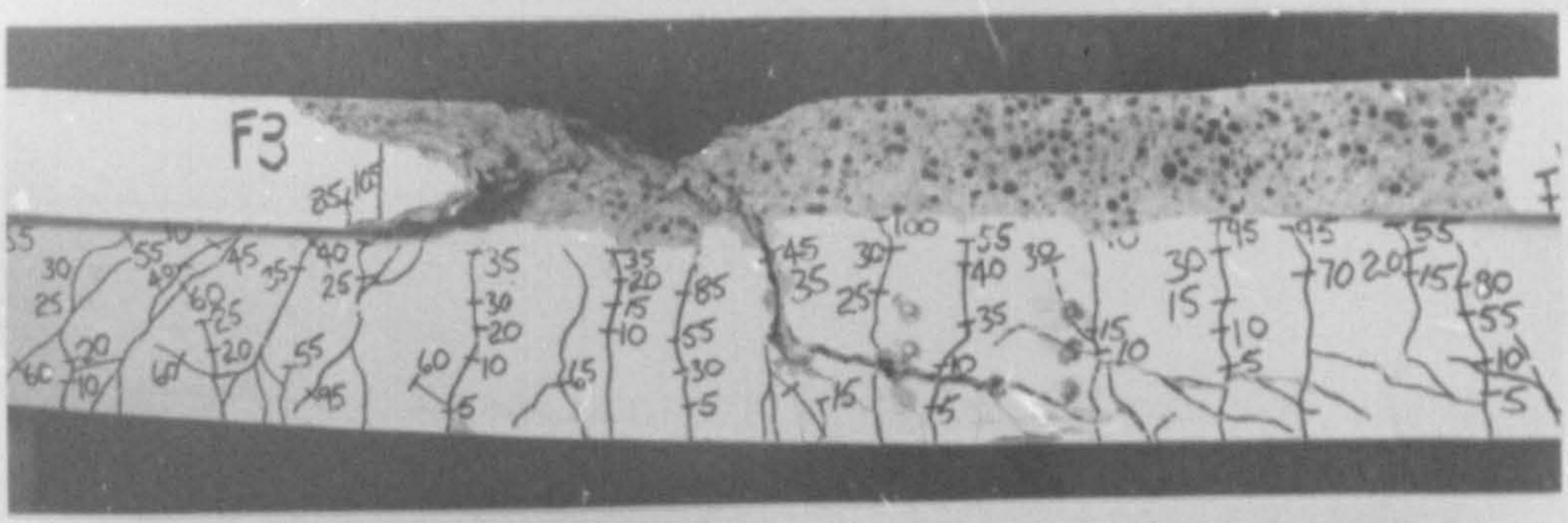

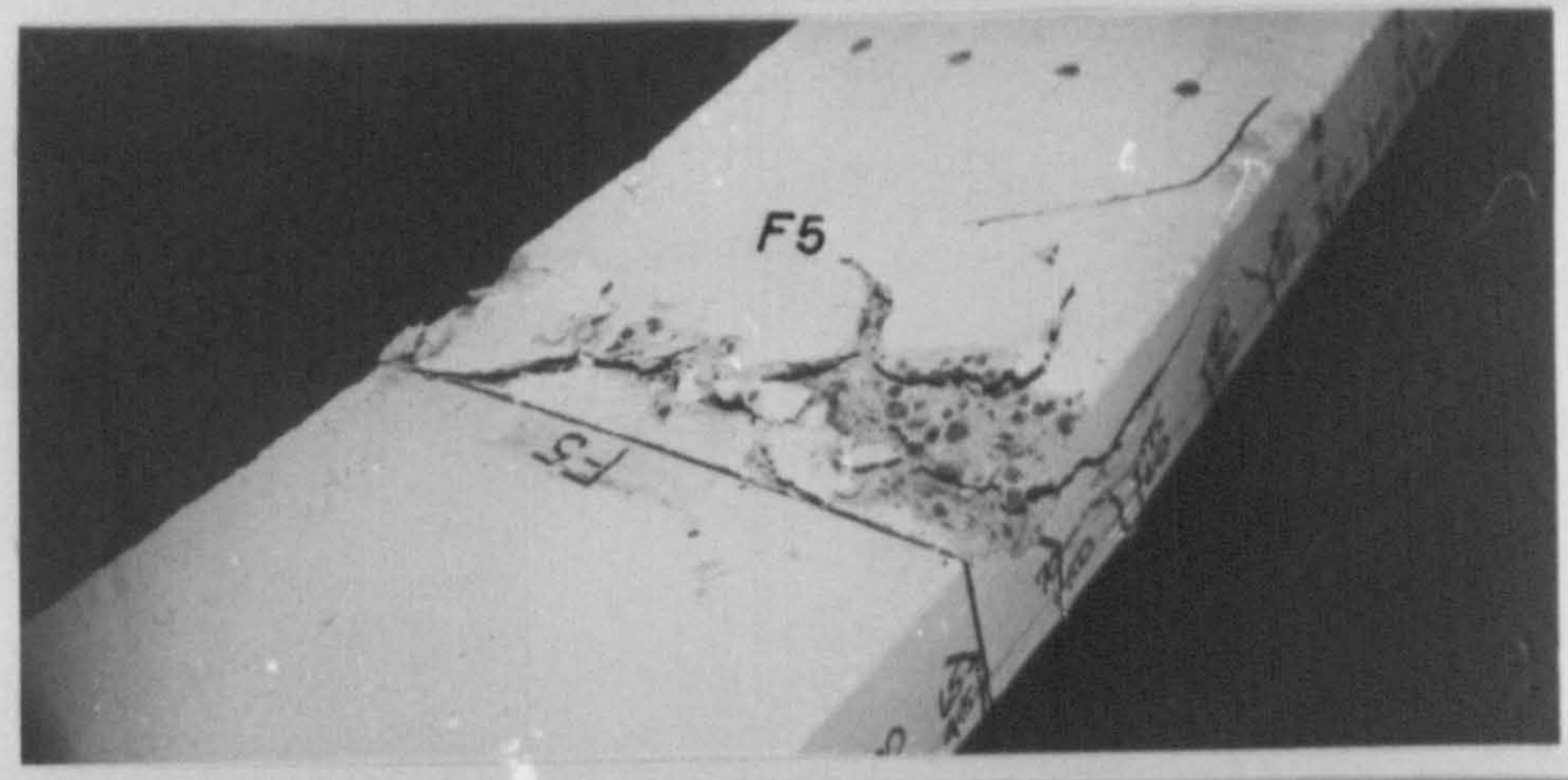

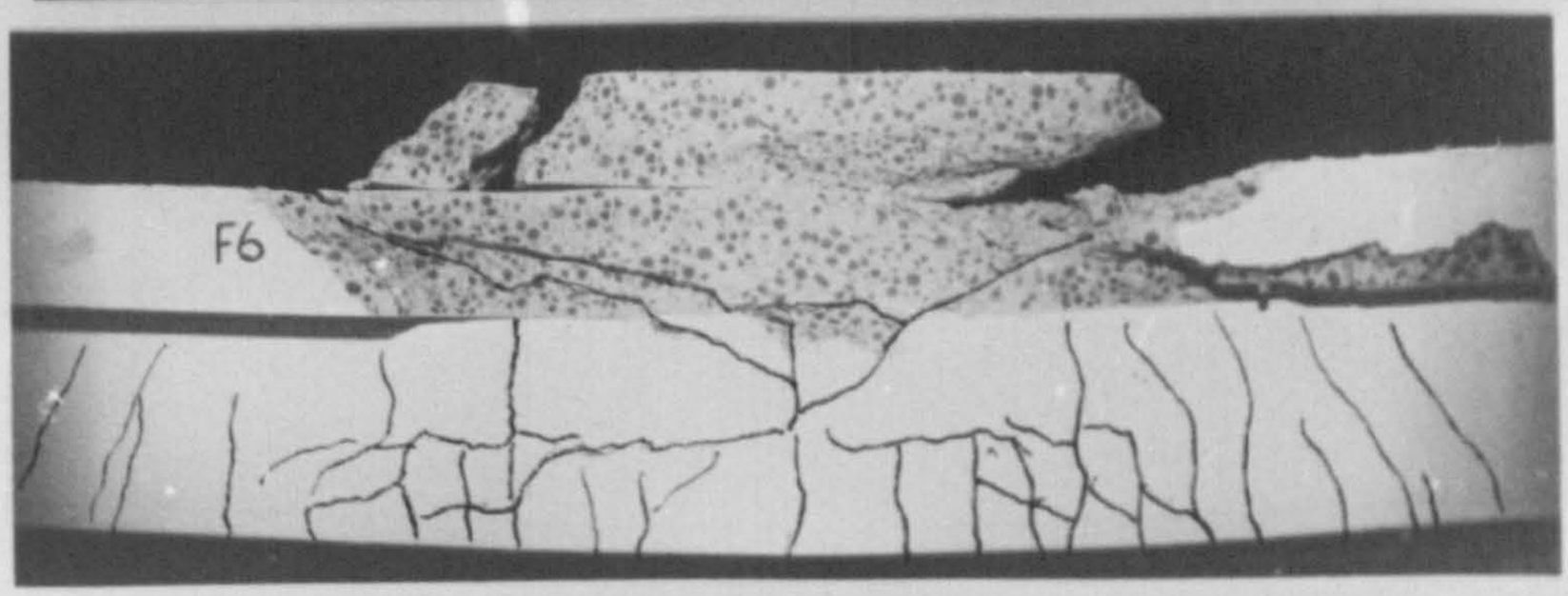

PLATE 8.3 COMPRESSION ZONE FAILURES IN FLEXURAL BEAMS

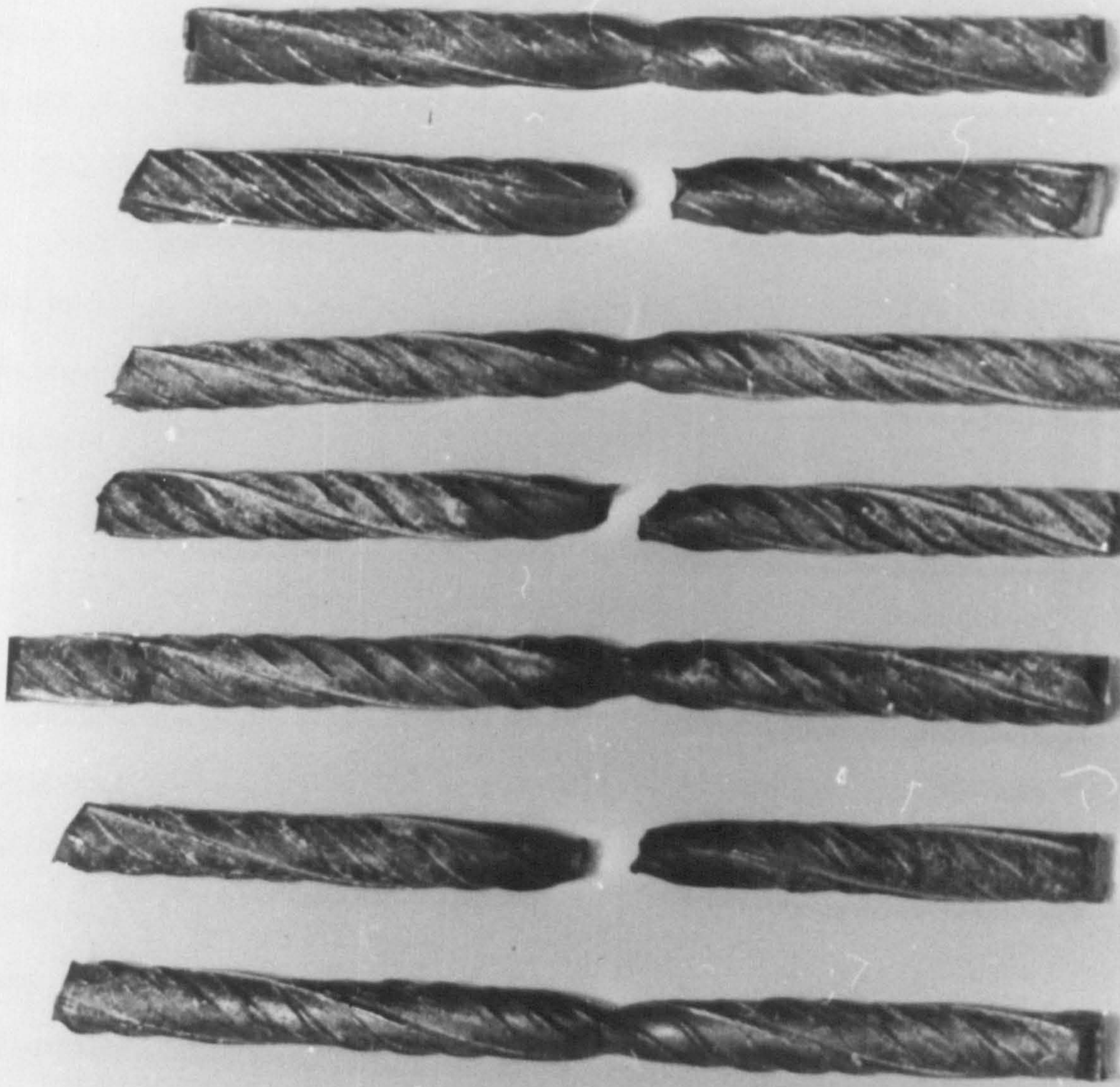

PLATE 8.4 TENSILE STEEL SPECIMENS FROM FLEXURAL BEAMS

reduction in cross-sectional area "necking" prior to fracture.

For all the beams tested, the primary mode of failure was yielding of the tensile steel which for beams F3, F5 and F6 led to concrete cushing as the neutral axis rose and the compressive stress on the concrete exceeded the crushing stress. For the remaining beams, F1, F2 and F4, the low area of tensile steel meant that sufficiently high concrete stresses, to cause failure, were not developed before the steel fractured.

8.4.9 Compliance With the Limit States of Deflection and Cracking

Under normal working loads, the deflection of a reinforced concrete beam should be such that it does not cause distress to adjacent members, fixings, partitions or finishes. Crack widths should be small enough to reduce the possibility of corrosion of the steel reinforcement due to the ingress of water and air.

CP 110 (54) suggests an upper limit on deflection of span/250 for the total deflection (including the effects of creep and shrinkage). In the present investigation the span/deflection ratio's varied from 270-396 at working load. This suggests that in the long term some of these beams may not satisfy the span-effective depth ratio limits given in CP 110 (54). These values are based on instantaneous deflection and do not allow for the time-dependent effects of creep and shrinkage which may amount to some 100-200 percent of the instantaneous deflection. Investigations at Laing R. & D. (62), on All-Lytag concrete beams, and comparable gravel concrete beams showed that the ratio of the total to instantaneous deflection at approximately 18 months is lower for Lytag concrete than for gravel concrete.

For crack widths, CP 110 (54) recommends a maximum value at the surface of the member of 0.3 mm in general. For aggressive environments values should not exceed 0.004 times the minimum cover to the main reinforcement.

From Tables 8.2 and 8.3 it can be seen that Lytag-sand concrete T-beams designed for the serviceability limit states of deflection and cracking, in accordance with CP 110 (54) will behave satisfactorily under working load in practice.

8.4.10 Conclusions

From the limited series of tests carried out on the flexural behaviour of Lytag-sand concrete T-beams, the following conclusions can be drawn:

1. The deflection prediction equations given in design codes (26, 54) underestimate the measured deflections. The standard A.C.I. equation predicts the values to within 8-18% whereas the standard CP 110 equation predicts the values to within 25-53%. If however the moment capacity of the concrete in the tension zone is neglected the CP 110 equation predicts the measured values to within 2-18%.
2. Crack widths at design service load vary between 0.10 and 0.18 mm and are within the durability requirements given in CP 110 (54).
3. The ultimate moments of Lytag-sand concrete T-beams are safely predicted by the present U.K. and American design codes (26, 54).
4. The load factor against failure, at design service load varied between 2.29 and 2.40 and is therefore fairly constant.
5. The assumption in the elastic analysis of sections, that plane sections remain plane, is generally a valid one especially within the concrete compression zone.
6. For beams which failed by crushing of the concrete compression zone, high strain capacities in excess of 4000 microstrain were recorded.
7. Crack spacings in Lytag-sand concrete beams appear to be smaller when compared to those of other concrete types tested by various investigators.

CHAPTER 9

LIMITATIONS OF THE PRESENT WORK, OVERALL CONCLUSIONS AND RECOMMENDATIONS FOR FUTURE WORK

9.1 Limitations of the Present Work

Lytag has been commercially available since the early sixties. Although concretes made with Lytag coarse and fine material have been the subject of several investigators, only a very limited amount of work has been carried out into the effects of sand replacement in Lytag concrete. The work reported in this thesis constitutes the most comprehensive study to date on Lytag-sand concrete. The range of work covered and the extent to which individual characteristics and behavioural properties were investigated was, however, limited by the time available. The main aim of this work was to produce useful design data for Lytag-sand concrete. The limitations within which this work was carried out were as follows:

1. Microstructure and Water Absorption

(a) For the microstructure examination, only the internal structure of Lytag pellets was investigated. No observations were made of the external surface of the pellet.

(b) The water absorption of Lytag aggregate was only measured up to a period of 24 hours.

2. Properties

(a) Only one type of cement, O.P.C., was used throughout the investigation.

(b) The tensile strength, elastic moduli and Poisson's ratio were only determined up to an age of 28 days.

(c) The complete-stress strain curves for Lytag-sand concrete were only determined for wet-cured specimens, and concrete strains were measured indirectly.

3. Unrestrained Shrinkage

(a) Only one specimen size was used throughout the tests.

(b) The shrinkage of plain concrete, only, was investigated.

4. Creep

(a) Only one curing regime was used.

(b) Creep of plain specimens under axial load, only, was investigated.

5. Shear

(a) The shear resistance of beams containing web reinforcement or compression reinforcement was not investigated.

(b) Only one beam cross-section was used.

6. Flexure

(a) Only one beam cross-section was used.

(b) The maximum steel percentage used was 45% of the balanced steel ratio.

9.2 Overall Conclusions

The conclusions drawn from this investigation are listed at the end of each chapter, but the main conclusions are summarised below:

9.2.1 Microstructure and Water Absorption

1. Lytag pellets are composed of unreacted p.f.a. cenospheres which are fused together at their points of contact and/or surrounded by a solidified honeycomb type material mass.

2. The unreacted cenospheres range in diameter from approximately 75-100 μm down to less than 1 μm.

3. Voids range in size from approximately 200 μm down to less than 1 μm and are predominantly interconnected, although discrete voids do exist.

9.2.2 Strength Characteristics

1. 28 day compressive strengths of 60 N/mm^2 can be obtained with Lytag-sand concrete.

2. In general, Lytag-sand concrete requires less cement than other sand replaced lightweight concretes in order to achieve a given compressive strength.

3. On average the increase in density of Lytag concrete by the addition of natural sand fines is approximately 15%.

4. The compressive strength of water stored specimens increases up to an age of 18 months.

5. The compressive strength of dry cured specimens may decrease after 28 days by as much as 7% but the strength is generally regained by 2 years.

6. The tensile strength of Lytag-sand concrete is affected by curing conditions at early ages.

7. A power law type of equation is able to sensibly describe the various relationships between tensile and compressive strengths.

9.2.3 Short Term Deformation Properties

1. The relationship between static modulus of elasticity and cube strength, for sand replaced lightweight concrete is, $E_S = 6.84\ f_{cu}^{0.28}$.

2. The relationship between dynamic modulus of elasticity and cube strength, for sand replaced lightweight concrete is, $E_D = 9.92\ f_{cu}^{0.24}$.

3. The static modulus of elasticity can be estimated from the dynamic modulus of elasticity by the equation $E_S = 0.93\ E_D - 2.56$.

4. Sand replacement increases the elastic modulus of Lytag concrete by 20-25%.

5. The elastic modulus of Lytag-sand concrete is approximately 60% of that of dense concrete as given in CP 110 (54).

6. The value of static Poisson's ratio for sand replaced lightweight concrete in general should be taken as 0.19.

9.2.4 Shrinkage, Moisture Movement and Creep

1. Shrinkage specimens cured outside, protected from direct rain and sunlight, show a lower ultimate shrinkage than for internally cured specimens.

2. The shrinkage and creep of Lytag-sand concrete may be greater than or less than that of dense concrete, depending on the dense aggregate type, for similar mix proportions.

3. Regardless of concrete strength and curing condition the ratio of the shrinkage, at various ages, to the shrinkage at 500 days remains sensibly constant particularly at ages of 90 days or more.

4. For a 60 day drying and 45 day wetting cycle, the moisture movement in Lytag-sand concrete is of the order of 300-350 m/m x 10^{-6}, for concrete strengths of 30 to 60 N/mm^2 respectively.

5. Creep in Lytag-sand concrete increases with increasing water-cement ratio.

6. The creep of Lytag-sand concrete is directly proportional to the stress-strength ratio for values of stress-strength ratio between 0.3 and 0.5.

3. The ultimate moments of Lytag-sand concrete T-beams are safely predicted by the present British and American design codes (26, 54).

4. The load factor against failure at design service load varied between 2.29 and 2.40 and was, therefore, sensibly constant.

5. For beams which failed by crushing of the concrete compression zone, high strain capacities in excess of 4000 microstrain were recorded.

9.3 Recommendations for Future Work

During this study several interesting questions have been raised which have not been investigated because of the limited time and resources available. Further investigation in the following fields is therefore suggested:

1. Basic properties of Lytag-sand concrete using rapid hardening Portland cement for both the short and the long term.

2. The restrained shrinkage behaviour of Lytag-sand concrete and the effect of restraint on cracking. Bandyopadhyay (49) carried out a series of tests on Solite concrete rings, which were restrained by an internal steel ring, in order to assess the incidence of cracking due to restraint. A similar series of tests is suggested for Lytag-sand concrete.

3. Creep tests under different curing conditions and for reinforced concrete specimens in bending.

4. It has been shown (155) that the shear resistance of a beam is dependent on the depth of section. In the shear test series carried out during this study the effective depth of the section remained constant. It is suggested that the work carried out in this study on the shear resistance of Lytag-sand concrete T-beams be extended to cover the effect of varying the effective depth with particular reference to deep beams.

5. For several of the flexural beams tested during this study the instantaneous deflections at design service load suggest that in the long-term the span-depth ratios, generally accepted as producing an adequate serviceability state, may be exceeded, and this requires further investigation.

APPENDIX A

STANDARD LYTAG-SAND MIXES (62)

Grade	28 Day Target Strength (N/mm^2)	Quantities per m^3 of Compacted Concrete				Optimum Slump Range (mm)
Characteristic Strength at 28 Days (N/mm^2)		Cement O.P.C. (kg)	Sand Zone 2-3 to BS 882 (83)		Effective (Free) Water Content (kg) (l)	
			Sand Dry Weight (kg)	Lytag 12 mm (m^3)		
15	22.5	260	685	0.87	180	75-100
20	27.5	290	660	0.87	180	75-100
25	32.5	330	625	0.87	180	75-100
30	37.5	370	590	0.87	180	75-100
35	42.5	410	560	0.87	180	75-100
40	47.5	460	505	0.87	185	50-75
45	52.5	520	440	0.87	190	50-75
50	57.5	600	345	0.87	200	50-75

Note: When conversion from volume to weight is required, the oven-dry, loose bulk density of the Lytag 12 mm aggregate should be taken as 800 kg/m^3. The bulk density may vary slightly and should be checked with the supplier.

APPENDIX B

CP 110 PARABOLIC STRESS BLOCK

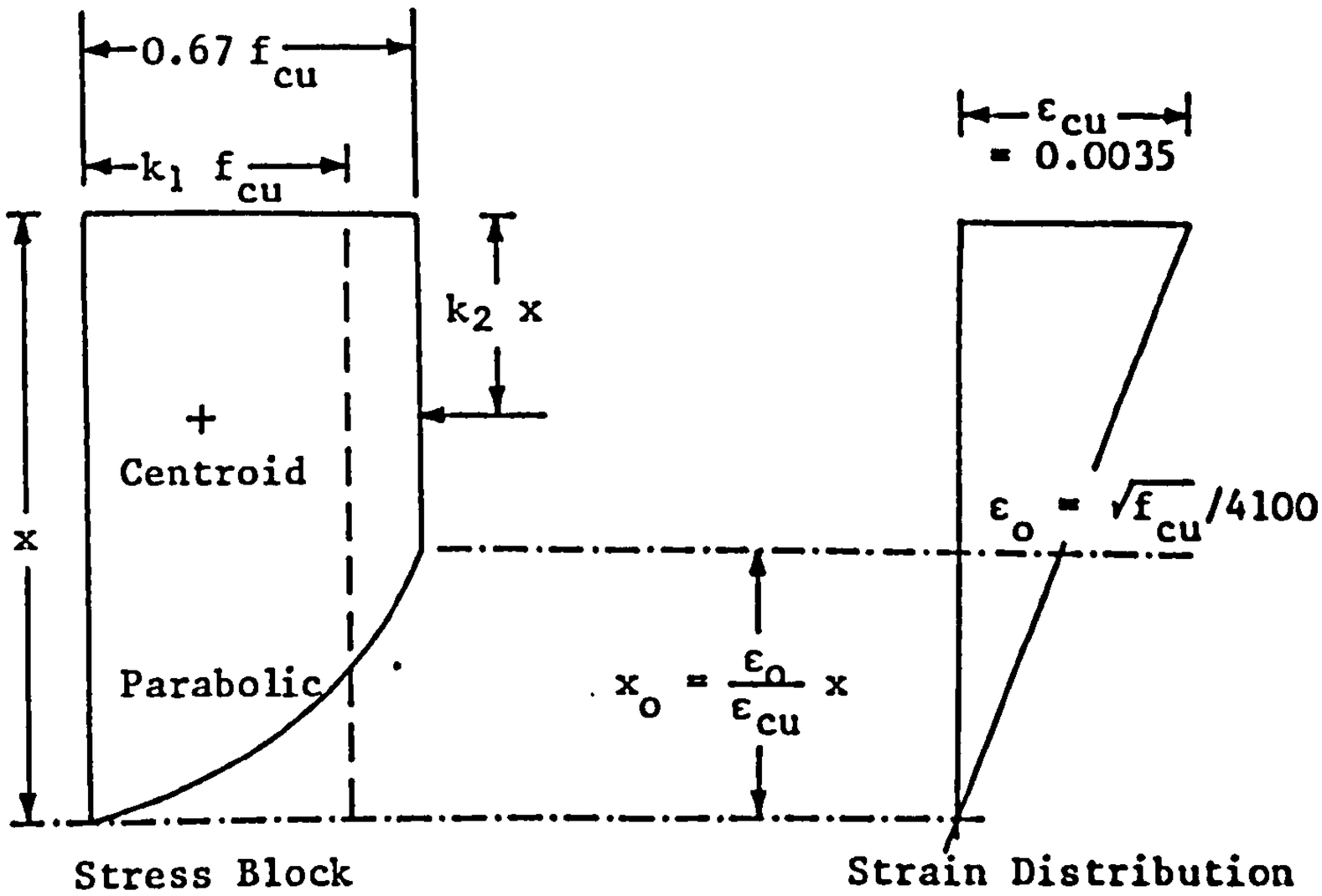

The above figures show the idealised stress block, adopted in CP 110 for ultimate strength calculations in design, without the concrete safety factor $\gamma_m = 1.5$, and the idealised strain distribution corresponding to the stress block.

$$\text{Area of parabolic section of stress block} = \frac{2}{3} \cdot \frac{\varepsilon_o}{\varepsilon_{cu}} x \cdot 0.67 \cdot f_{cu}$$

$$\therefore \text{Total area of equivalent stress block: } k_1 . f_{cu} . x = 0.67\ f_{cu}\ x\ (1 - \varepsilon_{o/3\varepsilon_{cu}})$$

$$\underline{k_1 = 0.67\ (1 - \sqrt{f_{cu}/43.1})}$$

Taking moments about the top of the stress block we have:

$$k_1\ k_2\ f_{cu}\ x^2 = 0.67\ f_{cu}\ \frac{(x - x_o)^2}{2} + 0.67\ f_{cu} \cdot \frac{2}{3} x_o\ (x - \frac{5}{8} x_o)$$

which reduces to:

$$k_2 = \frac{\left[2 - \frac{\sqrt{f_{cu}}}{14.4}\right]^2 + 2}{4\left[3 - \frac{\sqrt{f_{cu}}}{14.4}\right]}$$

For a tensile steel area A_{st} at a stress f_s balancing the compressive force in the concrete $k_1.f_{cu}.b.x$, the depth to the neutral axis, x, is given by:

$$x = \frac{A_{st} \cdot f_s}{k_1 \cdot f_{cu} \cdot b}$$ where b = section width.

For a balanced section in which the failure strain of the concrete ($\varepsilon_{cu} = 0.0035$) and the failure strain of the steel ($\varepsilon_s = 0.002$) are reached simultaneously, the balanced steel ratio ρ_b is given by:

$$\rho_b = k_1 \frac{f_{cu}}{f_y} \cdot \frac{\varepsilon_{cu}}{\varepsilon_{cu} + \varepsilon_y}$$

where f_y = the characteristic yield stress of the tensile steel = 465 N/mm^2.

For a value of A_{st} less than the balanced steel area, the beam fails by yielding of the steel and, therefore, the ultimate flexural moment of the section, M_f, is given by:

$$M_f = A_{st} \cdot f_y \left[1 - \rho \frac{k_2}{k_1} \frac{f_y}{f_{cu}}\right] d$$

REFERENCES

1. RILEM, LIGHTWEIGHT CONCRETE COMMITTEE. 'Terminology and definitions.' Materials and Structures, V. 3, No. 13, Jan.-Feb. 1970, pp. 60-69.

2. SHARPE, N.R., 'Comparing the use of lightweight concrete in New York and London.' Civ. Engng. publ. Wks Rev., V. 59, Aug. 1964, pp. 960-961.

3. ANON. 'Case for lightweight concrete.' Engineering, V. 206, No. 7, July 1968, pp. 14-15.

4. BOBROWSKI, J. and BARDHAN-ROY, B.K. 'Structural assessment of lightweight aggregate concrete.' Concrete, V. 5, No. 7, July 1971, pp. 229-234.

5. VARIOUS AUTHORS. 'Lightweight concrete.' (Seven articles). Concrete, V. 6, No. 12, Dec. 1972, pp. 20-36.

6. LYDON, F.D. 'Artificial aggregates for concrete.' Concrete, V. 9, No. 9, Sept. 1975, pp. 49-52.

7. FORREST, J.M.C. 'The emerging potential of lightweight aggregate concrete.' Concrete, V. 9, No. 12, Dec. 1975, pp. 17-19.

8. BOBROWSKI, J. 'Why not lightweight concrete.' Civil Engineering, Mar. 1977, pp. 32-33.

9. LITTLE, M.E.R. 'The use of lightweight aggregates for structural concrete.' The Structural Engineer, V. 55, No. 12, Dec. 1977, pp. 539-546.

10. GRIMER, F.J. 'The durability of steel embedded in lightweight concrete.' Concrete, V. 1, No. 4, Apr. 1967, pp. 125-131.

11. TEYCHENNÉ, D.C. 'Structural concrete made with lightweight aggregates.' Concrete, V. 1, No. 4, Apr. 1967, pp. 111-124.

12. LYDON, F.D. 'The problem of water absorption by lightweight aggregates.' Mag. Concr. Res., V. 21, No. 68, Sept. 1969, pp. 131-140.

13. LYDON, F.D. 'Research on lightweight concrete in the U.K. 1967-1976.' Mag. Concr. Res., V. 28, No. 95, June 1976, pp. 101-104.

14. SHORT, A. 'Lightweight aggregate concrete.' Concrete, V. 8; No. 7, July 1974, pp. 47-48, No. 8, Aug. 1974, pp. 41-42 & No. 9, Sept. 1974, pp. 49-50.

15. CONCRETE SOCIETY. 'Structural lightweight aggregate concrete for marine and offshore applications.' Report of a Concrete Society working party. Technical report No. 16, May 1978, pp. 29.

16. ZUNZ, G.J. 'Some notes of the use of lightweight concrete in structures in the U.K.' Proceedings of the First International Congress on Lightweight Concrete, V. 1, May 1968, C. & C.A., pp. 187-202.

17. CONCRETE SOCIETY. 'A comparative study of the economics of lightweight structural concrete floor slabs in building.' International Journal of Lightweight Concrete, The Construction Press Ltd., V. 1, No. 1, Oct. 1979, pp. 9-27.

18. SKOYLES, E.R. 'Lightweight concrete: A look at economic factors.' Concrete, V. 6, No. 12, Dec. 1972, pp. 20-22.

19. SHIDELER, J.J. 'Lightweight aggregate concrete for structural use.' J. Am. Concr. Inst. Proc., V. 54, Oct. 1957, pp. 299-328.

20. BRITISH STANDARDS INSTITUTION. 'Clinker aggregate for concrete.' B.S. 1165, 1966, London, 8 p.

21. BRITISH STANDARDS INSTITUTION. 'Foamed or expanded blast furnace slag lightweight aggregate for concrete.' B.S. 877, Part 2, 1973, London, 8 p.

22. BRITISH STANDARDS INSTITUTION. 'The structural use of reinforced concrete in buildings.' C.P. 114, 1957, London. Revised 1965, 95 p.

23. HORLER, D.B. 'An update of lightweight aggregate production in U.K.' Proceedings of the Second International Congress on Lightweight Concrete, (CI80), London, Apr. 1980, Construction Press Ltd., 202 p.

24. RICHART, F.E. and JENSEN, V.P. 'Tests on plain and reinforced concrete made with Haydite aggregates.' Bulletin No. 237, University of Illinois, Engineering Experimental Station, Oct. 1931, pp. 7-79.

25. WASHA, G.W., KLUGE, R.W., CARLSON, C.C. and VALORE, R.C. (i) 'Properties of lightweight aggregates and lightweight concretes.' (ii) 'Structural lightweight aggregate concrete.' (iii) 'Lightweight aggregates for concrete masonary units.' (iv) 'Insulating concretes.' J. Am. Concr. Inst. Proc., V. 53, 1956-1957, pp. 375-382, 383-402, 491-508 and 509-532.

26. AMERICAN CONCRETE INSTITUTE. 'Building code requirements for reinforced concrete.' ACI-318-51, Detroit, 1951. Revised 1963, ACI-318-63. Revised 1971, ACI-318-71. Revised 1977, ACI-318-77, 144 p.

27. HANSON, J.A. 'Shear strength of lightweight reinforced concrete beams.' J. Am. Concr. Inst. Proc., V. 55, No. 3, Sept. 1958, pp. 387-403.

28. HANSON, J.A. 'Tensile strength and diagonal tension resistance of structural lightweight concrete.' J. Am. Concr. Inst. Proc., V. 58, No. 1, July 1961, pp. 1-39.

29. GRIEB, W.E. and WERNER, G. 'Comparison of splitting tensile strength of concrete with flexural and compressive strengths.' Proc. Am. Soc. Test Mater., V. 62, 1962, pp. 972-995.

30. A.C.I. COMMITTEE 213. 'Guidelines for structural lightweight aggregate concrete.' Concrete International, V. 1, No. 2, Feb. 1979, pp. 33-62.

31. SHORT, A. 'The use of lightweight concrete for reinforced concrete construction.' Reinforced Concrete Review, V. 5, Sept. 1959, pp. 141-188.

32. TEYCHENNÉ, D.C. 'Lightweight aggregates: their properties and uses in concrete in the U.K.' Proceedings of the First International Congress on Lightweight Concrete, V. 1, May 1968, pp. 23-37.

33. TAYLOR, R. and BREWER, R.S. 'The effect of type of aggregate on the diagonal cracking of reinforced concrete beams.' Mag. Concr. Res., V. 15, No. 44, July 1963, pp. 87-92.

34. EVANS, R.H. and HARDWICK, T.R. 'Lightweight concrete with sintered clay aggregate.' Reinforced Concrete Review, V. 5, June 1960, pp. 369-400.

35. EVANS, R.H. and DONGRE, A.V. 'The suitability of a lightweight aggregate (Aglite) for structural concrete.' Mag. Concr. Res., V. 15, July 1963, pp. 93-100.

36. EVANS, R.H. and ORANGUN, C.O. 'Behaviour in flexure of reinforced lightweight aggregate (Lytag) concrete beams.' Civ. Engng. publ. Wks. Rev., V. 59, May-June 1964, pp. 597-601 and 740.

37. EVANS, R.H. and ORANGUN, C.O. 'The use in prestressed concrete structures of lightweight aggregate (Lytag) concrete.' Civ. Engng. publ. Wks Rev., V. 60, Jan. 1965, pp. 90-92.

38. EVANS, R.H. and PATTERSON, W.S. 'Long term deformation characteristics of Lytag lightweight aggregate concrete.' The Structural Engineer, V. 45, No. 1, Jan. 1967, pp. 13-21.

39. NEVILLE, A.M. and LISZKA, W.Z. 'Accelerated determination of creep of lightweight aggregate concrete.' Civ. Engng. publ. Wks Rev., V. 68, June 1973, pp. 515-519.

40. BROOKS, J.J. and NEVILLE, A.M. 'Estimating long-term creep and shrinkage from short-term tests.' Mag. Concr. Res., V. 27, No. 90, Mar. 1975, pp. 3-12.

41. BROOKS, J.J. and NEVILLE, A.M. 'Predicting long-term creep and shrinkage from short-term tests.' Mag. Concr. Res., V. 30, No. 103, June 1978, pp. 51-61.

42. SWAMY, R.N. 'Prestressed lightweight concrete.' Chapter 5 'Developments in prestressed concrete - 1.' Ed. F. Sawko, Applied Science Publishers Ltd., London, 1978, pp. 149-191.

43. SWAMY, R.N. and BANDYOPADHYAY, A.K. 'Durability of steel embedded in structural lightweight concrete.' Materials and Structures, V. 8, No. 45, May-June 1975, pp. 203-210.

44. SWAMY, R.N. and BANDYOPADHYAY, A.K. 'The elastic properties of structural lightweight concrete.' Proc. Instn. Civ. Engrs., V. 59, Sept. 1975, pp. 381-394.

45. SWAMY, R.N. and BANDYOPADHYAY, A.K. 'Shear behaviour of structural lightweight concrete T-beams without web reinforcement.' Proc. Instn. Civ. Engrs., V. 67, June 1979, pp. 341-354.

46. SWAMY, R.N. and IBRAHIM, A.B. 'Shrinkage and creep properties of high early strength structural lightweight concrete.' Proc. Instn. Civ. Engrs., V. 55, Sept. 1973, pp. 635-645.

47. SWAMY, R.N., IBRAHIM, A.B. and ANAND, K.L. 'The strength and deformation characteristics of high early strength structural concrete.' Materials and Structures, V. 8, No. 48, Nov.-Dec. 1975, pp. 413-423.

48. IBRAHIM, A.B. 'Structural properties and behaviour of high early strength lightweight aggregate (Solite) concrete.' Ph.D. Thesis, University of Sheffield, 1972.

49. BANDYOPADHYAY, A.K. 'Material properties and structural behaviour of lightweight (Solite) concrete.' Ph.D. Thesis, University of Sheffield, 1974, 376 p.

50. AJIBADE, A.O. 'Some material properties of high early strength lightweight (Lytag) concrete.' M. Eng. Thesis, Univeristy of Sheffield, 1978, 72 p.

51. JOJAGHA, A.H. 'Workability and strength characteristics of structural lightweight concrete with and without fibres.' M. Eng. Thesis, University of Sheffield, 1979, 99 p.

52. SITTAMPALAM, K. 'Flexural behaviour of limited prestressed lightweight (Lytag) concrete beams with and without fibre reinforcement.' M. Eng. Thesis, University of Sheffield, 1979, 89 p.

53. WINATA, R. 'A study of shrinkage characteristics of (Lytag) lightweight concrete using high early strength Portland cement.' M. Eng. Thesis, University of Sheffield, 1978, 89 p.

54. BRITISH STANDARDS INSTITUTION. 'The structural use of concrete: Part 1. Design, materials and workmanship.' CP 110, 1972, 154 p.

55. LYDON, F.D. 'Some points on water absorption by lightweight aggregates.' Proceedings of the First International Congress on Lightweight Concrete, London, May 1968, V. 2: Discussion, pp. 12-18.

56. LYDON, F.D. 'Does moisture content of aggregate or concrete affect strength.' Proceedings of the First International Congress on Lightweight Concrete, London, May 1968, V. 2: Discussion, pp. 109-110.

57. LYDON, F.D. 'Concrete mix design.' Chapter 9 Lightweight aggregate concrete, Applied Science Publishers Ltd., London, 1972, pp. 104-115.

58. LYDON, F.D. 'Some criteria for the choice and use of lightweight concrete.' Build International, V. 6, No. 3, May-June 1973, pp. 321-338.

59. LYDON, F.D. (Ed.) 'Developments in concrete technology - 1.' Applied Science Publishers Ltd., London, 1979, 325 p.

60. LYDON, F.D. Discussion of Reference No. 9. Structural Engineer, V. 57, May 1979, pp. 158-166.

61. BALENDRAN, R.V. 'Properties of high strength lightweight concrete.' Ph.D. Thesis, U.W.I.S.T., 1980, 387 p.

62. LYTAG LTD. Private Communication.

63. HANSON, J.A. 'Replacement of lightweight aggregate fines with natural sand in structural concrete.' J. Am. Concr. Inst. Proc., V. 61, No. 7, July 1964, pp. 779-794.

64. PFEIFER, D.W. 'Sand replacement in structural lightweight concrete: Splitting tensile strength.' J. Am. Concr. Inst. Proc., V. 64, No. 7, July 1967, pp. 384-392.

65. PFEIFER, D.W. 'Sand replacement in structural lightweight concrete: Freezing and thawing tests.' J. Am. Concr. Inst. Proc., V. 64, No. 11, Nov. 1967, pp. 735-744.

66. PFEIFER, D.W. 'Sand replacement in structural lightweight concrete: Creep and shrinkage studies.' J. Am. Concr. Inst. Proc., V. 65, No. 2, Feb. 1968, pp. 131-139.

67. PFEIFER, D.W. 'Fly Ash aggregate lightweight concrete.' J. Am. Concr. Inst. Proc., V.68, Mar. 1971, pp. 213-216.

68. PFEIFER, D.W. and HANSON, J.A. 'Sand replacement in structural lightweight concrete - sintering grate aggregates.' J. Am. Concr. Inst. Proc., V. 64, Mar. 1967, pp. 121-127.

69. F.I.P. COMMISSION REPORT. 'Prestressed lightweight concrete.' Prestressed Concrete Institute Journal, V. 12, June 1967, pp. 68-93.

70. COMITÉ EUROPÉEN DU BÉTON. 'Manual lightweight concrete.' Bulletin D'Information No. 85, May 1972. Revised May 1973, Bulletin D'Information No. 95.

71. CEMBUREAU. 'Lightweight aggregate concrete: Technology and world applications.' Ed. G. Bologna, AITEC, Rome, 1974.

72. C.E.B./F.I.P. 'Lightweight aggregate concrete.' Ed. A. Short, Construction Press Ltd., Lancaster, 1977, 169 p.

73. C.E.B./F.I.P. 'Model code for concrete structures.' CEB/FIP International Recommendations, 3rd. Ed., C.E.B., 1978, 348 p.

74. KINNIBURGH, W. 'Lightweight aggregate from pulverised-fuel ash.' Concrete and Constructional Engineering, V. 51, No. 12, Dec. 1956, pp. 571-574.

75. HOBBS, C. 'Building materials from pulverised-fuel ash.' British Chemical Engineering, V. 4, No. 4, April 1959, pp. 212-216.

76. ORCHARD, D.F. 'Concrete technology: Volume 1 - Properties of materials.' 4th Ed. Applied Science Publishers, London, 1979, 487 p.

77. SHORT, A. and KINNIBURGH, W. 'Lightweight concrete.' Applied Science Publishers Ltd., London, Revised edition, 1968, 368 p.

78. GUTT, W. and NIXON, P.J. 'Alkali aggregate reactions in concrete in the U.K.' Concrete, V. 13, No. 5, May 1979, pp. 19-21.

79. BRITISH STANDARDS INSTITUTION. 'Methods of sampling and testing of mineral aggregates, sands and fillers.' B.S. 812, 1975, London, 4 parts.

80. HOSKING, J.R. 'Synthetic aggregates of high resistance to polishing: Part 3 - Porous aggregates.' Transport and Road Research Laboratory, Report No. 655, Crowthorne, 1974, 27 p.

81. ROAD RESEARCH LABORATORY. 'Design of concrete mixes.' Road Note 4. 2nd Ed., H.M.S.O., London, reprinted 1970, 16 p.

82. TEYCHENNÉ, D.C., FRANKLIN, R.E. and ERNTROY, H.C. 'Design of normal concrete mixes.' Department of the Environment, H.M.S.O., London, 1975, 30 p.

83. BRITISH STANDARDS INSTITUTION. 'Aggregates from natural sources for concrete.' B.S. 882, Part 2, London, 1973, 16 p.

84. BRITISH STANDARDS INSTITUTION. 'Methods of sampling and testing of lightweight aggregates for concrete.' B.S. 3681, Part 2, 1973, London, 16 p.

85. BRITISH STANDARDS INSTITUTION. 'Specification for lightweight aggregates for concrete.' B.S. 3797, Part 2, 1976, London, 4 p.

86. BRITISH STANDARDS INSTITUTION. 'Methods of testing concrete.' B.S. 1881, 1970, London, 6 parts.

87. OWENS, P.L. 'Lightweight concrete - Development of mixes suitable for structural applications.' Proc. Advances in Concrete, Symposium, University of Birmingham, England, 1971.

88. OWENS, P.L. 'Mix design charts for lightweight aggregate concrete.' Proceedings First International Congress on Lightweight Concrete, V. 2, Cement and Concrete Association, May 1968, pp. 24-25.

89. BROOKS, J.J. and NEVILLE, A.M. 'A comparison of creep, elasticity and strength of concrete in tension and compression.' Mag. Concr. Res., V. 29, No. 100, Sept. 1977, pp. 131-141.

90. PRICE, W.H. 'Factors influencing concrete strength.' J. Am. Concr. Inst. Proc., V. 47, No. 6, Feb. 1951, pp. 417-432.

91. ORANGUN, C.O. 'Influence of properties of lightweight aggregate (Lytag) concrete on behaviour of reinforced and prestressed concrete members.' Ph.D. Thesis, University of Leeds, England, June 1963, 133 p.

92. KOMLOS, K. 'Comments on the long-term tensile strength of plain concrete.' Mag. Concr. Res., V. 22, No. 73, Dec. 1970, pp. 232-238.

93. WANG, P.T., SHAH, S.P. and NAAMAN, A.E. 'Stress-strain curves of normal and lightweight concrete in compression.' J. Am. Concr. Inst. Proc., V. 75, No. 11, Nov. 1978, pp. 603-611.

94. SWAMY, R.N. and RIGBY, G. 'Dynamic properties of hardened paste, mortar and concrete.' Materials and Structures, V. 4, No. 19, Jan.-Feb. 1971, pp. 13-40.

95. BAKER, A.L.L. 'A criterion of concrete failure.' Proc. Instn. civ. Engrs., V. 45, Feb. 1970, pp. 269-278.

96. SWAMY, R.N. 'Fracture mechanics applied to concrete.' Chapter 6, 'Developments in concrete technology - 1.' Ed. F.D. Lydon, Applied Science Publishers Ltd., London, 1979, pp. 221-282.

97. BROCK, G. 'Concrete: complete stress-strain curves.' Engineering, V. 193, No. 5011, May 1962, p. 606.

98. BARNARD, P.R. 'Researches into the complete stress-strain curve for concrete.' Mag. Concr. Res., V. 16, No. 49, Dec. 1964, pp. 203-210.

99. TURNER, P.W. and BARNARD, P.R. 'Stiff constant strain rate testing machine.' The Engineer, V. 214, No. 5557, July 1962, pp. 146-148.

100. SANGHA, C.M. and DHIR, R.K. 'Strength and complete stress-strain relationships for concrete, tested in uniaxial compression under different test conditions.' Materials and Structures, V. 5, No. 30, Nov.-Dec. 1972, pp. 361-370.

101. PHIPPS, M.E. 'The strain capacity of compression zone concrete and its effect upon the deformation of simply supported reinforced concrete beams.' Ph.D. Thesis, University of Sheffield, England, Nov. 1974.

102. BEST, C.H. and POLIVKA, M.S. 'Creep of lightweight concrete.' Mag. Concr. Res., V. 11, No. 33, Nov. 1959, pp. 129-134.

103. BLAKEY, F.A. and LEWIS, R.K. 'A review of elastic deformation, creep and shrinkage of expanded shale concrete.' Constructional Review, June 1964, pp. 19-22.

104. JONES, R.T. and HIRSCH, T.J. 'Creep and shrinkage in lightweight concrete.' Proceedings Highway Research Board, V. 38, 1959, pp. 74-89.

105. NEVILLE, A.M. 'Creep of concrete: Plain, reinforced and prestressed.' North-Holland Publishing Co., Amsterdam, 1970, 622 p.

106. TYLER, R.G. 'Creep, shrinkage and elastic strain in concrete bridges in the United Kingdom, 1963-71.' Mag. Concr. Res., V. 28, No. 95, June 1976, pp. 55-84.

107. A.C.I. COMMITTEE 209. 'Annotated bibliography on shrinkage and creep in concrete - 1905-1964.' A.C.I. Bibliography No. , Detroit, 1967, 102 p.

108. LORMAN, W.R. 'List of additional references to creep and volume changes of concrete 1901-1964.' A.C.I., Detroit, June 1967, 58 p.

109. A.C.I. COMMITTEE 209. 'Shrinkage and creep in concrete: 1966-1970.' A.C.I. Bibliography No. 10, Detroit, 1972, 93 p.

110. BENNETT, E.W. and LOAT, D.R. 'Shrinkage and creep of concrete as affected by the fineness of Portland cement.' Mag. Concr. Res., V. 22, No. 71, June 1970, pp. 69-78.

111. HOBBS, D.W. 'Influence of aggregate restraint on the shrinkage of concrete.' J. Am. Concr. Inst. Proc., V. 71, No. 9, Sept. 1974, pp. 445-450.

112. LYSE, I. 'The shrinkage and creep of concrete.' Mag. Concr. Res., V. 11, No. 33, Nov. 1959, pp. 135-142.

113. EVANS, R.H. and KONG, F.K. 'Estimation of shrinkage of concrete in reinforced and prestressed concrete design.' Civ. Engng. publ. Wks Rev., V. 62, May 1967, pp. 559-561.

114. TROXELL, G.E., RAPHAEL, J.M. and DAVIS, R.E. 'Long-term creep and shrinkage tests on plain and reinforced concrete.' Proc. Am. Soc. Test Mater., V. 58, 1958, pp. 1101-1120.

115. REICHARD, T.W. 'Creep and drying shrinkage of lightweight and normal weight concrete.' National Bureau of Standards, Monograph 74, Mar. 1964, 30 p.

116. HARDWICK, T.R. 'Lightweight structural concrete.' Ph.D. Thesis, University of Leeds, 1961.

117. NASSER, K.W. and NEVILLE, A.M. 'Creep of concrete at elevated temperatures J. Am. Concr. Inst. Proc., V. 62, No. 12, Dec. 1965, pp. 1567-1579.

118. NASSER, K.W. and NEVILLE, A.M. 'Creep of old concrete at normal and elevated temperatures.' J. Am. Concr. Inst. Proc., V. 64, No. 2, Feb. 1967, pp. 97-103.

119. MULLEN, W.G. and DOLCH, W.L. 'Creep of Portland cement paste.' Proc. Am. Soc. Test Mater., V. 64, 1964, pp. 1146-1170.

120. ROSS, A.D. 'Shrinkless and creepless concrete.' Civ. Engng. Publ. Wks Rev., V. 64, No. 545, 1951, pp. 853-854.

121. HOBBS, D.W. and PARROTT, L.J. 'Prediction of drying shrinkage.' Concrete, V. 13, No. 2, Feb. 1979, pp. 19-24.

122. A.C.I. COMMITTEE 209. 'Designing for effects of creep, shrinkage and temperature in concrete structures.' A.C.I. Publication SP-27, Detroit, 1971, 430 p.

123. ROSS, A.D. 'Shape, size and shrinkage.' Concrete and Constructional Engineering, Aug. 1944, pp. 193-199.

124. DAVIS, R.E., DAVIS, H.E. and HAMILTON, J.S. 'Plastic flow of concrete under sustained stress.' Proc. Am. Soc. Test Mater., V. 34, 1934, pp. 354-386.

125. HANSON, T.C. and MATTOCK, A.K. 'Influence of size and shape of member on the shrinkage and creep of concrete.' J. Am. Concr. Inst., V. 63, No. 2, Feb. 1966, pp. 267-290.

126. L'HERMITE, H.G. and MAMILLAN, M. 'The structure of concrete and its behaviour under load.' Proc. of an International Conference, London, Sept. 1965, C. & C.A., London, 1968, pp. 423-433.

127. HOBBS, D.W. and MEARS, A.R. 'The influence of specimen geometry upon weight change and shrinkage of air dried mortar specimens.' Mag. Concr. Res., V. 23, No. 75-76, June-Sept. 1971, pp. 89-98.

128. CAMPBELL-ALLEN, D. and ROGERS, D.F. 'Shrinkage of concrete as affected by size.' Materials and Structures, V. 8, No. 45, 1975, pp. 193-202.

129. HOBBS, D.W. 'Influence of specimen geometry upon weight change and shrinkage of air-dried concrete specimens.' Mag. Concr. Res., V. 29, No. 99, June 1977, pp. 70-80.

130. RUETZ, W.A. 'A hypothesis for the creep of hardened cement paste and the influence of simultaneous shrinkage.' Proc. of an International Conference, London, Sept. 1965, C. & C.A., London, 1968, pp. 365-387.

131. ROSS, A.D. 'Concrete creep data.' The Structural Engineer, V. 15, No. 8, 1937, pp. 314-326.

132. BRANSON, D.E. and CHRISTIASON, M.L. 'Time dependent concrete properties related to design strength and elastic properties, creep and shrinkage.' Symposium on Creep, Shrinkage and Temperature Effects, SP-27, A.C.I., Detroit, 1971, pp. 257-269.

133. C.E.B.-F.I.P. 'International recommendations for the design and construction of concrete structures.' C.E.B.-F.I.P., Paris, 1970, English translation, C. & C.A., London, 1970, 80 p.

134. MARTIN, I. 'Environment effect on thermal variations and shrinkage of lightweight concrete structures.' J. Am. Concr. Inst. Proc., V. 69, No. 3, March 1972, pp. 179-184.

135. FENWICK, R.C. and PAULAY, T. 'Mechanisms of shear resistance of concrete beams.' Jour. Struc. Div. Proc. A.S.C.E., V. 94, No. ST10, Oct. 1968, pp. 2325-2350.

136. HOGNESTAD, E. 'What do we know about diagonal tension and web reinforcement in concrete.' Circular Series No. 64, University of Illinois, Engineering Experiment Station, Mar. 1952, 47 p.

137. A.S.C.E.-A.C.I. COMMITTEE 326. 'Shear and diagonal tension - Pt. 1: General principles.' J. Am. Concr. Inst. Proc., V. 59, No. 1, Jan. 1962, pp. 3-30.

138. A.S.C.E.-A.C.I. TASK COMMITTEE 426. 'The shear strength of reinforced concrete members.' Jour. Struc. Div., Proc. A.S.C.E., V. 99, No. ST6, June 1973, pp. 1091-1187.

139. INSTITUTION OF STRUCTURAL ENGINEERS. 'The shear strength of reinforced concrete beams.' Report of shear study group, Jan. 1969, 170 p.

140. HAMMAD, Y.M.H. 'Influence of the flange on the ultimate shear capacity of reinforced concrete T-beams.' Ph.D. Thesis, University of Sheffield, 1978.

141. QURESHI, S. 'Shear strength of simply supported reinforced concrete T-beams.' Ph.D. Thesis, University of Sheffield, 1971.

142. SWAMY, R.N., BANDYOPADHYAY, A.K. and ERIKITOLA, M.K. 'Influence of the flange width on the shear behaviour of reinforced concrete T-beams. Proc. Instn. civ. Engrs., V. 55, Mar. 1973, pp. 167-190.

143. FERGUSON, P.M. and THOMPSON, J.N. 'Discussion of reference 27.' J. Am. Concr. Inst. Proc., V. 55, No. 9, Mar. 1959, pp. 1057-1068.

144. IVEY, D.L. and BUTH, E. 'Shear capacity of lightweight concrete beams.' J. Am. Concr. Inst. Proc., V. 64, No. 10, Oct. 1967, pp. 634-643.

145. A.C.I. 'Concrete Design: U.S. and European practices.' A.C.I. Publication SP-59, Detroit, Michigan, U.S.A., 1979, 346 p.

146. W. CRANSTON. Private Communication.

147. B.K. BARDHAN-ROY. Private Communication.

148. SWAMY, R.N. and QURESHI, S.A. 'Strength, cracking and deformation similitude in reinforced concrete T-beams under bending and shear.' J. Am. Concr. Inst. Proc., V. 68, No. 3, Mar. 1971, pp. 187-196.

149. MATHEY, R.G. and WATSTEIN, D. 'Strains in beams having diagonal tension cracks.' J. Am. Concr. Inst. Proc., V. 55, No. 6, Dec. 1958, pp. 717-728.

150. MATHEY, R.G. and WATSTEIN, D. 'Shear strength of beams without web reinforcement containing deformed bars of different yield strength.' J. Am. Concr. Inst. Proc., V. 60, No. 2, Feb. 1963, pp. 183-205.

151. SWAMY, R.N., ANDRIOPOULOS, A. and ADEPEGBA, D. 'Arch action and bond in concrete shear failures.' Jour. Struc. Div., Proc. A.S.C.E., Vol. 96, No. ST6, June 1970, pp. 1069-1091.

152. SWAMY, R.N. and ADEPEGBA, D. 'Discussion of reference No. 149.' J. Am. Concr. Inst. Proc., V. 63, No. 6, June 1966, pp. 1754-1755.

153. BOWER, J.E. and VIEST, I.M. 'Shear strength of restrained concrete beams without web reinforcement.' J. Am. Concr. Inst. Proc., V. 57, No. 1, July 1960, pp. 73-98.

154. WHITNEY, C.S. 'Plastic theory of reinforced concrete design.' Transactions A.S.C.E., V. 107, 1942, pp. 251-326.

155. WALRAVEN, J.C. 'The influence of depth on the shear strength of lightweight concrete beams without shear reinforcement.' Report No. 5-78-4, Stevin Laboratory, Delft University of Technology, Netherlands, 1978, 36 p.